Identification of plasma biomarkers for the early Alzheimer Disease diagnosis through lipid peroxidation and multi-omics studies

Instituto de Investigación Sanitaria La Fe

Universitat de València

Doctoral Thesis presented by

María del Carmen Peña Bautista

Programa de doctorado en Medicina (R.D. 99/2011)

PhD Program in Medicine (Faculty of Medicine and Dentistry)

Directed by: Dra. Consuelo Cháfer Pericás & Dr. Máximo Vento Torres

Tutored by: Dra. Ana Lloret Alcañiz

October 2023

Dña. Consuelo Cháfer Pericás, Investigadora Principal del Grupo de Investigación en Enfermedad de Alzheimer del Instituto de Investigación Sanitaria La Fe de Valencia,

D. Máximo Vento Torres, Investigador Principal del Grupo de Investigación en Perinatología del Instituto de Investigación Sanitaria La Fe de Valencia,

Dña. Ana Isabel Lloret Alzañiz, Catedrática de universidad de Valencia, Departamento de Fisiología, Instituto de Investigacion Sanitaria-INCLIVA, Valencia

CERTIFICAN:

Que la presente memoria, titulada "Identification of plasma biomarkers for the early Alzheimer Disease diagnosis through lipid peroxidation and multi-omics studies", corresponde al trabajo realizado bajo su dirección por

D. María del Carmen Peña Bautista, para su presentación como Tesis Doctoral en el Programa de Doctorado en Medicina de la Universitat de València.

Y para que conste firman el presente certificado en Valencia, a 29 de Septiembre de 2023.

Consuelo Cháfer-Pericás

MARIA CONSUELO\| CHAFER\| PERICAS

Firmado digitalmente por MARIA CONSUELO\| CHAFER\|PERICAS
Fecha: 2023.10.05 08:47:12 +02'00'

Máximo Vento Torres

MAXIMO\| VENTO\| TORRES

Firmado digitalmente por MAXIMO\|VENTO\| TORRES
Fecha: 2023.10.03 16:23:04 +02'00'

Ana Lloret Alcañiz

ANA ISABEL LLORET ALCAÑIZ - NIF:20162077R

Firmado digitalmente por ANA ISABEL LLORET ALCAÑIZ - NIF:20162077R
Fecha: 2023.10.04 14:34:51 +02'00'

A mis padres y mi hermana Alba

Agradecimientos

Ya lo decía Newton, “Si he logrado ver más lejos ha sido porque he subido a hombros de gigantes”. Quienes me conocen saben que no soy especialmente buena con las palabras pero en estos momentos, casi al final de la etapa de doctorado, es inevitable acordarse de todos y cada uno de esos gigantes que han formado parte de este camino y que de alguna forma han aportado su tiempo y cariño.

En primer lugar, me gustaría agradecer a mis directores, los doctores Consuelo Cháfer y Máximo Vento. A Consuelo por haber confiado en mí desde el primer momento, por haberme permitido iniciarme en este camino cuando casi pensaba en abandonarlo. Y por supuesto por haberme dado la oportunidad de formar parte del grupo de Investigación en Alzheimer desde el inicio y de poder ver cómo ha ido creciendo durante estos años. ¡Es un orgullo poder aportar mi granito de arena a este excelente equipo! También por el apoyo y la ayuda constante durante estos años. A Max por haberme acogido en su grupo (Perinatología), haberme permitido trabajar de cerca con investigadores excepcionales y sobre todo por sus siempre acertados consejos.

Un agradecimiento muy especial a todos y cada uno de los compañeros y estudiantes de prácticas que han pasado por el laboratorio 6.28 durante estos años. Pero especialmente a mi compañera de batallas y amiga Laura, por estar en cada una de las crisis pero también en todos los buenos momentos.

Por supuesto, no puedo dejarme a ninguno de los miembros de GINEA, a todo el equipazo que año a año ha ido creciendo. Un millón de gracias a todas por el apoyo constante, en lo profesional y también lo personal. Por supuesto al Dr. Baquero por aportar siempre su visión clínica que va siempre un paso más allá de lo que el resto somos capaces de ver. A Lourdes por ser mi neuróloga de confianza, pero también al resto de neuros, las nuevas incorporaciones y los que estuvieron en el inicio. A las enfermeras, especialmente a Aitana, con la que más momentos he podido compartir este tiempo y también a Bea, Inés y Silvia, sois un gran ejemplo de organización y calma ante los problemas que espero haber aprendido y poder usar en mi camino. Y por supuesto a mis psicólogas Inés, Lorena, Luis y Mar P, ¡Qué suerte tener un equipo tan bueno de psicólogas y no psicólogas que bien podrían dedicarse a ello! Un millón de gracias especialmente a mis chicas que durante estos años no han sido compañeras de trabajo sino amigas. Y por último,

agradecimiento doble a las que compartís conmigo en este camino de doctorado (Laura, Gemma, Inés, Lourdes, Mar G), juntas hemos crecido y estoy segura de que lo seguiremos haciendo. Ginea, hacéis muy fácil el trabajo, ¡un millón de gracias!

Mención especial al doctor Daniel Ferreira, por haberme acogido en su grupo como una más desde el inicio y por todo el aprendizaje. I also would like to extend this gratitude to all Dr. Ferreira's group and all people at Karolinska Institute. Thank you for showing me your exceptional way of doing science, for the collaboration, good predisposition and constant help.

No podría acabar sin acordarme de mis bioquímicos que siguen estando después de tantos años. Con ellos empezó el camino y es un orgullo poder decir que siguen estando.

Casi al final de mis agradecimientos, me gustaría acordarme de aquellos que se convirtieron en piedras en el camino, sin los cuales tampoco habría llegado hasta aquí. Pero también a los amigos que han empujado.

Por último pero no por ello menos importante, mi mayor agradecimiento es para mi familia, especialmente a mis padres y mi hermana por estar a mi lado en todo momento y ayudarme en los malos momentos, que sí, los hay. Para ellos va un gran reconocimiento.

Contents

De acuerdo con las regulaciones aprobadas por la Escuela de Doctorado y el Comité Académico del Programa de Doctorado en Medicina de la Universitat de València, la presente Tesis Doctoral se ha estructurado en el formato de compendio de publicaciones. El núcleo de la tesis está compuesto por doce artículos originales de la doctoranda como primera autora, publicados en revistas Q1 y Q2 según la base de datos "Journal Citation Reports".

New screening approach for Alzheimer's disease risk assessment from urine lipid peroxidation compounds. **Peña-Bautista C**, Vigor C, Galano JM, Oger C, Durand T, Ferrer I, Cuevas A, López-Cuevas R, Baquero M, López-Nogueroles M, Vento M, Hervás-Marín D, García-Blanco A, Cháfer-Pericás C. **Scientific Reports**. 2019 Oct 2;9(1):14244. doi: 10.1038/s41598-019-50837-2.

Factor de impacto en Journal Citation Reports (JCR) 2019: 3.998. Categoría y posición (JCR) 2019: Multidisciplinary Sciences 17/71, Q1.

Plasma lipid peroxidation biomarkers for early and non-invasive Alzheimer Disease detection. **Peña-Bautista C**, Vigor C, Galano JM, Oger C, Durand T, Ferrer I, Cuevas A, López-Cuevas R, Baquero M, López-Nogueroles M, Vento M, Hervás D, García-Blanco A, Cháfer-Pericás C. **Free Radical Biology and Medicine**. 2018 Aug 20;124:388-394. doi: 10.1016/j.freeradbiomed.2018.06.038.

Factor de impacto en Journal Citation Reports (JCR) 2018: 5.657. Categoría y posición (JCR) 2018: Biochemistry & Molecular Biology 43/299, Q1.

Assessment of lipid peroxidation and artificial neural network models in early Alzheimer Disease diagnosis. **Peña-Bautista C**, Durand T, Oger C, Baquero M, Vento M, Cháfer-Pericás C. **Clinical Biochemistry**. 2019 Oct;72:64-70. doi: 10.1016/j.clinbiochem.2019.07.008.

Factor de impacto en Journal Citation Reports (JCR) 2019: 2.573. Categoría y posición (JCR) 2019: Medical Laboratory Technology 12/29, Q2.

Isoprostanoids Levels in Cerebrospinal Fluid Do Not Reflect Alzheimer's Disease. **Peña-Bautista C**, Baquero M, López-Nogueroles M, Vento M, Hervás D, Cháfer-Pericás C. **Antioxidants (Basel)**. 2020 May 10;9(5):407. doi: 10.3390/antiox9050407.

Factor de impacto en Journal Citation Reports (JCR) 2020: 7.675. Categoría y posición (JCR) 2020: Chemistry, medicinal 4/63, D1.

Clinical Utility of Plasma Lipid Peroxidation Biomarkers in Alzheimer's Disease Differential Diagnosis. **Peña-Bautista C**, Álvarez L, Durand T, Vigor C, Cuevas A, Baquero M, Vento M, Hervás D, Cháfer-Pericás C. **Antioxidants (Basel)**. 2020 Jul 22;9(8):649. doi: 10.3390/antiox9080649.

Factor de impacto en Journal Citation Reports (JCR) 2020: 6.313. Categoría y posición (JCR) 2020: Chemistry, medicinal 6/62, D1.

Lipid Peroxidation Assessment in Preclinical Alzheimer Disease Diagnosis. **Peña-Bautista C**, Álvarez-Sánchez L, Ferrer I, López-Nogueroles M, Cañada-Martínez AJ, Oger C, Galano JM, Durand T, Baquero M, Cháfer-Pericás C. **Antioxidants (Basel)**. 2021 Jun 29;10(7):1043. doi: 10.3390/antiox10071043.

Factor de impacto en Journal Citation Reports (JCR) 2021: 6.313. Categoría y posición (JCR) 2021: Chemistry, medicinal 6/62, D1.

Lipid peroxidation biomarkers correlation with medial temporal atrophy in early Alzheimer Disease. **Peña-Bautista C**, López-Cuevas R, Cuevas A, Baquero M, Cháfer-Pericás C. **Neurochemistry International**. 2019 Oct;129:104519. doi: 10.1016/j.neuint.2019.104519.

Factor de impacto en Journal Citation Reports (JCR) 2019: 3.881. Categoría y posición (JCR) 2019: Neurociences 95/272, Q2.

Plasma metabolomics in early Alzheimer's disease patients diagnosed with amyloid biomarker. **Peña-Bautista C**, Roca M, Hervás D, Cuevas A, López-Cuevas R, Vento M, Baquero M, García-Blanco A, Cháfer-Pericás C. **Journal of Proteomics**. 2019 May 30;200:144-152. doi: 10.1016/j.jprot.2019.04.008.

Factor de impacto en Journal Citation Reports (JCR) 2019: 3.509. Categoría y posición (JCR) 2019: Biochemical Research Methods 21/77, Q2.

Metabolomics study to identify plasma biomarkers in alzheimer disease: ApoE genotype effect. **Peña-Bautista C**, Roca M, López-Cuevas R, Baquero M, Vento M, Cháfer-Pericás C. **Journal of Pharmaceutical and Biomedical Analysis**. 2020 Feb 20;180:113088. doi: 10.1016/j.jpba.2019.113088

Factor de impacto en Journal Citation Reports (JCR) 2020: 3.935. Categoría y posición (JCR) 2020: Chemistry, Analytical 24/87, Q2.

Plasma Lipidomics Approach in Early and Specific Alzheimer's Disease Diagnosis. **Peña-Bautista C**, Álvarez-Sánchez L, Roca M, García-Vallés L, Baquero M, Cháfer-Pericás C. **Journal of Clinical Medicine**. 2022 Aug 27;11(17):5030. doi: 10.3390/jcm11175030.

Factor de impacto en Journal Citation Reports (JCR) 2022: 3.9. Categoría y posición (JCR) 2021: Medicine, General & Internal 58/167, Q2.

Plasma microRNAs as potential biomarkers in early Alzheimer disease expression. **Peña-Bautista C**, Tarazona-Sánchez A, Braza-Boils A, Balaguer A, Ferré-González L, Cañada-

Martínez AJ, Baquero M, Cháfer-Pericás C. **Scientific Reports**. 2022 Sep 16;12(1):15589. doi: 10.1038/s41598-022-19862-6

Factor de impacto en Journal Citation Reports (JCR) 2021: 4.6. Categoría y posición (JCR) 2021: Multidisciplinary Sciences 22/73, Q2.

Epigenomics and Lipidomics Integration in Alzheimer Disease: Pathways Involved in Early Stages. **Peña-Bautista C**, Álvarez-Sánchez L, Cañada-Martínez AJ, Baquero M, Cháfer-Pericás C. **Biomedicines**. 2021 Dec 2;9(12):1812. doi: 10.3390/biomedicines9121812.

Factor de impacto en Journal Citation Reports (JCR) 2021: 4.757. Categoría y posición (JCR) 2021: Biochemistry & Molecular Biology 121/297, Q2.

RESUMEN GLOBAL

1. Introducción

Enfermedad de Alzheimer: fisiopatología, diagnóstico y tratamiento.

La Enfermedad de Alzheimer (EA) es la enfermedad neurodegenerativa más común siendo la causa de alrededor del 70% de las demencias. En 2018 la EA afectaba a alrededor de 50 millones de personas en todo el mundo [1,2], y se espera que la incidencia en países desarrollados continue aumentando debido al envejecimiento de la población, superando los 150 millones en 2050. La EA genera un gran impacto social y económico [3], debido a factores como el coste médico, la falta de productividad, la disminución de la calidad de vida de enfermos y cuidadores, y la dependencia. Sin embargo, los tratamientos disponibles no consiguen curar ni detener la enfermedad, siendo en su mayoría tratamientos sintomatológicos [4]. Actualmente, se están desarrollando numerosos ensayos clínicos con nuevos fármacos con acción frente a diferentes mecanismos fisiopatológicos potencialmente implicados en el desarrollo de la EA [4]. En general, estos tratamientos están dirigidos a fases iniciales de la enfermedad, en las que muestran conseguir una mayor efectividad. Por ello, es necesario un diagnóstico temprano de la EA. Actualmente la complejidad e invasividad de los métodos diagnósticos utilizados (biomarcadores en líquido cefalorraquídeo, técnicas de neuroimagen), dificulta la detección temprana. Por ello, es necesario identificar biomarcadores diagnósticos fiables, tempranos y mínimamente invasivos, así como avanzar en el conocimiento de los mecanismos fisiopatológicos implicados en la aparición y desarrollo de la enfermedad.

Clínicamente, la EA se caracteriza por un deterioro cognitivo progresivo que afecta a diferentes dominios como la memoria episódica, la fluidez verbal o las funciones ejecutivas [5]. En la mayoría de casos se trata de una enfermedad esporádica, de hecho los casos de EA familiar debida a mutaciones en genes (proteína precursora de amiloide (APP), presenilinas 1 y 2 (PS1) (PS2)) no llegan al 2% [6]. Además, entre los factores de riesgo de la EA destaca el gen que codifica la Apolipoproteína E (ApoE), concretamente el alelo Ɛ4; así como otros factores relacionados con el estilo de vida (hipercolesterolemia, diabetes, hipertensión), considerados factores modificables [7].

Mecanismos fisiopatológicos

A nivel fisiopatológico, la EA se caracteriza principalmente por dos marcas histopatológicas: i) agregados intracelulares de la proteína Tau fosforilada (p-Tau) en forma de ovillos neurofibrilares, y ii) acúmulos extracelulares de la proteína beta amiloide (βA) anormalmente plegada en forma de placas seniles que ocurre principalmente en el lóbulo temporal medial y estructuras neocorticales, que acaban dando lugar a una pérdida de sinapsis [4]. En general, las principales hipótesis sobre el origen de la enfermedad son la cascada amiloide, la hipótesis de Tau y la colinérgica [4].

La hipótesis amiloide. En 1992 se hipotetizó por primera vez el papel central de la proteína amiloide β (Aβ) como el agente causante de la EA [8]. En ella se describía cómo a partir de un procesamiento específico de la proteína precursora amiloide (PPA) se generaba un péptido que precipitaba dando lugar a la muerte celular, además de promover la acumulación de Tau en ovillos neurofibrilares [8]. La PPA es una proteína transmembrana que puede ser escindida por dos vías: i) la "normal" o no patológica, en la que actúa la enzima α-secretasa y posteriormente la γ-secretasa dando lugar a un péptido extracelular soluble; y ii) la amiloidogénica, en la que actúa la enzima β-secretasa (BACE) y posteriormente la enzima γ-secretasa produciendo péptidos de diferentes longitudes, entre los que se encuentra Aβ42 [9]. Como apoyo a esta teoría se encuentra los factores de riesgo genéticos. Así pues, la Apolipiproteína E (ApoE) tiene influencia sobre la eliminación de amiloide β42 siendo menor con la isoforma Apoε4 [10]. Además, mutaciones en los genes PS1, PS2 y BACE contribuyen al desarrollo de la enfermedad.

El aumento en la producción de este péptido Aβ42, considerado tóxico y la reducción en los mecanismos de eliminación del mismo da lugar a la formación primero de oligómeros afectando a la función sináptica. Esto desencadena una respuesta inflamatoria y un aumento de estrés oxidativo, dando lugar finalmente a la formación de las placas seniles [11]. Esta respuesta inflamatoria contribuye a la fosforilación de Tau que también juega un papel relevante en el desarrollo de la enfermedad [11].

Hipótesis de Tau. Algunos estudios sugieren que en primer lugar aparece la cascada amiloide y la toxicidad generada da lugar a la hiperfosforilación de Tau generando un aumento en la toxicidad celular y pérdida de neuronas. Sin embargo, otros sostienen que

la patología Tau es la que desencadena los mecanismos patológicos de la enfermedad [12,13].

Tau es una proteína intracelular que forma parte del citoesqueleto y es especialmente importante en las neuronas donde realiza funciones estructurales y de transporte de sustancias como los neurotransmisores [13]. En condiciones fisiológicas, esta proteína sufre fosforilaciones en diversos residuos, sin embargo, en condiciones patológicas como la EA se produce una hiperfosforilación [13], que aumenta su toxicidad. Además, facilita la formación de agregados de proteínas Tau u ovillos neurofibrilares (NFT) pudiendo dar lugar a muerte celular y por tanto a la pérdida de neuronas [13].

Hipótesis colinérgica. La acetilcolina (ACh) es un neurotransmisor que se forma en el citoplasma de las neuronas colinérgicas a partir de colina y Acetil-CoA por acción de la enzima colina-acetil transferasa. Este neurotransmisor es transportado por vesículas al espacio sináptico tras la despolarización de la neurona presináptica. En la neurona postsináptica puede unirse a receptores muscarínicos o nicotínicos produciendo repuesta inhibitoria o activadora. En el espacio sináptico se hidroliza por la acetilcolinesterasa si no se ha unido a ningún receptor [14].

La acetilcolina (ACh) es un neurotransmisor implicado en procesos como el aprendizaje o la memoria, y las neuronas colinérgicas presentan una degeneración específica en la EA [14]. Concretamente, se ha observado una reducción de la actividad de la enzima acetiltransferasa de colina [11]. De hecho, los tratamientos convencionales actuales para la EA se basan en aumentar la señal colinérgica para contrarrestar la reducción de acetilcolina manteniendo el neurotransmisor un tiempo más prolongado en el espacio sináptico [15].

A pesar de haber discrepancias en la temporalidad de mecanismos implicados en la EA, todos ellos coexisten una vez la patología está instaurada, junto con otros mecanismos como la neuroinflamación, activación de microglía y astrocitos, estrés oxidativo, alteraciones en el metabolismo de lípidos, proteínas, ADN, neurotransmisores, etc [4,16–20].

Diagnóstico

En la práctica clínica el diagnóstico se basa principalmente en los síntomas clínicos. Sin embargo, desde este punto de vista la EA es muy heterogénea [21]. Se trata de una enfermedad progresiva que puede evolucionar a lo largo de 15-25 años desde que se instauran los mecanismos fisiopatológicos hasta que aparecen los síntomas clínicos y se agravan [22]. En el continuo que caracteriza a la EA se pueden definir varias etapas: i) EA preclínica en la que hay ausencia de síntomas clínicos, aunque se detecta la alteración de los biomarcadores propios de la enfermedad; ii) deterioro cognitivo leve (DCL) con presencia de síntomas iniciales pero sin afectación de las actividades de la vida diaria; y iii) demencia, caracterizada por síntomas más avanzados con afectación de las actividades de la vida diaria [5]. Las guías clínicas definidas por Instituto Nacional de envejecimiento y la Asociación de Alzheimer (NIA-AA) basan el diagnóstico en la etapa de deterioro cognitivo leve (DCL), concretamente en la detección de un cambio en la cognición por parte del paciente, un observador o bien un clínico experto [23]. Este deterioro se produce en uno o varios dominios cognitivos (memoria, función ejecutiva, atención, lenguaje, habilidades visoespaciales) [23]. Sin embargo, estos pacientes siguen manteniendo independencia en cuanto a la funcionalidad [23]. En etapas más avanzadas se basa en la presencia de demencia (deterioro en funcionalidad que no se explican por delirio o problemas psiquiátricos, deterioro cognitivo basado en valoraciones neuropsicológicas, alteraciones en el comportamiento), y una progresión de los síntomas durante meses o años [24]. Además, los principales síntomas cognitivos son el deterioro en el aprendizaje y recuerdo de la información aprendida recientemente en el caso de la variante amnésica, o bien alteraciones en el lenguaje, visoespaciales o en funciones ejecutivas en la variante no amnésica [24].

El NIA-AA publicó en 2018 una actualización de las guías diagnósticas para la EA de 2011 basadas en criterios clínicos encaminada a una definición más biológica de la enfermedad basada en biomarcadores [25]. Los biomarcadores se agrupan según la clasificación ATN (A: depósito de β-amiloide; T: Tau patológica; N: neurodegeneración). Este sistema de clasificación ATN incluye biomarcadores de imagen y líquido cefalorraquídeo (LCR) según el proceso patológico que cada uno mide. En cuanto a las medidas de depósito de amiloide (A) se encuentran los biomarcadores en LCR Aβ42 y el

ratio Aβ42/Aβ40 además de Tomografía por Emisión de Positrones (PET) amiloide. En cuanto a los depósitos de ovillos neurofibrilares o Tau patológica (T), se define por los niveles de p-Tau en LCR o PET Tau. Por último, la definición de neurodegeneración o daño neuronal (N) incluye resonancia magnética nuclear (RMN) estructural, PET-FDG o niveles de Tau total en LCR (t-Tau). En estas guías se remarca la flexibilidad del sistema para la incorporación de nuevos biomarcadores dentro de los grupos ATN y también nuevas categorías.

Tratamientos

Actualmente, los tratamientos frente a la EA únicamente consiguen reducir la sintomatología a nivel cognitivo y funcional. Los fármacos más extendidos para la EA son los inhibidores de la acetilcolinesterasa (donepezilo (Aricept™), rivastigmina (Exelon™), y galantamina (Razadyne™)) y antagonistas del receptor N-metil-D-aspartato (memantine (Namenda™)) [26]. En los últimos años se están desarrollando nuevos potenciales tratamientos que pueden dividirse en dos tipos: i) los dirigidos a actuar sobre la sintomatología de la enfermedad (cognición, agitación, agresividad, etc) y ii) tratamientos modificadores de la enfermedad [26]. Estos últimos se dirigen a diferentes dianas entre las que destacan los tratamientos anti-amiloide, encaminados específicamente a reducir la placa amiloide, los tratamientos anti-Tau dirigidos a reducir los ovillos neurofibrilares y los dirigidos a reducir o regular inflamación, metabolismo, bioenergética, plasticidad sináptica y neuroprotección o antioxidantes entre otros [22,26,27]. Algunos de estos tratamientos han mostrado una reducción en las placas amiloides aunque esto sólo se traduce en una reducción moderada en el deterioro cognitivo producido por la enfermedad [28]. En general, los tratamientos que se encuentran en investigación clínica tienen una alta tasa de fracaso que podría ser consecuencia de la complejidad de la enfermedad y la falta de una visión completa de los mecanismos fisiopatológicos implicados y la interacción entre ellos [26]. Por otro lado, cabe destacar que la mayoría de los ensayos llevados a cabo actualmente se dirigen a pacientes en etapas tempranas y algunos en etapas moderadas [26], por lo que es relevante obtener un diagnóstico precoz para poder acceder a los tratamientos en las etapas tempranas en las que muestran efectividad [27].

Estrés oxidativo y Enfermedad de Alzheimer

El estrés oxidativo juega un papel importante en el desarrollo de las enfermedades neurodegenerativas [29]. En circunstancias normales, existe en el organismo un equilibrio entre sustancias oxidantes y antioxidantes que permite al organismo realizar sus funciones metabólicas y de señalización necesarias [30]. Sin embargo, cuando los sistemas antioxidantes no son capaces de compensar el nivel de oxidantes se desencadena un desequilibrio conocido como estrés oxidativo [30]. Cuando este desequilibrio ocurre existe un aumento en el estrés celular dando lugar en última instancia a procesos de muerte celular y apoptosis, necrosis o autofagia [31].

Específicamente, el estrés oxidativo mantiene una relación bidireccional con la cascada amiloide, por un lado el estrés oxidativo favorece la vía amiloidogénica de procesamiento de APP aumentando la producción del péptido tóxico Aβ42, y por otro lado, las placas amiloides favorecen el aumento de estrés oxidativo llevando a la muerte celular [32,33]. De forma similar, el estrés oxidativo interacciona con las quinasas encargadas de la fosforilación de Tau y a su vez los ovillos neurofibrilares producen un aumento de especies reactivas de oxígeno (ROS) [32].

El ambiente oxidante genera daño en biomoléculas celulares como proteínas, ADN y lípidos [34]. Compuestos derivados de este proceso pueden ser detectados en muestras periféricas como sangre u orina sirviendo como una aproximación al estado oxidativo del organismo [35]. Específicamente, los biomarcadores de estrés oxidativo más utilizados son proteínas carboniladas, nitrotirosina, productos de oxidación avanzada de proteínas (ej. Cloro-tirosina) como derivados de la oxidación de proteínas; 7,8-dihydroxy-8-oxo-2′-deoxyguanosine (8oxodG), como derivados de la oxidación de ADN; y malondialdehído (MDA), 4-hidroxi-2-nonenal (HNE) e isoprostanos como derivados de la oxidación lipídica [36].

El cerebro es un órgano con una gran actividad metabólica, alto consumo de oxígeno y alto contenido en ácidos grasos poliinsaturados que lo hacen susceptible al daño oxidativo [37]. Concretamente, la oxidación de lípidos podría tener un papel importante en el desarrollo de enfermedades neurodegenerativas y específicamente en la EA [38]. De hecho, estudios previos han encontrado co-localización de productos de la oxidación de

lípidos con placas amiloides evidenciando la relación entre el estrés oxidativo y los lípidos con el desarrollo de los mecanismos patológicos de la EA [39].

Los lípidos pueden ser oxidados por dos vías independientes (enzimática y no enzimática o por radicales libres) [40]. En esta tesis nos centramos en los compuestos derivados de la oxidación de tres ácidos grasos polinsaturados (PUFA): ácido araquidónico (AA), ácido docosahexanoico (DHA) y ácido adrénico (AdA). En cuanto al AA su oxidación da lugar a dos familias de compuestos: i) isoprostanos e isofuranos como (15(*R*)-15-F_{2t}-IsoP; 2,3-dinnor-15-*epi*-15-F_{2t}-IsoP; 15-keto-15-E_{2t}-IsoP; 15-keto-15-F_{2t}-IsoP; 15-E_{2t}-IsoP;15-F_{2t}-IsoP; 5-F_{2t}-IsoP), originándose los segundos bajo unas condiciones con más tensión de oxígeno, y ii) prostaglandinas (PGE_2; $PGF_{2\alpha}$; 1a,1b-dihomo- $PGF_{2\alpha}$) [41]. EL AA se encuentra en una gran cantidad en el cerebro formando parte de las membranas celulares [42,43]. Por otro lado, la oxidación del DHA localizado principalmente en la materia gris del cerebro, y del AdA localizado principalmente en la materia blanca del cerebro, dan lugar a los neuroprostanos (10-*epi*-10-F_{4t}-NeuroP; 14(*RS*)-14-F_{4t}-NeuroP; 4(*RS*)-F_{4t}-NeuroP) y dihomo-isoprotanos (17-*epi*-17-F_{2t}-dihomo-IsoP; 17-F_{2t}-dihomo-IsoP; *ent*-7(*RS*)-7-F_{2t}-dihomo-IsoP; 17(*RS*)-10-*epi*-SC-Δ^{15}-11-dihomo-IsoF; 7(*RS*)-ST-Δ^{8}-11-dihomo-IsoF), respectivamente [43].

Análisis ómicos y Enfermedad de Alzheimer

Otra herramienta de gran utilidad en el estudio de enfermedades complejas como la EA son los análisis ómicos en muestras biológicas, que proporcionan información acerca de las vías patológicas implicadas, así como generando nuevos potenciales biomarcadores y dianas terapéuticas [44,45]. Este tipo de análisis implican un tratamiento previo de la muestra, así como un procesado e interpretación posterior de los resultados [46]. En esta tesis centramos el estudio ómico en análisis metabolómico, lipidómico y epigenómico.

Metabolómica en EA

La metabolómica permite caracterizar el perfil de metabolitos en cualquier tipo de muestras como sangre o LCR, siendo especialmente útil en la detección de potenciales biomarcadores dada su capacidad para detectar pequeños cambios y para el estudio de mecanismos fisiológicos y patológicos [47]. Los estudios metabolómicos pueden enfocarse desde un análisis no dirigido, que permite una visión global; y un análisis

dirigido, que permite validar y confirmar los resultados obtenidos con los métodos no dirigidos [48]. Una de las técnicas analíticas más utilizadas es la espectrometría de masas (MS), que se caracteriza por su elevada sensibilidad y especificidad [49]

Los estudios metabolómicos dirigidos y no dirigidos han permitido identificar biomarcadores para la EA en fluidos biológicos como LCR, plasma u orina [50–52] postulando esta técnica como una herramienta útil en la búsqueda de nuevos biomarcadores.

Lipidómica en EA

La lipidómica consiste en el estudio del perfil lipídico en una determinada muestra biológica.

El cerebro tiene una alta composición lipídica, por ello tiene gran interés el estudio lipidómico en pacientes con EA, evidenciando la desregulación de esta familia de biomoléculas tanto en diferentes áreas cerebrales como en otros fluidos biológicos [53]. Además, estos metabolitos presentan una potencial utilidad como fuente de biomarcadores diagnósticos específicos de la enfermedad [53].

Epigenómica en EA

La epigenómica se encarga del estudio de la regulación de genes siendo las vías más estudiadas la metilación de ácido desoxirribonucleico (DNA), las modificaciones de histonas y los áidos ribonucleico (RNAs) no codificantes [54]. Dentro de estos últimos, se encuentran los microRNAs (miRNA) que son secuencias de RNA de entre 19 y 25 nucleótidos implicados en la regulación de genes tanto positiva como negativamente [55]. Por tanto, la epigenética guarda una estrecha relación con los procesos patológicos siendo de gran utilidad en la compresión de los mecanismos fisiopatológicos así como proporcionando potenciales biomarcadores [56].

En la EA diversos miRNAs han mostrado niveles diferenciales en comparación con sujetos sin la enfermedad, tanto en cerebro como en fluidos biológicos (LCR, derivados sanguíneos [57]. Las metilaciones de DNA, modificaciones de histonas y los RNA no codificantes están implicados en rutas relacionadas con la enfermedad y sus factores de riesgo [58]. Por tanto, pueden constituir una importante fuente de biomarcadores.

Integración de datos experimentales de diferente naturaleza

La integración de resultados de diferentes técnicas ómicas permite la identificación de vías implicadas en la EA permitiendo una caracterización más completa de los pacientes con EA [59]. Esto puede ayudar a una descripción más exhaustiva de la heterogeneidad de los pacientes con EA y sus implicaciones clínicas con el fin de obtener un diagnóstico temprano, generalizado, fiable y fácil acceso a tratamientos personalizados [60].

Estudios previos han integrado datos de diferente naturaleza con el objetivo común de profundizar en las vías patológicas de la EA. Específicamente, la integración de análisis metabolómicos y genómicos permitió detectar metabolitos alterados y sus reguladores [61]. Además, la visión conjunta incluyendo metabolómica y genómica ayudan a la compresión de los mecanismos subyacentes que contribuyen al riesgo de EA [62]. Por tanto, estos estudios permiten una visión global y más completa de la enfermedad.

2. Hipótesis y Objetivos

La hipótesis de la presente Tesis Doctoral es que los compuestos de peroxidación lipídica y otros obtenidos mediante análisis ómicos (metabolómica, lipidómica, epigenómica) en muestras mínimamente invasivas, pueden ser potenciales biomarcadores para el diagnóstico temprano de la EA, además de proporcionar información sobre las vías metabólicas implicadas en el desarrollo de la enfermedad.

El objetivo principal de la tesis fue estudiar los compuestos derivados de peroxidación lipídica como potenciales biomarcadores diagnósticos específicos de la EA y su relación con las variables clínicas de la enfermedad, e identificar nuevos biomarcadores y vías patológicas alteradas en las primeras etapas de la EA mediante una aproximación multiómica (metabolómica, lipidómica, epigenómica).

Los objetivos específicos fueron:

i) Identificar potenciales biomarcadores basados en peroxidación lipídica para la detección de la EA en muestras de orina (*Capítulo 1*) y plasma (*Capítulo 2*).

ii) Desarrollo de modelos diagnóstico de la EA basados en biomarcadores de peroxidación lipídica (*Capítulos 1, 2 y 5*).

iii) Seleccionar el mejor tipo de muestra para el diagnóstico de la EA a partir de los niveles de los compuestos de peroxidación lipídica (*Capítulo 3*).

iv) Analizar la utilidad de los potenciales biomarcadores (compuestos de peroxidación lipídica) para el diagnóstico temprano o preclínico de la EA (*Capítulo 6*).

v) Establecer la relación entre los compuestos de peroxidación lipídica y las variables clínicas de la EA: atrofia cerebral mediante escalas visuales (*Capítulo 7*), biomarcadores estándar en Líquido cefalorraquídeo (LCR) y deterioro cognitivo mediante evaluaciones neuropsicológicas (*Capítulos* 2, 4 y 6)

vi) Búsqueda de nuevos biomarcadores plasmáticos para el diagnóstico de la EA en plasma mediante técnicas ómicas: metabolómica (*Capítulos 8 y 9*), lipidómica (*Capítulo 10*), epigenómica (*Capítulo 11*).

vii) Estudio de potenciales vías metabólicas alteradas en la EA mediante el análisis ómico (*Capítulos 10 y 11*) y la integración de diferentes resultados ómicos (*Capítulo 12*).

3. Metodología

Participantes y obtención de muestras

Los participantes incluidos en estos estudios son pacientes de la Unidad de Neurología del Hospital Universitario La Fe (Valencia). El diagnóstico y clasificación de estos pacientes en grupos de estudio se realiza siguiendo los criterios del NIA-AA teniendo en cuenta la valoración neuropsicológica (*Clinical Dementia Rating* (CDR), *Mini-mental State Examination* (MMSE), *Repeatable Battery for the Assessment of Neuropsychological Status* (RBANS), *Functional Activities Questionnaire* (FAQ)), niveles de biomarcadores (Aβ42, t-Tau, p-Tau181) en LCR o PET amiloide, y cambios estructurales cerebrales mediante resonancia magnética nuclear (RMN). De esta forma los participantes se clasifican en los siguientes grupos: i) control, presentan niveles normales de biomarcadores en LCR y no tienen alteración cognitiva; ii) EA preclínica, presentan niveles alterados de biomarcadores en LCR pero no tienen alteración cognitiva; iii) DCL debido a EA, presentan niveles alterados de biomarcadores en LCR y alteración cognitiva, sin perder la capacidad para la realización de las actividades de la vida diaria; iv) DCL no debido a EA, presentan niveles normales de biomarcadores en LCR y alteración cognitiva. El grupo "EA" o "caso" que aparece en algunos capítulos incluye pacientes con DCL-EA o demencia leve debida a EA y el grupo EA temprana incluye pacientes con DCL-EA y EA preclínica. Además el grupo control está referido en algunos capítulos como controles sanos o sanos.

Determinación de biomarcadores

En cuanto a los biomarcadores analizados en los diferentes estudios que componen la presente tesis, en la primera sección se determinan biomarcadores procedentes de la peroxidación lipídica y en la segunda sección biomarcadores de distinta naturaleza mediante técnicas ómicas (metabolómica, lipidómica, epigenómica)

En cuanto a los biomarcadores de peroxidación lipídica, se determinaron en muestras de orina, plasma y LCR mediante un método analítico basado en cromatografía líquida de alta resolución acoplado a espectrometría de masas (UPLC-MS/MS). Previamente se realizó un tratamiento a las muestras, diferente para cada matriz biológica, que en general incluía una etapa de purificación y pre-concentración.

En cuanto a las técnicas ómicas en muestras de plasma se realizaron estudios de metabolómica y lipidómica mediante los métodos validados de la Unidad Analítica del Instituto de Investigación Sanitaria La Fe (IIS LaFe) basados en espectrometría de masas; y epigenómica mediante secuenciación masiva. Previamente al análisis metabolómico y lipidómico se realizó una etapa de precipitación de proteínas y para los estudios epigenómicos se requirió de una etapa de extracción de RNA. Posteriormente, en todas las técnicas se realizó un pre-procesamiento de datos y los controles de calidad pertinentes.

Análisis estadísticos

Los análisis estadísticos realizados fueron por un lado univariantes, incluyendo el estudio de diferencias entre grupos mediante Mann-Whitney o Kruskal-Wallis para las variables numéricas y Chi-Cuadrado para las variables categóricas, y el estudio de correlaciones mediante el Test de Correlación de Pearson.

Por otro lado, se realizaron análisis multivariantes para estudiar la capacidad diagnóstica de paneles de biomarcadores y la selección de variables influyentes en la discriminación entre los grupos de estudio. Los principales modelos utilizados fueron: i) Regresión por mínimos cuadrados parciales (PLS), ii) Regresión lineal Elastic Net, iii) Máquinas de vectores de soporte (SVM), iv) Redes neuronales artificiales (ANN), y v) Random Forest.

Se utilizaron los softwares R studio y SPSS y se consideró el p valor <0.05 para establecer la significación estadística.

4. Resultados

La tesis está dividida en dos secciones, ambas centradas en los biomarcadores diagnósticos para la EA. La primera parte incluye 7 capítulos en los que se evalúa la capacidad de los compuestos de peroxidación lipídica en orina y plasma, en el diagnóstico de la EA. La segunda parte incluye los capítulos del 8 al 12 dedicados al estudio de la utilidad diagnóstica de los análisis ómicos (metabolómica, lipidómica, epigenómica) en la EA. A continuación, se detallan los principales resultados obtenidos.

En los dos primeros capítulos se realizaron análisis en pacientes con EA temprana (DCL-EA y demencia leve debida a EA) y controles en muestras de plasma y orina. En las muestras de orina (capítulo 1), se encontraron algunos biomarcadores diferencialmente expresados entre los grupos caso (n=70) y control (n=29). Los compuestos 5-F_{2t}-IsoP, 2,3-dinor-15-*epi*-15-F_{2t}-IsoP, 15-E_{2t}-IsoP, PGE_2, $PGF_{2\alpha}$, 10-*epi*-10-F_{4t}-NeuroP, 4(*RS*)-4-F_{4t}-NeuroP, *ent*-7(*RS*)-7-F_{2t}-dihomo-IsoP) mostraron niveles elevados en los pacientes con EA con respecto a los controles, mientras que 15-keto-15-E_{2t}-IsoP, 15-keto-15-F_{2t}-IsoP presentaban niveles más bajos en el grupo con EA. Con estos resultados, se desarrolló un modelo de regresión lineal (Elastic Net) que seleccionó 6 variables (15(*R*)-15-F_{2t}-IsoP, 15-E_{2t}-IsoP, $PGF_{2\alpha}$, 4(*RS*)-F_{4t}-NeuroP, 14(*RS*)-14-F_{4t}-NeuroP, *Ent*-7(*RS*)-7-F_{2t}-dihomo-IsoP) además de género y edad. La exactitud del modelo fue de 0.682. En paralelo se desarrolló un modelo basado en Random Forest que seleccionó las mismas variables con una exactitud de 0.71. Cabe destacar en el modelo de Elastic Net que para poder ser útil como herramienta de cribado y obtener una buena sensibilidad se debe sacrificar la especificidad.

En las muestras de plasma (capítulo 2) se encontraron algunos de los biomarcadores diferencialmente expresados entre los grupos caso (pacientes con EA) y control. Los compuestos 15(*R*)-15-F_{2t}-IsoP, 15-keto-15-E_{2t}-IsoP, 15-keto-15-F_{2t}-IsoP, 15-E_{2t}-IsoP, 4(*RS*)-F_{4t}-NeuroP and *ent*-7(*RS*)-7-F_{2t}-dihomo-IsoP mostraron niveles elevados en el grupo caso con respecto a los controles, mientras que $PGF_{2\alpha}$, 5-F_{2t}-IsoP, 7(*RS*)-ST-Δ^8–11-dihomo-IsoF presentaban niveles más bajos en el grupo de EA. Con estos resultados, se desarrolló un modelo de regresión lineal (Elastic Net) que seleccionó 6 variables 15-keto-15-F_{2t}-IsoP, 4(*RS*)-4-F_{4t}-NeuroP, 1a,1b-dihomo-$PGF_{2\alpha}$, ent-7(*RS*)-7-F_{2t}-dihomo-IsoP, 17-*epi*-17-F_{2t}-dihomo-IsoP), además de género y edad. La exactitud del modelo fue de 0.88

(IC 95%, 0.82-0.95) y el área bajo la curva- Característica Operativa del Receptor (AUC-ROC) de validación de 0.817.

En el capítulo 3 nos planteamos comparar la capacidad diagnóstica de los paneles de biomarcadores determinados en ambas matrices (plasma y orina) en la diferenciación entre controles sanos y pacientes con DCL-EA. Para ello, se desarrollaron modelos estadísticos basados en ANN, SVM y PLS. Los resultados obtenidos fueron los siguientes: en orina (ANN AUC: 0.839 (IC 95%, 0.746–0.933), PLS AUC: 0.653 (IC 95%, 0.526–0.780), SVM AUC: 0.644 (IC 95%, 0.539–0.749) con función polinomial y 0.659 (IC 95%, 0.558–0.759) con función radial); en plasma: (ANN AUC: 0.882 (IC 95%, 0.814–0.949), PLS AUC 0.765 (CI 95%, 0.633–0.868) y SVM AUC: 0.817 (IC 95%, 0.712–0.922) con función polinomial y 0.827 (IC 95%, 0.739–0.915) con función radial. En general, los modelos basados en redes neuronales fueron los que presentaron mejores índices diagnósticos y los modelos basados en biomarcadores en plasma presentaron mayor exactitud que los de orina.

En el capítulo 4, se estudió la relación de los niveles de los compuestos peroxidación lipídica entre muestras de LCR y plasma para valorar su posible procedencia cerebro-específica. Las correlaciones entre estas dos matrices no fueron satisfactorias. Únicamente 17(*RS*)-10-*epi*-SC-Δ^{15}-11-dihomo-IsoF mostró una correlación significativa entre las dos matrices (CCP 0.248, p = 0.031). Analizando por separado los grupos de participantes (EA y no EA) con el fin de evaluar la influencia de la alteración en la barrera hematoencefálica, se obtuvieron correlaciones significativas entre las dos matrices para 15(*R*)-15-F_{2t}-IsoP (CCP = 0.388, p = 0.024), 15-keto-15-F_{2t}-IsoP (CCP = 0.360, p = 0.037) y 5-F_{2t}-IsoP (CCP = 0.345, p = 0.046) en el grupo no EA y para 17-F_{2t}-dihomo-IsoP (CCP = 0.399, p = 0.009), 17(*RS*)-10-*epi*-SC-Δ^{15}-11-dihomo-IsoF (CCP = 0.345, p = 0.045) en el grupo EA. A pesar de no encontrarse en general una buena relación entre las dos matrices, sí se encontraron algunas relaciones con los biomarcadores propios de la EA y el estado cognitivo. De hecho, los niveles de Aβ42 en LCR mostraron correlación negativa significativa con los niveles en LCR de 7(*RS*)-ST-Δ^{8}-11-dihomo-IsoF, 5-F_{2t}-IsoP, neurofuranos e isofuranos totales. Además, p-Tau181 en LCR mostró correlación negativa con PGE_2 en LCR. En cuanto al estado cognitivo, RBANS y especialmente su dominio viso/espacial mostró correlación con los niveles de 15-F_{2t}-IsoP, *Ent*-7(*RS*)-F_{2t}-

dihomo-IsoP and 15-keto-15-F_{2t}-IsoP LCR. Además, 15-keto-15-F_{2t}-IsoP también correlacionaba con el dominio de atención de RBANS y MMSE, y 15-keto-15-E_{2t}-IsoP correlacionaba con FAQ y CDR.

Hasta el momento, habíamos valorado la potencial capacidad diagnóstica de este panel de biomarcadores de EA frente a controles con mínimo deterioro cognitivo, pero tratando de acercarnos más a la práctica clínica, en el capítulo 5 se evaluó la capacidad diagnóstica específica de los compuestos de peroxidación lipídica en muestras de plasma para la EA.

Para ello, se evaluaron las diferencias entre pacientes con EA y pacientes sin EA (controles y pacientes con DCL por otras causas distintas a EA). En este caso, los compuestos 15-E_{2t}-IsoP, $PGF_{2\alpha}$, 4(*RS*)-F_{4t}-NeuroP, 10-*epi*-10-F_{4t}-NeuroP e IsoP totales presentaron diferencias entre los grupos de estudio (EA (n = 138), no EA (DCL y otras demencias no debidas a EA) (n = 70), control sano (n = 50)). Además, se desarrolló un modelo diagnóstico en 2 etapas basado en regresión lineal. La primera etapa consistía en una evaluación neuropsicológica (CDR, RBANS.MR) que diferenciaba ente controles y casos (incluyendo grupos de pacientes con EA y sin EA) con un AUC de 0.99. La segunda etapa incluía las determinaciones en plasma de 10-*epi*-10-F_{4t}-NeuroP e isoprostanos totales (IsoPs) y diferenciaba pacientes con EA frente a pacientes no EA. Se obtuvo un AUC global de 0.74 siendo de 0.99 para la primera etapa y 0.79 en la segunda.

En el capítulo 6, se valoró la capacidad de estos compuestos de peroxidación lipídica para la detección de EA en sus etapas más iniciales, es decir, en pacientes preclínicos. Ninguno de los compuestos mostró diferencias entre los pacientes con EA preclínica y controles de forma individual. Solo se observaron pequeñas diferencias no significativas con niveles en general, más bajos en EA. Sin embargo, algunos de estos potenciales biomarcadores sí mostraron relación con el estado cognitivo (RBANS.MR, CDR) y con los biomarcadores estándar de EA en LCR. Específicamente RBANS.MR correlacionaba con 2,3-dinor-15-*epi*-15-F_{2t}-IsoP (r = -0.314, p = 0.040), 15-E_{2t}-IsoP (r = -0.432, p = 0.025), 5-F_{2t}-IsoP (r = -0.335, p = 0.028), 15-F_{2t}-IsoP (r = -0.390, p = 0.10), and $PGF_{2\alpha}$ (r = -0.342, p = 0.025) y CDR con 15-*epi*-15-F_{2t}-IsoP (r = 0.329, p = 0.031), PGE_2 (r = 0.329, p = 0.031), 2,3-dinor-15-*epi*-15-F_{2t}-IsoP (r = 0.316, p = 0.039), 15-keto-15-E_{2t}-IsoP (r = 0.333, p = 0.029), 15-keto-15-F_{2t}-IsoP (r = 0.319, p = 0.037), 15-E_{2t}-IsoP (r = 0.363, p = 0.017), and 4(*RS*)-4-F_{4t}-NeuroP (r = 0.332, p = 0.030). Por otro lado, t-Tau en

LCR correlacionó significativamente con 15-F2t-IsoP (r = 0.397, p = 0.008), and PGF2 (r = 0.339, p = 0.026), mientras que p-Tau lo hizo con 15-F2t-IsoP (0.401, p = 0.008), and $PGF_{2\alpha}$ (r = 0.329, p = 0.031). Por tanto, a pesar de no mostrar diferencias entre los grupos, estos compuestos mostraron cierta relación con la EA en fase preclínica. Por tanto, se desarrolló un modelo estadístico multivariante basado en regresión logística Elastic Net, que incluía 10 compuestos (15-*epi*-15-F_{2t}-IsoP, PGE_2, 15-keto-15-E_{2t}-IsoP, 15-keto-15-F_{2t}-IsoP, 15-E_{2t}-IsoP, $PGF_{2\alpha}$, 4(*RS*)-4-F_{4t}-NeuroP, 1a,1b-dihomo-$PGF_{2\alpha}$, 10-*epi*-10-F_{4t}-NeuroP, 14(*RS*)-14-F_{4t}-NeuroP) además de sexo y edad, obteniendo una AUC de 0.96 (IC 95% 0.903-1) y una AUC de validación de 0.90 con una sensibilidad de 91% y una especificidad de 93 %.

En el capítulo 7, se valoró la relación de los niveles de los compuestos de peroxidación lipídica en plasma con los resultados de RMN en EA, concretamente con la atrofia cerebral evaluada mediante escalas visuales. Algunos compuestos correlacionaban con las escalas visuales de atrofia temporal medial (MTA) y patología vascular Fazekas. Concretamente, se observó relación entre MTA en el lado derecho con neuroprostanos totales (r=0.242, p=0.010), 17-*epi*-17-F_{2t}-dihomo-IsoP (r=0.223, p=0.018) y $PGF_{2\alpha}$ (r=−0.259, p=0.006); MTA en el lado izquierdo con neuroprostanos (r=0.213, p=0.024), 17-*epi*-17-F_{2t}-dihomo-IsoP (r=0.214, p=0.024) y $PGF_{2\alpha}$ (r=−0.305, p=0.001); suma de MTA con neuroprostanos (r=0.234, p=0.013), 17-*epi*-17-F_{2t}-dihomo-IsoP (r=0.224, p=0.018) y $PGF_{2\alpha}$ (PCC=−0.288, p=0.002); Fazekas con 17-F_{2t}-dihomo-IsoP (r=0.215, p=0.023).

En la segunda sección de la tesis se describen los estudios ómicos. En primer lugar, se realizó un estudio metabolómico (capítulo 8) en el que se compararon muestras de plasma de pacientes con DCL-EA y controles. El modelo de regresión basado en Elastic Net seleccionó 24 variables discriminantes en el modo de ionización positivo (con una AUC de 0.993) y 29 variables en el modo de ionización negativo (AUC 0.990). De esas 53 variables seleccionadas, se identificaron 16 metabolitos como potenciales biomarcadores, relacionados con vías como neurotransmisión, metabolismo energético, de lípidos o aminoácidos. De ellas, 4 variables se identificaron con los patrones de fragmentación (MS/MS y todos los iones de fragmentación) (colina, rescinamina, soraphen A, Lyso

PE(20:0/0:0) o Lyso PE(0:0/20:0)). Finalmente, 1 variable, el metabolito colina, se confirmó con el patrón correspondiente.

En el Capítulo 9, el análisis de los resultados metabolómicos mediante volcano plot y la regresión por PLS reveló un conjunto de variables principalmente relacionadas con el metabolismo lipídico que discriminaba entre pacientes con EA temprana (DCL-EA) y controles. Sin embargo, con el fin de explicar la amplia dispersión observada en el grupo de pacientes con EA en el gráfico de puntuaciones del PLS, se estudió la influencia del genotipo ApoE en la capacidad discriminante del modelo. Finalmente, se seleccionaron 8 variables principalmente identificadas como glicerofosfolípidos que mostraban niveles inferiores en los pacientes portadores del alelo ε4. Entre ellas, el LysoPC (18:0) se confirmó con patrón y otras tres variables (LysoPC (18:0), LysoPE (0:0/22:1 (13Z) y cardiolipinas) fueron caracterizadas putativamente.

Dado que los resultados obtenidos en los estudios metabolómicos revelaban un importante papel de los lípidos en la distinción entre pacientes con EA y controles, nos propusimos realizar un estudio lipidómico con el fin de estudiar las diferencias en el perfil lipídico plasmático entre individuos controles y con EA en etapas iniciales, además de identificar potenciales biomarcadores (Capítulo 10). En primer lugar, realizamos un análisis no dirigido con el que se estudiaron diferencias en cuanto a clases lipídicas entre controles, pacientes con EA preclínica y pacientes con DCL-EA. Las familias diacilgliceroles (DGs), lisofosfatidoletanolaminas (LPE), lisofosfatidilcolinas (LPC), monoacilgliceroles (MG), esfingomielinas (SM) mostraron diferencias entre los grupos. En general, los niveles de estas familias se encontraban elevados en los pacientes preclínicos y reducidos en el grupo DCL-EA. Por otro lado, los resultados obtenidos del análisis no dirigido se analizaron mediante volcano plot y modelo de regresión por PLS. Se identificaron variables discriminantes entre controles y DCL-EA (fosfocolina), y entre controles y pacientes con EA preclínica (pisumionoside, 1-O-Palmitoil-2-O-acetil-sn-glycero-3-phosphorilcolina). A partir de estos resultados y los de estudios previos, se desarrolló el método analítico para cuantificar un panel de 10 lípidos de los que finalmente 4 pudieron ser cuantificados de forma satisfactoria en muestras de plasma (18:1 LPE, 18:0 LPC, 16:1 SM, 16:0 SM). Entre ellos, el LPE 18:1 mostró una AUC-

ROC de 0.722 (95% IC, 0.595–0.848) discriminando EA (DCL y preclínico) frente a no EA (controles).

En el capítulo 11, nos propusimos estudiar mecanismos regulatorios que pudiesen estar alterados en las etapas iniciales de la EA a través de los microRNAs (miRNA) que además podrían servir como biomarcadores plasmáticos. En primer lugar, realizamos secuenciación de RNA de tres grupos de estudio (DCL-EA, n = 19), EA preclínica (n = 8) y controles (n = 19). A partir de estos resultados se seleccionó un panel de 11 miRNAs como potenciales biomarcadores discriminantes entre EA y no EA, de los que 8 fueron cuantificados satisfactoriamente mediante PCR cuantitativa. A pesar de que de forma individual no se observaron diferencias entre grupos para ninguno de ellos, de forma multivariante 3 miRNAs (hsa-miR-92a-3p, hsa-miR-486-5p, hsa-miR-29a-3p) mostraron tendencia a discriminar entre los tres grupos de estudio y 2 miRNAs (hsa-miR-92a-3p. hsa-miR-29a-3p) mostraron tendencia a discriminar entre pacientes con EA (DCL y preclínicos) y sin EA. Posteriormente, se estudiaron las potenciales vías que podrían estar reguladas por estos miRNAs y que podrían desempeñar un papel en la enfermedad mediante la base de datos miRDB. Primero, hsa-miR-92a-3p tiene como dianas genes implicados en la regulación de muerte celular o autofagia, proliferación celular y rutas de transporte de vesículas y transmisión sináptica. Segundo, hsa-miR-486-5p se relaciona con la señalización celular, funciones estructurales y transcripción, además de con el metabolismo de proteínas y lípidos. Tercero, hsa-miR-29a-3p podría regular las vías principales de proliferación celular y más específicamente diferenciación neuronal además de señalización, transcripción y función estructural.

Finalmente, en el capítulo 12, combinando los resultados obtenidos en los análisis lipidómicos y epigenómicos se estudiaron las potenciales vías metabólicas alteradas en la enfermedad. Se desarrolló un modelo PLS incluyendo los resultados lipidómicos y epigenómicos (secuenciación de miRNAs) obtenidos de controles sanos (n=5) y pacientes con DLC-EA (n=22) y se seleccionaron 25 variables lipídicas y 25 miRNAs como las variables más discriminantes entre ambos grupos de participantes. Entre los lípidos se encontraban principalmente fosfatidiletanolaminas, lisofosfatidilcolinas, ceramidas, fosfatidilcolinas, triglicéridos, y familias de ácidos grasos de cadena larga. Muchos de estos lípidos mostraron correlación con los miRNAs seleccionados. De hecho, estos

miRNAs podrían regular genes implicados en vías del metabolismo de ácidos grasos, específicamente en la elongación de ácidos grasos de cadena muy larga.

5. Conclusiones

-El estrés oxidativo y en concreto la peroxidación de lípidos parecen jugar un papel relevante en la EA desde las etapas más iniciales (preclínicos y DCL). Además, estas vías proporcionan biomarcadores diagnósticos para la enfermedad fácilmente accesible en muestras de plasma.

-Se han definido modelos basados en los niveles de biomarcadores de peroxidación lipídica en plasma y la evaluación del estado cognitivo, siendo capaces de establecer un diagnóstico diferencial de EA frente a individuos con otras demencias con manifestaciones clínicas similares y sujetos sin deterioro cognitivo.

-Además, estos biomarcadores se relacionan con la atrofia cerebral, el estado cognitivo de los pacientes y los biomarcadores estándar de la EA en LCR.

-Las técnicas ómicas (metabolómica, lipidómica, epigenómica) son herramientas útiles para la búsqueda de nuevos biomarcadores, así como para el estudio de las vías patológicas alteradas en la EA.

-El metabolismo de lípidos se encuentra alterado en la EA y el perfil lipídico podría ayudar al diagnóstico de la enfermedad.

-El estudio integrado de biomarcadores de diferente naturaleza (lípidos, miRNAs) puede proporcionar información sobre las vías alteradas en la EA y por tanto proporcionar nuevas dianas terapéuticas.

LIST OF ABBREVIATIONS

AA	Arachidonic Acid
Aβ	Amyloid β
Ach	Acetylcholine
AD	Alzheimer Disease
AdA	Adrenic Acid
AM	Accurate mass
ANN	Artificial Neural Network
APP	Amyloid Protein Precursor (APP)
AUC-ROC	Area Under the Receiver Operating Characteristics
BACE1	Beta-site amyloid precursor protein cleaving enzyme 1
BBB	Blood Brain Barrier
CAT	Computerized axial tomography
CDR	Clinical Dementia Rating
CE	Cholesterol esters
CEIC	Ethics Committee
Cer	Ceramides
CI	Confidence Interval
CMM	CEU Mass Mediator
CNS	Central Nervous System
CRP	C-reactive protein
CSF	Cerebrospinal fluid

CV	Coefficients of Variation
CVM	Cross-Validated Mean-squared Error
DG	Diglycerols
DHA	Docosahexaenoic Acid
DLB	Dementia with Lewy Bodies
DNA	Deoxyribonucleic Acid
DOPE	Dioleoyl phosphatidylethanol
DOR	Diagnostic Odds Ratio
DT	Difusion Tensor
EOAD	Early Onset Alzheimer Disease
ESI	Electrospray Ionization
FA	Fatty acids
FAQ	Functional Activities Questionnaire
FC	Fold change
GMS	Geriatric Mental State Schedule
HMDB	Human Metabolome Database
IQR	Interquartile Range
IS	Internal Standard
LPC	Lysophosphatidylcholine
LPE	Lysophosphatidylethanolamine
LR	Likelihood Ratio
Lyso PE	Lysophosphatidylethanolamines

MCI	Mild Cognitive Impairment
MG	Monoglycerides
miRNAs	microRNAs
MMSE	Mini-mental State Examination
NGS	Next Generation Sequencing
NIA-AA	National Institute on Aging-Alzheimer's Association
MRI	Magnetic Resonance Imaging
MRM	Multiple Reaction Monitoring
MTA	Medial Temporal Atrophy
OOB	Out of Bag
OR	Odds Ratio
OS	Oxidative stress
OxLDL	oxidised low-density lipoprotein
p-Tau	phosphorylated-Tau.
PC	Phosphatidylcholines
PCC	Pearson Correlation Coefficient
PD	Parkinson Disease
PD	Porbability of Directino
PE	Phosphatidylethanolamine
PET	Positron Emission Tomography
PI	Phosphatidylinositols
PLS	Partial Least Square

PSEN1	Presenilin-1
q-PCR	Quantitative Polymerase Chain Reaction
QC	Quality Control
RLC	Relative Light Changes
RBANS	Repeatable Battery for the Assessment of Neuropsychological Status
RNA	Ribonucleic acid
ROPE	Region of Practical Equivalence
RT	Retention time
RT-PCR	Real Time Polymerase Chain Reaction
SM	Sphingomyelin
SPE	Solid-phase extraction
SVM	Support Vector Machine
t-Tau	total-Tau
TG	Triglycerides.
UPLC-MS/MS	Ultra-Performance Liquid Chromatography coupled with tandem Mass Spectrometry
VIP	Variable Importance In Projection
WHO	World Health Organization

LIST OF TABLES

LIST OF FIGURES

ABSTRACT

This PhD thesis is focused on the identification and determination of reliable and minimally invasive biomarkers for Alzheimer Disease (AD) diagnosis in its early stages, as well as to advance in the knowledge of the pathophysiological mechanisms involved in the course of the disease.

AD is the most common cause of dementia and it generates a great social and economic impact. However, the lack of early accessible diagnosis biomarkers hinders the initiation of treatments and limits research into new therapies to cure or slow down the course of the disease. AD is a complex disease with multiple pathological pathways such as protein accumulation (amyloid β42 (Aβ42, hyperphosphorylated Tau (p-Tau)), but also pathophysiological pathways such as oxidative stress (OS), lipid dysregulation, dysregulation of the clearance machinery, etc. Therefore, this PhD thesis is divided into two parts, the first one dedicated to the studies of lipid peroxidation compounds as biomarkers of the disease and the second part dedicated to the omics studies (metabolomic, lipidomic, epigenomic) in patients with early AD to examine the pathways involved in early AD and to provide new potential diagnosis biomarkers.

Regarding lipid peroxidation-derived compounds, they were measured in urine and plasma samples by a validated method on based ultra-performance liquid chromatography coupled to tandem mass spectrometry (UPLC-MS/MS). The developed diagnosis models showed discriminatory capacity between early AD and controls, especially for plasma samples. In addition, these compounds were able to discriminate controls from preclinical AD cases and AD from other dementias.

In addition, omic analyses (metabolomics, lipidomics, epigenomics) were carried out in plasma samples from AD and non-AD cases. These analyses revealed the dysregulation of some metabolites (choline, rescinamine, soraphen A, Lyso PE(20:0/0:0), Lyso PE(0:0/20:0), lipids (LysoPC (18:0), LysoPE (0:0/22:1 (13Z)), cardiolipins, phosphocholine, 1-O-Palmitoil-2-O-acetil-sn-glycero-3-phosphorilcholine, 18:1 LPE, 18:0 LPC, 16:1 SM, 16:0 SM) and miRNAs (hsa-miR-92a-3p, hsa-miR-486-5p, hsa-miR-29a-3p). In fact, these miRNAs could be involved in fatty acids metabolism.

The complete characterization of plasma biomarkers from AD patients with special attention on OS and lipid metabolism could help to obtain an early diagnosis and to define

the metabolic pathways altered in each individual allowing an early and personalized treatment.

INTRODUCTION

1. Alzheimer Disease: pathophysiology, diagnosis and treatment.

AD is the most common neurodegenerative disease being the cause of about 70% of dementia cases. In 2018, AD affected around 50 million people worldwide [1,2], and the incidence in developed countries is expected to continue increasing due to the rise in life expectancy, exceeding 150 million cases in 2050. AD has a major social and economic impact [3], due to factors such as medical costs, lack of productivity, reduced quality of life for patients and caregivers, and dependency. However, available treatments fail to cure or stop the disease, being mostly symptomatologic treatments [4]. Numerous clinical trials are currently underway with new drugs targeting different pathophysiological mechanisms potentially involved in the development of AD [4]. In general, these treatments are directed to the early stages of the disease, where they are expected to be more effective. Therefore, early AD diagnosis is crucial. Currently, the complexity and invasiveness of the diagnostic methods (biomarkers in cerebrospinal fluid) difficult its early detection. Therefore, it is necessary to identify reliable, early, and minimally invasive diagnostic biomarkers, as well as to advance in the knowledge of the pathophysiological mechanisms involved in the onset and development of the disease.

Clinically, AD is characterized by progressive cognitive impairment affecting different domains such as episodic memory, verbal fluency, or executive function [5]. In most cases, it is a sporadic disease. In fact, AD familial cases which are mainly due to mutations in genes such as amyloid precursor protein (APP) and presenilins 1 and 2 (PS1) (PS2), do not reach 2%.[6]. However, among the risk factors for AD, it highlights the gene encoding Apolipoprotein E, specifically the Ɛ4 allele. In addition, there are several of lifestyle-related risk factors (hypercholesterolemia, diabetes, hypertension) that can be considered modifiable factors [7].

1.1. Pathophysiological mechanisms

At the pathophysiological level, AD is mainly characterized by two histopathological hallmarks: i) intracellular accumulations of phosphorylated Tau (p-Tau) in the form of neurofibrillary tangles, and ii) extracellular accumulations of abnormally folded amyloid β (Aβ) protein forming senile plaques mainly in the medial temporal lobe and neocortical structures that eventually result in loss of synapses[4]. In general, the main hypotheses

about the origin of the disease are the amyloid cascade, Tau hyperphosphorylation, and cholinergic misfunction [4]. Figure 1 describes the mechanisms involved in AD.

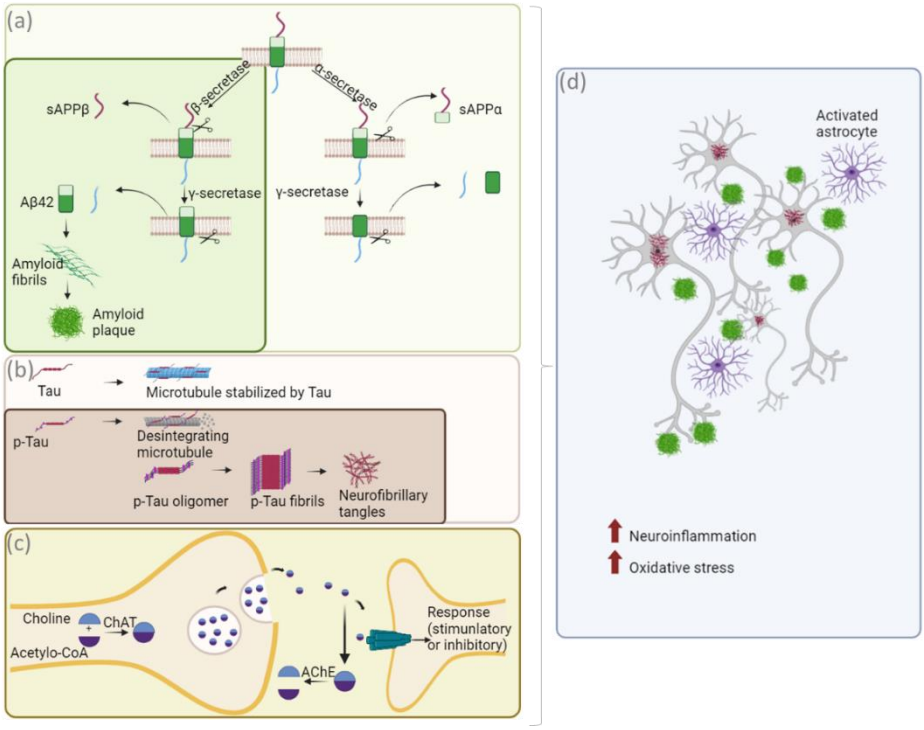

Figure 1. Alzheimer Disease pathophysiological mechanisms. (a) Describes the amyloid hypothesis. Amyloid precursor protein (transmembrane protein) can be cleaved by α-secretase and γ-secretase generating soluble peptides. However, when APP is cleaved by the enzymes β-secretase and γ-secretase (as it occurs in AD) it can generate amyloid β (Aβ) peptides such as Aβ42, an insoluble peptide with a tendency to form fibrils and finally amyloid plaques. (b) Describes the Tau pathology. The Tau protein is found forming part of the microtubules, stabilizing them. When it is hyperphosphorylated microtubules can be destabilized and hyperfosforilated Tau (p-Tau) can form first oligomers and fibrils and, finally neurofibrillary tangles. (c) The cholinergic hypothesis. Cholinergic neurons use acetylcholine (Ach) as a neurotransmitter. When the neuron receives stimulation (action potential), Ach is released into the synaptic space. This Ach is formed from choline and Acetyl-CoA by the enzyme Choline acetyltransferase. Ach in the synaptic space can be captured by muscarinic and nicotinic receptors, generating stimulatory or inhibitory responses. If Ach is not bound to any receptor, the enzyme acetylcholinesterase forms again choline and acetyl-CoA, which is taken again by the presynaptic neuron. In AD it occurs a reduction in these neurotransmission pathway activity (d) In AD, these mechanisms cause senile plaques, neurofibrillary tangles, and the loss of synaptic function. In addition, this generates an oxidizing and pro-inflammatory environment that positively feedback the disease's pathophysiological mechanisms. Created with BioRender.com.

The amyloid hypothesis. In 1992, the central role of the Aβ protein as the causative agent of AD was first hypothesized [8]. It described how specific processing of the amyloid precursor protein (APP) generates a precipitating peptide that leads to cell death and promotes the accumulation of Tau in neurofibrillary tangles [8]. APP is a transmembrane protein that can be cleaved by two pathways: i) the "normal" or non-pathological one, in which the enzyme α-secretase and subsequently the γ-secretase acts giving rise to a soluble extracellular fragment; and ii) the amyloidogenic one, in which the enzyme β-secretase (BACE) and subsequently the enzyme γ-secretase acts producing peptides of different lengths, including Aβ42, an insoluble peptide that forms precipitates [9]. Supporting this theory are genetic risk factors. Actually, ApoE influences Aβ42 clearance [10], and mutations in the PS1, PS2, and BACE genes contribute to the development of the disease.

Increased production of this peptide (Aβ42) is considered toxic and a reduction in its clearance mechanisms results in the formation of oligomers affecting synaptic function, triggering an inflammatory response and increasing oxidative stress (OS), and finally the formation of plaques [11]. This inflammatory response contributes to the phosphorylation of Tau, which also plays a relevant role in the disease [11].

Tau hypothesis. Some studies suggest that the amyloid cascade is the first mechanism that appears and the toxicity associated results in the hyperphosphorylation of Tau leading to an increase in cellular toxicity and neuronal loss. However, other theories argue that Tau pathology is the trigger of pathological mechanisms [12,13].

Tau is an intracellular cytoskeleton protein with functions of transport of molecules such as neurotransmitters in neurons [13]. Under physiological conditions, this protein undergoes phosphorylations at various residues; however, in pathological conditions such as AD, hyperphosphorylation occurs [13]. This hyperphosphorylation increases toxicity but also facilitates the formation of Tau protein aggregates or neurofibrillary tangles (NFT) leading to cell death and thus to neuronal loss [13].

Cholinergic hypothesis. Acetylcholine (ACh) is a neurotransmitter generated in the cytoplasm of cholinergic neurons from choline and acetyl-CoA by the action of the enzyme choline acetyltransferase. This neurotransmitter is transported by vesicles to the synaptic space after depolarization of the presynaptic neuron. In the postsynaptic neuron,

it can bind to muscarinic or nicotinic receptors producing an inhibitory or activatory response. In the synaptic space, it is hydrolyzed by acetylcholinesterase if it has not bound to any receptor [14].

Acetylcholine (ACh) is a neurotransmitter involved in cognitive processes such as learning or memory and cholinergic neurons show a specific degeneration in AD [14]. Specifically, a reduction in the activity of the choline acetyltransferase enzyme has been observed under AD pathological conditions [11]. In fact, current conventional treatments for AD are based on increasing the cholinergic signal to compensate for the Ach reduction by maintaining the neurotransmitter for a longer time in the synaptic space [15].

Despite discrepancies in the order of appearance of these mechanisms in AD, all of them coexist once the pathology is established, along with other mechanisms such as neuroinflammation, activation of microglia and astrocytes, OS, alterations in the metabolism of lipids, proteins or DNA, neurotransmission, etc [4,16–20].

Both amyloid and Tau pathologies usually spread from medial temporal lobe grey matter to the rest of cortical grey matter in a relatively predictable pattern [63]. Initial involvement in medial temporal lobe structures that are involved in the correct episodic memory, explains the memory impairment as the first disease symptom. Nevertheless, variations in pathology spreading would explain the different damage degrees in the brain cortex among patients, involving in some cases also language disturbance, frontal lobe dysfunction, or apraxia syndromes. Moreover, advanced-age patients show concurrent brain comorbidities (e.g. depression, psychiatric disorders…).

1.2. Diagnosis

In clinical practice, the diagnosis is mainly based on clinical symptoms. In this sense, AD is a highly heterogeneous disease [21]. It is a progressive disease that can evolve over 15-25 years from the onset of pathophysiological mechanisms to the severe clinical manifestations [22]. In the AD continuum, the following stages can be distinguished: i) Preclinical AD, characterized by the absence of clinical symptoms although impairment of the CSF AD biomarkers is detected; ii) mild cognitive impairment (MCI), characterized by the presence of initial symptoms but maintaining functionality in daily living activities and CSF AD biomarkers alteration; and iii) dementia, characterized by

more advanced symptoms with alteration of activities of daily living activities [5]. The clinical guidelines defined by the NIA-AA base the diagnosis at the stage of MCI on the detection of a change in cognition by the patient, an observer, or an expert clinician [23]. This impairment occurs in one or more cognitive domains (memory, executive function, attention, language, visuospatial skills) [23], but maintaining patients' functional independence [23]. In more advanced stages, the diagnosis is based on the presence of dementia (impairment in functionality not explained by delirium or psychiatric problems, cognitive impairment based on neuropsychological assessments, and behavioral disturbances), and a progression of symptoms over months or years [24]. The main cognitive symptoms are impairment in learning and recall of recently learned information in the case of the AD amnestic variant, or alterations in language, visuospatial, or executive functions in the non-amnestic variant [24].

The NIA-AA published in 2018 an update to the 2011 diagnostic guidelines for AD. The new criteria changed from a clinical diagnosis to a biological definition based on biomarkers [25]. Biomarkers were grouped according to the ATN classification (A: Aβ deposition; T: pathological Tau; N: neurodegeneration). This ATN classification system includes imaging and CSF biomarkers. For amyloid (A) deposition measures are CSF biomarkers (Aβ42, Aβ42/Aβ40) and amyloid Positron Emission Tomography (PET). Neurofibrillary tangle deposits or pathological Tau (T) are defined by CSF p-Tau levels or PET Tau. Finally, the definition of neurodegeneration or neuronal damage (N) includes structural magnetic resonance imaging (MRI), FDG-PET or CSF biomarkers t-Tau and NfL levels. These guidelines emphasize the flexibility of the system for the incorporation of new biomarkers within the ATN groups and also new categories.

1.3. Treatments

Currently, treatments are only able to reduce symptoms at cognitive and functional level. The most widespread drugs for AD are acetylcholinesterase inhibitors (donepezil (Aricept™), rivastigmine (Exelon™), and galantamine (Razadyne™)) and N-methyl-D-aspartate receptor antagonists (memantine (Namenda™)) [26]. The new potential treatments under development can be divided into two types: i) those aimed at acting on the symptomatology of the disease (cognition, agitation, aggressiveness, etc.), and ii) disease-modifying treatments [26]. The latter are directed to different targets. Most of

them are anti-amyloid treatments, specifically aimed at reducing amyloid plaque; anti-Tau treatments and those aimed at reducing or regulating inflammation, metabolism, bioenergetics, synaptic plasticity, and neuroprotection or antioxidants among others [22,26,27]. Some of these anti-amyloid treatments have shown a reduction in amyloid plaque. However, it only generates a moderate reduction in the normal deterioration produced by the disease [28]. In general, the treatments under clinical investigation have a high failure rate, which could be a consequence of the complexity of the disease and the lack of a complete view of the pathophysiological mechanisms involved, as well as the interaction between the different pathways [26]. On the other hand, it should be noted that most of the trials carried out are addressed to patients in the early stages and some at moderate stages [26]. So, it is relevant to obtain an early diagnosis to access the treatments in the early stages, in which they show higher effectiveness [27].

2. New potential biomarkers for AD

AD is a complex and multifactorial disease, whose pathological pathways are currently not fully understood [64]. Molecular perturbations may occur at a systemic level in the early stages, before the appearance of characteristic symptoms, and plasma constitutes a promising minimally invasive sample to study these alterations. In addition, this biological biofluid could be useful to advance in the knowledge of AD pathophysiological mechanisms and the identification of new biomarkers, as well as for the discovery of new therapeutic targets. In this sense, omic techniques are useful tools that provide a large amount of information. [65–67] In addition, OS that plays a central role in AD may be a source of biomarkers for the disease.

2.1 Oxidative Stress and AD

2.1.1 Mechanism

OS is described as an imbalance between oxidant and antioxidant species in favor of oxidants [68]. Under normal circumstances, there is a balance in the body between oxidant and antioxidant substances that provides the necessary conditions for the correct metabolic and signaling functions [30]. However, when the antioxidant systems are not able to compensate for the level of oxidants, it occurs an imbalance known as OS [30]. It

consists of an increase in cellular stress leading to processes of cell death and apoptosis, necrosis, or autophagy [31]. The main causes of OS are decrease or inactivation of antioxidant molecules, increase of reactive oxygen species (ROS) and other oxidant molecules, as well as increase of endogenous metabolites capable of autoxidation [69].

Among oxidant species, ROS and Reactive Nitrogen Species (RNS) (e.g. superoxide anion, hydrogen peroxide, hydroxyl radical, nitric oxide) are produced predominantly in the mitochondria from molecular oxygen and nitrogen [70]. Other sources of ROS are the endoplasmic reticulum, and nuclear or plasmatic membranes, as well as, oxidase enzymes (xanthine oxidase, NADPH) [69]. Glutathione (GSH) is the most abundant non-enzymatic antioxidant in the human body, being able to avoid damage caused by ROS to important cellular components. In general, OS is involved in most of chronic diseases, such as cancer [71], respiratory diseases [71] and neurodegeneration [72]. Therefore, OS mechanisms have been largely studied to clarify the pathogenesis of neurodegeneration [29]. Specifically, OS maintains a bidirectional relationship with the amyloid cascade. On the one hand, OS favors the amyloidogenic pathway of APP increasing the production of toxic Aβ42 peptide. On the other hand, amyloid plaques favor an increase in OS leading to cell death [32,33]. Similarly, OS interacts with kinases responsible for Tau phosphorylation and neurofibrillary tangles produce an increase in ROS [32]. In this sense, currently, 7 clinical trials for AD treatment are focused on OS [73].

2.1.2. Oxidative stress biomarkers

OS causes oxidation of biomolecules such as proteins, DNA, or lipids. Regarding lipid peroxidation, it generates cellular damage and new oxidizing molecules [74], altering membrane lipids and circulating lipids, and also cellular functions [75]. Specifically, at the brain level, OS could modify lipid and protein levels, generating morphological brain changes [76–78]. In this sense, throughout the AD course, different brain areas could be affected [79]. One area with a remarkable atrophy grade during AD progression is the medial temporal lobe, where the hippocampus is located [80].

The most commonly used biomarkers of OS are carbonyl proteins, nitrotyrosine, advanced oxidation products of proteins (e.g., chloro-tyrosine) as derivatives of protein oxidation; 7,8-dihydroxy-8-oxo-2′-deoxyguanosine (8oxodG), as derivatives of DNA

oxidation; and malondialdehyde (MDA), 4-hydroxy-2-nonenal (HNE) and isoprostanes as derivatives of lipid oxidation [36]. Compounds derived from this process can be detected in peripheral samples, such as blood or urine, serving as an approach for oxidative status [35].

Lipid peroxidation biomarkers in AD

The brain is an organ with high metabolic activity, high oxygen consumption, and high polyunsaturated fatty acid content that make it susceptible to oxidative damage [37]. Therefore, lipid oxidation could play an important role in the development of neurodegenerative diseases and specifically in AD [38]. Previous studies have found co-localization of lipid oxidation products with amyloid plaques, evidencing the relationship between OS and lipids with the development of AD pathological mechanisms [39].

In this sense, some lipid peroxidation products (e.g. isoprostanes, MDA, thiobarbituric acid-reactive substances (TBARS), and fluorescent lipofuscin-like pigments (LPF)) have been evaluated as AD biomarkers in different human samples [81], mainly blood (plasma, serum) and urine[81].

Lipids can be oxidized by two independent pathways (enzymatic and non-enzymatic or by free radicals) [40]. In this thesis we focus on compounds derived from the oxidation of three polyunsaturated fatty acids (PUFA): i) arachidonic acid (AA), ii) docosahexaenoic acid (DHA), and iii) adrenic acid (AdA) (see Figure 2). For AA, its oxidation generates two families of compounds, isoprostanes and isofurans (e.g. 15(*R*)-15-F_{2t}-IsoP; 2,3-dinnor-15-*epi*-15-F_{2t}-IsoP; 15-keto-15-E_{2t}-IsoP; 15-keto-15-F_{2t}-IsoP; 15-keto-15-E_{2t}-IsoP; 15-keto-15-F_{2t}-IsoP; 15-E_{2t}-IsoP;15-F_{2t}-IsoP; 5-F_{2t}-IsoP), the latter originated under higher oxygen tension conditions, and prostaglandins (PGE_2; $PGF_{2\alpha}$; 1a,1b-dihomo-$PGF_{2\alpha}$) [41]. AA is present in large quantities in the brain as part of cell membranes [42,43]. On the other hand, the oxidation of DHA, located mainly in brain grey matter, and AdA located mainly in the white matter of the brain, generate neuroprostanes (e.g. 10-*epi*-10-F_{4t}-NeuroP; 14(*RS*)-14-F_{4t}-NeuroP; 4(*RS*)-F_{4t}-NeuroP) and dihomo-isoprotanes (e.g. 17-*epi*-17-F_{2t}-dihomo-IsoP; 17-F_{2t}-dihomo-IsoP; *ent*-7(*RS*)-7-F_{2t}-dihomo-IsoP; 17(*RS*)-10-*epi*-SC-Δ^{15}-11-dihomo-IsoF; 7(*RS*)-ST-Δ^{8}-11-dihomo-IsoF), respectively [43].

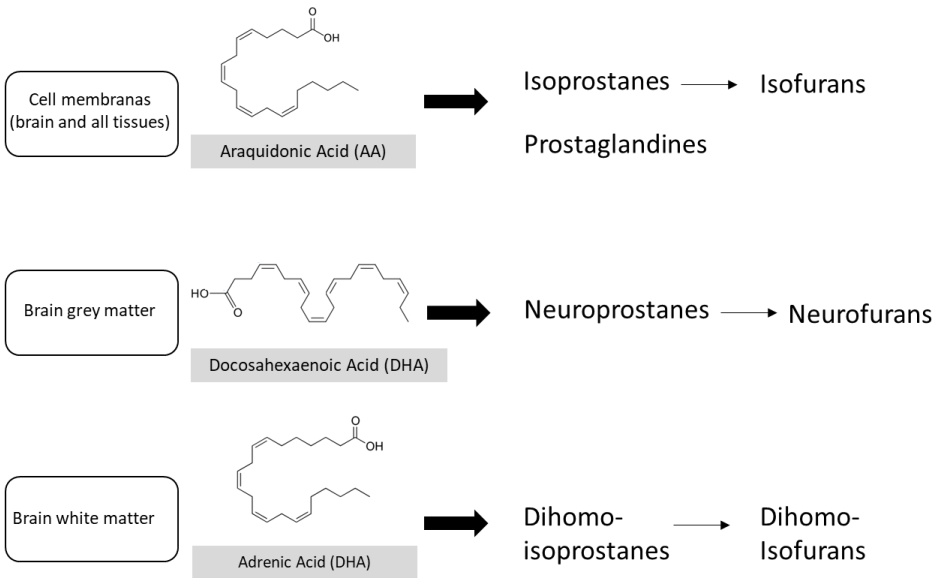

Figure 2. Lipid peroxidation metabolites origin.

2.2. Omics Analysis and AD

In the initial stages of AD, there is an imbalance in the interactions among different brain cell types, pathogenic forms of Tau and amyloid proteins, and the brain signaling pathways impairment [67,82]. In this way, the neurodegenerative process would affect each cell type at multiple levels (epigenomic, transcriptomic, metabolomic/lipidomic, proteomic). Therefore, a complete knowledge of the AD mechanisms could be achieved from a multi-omic approach applied to different biological samples. In this sense, the omic tools would contribute importantly to the knowledge of the early AD pathophysiological mechanisms and the identification of specific and reliable AD biomarkers in biological samples.

The development of omic platforms and advances in bioinformatics are generating a large volume of data [83], which provide information about the pathological pathways involved in AD and new potential biomarkers and therapeutic targets [44,45,67]. This type of analysis involves prior treatment of the sample as well as subsequent processing and interpretation of the results [46]. Metabolomics, epigenomics, and proteomics are the

most widely employed omic tools in clinical studies [67]. In this thesis, we focus on the omics studies (metabolomic, lipidomic, epigenomic).

2.2.1. Metabolomics and AD

Metabolomics reflects changes in the metabolome representing a precise biochemical phenotype of the organism in health and disease [84]. This allows a reliable approach to the complex AD nature. Metabolomics let the characterization of the metabolite profile using any sample type such as blood or CSF. It is especially useful in the detection of potential biomarkers given the ability of metabolomics to detect small changes and for the study of physiological and pathological mechanisms [47].

Metabolomic studies can be carried out from an untargeted analysis, which allows a global view; and a targeted analysis, which allows validation and confirmation of the results obtained with non-targeted methods [48]. One of the most widely used analytical techniques is mass spectrometry (MS), which is characterized by its high sensitivity and specificity [49]. Targeted and untargeted metabolomic studies have allowed the identification of biomarkers for AD in biological fluids such as CSF, plasma, or urine [50–52], postulating this technique as a useful tool for new biomarkers identification.

Recent metabolomics studies in AD have identified some altered metabolic pathways, such as polyamine pathway, lysine metabolism, tricarboxylic acid cycle, lipid metabolism, neurotransmission, inflammation and OS [85] mitochondrial activity [86], as well as the impairment of some metabolite levels (tyrosine, glycylglycine, glutamine, lysophosphatic acid, platelet-activating factor, organic acids, isoprostanes, prostaglandines) [87] tryptophan and purines metabolisms [88], sphingolipids [89], amino acids and phospholipids [90]. Metabolomic studies in AD have been applied to different biological samples [91,92]. Nevertheless, there is an increasing interest in improving early AD diagnosis by means of minimally invasive samples, such as serum [89,93], plasma [87,94], urine [95], and saliva [96]. Specifically, plasma is a promising matrix since some biochemical pathways have shown disturbances in patients with AD, such as amino acids, amines, and polyamines metabolisms [52,94,97,98], aswell as lipid metabolism [87,89,92,99–101], even in mild-cognitive impairment (MCI) stage [94]. Nevertheless, most of metabolomics studies in plasma have been developed from animal

models [92,101,102], and among human studies few of them defined MCI-AD participants from the standard CSF biomarkers [87]. In this sense, the ambiguity in dementia type diagnosis is considered an important limitation in the development of AD reliable diagnostic models [52,94,97,103–105].

Previous studies found a relationship between different metabolite networks and the ApoE genotype [87], as well as between ApoE polymorphisms and metabolomic changes [106]. Moreover, targeted studies found differences in biomarkers such as CSF Synaptosoma-Associated Protein 25 (SNAP25), or blood metabolic biomarkers between ApoE4 carriers and non-carriers [107,108]. Therefore, it would be interesting to include ApoE genotype as a variable in metabolomics studies as it is one of the most important, although the mechanisms that relate it to the disease are still unknown [109]. ApoE4 genotype is associated with earlier amyloid deposition [110]. In this sense, some patients showed different responses against therapies according to their ApoE genotype [111].

2.2.2 Lipidomics and AD

Lipidomics consists of the study of the lipid profile in a given biological sample. The brain has a high lipid composition, and therefore numerous lipidomic studies have been carried out in AD patients, showing the dysregulation of this family of biomolecules both in the brain and in other biological fluids [53]. These metabolites have potential utility as a source of disease-specific diagnostic biomarkers [53] in different biological sample types [112]. In fact, several lipid families, such as sphingomyelins (SM), cholesterol esters (CE), phosphatidylcholines (PC), phosphatidylethanolamines (PE), phosphatidylinositols (PI), ceramides (Cer), and triglycerides (TG), have been related to AD [113,114]. Lipid biomarkers could be useful not only for diagnosis but also for disease progression prediction. Specifically, LysoPE (LPE) and PE could be useful biomarkers for monitoring the conversion of MCI to AD [115,116], and plasma sphingomyelins have been related to cognitive decline in probable AD patients [116]. In fact, lipidomic analyses have been carried out to study the involvement of lipids in AD pathology and progression [117]. Brain tissue from elderly healthy participants and patients with different stages of AD showed differential expression of lipids such as glycerolipids, glycerophospholipids, and sphingolipids [53]. In addition, the

lipidomics research field focusing on lipids as potential biomarkers in peripheral biofluids (e.g., plasma and serum) is gaining attention [118–120].

2.2.3. Epigenomics and AD

Epigenomics focuses on the study of gene regulation mechanisms (e.g. deoxyribonucleic acid (DNA) methylation, histone modifications, non-coding ribonucleic acid (RNAs)) [54]. This omic science constitutes an interesting approach to the advance in the knowledge of the pathophysiology of AD since the expression patterns of certain genes implicated in the development of the disease (APP, PSEN1, PSEN2, BACE1), as well as secretase enzymes and inflammatory response genes, are altered by epigenetic modifications (DNA methylation [24], histone modifications, expression of non-coding genes transcripts (microRNAs [25])). Specifically, some microRNAs (miRNAs) (RNA sequences of 19-25 nucleotides involved in both positive and negative gene regulation) [55] have been related to the regulation of amyloid protein precursor (APP) cleavage, presenilin-1 (PSEN1) and beta-site amyloid precursor protein cleaving enzyme 1 (BACE1), as well as in OS and other AD risk factors[121].

Currently, few studies evaluate the diagnostic capacity of epigenetic changes in peripheral fluids from AD patients [26]. However, next generation sequencing (NGS) technology is postulated as a viable approach to carry it out [27]. MiRNAs from AD patients have shown differential levels compared to non-diseased subjects in brain and biological fluids such as CSF or blood derivatives using NGS [57,122,123]. They may therefore constitute an important source of biomarkers. Among epigenetic biomarkers, the miRNAs constitute a key element in cell signaling pathways. In recent years, they have been postulated as powerful biomarkers for the diagnosis of neurodegenerative diseases [61]. In fact, there is evidence that they could be more sensitive than messenger RNA, or even proteins used as clinical markers [62]. MiRNAs showed good performance as biomarkers and miRNAs panels showed dysregulation several years before the onset of disease symptoms [124]. Several panels have been developed from plasma, serum, or exosomes, showing their potential for a minimally invasive disease diagnosis[125–127].

Therefore, epigenetic is closely related to diseases and is useful in the understanding of pathophysiological mechanisms as well as providing potential biomarkers [56].

2.2.4. Integration of experimental data of different nature

The integration of results from different omics techniques allows the identification of pathways involved in AD enabling a more complete characterization of AD patients [59]. This may provide a more comprehensive description of the heterogeneity of AD patients and its clinical implications to obtain an early, generalized, reliable diagnosis and access to personalized treatments [60].

Different studies have integrated data from different nature with the common goal of deepen into the pathological pathways of AD. Specifically, the integration of metabolomic and genomic analyses allowed the detection of altered metabolites and their regulators [61]. In addition, the combined view including metabolomics, and genomics helps with the understanding of the underlying mechanisms contributing to AD risk [62]. Moreover, epigenomic–lipidomic integration would allow the global study of the regulatory mechanisms involved in AD such as lipid homeostasis, OS, synaptic vesicle trafficking, inflammation, etc. [59]. Previous works based on the analysis of genome-wide DNA methylation showed that an epigenetic pattern was associated with cholesterol regulation [128]. Thus, the study of the integration between epigenomics and lipidomics could reveal lipid regulation mechanisms involved in AD. Therefore, integrative studies allow a global and more complete view of the disease and its pathophysiological mechanisms.

HYPOTHESIS AND OBJECTIVES

This PhD Thesis hypothesizes that lipid peroxidation and other compounds obtained by omics analyses (metabolomics, lipidomics, epigenomics) in minimally invasive samples, may be potential biomarkers for the early AD diagnosis and can provide information on the metabolic pathways involved in the development of the disease.

Therefore, the main objective of the thesis was to study compounds derived from lipid peroxidation as potential specific AD diagnostic biomarkers and their relationship with clinical features of the disease, and to identify new biomarkers and pathological pathways altered in the early stages of AD from a multi-omics approach (metabolomics, lipidomics, epigenomics).

The specific objectives were:

(i) Identifying potential biomarkers based on lipid peroxidation for detection of AD in urine (Chapter 1) and plasma (Chapter 2) samples.

(ii) Developing diagnostic models for AD based on lipid peroxidation biomarkers (Chapters 1, 2,3, and 5).

(iii) Selecting the best sample type for AD diagnosis based on the levels of lipid peroxidation compounds (Chapter 3).

(iv) Analyzing the usefulness of lipid peroxidation compounds as potential biomarkers for early or preclinical diagnosis of AD (Chapter 6).

(v) Establishing the relationship between lipid peroxidation compounds and clinical AD variables: brain atrophy by visual scales (Chapter 7), standard biomarkers in cerebrospinal fluid (CSF), and cognitive impairment by neuropsychological evaluations (Chapters 2, 4, and 6).

(vi) Searching for new plasma biomarkers for AD diagnosis using omics techniques: metabolomics (Chapters 8 and 9), lipidomics (Chapter 10), epigenomics (Chapter 11).

(vii) Studying potential metabolic pathways altered in AD by omics analyses (Chapters 10 and 11) and integration of different omics results (Chapter 12).

MATERIAL AND METHODS

1. Study design and participants

All the studies included in the present thesis were prospective observational studies carried out including patients form the Neurology Unit at the University and Polytechnic Hospital La Fe, Valencia (Spain). The study protocols were approved by the Ethics Committee (CEIC) from Health Research Institute La Fe (Valencia, Spain), the methods were carried out in accordance with the relevant guidelines and regulations, and informed consent from all participants was obtained. The studies included in the present doctoral thesis are included in the projects CP16/00082 and PI19/00570 and the references for CEIC approvals were 2016/0257 and 2019/0105, respectively.

The eligible participants were people between 50 and 80 years old who suffered from MCI due to AD (MCI-AD), dementia due to AD (dementia-AD), patients with preclinical AD, participants with dementia not due to AD (non-AD), and participants without cognitive impairment or minimally impaired (control). The exclusion criteria included other known neurological impairments (stroke, brain tumor, severe head trauma, epilepsy, brain injury, multiple sclerosis…) or major psychiatric disorders (major depressive disorder, bipolar disorder, schizophrenia…), as well as patients with moderate to severe dementia, major sensory impairment or an invalidating previous pathology or that were unable to undergo neuropsychological evaluations.

Participants were recruited from the Neurology Unit and they were classified following the NIA-AA recommendations [23,24] that include neuropsychological evaluation, structural and functional neuroimaging, and CSF biomarkers. Specifically, there were used *the Repeatable Battery for the Assessment of Neuropsychological Status* (RBANS), *Clinical Dementia Rating* (CDR), *Mini-Mental State Examination* (MMSE), *Functional Activities Questionnaire* (FAQ)) [129–132] for neuropsychological evaluation, MRI or computerized axial tomography (CAT) for brain structural evaluation [133], and CSF biomarkers (Aβ, t-Tau, p-Tau) [134,135] to assess the abnormal amyloid and Tau proteins processing [134,135]. From 1–10 mL of CSF were collected under a standardized lumbar puncture procedure at 8-10 a.m. Aβ42, t-Tau, and p-Tau were measured by Innotest Elisa kit (Fujirebio Diagnostics, Ghent, Belgium) using a fully automated system (Lumipulse G, Fujirebio). Table 1 describes the classification criteria for each participant group: i) the control group included participants with normal levels of CSF

AD biomarkers and normal cognitive tests; ii) the preclinical AD group included participants with impaired CSF AD biomarkers and normal cognitive evaluation test scores; iii) the MCI-AD group were patients with impaired CSF biomarkers and cognitive impairment, but without daily living activities impairment; iv) the non-AD group included patients with MCI not due to AD, (e.g. frontotemporal dementia, vascular dementia, or dementia with Lewy bodies (DLB)), with normal CSF biomarkers and cognitive impairment. In general, the AD or "case" group included patients with MCI-AD and mild dementia due to AD, who showed cognitive complaints without daily living activities impairment or with minor daily living activities impairment. In addition, the control group is called healthy control or healthy in some of the chapters.

Table 1. Participants' classification attending to neuropsychological evaluation, neuroimage and cerebrospinal fluid biomarkers.

Test	MCI-AD Group	Preclinical AD	Non-AD Group	Control
Neuropsychological test				
CDR	0.5–1	0	0.5–1	0
RBANS.DM	≤85	>85	≤85	>85
MMSE	20-26	≥ 27	<27	≥ 27
FAQ	<9	<9	-	<9
Neuroimage test				
Amyloid PET	Positive	Positive	Negative	Negative
CSF biomarkers				
Aβ42 (pg mL^{-1})	<725	<725	≥725	≥725
p-Tau (pg mL^{-1})	>350	>350	≤350	≤350
t-Tau (pg mL^{-1})	>85	>85	≤85	≤85

CDR: Clinical dementia rating; RBANS.DM: Repeatable Battery for the Assessment of Neuropsychological Status-Delayed Memory; CSF: cerebrospinal fluid; Aβ42: amyloid β 42; t-Tau: total Tau; p-Tau: phosphorylated Tau.

*When only one of the neuropsychological tests has an altered score it is considered a normal cognition.

The present doctoral thesis is divided into two sections. Section I is focused on lipid peroxidation studies and Section II in omic studies. Therefore, the analytical methods are described separately.

2. Section I. Experimental procedures

2.1. Materials and reagents

As regards the lipid peroxidation products, standards of IsoPs and prostaglandins used for calibration include 15(*R*)-15-F_{2t}-IsoP, 2,3-dinor-15-*epi*-15-F_{2t}-IsoP, 5-F_{2t}-IsoP, 15-keto-15-E_{2t}-IsoP, 15-keto-15-F_{2t}-IsoP, 15-E_{2t}-IsoP, 15-F_{2t}-IsoP, 1a,1b-dihomo-$PGF_{2\alpha}$, PGE_2, and $PGF_{2\alpha}$, as well as the deuterated internal standard (IS) $PGF_{2\alpha}$-D_4 and they were purchased from Cayman Chemical Company (Ann Arbor, Michigan, USA). The other standards corresponding to neuroprostanes (NeuroPs), dihomo-isoprostanes (dihomo-IsoPs) and dihomo-isofurans (dihomo-IsoFs) (7(*RS*)-ST-Δ^8–11-dihomo-IsoF, 10-*epi*-10-F_{4t}-NeuroP, D_4–10-*epi*-10-F_{4t}-NeuroP, 4(*RS*)-F_{4t}-NeuroP, 17-*epi*-17-F_{2t}-dihomo-IsoP, 17-F_{2t}-dihomo-IsoP, 17(*RS*)− 10-*epi*-SC-Δ^{15}-11-dihomo-IsoF, *ent*- 7(*RS*)− 7-F_{2t}-dihomo-IsoP, 14(*RS*)− 14-F_{4t}-NeuroP) were synthesized by Durand's team at the Institute des Biomolécules Max Mousseron (IBMM) (Montpellier, France)[136–140]. The calibration curves were prepared by serial dilutions in H_2O (pH 3): CH_3OH (85:15 v/v) with CH_3COOH 0.01%, in concentrations from 300 nmol L^{-1} to 0.004 nmol L^{-1} of each analyte.

The centrifuge (multiSPIN) was from Cleaver Scientific Ltd. (Warwickshire, United Kingdom) and the vortex mixer was from Velp Scientifica (Usmate, Italy). The speed vacuum concentrator (mi Vac) was from Genevac LTD (Ipswich, United Kingdom). The thermomixer HLC was from Ditabis (Pforzheim, Germany). The Strata X-AW (100 mg, 3 mL) solid phase extraction cartridges used for sample solid- phase extraction (SPE) and the SPE 12-position vacuum manifold were from Phenomenex (Madrid, Spain).

2.2. Sample treatment

In this section urine, plasma, and CSF samples were analyzed. The sample treatment for each matrix is described in Figure 3.

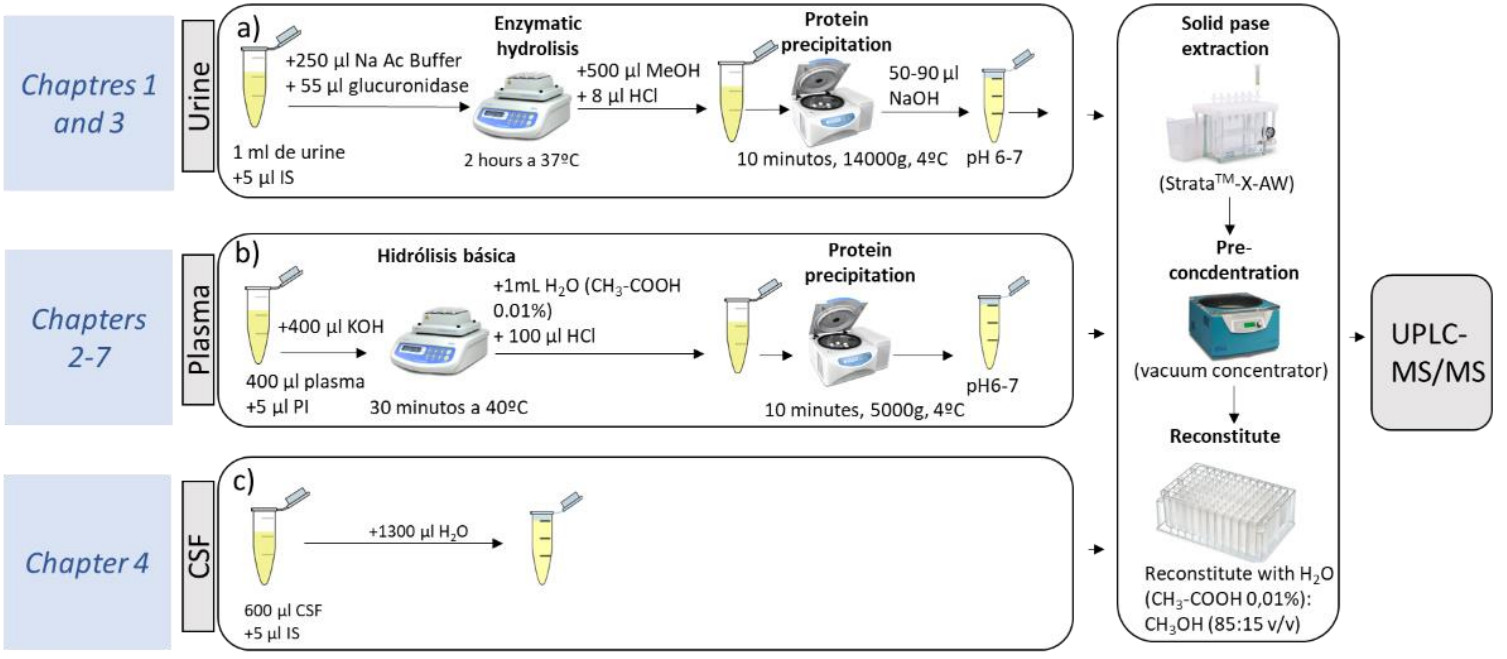

Figure 3. Samples treatment for lipid peroxidation analyses. a) treatment for urine samples; b) treatment for plasma samples; c) treatment for CSF samples.

2.2.1 Urine samples

Urine samples (Chapters 1 and 3) were collected in a sterile bottle and immediately stored at −80 °C until analysis (~6 months). As stated in a previous study, no deterioration was observed for the lipid peroxidation compounds at long-term, since samples were not subjected to freeze-thaw cycles [141]. Then, they were treated following the optimum procedure established in a previous work [141]. Briefly, samples were thawed on ice and 5 µL of the internal standard solution (PI) ($PGF_{2\alpha}$-d_4 10 µmol L^{-1} and d_4-10-*epi*-10-F_{4t}-NeuroP 6 µmol L^{-1}) were added to 1 mL of sample. Then, enzymatic hydrolysis was performed by adding the enzyme β-glucuronidase and sodium acetate buffer (100 mmol L^{-1}, pH 4.9) and incubated for 2 hours at 37 °C. Then, the reaction was stopped and the enzyme was precipitated with cold methanol and chlorhydric acid (37%, v/v) and centrifuged for 10 min (14000 g, 4 °C). The supernatant pH was adjusted to 6–7 with sodium hydroxide (2.5 mol L^{-1}). Finally, a solid phase extraction procedure was carried out.

The results were standardized by the creatinine levels measured using a colorimetric kit (MicroVue creatinine EIA) and a spectrophotometer following the manufacturer's protocol.

2.2.2 Plasma Sample

Plasma samples were collected from peripheral blood employing cryo-tubes with ethylenediaminetetraacetic acid. Then they were centrifuged for 15 min at 1160*g* at room temperature. Plasma was separated in a tube containing butylated hydroxytoluene (0.25% (w/v) in ethanol) to avoid further oxidation of the sample. Afterward, samples were frozen at − 80 °C until analysis.

The sample treatment consisted of the addition of 5 µL of an internal standard solution ($PGF_{2\alpha}$-D_4 2 µmol L^{-1} and D_4–10-*epi*-10-F_{4t}-NeroP 1.2 µmol L^{-1}) and 400 µL of a potassium hydroxide solution (15% w/v) to 400 µL of plasma to carry out the hydrolysis (40 °C, 30 min). After that, the samples were placed on ice, diluted with 1 mL of H_2O (0.01% v/v acetic acid), acidified with hydrochloric acid (37%), and centrifuged for 10 min (5000*g*, 4 °C). Then, the supernatant final pH was adjusted to 7 by adding NaOH 2.5 mol L^{-1}. For clean-up and pre-concentration, a SPE procedure using Strata X-AW

cartridges was carried out [141].

2.2.3 CSF samples

CSF samples were obtained by lumbar puncture as part of the diagnostic protocol in the Polytechnic University Hospital La Fe (Valencia, Spain), and they were kept at –80 °C. The analysis consisted of samples thawing on ice and adding 5 µL of the internal standard solution (IS) (d_4-10-*epi*-10-F_{4t}-NeuroP at 6 µmol L^{-1}, and PGF2α-d_4 at 10 µmol L^{-1}) to 600 µL CSF. Then, they were diluted with 1300 µL of water.

2.2.4 Solid phase extraction

After the samples pretreatment, a cleaning and pre-concentration step was carried out by solid-phase extraction SPE for all sample types (urine, plasma and CSF). For this, the cartridges were first conditioned with 1 mL methanol and 1 mL H_2O. Then the samples were loaded into the SPE cartridge and the cartridge was washed with 1 mL ammonium acetate (100 mmol L^{-1}, pH 7) and 1 mL heptane. Elution was carried out with 2 × 500 µL of methanol (5% v/v CH_3COOH). After that, the samples were evaporated to dryness in the vacuum concentrator and reconstituted in 100 µL of H_2O (pH 3):CH_3OH (85:15 v/v) containing 0.01% (v/v) CH_3COOH. Finally, the samples were injected into ultra-performance liquid chromatography coupled to tandem mass spectrometry (UPLC-MS/MS)(Waters Acquity UPLC-Xevo TQD system (Milford, MA, USA)).

2.3. Chromatographic system

The chromatographic system consisted of a UPLC system (Waters Acquity) coupled to a Xevo TQD system mass spectrometry system (Waters, United Kingdom). The conditions used were: ionization in negative mode (ESI-), capillary tension 2.0 kV, source temperature of 150 °C, desolvation temperature of 395 °C nitrogen cone and desolvation gas flows were 150 and 800 L h^{-1}, respectively, and dwell time was 10 ms.

The UPLC conditions were selected to achieve appropriate chromatographic retention and resolution by using a C_{18} column (2.1 × 100 mm, 1.7 µm) (Acquity UPLC BEH, Waters). Mobile phases consisted of water (0.01% v/v CH_3COOH as mobile phase A) and acetonitrile (0.01% v/v acetic acid as mobile phase B). The temperatures of the column and the

autosampler were set at 55 °C and 4 °C, respectively. The injection volume was set at 8 µL and the flow rate was set to 0.45 mL min^{-1}. A total 8.5 min elution gradient was performed. It consisted of 0.5 min with eluent composition at 80% A and 20% B, which was gradually changed to 55% A and 45% B at 6 min; then B was increased to 95% along 0.2 min, and kept constant for 0.8 min. Finally, the mobile phase composition returned to the initial conditions, and it was maintained for 1.3 min for system conditioning.

The detection was performed by multiple reaction monitoring (MRM) using the acquisition parameters obtained in a previous work [141].

2.4. Neuroimaging data acquisition

MRI was performed as part of the routine clinical assessment. Images were obtained using three MRI scanners (Siemens): two 1.5 T and one 3T machines were used. Imaging protocol included axial, sagittal and coronal views of the brain using T1, T2, gradient echo and fluid attenuation inversion recovery (FLAIR) sequences. Medial temporal atrophy (MTA) was assessed visually by a single rater relative light changes (RLC) using FLAIR or T1 coronal images at the level of the hippocampus. The visual assessment of MTA was ranged from 0 (no atrophy) to 4 (severe atrophy) and was based on criteria and score system proposed by Scheltens et al.[142].

2.5. Statistical analyses

2.5.1 Univariate analyses

Data were summarized using median and interquartile range (IQR) in the case of continuous variables, and with relative and absolute frequencies in the case of categorical variables.

Regarding univariate analysis, differences between groups for numerical variables were analyzed by the Mann-Whitney or Kruskal Wallis tests. Categorical variables were analyzed by the Chi-square test. Finally, correlations among the biomarkers, as well as between the biofluids were analyzed by Pearson Correlation. In addition, as descriptive analysis, correlations among the different variables (18 lipid peroxidation compounds in plasma and 3 biomarkers in CSF) were assessed by constructing a correlation network

based on the spearman correlation matrix of the variables (Chapter 2). Correlations with an absolute value under 0.3 were excluded from the network to avoid spurious effects. Variables distribution was studied using a Kolmogorov–Smirnov test. Analysis were carried out with the software SPSS version 20.0 software (SPSS, Inc., Chicago, IL, USA) and R software (different versions). For all the analysis, significance value was p value < 0.05. Box-plots were used to represent the levels of isoprostanoids biomarkers.

2.5.2. Multivariate analysis

Multivariate analysis based on Elastic Net was developed in Chapter 1. Elastic net is able to perform variable selection at the same time of model fitting and produces parsimonious predictive models. This property improves generalization of the model to new data by avoiding overfitting. It is an adequate variable selection technique compared to other commonly used methods such as stepwise algorithms or univariate screening, which suffer from many consistency problems [143]. Prior to modelling, variables were log-transformed to avoid potential strongly influential outliers due to the highly skewed nature of some variables. Then, a logistic regression model based on elastic-net-penalized was developed including gender and age as covariates. The penalization parameter lambda was selected by performing 500 replications of ten-fold cross validation. The minimum cross-validated error was selected on each replication and the median from the selected lambda values was considered the consensus lambda. Since the minimum lambda value was used, an alternative variable selection method was performed as a sensitivity analysis. This alternative analysis consisted on a random forest using the Altmann et al. method [144]. The final elastic net model was validated using bootstrap validation. For this, the procedure of Steyerberg et al. was followed [145]. Statistical analyses were performed using the softwares R (version 3.5.0), the BootValidation R (version 0.1.3), glmnet R (version 2.0–16), and ranger (version 0.9.0).

In chapter 2, as descriptive analysis, correlations among the different variables (18 lipid peroxidation compounds in plasma and 3 biomarkers in CSF) were assessed by constructing a correlation network based on the spearman correlation matrix of the variables. Correlations with an absolute value under 0.3 were excluded from the network to avoid spurious effects. Then, multivariate analyses based on Elastic-Net was carried

out. Prior to modelling, variables with near zero variance were excluded (1a,1b-dihomo-$PGF_{2\alpha}$ and 2,3-dinor-15-*epi*-15-F_{2t}-IsoP). With the remaining variables, an elastic-net-penalized logistic regression model was adjusted. Age and gender were included in the models as covariates. Selection of the penalization parameter lambda, which controls the complexity of the model by decreasing the number of variables included in the model as it grows larger, was performed by estimating the bias-variance error curve of the population using 500 replications of ten-fold cross validation. The lambda value at one standard error from the minimum cross-validated error was selected on each replication and the median from the selected lambda values was chosen as the consensus lambda. The fitted elastic net model performance measured as optimism corrected AUC was validated using bootstrap, following the procedure of Smith et al. [146]. Statistical analyses were performed using R (version 3.4.3) and the BootValidation R (version 0.1.3) and glmnet (version 2.0–13) R packages.

In chapter 3 different regression models, based on linear discriminant analysis (PLS) and non-linear discriminant analysis (support vector machine (SVM); artificial neural networks, (ANN)), were developed from lipid peroxidation compounds levels determined in urine and plasma samples from healthy and MCI-AD participants. Each model was trained and tested multiple times, and the diagnostic performance obtained for each model was evaluated.

The PLS analysis was carried out with the Unscrambler software version 7.6 (Camo, Woodbridge, USA), the SVM analysis with radialand polynomial kernel functions was carried out with IBM SPSS Modeler software version 1.0 (IBM, New York, USA) and the ANN analysis was carried out with SPSS software version 20.0 (SPSS, Inc., Chicago, IL, USA). These statistical multivariate models were developed for each sample matrix that was analyzed.

The PLS models were constructed from 24 independent variables (22 lipid peroxidation compounds, gender and age) as predictor variables, 1 dependent variable (participant group (MCI-AD/healthy control)) and 5 principal components. All variables were normalized, and a random cross validation (one left out) was carried out.

The SVM models with radial and polynomial kernel functions were developed from 24 independent variables (22 lipid peroxidation analytes, gender and age) and 1 dependent

variable (participant group (MCI-AD/healthy control)). The dataset was randomly divided into training sample (70%), testing sample (15%) and validating sample (15%). The parameters utilized were detention criteria of $1.0E^{-3}$, regularization parameter (C) of 10, precision of regression of 0.1, and the kernel functions employed were radial basis function (gamma (γ) of 0.1) and polynomial function (γ of 1).

The ANN models were constructed from the 24 independent variables (gender and age as factors, 22 analytes as covariables), and 1 dependent variable (participant group (MCI-AD/healthy control)). In the first step, the dataset was randomly divided into training sample (70%), testing sample (15%) and validating sample (15%) [147], before model development. The training sample is used to train the network in several iterations improving the ANN performance. Then, the optimum values of weights and biases are determined, and the ANN performance is examined in the testing sample. The feedforward architecture was based on the predictors function Multilayer Perceptron (MPL), as training algorithm, that minimizes the prediction error of outputs, and the form of this function consists of input, hidden and output layers, but the number of neurons in each layer as well as the number of layers depend on the complexity of the studied system. The automatic architecture selection builds a network with one hidden layer, and the number of units in the hidden layer was tested between 1 and 50, 1 unit being the optimum number. The transfer functions for the hidden and output layers were hyperbolic tangent and normalized exponential function, respectively. These functions have the following forms:

$$\gamma\,(x) = \tanh\,(x) = (e^{x} - e^{-x})/(e^{x} + e^{-x})$$

$$\gamma(x_k) = \exp.(x_k)/\Sigma_j \exp(x_j), \text{ for } j = 1, \ldots, k \text{ (dimensions)}$$

In this sense, a three-layer 24-1-1-feed-forward propagation ANN model was trained and developed from 24 predictor variables (age, gender, lipid peroxidation compounds).

Regarding the training type, it was in batch, and the optimization algorithm to estimate the synaptic weights was based on scaled conjugate gradient including an initial lambda and an initial sigma values of 0.0000005 and 0.00005, respectively, as initial values for the weights and biases to optimize them in successive iterations.

In chapter 5, a two-stage model for Alzheimer's disease diagnosis was developed by

adjusting two nested logistic regression models. The first model was based on the discrimination capacity of the neuropsychological evaluation to differentiate between control and case (including AD and non-AD groups) participants. Specifically, the clinical variables RBANS.DM and CDR were used as predictors in this first model. The second model was based on the discrimination capacity of lipid peroxidation products from plasma samples to diferentiate between AD and non-AD patients in the case group. Specifically, the potential predictors in this second model were 15(*R*)-15-F_{2t}-IsoP, PGE_2, 2,3-dinor-iPF2-III, 15-keto-15-E_{2t}-IsoP, 15-keto-15-F_{2t}-IsoP, 15-E_{2t}-IsoP, 5-F_{2t}-IsoP, 15-F_{2t}-IsoP, $PGF_{2\alpha}$, 1a,1b-dihomo-$PGF_{2\alpha}$, 4(*RS*)-F_{4t}-NeuroP, 10-*epi*-10-F_{4t}-NeuroP, 14(*RS*)-14-F_{4t}-NeuroP, *Ent*-7(*RS*)-F_{2t}-dihomo-IsoP, 17-F_{2t}-dihomo-IsoP, 17-*epi*-17-F_{2t}-dihomo-IsoP, 17(*RS*)-10-*epi*-SC-D^{15}-11-dihomo-IsoF, 7(*RS*)-ST-D^{8}-11-dihomo-IsoF, as well as the total parameters IsoP, IsoF and NeuroF. Selection of the final predictors in the model was performed using Elastic Net [148].

Performance of the model was assessed by estimating optimism-corrected AUC using 200 bootstrap replications. All statistical analyses were performed using R (version 3.6) and R packages pROC (version 1.14.0) and brms (version 2.8.0).

In Chapter 6, the elastic net logistic regression model was used to select "variables" with the glmnet package in order to discriminate between participants groups [149], due to the collinear nature and high dimensionality of the data. The elastic net regularization method of the estimated beta coefficients improves upon ordinary least squares. It linearly combines the L1 and L2 penalties of the lasso and ridge methods. Regularization parameter λ determines the amount of regularization. An optimal value for λ was determined performing a 5-fold cross-validation, which yielded the minimum cross-validated mean-squared error (CVM). A median of 500 repetitions of the cross validation was calculated in order to improve lambda´s robustness.

In Chapter 7, discriminant analysis was performed by PLS.

The multivariate statistical analysis was carried out using the Minitab software version 18 (USA). Then, the Receiver operating characteristic curve (ROC) of the discriminant model was obtained. Two models were constructed, the first included plasma biomarkers (isoprostanes, neuroprostanes, isofurans, neurofurans, 17-*epi*-17-F_{2t}-dihomo-IsoP, $PGF_{2\alpha}$), gender and age as predictor variables; and the second included image data (MTA-

R (right), MTA-L (left) and MTA-S (sum)), gender and age as predictor variables. The response variable used was group (control-case). All the variables were standardized and cross-validation of the models was carried out.

4.2.5.3. Diagnostic models performance evaluation

For diagnostic performance evaluation of the receiver operating characteristic (ROC) curves were constructed from the corresponding validation results from developed models, indicating the area under the curve (AUC)-ROC as a parameter that represents the accuracy of each model. For the PLS model, it was cross validatied leaving one out, while for the SVM and ANN models, validation consisted of using data sets randomly divided. The corresponding area under the curve (AUC, 95% confidence interval (CI)), and the optimum cut-off values (the highest sum of sensitivity and specificity) were determined. Finally, the diagnostic indices (sensitivity, specificity, positive likelihood ratio (LR+), negative likelihood ratio (LR−), diagnostic odds ratio (DOR)) were calculated.

3. Section II. Experimental procedures

3.1 Sample treatment

Figure 4 represents the plasma sample treatment for each chapter.

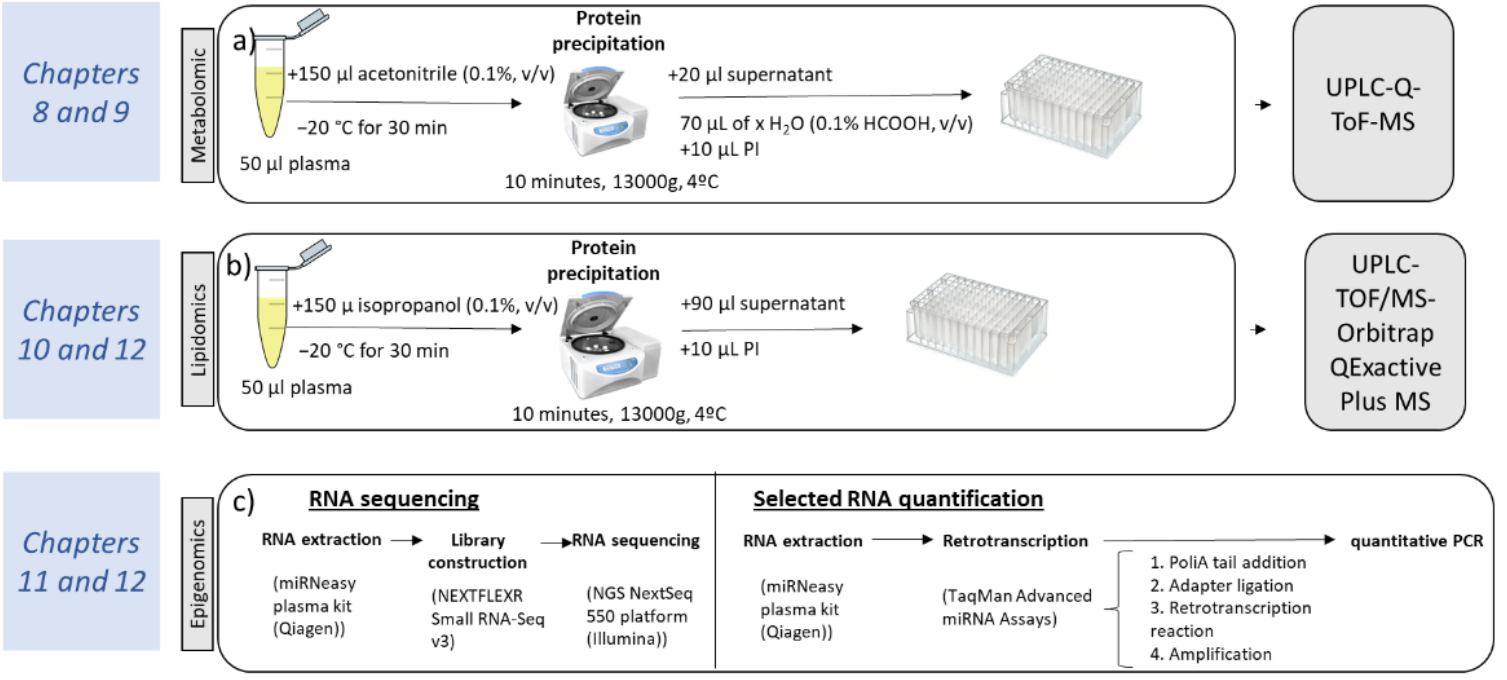

Figure 4. Plasma samples treatment for omics analyses. a) treatment for metabolomic analyses; b) treatment for lipidomic analyses; c) treatment for epigenomic (miRNomic) analyses.

3.1.1 Metabolomics

Plasma samples were thawed on ice, 150 µL of cold acetonitrile (0.1%, v/v) were added to 50 µL of plasma, vortexed and kept at −20 °C for 30 min, for protein precipitation. After centrifugation at 13000 *g* (10 min, 4 °C), 20 µL of the supernatant were transferred to a 96-wells plate for liquid chromatography coupled to mass spectrometry (LC-MS) analysis. Then, 70 µL of H_2O (0.1% HCOOH, v/v), and 10 µL of internal standard mix solution (reserpine, leucine enkephaline, phenylalanine-d5, 20 µM each one) were added to each sample.

3.1.2 Lipidomics

Briefly, 150 µL of cold isopropanol (IPA) were added to 50 µL of plasma, vortexed, and kept at - 20 ˚C for 30 min. Then, it was centrifuged (13,000 *g*, 10 min, 4 ˚C), and 90 µL of supernatant was transferred to a 96-well plate. After that, 10 µL of an internal standard (IS) mix solution (17:0 LPC, d18:1/17:0 SM, and 17:0 PE) (100 µg/mL, each compound) wwere added to each sample.

For both, metabolomics and lipidomics, Quality control (QC) was prepared by mixing 10 µL from each plasma sample. Blank was prepared replacing plasma by ultrapure water in order to identify potential artefacts from the tube, reagents and other materials. Finally, plasma samples, QCs and blanks were injected in the chromatographic system. In order to avoid intra-batch variability, as well as to enhance quality and reproducibility, the analysis scheme consisted of random injection order and analysis of QC every 6 plasma samples. Blank analysis was performed at the end of the sequence. Sample stability and analytical drift were investigated through the internal standard intensities.

3.1.3 Epigenomics.

RNA was isolated for RNA sequencing using the miRNeasy plasma kit (Qiagen, Germany) following the manufacturer's protocol. Briefly, 200 µL of plasma and 700 µL of QIAzol lysis reagent wereincubated for 5 min at room temperature (RT). Then, 140 µL of chloroform were added and incubated at RT for3 min and centrifuged at 1200 g (15 min, 4 °C). The aqueous phase was mixed in a new tube with 525 µL of ethanol and transferred to a RNeasy MinElute spin column followed by a centrifugation step at 10000 g (30 s, RT).

The column was then washed with RWT buffer (700 µL) and RPE buffer (500 µL) and dried for 90 s at 10000 g.Finally, the elution step was performed with 15 µL of RNase-free water (13000 g, 1 min).

For Polymerase Chain Reaction (PCR) validation, RNA extraction was carried out in a similar way but including a previous step, which consisted on the addition of RNA spike-in before the protocol.

3.2 Analytical methods

3.2.1 Metabolomics

Metabolomic analysis was performed on an UPLC system coupled to an iFunnel quadrupole time of flight (Q-ToF) Agilent 6550 mass spectrometer (Agilent Technologies, CA, USA). Chromatographic separation was performed by using an UPLC BEH C_{18} (100 × 2.1 mm, 1.7 µm, Waters, Wexford, Ireland) column from Waters (Wexford, Ireland). Autosampler and column temperatures were set to 4 °C and 40 °C, respectively. The injection volume was 5 µL. A gradient elution with a total run time of 14 min was performed at a flow rate of 400 µL min^{-1} as follows: 98% of mobile phase A (H_2O, 0.1% v/v HCOOH) for 1 min, a linear gradient from 2% to 15% of mobile phase B (CH3CN, 0.1% v/v HCOOH) for 2 min, from 15% to 50% B for 3 min and from 50% to 95% for 3 min. Finally, 95% B was held for 3 min and a 0.55 min gradient was used to return to the initial conditions, which were held for 2.5 min to totally column recovery. Full scan MS data from 50 to 1700 m/z with a scan frequency of 6 Hz was collected. Both positive and negative electrospray ionization modes (ESI +, ESI –) were used and the conditions were set as follows: gas temperature, 200 °C; drying gas, 14 L min^{-1}; nebulizer, 60 psi; sheath gas temperature, 350 °C; sheath gas flow, 11 L min^{-1}. Automatic MS spectra recalibration was carried out introducing a reference standard into the source via a reference sprayer valve during the analysis. Q-ToF-MS was also used under auto MS/MS and all-ions (MS^E) fragmentation modes for the simultaneous acquisition at low and high collision energies, which provide useful information about the (de)protonated molecules and main fragment ions for the identification of discovered metabolites.

3.2.2 Lipidomics

Samples were analyzed by UPLC coupled to time-of-flight mass spectrometry (UPLC-TOF/MS-Orbitrap QExactive Plus MS) following the normalized protocol from the Analytical Unit in Health Research Unit La Fe (Valencia, Spain). Briefly, the chromatographic conditions consisted of using an Acquity UPLC CSH C18 column (100 x 2.1 mm, 1.7 µm) from Waters. The mobile phase in the positive ionization mode was acetonitrile/water (60:40) with formic acid (10 mM) (A) and isopropyl alcohol/acetonitrile (90:10) with formic acid (10 mM) (B); in the negative ionization mode, it was acetonitrile/water (60:40) with acetic acid (10 mM) (A) and isopropyl alcohol/acetonitrile (90:10) with acetic acid (10 mM) (B). The flow rate was 0.40 mL min^{-1}, the column temperature was 65 °C, and the injection volume was 5 µL.

Untargeted Analysis

For the untargeted analysis, the mass spectrometry conditions consisted of positive and negative ionization, an *m/z* range of 70–1700 Da, a resolution full scan of 70,000, a capillary voltage of 2.5 kV, a sheath gas flow rate of 35, an auxiliary gas flow rate of 15, a sweep gas flow rate of 0, a capillary temperature of 250 °C, an s-lens RF level of 65, and an auxiliarygas heater temperature of 200 °C. Samples were randomly injected in the chromatographic system in order to avoid intra-batch variability. Regarding the QC sample, it was analyzed every seven injections to monitor and correct changes in the instrument response. Moreover, it was repeatedly analyzed under the auto MS/MS and all-ion (MSE) fragmentation modes to provide useful information of fragment ions for identification purposes. The stability of the analytical system during the analysis was investigated through the trends and drifts of IS intensities over the course of the batch analysis. A blank analysis was performed at the end of the sequence and was used to identify artefacts from sampling, the preparation of samples, and analysis.

Then, some variables were annotated, with a mass error <5 ppm, and some of them were selected for a subsequent targeted analysis.

Targeted analysis

Some of previous variables were selected for a targeted analysis. First, lipid families that showedstatistically significant differences among the participant groups were selected. Then, individual compounds from these families that showed statistically significant differences between groups were selected. In the case of no commercially available standards, similar lipid compounds from the same family were selected.

Table 2. Acquisition parameters for targeted lipid analysis.

Compound	Mass to Charge (*m/z*) Precursor Ion	Chemical Formula (M)	Product Ion (*m/z*) (Quantitative)	Product Ion (*m/z*) (Qualitative)
18:1 LPE	480.30847	C23H46NO7P	308.294	
18:0 LPC	524.37107	C26H54NO7P	184.073	104.107
16:1 SM (d18:1/16:1)	701.5592	C39H77N2O6P	184.073	104.107
16:0 SM (d18:1/16:0)	703.57485	C39H79N2O6P	184.073	104.107
18:0 SM (d18:1/18:0)	731.60615	C41H83N2O6P	184.073	104.107
18:1 (9-Cis) PE (DOPE)	744.55378	C41H78NO8P	308.294	
24:0 SM	815.70005	C47H95N2O6P	184.073	86.0963
17:0 LPC	568.3626	C25H52NO7P	184.073	
17:0 SM (d18:1/17:0)	717.5905	C40H81N2O6P	184.073	
17:0 PE	720.22537	C39H78NO8P	184.073	

LPE: lysophosphatidylethanolamine; LPC: lysophosphatidylcholine; SM: sphingomyelin; PE: phosphatidylethanolamine; DOPE: dioleoyl phosphatidylethanolamine.

The sample treatment and the MS/MS method were developed for the simultaneous targeted analysis of seven lipid compounds (18:1 LPE, 18:0 LPC, 16:1 SM (d18:1/16:1), 16:0 SM (d18:1/16:0), 18:0 SM (d18:1/d18:0), 18:1 (9-Cis) PE (DOPE), and 24:0 SM). In addition, 17:0 LPC, 17:0 SM (d18:1/17:0), and 17:0 PE were used as internal standards. Metabolite concentrations were calculated by an internal calibration using a reaction and multiple reaction monitoring (MRM) method. The employed mass spectrometry conditions consisted of positive ionization, a capillary voltage of 3 kV, a sheath gas flow rate of 35, an auxiliary gas flow rate of 15, a sweep gas flow rate, a capillary temperature of 250 ˚C, an s-lens RF level, and an

auxiliary gas heater temperature of 200 °C. The normalized collision energy was 25 for all compounds. The MRM methodparameters are summarized in Table 2.

Analytical Method Validation

The analytical characteristics assayed during the validation procedure were the linearity range, precision, accuracy, limit of detection (LOD), and limit of quantification (LOQ).The accuracy was evaluated by means of the recovery test. For this, standards were spiked at three concentration levels, and they were analyzed in triplicate. The precision was estimated from the analysis of standards and spiked samples at three concentration levels (i.e., low, medium, and high) in triplicate. The LOD and LOQ were established experimentally as the concentrations required to generate signal-to-noise ratios of 3 and 10, respectively.

3.2.3 Epigenomics

RNA sequencing method.

Construction of RNA libraries. The miRNA libraries were prepared from total RNA using the NEXTFLEX® Small RNA-Seq v3 Kit for Illumina Platforms (Bioo Scientific Corporation, Texas, USA). Briefly, the small RNA molecules were first ligated to the 3'-4 N adenylated adapters, taking advantage ofthe phosphate group at their terminal end, which allows the exclusive targeting of these molecules. Secondly, the 5'-4 N adapters were ligated. Later, reverse transcription of the molecule into cDNA was carried out. The generated cDNA fragments were then amplified and indexed by PCR using different barcode primers for each sample.Finally, a size-selective purification was carried out.

The quality control and concentration of the libraries were verified with the Agilent Technologies 2100 bioanalyser using highly sensitivity DNA chips (Central Unit for Research in Medicine (Universitat de València)). Subsequently, an equimolecular pool of each library was prepared for sequencing.

Sequencing on an Illumina equipment. Sequencing was carried out on the NGS NextSeq 550 platform (Illumina, San Diego, CA, USA) by single read sequencing of 50 cycles (1 × 50 bp).

miRNAs validation by quantitative PCR.

Quantitative PCR procedure. From the extracted RNA, retro-transcription and amplification steps were carried out following the manufacturer's recommendation (TaqMan Advanced miRNA Assays) [https://tools.thermofisher.com/content/sfs/manuals/100027897_TaqManAdv_miRNA_Assays_UG.pdf]. Briefly, the protocol consisted of four steps. First, the addition of a polyA tail, after the adapter ligation, followed by the retro-transcription step, and then the specific miRNA amplification. Finally, samples were diluted, and real time PCR (RT-PCR) was carried out in duplicate using the thermocycler (ViiA7, Applied Biosystems, California, USA).

3.3 Data pre-processing

3.3.1 Metabolomics

First, pre-processing of acquired data from the full scan analysis by UPLC-Q-ToF-MS is required to detect molecular features. Data processing was done by using the XCMS package in R [150], for peak detection, noise filtering, peak alignment, grouping, and normalization of data; and the CAMERA package [151], for identification of isotopes and most probable adducts. Finally, a data matrix was generated including molecular features (m/z-retention time), sample ID (observations) and peak intensities.

3.3.2 Lipidomics

The results from the untargeted analytical method were converted to the mzXML file format, and the data were processed (peak detection, noise filtering, and peak alignment) using an *in-house* R processing script based in the LipidMS package published by Alcoriza-Balaguer et al. and developed in the Analytical Unit of the Health Research Institute of La Fe (Valencia) [152].

For both analyses metabolomics and lipidomics, before the statistical analysis, data quality (reproducibility, stability) was evaluated by means of the internal standards stability and the QC's coefficients of variation (CV). Those molecular features with CV $>$ 30% or not present in 60% of the samples in at least one of the compared groups were removed from the data matrix. Prior to statistical analysis, normalization was performed

in order to find the most appropriate method for this study to eliminate intra-batch variability due to technical differences. They were two approaches based on multiple internal standard (IS), a median fold change normalization, and a QC-based robust locally weighted scatter plot smoothing (LOESS) for signal correction. After evaluation, LOESS data normalization was selected for statistical analysis. Finally, the obtained peaks table was used for statistical analysis.

3.3.3 Epigenomics

Pre-processing, quality control and normalization. NGS data (raw fastq files from sRNA sequencing) were processed following the standard protocol proposed by Cordero et al. [153] implemented in the function mirnaCounts from docker4seq package [154] with default parameters in R[155]. First, a sequence quality control check was generated using FastQC[156] and then cutadapt[157] program was used for the adapter trimming. Specifically, adapters and low-quality reads (Phred Score < 10) were trimmed and removed (44.014.980 reads). Once adapters were removed, sequence reads (219.207.246 good quality reads) were mapped against miRNA precursors from miRBase (v.21)[158], using SHRIMP[158,159] , filtering out a total of 95.03% reads. Finally, miRNA quantification from the resulting 4.97% of mapped reads were generated using the function count Overleaps from GenomicRanges package [160], resulting in a total of 9.799.858 miRNA counts in a total of 2.386 miRNAs.

miRNAs selection. From the miRNAs identified in the pre-processing, quality control and normalization process, some of them were selected. Specifically, those miRNAs which showed a number of counts different from zero in at least 80% of the samples and that were corroborated in literature. Finally, the selected miRNAs were validated by means of qPCR in the same plasma samples.

3.4. Statistical analysis

Demographic and clinical data from participants were summarized using median and interquartile range for continuous variables, and relative and absolute frequencies for categorical variables. Univariate analysis was carried comparing medians between participants groups by Mann Whitney and Kruskal Wallis tests for numerical variables and Chi-square test for categorical variables. All these analysis were carried out with

SPSS software version 20.0 (SPSS, Inc., Chicago, IL, USA). Correlation analyses were carried out by Pearson correlation test. Statistically significant differences were considered from p value < 0.05. In addition, the fold change (FC) ratios for metabolomic analyses were calculated as MCI-AD mean/control group mean for each metabolite.

3.4.1 Metabolomics

Multivariate analyses were carried out with metabolomic data. First, multivariate analysis based on an Elastic Net penalized logistic regression [149] (Chapter 8). It was adjusted to identify the most influential variables in the differentiation between healthy individuals and MCI-AD patients using R (version 3.5), R packages glmnet (version 2.0-16), and BootValidation (version 0.1.5). Penalized regression methods consist on fitting a regression model subject to a specific restriction (a bound on the value of the coefficients). This method forces the shrinkage of the parameters to zero, potentially performing variable selection at the model-fitting step. Penalization factor for the Elastic Net was selected using 500 repetitions of 10-fold cross-validation. From each repetition the highest lambda at one standard error from the minimum was selected (one-standard-error rule) and the median of the 500 lambda values was used as the final penalization factor. With the selected features, the Elastic net models obtained for each ionization mode were evaluated by estimating its optimism corrected AUC-ROC by bootstrapping, following the procedure of Gordon et al. [146]. On chapter 9, for multivariate statistical analysis, data from positive and negative ionization modes were treated simultaneously. First, the normalized variables obtained from data processing were visualized in a Volcano Plot to show which variables present a stronger combination of FC and statistical significance (p-value) from a t-test. Significant variables (p value t-test 1) were selected for a supervised orthogonal-least-squares discriminant analysis (PLS) validated by an iterative 7-fold cross-validation (CV) approach. The validity and robustness of the models were evaluated by R^2 (Y) (model fit) and Q^2 (Y) (predictive ability) diagnostic parameters. Quality of CV Q^2 (Y) was assessed by using the p-value from CV-anova analysis. R^2 Y intercepts and Q2 Y intercepts from 1000 times permutation test in the PLS model was also used to evaluate the overfitting risk. Most discriminant variables were selected according to their Variance Importance in Projection plot values (VIP >1.0), and a jackknife confidence interval that did not include zero. Finally, the potential metabolites

were submitted to identification process. Volcano plots were carried out using the R platform, while the multivariate analysis was carried out using Simca 14.1 software (Sartorius Stedim Biotech, Aubagne, France).

3.4.2 Lipidomics

The variables identified by the LipidMS package [152] were grouped into lipid families (CE, Cer, diglycerol (DG), fatty acid (FA), lysophosphatidylethanolamine (LPE), lysophos-phatidylcholine (LPC), monoglyceride (MG), PC, PE, PI, SM, and TG). In addition, we calculated the variables monounsaturated (MUFAS), polyunsaturated (PUFAS), and saturated (SFAS) fatty acids as the sum of levels (MUFAS, PUFAS, and SFAS, respectively), including all previous lipid families.

On the other hand, a multivariate statistical analysis was carried out with the variables detected in the untargeted analysis in order to identify other potential biomarkers (not identified by the LipidMS package). For this, data from the positive and negative ionization modes were considered simultaneously. First, the normalized variables were visualized in a volcano plot carried out using an *in-house* script in R platform. From this, variables with a stronger combination of FC (abs (log2 FC) > 1) and statistical significance (*p* value of *t*-test < 0.05) in each comparison (MCI-AD vs. control and preclinical AD vs. control) were False Discovery Rate-adjusted and selected for a supervised PLS. The PLS was carried out using Simca 14.1 software (Sartorius Stedim Biotech, Aubagne, France), and it was validated by a seven cross-validation procedure (CV, dataset split into seven subsets). The corresponding models were evaluated by R^2 (Y) (model fit) and Q^2 (Y) (predictive ability) diagnostic indices, the *p*-value of the CV-anova model, and a permutation test. The most discriminant variables were selected according to their variance importance in projection plot values (VIP > 1.0). Once selected, these features were annotated as potential metabolites by the CEU mass mediator database according to the Schymanski levels of identification [161]. In summary, Figure 5 describes the workflow of these analyses.

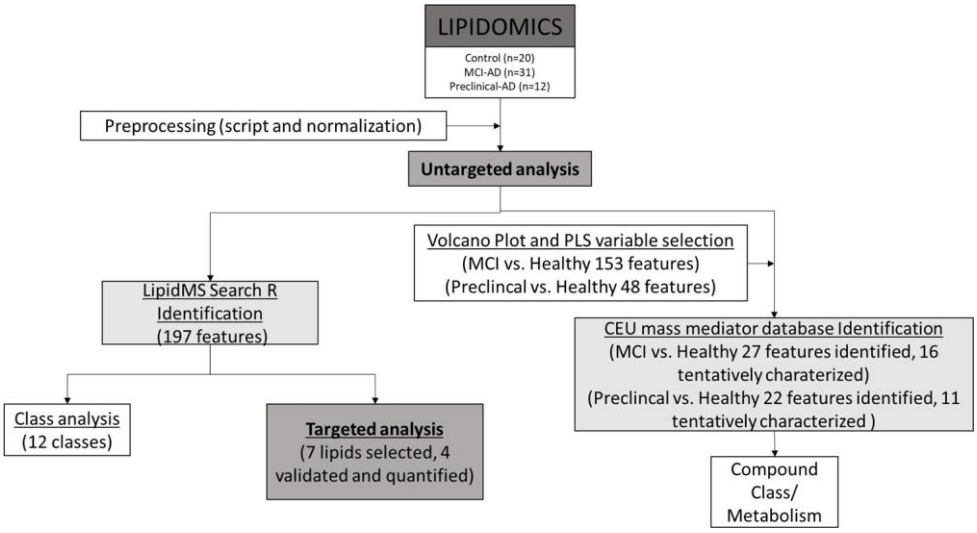

Figure 5. Workflow of the analyses.

3.4.3 Epigenomics

The number of counts obtained from RT-PCR were averaged for duplicates, discarding replicates with values within ± 2 counts from mean. Then, samples were normalized using the mean and standard deviation. The miRNAs detected in at least 80% of the samples and with a difference between replicates < 1 count were satisfactorily quantify. The effect of each biomarker on pathology was then analyzed by Bayesian models: the first model discriminates among control, MCI-AD and preclinical AD groups; and the second model discriminates between AD (preclinical AD, MCI-AD) and control groups. For these models, some parameters were calculated (estimate, which indicates the direction of the miRNAs levels; Odds Ratio; Percentage Inside Rope, which defines the percentage of the area that is within the region of practical equivalence (equivalent to null effect); probability of direction (PD), which indicates the probability that the effect has in a particular direction (indicated by the estimate). PD > 80% was considered significative).

3.4.4 Lipidomics-Epigenomics Integration

Sparse Partial Least Squares (PLS) regression was applied to the previous data sets to select variables (miRNAs, lipids) and integrate them. The PLS approach combines both integration and variable selection on two data sets in a one-step strategy [154].

Then, the graphical representations (correlation circle plots, heatmaps, relevance networks) resulting from the statistical approach were plotted.

Individual differences between groups were carried out by Mann–Whitney test, and correlations by Pearson Correlation. In all the cases, statistical significance was fixed in a *p* value of 0.05.

Statistical analyses were performed using R software (v 4.0.3, Auckland, CA, USA) and mixOmics (v 6.16.2) and clickR (v 0.7.35) packages and SPSS software version 20.0 (SPSS, Inc., Chicago, IL, USA).

3.5 Metabolite annotation

3.5.1 Metabolomics

Metabolite annotation. Molecular features selected by Elastic Net analysis were preliminarily identified by querying their exact mass against those presented in the online Human Metabolome Database (HMDB) (http://www.hmdb.ca/) and the Metlin database (https://metlin.scripps.edu) within a mass range of ± 10 ppm. The identities of the selected features were verified by comparing the MS/MS and all-ions spectra with those of the proposed metabolites in the cited online databases, as well as by using authentic standards whenever available.

Variables selected by PLS analysis were identified by using the online CEU Mass Mediator ((CMM), 3.0, Gil de la Fuente et al, 2019) [162] which combines the results of several online databases, among which Human Metabolome Database (HMDB) (http://hmdb.ca/), Metlin (https://metlin.scripps.edu/), LipidMaps (http://www.lipidmaps.org) and Kegg (http://www.kegg.jp) are used. Annotation of variables (m/z) was carried by querying their accurate mass (AM) against those presented in these sources within a mass range of ±5 ppm. Only those metabolites that appeared at least in the HMDB were finally selected. The adducts included were [M+H], [M+Na], [2M+H], and [2M+Na] for positive ionization mode, and [M-H], [M+HCOOH-H], [2M-H] for negative ionization mode. Also, neutral water loss was taken into account for both ionization modes. A scoring of annotation was calculated by the CMM based on the probability to form specific adducts, as well as their retention time (RT), and lipid elution

order based in RT and the number of carbons and double bonds. Metabolites' annotation was also supported by comparing the obtained MS/MS fragmentation spectra with those experimental spectra proposed in databases. Annotation confidence levels were determined according to the categorical scoring system proposed by the Metabolomics Community. They were level 1, identification of molecular feature through AM and RT, matching with its chemical standard; level 2, putatively annotation through AM and MS/MS spectra matching with online databases; level 3, putatively characterization of compounds by AM matching with online databases; and level 4, feature without annotation (unknown compound) [163,164].

3.5.2 Lipidomics

In order to increase the metabolic coverage, two data analysis strategies were used. The variables were identified by two complementary methods in order to identify more metabolites with different polarity ranges. As a first method, annotation using the LipidMS package and statistical analysis was carried out with the variables. As a second method, annotation by means of the variable AM, using the CEU mass mediator database (including the Kegg, LipidMaps, Metlin, and Human Metabolome databases),a mass range of 5 ± ppm, and some adducts ([M+H], [M+Na], [2M+NH4], [M+NH4],and [M+H-2O] for the positive ionization mode and [M-H], [M+HCOOH-H], [2M-H], and [M+Na-2H] for the negative ionization mode), was carried out. In this second approach, the identity of the metabolites was confirmed by comparing the obtained MS/MS fragmentation spectra with those predicted and proposed in the databases. In this sense, four annotation confidence levels were evaluated, as proposed by E. Schymanski et al. (2014) [161,165]. They were level 1 (identified compounds with structures confirmed by AM, MS/MS spectra, retention time (rt), and reference standards); level 2 (compounds putatively annotated through AM and experimental or predicted MS/MS spectra matched with online libraries); level 3 (compounds putatively characterized by AM matched with online databases); and level 4 (unknown compounds) [165,166].

The results from the targeted analytical method were the signal intensities (arbitrary units) obtained for each lipid compound in plasma samples, and their concentrations were determined from the corresponding calibration curves.

3.5.3 Epigenomics: pathway analyses

The target genes of the differentially expressed miRNAs were studied using the miR data base (miRDB). The selected target genes were those with a target score ≥ 95. Then, the targets were classified according to cellular pathways and functions in order to analyze the implication in AD.

RESULTS, DISCUSSION AND CONCLUSIONS.

SECTION I. Lipid peroxidation studies

Chapter 1. New screening approach for Alzheimer's disease risk assessment from urine lipid peroxidation compounds

1. Summary

The aim of this chapter was to evaluate the capacity of lipid peroxidation compounds from urine samples to disctiminate patients with AD (case grup, n=70) from non-AD cases (control group, n=29). Lipid peroxidation compounds were determined in urine using a validated analytical method based on UPLC-MS/MS. Statistical studies consisted of the evaluation of two different linear (Elastic Net) and non-linear (Random Forest) regression models to discriminate between groups of participants.

2. Results

2.1 Participant' characteristics

Table 3. Demographic and clinical variables of the study participants.

Variable	Case (n = 70)	Control (n = 29)
Age (years) (median (IQR))	70.5 (68, 74)	66 (62, 72)
Gender (female) (n (%))	28 (40%)	18 (62%)
Secondary Studies (n (%))	10 (14%)	10 (34%)
Alcohol consumption (yes) (n (%))	6 (8%)	6 (21%)
Smoking status (yes) (n (%))	8 (11%)	1 (3%)
Medications (yes) (n (%))	54 (77%)	18 (62%)
Comorbidity (yes) (n (%))	53 (76%)	18 (62%)
RBANS.DM (median (IQR))	44 (40, 49)	100 (91, 106)
CDR (median (IQR))	0.5 (0.5,1)	0 (0,0)
FAQ (median (IQR))	7 (3, 13)	0 (0, 0)
MMSE (median (IQR))	22 (18, 26)	30 (28, 30)
CSF Aβ (pg mL^{-1}) (median (IQR))	568 (441, 668)	1227 (1143, 1144)
CSF t-Tau (pg mL^{-1}) (median (IQR))	553 (377, 790)	208 (141, 333)
CSF p-Tau (pg mL^{-1}) (median (IQR))	88 (71, 116)	51 (38, 70)
Temporal atrophy (yes) (n (%))	51 (72%)	2 (7%)
Depression (yes) (n (%))	9 (13%)	3 (10%)

IQR: Interquartilic range; RBANS-DM,Repeatable Battery for the Assessment of Neuropsychological Status-Delayed Memory (Standard Score; cut- off point <85); CDR, Clinical Dementia Rating, values: 0, 0.5, 1, 2; FAQ, Functional Activities Questionnaire (Direct Score; cut-off point >9); MMSE, Minimental State Examination.

Table 3 shows the demographic and clinical data for both groups. Small differences were shown for age and gender between groups, so these variables were considered covariates. Regarding the neuropsychological variables (CDR, RBANS, FAQ, MMSE) and biological

measures (CSF Aβ, CSF t-Tau, CSF p-Tau, temporal atrophy) used in the standard diagnosis, they showed significant differences between groups. However, the demographic variables (age, gender, studies, alcohol, smoking status, medication, comorbidity) did not show statistical differences between groups.

2.2 Determination of urine lipid peroxidation biomarkers

Table 4. Concentrations of lipid peroxidation biomarkers in urine samples

Biomarkers	Case (n = 70) Median (IQR) (ng mg^{-1} creatinine)	Control (n = 29) Median (IQR) (ng mg^{-1} creatinine)
15(R)-15-F_{2t}-IsoP	0.72 (0.5, 1.56)	0.7 (0.48, 0.94)
PGE_2	1.98 (0.62, 3.5)	1.69 (0.93, 4.26)
15-keto-15-E_{2t}-IsoP	0.93 (0.53, 1.47)	1.02 (0.65, 1.54)
15-keto-15-F_{2t}-IsoP	0.84 (0.22, 1.94)	1.33 (0.58, 2)
2,3-dinor-15-epi-15-F_{2t}-IsoP	0.78 (0.53, 1.22)	0.65 (0.47, 1.09)
15-E_{2t}-IsoP	0.23 (0.06, 1.31)	0.16 (0.07, 0.58)
5-F_{2t}-IsoP	2.67 (1.68, 5.07)	2.37 (1.76, 3.37)
15-F_{2t}-IsoP	0.01 (0, 0.02)	0.01 (0, 0.02)
$PGF_{2\alpha}$	3.72 (2.79, 7.32)	3.38 (2.35, 5.17)
4(RS)-4-F_{4t}-NeuroP	0.89 (0.67, 1.36)	0.72 (0.5, 1.01)
1a,1b-dihomo-$PGF_{2\alpha}$	1.33 (0.64, 2.48)	1.67 (1.05, 2.23)
10-epi-10-F_{4t}-NeuroP	0.03 (0, 0.06)	0.01 (0, 0.05)
14(RS)-14-F_{4t}-NeuroP	1.21 (0.76, 2.16)	1.27 (0.74, 1.94)
ent-7(RS)-7-F_{2t}-dihomo-IsoP	0.33 (0.14, 0.63)	0.28 (0.19, 0.36)
17-F_{2t}-dihomo-IsoP	0.09 (0, 0.38)	0.11 (0, 0.26)
17-epi-17-F_{2t}-dihomo-IsoP	0.01 (0, 0.07)	0 (0, 0)
17(RS)-10-epi-SC-Δ^{15}-11-dihomo-IsoF	0.03 (0, 0.1)	0.05 (0.03, 0.08)
7(RS)-ST-Δ^{8}-11-dihomo-IsoF	0 (0, 0.02)	0 (0, 0.03)

IQR, inter-quartile range; IsoP, isoprostane; dihomo-IsoP, dihomo-isoprostane; dihomo-IsoF, dihomo-isofuran, NeuroP, neuroprostane.

Urine levels of lipid peroxidation compounds obtained for each group are shown in Table 4. Some of them (5-F_{2t}-IsoP, 2,3-dinor-15-epi-15-F_{2t}-IsoP, 15-E_{2t}-IsoP, PGE_2, $PGF_{2\alpha}$, 10-*epi*-10-F_{4t}-NeuroP, 4(*RS*)-4-F_{4t}-NeuroP, *ent*-7(*RS*)-7-F_{2t}-dihomo-IsoP) showed higher levels in early AD patients than in healthy controls, and some analytes (15-keto-15-E_{2t}-IsoP, 15-keto-15-F_{2t}-IsoP) showed lower values in the case group than in the control group. Figure 6 shows the box plots for each analyte.

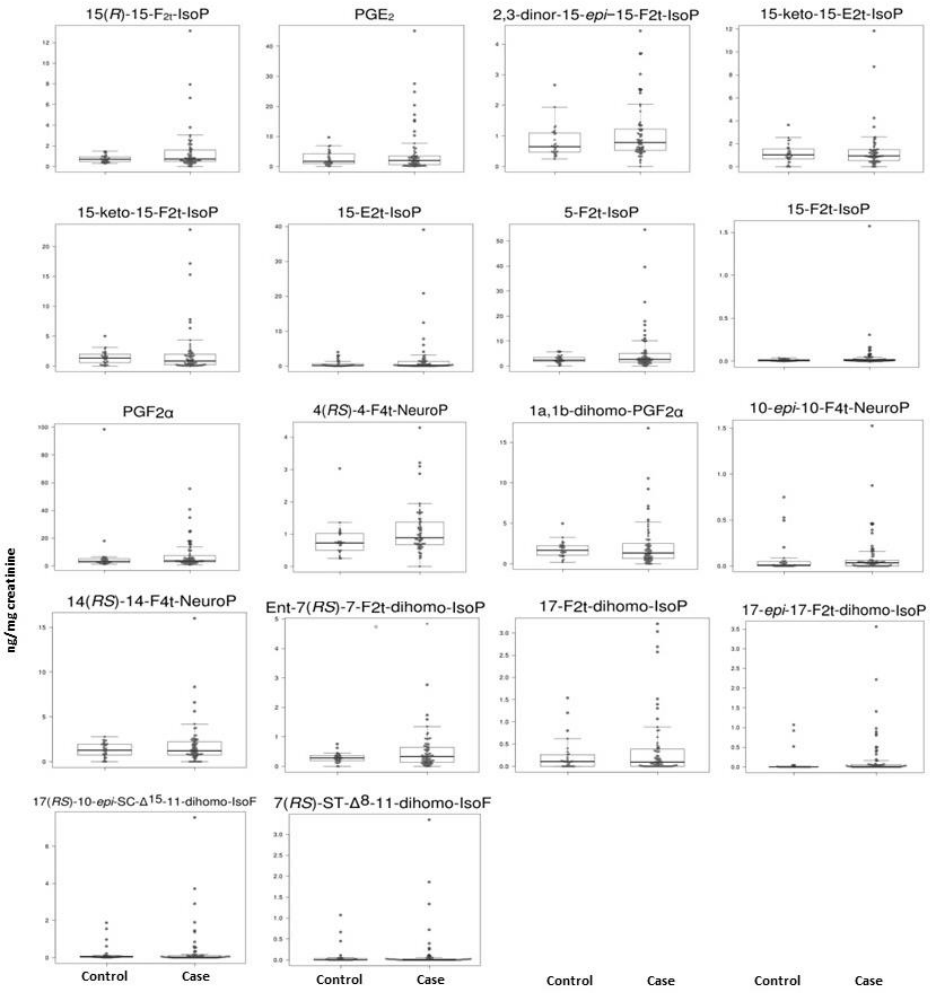

Figure 6. Box-Plot of the differences in different lipid peroxidation analytes levels between early AD (case) and healthy (control) groups.

2.3 Screening model from urine lipid peroxidation biomarkers

The elastic net model selected five variables corresponding to one isoprostane, one neuroprostane, one prostaglandin and two dihomo-isoprostanes shown in Table 5. The model also included gender and age, which were introduced as covariates. These predictor

variables were combined as it is indicated in the formula below in order to estimate the individual probability (Pr) of suffering from AD.

$$\Pr(Y)\frac{e^{-4.187+0.51*female+0.064*age-0.13*(A)+0.622*(B)-0.048*(C)+0.554*(D)+0.072*(E)}}{1+e^{-4.187+0.463*female+0.064*age-0.13*(A)+0.622*(B)-0.048*(C)+0.554*(D)+0.072*(E)}}$$

A: 15-keto-15-F_{2t}-IsoP; B: 4(*RS*)-4-F_{4t}-NeuroP; C: 1a,1b-dihomo-$PGF_{2\alpha}$; D: *ent*-7(*RS*)-7-F_{2t}-dihomo-IsoP; E:17-*epi*-17-F_{2t}-dihomo-IsoP.

Table 5. Results of the elastic net and random forest analyses.

Variable	Coefficient (elastic net)	Importance (random forest)	p-value (random forest)
Gender (female)	0.463	0.17	0.08*
Age	0.064	1.09	0.012*
15-keto-15-F_{2t}-IsoP	−0.13	0.71	0.043*
4(RS)-F_{4t}-NeuroP	0.62	0.74	0.046*
1a,1b-dihomo-$PGF_{2\alpha}$	−0.048	0.73	0.035*
ent-7(RS)-7-F_{2t}-dihomo-IsoP	0.55	0.64	0.044*
17-epi-17-F_{2t}-dihomo-IsoP	0.072	0.58	0.029*
10-epi-10-F_{4t}-NeuroP	0	0.48	0.075
17-F_{2t}-dihomo-IsoP	0	0.35	0.133
17(RS)-10-epi-SC-Δ^{15}-11-dihomo-IsoF	0	0.21	0.219
15-E_{2t}-IsoP	0	0.17	0.293
5-F_{2t}-IsoP	0	0.14	0.325
2,3-dinor-15-epi-15-F_{2t}-IsoP	0	0.11	0.381
15(R)-15-F_{2t}-IsoP	0	0.10	0.379
PGE_2	0	0.08	0.405
15-keto-15-E_{2t}-IsoP	0	0.05	0.436
7(RS)-ST-Δ^{8}-11-dihomo-IsoF	0	−0.08	0.636
$PGF_{2\alpha}$	0	−0.09	0.603
14(RS)-14-F_{4t}-NeuroP	0	−0.25	0.755

The alternative analysis using random forest selected the same five variables as the most important ones (Table 5), and they were also all considered statistically significant by the Altmann method [144]. Classification performance of the models was assessed using bootstrap in the case of elastic net and by the Out of Bag (OOB) estimate in the case of random forest. Bootstrap validated AUC-ROC for the elastic net model was 0.682 and OOB accuracy for the random forest model was 0.71, so their performance can be considered similar. Remarkably for the elastic net results, the sensitivity and specificity profile shows

a sharp decrease of the sensitivity values as the specificity increases, forcing a decision between high sensitivity (0.97) at a cost of low specificity (0.31) or high specificity (0.93) at a cost of mediocre sensitivity (0.5) (Figure 7).

Coefficients of the elastic net model are interpreted as log-odds, so negative values indicate a negative association between higher concentration levels and risk of disease, and positive values indicate a positive association between higher concentration levels and risk of disease. Importance values and p-values for random forest are derived from the gini index using Altman method.

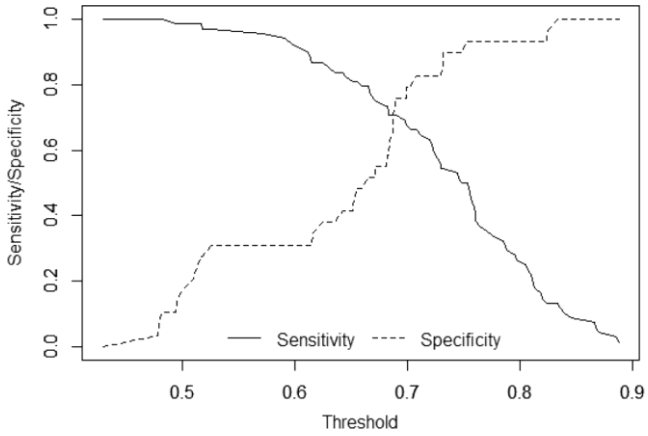

Figure 7. Sensitivity and specificity profile plot. The continuous line depicts the relationship between the probability threshold set in the model's prediction and its corresponding sensitivity and the dashed line represent the relationship between the probability threshold and the specificity.

3. Discussion

The reliable determination of lipid peroxidation products levels in urine samples from well-defined healthy and early AD participants, and the satisfactory classification performance of two complementary regression models allowed to develop an early and non-invasive screening model to identify individuals with high risk to develop the AD.

The role of lipid peroxidation in AD development has been largely studied [167] but few studies have been carried out determining isoprostanoids as target metabolites in AD

[168,169]. In addition, the analytical methods used in most of these works were based on commercial kits or immunoassays what is associated to low specificity on isomers determinations (Puertas et al., 2012). Nevertheless, in the present study a previously validated analytical method based on mass spectrometry detection has been used, providing high selectivity and sensitivity, as well as high reliability to determine simultaneously several isoprostanoids isomers [141].

Regarding the development of early and non-invasive diagnosis, urine could be considered a promising matrix. However, few studies in literature have focused on this matrix [171,172]. Specifically, in the present work some compounds (PGE_2, 2,3-dinor-15-epi-15-F_{2t}-IsoP, 15-E_{2t}-IsoP, 5-F_{2t}-IsoP, $PGF_{2\alpha}$, 10-*epi*-10-F_{4t}-NeuroP, 4(*RS*)-4-F_{4t}-NeuroP and 17-*epi*-17-F_{2t}-dihomo-IsoP) showed higher concentrations in urine from AD patients than in healthy participants. Similarly, previous studies showed higher levels of some F_2-IsoPs in urine from patients with AD than in the control group [173–175]. However, further studies to clinically validate these potential biomarkers, using a larger number of samples from well-defined participants, and predictive models are required.

In this work, two alternative modelling methods with completely different characteristics were used. First, elastic net logistic regression is based on standard generalized linear regression models, thus assuming linearity of the relationship between predictors and the linear predictor, no interactions are assessed and the results are fully interpretable as in a standard logistic regression. On the other hand, random forest is a non-linear non-parametric model, that enable the assessment of higher order interactions between variables at a cost of lower statistical power compared to elastic net model when the relationship is linear [50,176]. Random forest does not provide an interpretable model, but provides a list of the most important variables in predicting the response. The fact that both methods obtained very similar results, provides robustness to our results.

In literature, few AD predictive models using these sophisticated statistical tools can be found [50,177–179], and most of them are based on neuroimaging measures [180]. However, none of them were based on non-invasive determination of lipid peroxidation biomarkers in early AD patients.

The diagnostic indices obtained from both models indicated that the results could constitute a satisfactory screening approach from early AD stages with the consequent

benefits for patients and health public system. In fact, the high sensitivity obtained would allow a reliable identification of high-risk patients in the early stages of AD, and they would be derived to a method with higher specificity to rule out false positives [168]. Nevertheless, further clinical validation using an external cohort of participants would be required in order to obtain a reliable diagnostic model.

Regarding the study limitations, the low number of controls compared to cases would be explained by the difficulty to obtain healthy participants with CSF biomarkers. Also, we did not include participants with other similar dementias, so differential AD diagnosis was not achieved. Further clinical validation work will be developed by including a higher number of controls, as well as patients with similar pathologies. In addition, a follow-up study will be carried out in order to evaluate the variation of these compounds' levels along the time.

4. Conclusion

A set of new lipid peroxidation biomarkers has been determined in urine samples from well-defined participants (early AD, healthy) by means of a previously validated analytical method. So, reliable results have been obtained and used to develop a preliminary early and non-invasive screening model in order to identify potential individuals with high risk of suffering AD, although it could not be considered AD specific. For this, two different regression models (linear, elastic net; non-linear, random forest) were developed, obtaining similar performance in terms of variable selection and accuracy, in spite of being based on different analytical principles, and so providing robustness to the results.

Chapter 2. Plasma lipid peroxidation biomarkers for early and non-invasive Alzheimer Disease detection

1. Summary

The aim of this chapter was to evaluate the capacity of lipid peroxidation compounds from plasma samples to discriminate patients with AD (case group, n=68) from non-AD cases (control group, n=26). First, the analytical method for lipid peroxidation compounds in plasma samples was validated and then plasa from participantes were analysed using a validated analytical method based on UPLC-MS/MS. Statistical studies consisted of an elastic-net-penalized logistic regression adjustment.

2. Results

2.1. Patients' characteristics

Demographic, clinical and CSF biomarker data for both groups are summarized in Table 6. Age and gender showed small differences between groups, so they were included in the predictive model as covariates. As expected, RBANS, CDR, FAQ, Aβ42, t-Tau and p-Tau were clearly different between both groups. C-reactive protein (CRP) was also different, with the AD patients displaying higher values. Depression was similar between both groups.

Table 6. Demographic and clinical characteristics, and biomarkers levels of the participants.

Variable		Case (n=68)	Control (n=26)
Age (years) (median, IQR)		71 (68, 74)	66 (62.25, 71.5)
Gender (female) (n, (%))		39 (57.35%)	9 (34.62%)
Studies levels (%)	**Primary**	31 (45%)	14 (53%)
	Secondary	15 (22%)	5 (20%)
	Academic	22 (33%)	7 (27%)
Alcohol consumption (yes, n (%))		9 (13%)	6 (23%)
Smoking status (n, (%))	**Yes**	10 (15%)	2 (8%)
	Former smoker (more than 10 years)	11 (16%)	8 (31%)
Medications (n, (%))		54 (79%)	18 (69%)
Comorbidiyt (n, (%))	**None**	15 (22%)	8 (31%)
	Dyslipemia	17 (25%)	6 (23%)
	Heart disease	1 (1%)	0 (0%)
	Arterial hypertension	8 (12%)	6 (23%)
	Two or more	23 (34%)	3 (11,5%)
	Others	4 (6%)	3 (11,5%)
Triglycerides (median, IQR)		90 (75.5, 120)	94.5 (83.75, 113.75)
Cholesterol (median, IQR)		195.5 (171.25, 220)	202.5 (193, 237)
CRP (median, IQR)		0 (0, 1.3)	0 (0, 0)
RBANS.DM (median, IQR)		44 (40, 49)	100 (91.25, 105.25)
CDR (median, IQR)		0.5 (0.5,1)	0 (0,0)
FA[c] (median, IQR)		8 (3, 13)	0 (0, 0)
CSF Aβ42 (pg mL^{-1}) (median, IQR)		565 (444.5, 673)	1197 (1150, 1423.5)
CSF t-Tau (pg mL^{-1}) (median, IQR)		543 (386.5, 788.5)	208 (142, 326)
CSF p-Tau (pg mL^{-1}) (median, IQR)		87 (71.5, 108)	52 (41, 68.5)
Temporal atrophy (n, (%))		51 (79.69%)	2 (8%)
Depression (n, (%))		18 (28.57%)	4 (15.38%)

IQR: inter-quartile range; CRP: C-reactive protein; CSF: cerebrospinal fluid; Aβ42: amyloid β 42; t-Tau: total Tau; p-Tau: phosphorylated Tau. RBANS-DM, Repeatable Battery for the Assessment of Neuropsychological Status- Delayed Memory (Standard Score; cut-off point<85). CDR, Clinical Dementia Rating, values: 0, 0.5, 1, 2. FAQ, Functional Activities Questionnaire (Direct Score; cut-off point>9).

2.2. Analytical method validation

The analytical method showed an adequate linearity for all the analytes within the corresponding concentration ranges and coefficients of determination (R^2) ranged between 0.990 and 0.999. It also provided suitable precision, with intra-day and inter-day coefficients of variation of 2–11% (n = 3) and 5–13% (n = 6), respectively (at medium concentration level within the linearity interval). The limits of detection (signal to noise ratio of 3) obtained for each analyte ranged between 0.02 and 2 nmol L^{-1}, and the limits of quantification (signal to noise ratio of 10) were between 0.07 and 8 nmol L^{-1}.

The accuracy of the method was evaluated by analyzing standard solutions and spiked

plasma samples containing the analytes at different concentration levels. In all the cases, the proposed method provided values close to the real concentrations, and matrix effect was considered negligible, with the exemption of 15-keto-15-E_{2t}-IsoP, for which only a semi-quantitative determination was achieved.

2.3. Determination of plasma lipid peroxidation biomarkers and correlation analysis

Regarding plasma levels of lipid peroxidation compounds, some of them (15(*R*)-15-F_{2t}-IsoP, 15-keto-15-E_{2t}-IsoP, 15-keto-15-F_{2t}-IsoP, 15-E_{2t}-IsoP, 4(*RS*)-F_{4t}-NeuroP and *ent*-7(*RS*)−7-F_{2t}-dihomo-IsoP) showed higher levels in AD patients than in healthy controls (control). Figure 8 shows the same results by means of box plots for each analyte, and some analytes showed lower values in the case group than in the control group ($PGF_{2\alpha}$, 5-F_{2t}-IsoP, 7(*RS*)-ST-Δ^8-11-dihomo-IsoF).

Correlation analysis among the plasma lipid peroxidation biomarkers and the CSF biomarkers (Aβ42, t-Tau and p-Tau) was carried out by constructing a correlation network (Figure 9). Red lines represent positive correlations, while blue lines show negative correlations. Besides, the width of the line corresponds to the strength of the correlation. The figure shows an evident association between the CSF biomarkers (t-Tau, p-Tau, Aβ42) and some plasma analytes, such as 15(*R*)-15-F_{2t}-IsoP formed from the AA peroxidation, and *ent*-7(*RS*)-7-F_{2t}-dihomo-IsoP formed from the AA peroxidation. As observed in Figure 8, these two plasma analytes showed higher levels in AD patients than in healthy participants, corroborating their high association with standard AD biomarkers. Other interesting associations were the correlation between *ent*-7(*RS*)-7-F_{2t}-dihomo-IsoP and PGE_2, which belongs to the prostaglandins family and may play an important role in the inflammatory response associated to AD; the correlation between the prostaglandin $PGF_{2\alpha}$, the isoprostane isomer 15-F_{2t}-IsoP that is studied in depth in a variety of biological systems, and 10-*epi*-10- F_{4t}-NeuroP formed from the DHA peroxidation; as well as the correlation between 15-E_{2t}-IsoP and 15-keto-15-F_{2t}-IsoP (Figure 9). Also, some negative correlations were found between the prostaglandin $PGF_{2\alpha}$ and both 17-*epi*-17-F_{2t}-dihomo-IsoP and 4(*RS*)-F_{4t}-NeuroP. However, 14(*RS*)-14-F_{4t}-NeuroP does not show any correlation with the other compounds.

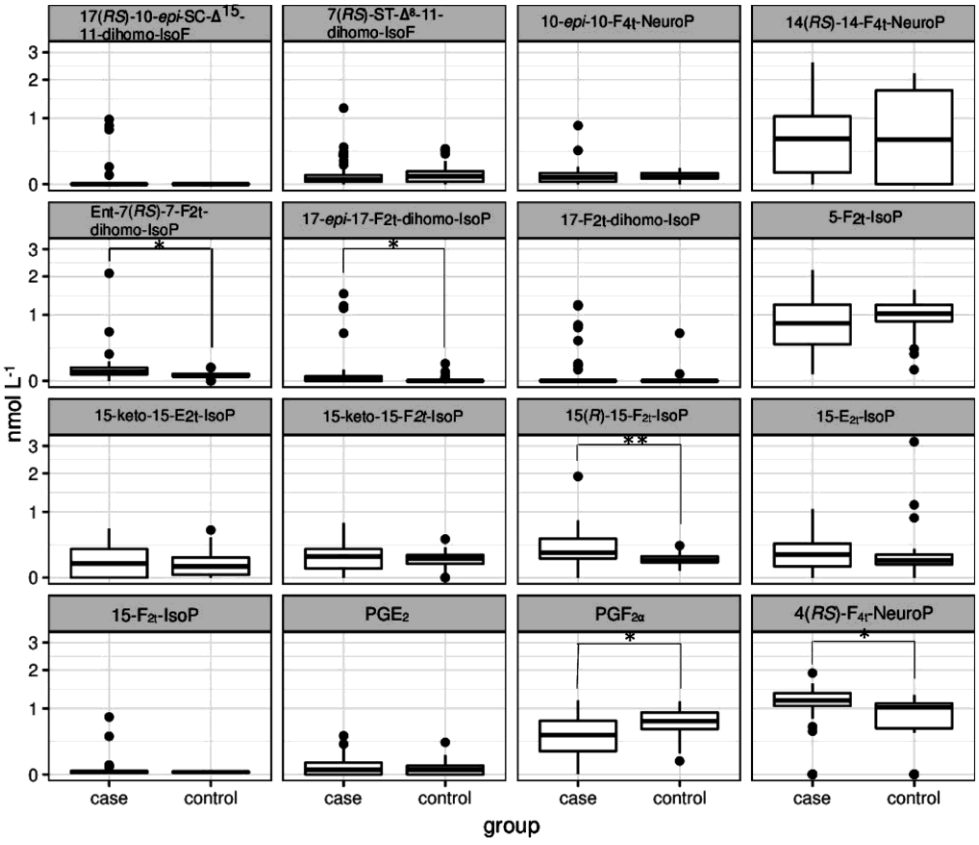

Figure 8. Box plot graphs representing the concentration in plasma samples for each analyte in case and control groups. Boxes represent the 1st and 3rd quartiles, the black lines the median, and whiskers encompass from 1st quartile − 1.5 times the interquartile range to 3rd quartile + 1.5 times the interquartile range (* $p < 0.01$,** $p < 0.001$).

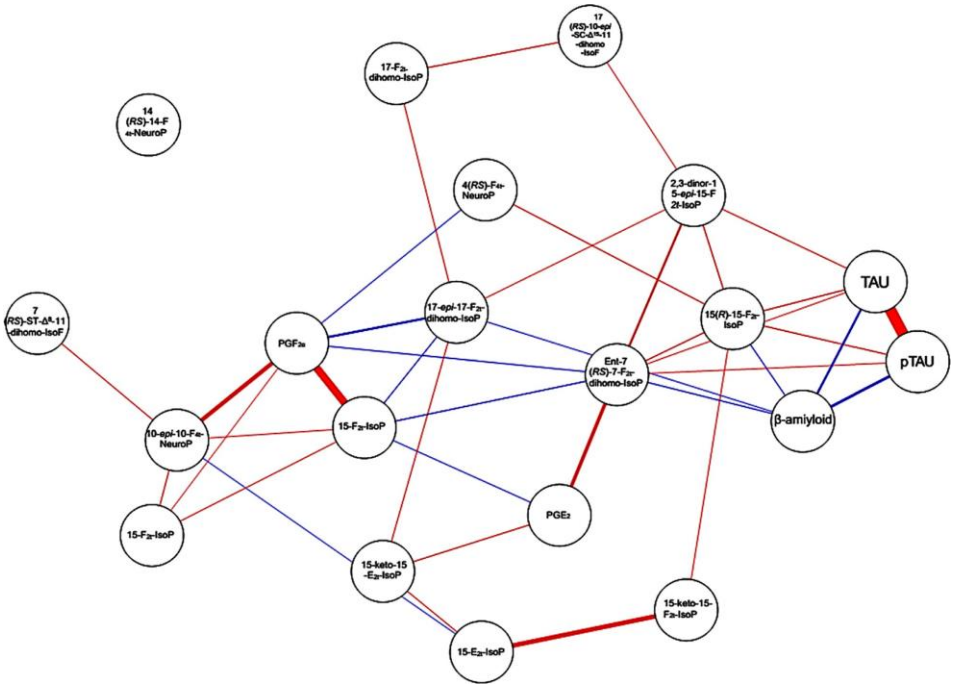

Figure 9. Correlation network for all the lipid peroxidation products in plasma and CSF biomarkers (Aβ42, t-Tau and p-Tau). The width of the line corresponds to the strength of the correlation, red lines represent positive correlations and blue lines represent negative correlations.

2.4. Diagnostic model from plasma lipid peroxidation biomarkers

The elastic-net logistic regression model fitted to the data selected six variables as potential predictors of AD. The model was also forced to include age and gender as covariates. These predictors were combined using the following formula in order to calculate the individual probability of suffering from AD (Pr):

$$\Pr(AD) = \frac{e^{LP}}{1 + e^{LP}}$$

where LP= – 3.55 + 2.23 * 15(*R*)-15-F_{2t}-IsoP – 0.239 * 15-E_{2t}-IsoP –1.424 * $PGF_{2\alpha}$ + 0.5098 * 4(*RS*)-F_{4t}-NeuroP – 0.08 * 14(*RS*)-14-F_{4t}-NeuroP + 0.154 * *Ent*-7(*RS*)-7-F_{2t}-dihomo-IsoP + 0.596 * gender + 0.059 * age

This model achieved an apparent AUC-ROC of 0.883 (95% Confidence Interval, 0.817–0.95, p-value < 0.001) (Figure 10) and a bootstrap-validated AUC- ROC of 0.817. Calibration of the model was also assessed, obtaining very low deviations when comparing the fitted versus the real probabilities, except around the 30–40% mark, where the deviations toped at -10% (Figure 11).

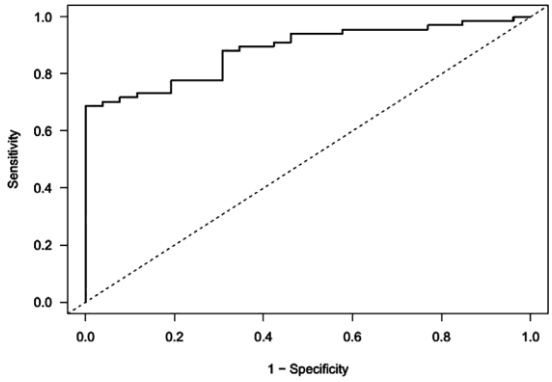

Figure 10. Receiver operating characteristic curve for the diagnostic model. The AUC is 0.883 with a $p < 0.001$.

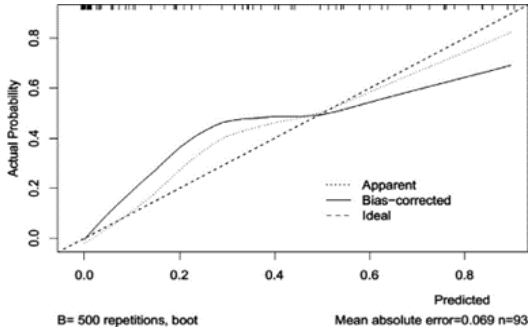

Figure 11. Calibration plot of the model. The dotted line represents an empirical estimation of the in-sample observed probability versus the model-predicted probability. The continuous line represents the bias-corrected estimation of the observed probability versus the predicted probability. The dashed line represents the ideal 1:1 relationship between observed and predicted probabilities.

3. Discussion and conclusion

In this study, we have used a validated analytical method to determine levels of 18 isoprostanoids in plasma from well-defined participants groups (early AD patients and healthy participants). Nowadays, the standard diagnosis criteria employed to classify the participants are based on the review from the NIA-AA [23,24]. However, since it shows some disadvantages, an early and reliable potential diagnosis method has been studied in this work.

The results obtained from the determination of 18 lipid peroxidation biomarkers in plasma samples indicate that higher concentrations of some compounds (15(*R*)-15-F_{2t}-IsoP, 15-keto-15-E_{2t}-IsoP, 15-keto- 15-F_{2t}-IsoP, 15-E_{2t}-IsoP, 4(*RS*)-F_{4t}-NeuroP, *ent*-7(*RS*)-7-F_{2t}-dihomo- IsoP) were found in early AD patients than in healthy participants. This finding corroborates the results obtained by Şirin et al. in which plasma levels of 15-F_{2t}-IsoP were higher in AD than in healthy individuals [181]. As regards the descriptive correlation analysis among plasma and CSF biomarkers, we considered that a correlation with an absolute value ≥ 0.3 may be relevant in the lipid peroxidation associated to early AD. Although it is not possible to explain the implications of all these correlations, some of these metabolites' levels were altered in MCI-AD. Of note, 15(*R*)-15-F_{2t}-IsoP and *ent*-7(*RS*)-7-F_{2t}-dihomo IsoP in plasma showed positive correlation with t-Tau and p-Tau in CSF, and negative correlation with Aβ42 in CSF. In this sense, a potential relationship between lipid peroxidation and the protein biology in brain was observed, confirming previous studies [182]. Actually, in a previous study it was found that the insert of Aβ aggregates into the lipid bilayer in cellular membrane, may lead to the formation of lipid peroxidation compounds [167]. On the other hand, some compounds in plasma were highly correlated, such as, $PGF_{2\alpha}$ and 15-F_{2t}-isoP, as well as $PGF_{2\alpha}$ and 10-*epi*-10-F_{4t}-NeuroP, and finally PGE_2 and *ent*-7(*RS*)-7-F_{2t}-dihomo-IsoP, indicating the presence of both enzymatic and non-enzymatic lipid oxidation since early AD, as well as inflammatory response also observed in previous studies [183,184]. Moreover, an important inverse relationship was observed between $PGF_{2\alpha}$ and 17-*epi*- 17-F_{2t}-dihomoIsoP.

From these preliminary results, we elaborated a regression model showing good diagnostic accuracy from the biomarkers 15(*R*)-15-F_{2t}- IsoP, 15-E_{2t}-IsoP, $PGF_{2\alpha}$,

4(*RS*)-F_{4t}-NeuroP, 14(*RS*)-14-F_{4t}-NeuroP and *ent*-7(*RS*)-7-F_{2t}-dihomo-IsoP. Although these biomarkers are not able to discriminate between both groups when considered alone, they improve their discriminative ability when they are included in the diagnostic model with age and gender as covariates. Developing reliable diagnostic models in small data sets is difficult because the issue of overfitting is especially prominent in these cases. Common methods employed in medical literature include univariate screening, stepwise variable selection and, most recently, shrinkage or regularization methods such as lasso or elastic net. Of these, only regularization methods are able to produce stable estimates of the predictors and achieve good generalization of its predictive capacity [145]. In this study we used an elastic net penalized logistic regression model for AD diagnosis. Elastic net is a generalization of lasso and improves its prediction accuracy as it allows to deal with multicollinearity (high correlations between the different covariates) which was a property of our dataset. Our model achieved a promising validated AUC of 0.82 and has the advantage of providing an equation that can be used to obtain individualized estimates for each patient. The possibility to estimate the probability of AD opens the door to personalized decision making in the handling of potential AD patients. This would leave the use of CSF biomarkers, the gold standard for diagnosis, only for cases considered as high risk by our model.

Although the diagnostic accuracy of this model was not superior to the employment of CSF biomarkers this model has the advantage of being based on non-invasive sampling.

In literature, we can find some AD diagnosis models developed using different biomarkers. For instance, Nazeri et al. showed that different plasma proteins (interleukin-16, thyroxine-binding globulin, peptide tyrosine tyrosine, apolipoprotein E, eselectin, matrix metallopeptidase (10)) could be used to achieve the diagnosis and follow-up of the AD quite accurately against neuroimaging techniques, but these proteins are required to be clinically validated as possible AD indicators [185]. In addition, Marmarelis et al. proposed a diagnostic model based on cerebral hemodynamics through measures of pressure changes and cerebral CO_2 vasomotor reactivity, but the specificity of this diagnosis has not been assessed and the number of participants is low [186]. Another model was based on the determination of CSF biomarkers by means of capillary

electrophoresis coupled to mass spectrometry [187]. Also, a diagnostic model based on image techniques was described by Liao et al., in which age could explain some metabolic alterations, but the imaging techniques involve high economic costs [188].

4. Conslusion

To conclude, a satisfactory AD diagnostic model has been obtained from plasma lipid peroxidation biomarkers, indicating the individual probability of suffering from AD. To our knowledge, this is the first study evaluating the AD diagnostic accuracy of lipid peroxidation compounds in plasma from well-defined participants groups and using a validated analytical method. This is an important contribution in the study of an early and non-invasive AD diagnosis. In addition, the results from this work are relevant in the evaluation of OS as a molecular mechanism between amyloid deposition and neurodegeneration in AD. Prospective clinical validation of this potential diagnostic model will be carried out using an external group of patients.

Chapter 3. Assessment of lipid peroxidation and artificial neural network models in early Alzheimer Disease diagnosis

1. Summary

The aim of this chapter was to evaluate the capacity of lipid peroxidation biomarkers from plasma and urine samples to discriminate between MCI-AD and healthy control groups participants with different statistical strategies. For this, lipid peroxidation compounds were determined in urine and plasma samples from patients diagnosed with early Alzheimer Disease (n=70) and controls (n=26) by means of UPLC-MS/MS. The obtained results were analysed by means of different statistical models (PLS, SVM, ANN) to evaluate the diagnostic capacity for sample type.

2. Results

2.1. Demographic, clinical and analytical variables

The demographic and clinical variables for each group of participants are described in Table 7. All of them showed a non-normal distribution, so medians were compared between groups by means of Mann Whitney test for numerical variables, and Chi-square and Fisher exact tests for categorical variables. The clinical variables (RBANS, CDR, FAQ, MMSE), cerebrospinal fluid (CSF) Aβ42, CSF t-Tau and CSF p-Tau) showed statistically significant differences between MCI-AD and healthy control groups. On the other hand, demographic variables did not present statistically significant differences between both groups except of gender and age, so these variables were taken into account in the subsequent analyses.

The concentrations obtained for each analytical variable (22 analytes) in both matrices (urine, plasma) are summarized in Table 8. As we can see, statistically significant differences between groups were obtained for 17-*epi*-17-F_{2t}-dihomo-IsoP in urine samples, and for 15(*R*)-15-F_{2t}-IsoP, $PGF_{2\alpha}$, 4(*RS*)-4-F_{4t}-NeuroP, *ent*-7(*RS*)-7-F_{2t}-dihomo-IsoP, 17-*epi*-17-F_{2t}-dihomo-IsoP, isoprostanes, isofurans, neuroprostanes and neurofurans in plasma samples.

Table 7. Demographic and clinical variables of the studied population.

Variable		MCI-AD (n=70)	Healthy control (n=26)	P-value
Gender (Female, n (%))		41 (58.6%)	9 (34.6%)	0.037*
Age (Median, (IQR))		70 (68-74)	66 (62-70)	0.044*
Depression (Yes, n (%))		9 (13%)	5 (19%)	0.566
Anxiety (Yes, n (%))		6 (9%)	2 (8%)	0.629
Studies levels (n (%))	Primary	28 (40%)	16 (61%)	0.173
	Secondary	20 (29%)	3 (12%)	
	Academic	22 (31%)	7 (27%)	
Smoking status (smoker or former smoker) (n (%))		50 (71%)	13 (50%)	0.124
Alcohol consumption (yes, n (%))		12 (17%)	2 (8%)	0.307
Medications (n, (%))	None	15 (22%)	8 (31%)	0.269
	psychotropic drugs	3 (4%)	2 (8%)	
	Antihypertensive	10 (14%)	7 (27%)	
	Statins	12 (17%)	3 (11%)	
	Two or more	30(43%)	6 (23%)	
Comorbidity (n, (%))	None	18 (26%)	10 (39%)	0.071
	Dyslipemia	18 (26%)	3 (11%)	
	Hypertension	10 (14%)	7 (27%)	
	Heart disease	0 (0%)	1 (4%)	
	Two or more	24 (34%)	5 (19%)	
RBANS-DM		42 (40-49)	100 (90-106)	0.000*
CDR		0.5 (0.5-1)	0 (0-0)	0.000*
FAQ		7 (2-13)	0 (0-0)	0.000*
MMSE		25 (19-29)	24 (21-27)	0.000*
CSF Aβ42 (pg mL^{-1})		597 (445-687)	1186 (1033-1403)	0.000*
CSF t-Tau (pg mL^{-1})		572 (396-857)	202 (139-320)	0.000*
CSF p-Tau (pg mL^{-1})		88 (72-111)	49 (35-67)	0.000*

IQR: Interquartile range. Data were expressed as median (interquartile range (IQR)) for non-parametric continuous variables, and number of cases (percentages) for categorical cases. The statistical calculations to compare between the two groups employed Mann-Whitney test, Chi-Square test and Fisher exact test, respectively; RBANS-DM, Repeatable Battery for the Assessment of Neuropsychological Status- Delayed Memory (Standard Score; cut-off point < 85); CDR, Clinical Dementia Rating, values: 0, 0.5, 1, 2; FAQ, Functional Activities Questionnaire (Direct Score; cut-off point > 9); MMSE, Minimental State Examination; CSF, Cerebrospinal fluid; Aβ42: amyloid β 42; t-Tau, total-Tau; p-Tau, phosphorylated-Tau; * $p < .05$.

Table 8. Concentrations determined by UPLC-MS/MS for each analyte in plasma and urine samples from MCI-AD and healthy control participants.

Analyte	**Plasma (nmol L^{-1})**							**Urine (ng mg creatinine $^{-1}$)**						
	MCI-AD (n= 70)			**Healthy control (n= 26)**			**P-value**	**MCI-AD (n= 70)**			**Healthy control (n= 26)**			**P-value**
	Median	quartile		Median	quartile			Median	quartile		Median	quartile		
		1st	3rd		1st	3rd			1st	3rd		1st	3rd	
15(*R*)-15-F_{2t}-IsoP	0.30	0.23	0.46	0.20	0.15	0.26	0.000*	0.69	0.47	1.42	0.71	0.49	1.00	0.830
PGE_2	0.05	0.00	0.13	0.05	0.00	0.10	0.520	1.93	0.43	3.48	1.85	0.92	4.62	0.615
2,3-dinor-15-*epi*-15-F_{2t}-IsoP	0.00	0.00	0.03	0.00	0.00	0.00	0.067	0.73	0.49	1.22	0.65	0.47	1.12	0.458
15-keto-15-E_{2t}-IsoP	0.15	0.00	0.35	0.13	0.04	0.27	0.874	0.92	0.51	1.46	0.88	0.52	1.65	0.644
15-keto-15-F_{2t}-IsoP	0.23	0.09	0.35	0.23	0.14	0.28	0.599	0.79	0.16	1.85	1.52	0.60	2.20	0.094
15-E_{2t}-IsoP	0.26	0.12	0.43	0.19	0.09	0.28	0.320	0.18	0.05	1.29	0.19	0.06	0.76	0.830
5-F_{2t}-IsoP	0.78	0.40	1.26	0.99	0.73	1.23	0.362	2.66	1.61	4.85	2.70	1.77	3.85	0.817
15-F_{2t}-IsoP	0.02	0.01	0.04	0.02	0.02	0.03	0.638	0.01	0.00	0.02	0.01	0.00	0.02	0.113
$PGF_{2\alpha}$	0.51	0.24	0.76	0.74	0.48	0.94	0.008*	3.67	2.69	7.90	2.98	2.34	4.98	0.295
4(*RS*)-4-F_{4t}-NeuroP	1.14	0.96	1.33	1.03	0.00	1.13	0.003*	0.91	0.67	1.40	0.72	0.50	1.05	0.051
1a,1b-dihomo-$PGF_{2\alpha}$	0.00	0.00	0.00	0.00	0.00	0.00	0.784	1.26	0.61	2.35	1.63	1.01	2.32	0.232
10-*epi*-10-F_{4t}-NeuroP	0.08	0.03	0.15	0.09	0.03	0.14	0.731	0.03	0.00	0.06	0.01	0.00	0.04	0.094
14(*RS*)-14-F_{4t}-NeuroP	0.53	0.06	1.03	0.60	0.00	1.74	0.671	1.22	0.76	2.38	1.37	0.78	1.98	0.837
***ent*-7(*RS*)-7-F_{2t}-dihomo-IsoP**	0.10	0.05	0.15	0.05	0.04	0.08	0.002*	0.32	0.13	0.60	0.29	0.21	0.39	1.000
17-F_{2t}-dihomo-IsoP	0.00	0.00	0.00	0.00	0.00	0.00	0.555	0.08	0.00	0.36	0.10	0.00	0.23	0.625

17-*epi*-17-F_{2t}-dihomo-IsoP	0.03	0.00	0.05	0.00	0.00	0.01	0.015*	0.01	0.00	0.06	0.00	0.00	0.00	0.019*
17(*RS*)-10-*epi*-SC-Δ^{15}-11-dihomo-IsoF	0.00	0.00	0.00	0.00	0.00	0.00	0.164	0.03	0.00	0.11	0.05	0.02	0.08	0.330
7(*RS*)-*ST*-Δ^{8}-11-dihomo-IsoF	0.04	0.03	0.08	0.09	0.02	0.16	0.067	0.00	0.00	0.02	0.00	0.00	0.03	0.849
Neurofurans[a]	0.09	-0.05	0.17	-0.10	-0.15	0.07	0.000*	3.13	1.76	6.62	4.15	2.51	5.95	0.356
Isofurans[a]	0.09	0.07	0.12	0.07	0.06	0.09	0.013*	4.36	2.53	7.25	4.29	3.37	9.64	0.343
Neuroprostanes[a]	-0.22	-0.70	0.19	-0.65	-0.76	-0.48	0.010*	3.52	2.25	4.97	3.77	2.02	6.17	0.650
Isoprostanes[a]	0.30	0.22	0.39	0.20	0.17	0.27	0.000*	6.20	3.82	12.37	7.30	4.67	11.45	0.49

* $p < 0.05$.

[a], Total parameters results expressed as intensity of signal units in plasma and as signal units mg^{-1} creatinine in urine.

2.2. Multivariate statistical models

In this work we developed different multivariate models in order to improve the diagnostic utility of lipid peroxidation products from plasma and urine samples [141,168], since they do not have a high diagnostic capacity individually. For this, different multivariate models based on linear and non-linear regression were developed for each kind of biological sample and they were compared in terms of diagnostic performance.

(a) (b)

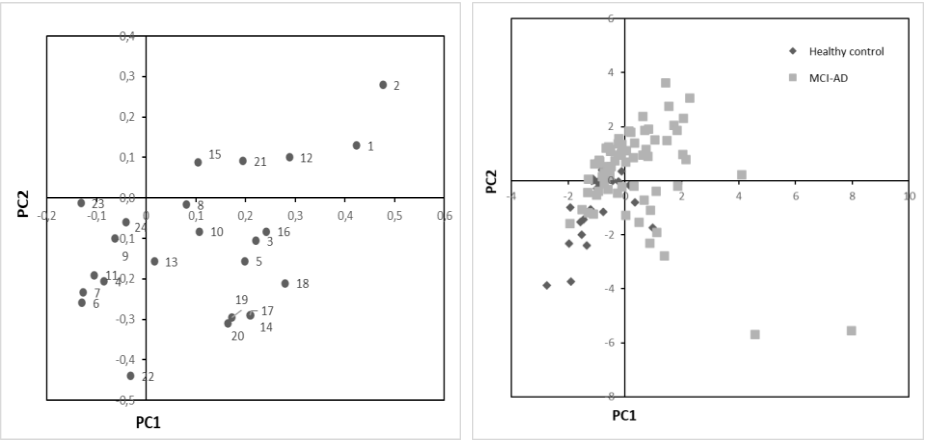

Figure 12. Plots representing results of the partial least squares regression model in urine samples. (a) Loadings plot. 1: Gender; 2: Age; 3: 15(*R*)-15-F_{2t}-IsoP; 4: PGE_2; 5: 2,3-dinor-15-*epi*-15-F_{2t}-IsoP; 6: 15-keto-15-E_{2t}-IsoP; 7: 15-keto-15-F_{2t}-IsoP; 8: 15-E_{2t}-IsoP; 9: 5-F_{2t}-IsoP; 10: 15-F_{2t}-IsoP; 11: $PGF_{2\alpha}$; 12: 4(*RS*)-F_{4t}-NeuroP; 13: 1a,1b-dihomo-$PGF_{2\alpha}$; 14: 10-*epi*-10-F_{4t}-NeuroP; 15: 14(*RS*)-14-F_{4t}-NeuroP; 16: *ent*-7(*RS*)-7-F_{2t}-dihomo-IsoP; 17: 17-F_{2t}-dihomo-IsoP; 18: 17-*epi*-17-F_{2t}-dihomo-IsoP; 19: 17(*RS*)-10-*epi*-SC-Δ^{15}-11-dihomo-IsoF; 20: 7(*RS*)-ST-Δ^{8}-11-dihomo-IsoF; 21: neurofurans; 22: isofurans; 23: neuroprostanes; 24: isoprostanes. (b) Scores plot.

First, PLS linear regression models were developed. For PLS in urine, in Figure 12 we can see that the MCI-AD group showed higher levels for the compounds 15(*R*)-15-F_{2t}-IsoP, 2,3-dinor-15-*epi*-15-F_{2t}-IsoP, 4(*RS*)-4-F_{4t}-NeuroP, *ent*-7(*RS*)-7-F_{2t}-dihomo-IsoP, 17-*epi*-17-F_{2t}-dihomo-IsoP, 10-*epi*-10-F_{4t}-NeuroP, 17-F_{2t}-dihomo-IsoP and neurofurans, as well as higher age and female proportion (Figure 12a). However, the healthy

participants are grouped on the left side of the score plot (Figure 12b) because they showed lower levels for the previous compounds. Similarly, for PLS in plasma, in Figure 13 we can see that the MCI-AD group showed higher levels for the compounds 15(*R*)-15-F_{2t}-IsoP, 4(*RS*)-4-F_{4t}-NeuroP, neuroprostanes, isoprostanes, *ent*-7(*RS*)-7-F_{2t}-dihomo-IsoP, neurofurans and isofurans, as well as higher age and female proportion (Figure 13a). However, the healthy individuals are grouped in the left side of the score plot (Figure 13b) due to their lower levels for the previous compounds.

(a) (b)

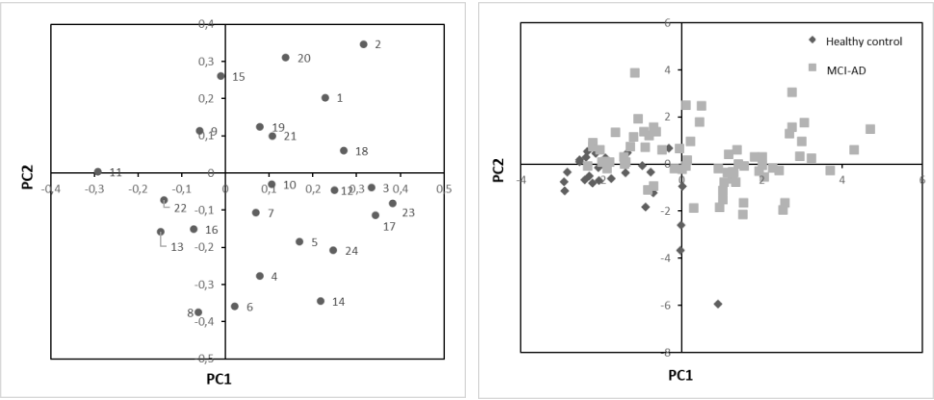

Figure 13. Plots representing results of the partial least squares regression model in plasma samples. (a) Loadings plot. 1: Gender; 2: Age; 3: 15(*R*)-15-F_{2t}-IsoP; 4: PGE_2; 5: 2,3-dinor-15-*epi*-15-F_{2t}-IsoP; 6: 15-keto-15-E_{2t}-IsoP; 7: 15-keto-15-F_{2t}- IsoP; 8: 15-E_{2t}-IsoP; 9: 5-F_{2t}-IsoP; 10: 15-F_{2t}-IsoP; 11: $PGF_{2\alpha}$; 12: 4(*RS*)-4-F_{4t}-NeuroP; 13: 1a,1b-dihomo-$PGF_{2\alpha}$; 14: neuroprostanes; 15: 10-*epi*-10-F_{4t}-NeuroP; 16: 14(*RS*)-14-F_{4t}-NeuroP; 17: isoprostanes; 18: *ent*-7(*RS*)-7-F_{2t}-dihomo-IsoP; 19: 17-F_{2t}-dihomo-IsoP; 20: 17-*epi*-17-F_{2t}-dihomo-IsoP; 21: 17(*RS*)-10-*epi*-SC-Δ^{15}-11-dihomo-IsoF; 22: 7(*RS*)-ST-Δ^{8}-11-dihomo-IsoF; 23: neurofurans; 24: isofurans. (b) Scores plot.

Secondly, SVM models with radial and polynomial kernel functions were developed from results in plasma and urine samples. Non-linear functions were used in order to obtain a better classification of the participants.

Thirdly, non-linear regression models based on ANN were developed for urine and plasma samples in order to classify the two groups of participants. As shown in Figure 14, 22 analytes, gender and age were included in the input layer. For the hidden and output

layers, the transfer functions were hyperbolic tangent and normalized exponential functions, respectively.

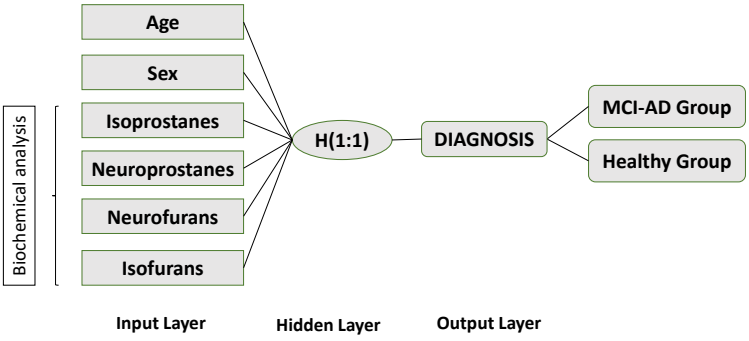

Figure 14. General structure of the developed neural network for the prediction of early AD consisting of 24 input variables, 1 hidden layer with 1 node, and 1 output variable.

2.3. Diagnostic performance for the statistical multivariate developed models

The diagnostic performance of each model was estimated from the corresponding ROC curves (Figure 15). In urine samples, the ANN model provided an AUC of 0.839 (CI 95%, 0.746–0.933), while for the PLS model it was 0.653 (CI 95%, 0.526–0.780), and for the SVM models it was 0.644 (CI 95%, 0.539–0.749) with the polynomial function and 0.659 (CI 95%, 0.558–0.759) with the radial function. Similarly, in plasma samples, the ANN model provided an AUC of 0.882 (CI 95%, 0.814–0.949), while for PLS it was 0.765 (CI 95%, 0.633–0.868), and for SVM models it was 0.817 (CI 95%, 0.712–0.922) with the polynomial function and 0.827 (CI 95%, 0.739–0.915) with the radial function. Therefore, ANN models provided better diagnostic accuracy than PLS and SVM models in both matrices. Moreover, plasma matrix showed higher diagnostic accuracy than urine.

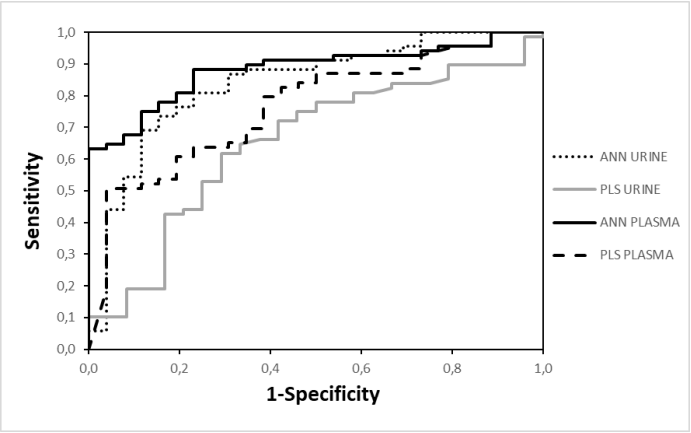

Figure 15. Receiver operating Characteristic curves for PLS and ANN models in plasma and urine samples.

From the estimated optimal cut-off values, the diagnostic indices in the prediction of early AD were calculated for each developed model in plasma and urine samples (Table 9). For urine, the ANN model provided a sensitivity of 80.9%, while its specificity was 76.9%. In addition, DOR value for ANN model in urine revealed that there was strong association between the model results and the AD occurrence. Regarding the ANN model in plasma samples, it provided a sensitivity of 88.2%, while its specificity was 76.9%. This model also showed an elevated DOR value that supported its diagnostic value. DOR values were quite similar among plasma models, but ANN model showed better accuracy (AUC- ROC 0.882) than PLS (AUC-ROC 0.765) and SVM (AUC-ROC 0.827).

Moreover, ANN model showed better sensitivity and a satisfactory balance between sensitivity and specificity. ANN model showed better balance, obtaining a higher number of participants correctly classified. By contrast, PLS model showed high specificity but low sensitivity, classifying the AD participants as healthy subjects; while SVM model showed high sensitivity but low specificity, classifying the healthy subjects as AD patients. In general, for both matrices, the PLS model was the most specific, the SVM model was the most sensitive, and the ANN model showed the best balance of sensitivity/specificity.

Table 9. Diagnostic indices for each developed statistical model in the prediction of MCI-AD from lipid peroxidation compounds determined in urine and plasma samples.

	Urine				**Plasma**			
	PLS	**ANN**	**SVM**		**PLS**	**ANN**	**SVM**	
			Radial	**Polynomial**			**Radial**	**Polynomial**
AUC (CI 95%)	0.653 (0.526-0.780)	0.839 (0.746-0.933)	0.659 (0.558-0.759)	0.644 (0.539-0.749)	0.765 (0.663-0.868)	0.882 (0.814-0.949)	0.827 (0.739-0.915)	0.817 (0.712-0.922)
Sensitivity (%, CI 95%)	63.2 (51.4-73.7)	80.9 (70.0-88.5)	92.9 (68.5-98.7)	92.3 (66.7-98.6)	50.7 (39.2-62.2)	88.2 (78.5-93.9)	92.3 (66.7-98.6)	100.0 (77.2-100)
Specificity (%, CI 95%)	70.8 (50.8-85.1)	76.9 (57.9-89.0)	11.1 (2.0-43.5)	37.5 (13.7-69.4)	96.2 (81.1-99.3)	76.9 (57.9-89.0)	50.0 (21.5-78.5)	25.0 (7.1-59.1)
LR+ (CI 95%)	2.17 (1.13-4.15)	3.50 (1.72-7.14)	1.04 (0.80-1.37)	1.48 (0.84-2.58)	13.19 (1.90-91.40)	3.82 (1.89-7.75)	1.85 (0.91-3.76)	1.33 (0.89-1.99)
LR- (CI 95%)	0.52 (0.36-0.74)	0.25 (0.15-0.41)	0.64 (0.07-6.06)	0.21 (0.03-1.49)	0.51 (0.40-0.66)	0.15 (0.08-0.30)	0.15 (0.02-1.08)	-
DOR (CI 95%)	4.18 (1.52-11.46)	14.10 (4.72-42.13)	1.63 (0.09-29.78)	7.20 (0.60-87.02)	25.74 (3.30-200.67)	25.00 (7.73-80.81)	12.0 (1.02-141.34)	-

PLS, partial least squares; ANN, artificial neural network; SVM, support vector machine; AUC, area under the curve; LR+, positive likelihood ratio; LR-, negative likelihood ratio; CI, confidence interval; DOR, diagnostic odds ratio.

3. Discussion

Some of the analytes studied in this work showed statistically significant differences, such as 17-*epi*-17-F_{2t}-dihomo-IsoP in urine samples, and 15(*R*)-15-F_{2t}-IsoP, $PGF_{2\alpha}$, 4(*RS*)-4-F_{4t}-NeuroP, *ent*-7(*RS*)-7-F_{2t}- dihomo-IsoP, 17-*epi*-17-F_{2t}-dihomo-IsoP, isoprostanes, isofurans, neuroprostanes and neurofurans in plasma samples. Nevertheless, each analyte individually did not provide a reliable AD diagnosis. In contrast, a multivariate model based on ANN showed better accuracy than PLS and SVM models, and analytes from plasma samples were more useful than those in urine samples to achieve a reliable AD diagnosis.

Some studies found lipid peroxidation products as biomarkers for AD diagnosis, and most of them were based on individual biomarkers, such as lipid peroxidation end products [189] or TBARS [170]. However, multivariate models could reflect the OS status of patients better, showing superior diagnostic indices and higher accuracy. Specifically, a previous work developed an ANN model based on different AD risk factors studied the predictive value of these factors [190]. It showed high capacity to integrate different data and achieve a general evaluation. Other developed ANN models to diagnose AD or MCI were based on image, genetics, neuropsychology or other biomarkers [191,192], but the present study is the first one using lipid peroxidation compounds as biomarkers. In general, previous studies based on ANN showed model accuracies around 90%, similar to our results. Also, PLS models have been developed for AD diagnosis. They were mainly based on gene expression and neuroimaging [193–195], but none of them was based on our set of lipid peroxidation products. In addition, a previous study for MCI diagnosis compared PLS model to other statistical tests, such as Random Forest showing the higher PLS diagnostic power [196]. The diagnostic indices obtained for each model in the present study indicated that the ANN model in both matrices showed a satisfactory accuracy (> 80%). In addition, the plasma ANN model showed, in general, better diagnostic indices than the urine model, corroborating previous studies in the literature [197,198]. Specifically, the ANN model based on the plasma levels of lipid peroxidation products showed high DOR value, sensitivity, and accuracy, as well as, satisfactory specificity, so it is considered a reliable diagnostic model. In this sense, Quintana et al. also found that ANN models

showed better discriminant capacity than linear models in AD diagnosis [199]. AD is a complex disease process, in which multiple factors are involved and that could be the reason why non-linear regression models showed a better predictive capacity than those models based on linear regression [190].

Regarding the biological matrix, the proposed ANN diagnostic model in plasma samples constitutes a promising minimally invasive approach that could avoid, in some cases, the current diagnostic methods, which involve invasive sampling and expensive techniques [200]. In this sense, the ANN models have a satisfactory diagnostic capacity, and they are able to classify the participants into healthy and MCI-AD, with high accuracy in both matrices as an early screening tool.

4. Conclusion

The non-linear regression model based on ANN explained the non-linear relationship between the levels of lipid peroxidation compounds and the diagnosis of a complex pathophysiological process, such as AD, constituting a promising screening approach. Specifically, the developed ANN model in plasma samples showed high accuracy and suitable diagnostic indices in early AD prediction. Nevertheless, further research will need to be carried out to clinically validate this diagnostic model. This approach constitutes a significant advance in early AD diagnosis, using minimally invasive sampling techniques, and offers important economic cost reduction for the public health system.

Chapter 4. Isoprostanoids levels in cerebrospinal fluid do not reflect Alzheimer's Disease

1. Summary

The aim of this chapter was to evaluate the capacity of lipid peroxidation biomarkers in CSF to reflect neurodegeneration and neuropsychological status and to establish a correlation between CSF and plasma lipid peroxidation biomarker levels in order to evaluate the latter as minimally invasive diagnosis biomarkers. For this, there were analysed plasma and CSF samples from AD and non-AD (including other neurological pathologies) participants, by means of an analytical method based on UPLC-MS/MS. Then correlations between biological matrices (plasma and CSF) and between CSF lipid biomarkers and CSF standard AD biomarkers and neuropsychological tests.

2. Results

2.1. Participants' characteristics

The clinical and demographic characteristics of the population are summarized in Table 10. There were no differences between groups for age and gender. By contrast, CSF biomarkers (Aβ, t-Tau and p-Tau) showed statistically significant differences between participant groups as was expected. The CSF Aβ levels were lower in the AD than in the non-AD patients. It could be explained by the aggregation of Aβ in the brain, hindering its transport to the CSF [201]. Similarly, the neuropsychological status (RBANS, MMSE, FAQ) showed differences between the groups while CDR did not show differences.

Table 10. Demographic and clinical variables of the study participants.

Variables	Non-AD (n = 34)$^{\$}$	AD (n = 42)	p-Value (Mann-Whitney)
Age (years) Median (IQR)	66 (63, 72)	70 (68, 73)	0.102
Gender (Female) (n, %))	17 (50%)	28 (67%)	0.142
CSF Aβ42 (pg Ml^{-1}) Median (IQR)	1236.50 (950, 1435)	630 (535, 735)	0.000*
CSF t-Tau (pg Ml^{-1}) Median (IQR)	230 (159, 347)	573 (436, 1005)	0.000*
CSF p-Tau (pg Ml^{-1}) Median (IQR)	47 (32, 61)	86 (71, 122)	0.000*
CDR Median (IQR)	0.5 (0, 0.5)	0.5 (0.5, 1)	0.071
MMSE Median (IQR)	27 (21, 28)	24 (18, 25)	0.004*
RBANS.IM Median (IQR)	73 (69, 90)	57 (40, 67)	0.000*
RBANS.V/C Median (IQR)	87 (75, 100)	75 (57, 87)	0.016*
RBANS.L Median (IQR)	85 (60, 92)	60 (51, 82)	0.031*
RBANS.A Median (IQR)	79 (60, 88)	60 (49, 79)	0.004*
RBANS.DM Median (IQR)	68 (56, 88)	40 (40, 53)	0.000*
FAQ Median (IQR)	3 (0, 8)	7 (3, 13)	0.015*

* $p < 0.05$; IQR: inter-quartile range; RBANS.IM: Repeatable Battery for the Assessment of Neuropsychological Status–Immediate Memory; RBANS.V/C: RBANS-Visuospatial/Constructional; RBANS.L: RBANS-Language; RBANS.A: RBANS-Attention; RBANS.DM: RBANS-Delayed Memory; CDR: Clinical Dementia Rating values; FAQ: Functional Activities Questionnaire;CSF: cerebrospinal fluid. $^{\$}$The non-AD group is composed of healthy controls (n = 4) and other dementias and cognitive impairments not caused by AD (n = 30).

2.2. Correlation between CSF isoprostanoids and standard CSF biomarkers

We analyzed possible correlations between the different isoprostanoids families (isoprostanes, neuroprotanes, dihomo-isoprostanes), and CSF AD-specific biomarkers (Aβ, t-Tau, p-Tau) in order to establish a possible relationship between OS (brain grey and white matter damage) and amyloid pathology. Table 11 shows that Aβ correlates negatively with 7(*RS*)-ST-Δ^8-11-dihomo-IsoF, 5-F_{2t}-IsoP, total neurofurans and isofurans. In addition, p-Tau showed negative correlation with PGE_2.

2.3. Correlations between CSF isoprostanoids and neuropsychological evaluation

Regarding correlations between the isoprostanoids biomarkers and neuropsychological evaluation of the participants, Table 11 shows that RBANS and especially its visuospatial/constructional domain showed correlations with 15-F_{2t}-IsoP, Ent-7(*RS*)-F_{2t}-dihomo-IsoP and 15-keto-15-F_{2t}-IsoP. The latter also showed correlation with the RBANS attention domain and with MMSE. Moreover, 15-keto-15-E_{2t}-IsoP correlated with FAQ and CDR scores.

2.4. CSF and plasma lipid peroxidation biomarkers

A previous study described a diagnosis model for early AD based on the quantification of these isoprostanoid compounds in plasma samples. In the present study it was evaluated if these plasma levels reflected brain damage by means of the determination of the corresponding levels in CSF samples. In this sense, only 17(*RS*)-10-epi-SC-Δ^{15}-11-dihomo-IsoF showed correlation between both matrices (PCC = 0.248, p = 0.031). In addition, when we analysed the results separately for AD and non-AD groups, we found that the non-AD group showed correlations between the two matrices for 15®-15-F_{2t}-IsoP (PCC = 0.388, p = 0.024), 15-keto-15-F_{2t}-IsoP (PCC = 0.360, p = 0.037) and 5-F_{2t}-IsoP (PCC = 0.345, p = 0.046). However, these analytes did not show correlation between plasma and CSF samples in AD patients. In this AD group, 17-F_{2t}-dihomo-IsoP (PCC = 0.399, p = 0.009) and 17(*RS*)-10-epi-SC-Δ^{15}-11-dihomo-IsoF (PCC = 0.345, p = 0.045) showed correlation between CSF and plasma samples.

Table 12 shows the plasma levels of isoprostanoids biomarkers. Some metabolites showed statistically significant differences between the groups for 15®-15-F_{2t}-IsoP (p < 0.001), 2,3-dinor-15-*epi*- 15-F_{2t}-IsoP (p = 0.028), 5-F_{2t}-IsoP (p = 0.021), 15-F_{2t}-IsoP (p < 0.001), $PGF_{2\alpha}$ (p = 0.011), neuroprostanes (p = 0.029), 10-*epi*-10-F_{4t}-NeuroP (p < 0.001), isoprostanes (p < 0.001), Ent-7(*RS*)-7-F_{2t}-dihomo-IsoP(p < 0.001), and 17-*epi*-17-F_{2t}-dihomo-IsoP (p < 0.001). However, none of the CSF compounds showed statistically significant differences between the AD and non-AD groups.

Table 11. Correlations between CSF isoprostanoids and clinical variables (standard CSF biomarkers, neuropsychological evaluation).

		CSF Aβ42	CSF t-Tau	CSF p-Tau	CDR	MMSE	RBANS.IM	RBANS.VC	RBANS.L	RBANS.A	RBANS.DM	FAQ
15®-15-F_{2t}-IsoP	**PCC**	-0.196	-0.094	-0.032	-0.038	0.159	-0.030	0.124	-0.031	0.147	-0.022	-0.076
	P value	0.089	0.419	0.783	0.770	0.226	0.818	0.344	0.811	0.262	0.865	0.564
PGE_2	**PCC**	0.013	-0.205	-0.267	-0.031	0.095	0.136	0.043	0.219	0.106	0.061	-0.044
	P value	0.908	0.076	0.020*	0.814	0.471	0.298	0.743	0.092	0.418	0.643	0.738
2.3-dinor-15-epi-15-F_{2t}-IsoP	**PCC**	-0.107	0.128	0.100	-0.047	0.081	0.010	0.021	0.019	0.074	-0.122	-0.025
	P value	0.358	0.272	0.391	0.724	0.538	0.939	0.875	0.887	0.574	0.352	0.852
15-keto-15-E_{2t}-IsoP	**PCC**	-0.088	-0.074	-0.015	0.297	-0.181	-0.113	-0.034	-0.037	-0.101	-0.120	0.275
	P value	0.449	0.524	0.897	0.021*	0.167	0.391	0.799	0.782	0.442	0.361	0.034*
15-keto-15-F_{2t}-IsoP	**PCC**	-0.109	-0.107	-0.101	-0.117	0.259	0.149	0.344	0.216	0.280	0.019	-0.230
	P value	0.350	0.359	0.385	0.374	0.045*	0.254	0.007*	0.097	.0030*	0.884	0.077
15-E_{2t}-IsoP	**PCC**	-0.106	0.039	0.108	-0.137	0.072	0.086	-0.017	-0.047	0.146	0.051	-0.085
	P value	0.360	0.741	0.353	0.296	0.587	0.514	0.895	0.724	0.265	0.697	0.517
5-F_{2t}-IsoP	**PCC**	-0.242	-0.031	0.020	-0.005	0.103	-0.175	-0.079	-0.101	-0.032	-0.067	-0.050
	P value	0.035*	0.789	0.866	0.967	0.435	0.181	0.550	0.444	0.808	0.613	0.703
15-F_{2t}-IsoP	**PCC**	-0.014	-0.068	-0.024	0.038	0.120	-0.022	0.265	-0.051	0.178	-0.007	-0.058
	P value	0.903	0.562	0.834	0.773	0.360	0.870	0.041*	0.699	0.173	0.959	0.659
$PGF_{2\alpha}$	**PCC**	-0.171	0.022	0.051	-0.075	0.031	-0.113	-0.138	-0.066	-0.070	-0.127	-0.097
	P value	0.140	0.849	0.660	0.569	0.814	0.390	0.292	0.615	0.593	0.332	0.459
4*(RS)*-F_{4t}-NeuroP	**PCC**	-0.018	-0.167	-0.130	-0.175	-0.049	0.109	-0.078	0.082	-0.123	-0.060	-0.149
	P value	0.877	0.150	0.263	0.181	0.709	0.406	0.554	0.532	0.348	0.647	0.256
10-epi-10-F_{4t}-NeuroP	**PCC**	-0.106	-0.045	-0.017	0.103	0.048	-0.077	0.068	-0.108	0.098	-0.047	0.015
	P value	0.361	0.699	0.885	0.434	0.717	0.557	0.606	0.412	0.455	0.720	0.912
14*(RS)*-14-F_{4t}-NeuroP	**PCC**	0.017	-0.167	-0.124	-0.074	0.071	0.029	-0.006	-0.006	0.135	0.105	-0.150
	P value	0.886	0.150	0.284	0.574	0.591	0.824	0.965	0.962	0.304	0.423	0.252
	PCC	-0.004	-0.081	-0.086	-0.050	0.186	0.055	0.349	0.011	0.240	-0.066	-0.173

Ent-7*(RS)*-7-F_{2t}-dihomo-IsoP	**P value**	0.974	0.487	0.462	0.707	0.156	0.679	0.006*	0.931	0.065	0.618	0.186
17-F_{2t}-dihomo-IsoP	**PCC**	0.010	-0.086	-0.036	-0.009	-0.026	-0.099	0.153	-0.139	0.017	-0.102	-0.053
	P value	0.935	0.460	0.760	0.947	0.842	0.451	0.242	0.290	0.899	0.440	0.688
17-epi-17-F_{2t}-dihomo-IsoP	**PCC**	-0.003	-0.079	-0.073	-0.006	0.012	-0.129	0.076	-0.180	0.034	-0.014	-0.018
	P value	0.982	0.497	0.530	0.963	0.928	0.326	0.564	0.168	0.797	0.914	0.893
17*(RS)*-10-epi-SC-Δ^{15}-11-dihomo-IsoF	**PCC**	-0.093	0.014	-0.012	-0.055	0.226	0.026	0.170	-0.054	0.242	0.156	-0.014
	P value	0.422	0.901	0.916	0.675	0.083	0.847	0.194	0.683	0.062	0.233	0.913
7*(RS)*-ST-Δ^{8}-11-dihomo-IsoF	**PCC**	-0.262	0.030	0.035	0.048	-0.030	-0.155	-0.040	-0.230	-0.110	-0.029	0.131
	P value	0.022*	0.797	0.765	0.715	0.821	0.238	0.761	0.077	0.405	0.828	0.318
Isoprostanes$^{\$}$	**PCC**	-0.196	-0.022	-0.020	-0.085	0.004	-0.150	-0.238	-0.193	-0.141	-0.040	0.010
	P value	0.089	0.852	0.863	0.520	0.976	0.253	0.067	0.139	0.284	0.761	0.940
Neurorostanes$^{\$}$	**PCC**	-0.001	-0.011	-0.033	0.102	-0.019	-0.077	0.207	-0.029	0.055	0.028	-0.026
	P value	0.995	0.924	0.775	0.437	0.883	0.556	0.113	0.825	0.678	0.831	0.841
Neurofurans$^{\$}$	**PCC**	-0.246	-0.032	0.019	-0.159	0.142	0.122	-0.008	-0.013	0.093	0.135	-0.057
	P value	0.032*	0.784	0.871	0.224	0.278	0.355	0.953	0.920	0.481	0.304	0.667
Isofurans$^{\$}$	**PCC**	-0.309	0.013	0.062	-0.098	-0.051	-0.120	-0.084	-0.083	-0.083	-0.132	0.040
	P value	0.007*	0.914	0.595	0.458	0.698	0.359	0.525	0.530	0.527	0.315	0.760

PCC: Pearson correlation coefficient; *$p < 0.05$; $^{\$}$Total parameters.

Table 12. Concentrations of lipid peroxidation biomarkers in plasma samples.

Concentration (nmol L^{-1})	**Non-AD (*n* = 34) (Median (IQR))**	**AD (*n* = 42) (Median (IQR))**	***p*-Value Mann-Whitney**
15®-15-F2t-IsoP	0.075 (0, 0.231)	0.300 (0.188, 0.394)	<0.001 *
PGE_2	0.050 (0, 0.100)	0.038 (0, 0.125)	0.590
2,3-dinor-15-*epi*-15-F2t-IsoP	0 (0, 0)	0 (0, 0.006)	0.028 *
15-keto-15-E2t-IsoP	0.150 (0, 0.250)	0.163 (0, 0.325)	0.541
15-keto-15-F2t-IsoP	0.113 (0.044, 0.181)	0.225 (0.069, 0.331)	0.065
15-E2t-IsoP	0.200 (0.100, 0.325)	0.213 (0.019, 0.525)	0.900
5-F2t-IsoP	0.263 (0.056, 0.831)	0.700 (0.350, 1.125)	0.021 *
15-F2t-IsoP	0 (0, 0)	0.020 (0.009, 0.035)	<0.001 *
$PGF_{2\alpha}$	0.238 (0.044, 0.363)	0.413 (0.194, 0.706)	0.011 *
4*(RS)*-F4t-NeuroP	0 (0, 1.475)	1.100 (0.763, 1.425)	0.119
1a,1b-dihomo-$PGF_{2\alpha}$	0 (0, 0)	0 (0, 0)	0.219
10-*epi*-10-F4t-NeuroP	0.225 (0.175, 0.281)	0.079 (0.025, 0.175)	<0.001 *
14*(RS)*-14-F4t-NeuroP	0.300 (0.019, 0.850)	0.563 (0.131, 1.044)	0.316
Ent-7*(RS)*-7-F2t-dihomo-IsoP	0 (0, 0.050)	0.075 (0.050, 0.150)	<0.001 *
17-F2t-dihomo-IsoP	0 (0, 0)	0 (0, 0)	0.096
17-epi-17-F2t-dihomo-IsoP	0 (0, 0)	0 (0, 0.025)	<0.001 *
7(*RS*)-*epi*-SC-Δ^{15}-11-dihomo-IsoF	0 (0, 0)	0 (0, 0)	0.066
7*(RS)*-ST-Δ^{8}-11-dihomo-IsoF	0.013 (0, 0.050)	0.025 (0, 0.075)	0.098
Isoprostanes$	0.449 (0.396, 0.488)	0.345 (0.234, 0.409)	<0.001 *
Neuroprostanes$	0.142 (0.050, 0.207)	0 (0, 0.268)	0.029 *
Isofurans$	0.073 (0.058, 0.105)	0.085 (0.069, 0.115)	0.202
Neurofurans$	0.114 (0.082, 0.173)	0.095 (0, 0.169)	0.111

$Arbitrary units: intensity of signal units x (internal standard concentration, mg L^{-1}); * *p*-value < 0.05.

3. Discussion

The reliable determination of lipid peroxidation product levels in CSF samples from biologically defined groups (AD and non-AD), based on specific AD biomarkers, was carried out. A previous study showed that these biomarkers were useful to diagnose AD with high accuracy when they were measured in plasma samples [168]. Previous studies also showed an increase of CSF isoprostanes in AD patients when their levels were corrected by ventricular volume, and these levels correlated with other clinical variables [202]; although Dutis et al. did not find any differences for CSF isoprostanes between AD, MCI and healthy control groups [203]. Therefore, ventricular volume could affect the concentration measured in CSF samples and that could be the reason why no differences were found between participant groups with or without AD.

In the present work, although isoprostanoids did not show differences between AD and non-AD groups, some lipid peroxidation products determined in CSF correlated with CSF Aβ and p-Tau levels. These results are consistent with those obtained by Kuo et al. who did not find differences between AD and non-AD groups for CSF levels of F_2-isoprostanes and F_4-neuroprostanes, but showed correlations with these metabolites and CSF Aβ levels [204]. By contrast, Yao et al. found that 12(S)-hydroxyeicosatetraenoic (HETE) acid and 15(S)-HETE correlated with CSF Tau but not with CSF Aβ [205]. As amyloid biomarkers are specific for AD, isoprostanes seem to be more specific for amyloid pathology and AD than other biomarkers, such as HETE.

In our study, there is a correlation between isoprostanoids, such as 15-keto-15-F_{2t}-IsoP, and cognitive impairments identified through MMSE scale examination. Similar results were obtained by Duits et al. that found a correlation between MMSE and F_2-isoprostanes in ApoE ε4 carriers [203]. Moreover, Kester et al. did not find differences for CSF isoprostanes levels between non-demented, MCI and AD patients, but these analytes showed an increase in the follow up of these participants showing an association with cognitive decline and MMSE examination [206]. In fact, CSF isoprostanes were described by de Leon et al. as good, not only in diagnosis, but also in AD progression study [207]. However, Yao et al. did not find any correlation between MMSE score and 12(S)-HETE and 15(S)-HETE, while in the present study 8-iso-15-keto-$PGF_{2\alpha}$ correlated with this neuropsychological status evaluation [205].Therefore, ApoE ε4 could be another important variable that affects

isoprostanes levels in CSF.

In this study, correlations between lipid peroxidation levels in CSF and plasma samples were not found. Similarly, plasma and CSF levels of other metabolites, such as neurogranin, did not show any correlation [208]. Moreover, Aβ42 measured in plasma and CSF samples did not show any correlation [209], while Mehta et al. did not find correlation for Aβ40 and Aβ42 between these two biofluids [210]. However, Sun et al. studied correlations between different analytes such as α(1)-antichymotrypsin (ACT), α(1)-antitrypsin (AAT), interleukin-6 (IL-6), monocyte chemoattractant protein-1 (MCP-1) and oxidised low-density lipoprotein (oxLDL) between plasma and CSF samples.They found correlations for ACT, IL-6, MCP-1 and oxLDL, the latter showing a weaker correlation [211]. In addition, other analytes, such as adiponectin showed a correlation between these two matrices [212]. Moreover, different metabolites from the kyneurine pathway showed correlation between plasma and CSF samples, some showing a relationship with other CSF biomarkers (t-Tau, p-Tau) [213]. Therefore, metabolites exchange between blood brain barrier (BBB) is not always equal, and concentrations between both biofluids could show differential distribution depending on the metabolite characteristics. As a hypothesis, CSF is continuously filtrating, so isoprotanes are not accumulated in this fluid, and the analyte concentrations in CSF are dependent on ventricular volume. By contrast, metabolites accumulating in the blood system for longer could be more easily measured. Previous studies showed that BBB permeability is increased under pathologic conditions, such as AD [214,215], and this permeability depends on inflammatory processes [216]. BBB alteration in AD could be responsible for the differences in correlation between plasma and CSF levels of different analytes in AD and non-AD. In addition, ventricular volume could influence the concentration of different metabolites in CSF, so corrections to this volume could result in a better correlation between plasma and CSF levels.

4. Conclusions

New lipid peroxidation biomarkers were satisfactorily measured in CSF samples from participants with AD and without AD (including healthy controls and other neurological pathologies) by an analytical method based on UPLC-MS/MS. These CSF metabolites are not able to discriminate between AD and non-AD groups, although some of them correlate with neuropsychological evaluations, as well as standard AD CSF biomarkers (Aβ42, p-Tau).

On the other hand, the levels of each isoprostanoid in plasma and CSF did not show correlation. It could be that changes in the transportation of substances through the BBB, the clearance of these compounds did not allow their accumulation and quantification in CSF, due to the necessity to correct CSF biomarker levels with ventricular volume. However, the CSF isoprostanoids levels could be useful in the evaluation of cognitive capacity.

Chapter 5. Clinical utility of plasma lipid peroxidation biomarkers in Alzheimer's Disease differential diagnosis

1. Summary

The aim of this chapter was to develop an early AD diagnosis model based on plasma lipid peroxidation biomarkers for a differential diagnosis from other similar neurological

And neurodegenerative diseases with shared clinical symptoms. For this, plasma lipid peroxidation compounds in plasma samples from participants classified into AD (n = 138), non-AD (including MCI and other dementias not due to AD) (n = 70) and healthy controls (n = 50) were analysed by UPLC-MS/MS. A two-stage model for Alzheimer's disease diagnosis was developed by adjusting two nested logistic regression models. The first stage was based on neuropsychological status and the second stage on lipid peroxidation.

2. Results

Table 13. Clinical and demographic variables for the participants.

Variables	**AD Group (*n* = 138)**	**Healthy Group (*n* = 50)**	**Non-AD Group (*n* = 70)**
Age (years, median (IQR))	71 (68, 74)	67 (62, 69)	66 (62, 71)
Gender (female, *n* (%))	80 (59.7%)	19 (38.78%)	31 (48.44%)
RBANS.DM (median (IQR))	44 (40, 56)	100 (92, 106)	64 (52, 81)
CDR (median (IQR))	0.5 (0.5–1)	0 (0–0)	0.5 (0.5–1)
Aβ42 (pg mL^{-1}, median (IQR))	580 (464, 694)	1085 (924, 1308)	1049 (850, 1264)
t-Tau (pg mL^{-1}, median (IQR))	707 (428, 830)	255 (144, 313)	322 (190, 395)
p-Tau (pg mL^{-1}, median (IQR))	99 (71, 110)	47 (32, 60)	52 (34, 61)

CDR: Clinical dementia rating; RBANS.DM: Repeatable Battery for the Assessment of Neuropsychological Status-Delayed Memory; CSF: cerebrospinal fluid; t-Tau: total Tau; p-Tau: phosphorylated Tau.

The demographic and clinical data from the participants are summarized in Table 13. The clinical variables allowed to differentiate among participants groups. Specifically, the CSF biomarkers (Aß42, t-Tau, p-Tau) levels identify AD patients from control and non-AD

participants. Moreover, the neuropsychological evaluation (RBANS.DM, CDR) identifies control participants.

Table 14. Analytes concentrations in plasma samples from participants groups.

Variable **Median (IQR) (nmol L^{-1})**	**AD Group** **(*n* = 138)**	**Healthy Group** **(*n* = 50)**	**Non-AD Group** **(*n* = 70)**	***P*-Value** **(Kruskal–Wallis)**
	Median (IQR)	**Median (IQR)**	**Median (IQR)**	
15(*R*)-15-F_{2t}-IsoP	0.21 (0.12, 0.32)	0.19 (0.13, 0.29)	0.19 (0.09, 0.33)	0.361
PGE_2	0.08 (0, 0.38)	0.08 (0.02, 0.36)	0.12 (0.03, 0.36)	0.913
2,3-dinor-$iPF_{2\alpha}$-III	0 (0, 0)	0 (0, 0)	0 (0, 0)	0.418
15-keto-15-E_{2t}-IsoP	0.04 (0, 0.13)	0.03 (0, 0.14)	0 (0, 0.2)	0.924
15-keto-15-F_{2t}-IsoP	0.14 (0.06, 0.37)	0.14 (0.09, 0.23)	0.16 (0.1, 0.33)	0.872
15-E_{2t}-IsoP	0.2 (0.09, 0.93)	0.2 (0.12, 0.64)	0.48 (0.18, 1.05)	0.041 *
5-F_{2t}-IsoP	0.77 (0.37, 1.45)	1.12 (0.54, 1.46)	1.08 (0.45, 1.55)	0.542
15-F_{2t}-IsoP	0.03 (0.01, 0.06)	0.02 (0.01, 0.04)	0.01 (0, 0.07)	0.129
$PGF_{2\alpha}$	0.43 (0.17, 0.91)	0.78 (0.4, 1.08)	0.62 (0.3, 1.13)	0.005 *
4(*RS*)-F_{4t}-NeuroP	1.2 (0.59, 1.44)	1.22 (0.7, 1.43)	0.5 (0, 1.43)	0.006 *
1a,1b-dihomo-$PGF_{2\alpha}$	0 (0, 0)	0 (0, 0)	0 (0, 0)	0.178
10-*epi*-10-F_{4t}-NeuroP	0.13 (0.05, 0.2)	0.13 (0.07, 0.18)	0.22 (0.17, 0.31)	<0.001 *
14(*RS*)-14-F_{4t}-NeuroP	0.56 (0.1, 1.2)	0.62 (0, 1.33)	0.52 (0.1, 1.48)	0.891
IsoP[$]	0.36 (0.26, 0.55)	0.31 (0.19, 0.45)	0.54 (0.42, 0.93)	<0.001 *
Ent-7(*RS*)-F_{2t}-dihomo-IsoP	0.12 (0.08, 0.17)	0.11 (0.07, 0.15)	0.13 (0, 0.45)	0.181
17-F_{2t}-dihomo-IsoP	0 (0, 0)	0 (0, 0)	0 (0, 0)	0.989
17-*epi*-17-F_{2t}-dihomo-IsoP	0 (0, 0.02)	0 (0, 0)	0 (0, 0.18)	0.168
17(*RS*)-10-*epi*-SC-Δ^{15}-11-dihomo-IsoF	0 (0, 0)	0 (0, 0)	0 (0, 0)	0.536
7(*RS*)-ST-Δ^{8}-11-dihomo-IsoF	0.06 (0, 0.12)	0.11 (0, 0.18)	0.02 (0, 0.1)	0.155
NeuroF[$]	0.13 (0.06, 0.25)	0.07 (−0.1, 0.25)	0.14 (0.08, 0.2)	0.022*
IsoF[$]	0.14 (0.08, 0.29)	0.11 (0.07,0.3)	0.2 (0.08, 0.39)	0.336

[$] Arbitrary units: (intensity of signal units × (internal standard concentration, nmol L^{-1}); * $P<0.05$; IQR: Interquartile range.

The analytes concentrations found in plasma samples from participants groups are summarized in Table 14. All these variables showed non-normal distribution, so the non-parametric test (Kruskal-Wallis) was applied showing statistically significant differences among groups for some lipid peroxidation compounds (15-E_{2t}-IsoP, $PGF_{2\alpha}$, 4(*RS*)-F_{4t}-NeuroP, 10-*epi*-10-F_{4t}-NeuroP, IsoP).

The first model, using these neuropsychological variables, was able to discriminate between control and patients. It achieved a very high accuracy, with an AUC of 0.99 and a bootstrap validated AUC of 0.99. These results show that separating control participants from case patients (AD, non-AD) is straightforward using standard neuropsychological evaluation tests. In Figure 16a, it can be seen that participants without any neurological or neurodegenerative disease (healthy participants) are grouped in the left and upper side, indicating higher RBANS.DM and lower CDR punctuations. The formula for this first prediction step is the following:

$$\Pr(Case/Control) = \frac{e^{9.25-0.13xRBANS+22.71xCDR}}{1+e^{9.25-0.13xRBANS+22.71xCDR}}$$

The second model, for discriminating between AD and non-AD patients in the case group included the variables 10-*epi*-10-F_{4t}-NeuroP and IsoPs (Figure 16b), and it achieved an AUC of 0.79 and a bootstrap validated AUC of 0.74. Calibration of the model was satisfactory. It was assessed using bootstrapping and comparing predicted *vs.* obtained values, observing very low deviations. The formula for this final prediction step, to be applied only to the individuals predicted as patients (case) by the first step, is the following:

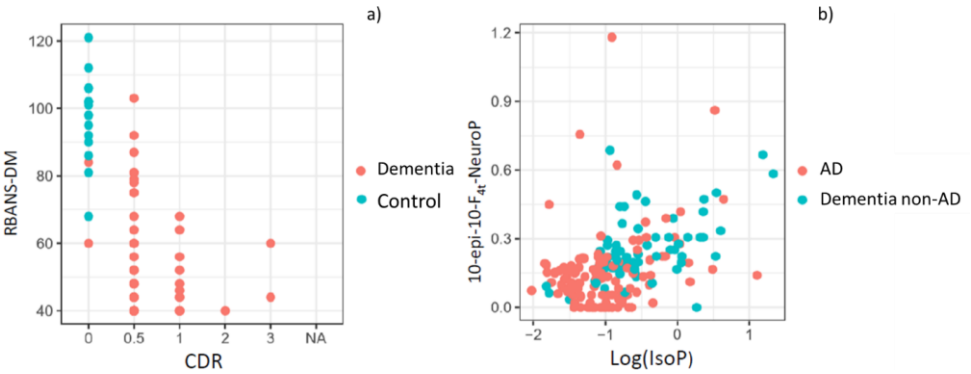

Figure 16. (a) Representation of control and dementia patients by using standard neuropsychological evaluation tests (RBANS-DM, CDR); (b) Representation of AD and non-AD patients by using the variables 10-*epi*-10-F4t-NeuroP and IsoP.

$$\Pr(Case/Control) = \frac{e^{-0.14+1.15xlog(IsoPs)+2.24x10-epi-10-F4t-NeuroP}}{1+e^{-0.14+1.15xlog(IsoPs)+2.24x10-epi-10-F4t-NeuroP}}$$

3. Discussion

In this work it is described a new diagnosis model based on plasma lipid peroxidation biomarkers and neuropsychological scores, which evaluate memory, cognition and functional performance.

This model could be able to differentiate AD from healthy subjects and participants with other pathologies, such as MCI not due to AD, frontotemporal dementia, vascular dementia, or DLB. Differential diagnosis between AD and non-AD pathologies are commonly a challenge in neurology units especially in early stages [217], since some pathologies show similar clinical symptoms. Therefore, a reliable early diagnosis model is required to be applied to clinical practice.

Recent research has shown an increasing interest in the clinical validation of potential biomarkers to early and specific diagnose AD using minimally invasive biological samples [44]. Among the physiological mechanisms that are already impaired in early disease stages, lipid peroxidation has shown some promising results, and plasma samples constitute an interesting matrix in the search for the corresponding biomarkers [141,170,189,218–222].

Among lipid peroxidation biomarkers evaluated in plasma, some AD studies found

altered levels for malondialdehyde [170,218–220], 4-hydroxynonenal [221], lipophilic fluorescent products [189,222], and isoprostanes [168]. In general, these potential biomarkers showed elevated levels in AD in comparison with healthy participants, reflecting high OS at systemic level. However, OS is common in many pathologies, such as cancer [223] or vascular diseases [224], as well as in other neurodegenerative diseases [225]. For that reason, the present work focused on the need to develop a specific diagnosis model for AD. In fact, AD shows similar clinical symptoms to other pathologies, and the differential AD diagnosis constitutes the real diagnostic challenge. In this sense, lipid peroxidation biomarkers were evaluated as potential specific AD biomarkers, as the brain has a high lipid composition (polyunsaturated fatty acids…) [167]. For this, a previously developed and validated analytical method was applied [168]. This method showed adequate linearity for all the analytes within the corresponding concentration ranges, and suitable precision. The limits of detection and accuracy were satisfactory, and matrix effect was considered negligible. Among studied compounds, statistically significant results were obtained for two prostaglandins (derived from araquidonic acid), two neuroprostanes (derived from DHA), and isoprostanes as total parameter (15-E_{2t}-IsoP, $PGF_{2\alpha}$, 4(*RS*)-F_{4t}-NeuroP, 10-*epi*-10-F_{4t}-NeuroP, IsoP). In contrast to the results in this work, some studies determining isoprostanoids did not obtain satisfactory results [226,227]. It could be explained by the limited list of compounds assessed in literature. However, in the present study a set of 18 compounds were evaluated simultaneously, and it could provide more information about the oxidative state of each individual.

In addition, the present study shows the strengths of using standard diagnosis based on biological definition (CSF biomarkers) to identify accurately the participants (early AD patients, healthy controls, non-AD patients). Furthermore, it is important to highlight the relevant discrimination capacity of the neuropsychological evaluation to identify accurately the healthy controls. From this accurate participant's classification, a further AD specific and minimally invasive diagnosis was developed. For this, a two-step model was required using the advantages of the neuropsychological evaluation (first step), and the plasma lipid peroxidation determinations (second step). In the developed model, the first step identified the healthy participants, while the second step increased the diagnosis specificity, differentiating AD patients from other patients with other

pathologies with similar symptoms. In this sense, a one-step model would not be able to distinguish accurately among AD, non-AD and healthy patients. Therefore, the two-step developed model was required to achieve the minimally invasive and differential AD diagnosis.

Regarding AD differential diagnosis, our study achieved high discriminative power. Albeit not outstanding, it serves as a first approach for developing a differential diagnosis model based on lipid peroxidation compounds. Some studies can be found in literature identifying different biomarkers that differentiate AD from vascular dementia [228], and diabetes-related dementia [229]. However, there is a lack of preliminary studies with clinical validation. A recent study focused on differentiating AD and DLB by means of different pathological signatures of gait [230] supported the theory of interacting cognitive-motor networks [231]. In addition, a previous study found that the CSF p-Tau/Aβ42 ratio might reliably detect AD pathology in patients suffering from different types of dementia [232]. In the present work the non-AD group included a large variety of pathologies, such as MCI not due to AD, frontotemporal dementia, vascular dementia, and DLB. The different lipid peroxidation pattern observed between AD and non-AD subjects could be corroborated by a previous study, which suggested that high lipid peroxidation levels preceded Aβ accumulation in brain [233]. Among the physiological mechanisms that could explain the different lipid peroxidation levels between AD and non-AD pathologies, it is important to highlight the role of potential mediators between lipid peroxidation products and AD pathology [234]. Specifically, thromboxane A2 receptor is activated by isoprostanes and promotes amyloid aggregation [235,236]. In fact, previous studies have shown that agonists for this receptor reduced this amyloid increase and they could be potential treatments for AD [235]. On the other hand, another study found co-localization of lipid oxidation and amyloid plaques in brain [39]. From the clinical point of view, the specificity described in the developed diagnosis model could have a great value due to the high clinical similarity among pathological symptoms.

As regards biomarkers and neuropsychological tests, they were selected from our previous experience. In fact, a study carried out with the same lipid peroxidation compounds in plasma samples from AD and healthy participants showed the capacity of these analytes

as potential biomarkers for AD [168]. In that work, a one-step diagnosis model was developed from the levels obtained for six lipid peroxidation compounds. The corresponding diagnosis model could differentiate early AD patients from healthy participants with satisfactory accuracy (AUC-ROC 0.817). Nevertheless, it showed the disadvantage of low sample size. Moreover, the differential diagnosis power from non-AD pathologies, which constitutes an important diagnostic problem in clinical practice, was not evaluated [168]. On the other hand, a previous model for early AD diagnosis was developed from the RBANS.DM test. It showed a high discriminative power between AD and non-AD participants [237,238]. For that reason, RBANS.DM was included in the first step of the present model, improving biomarkers diagnosis power. In this sense, the present developed diagnosis model is based on two steps, the sample size has been suitable to carry out an internal clinical validation, and the differential diagnosis has been included.

Finally, few studies have carried out an external clinical validation of potential biomarkers (plasma proteins, magnetic resonance imaging scans) differentiating two groups of participants (discovery group, validation group) [238,239]. In order to improve the statistical power, other studies developed an internal clinical validation [240,241]. Similarly, in this work, an internal clinical validation was carried out obtaining a satisfactory diagnostic power, since a large sample size was available. Most of previous works were based on CSF biomarkers or neuroimaging biomarkers, so the internal clinical validation based on plasma lipid peroxidation biomarkers constitutes a promising new approach.

The two-step diagnosis model developed in the present work provides the probability of suffering AD from early stages. In the first step, in a given population, it is possible to discriminate the control patients of case patients and thus putative AD patients. In the second step, AD diagnosis can be differentiated from other neurodegenerative diseases also involving cognitive impairment. These results combined with other factors (e.g., age, gender, familiar background, risk factors…) could decide upon the further need of using invasive techniques to establish the patient's diagnosis [242]. Therefore, the present diagnosis model could be considered a relevant approach in the clinical practice field.

4. Conclusions

A two-step early and differential diagnostic model has been developed indicating the individual probability of suffering from early AD, using low cost and minimally invasive procedures for the potential diagnosis. It consisted of a simultaneous approach from neuropsychological and biochemical fields. Lipid peroxidation has been assayed as a physiological mechanism which is impaired at early stages in AD. In this sense, a large set of related biomarkers were determined in plasma samples, selecting two compounds in the development of an AD differential diagnosis model. The corresponding internal validation was satisfactory, and further external validation of the developed model will be carried out as a fundamental stage before being applied in the clinical routine use. This is a promising screening test that could avoid the current invasive diagnosis method and could be useful in diagnosis and investigation.

Chapter 6. Lipid peroxidation assessment in preclinical Alzheimer Disease diagnosis

1. Summary

The aim of this chapter was to evaluate the capacity of lipid peroxidation compounds as minimally invasive biomarkers of preclinical AD. For this, a panel of lipid peroxidation biomarkers were determined in plasma samples from preclinical AD participants (n = 12) and controls (n = 31) by UPLC-MS/MS. Then, the results were analysed using an elastic net logistic regression model.

2. Results

2.1. Patients' characteristics

Demographic characteristics of the participants are described in Table 15. Participants showed median ages between 62 and 70 years old and they showed comparable normal cognitive status, with similar median RBANS.DM and CDR scores. As expected, the control group showed higher median levels of Aβ42 than the preclinical group, and the control group showed lower levels of t-Tau and p-Tau than the preclinical group. Additionally, both groups showed similar use of medications, comorbidities and educational levels.

Table 15. Participants' clinical and demographic description.

Variable		Control group (n=31) Median (1st, 3rd quartile)	Preclinical group (n=12) Median (1st, 3rd quartile)
Age (years)		62 (58.5, 67)	70 (60.75, 74)
Gender (Female, n (%))		19 (61.29%)	6 (50%)
Smoke (Yes, n (%))		6 (27.27%)	1 (14.29%)
Alcohol (Yes, n (%))		6 (27.27%)	0 (0%)
RBANS.DM (score)		98 (94, 102)	94.5 (87, 100.25)
RBANS.A (score)		91 (82, 98.5)	85 (78, 91)
RBANS.L (score)		90 (83, 94)	88.5 (82.5, 94.25)
RBANS.VC (score)		92 (84, 105)	87 (75, 105)
RBANS.IM (score)		87 (83, 98.5)	85 (81.75, 94)
CDR (score)		0.5 (0, 0.5)	0.5 (0, 0.5)
CSF Aβ42 (pg mL^{-1})		1224 (975.5, 1409.5)	571.5 (407, 683.29)
CSF t-Tau (pg mL^{-1})		212 (181.5, 259)	443.5 (256.75, 607.75)
CSF p-Tau (pg mL^{-1})		34 (26.5, 38.5)	74 (40.75, 86)
CSF t-Tau/ Aβ42		0.18 (0.16-0.21)	0.70 (0.51-0.97)
FAQ (score)		1 (0, 3.5)	1 (0, 3)
GDS (score)		11 (5.5, 13)	5 (3.75, 9)
Educational level (n, (%))	**Basic/primary**	10 (32.26%)	4 (33.33%)
	Secondary	7 (22.58%)	2 (16.67%)
	Universitary	14 (45.16%)	6 (50%)
Medication (n, (%))			
Statins		9 (40.91%)	3 (42.86%)
Fibrates		0 (0%)	1 (14.29%)
Morphics		0 (0%)	0 (0%)
IACE		1 (4.55%)	0 (0%)
Neuroleptics		2 (9.09%)	0 (0%)
Benzodiazepines		6 (27.27%)	2 (28.57%)
Antiepileptics		1 (4.55%)	0 (0%)
Anticoagulants		0 (0%)	0 (0%)
Antihipertensives		7 (31.82%)	2 (28.57%)
Corticoids		1 (4.55%)	0 (0%)
Anti-inflammatory		3 (13.64%)	0 (0%)
Comorbidity (n, (%))			
Dyslipidemia		11 (50%)	3 (42.86%)
Diabetes		9 (40.91%)	1 (14.29%)
Hypertension		8 (36.36%)	2 (28.57%)
Heart Disease		1 (4.55%)	0 (0%)
Cerebrovascular		1 (4.55%)	0 (0%)
Depression (n, (%))		4 (18.18%)	2 (28.57%)
Anxiety (n, (%))		3 (13.64%)	2 (28.57%)

RBANS, Repeatable Battery for the Assessment of Neuropsychological Status (DM, delayed memory; A, attention; L, learning; VC, visuospatial/constructional; IM, immediate memory); CDR, clinical dementia rating; CSF cerebrospinal fluid; FAQ, functional activities questionnaire; GDS, geriatric depression scale; ACEI, acetylcholinesterase inhibitors.

2.2. Plasma levels of lipid peroxidation compounds

The plasma levels obtained for the determined lipid peroxidation compounds are summarized in Table 16 for each participant group. As can be seen, these potential biomarkers did not show statistically significant differences between preclinical AD patients and healthy participants (Table 16). Figure 17 shows the corresponding boxplots, observing slight differences in median values between groups. In general, lower levels were obtained for the preclinical AD group.

Table 16. Plasma levels of lipid peroxidation compounds.

Variable (nmol L^{-1})	Control (n=31) Median (1st, 3rd quartile)	Preclinical (n=12) Median (1st, 3rd quartile)	P value
15-*epi*-15-F_{2t}-IsoP	0.62 (0.48, 0.82)	0.51 (0.34, 0.74)	0.414
PGE_2	0.3 (0.26, 0.38)	0.29 (0.27, 0.36)	0.738
2,3-dinor-15-*epi*-15-F_{2t}-IsoP	0.03 (0, 0.03)	0.03 (0.02, 0.03)	0.602
15-keto-15-E_{2t}-IsoP	1.02 (0.72, 1.35)	0.94 (0.69, 1.27)	0.384
15-keto-15-F_{2t}-IsoP	0.65 (0.45, 0.85)	0.66 (0.34, 0.89)	0.926
15-E_{2t}-IsoP	1.05 (0.8, 1.39)	1.26 (0.89, 1.46)	0.478
5-F_{2t}-IsoP	2.75 (2.16, 3.19)	2.35 (1.63, 2.9)	0.414
15-F_{2t}-IsoP	0.05 (0.05, 0.05)	0.05 (0.05, 0.07)	0.430
$PGF_{2\alpha}$	0.32 (0.25, 0.51)	0.34 (0.22, 0.65)	0.968
4(*RS*)-4-F_{4t}-NeuroP	3.62 (2.72, 4.9)	3.45 (2.36, 4.58)	0.800
1a,1b-dihomo-$PGF_{2\alpha}$	3.67 (3.06, 4.43)	3.14 (2.31, 4.34)	0.478
10-*epi*-10-F_{4t}-NeuroP	0.17 (0.11, 0.26)	0.15 (0.07, 0.25)	0.698
14(*RS*)-14-F_{4t}-NeuroP	1.77 (1.29, 2.31)	1.35 (1.03, 2.08)	0.355
***ent*-7(*RS*)-7-F_{2t}-dihomo-IsoP**	0 (0, 0)	0 (0, 0.01)	0.414
17-F_{2t}-dihomo-IsoP	0 (0, 0)	0 (0, 0)	1.000
17-*epi*-17-F_{2t}-dihomo-IsoP	0 (0, 0)	0 (0, 0)	1.000
17(*RS*)-10-*epi*-SC-Δ^{15}-11-dihomo-IsoF	0 (0, 0)	0 (0, 0)	0.679
7(*RS*)-ST-Δ^{8}-11-dihomo-IsoF	0 (0, 0.22)	0 (0, 0)	0.165
Neurofurans	0.27 (0.19, 0.37)	0.24 (0.21, 0.41)	0.679
Isofurans	0.52 (0.4, 0.65)	0.5 (0.41, 0.69)	0.718
Dihomo-isoprostanes	0.15 (0.14, 0.17)	0.15 (0.13, 0.17)	0.883
Dihomo-isofurans	0.01 (0.01, 0.02)	0.01 (0.01, 0.02)	0.883
Neuroprostanes	0.64 (0.49, 0.76)	0.59 (0.45, 0.77)	0.679
Isoprostanes	1.5 (1.25, 1.84)	1.32 (1.14, 1.67)	0.328

Correlations were computed between CSF biomarkers (Aβ42, t-Tau and p-Tau) and plasma lipid peroxidation biomarkers (see Figure 18). Results showed that t-Tau

correlated with 15-F_{2t}-IsoP (r = 0.397, p = 0.008), and $PGF_{2\alpha}$ (r = 0.339, p = 0.026); and p-Tau correlated with 15-F_{2t}-IsoP (0.401, p = 0.008), and $PGF_{2\alpha}$ (r = 0.329, p = 0.031). In addition, correlations were assayed between neuropsychological status and plasma biomarkers. Specifically, RBANS.DM correlated with 2,3-dinor-15-*epi*-15-F_{2t}-IsoP (r = - 0.314, p = 0.040), 15-E_{2t}-IsoP (r = - 0.432, p = 0.025), 5-F_{2t}-IsoP (r = 0.335, p = 0.028), 15-F_{2t}-IsoP (r = 0.390, p = 0.10), and $PGF_{2\alpha}$ (r = - 0.342, p = 0.025). Additionally, CDR showed correlation with 15-*epi*-15-F_{2t}-IsoP (r = 0.329, p = 0.031), PGE_2 (r = 0.329, p = 0.031), 2,3-dinor-15-*epi*-15-F_{2t}-IsoP (r = 0.316, p = 0.039), 15-keto-15-E_{2t}-IsoP (r = 0.333, p = 0.029), 15-keto-15-F_{2t}-IsoP (r = 0.319,p = 0.037), 15-E_{2t}-IsoP (r = 0.363, p = 0.017), and 4(*RS*)-4-F_{4t}-NeuroP (r = 0.332, p = 0.030).

2.3. Potential diagnosis model

The developed model included 10 analytical variables (15-*epi*-15-F_{2t}-IsoP, PGE2, 15-keto-15-E_{2t}-IsoP, 15-keto-15-F_{2t}-IsoP, 15-E_{2t}-IsoP, PGF2α, 4(*RS*)-4-F4t-NeuroP, 1a,1b-dihomo- PGF2α, 10-*epi*-10-F_{4t}-NeuroP, 14(*RS*)-14-F_{4t}-NeuroP), as well as age and gender. Table 17 shows the model characteristics and the tendency of the different selected biomarkers.The conditional effect for each variable is represented in Figure 19, showing the increase or decrease in preclinical-AD probability according to the levels for each variable. This model showed an AUC of 0.96 (CI 95%, 0.903–1.000) (Figure 20), and a validation AUC of 0.90. The sensitivity and specificity profile shows a satisfactory compromise, with high sensitivity (0.91) at a high specificity (0.93), constituting the optimum cut-off point (0.44) (Figure 21). The equation of the developed model determining the probability of sufferingfrom preclinical-AD status is shown.

$$\Pr(preclinical - AD) = \frac{e^{LP}}{1 + e^{LP}}$$

where LP = −6.566–0.153 * Female + 0.164 *Age—11.622 * A − 28.241 * B − 3.277 * C + 2.457 * D + 6.391 * E + 8.988 * F − 0.174 * G + 0.315 * H + 9.298 * I − 0.323 * J

A: 15-*epi*-15-F_{2t}-IsoP; B: PGE_2; 15-keto-15-E_{2t}-IsoP; D: 15-keto-15-F_{2t}-IsoP; E: 15-E_{2t}-IsoP; F: $PGF_{2\alpha}$; G: 4(*RS*)-4-F_{4t}-NuroP; H: 1a,1b-dihomo-$PGF_{2\alpha}$; I: 10-*epi*-10-F_{4t}-NeuroP; J: 14(*RS*)-14-F_{4t}-NeuroP

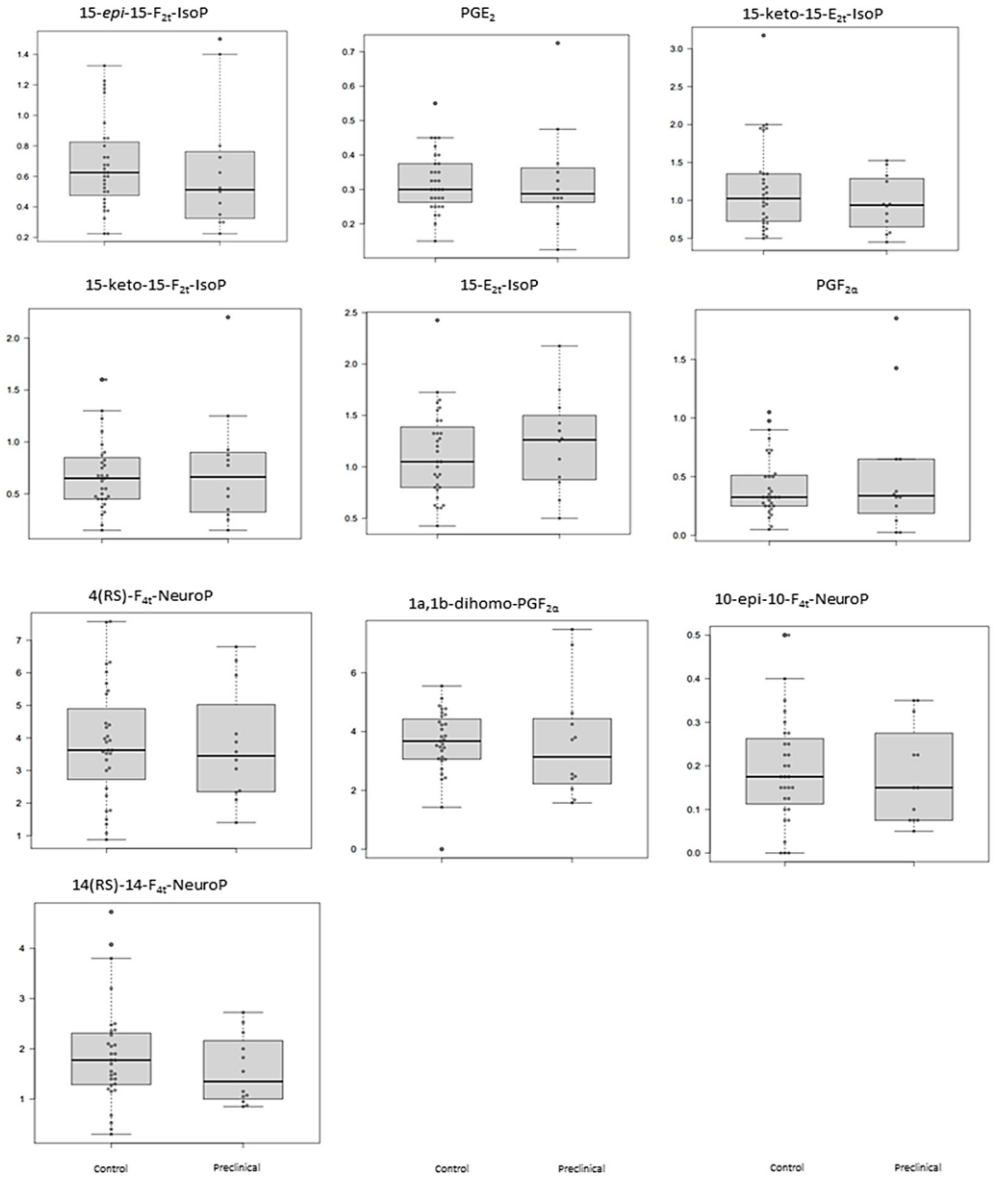

Figure 17. Box plots representing the concentrations in plasma samples for each analyte in control and preclinical-AD groups. Boxes represent the 1st and 3rd quartiles, and the black lines, the median.

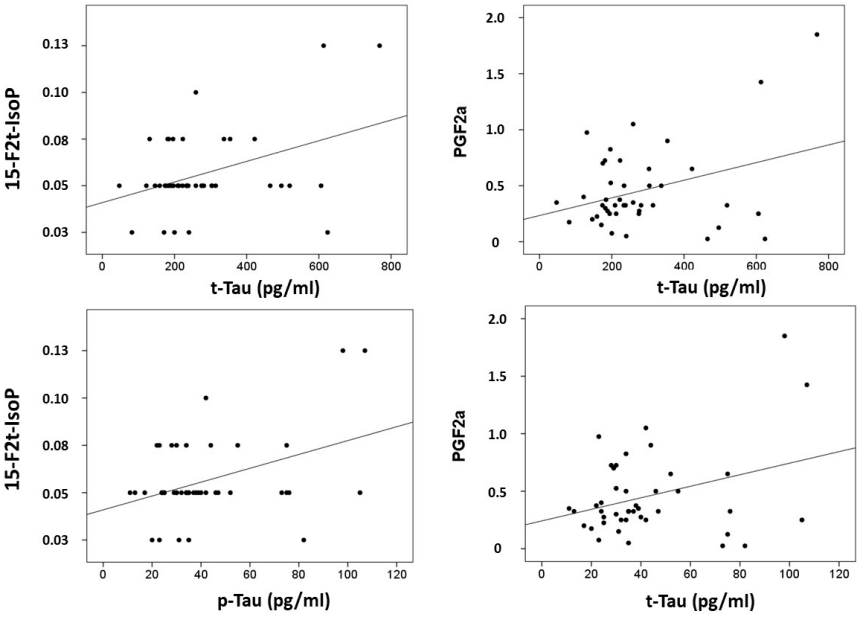

Figure 18. Correlation plots between plasma metabolites and CSF biomarkers.

Table 17. Model parameters.

Variables	*Estimate*	*exp.Estimate.*
(Intercept)	-6.566	0.001
Gender (Females)	-0.153	0.858
Age	0.164	1.178
15-epi-15-F_{2t}-IsoP	-11.622	0
PGE_2	-28.241	0
15-keto-15-E_{2t}-IsoP	-3.277	0.038
15-keto-15-F_{2t}-IsoP	2.457	11.671
15-E_{2t}-IsoP	6.391	596.158
$PGF_{2\alpha}$	8.988	8003.721
4(RS)-4-F_{4t}-NeuroP	-0.174	0.841
1a,1b-dihomo-$PGF_{2\alpha}$	0.315	1.371
10-*epi*-10-F_{4t}-NeuroP	9.289	10823.421
14(*RS*)-14-F_{4t}-NeuroP	-0.323	0.724
Lambda	0.004	

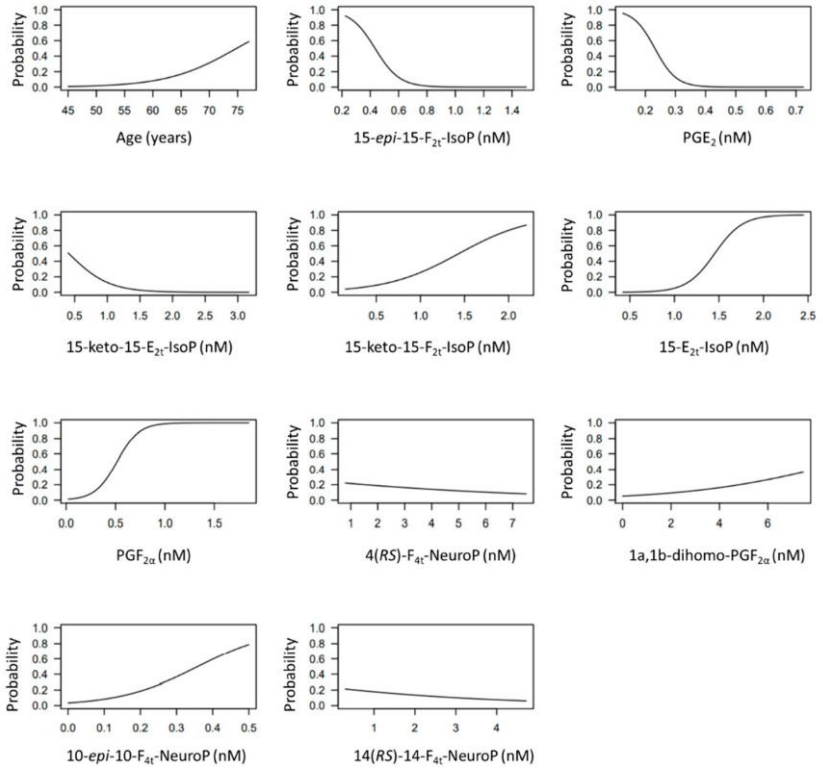

Figure 19. Conditional effect plots for each variable included in the model to predict the probability of preclinical-AD.

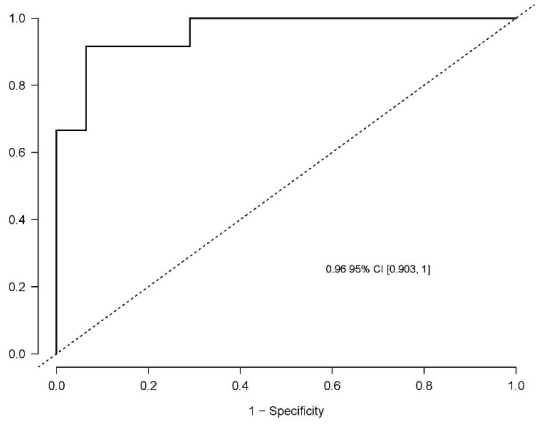

Figure 20. Receiver operating characteristic curve for the diagnostic model. The area under curve (AUC) is 0.96 (95% Confidence interval (CI), 0.903–1).

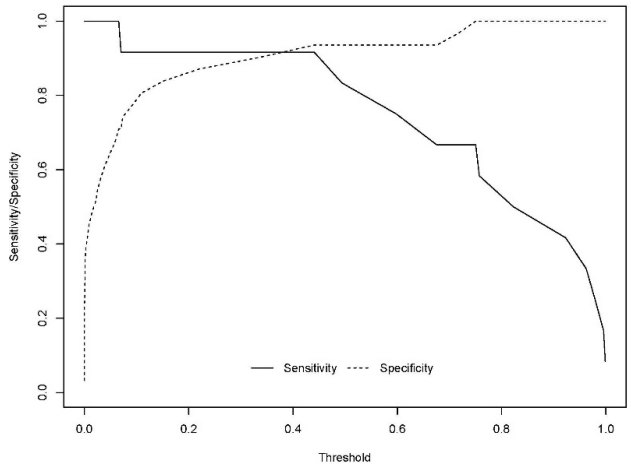

Figure 21. Sensitivity and specificity profile plot. The continuous line represents the relationship between the probability threshold set in the model's prediction and the sensitivity. The dashed line represents the relationship between the probability threshold and the specificity.

3. Discussion

In this work, some lipid peroxidation compounds were measured simultaneously in plasma samples from preclinical AD and healthy elderly participants, using UPLC-MS/MS as an analytical technique. These biomarkers did not show statistically significant different levels between both groups, although small differences could be observed for each metabolite. In addition, some of them showed a correlation with specific CSF biomarkersfor AD (t-Tau, p-Tau) and with neuropsychological tests (RBANS.DM, CDR), showing a certain relationship with early AD development. Thus, a multivariate model was developed including some of these lipid peroxidation compounds, and showing their potential utility in discrimination between preclinical AD patients and healthy participants. In fact, the multivariate model takes into account the effect of each individual predictor, which could change in the presence of other variables, generating a composed algorithm, and it provides accurate predictions. These compounds were studied because they can reflect specific impairment of brain white matter or grey matter. However, their specificity would be determined in further studies, because there is no clear evidence that potentially detectable changes would be

AD-specific, or if they would be general biomarkers of impairment of brain lipid metabolism.

In the literature, some studies focused on searching for AD plasma biomarkers, mainly lipidic molecules were assayed [163,168]. However, most of them were based on participants with MCI and AD, all of them were patients with clinical symptoms (memory loss, cognitive decline), but none of them evaluated the group of well-characterized preclinical participants [118,168,243]. In fact, a previous work from our group was focused on the determination of lipid peroxidation compounds (isoP, NeuroP, isoF, NeuroF) in plasma samples from MCI-AD patients, developing a diagnosis model [168]. In that model, the selected compounds were 15-*epi*-15-F_{2t}-IsoP, 15-E_{2t}-IsoP, $PGF_{2\alpha}$, 4(*RS*)-F_{4t}-NeuroP, 14(*RS*)-14-F_{4t}- NeuroP, and *ent*-7(*RS*)-7-F_{2t}-dihomo-IsoP. All of them, except *Ent*-7(*RS*)-7-F_{2t} dihomo-IsoP, were included in the present diagnosis model to predict AD in presymptomatic stage (preclinical AD). However, higher concentrations for these compounds were found in MCI- AD patients than in healthy participants; while lower concentrations were obtained for 15-*epi*-15-F_{2t}-IsoP and 4(*RS*)-F_{4t}-NeuroP in preclinical AD patients. These differences could be explained by the disease progression. In addition, the new developed model included more variables (PGE_2, 15-keto-15-E_{2t}-IsoP, 15-keto-15-F_{2t}-IsoP, 1a,1b-dihomo-$PGF_{2\alpha}$, 10-*epi*-10-F_{4t}-NeuroP) in order to improve the accuracy (AUC validated = 0.90) in comparison with the previous model (AUC validated = 0.82) [168].

Recent research has focused on earlier AD stages, before the appearance of the first clinical manifestations of the disease. In general, these studies were about plasma Aβ42/Aβ40 ratio, showing an AUC of 0.78 in the discrimination between normal cognitive individuals with PET Aβ positivity and negativity [244]. In addition, plasma Aβ levels showed an association with dementia (MMSE and the Geriatric Mental State Schedule (GMS)) and AD [245]. However, other study showed that plasma Aβ levels could not predict AD in preclinical participants [246,247]. A further study focused on plasma p-Tau revealed its utility in AD diagnosis and prognosis, showing increased values since preclinical stages and an accuracy of 85% in AD dementia diagnosis [247]. However, the present work is thefirst study evaluating lipid peroxidation compounds in preclinical AD patients accurately diagnosed by CSF

biomarkers.

Similarly, some of the studied biomarkers were lipidic compounds in plasma from preclinical AD participants [248]. In fact, the study carried out by Mapstone et al. analyzed lipids (phosphatidylcholine, Lysophosphatidylcholine, acylcarnitines, etc.), and it was carried out following the progression along 5 years, showing their potential utility as progression AD biomarkers [243].

The model developed in the present work was based on the plasma levels of 10 lipid peroxidation compounds. It is shown that an increase in the levels of these biomarkers (15-keto-15-F_{2t}-IsoP, 15-E_{2t}-IsoP, $PGF_{2\alpha}$, 10-*epi*-10-F_{4t}-NeuroP) could increase the probability of suffering from AD. Previous studies showed the utility of models based on plasma lipids as predictor approach of conversion amnestic MCI to AD or AD progression since preclinical stages [243,249]. The biomarkers determined in these studies are mainly related to membrane integrity, while ours are derived from OS. Another panel including 17 lipids can predict cognitive decline and brain atrophy in AD and it is related to clinical diagnosis in AD and t-Tau CSF levels [250].

Early AD diagnosis remains a big challenge for human sciences. There is a high need for easily available biomarkers now that specific biomarkers have been described. These specific biomarkers are invasive and expensive; so minimally invasive biomarkers are in demand. The utility of these putative biomarkers can be found in the diagnostic paradigm, identifying people at risk for developing cognitive impairment, with a biological suspicion of specific or non-specific neurodegeneration, or other pre-diagnostic characteristics. In addition, these biomarkers could be useful in identifying subgroups with different disease evolution, different therapeutic response, and different neuropsychological dysfunction.

Among the study limitations, it is important to highlight the small sample used. This limitation is an evident issue and the results of a study with a higher number of cases cannot be anticipated. However, the present study could be considered exploratory. It is important to remark that the participants were selected in an asymptomatic stage, and highlight the difficulties of realizing CSF studies in asymptomatic cases. Another limitation is the exclusion of cases with other similar neurodegenerative diseases. Different patterns of biomarkers are expected in other neurodegenerative diseases, but

in the present study, they were not evaluated. Therefore, these are preliminary results and further analysis in a large external cohort is required.

4. Conclusions

Lipid peroxidation biomarkers were determined in plasma from participants with preclinical AD and healthy elderly participants, showing no differences individually. However, these biomarkers showed a correlation with other specific AD CSF biomarkers and neuropsychological status. The multivariate model including 10 of these biomarkers constitutes a promising diagnostic tool to be applied to the general population in early AD detection. However, further validation studies are necessary to confirm the utility of this potential model for preclinical AD diagnosis.

Chapter 7. Lipid peroxidation biomarkers correlation with medial temporal atrophy in early Alzheimer Disease

1. Summary

The aim of this chapter was to evaluate the correlation between plasma lipid peroxidation biomarkers and anatomical brain changes, specifically medial temporal atrophy. For this, there were evaluated the temporal brain atrophy by means of visual ratings from magnetic resonance imaging (MRI) and a set of lipid peroxidation biomarkers from plasma samples were analysed in participants with AD (n=80) and healthy controls (n=32). The correlation between plasma lipid peroxidation biomarkers and atrophy visual ratings was evaluated. In addition, two statistical models using PLS analyses were carried out, the first based on neuroimaging analysis (visual ratings) and the second based on plasma lipid peroxidation biomarkers levels.

2. Results.

2.1. Participants' description

In Table 18, demographic and clinical characteristics from the study population are summarized. Age and gender showed statistically significant differences between both groups, so they were included as covariates in the multivariate models. As expected, clinical variables (CSF Aβ42, CSF t-Tau, CSF p-Tau, RBANS-DM, CDR, FAQ, MMSE) showed statistically significant differences between case and control groups.

Table 18. Demographic and clinical variables for the participants.

Variables	Control (n=32)	Case (n=80)	P value
Age (years, median (IQR))	66 (62-69)	71 (68-74)	0.000*
Gender (female, n (%))	11 (34%)	47 (59%)	0.020*
Aβ42 (pg mL^{-1}, median (IQR))	1192 (1051-1444)	588 (441-676)	0.000*
t-Tau (pg mL^{-1}, median (IQR)))	171 (108-284)	523 (361-775)	0.000*
p-Tau (pg mL^{-1}, median (IQR)))	44 (27-57)	82 (66-116)	0.000*
CDR (median (IQR))	0 (0-0)	0.5 (0.5-1)	0.000*
MMSE (median (IQR))	30 (28-30)	22 (18-26)	0.000*
RBANS.DM (median (IQR))	100 (92-106)	44 (40-52)	0.000*
FAQ (median (IQR))	0 (0-0)	7 (3-13)	0.000*
GDS (median (IQR))	3 (1-7)	7 (4-11)	0.021*
Fazekas (median (IQR))	0 (0-1)	1 (0-1)	0.018*
MTA-RIGHT (median (IQR))	0 (0-0)	2 (1-2)	0.000*
MTA-LEFT (median (IQR))	0 (0-0)	1 (1-2)	0.000*
MTA (R+L) (median (IQR))	0 (0-0)	3 (2-4)	0.000*

2.2. Image measurement data

Using neuroimaging techniques, the variables determined were MTA right (MTA-R), left (MTA-L), sum (MTA-S) and Fazekas. As can be seen in Table 18, the three MTA indices showed statistically significant differences between groups, as well as Fazekas.

2.3. Analyte determination

In Table 19 medians of analytes levels determined in plasma from case and control groups are summarized. 8-iso-15(*R*)-$PGF_{2\alpha}$, 2,3-dinor- $iPF_{2\alpha}$-III, 8-iso-15-keto-PGE_2, 4(*RS*)-F_{4t}-NeuroP, neuroprostanes, isoprostanes, *Ent*-7(*RS*)-F_{2t}-dihomo-IsoP and 17-*epi*-17-F_{2t}-dihomo-IsoP, showed higher levels in the case group than in the control group. Inversely, $PGF_{2\alpha}$, 14(*RS*)-14-F_{4t}-NeuroP, 5-$iPF_{2\alpha}$-VI and 7(*RS*)-*ST*-Δ^8-11-dihomo-IsoF showed higher levels in the control group. Nevertheless, only 8-iso-15(*R*)-$PGF_{2\alpha}$ ($p = 0.042$), $PGF_{2\alpha}$ ($p = 0.001$), 4(*RS*)-F_{4t}-NeuroP ($p = 0.030$), neuroprostanes

(p = 0.001), isoprostanes (p = 0.006) and 17-*epi*-17-F_{2t}-dihomo-IsoP (p = 0.008) showed statistically significant differences between groups.

Table 19. Concentrations of analytes in plasma samples from participants groups.

	Control (n=32)	Case (n=80)	P value
8-iso-15(R)-$PGF_{2\alpha}$	0.25 (0.20-0.35)	0.30 (0.23-0.49)	0.042*
PGE_2	0.06 (0.01-0.75)	0.09 (0.00-0.28)	0.693
2,3-dinor-$iPF_{2\alpha}$-III	0.00 (0.00-0.00)	0.00 (0.00-0.03)	0.950
8-iso-15-keto-PGE_2	0.06 (0.00-0.17)	0.13 (0.00-0.34)	0.425
8-iso-15-keto- $PGF_{2\alpha}$	0.25 (0.18-0.33)	0.26 (0.13-0.35)	0.754
8-iso-PGE_2	0.28 (0.15-1.98)	0.39 (0.18-0.78)	0.689
5-$iPF_{2\alpha}$-VI	0.94 (0.67-1.22)	0.71 (0.35-1.22)	0.123
8-iso-$PGF_{2\alpha}$	0.02 (0.01-0.03)	0.02 (0.01-0.03)	0.841
$PGF_{2\alpha}$	0.74 (0.60-0.94)	0.48 (0.25-0.78)	0.001*
4(RS)-F_{4t}-NeuroP	1.03 (0.71-1.24)	1.15 (0.96-1.33)	0.030*
1a,1b-dihomo-$PGF_{2\alpha}$	0.00 (0.00-0.00)	0.00 (0.00-0.00)	0.326
Neuroprostanes	0.29 (0.22-0.38)	0.83 (0.26-1.52)	0.001*
10-epi-10-F_{4t}-NeuroP	0.11 (0.07-0.18)	0.09 (0.03-0.18)	0.390
14(RS)-14-F_{4t}-NeuroP	0.90 (0.00-1.51)	0.80 (0.29-1.27)	0.930
Isoprostanes	0.22 (0.18-0.34)	0.32 (0.23-0.40)	0.006*
Ent-7(RS)-F_{2t}-dihomo-IsoP	0.08 (0.05-0.17)	0.13 (0.08-0.18)	0.145
17-F_{2t}-dihomo-IsoP	0.00 (0.00-0.00)	0.00 (0.00-0.00)	0.302
17-epi-17-F_{2t}-dihomo-IsoP	0.00 (0.00-0.00)	0.00 (0.00-0.03)	0.008*
7(RS)-10-epi-SC-Δ^{15}-11-dihomo-IsoF	0.00 (0.00-0.00)	0.00 (0.00-0.00)	0.150
7(RS)-ST-Δ^{8}-11-dihomo-IsoF	0.10 (0.01-0.25)	0.05 (0.01-0.19)	0.199
Neurofurans	0.18 (0.11-0.26)	0.18 (0.13-0.27)	0.762
Isofurans	0.09 (0.06-0.22)	0.10 (0.08-0.16)	0.399

2.4. Correlation between plasma lipid peroxidation biomarkers levels and image indices

Relationship between neuroimaging indices and plasma biomarker levels was analyzed, and some statistically significant correlation was observed. In fact, MTA in right brain lobe showed positive correlation with neuroprostanes ($r = 0.242$, $p = 0.010$), and 17-*epi*-17-F_{2t}-dihomo-IsoP ($r = 0.223$, $p = 0.018$), while it showed negative correlation with $PGF_{2\alpha}$ ($r = -0.259$, $p = 0.006$). Similar results were obtained with MTA in the left side, positive correlation was observed with neuroprostanes ($r = 0.213$, $p = 0.024$), and 17-*epi*-17-F_{2t}-dihomo-IsoP ($r = 0.214$, $p = 0.024$), while it showed negative correlation with $PGF_{2\alpha}$ ($r = -0.305$, $p = 0.001$). In the same sense, the sum of MTA in both brain lobes showed correlation with neuroprostanes ($r = 0.234$, $p = 0.013$), 17-*epi*-17-F_{2t}-dihomo-IsoP ($r = 0.224$, $p = 0.018$) and $PGF_{2\alpha}$ (PCC $= -0.288$, $p = 0.002$). In addition, Fazekas, index related to vascular brain disease, showed correlation with 17-F_{2t}-dihomo-IsoP ($r = 0.215$, $p = 0.023$) (see Figure 22).

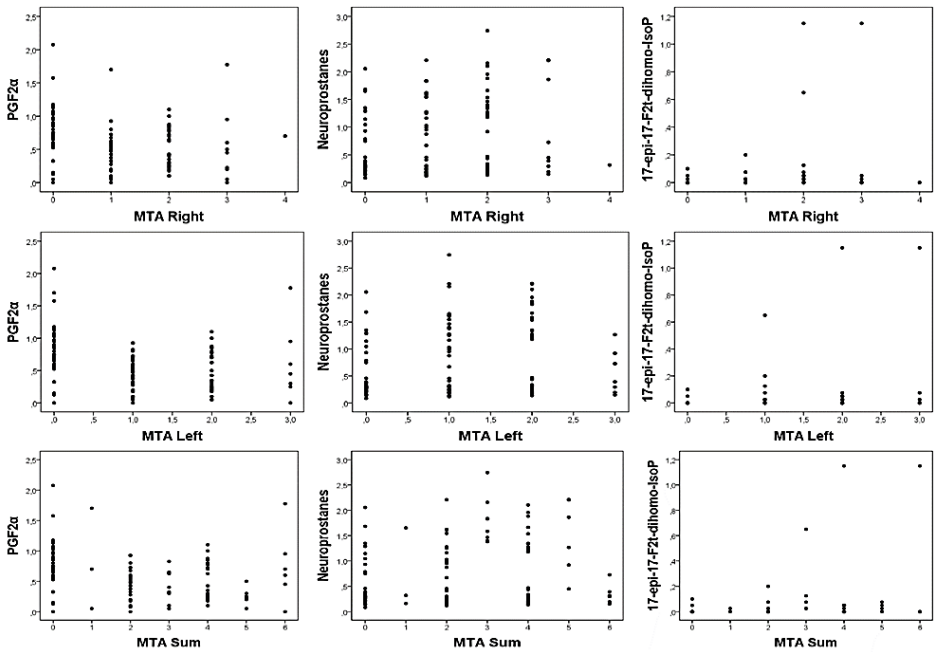

Figure 22. Correlations between neuroimaging variables and plasma biomarkers levels.

2.5. Multivariate analysis

Two statistical models were carried out, the first based on neuroimaging analysis and the second based on plasma lipid peroxidation biomarkers levels. As it is shown in Figure 23a, the model based on neuroimaging analysis showed a correlation between the different MTA measures (right and left lobe and total MTA), but age and gender did not correlate with them. Also, the scatter plot (Figure 23b) showed a satisfactory separation between participants groups. In this sense, the case group is characterized by higher levels of MTA. For this model, the AUC-ROC is 0.929 (CI 95%, 0.882–0.977). Besides, this model has a sensitivity of 90.00%, a specificity of 84.38% and its positive and negative predictive values are 93.51% and 77.14, respectively.

(a) (b)

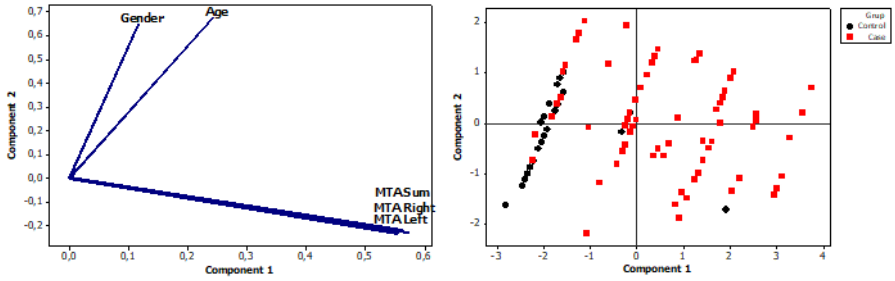

(c) (d)

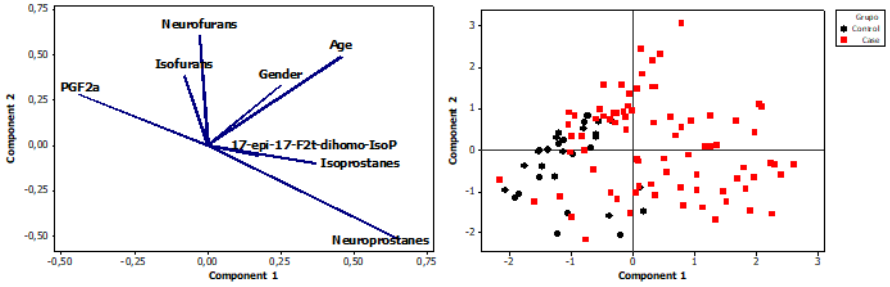

Figure 23. PLS models. First, model based on neuroimaging techniques (a) loading graph and (b) score plot. Second, model based on plasma biomarkers (c) loading plot and (d) score plot.

Regarding the model constructed by plasma biomarkers (neuroprostanes, isoprostanes, neurofurans, isofurans, 17-*epi*-17-F_{2t}-dihomo- IsoP, $PGF_{2\alpha}$), a negative correlation between $PGF_{2\alpha}$ and isoprostanes and isofurans was observed, but age and gender did not correlate with biomarkers (Figure 23c). Also, Figure 23d shows a satisfactory discrimination between case and control groups. This model could diagnose AD or not-AD with an accuracy of AUC-ROC = 0.900 (0.845–0.956). The diagnosis indices for this model were sensitivity 72.5%, specificity 100%, negative predictive value 59.26% and positive predictive value 100%.

3. Discussion

The parameter MTA is commonly related to cerebrovascular dementias [251]. Previous works showed that this morphological alteration is associated with MCI and AD, showing higher damage grade in AD than in MCI patients, as well as a correlation with neuropsychological evaluation tests (e.g. MMSE, CDR) [252]. In this sense, some cut-off values for MTA to be used as AD diagnosis and MCI prognosis were established [253]. In addition, MTA is related to cognitive impairment in patients with Dementia with Lewy Bodies [254]. Medial temporal lobe atrophy evaluation contributes to a better diagnosis accuracy [255]. Moreover, correlations between MTA and CSF biomarkers t-Tau and p-Tau for different variants of Early-Onset Alzheimer Disease (EOAD) were described [256]. Nowadays, neuropsychological tests and CSF biomarkers are employed as AD diagnosis, these two parameters could be related to MTA, so the evaluation of atrophy could be useful in AD diagnosis, as well as the lipid peroxidation study as a possible pathway implied in AD. Our results showed that a diagnosis model based only on this atrophy evaluation could diagnose AD with an accuracy of 0.929. It could avoid actual lumbar puncture used in AD diagnosis nowadays, as well as neuropsycological evaluations that require a considerable amount of time on part of specialized staff and is tiresome for patients. In this sense, other diagnosis models for AD based on neuroimaging techniques have been developed. Specifically, a model based on MRI and Positron Emission Tomography (PET) was able to differentiated between AD, MCI and healthy control groups with accuracies between 0.75 and 0.95 [257]. The model developed by [258] was able to distinguish between EOAD and behavioral variant of frontotemporal dementia with an accuracy of 0.82 based on cortical thickness and DT

(diffusion tensor) MRI measures [258]. Our model shows better accuracy, but its specificity is required to be evaluated employing other dementias or neurodegenerative diseases. This model shows good diagnosis indices, especially its high specificity that could allow the application of this model as a preliminary screening test although it probably needs other tests to give a reliable diagnosis.

Regarding the evaluation of possible correlations between neuroimaging results (MTA) and different lipid peroxidation products in plasma samples form AD and healthy participants, the highest correlations were between brain MTA and neuroprostanes. Therefore, specific brain alterations could be measured in plasma samples by means of these lipid peroxidation products [259]. As MTA scale is based mainly in grey matter atrophy, neuroprostanes could explain this alteration evaluation [142]. In addition, neuroprostanes levels were statistically significant different between AD and healthy participants. Therefore, they are satisfactory AD biomarkers. In addition, the dihomo-isoprostanes could be obtained from brain white matter oxidation. The correlation found between MTA and these compounds could be explained as some white matter atrophy that occurs together with the grey matter alterations in medial temporal lobe mainly in the hipocampus from AD patients. We also analyzed correlations between our biomarkers and Fazekas, which is a scale based on brain white matter lesions and it is usually related to vascular pathologies. This scale is not AD specific but it could help to discard AD as a cause of vascular dementia [260]. Punctuation for this scale showed statistically significant correlation with 17-F_{2t}-dihomo-IsoP that is a white matter lipid peroxidation product. So, this biomarker could be useful in the study of white matter lesions present in different neurodegenerative diseases, not only in AD, and sometimes it could serve to discard AD diagnosis or to differentiate it from frontotemporal dementia whose symptoms could be confused [261].

Regarding plasma biomarkers, neuroprostanes and neurofurans are derived from DHA oxidation, while isoprostanes and isofurans come from the AA oxidation [262], and dihomo isoprostanes (e.g. 17-*epi*-17-F_{2t}-dihomo- IsoP) come from AdA oxidation [263]. DHA is the major polyunsaturated fatty acid in the brain [43] so, the presence of neuroprostanes and neurofurans in different human biofluids is highly brain specific. For the quantification of these lipid peroxidation biomarkers in plasma samples, the analytical

method was previously described [168], and the developed model could distinguish between AD and healthy patients with an accuracy of 0.90. Therefore, it could reflect brain lipid peroxidation damage (neuroprostanes, neurofurans, 17-*epi*-17-F_{2t}-dihomo-IsoP), and OS at systemic level in AD patients. In fact, it was shown in previous works [264,265]. Also, the presence of a negative correlation between $PGF_{2\alpha}$ and MTA, and its capacity to discriminate between AD and control groups ($p = 0.001$) are remarkable. This analyte is an inflammatory mediator and it is derived from AA oxidation by an enzymatic pathway [266]. Previous studies showed that inflammation is related to AD progression [267], and inhibition of cyclooxygenases that are implied in prostaglandin pathway in AD models, showed beneficial effects. So, probably in very early stages of the disease these mechanisms try to avoid the disease progression [268]. In addition, it is known that in neurodegenerative diseases the BBB) is altered [214]. Specifically in AD, previous works showed an increase on BBB permeability [215], allowing that different lipid peroxidation products generated in brain could pass through the BBB, and being found at peripheral level. For this reason, we constructed a model based on plasma biomarkers levels that could reflect brain MTA including damage to white matter, grey matter and also inflammatory mediators. That model shows really satisfactory diagnosis indices. Its specificity of 100% is especially remarkable. In our study, all patients diagnosed as positive with our model were AD patients. By contrast, its weak point is the sensitivity (72.5%). For that reason, the new model could serve as a screening test. Only when the test result is negative, patients will have to undergo additional tests to confirm the diagnosis. It would improve the diagnosis based on only image tests because biomarkers reflecting specific brain atrophy in AD patients would constitute an integrative vision of oxidative status [269]. In any case, more studies are required to confirm this diagnosis capacity, and other dementias or neurodegenerative diseases have to be included in the study to evaluate the model specificity.

4. Conclusions

Correlation between plasma neuroprostanes and dihomo-isoprostanes with neuroimaging data could indicate that the neurodegeneration occurred in different brain areas is related to OS damage and brain lipid peroxidation. Lipid peroxidation biomarkers could reflect brain damage that accompanied neurodegenerative diseases. However, their specificity

should be studied comparing the results with other neurodegenerative and brain pathologies. AD diagnosis model based on lipid peroxidation biomarkers shows similar accuracy as the neuroimaging model, and it reflects the implication of this pathway in the pathology since its early stages. The model based on lipid peroxidation biomarkers (neuroprostanes, neurofurans, isoprostanes, isofurans, 17-*epi*-17-F_{2t}-dihomo-IsoP, $PGF_{2\alpha}$) could be used as a screening test for AD diagnosis avoiding in many cases invasive and expensive diagnosis techniques.

RESULTS, DISCUSSION AND CONCLUSIONS

SECTION II. Omic studies

Chapter 8. Plasma metabolomics in early Alzheimer's disease patients diagnosed with amyloid biomarker

1. Summary

The aim of this chapter was to identify reliable plasma biomarkers associated to MCI-AD by means of untargeted metabolomics. For this, an untargeted metabolomics study based on UPLC has been carried out using plasma samples from patients with MCI-AD (n=29) and controls (n=29). The differences between metabolomic profiles from MCI-AD and controls were investigated using ElasticNet. Then, an attempt was made to identify the selected variables by The Human Metabolome Database, all ions fragmentation modes, or confirmation with standard when it was possible.

2. Results

2.1. Participants demographic and clinical characteristics

The demographic and clinical characteristics of participants in this study are summarized in Table 20. As we can see, age and gender showed differences between groups and for that reason they were included in the multivariate model as co-variables. As expected from participants' classification, temporal atrophy was higher in MCI-AD, and the CSF biomarkers showed significant differences between groups. Regarding the neuropsychological evaluations, the RBANS (IM, V/C, L, A, DM) and MMSE scores were lower in MCI-AD patients than in control subjects, while the FAQ and CDR scores were higher in the MCI-AD group.

Table 20. Demographic and clinical characteristics of study participants.

Variable		Control (n = 29)	MCI-AD (n = 29)	P value
Age (years) (median (IQR))		65 (63, 70)	72 (69, 75)	0.002*
Gender (female) (n (%))		9 (31.03 %)	19 (65.52%)	0.016*
Studies levels (n (%))	**Basics**	6 (20 %)	17 (59 %)	0.010
	University	11 (38 %)	5 (17%)	
Medications (n (%))	**Statins**	10 (34%)	17 (59%)	0.149
	Fibrates	3 (10%)	2 (7%)	
	Benzodiazepines	2 (7%)	4 (13.79%)	
	Opiates	0 (0%)	0 (0%)	
	Antiepileptics	1 (3.45%)	0 (0%)	
	Antihipertensives	10 (35.71%)	14 (48.28%)	
	Corticoids	0 (0%)	2 (6.9%)	
Comorbidity (n (%))	**Dyslipidemia**	10 (35.71%)	16 (55.17%)	0.621
	Diabetes	3 (10%)	3 (10.34%)	
	Hypertension	11 (38%)	13 (44.83%)	
	Heart Disease	1 (3.45%)	0 (0%)	
Smoking status (n (%))	**Yes**	1 (3.45%)	2 (6.9%)	0.778
	Former smoker (more than 10 years)	9 (31%)	7 (24.14%)	
Alcohol or drugs consumption (n (%))		6 (21.43%)	3 (10.34%)	0.301
Presenile family background (n (%))	**None**	22 (76%)	22 (88%)	0.381
	First grade	5 (17%)	5 (17%)	
	Second grade	2 (7%)	0 (0%)	
Depression (n (%))		3 (10.34%)	4 (14%)	0.883
Anxiety (n (%))		1 (3.45%)	3 (10.34%)	0.246
Temporal atrophy (n (%))		2 (7.14%)	20 (69%)	0.000*
CSF Aβ42 (pg mL^{-1}) (median (IQR))		1256 (1164, 1464)	600 (496, 687)	0.000*
CSF t-Tau (pg mL^{-1}) (median (IQR))		196 (141, 298)	590 (465, 782)	0.000*
CSF p-Tau (pg mL^{-1}) (median (IQR))		48 (37, 60)	84 (73, 104)	0.000*
RBANS.MI (median (IQR))		93 (84,107)	61 (51,75)	0.000*
RBANS.V/C (median (IQR))		101 (86,112)	81 (75,92)	0.013*
RBANS.L (median (IQR))		92 (86,97)	71 (59,85)	0.000*
RBANS.A (median (IQR))		100 (82,112)	68 (56,81)	0.000*
RBANS.DM (median (IQR))		100 (92, 106)	48 (40, 66)	0.000*
MMSE (median (IQR))		30 (28,30)	25 (24,28)	0.000*
FAQ (median (IQR))		0 (0, 0)	5 (0, 8.5)	0.000
CDR (n (%))	**0**	29 (100%)	5 (17%)	0.000
	0.5	0 (0%)	18 (62%)	
	1	0 (0%)	6 (21%)	

IQR: Inter-quartile range.

2.2. Multivariable analysis and selection of discriminant variables

Elastic net models were used to select discriminant variables. Outcomes of these models identified 24 and 29 discriminant variables between MCI-AD and control subjects in positive and negative ionization mode, respectively. The different levels of these variables between participants groups were represented in heat map visualizations of the variables' values (Figure 24).

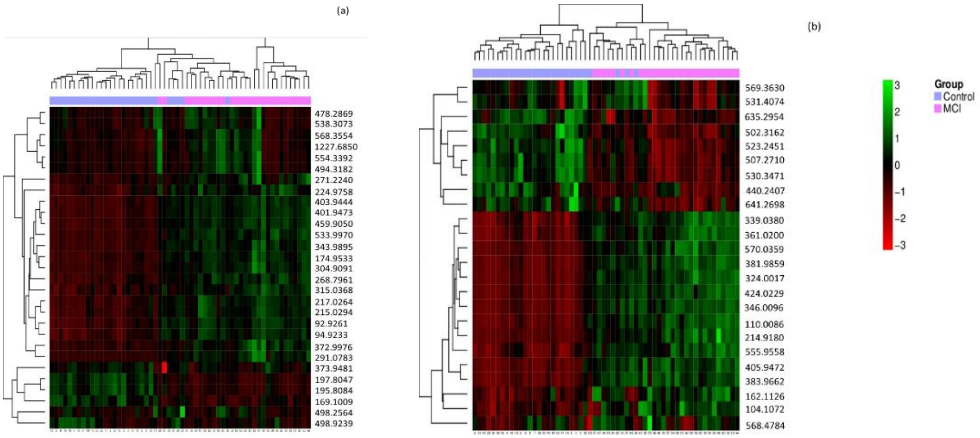

Figure 24. Heatmap including the selected variables by the elastic net logistic regression model. *Z*-scores for each variable are represented in a color-coded scale were values at the mean are black, values under the mean are red and values over the mean are green. Ordering of rows and columns of the heatmap is performed by hierarchical clustering of the observations (columns) and of the variables (rows). a) for the negative ionization mode, and b) for the positive ionization mode.

As we can see, the levels of relative increase were depicted in green, while the levels of relative decrease were depicted in red. In this sense, most of the metabolites showed higher levels in MCI-AD group than in control group. The discrimination power of these selected variables was measured as bootstrap validated AUC, being 0.993 and 0.990 in negative and positive ionization mode, respectively.

2.3. Metabolites identification

From the 53 variables selected by the elastic net models, 16 variables were preliminarily identified as potential metabolites, only 4 of these variables were tentatively identified with their MS fragments pattern (MS/MS and/or all-ions fragmentation), being only 1 variable finally confirmed with its pure standard (Table 21).

Table 21. Metabolomic variables selected by Elastic Net statistical models and preliminarily identified by The Human Metabolome Database.

Mass (m/z)	**Retention time (min)**	**Adduct**	**Formula**	**Annotation**	**Confirmation mode**	**Compound class/ Metabolism**	**[a]Fold change**
104.1072	0.60	$[M+H]^+$	C5H14NO	**Choline**	MS fragmentation confirmation Standard confirmation	Quaternary ammonium/ Cholinergic system	1.582436
162.1126	0.60	$[M+H]^+$	C7H15NO3	L-carnitine; Malonyl-Carnitin		Amines/ Energy metabolism and fatty acid oxidation	1.750063
		$[M+H]^+$	C7H16NO3	S-Carnitinium		Quaternary ammonium (Carnitines)/fatty acid oxidation	
324.0017	0.68	M^+		UNKNOWN			3.211441
339.0380	0.65	$[M+H]^+$	C14H10O10	2,3,4-trihydroxy-5-(3,4,5-trihydroxybenzoyloxy)benzoic acid; 2,4,5-trihydroxy-3-(3,4,5-trihydroxybenzoyloxy)benzoic acid; 3,4-dihydroxy-5-(2,3,4,5-tetrahydroxybenzoyloxy)benzoic acid; 4,4',5,5',6,6'-hexahydroxy-[1,1'-biphenyl]-2,2'-dicarboxylic acid		Organic compound (depsides and depsidones)/Benzene hydroxylation	1.60648
361.0200	0.65	$[M+Na]^+$					1.834496
346.0096	0.68	M^+		UNKNOWN			2.529556
381.9859	0.66	M^+		UNKNOWN			2.702668
383.9662	0.70	M^+		UNKNOWN			2.896863
405.9472	0.67	M^+		UNKNOWN			3.292516
424.0229	0.73	$[M+H]^+$	C16H13N3O7S2	5-Amino-4-hydroxy-3-(phenylazo)-2,7-naphthalenedisulfonic acid		Food dye	2.54245
485.2893	9.38	M^+		UNKNOWN			0.628327
502.3162	9.37	M^+		UNKNOWN			0.632845
507.2710	9.37	M^+		UNKNOWN			0.579632
523.2451	9.37	$[M+H]^+$	C28H39ClO7	4-Deoxyphysalolactone		Withanolides/inflammation pathways	

	0.00	$[M+H]^+$	C29H34N2O7	Bargustanine		Benzyllisoquinolines/Neuromuscular-blocking drugs	0.563752
530.3471	9.37	$[M+H]^+$		UNKNOWN			0.563486
531.4074	12.79	[M+H]+	C33H54O5	alpha-Tocopherol succinate		Vitamin E/Antioxidant activity	0.764254
555.9557	0.76	$[M+H]^+$		UNKNOWN			1.864629
568.4784	10.48	$[M+H]^+$		UNKNOWN			1.045444
569.3630	12.79	$[M+Na]^+$	C30H58O4S2	Dilauryl 3,3'-thiodipropionate		Dicarboxylic acids/Membrane formation	0.761616
570.0358	0.66	M^+		UNKNOWN			4.656571
635.2954	6.72	$[M+H]^+$	C35H42N2O9	**Rescinnamine**	MS fragmentation confirmation	Antihypertensive drug	0.903152
92.9260	0.62	M^-		UNKNOWN			1.424961
94.9233	0.62	M^-		UNKNOWN			1.400025
169.1009	1.03	M^-		UNKNOWN			0.780474
174.9533	0.54	M^-		UNKNOWN			1.731515
195.8083	0.65	M^-		UNKNOWN			0.515284
197.8046	0.65	M^-		UNKNOWN			0.48432
215.0294	0.62	$[M-H]^-$	C3H7ClO2	Chlorohydrin		Halohydrins/Cell membrane	1.648367
217.0264	0.62	$[M-H_20-H]^-$	C11H12N2S2	Brassinin		3-alkylindole (exogenous)	
		$[M+HCOO]^-$	C7H9O3P	Monomethyl phenylphosphonate		Exogenous	1.662713
		$[M-H_20-H]^-$	C7H12N2O5S	Cysteinyl-Aspartate		Dipeptide/Protein catabolism	
		$[M-H_20-H]^-$	C7H12N2O5S	Aspartyl-Cysteine		Dipeptide/Protein catabolism	
224.9758	0.72	M^-		UNKNOWN			1.577898
268.7960	0.61	M^-		UNKNOWN			1.513857
271.2240	9.61	M^-		UNKNOWN			1.564616
291.0783	0.70	M^-		UNKNOWN			8.59362
304.9090	0.53	M^-		UNKNOWN			2.562249
315.0368	0.64	$[M-H_20]^-$	C11H15N2O8P	Nicotinamide ribotide		Amide/Cellular energy maintenance	1.336687
		$[M-H_20]^-$	C11H16N2O8P	Beta-nicotinamide D-ribonucleotide			

343.9895	0.67	M^-		UNKNOWN			2.712838
372.9974	0.65	M^-		UNKNOWN			1.835085
373.9481	6.98	M^-		UNKNOWN			0.928195
401.9472	0.66	M^-		UNKNOWN			2.426884
403.9443	0.66	M^-		UNKNOWN			3.314504
459.9050	0.66	M^-		UNKNOWN			2.853813
478.2869	8.19	M^-		UNKNOWN			1.174307
494.3182	9.05						1.540692
498.2564	8.02	$[M-H]^-$	C25H42NO7P	Lyso PE(20:5/0:0); Lyso PE(0:0/20:5)		Lysophospholipid / Lipid metabolism	0.748392
498.9239	8.16	$[M-H]^-$	C6H16O18P4	Inositol 1,3,4,5-tetraphosphate; 1D-Myo-inositol 1,3,4,6-tetrakisphosphate; D-Myo-inositol 3,4,5,6-tetrakisphosphate; 1D-Myo-inositol 1,4,5,6-tetrakisphosphate		Second messengers in Ca2+ and Cl- regulation through membrane / Inositol metabolism	0.649237
533.9969	0.72			UNKNOWN			2.92495
538.3073	8.19	$[M-H_20]^-$	C29H44O8	**24,25-diacetylvulgaroside Cyasterone Soraphen A**	MS fragmentation confirmation	Exogenous Exogenous Macrolide/Lipid metabolism	1.185665
554.3392	9.05	$[M+HCOO]^-$	C25H52NO7P	**Lyso PE(20:0/0:0) or Lyso PE(0:0/20:0)**	MS fragmentation confirmation	Lysophospholipid / Lipid metabolism	1.534458
568.3554	9.39	M^-		UNKNOWN			1.351365
1227.6849	9.39	M^-		UNKNOWN			1.49062

[a]Fold change is calculated by the average value of the MCI-AD group compared to the control group.

Among the tentatively identified metabolites, first the variable m/z 635.2954 was identified as rescinnamine, a drug used for hypertension treatment. It is important to note that the incidence of hypertension did not show differences between control and MCI-AD groups (Table 20), so it is unlikely to be this compound. Second, the variable m/z 538.3073 was identified with three potential metabolites (24,25-diace- tylvulgaroside, cyasterone, soraphen A), 24,25-diacetylvulgaroside and cyasterone were exogenous products derived from fruits and plants [270,271], while soraphen A was a myxobacterium product that may be related to some infection in AD. So, we hypothesize that the metabolite with mass 538.3073 could be soraphen A. Third, the variable m/z 498.2564 was identified as lysophosphatidylethanolamines (Lyso PE (20:0/0:0) or Lyso PE (0:0/20:0)), breakdown products of phosphatidylethanolamine, present in cells of all organisms [272]. Finally, the variable m/z 104.1072 was also confirmed with its pure standard and identified as choline.

The relative levels of these variables in each group of participants are depicted in Figure 24. In general, the MCI-AD group showed increased levels for Lyso PE (m/z 498.2564), soraphen A (m/z 538.3073), and choline (m/z 104.1072). However, there is a small group of MCI-AD participants with decreased levels for Lyso PE (m/z 498.2564) and soraphen A (m/z 538.3073) (Figure 24). In Figure 25, the differences between MCI-AD and control groups are depicted for the metabolites verified by MS fragmentation patterns, showing statistically significant differences for choline ($p < 0.001$), rescinamine ($p < 0.001$) and Lyso PE ($p < 0.05$).

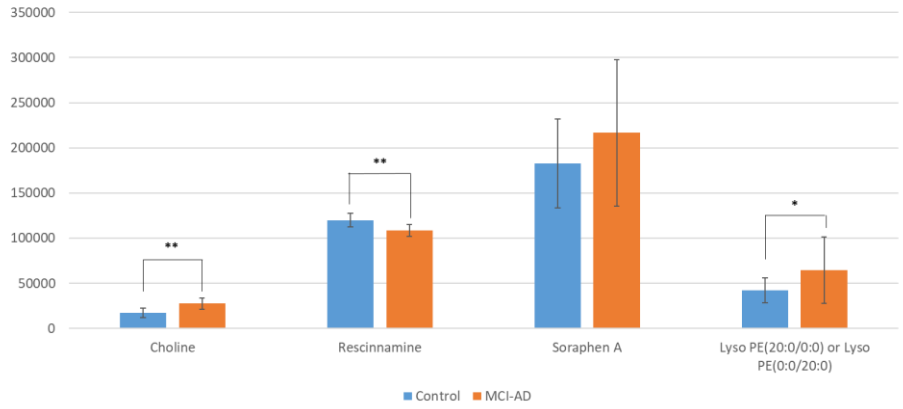

Figure 25. Bar graph representing the tentatively identified metabolites levels for each participants group (MCI-AD, control). (* $p < 0.05$, ** $p < 0.001$).

3. Discussion

An untargeted metabolomics study has been carried out in plasma samples to identify potential early AD biomarkers. For this, plasma samples from participants with CSF biomarker-confirmed diagnosis (healthy and MCI-AD), as well as a reliable and robust analytical method based on minimal sample treatment and UPLC-Q-ToF-MS chromatographic system were used. Specifically, the valuable samples from healthy and MCI-AD participants classified by specific AD biomarkers in CSF [25], together with the high quality, reproducibility and stability of the analytical method, provided high reliability to the experimental results. In fact, few studies in literature employed specific CSF biomarkers to identify clearly AD patients [87]. Also, few works have focused on AD patients at early stage [87,89,93,94,103], and few of them employed simple and robust untargeted analytical methods [94,103].

From the metabolomics results obtained in both mass spectrometry ionization modes, a multivariable statistical analysis was carried out to select the most discriminant variables between healthy individuals and MCI-AD patients. It was based on Elastic net penalized logistic regression, and the corresponding models obtained for each ionization mode provided high accuracy (AUC 0.990 and 0.993, respectively). However, most of previous works developed PLS discriminant models [52,92,94,97,101], adding all the studied variables into the model because PLS is not able to assign zero coefficients. Therefore,

PLS has the consequent limitations in metabolites selection and accuracy assessment. Nevertheless, elastic net is able to shrink the coefficients of uninformative variables exactly to zero, selecting automatically the most informative variables. This entails that the coefficients of elastic net model are more stable and reliable compared with those of PLS. Another difference between both statistical models is related to the selection of relevant variables. For elastic net, the variable selection is performed at the model-fitting step; while for PLS it relies on ranking methods, such as variable importance in projection (VIP) scores, which are affected by variable correlation, and they are sensitive to tuning parameters [273].

Among the discriminant molecular features selected for the elastic net models, some variables were preliminarily identified (choline, carnitine and nicotinamide derivatives, depsides, tocopherols, dipeptides, Lyso PEs, inositol derivatives). They are involved to cholinergic system, energy metabolism, amino acids and lipids metabolism, as well as nicotinamide pathways. These results agree with previous works in which lipids and amines biochemical pathways were altered in AD [52,87,97–101]. In addition, the nicotinamide pathway is involved in the mitochondrial transport chain that is related to the progression of AD through OS generation [274], so it could explain the higher levels found for nicotinamide ribotide or beta-nicotinamide D-ribonucleotide in the MCI group. Previous studies proposed nicotinamide riboside as a potential AD treatment since it showed beneficial effects on cognition and Aβ toxicity in AD mouse model [275], and in DNA repair [276]. This metabolite also showed beneficial effects on neuroprotection and energy metabolism that is directly implied in AD pathology [277]. Regarding inositol pathway, some metabolites were down-regulated in MCI-AD (inositol-1,3,4,5-tetraphosphate or 1D-myo-inositol-1,3,4,6-tetrakisphosphate or D-myo-inositol-3,4,5,6-tetrakisphosphate or 1D-myo-inositol-1,4,5,6-tetrakisphosphate). Similarly, inositol-1,4,5-trisphosphate receptor levels were lower in AD and it could be important in the neurofibrillary pathology [278]. In general, inositol is an important membrane component. Its brain derivates are implied in synaptic transport, and neurotransmitter secretion, and they regulate autophagy [279]. According to carnitine pathway, higher levels were found for MCI-AD group. Nevertheless, studies from literature found that serum acetyl-L-carnitine and other acyl-L-carnitine levels decreased in MCI and AD subjects [280,281], as well as in CSF samples [282]. A possible explanation to the higher

levels obtained for acetylcarnitine in the MCI-AD group may be that these compounds have antioxidant function [283], so natural mechanisms could be activated at early AD stages in order to face into the OS associated to further disease development. In addition, a mice model study demonstrated that acetyl-L-carnitine protects against neuroinflammation [284]. Therefore, the high levels found in early AD stages could be a compensatory mechanism, activating the protective mechanisms against the development of the disease.

The tentatively identified discriminant variables in this study were Lyso PE (20:0/0:0)/Lyso PE (0:0/20:0), choline and probably soraphen A. In spite of soraphen A was not confirmed by its standard, we discarded the other two possible compounds with the same mass (24,25- diacetylvulgaroside and cyasterone) as they are fruit and vegetables products, while soraphen A could show a possible relationship with fungal infection. So, Lyso PE (20:0/0:0)/Lyso PE (0:0/20:0), choline and soraphen A could be considered potential early AD biomarkers in plasma. In general, the MCI-AD group showed increased levels for soraphen A, Lyso PE and choline. First, soraphen A is produced by myxobacteria, and it can act as acetyl-CoA carboxylase inhibitor, which would alter the lipid synthesis pathways, avoiding the fatty acids elongation [285]. In the present study, most of MCI-AD patients showed increased levels of this metabolite. It may be indirectly related to the also higher levels of choline. Probably, the impairment in fatty acid elongation would lead to an increase in short-chain fatty acids levels, such as, choline. On the other hand, this potential myxobacteria infection is a controversial result that should be studied in depth, as well as other unexplained findings in literature relative to microscopic evidence of fungal infections in brain tissue from AD patients [286–288]. Second, Lyso PEs usually show low circulating levels, and they are considered biomarkers of the progression of AD [289]. In general, previous studies found that an alteration in lipid metabolism correlates with AD development [290]. However, a few participants from MCI-AD group showed decreased levels for soraphen A and Lyso PE, and further research is required to differentiate patients' subgroups. Third, choline was the only confirmed metabolite, constituting a promising biomarker in early AD diagnosis. It is a precursor metabolite in acetylcholine synthesis, so it plays an important role in this neurotransmitter function. In addition, it is a key component in some lipids with relevant brain functions, such as phosphatydilcholine [291], corroborating the impairment

observed in early AD stage. However, the choline levels found in AD patients from different metabolomics studies showed some discrepancy [285,292–294], probably due to the heterogeneous experimental conditions used (animal or human model, AD stage, sample matrix, analytical technique). In the present study, MCI-AD patients showed increased levels of this metabolite, as it was observed by Lin et al. 2017 [101,295]. It could be explained by the fact that in early AD stages the cholinergic transmission is reduced, and as compensatory response choline production would be increased. In addition, the pathology development involves a cellular integrity impairment, allowing the release of compounds out of the cell, such as choline [295]. Nevertheless, a recent study showed lower levels of choline in AD patients compared to healthy subjects [296]. Probably, the different disease phases show different biochemical profiles [98].

4. Conclusions

An untargeted metabolomics study has been carried out in plasma samples from patients with MCI due to AD and healthy participants, achieving the identification of some metabolites that could be involved in early AD development. They have important roles in some metabolic pathways related to neurotransmitters, energy metabolism, and lipids and amino acids pathways. However, only choline was confirmed, and further work will be carried out using a targeted analytical method based on UPLC-MS/MS in order to clinically validate this promising early AD biomarker. In addition, some tentatively identified compounds with neuroprotective or antioxidant effects were found elevated in MCI-AD patients. This may be explained by the activation of compensatory mechanisms to prevent AD development since its early stages.

Chapter 9. Metabolomics study to identify plasma biomarkers in alzheimer disease: ApoE genotype effect

1. Summary

The aim of this chapter was to identify metabolites altered in first AD stages to find new potential diagnosis biomarkers, as well as to evaluate the effect of ApoE genotype on the metabolomic profile of individuals with early AD. For this, metabolomic analysis was carried out for plasma samples from early AD patients and controls. Then data were analyzed by volcano plot and PLS to select discriminatory variables first between AD and non-AD participants and then between Apoε4 carriers and non-carriers.

2. Results and discussion

2.1. Demographic and clinical data of participants

Clinical and demographic characteristics from participants are summarized in Table 22. There were no differences between control and early AD groups for demographic variables except for gender and age. However, clinical variables (neuroimaging, CSF biomarkers (Aβ42, t-Tau, p-Tau), and neuropsychological evaluation tests (RBANS, CDR, FAQ)) showed differences between groups as it was expected.

Table 22. Demographic and clinical variables for the participants groups.

Variable		Control (n = 29)	Early AD (n = 29)
Age (years) (median (IQR))		65 (63, 70)	72 (69, 75)
Gender (female) (n (%))		9 (31.03 %)	19 (65.52%)
Studies levels (n (%))	**Basics**	6 (20 %)	17 (59 %)
	University	11 (38 %)	5 (17%)
Medications (n (%))	**Statins**	10 (34%)	17 (59%)
	Fibrates	3 (10%)	2 (7%)
	Benzodiazepines	2 (7%)	4 (13.79%)
	Opiates	0 (0%)	0 (0%)
	Antiepileptics	1 (3.45%)	0 (0%)
	Antihipertensives	10 (35.71%)	14 (48.28%)
	Corticoids	0 (0%)	2 (6.9%)
Comorbidity (n (%))	**Dyslipidemia**	10 (35.71%)	16 (55.17%)
	Diabetes	3 (10%)	3 (10.34%)
	Hypertension	11 (38%)	13 (44.83%)
	Heart Disease	1 (3.45%)	0 (0%)
Smoking status (n (%))	**Yes**	1 (3.45%)	2 (6.9%)
	Former smoker (more than 10 years)	9 (31%)	7 (24.14%)
Alcohol or drugs consumption (n (%))		6 (21.43%)	3 (10.34%)
Presenile family background (n (%))	**None**	22 (76%)	22 (88%)
	First grade	5 (17%)	5 (17%)
	Second grade	2 (7%)	0 (0%)
Depression (n (%))		3 (10.34%)	4 (14%)
Anxiety (n (%))		1 (3.45%)	3 (10.34%)
Temporal atrophy (n (%))		2 (7.14%)	20 (69%)
CSF Aβ42 (pg mL^{-1}) (median (IQR))		1256 (1164, 1464)	600 (496, 687)
CSF t-Tau (pg mL^{-1}) (median (IQR))		196 (141, 298)	590 (465, 782)
CSF p-Tau (pg mL^{-1}) (median (IQR))		48 (37, 60)	84 (73, 104)
RBANS.DM (median (IQR))		100 (92, 106)	48 (40, 66)
FAQ (median (IQR))		0 (0, 0)	5 (0, 8.5)
CDR (n (%))	**0**	29 (100%)	5 (17%)
	0.5	0 (0%)	18 (62%)
	1	0 (0%)	6 (21%)

2.2. Metabolomic differences between healthy and early AD subjects

The Volcano Plot analysis, carried out for the healthy control and early AD groups, showed 36 significant variables (Figure 26a). The supervised PLS analysis was carried out with those variables in order to find the most powerful discriminant metabolites between groups. As shown in Figure 26b, the PLS model revealed a clear separation between early AD cases and healthy controls (except for some misclassified controls), with good R^2Y (0.738) and Q^2Y (0.679) parameters, indicating biochemical changes

between groups. The model was satisfactorily validated with a 7-fold cross validation method (p CV-anova 1. Finally, 15 variables were studied and tentatively identified by using CMM tool and mass fragmentation strategies. Metabolite annotation based on AM, retention time and MS/MS spectra from chemical standard lead to the confirmation of m/z 1043.7008 as Lysophosphatidylcholine (18:1) (Lyso PC (18:1)). This metabolite showed levels with differences statistically significant between early AD and healthy control participants (Figure 26c). In addition, the variable m/z 1047.7345 was putatively characterized as NeuAcalpha2-3Galbeta-Cer(d18:1/20:0), LysoPE(21:0), LysoPC(18:0) or PC(O-16:0/2:0), all of them were glycerophospholipids. On the other hand, m/z 570.0359, and m/z 335.0450 were putatively characterized as chemical compound, and phenols, organic sulphuric acids, or fatty acyls classes, respectively. The other variables could not be identified by any of the databases. As previous works described, it seems that lipid metabolism plays an important role in AD physiopathology [297], and it could be useful in the discrimination between early AD and healthy controls. In this sense, previous studies showed that membrane lipid composition could be involved in the activity of gamma secretase, an enzyme acting in the appearance of Aβ peptide, the most characteristic hallmark of AD [162,165]. In addition, structural changes in lipid membrane could change the interaction with Aβ protein [298]. Regarding lipid metabolites, lysophosphatidylcholine is postulated as a potential plasma biomarker. Similarly, Liu et al. and Lin et al. found that lysophosphatidilcholines and phosphatidilcholines showed differential levels between AD and healthy elderly in plasma samples [299,300]. In fact, most of metabolomics studies carried out in plasma for AD biomarkers identification showed lipids as important potential biomarkers [301]. Oberacher et al. 2017 found similar results using soluble lysates from platelets where different phosphocholines seemed to discriminate between early AD and healthy controls [302]. Also, Dorninger et al. 2018 found that although lphosphatidylysocholine levels increased in normal aging, this increase is more remarkable in probable AD patients [303]. In addition, it was demonstrated that lysophosphatidylcholines increased the *in vitro* formation of Aβ1-42 oligomer [298,304]. On the contrary, Li et al. found decreased levels of lysophosphocholines in brain tissue from AD mice model [305].

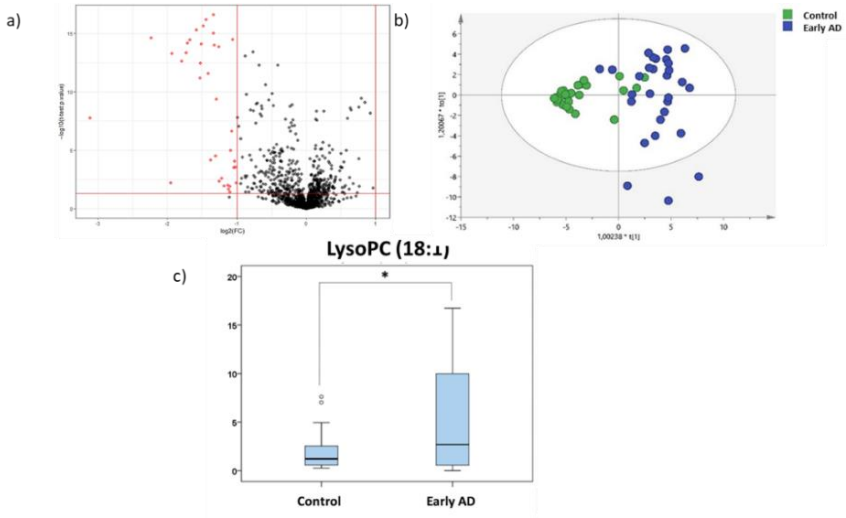

Figure 26. a) Volcano Plot representing the significant variables in the discrimination between early AD and healthy control groups. The non-significant variables are represented in grey, the significant variables are represented in red (p value t-test> 0.05 and FC> 2); b) PLS represents differential distribution between early AD and healthy control groups; c) Boxplot of plasma analytical responses of LysoPC(18:1). *p value < 0.05.

2.3. Metabolomic differences between ApoE4 genotypes

In Figure 26b, we appreciate a clear clustering in the control group, while the early AD case group showed high scattering, indicating a within class variation. In order to explain this variability, we proposed the ApoE4 genotype as a potential variable since it is considered an important risk factor in AD development. Specifically, ApoE genotype is related to AD pathogenesis as the ε4 allele is involved in cholesterol brain metabolism and in the maintenance of membrane integrity [48]. In addition, it is related to other pathways such as lipid metabolism, synaptic function, glucose metabolism microglial response, or Tau pathology, among others [306]. Therefore, ApoE genotype could generate differences in metabolomic profile. Previously, Karjalainen et al. indicated that ApoE-ε4 carriers and non-carriers showed differential serum metabolomics profile, it could be associated to different pathological status [106]. Therefore, in the present study, different metabolic profiles in plasma from early AD patients, as well as the ApoE genotype, influence were evaluated. The metabolomics differences were evaluated using the same statistical procedure described above. It was applied in early AD cases

previously classified as ε4-carriers and non ε4-carriers according to the PCR analysis results. In this sense, 20 significant variables were selected in the Volcano Plot (Figure 27a) for the following PLS analysis. As it is shown in the score plot (Figure 27b), few samples were misclassified and the model presented R^2Y (0.437) and Q^2Y (0.394) diagnostic parameters. Nevertheless, the model was reliable with a CV-anova p-value 1 and which their jackknife confidence interval did not include zero. Finally, 8 variables were tentatively identified by using the CMM tool (see Table 23). All these analytes showed lower values for ε4-carriers. Specifically, m/z 1043.7008 with a fold-change ratio of 0.26 was confirmed as LysoPC(18:1) by using a chemical standard, and it showed statistically significant differences between groups. This variable was previously confirmed in the metabolome comparison between healthy and early AD groups. Other variables were putatively characterized as LysoPC(P-18:0), LysoPE(0:0/22:1(13Z)), and cardiolipins. As can be seen in Figure 27c, some of these metabolites showed statistically significant differences between ε4-carriers and non ε4- carriers. Regarding the identified compounds class, most of them are glycerophospholipids (Table 23). Fonteh et al. previously described differences for different glycerophospholipids in CSF from AD patients and healthy controls [307]. However, Sharman did not find differences for glycerophospholipids levels in brain tissue nor plasma samples from knock-in mice with different human ApoE subtypes expression [308]. On the other hand, Igbavboa et al. found differential composition in synaptosomal lipid rafts depending on ApoE genotype [309]. In general, lipid metabolites are the most relevant compounds, since cardiolipins, lysophosphatidylcholines and lysophosphatidylethanolamines are discriminant variables between early AD and healthy control groups, as well as between ε4-carriers and non ε4-carriers. Regarding cardiolipins, they are phospholipids highly present in the mitochondrial membrane, and they have been related to brain disorders and neurodegenerative diseases, such as AD [310]. In this study, cardiolipins showed lower signals in ε4-carriers than non ε4-carriers. This dysregulation could be associated with mitochondrial dysfunction in AD synapsis [311]. Among lysophosphatidylcholines, LysoPC(18:1) is one of the most important discriminant variables between ε4-carriers and non ε4-carriers in this study, and its plasmatic levels were previously related to a lower risk of different cancer kinds [312]. In addition, Whiley et al. found that the determination of 3 different phosphatidylcholines combined with ApoE genotype, provided a

satisfactory discriminant capacity between AD and non-AD participants [313]. Nevertheless, the present study showed lower levels for this compound in the healthy and ε4-carrier groups in comparison with the non ε4- carrier group. This finding reinforces the idea that the ApoE genotype plays an important role in the development of AD. In this sense, LysoPC (18:1) levels and ApoE genotype could be a useful tool for early AD diagnosis. Regarding the limitations of the present study, it is important to highlight the low number of participants, since it is very difficult to achieve early AD patients and healthy people identified from CSF biomarkers levels.

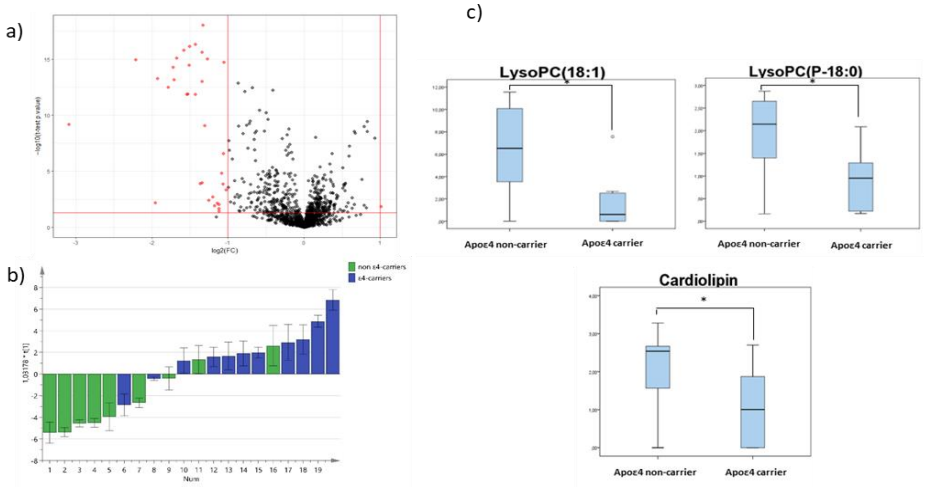

Figure 27. a) Volcano Plot representing the significant variables in the discrimination between early AD ε4-carrier and non ε4-carrier groups. The non-significant variables are represented in grey, the significant variables are represented in red (p value t-test> 0.05 and FC> 2); b) PLS represents differential distribution between ε4-carrier and non ε4-carrier groups; c) Boxplot of plasma analytical responses of LysoPC (18:1), LysoPC (P-18:0) and cardiolipin. *p value < 0.05.

3. Conclusions

Different levels for plasma metabolites are found in early AD patients compared to healthy controls, reflecting the different metabolic pathways that are affected in this disease. Among these analytes, different lipid compounds stand out, so lipid metabolism is an important pathway that seems to fail since early stages of the pathology. Therefore, it could constitute a source of biomarkers for the early AD diagnosis, as well as further

therapeutic targets. In addition, in the early AD patients, different metabolic profiles were obtained depending on their ApoE genotype (ε4-carriers, non ε4-carriers). Actually, different glycerophospholipids were altered between these groups. It could involve an important advancement in the knowledge of the different impaired mechanisms, as well as the improvement in precision medicine for diagnosis and treatment. Nevertheless, further work based on target analysis would be required for the quantification of these potential biomarkers in a larger number of participants in order to validate the diagnostic performance of these metabolites.

Table 23. Metabolites´ annotation from ApoE classification.

m/z	t_R (min)	Adduct Ion	Formula	Identification of variables		Compound class / Metabolism	FC[c]
				Metabolite annotation	Level #		
1087.6829	8.86	M-H	C6 H102O12P2	alpha-D-galactosyl undecaprenyl diphosphate	2	Prenol lipids/Lipid metabolism	0.46
1043.7008	8.85	2M+H	C26H52NO7P	LysoPC(18:1)	1	Glycerophospholipids / Lipid metabolism	0.26
508.3746	9.02	M+H	C26H54NO6P	LysoPC(P-18:0)	3[a]	Glycerophospholipids	0.48
530.3563	9.02	M+Na	C26H54NO6P	LysoPC(P-18:0)	3[b]	Glycerophospholipids	0.48
536.3696	9.16	M+H	C27H54NO7P	LysoPE(0:0/22:1(13Z)) LysoPE(22:1(13Z)/0:0)	3[a]	Glycerophospholipids	0.50
1261.8213	8.69	M+H	C67H122O17P2	CL(8:0/14:0/18:2(9Z,11Z)/18:2(9Z,11Z)) CL(8:0/i-14:0/18:2(9Z,11Z)/18:2(9Z,11Z))	3	Glycerophospholipids	0.50
1018.6680	8.70	+		Unknown	4		0.50
548.8109	8.85	+		Unknown	4		0.46

1: confirmed; 2: putative annotated; 3: putative characterized; 4: unknown.

[a] Score 1 for ionization rules (particular adducts formation depending on the lipid class, ionisation mode and mobile phase modifier used) based on CMM is very likely right (score range between 1.5-2)

[b] Score 1 for ionization rules (particular adducts formation depending on the lipid class, ionisation mode and mobile phase modifier used) based on CMM is likely right (score range between 1-1.5)

[c] FC: Fold Change was calculated as median signal of carriers divided to non-carriers

LysoPC: Lysophosphatidilcholine; LysoPE: lysophosphatidylethanolamine; CL: cardiolip

Chapter 10. Plasma lipidomics approach in early and specific Alzheimer's Disease diagnosis

1. Summary

The aim of this chapter is to evaluate plasma lipid profiles from untargeted and targeted approaches, identifying lipid families and single lipids involved in early AD as potential biomarkers. For this, an untargeted lipidomic analysis was carried out in plasma samples from preclinical AD (n = 11), MCI-AD (n = 31), and control (n = 20) participants. The, variables were identified by means of two complementary methods (LipidMS and CEU mass mediator database). Then, a targeted analysis was carried out to quantify some of the identified lipids.

2. Results

2.1. Participant's demographic and clinical data

In Table 24, the clinical and demographic characteristics of the participants are summarized. As was expected, neuropsychological variables (CDR, RBANS, FAQ, and MMSE) and CSF biomarkers (Aβ42, t-Tau, and p-Tau) showed statistically significant differences among the participant groups. In addition, age showed statistically significant differences among the groups. In this sense, the correlations between age and all lipids (from the untargeted and targeted analyses) were assessed, without obtaining significant results for any lipids.

Table 24. Clinical and demographic participant characteristics.

		Healthy (*n* = 31)	**MCI-AD (*n* = 20)**	**Preclinical AD (*n* = 11)**	***p* Value (Kruskal–Wallis)**
Median Age (years) (IQR)		62 (58, 68)	72 (69, 74)	70 (60, 74)	0.000
Gender (Female, *n* (%))		19 (61%)	10 (53%)	6 (50%)	0.737
Educational Level	**Primary (*n* (%))**	10 (32%)	7 (39%)	4 (33%)	0.023
	Secondary (*n* (%))	7 (23%)	10 (56%)	2 (17%)	
	University (*n* (%))	14 (45%)	2 (18%)	6 (50%)	
Concomitant Medication	**Statins (*n* (%))**	9 (41%)	12 (63%)	3 (25%)	0.335
	Fibrates (*n* (%))	0 (0%)	3 (17%)	1 (8%)	0.143
	Benzodiazepines (*n* (%))	6 (27%)	3 (16%)	2 (17%)	0.635
	Antidepressants (*n* (%))	7 (32%)	2 (11%)	0 (0%)	0.085
	Antiepileptics (*n* (%))	1 (5%)	0 (0%)	0 (0%)	0.547
	Antihypertensives (*n* (%))	7 (32%)	9 (50%)	2 (29%)	0.424
	Corticoids (*n* (%))	1 (5%)	0 (0%)	0 (0%)	0.547
	Anti-inflammatories (*n* (%))	3 (14%)	0 (0%)	0 (0%)	0.151
Comorbidities	**Dyslipidemia (*n* (%))**	11 (50%)	11 (58%)	3 (43%)	0.766
	Diabetes (*n* (%))	3 (14%)	2 (11%)	0 (0%)	0.589
	Hypertension (*n* (%))	8 (36%)	9 (47%)	2 (29%)	0.628
	Heart Disease (*n* (%))	1 (5%)	0 (0%)	0 (0%)	0.547
	Cerebrovascular (*n* (%))	1 (5%)	0 (0%)	0 (0%)	0.547
Smoke (Yes, *n* (%))		6 (27%)	3 (16%)	1 (14%)	0.598
Alcohol (Yes, *n* (%))		6 (27%)	2 (11%)	0 (0%)	0.157
Depression (Yes, *n* (%))		5 (23%)	5 (26%)	2 (29%)	0.939
Anxiety (Yes, *n* (%))		4 (18%)	3 (16%)	2 (29%)	0.757
Aβ42 (pg mL^{-1}) Median (IQR)		1224 (964, 1421)	495 (452, 622)	572 (383, 694)	0.000
t-Tau (pg mL^{-1}) Median (IQR)		212 (181, 259)	578 (449, 793)	444 (208, 611)	0.000
p-Tau (pg mL^{-1}) Median (IQR)		34 (25, 39)	91 (62, 109)	74 (28, 94)	0.000
CDR Median (IQR)		0.5 (0, 0.5)	0.5 (0.5, 0.5)	0.5 (0, 0.5)	0.001
MMSE Median (IQR)		29 (28, 29)	24 (22, 25)	29 (27, 30)	0.000
RBANS.DM Median (IQR)		98 (94, 103)	42 (40, 53)	95 (87, 101)	0.000
FAQ Median (IQR)		1 (0, 4)	7 (5, 10)	1 (0, 3)	0.000

IQR: Inter-quartile range; AD: Alzheimer Disease; MCI-AD: mils cognitive impairment due to Alzheimer Dis- ease; CDR: Clinical Dementia Rating; MMSE: Mini-Mental State Examination; FAQ: Functionality Assessment Questionnaire; RBANS: Repeatable Battery for Assessment of Neuropsychological Status; DM: Delayed memory

2.2. Lipids identified by LipidMS package

From the untargeted analysis, 197 features were annotated by the LipidMS package. They were grouped into some lipid families (4 CE, 16 Cer, 2 DG, 20 FA, 3 LPE, 16 LPC, 2 MG, 73 PC, 9 PE, 5 PI, 12 SM, and 35 TG). As can be seen in Figure 28, the main families were PC (37%), TG (18%), and FA (10%). In Table 25, the DG, LPE, LPC, MG, and SM families and monounsaturated lipids showed statistically significant differences among the three participant groups (preclinical AD, MCI-AD, and healthy). Moreover, the healthy and preclinical AD groups showed statistically significant differences in the levels of the Cer, LPE, LPC, MG, and SM families, while the MCI-AD and healthy groups showed statistically significant differences in the levels of DG, MG, and PE. In addition, Figure 29 shows the boxplots representing the levels of the lipid families in the participant groups (preclinical AD, MCI-AD, and healthy). In general, higher levels were obtained for the preclinical AD group, and lower levels were obtained for the MCI-AD group. A similar tendency was observed for monounsaturated, polyunsaturated, and saturated lipids, although only monounsaturated compounds showed statistically significant differences. In general, a trend was not found for any of the lipid families between the preclinical and MCI groups.

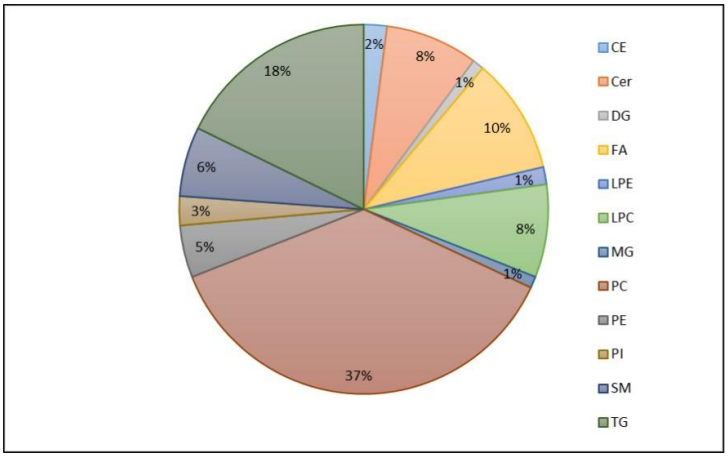

Figure 28. Lipid families identified from untargeted lipidomic analysis and identification by LipidMS package.
CE: Cholesterol esters; Cer: Ceramides; DG: Diglycerols; FA: Fatty acids; LPC: Lys phosphatidylcholines; LPE: Lysophosphatidylethanolamines; MG: Monoglycerides; PC: Phosphatidylcholines; PE: Phosphatidylethanolamines; PI: Phosphatidylinositols; SM: Sphingomyelins; TG: Triglycerides.

Table 25. Average sum of the different lipid families' levels in the participant groups (preclinical AD, MCI-AD, and healthy).

Lipid Family	Healthy Controls (HC) (*n* = 31)	MCI-AD (*n* = 20)	Preclinical AD (*n* = 11)	*p* Value (Kruskal–Wallis)	Healthy vs. Preclinical AD (Mann–Whitney, *p* Value)	Healthy vs. MCI-AD (Mann–Whitney, *p* Value)
CE (a.u.)	4.15 (2.86, 4.83)	3.60 (3.03, 5.04)	4.47 (3.86, 4.96)	0.416	0.350	0.685
Cer (a.u.)	4.39 (3.52, 4.39)	3.94 (2.42, 5.75)	5.67 (5.09, 6.87)	0.070	0.038 *	0.452
DG (a.u.)	2.05 (1.56, 2.22)	1.51 (1.25, 1.98)	2.20 (1.94, 2.73)	0.007 *	0.155	0.023 *
FA (a.u.)	15.04 (9.29, 22.21)	13.42 (9.44, 18.38)	22.32 (11.48, 26.24)	0.299	0.201	0.685
LPE (a.u.)	8.68 (7.16, 11.41)	7.61 (4.77, 12.73)	13.86 (10.32, 17.10)	0.006 *	0.002 *	0.418
LPC (a.u.)	18.48 (13.62, 12.39)	15.75 (8.93, 24.98)	27.37 (22.68, 35.24)	0.006 *	0.001 *	0.396
MG (a.u.)	1.48 (1.02, 2.83)	0.81 (0.48, 1.10)	2.52 (1.77, 3.56)	<0.001 *	0.017 *	0.002 *
PC (a.u.)	46.66 (35.34, 56.80)	41.08 (27.78, 55.27)	53.13 (43.75, 59.73)	0.202	0.257	0.316
PE (a.u.)	7.04 (5.09, 8.78)	4.76 (3.05, 9.53)	6.85 (6.13, 10.46)	0.061	0.572	0.034 *
PI (a.u.)	3.50 (2.86, 4.99)	3.08 (2.09, 5.00)	3.77 (2.70, 6.13)	0.366	0.553	0.307
SM (a.u.)	8.63 (6.13, 10.48)	5.79 (3.13, 10.02)	11.21 (9.65, 12.90)	0.001 *	0.003 *	0.061
TG (a.u.)	24.05 (19.40, 28.94)	21.00 (18.36, 29.71)	22.21 (17.83, 27.27)	0.625	0.381	0.537
Monounsaturated (a.u.)	39.78 (31.30, 47.49)	33.35 (22.55, 46.09)	47.79 (45.98, 60.65)	0.011 *	0.009 *	0.232
Polyunsaturated (a.u.)	93.13 (74.29, 113.90)	78.75 (58.62, 106.44)	104.67 (88.91, 111.74)	0.170	0.233	0.307
Saturated (a.u.)	156.73 (132.57, 189.15)	138.36 (99.15, 168.83)	191.35 (155.78, 203.83)	0.100	0.054	0.452

a.u.: arbitrary units. * $p < 0.05$. HC: healthy control.

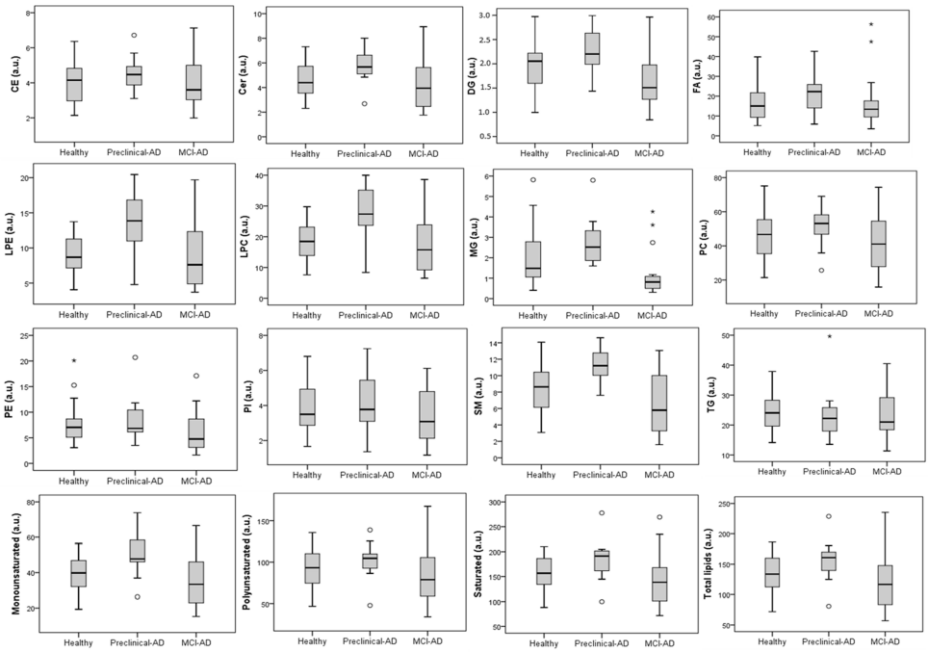

Figure 29. Boxplots representing the levels of lipid families for each participant group (healthy, preclinical AD, and MCI-AD. There were 4 CEs, 4 Cers, 2 DGs, 14 FAs, 3 LPEs, 8 LPCs, 2 MGs, 44 PCs, 7 PEs, 3 PIs, 9 SMs, and 25 TGs included in the analysis. (a.u.: arbitrary units)). o: outlayer; *: Extreme outlayer.

2.2.1. Targeted analysis

From previous results, the selected lipids were 18:1 LPE, 18:0 LPC, 16:1 SM (d18:1/16:1), 16:0 SM (d18:1/16:0), 18:0 SM (d18:1/d18:0), 18:1 (9-Cis) PE (DOPE), and 24:0 SM. The corresponding analytical method was developed and validated, obtaining satisfactory analytical performance for 18:1 LPE, 18:0 LPC, 16:1 SM (d18:1/16:1), and 16:0 SM (d18:1/16:0)(see Table 26). In fact, the accuracy was satisfactory, with recoveries around 100%, except for18:0 LPC with recoveries >130%, probably due to the matrix effect. Moreover, a suitable sensitivity was obtained, with LODs between 0.548 and 4.185 nmol L^{-1} and LOQs between 1.83 and 13.95 nmol L^{-1}. The other analytes did not show suitable analytical performance (18:0 SM (d18:1/d18:0), 18:1 (9-Cis) PE (DOPE), and 24:0 SM), and they were not determined in plasma samples.

Table 26. Analytical method validation.

Analyte	**Standard Concentration (nmol L^{-1})**	**Recovery (%)**	**LOD (nmol L^{-1})**	**LOQ (nmol L^{-1})**	**Linearity Range (nmol L^{-1})**	**Equation (y = a + bx)** **$a \pm s_a$** **$b \pm s_b$** **R^2**
18:1 LPE	6.25	108 ± 14	0.548	1.83	1.83–26.30	0.0019 ± 0.0008
	9.38	109 ± 15				0.0027 ± 0.000063
	12.5	104 ± 17				0.998
18:0 LPC	50	153 ± 15	4.185	13.95	13.95–209.38	0.012 ± 0.024
	75	147 ± 15				0.0072 ± 0.00022
	100	134 ± 21				0.997
16:1 SM (d18:1/16:1)	50	101 ± 11	2.857	9.52	9.52–208.11	0.0774 ± 0.021
	75	101 ± 11				0.0064 ± 0.00019
	100	96 ± 16				0.997
16:0 SM (d18:1/16:0)	12.5	108 ± 58	1.240	4.13	4.13–52.51	−0.0041 ± 0.0063
	18.75	102 ± 6				0.012 ± 0.00024
	25	82 ± 5				0.999
18:0 SM (d18:1/d18:0)	3.13		0.289	0.96	0.96–13.23	0.0014 ± 0.0011
	4.69	100 ± 26				0.0047 ± 0.00017
	6.25	119 ± 59				0.996
18:1 (9-Cis) PE (DOPE)	0.78		0.069	0.23	0.23–3.30	0.00019 ± 0.00015
	1.17	103 ± 65				0.0024 ± 0.000089
	1.56	62 ± 62				0.996
24:0 SM	6.25		0.306	1.02	1.02–26.02	0.24 ± 0.03
	9.38					0.044 ± 0.003
	12.50					0.990

2.2.2. Sample analysis

A panel of four lipids (previously selected) was determined in plasma samples from healthy participants (n = 20) and patients with preclinical AD (n = 11) and MCI-AD (n = 31). The concentrations of each lipid in the participant groups are summarized in Table 27. As can be seen, statistically significant differences were observed for 18:1 LPE among the three groups (p = 0.010) and between the AD (preclinical + MCI) and healthy groups (p = 0.003). In addition, this potential AD biomarker showed a correlation with some CSFbiomarkers (t-Tau (0.299, p = 0.022) and p-Tau (0.290, p = 0.026)). It should be mentioned that no correlation was observed between the lipid levels and age.

Table 27. Lipid concentrations in plasma from participant groups (healthy, MCI-AD, and preclinical AD).

Lipids	**Healthy Control (HC) (*n* = 31) Median (IQR) (nmol L^{-1})**	**MCI-AD (*n* = 20) Median (IQR) (nmol L^{-1})**	**Preclinical AD (*n* = 11) Median (IQR) (nmol L^{-1})**	**Kruskal-Wallis *p* Value (three groups)**	**Mann–Whitney *p* Value (AD vs. non-AD)**
18:1 LPE	1.37 (0.38, 1.83)	1.8 (1.2, 4.2)	1.8 (0.9, 3.7)	0.010 *	0.003 *
18:0 LPC	67 (61, 80)	65 (56, 96)	81 (60, 105)	0.504	0.569
16:1 SM	15 (7, 27)	13 (8, 24)	19 (15, 25)	0.501	0.647
16:0 SM	177 (137, 206)	168 (132, 213)	209 (159, 239)	0.374	0.371

* *p* value < 0.05.

In addition, LPE 18:1 showed an AUC-ROC of 0.722 (95% CI, 0.595–0.848), discriminating between early AD (preclinical + MCI) and healthy participants.

2.3. Compounds identified by CEU Mass Mediator Database

2.3.1. Preclinical AD vs. Healthy Subjects

The volcano plot analysis from the preclinical AD and healthy groups showed 48 significant variables (Figure 30a). The PLS analysis was carried out with these variables in order to identify the most discriminant variables between the groups. This model showed a *p* value <0.001 and a clear separation between preclinical AD cases and healthy participants (Figure 30b), with good R^2Y (0.637) and Q^2Y (0.566) parameters. The model was satisfactorily validated (1000 iterations) with R^2Y = 0.202 and Q^2Y = −0.373.

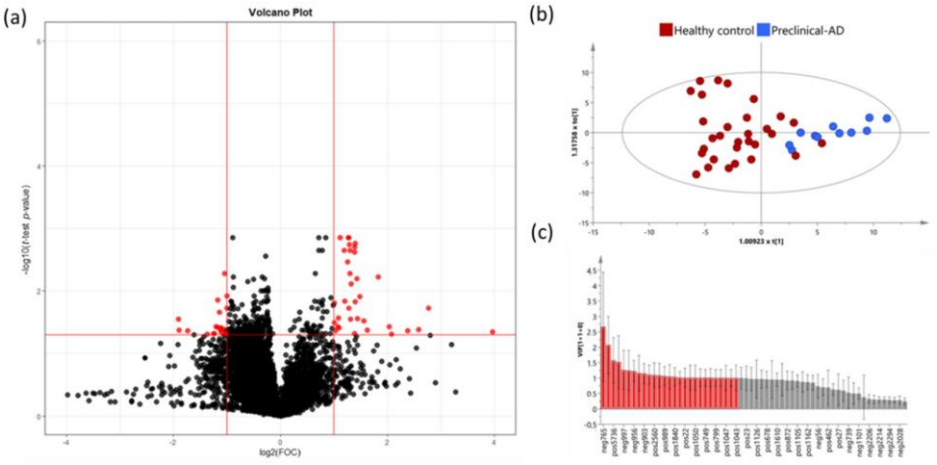

Figure 30. (a) Volcano Plot representing the significant variables in the discrimination between healthy controls and preclinical AD participants. Statistically significant variables are represented in red ($p < 0.05$, FC > 2); (b) PLS plot represents differential distribution between healthy controls and preclinical AD; (c) Threshold VIP plot value > 1 (red variables).

Potential compounds were subjected to identification and confirmation based on a threshold of VIP value >1 (27 variables) (Figure 30c). Finally, 16 variables were tentatively characterized by querying our experimental MS data with those provided in the commercial databases. From them, some variables showed more weight over the model (*m*/*z* 1484.140079, 508.3767054, 494.3609278, and 770.6063157). In addition, two

variables were putatively annotated through AM and MS/MS mass spectra with online databases. These variables were pisumionoside (*m/z* 405.2102471) and 1-O-Palmitoyl-2-O-acetyl-sn-glycero-3-phosphorylcholine (*m/z* 520.3404329).

2.3.2. Mild Cognitive Impairment-AD vs. Healthy Controls

The volcano plot analysis from the MCI-AD and healthy groups showed 153 significant variables (Figure 31a). The PLS analysis was carried out with these variables in order to identify the most discriminant lipids between the groups. This model showed a CV*p*-value <0.001 and a clear separation between MCI-AD and healthy control participants (Figure 31b), with good R^2Y (0.926) and Q^2Y (0.785) parameters. The model was satisfactorilyvalidated (1000 iterations) with R^2Y = 0.572 and Q^2Y = - 0.686.

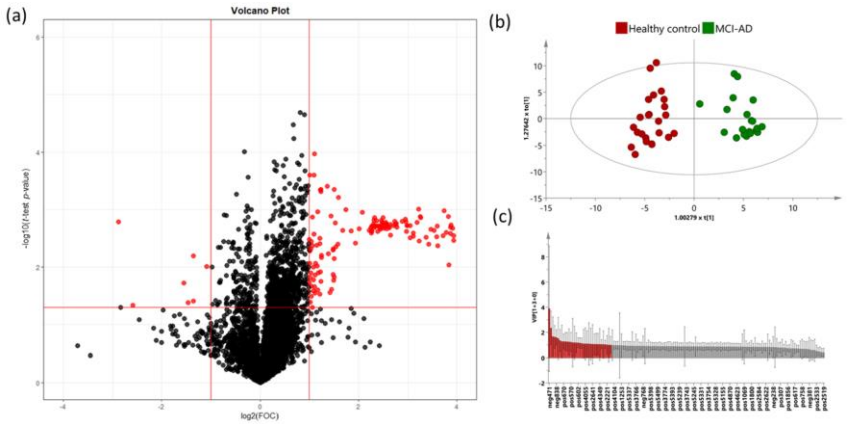

Figure 31. (a) Volcano plot representing the significant variables in the discrimination between healthy controls and MCI-AD. Statistically significant variables are represented in red ($p < 0.05$, FC > 2); (b) PLS plot represents differential distribution between healthy controls and MCI-AD. (c) Threshold VIP plot value > 1 (red variables).

Potential metabolites were subjected to identification and confirmation based on a threshold of VIP value > 1 (22 variables) (Figure 31c). Finally, 11 variables were tentatively characterized by using the corresponding databases. From them, some variables showed more weight over the model (*m/z* 409.3113, 362.2550, 350.3417, and 518.351396). In addition, the variable *m/z* 766.573457 was putatively annotated trough AM and MS/MS mass spectra with online databases, and it was identified as a phosphocholine.

3. Discussion

A lipidomic approach was developed in plasma samples from participants classified according to their amyloid status (CSF biomarkers) to identify lipid alterations involved in the onset of AD. For this, an untargeted analysis was carried out, and comparisons between early AD (preclinical or MCI) and healthy participants were evaluated. Some significant variables were identified in early AD deregulation, and lipid families were evaluated. Finally, a complementary multivariate analysis was carried out in order to identify other potential discriminative variables.

Lipid families identified by the LipidMS database revealed the potential implication of DG, LPE, LPC, MG, and SM in early AD. In the comparison between preclinical AD and healthy groups, some lipid families were identified as potential biomarkers (Cer, LPEs, LPCs, MGs, and SMs), as they were differentially expressed, especially the monounsaturated species. Similarly, Mielke et al. found an association between Cer and SMs with therisk of AD, although they described differential risks between men and women [314]. In addition, Jazvinšćak Jembrek et al. described the role of ceramides as mediators of neuronal apoptosis related to OS and Aβ accumulation [315]. Therefore, this deregulationof ceramides in the preclinical stages of the disease could contribute to the advancement of clinical manifestations contributing to neuronal loss. Moreover, Panchal et al. described ceramide accumulation in AD plaques [316]. In addition, SM/ceramide has been related toAD cognitive decline [116]. However, the utility of ceramides as biomarkers for dementias requires further investigation [317]. LPE was described as a biomarker for progression toAD [115], although our results suggest that it could be a potential biomarker for preclinicalstages. Similarly, LPCs could be a potential biomarker for the first stages of AD. In this sense, LPCs play a role in PUFAs transport across the BBB, perhaps controlling the availability of these essential compounds for the proper functioning of the brain [318]] In the comparison between MCI-AD and healthy controls, different lipid families were identified as potential biomarkers (DGs, MGs, and PEs). Similarly, Wood et al. found increased levels of DGs and MGs in early AD [319]. PEs could be involved in the physiopathology of AD due to their involvement in cell processessuch as oxidative phosphorylation, mitochondrial biogenesis, and autophagy [290]. Our results show

that MGs could be potential biomarkers of early AD, including both the preclinical and MCI-AD stages. In addition, LPE, LPC, and SM seem to be more specifically altered in the preclinical stage, while DGs could be useful as biomarkers for the MCI stage. On the other hand, the annotation of variables by means of other databases (HMDB, Kegg, and Metlin) reported other important annotated variables and metabolite classes. In the discrimination between preclinical AD and healthy subjects, some lipid families were found, such as phosphatidylglicerol, glicerophosphocholine, glicerophosphoserine, phosphoethanolamine, phosphocholine, glicoesphingolipid, diacilglicerol, terpenes, steroids, flavonoid classes, and vitamin E. Specifically, plasma glycerophosphocholine compounds were observed at higher levels in the preclinical AD group. Similarly, other studies showed elevated levels of this lipid in AD brains [320] as well as in cerebrospinal fluid samples from AD patients [307,321], indicating that abnormal phospholipid metabolism in the brain is characteristic of AD. In addition, the present study found that plasma phosphoethanolamine levels were lower in the preclinical AD group, and a previous work found lower levels for PE in AD brain samples [322]. In fact, PE is a precursor for phosphatidylcholine and a substrate for important posttranslational modifications [290]. Moreover, phosphocholine is a precursor of phosphatidylcholine, and higher levels were obtained for the preclinical AD group, indicating a potential membrane impairment in the early disease process [323]. Moreover, glycosphingolipids could be involved in preclinical AD since higher levels wereobtained in plasma samples from these participants. In this regard, ceramides, which are involved in sphingolipid metabolism, showed an association with neuropsychiatric symptoms [324]. Moreover, we found higher levels of DGs in the preclinical AD group, similar to the increased plasma levels in early AD, suggesting that lipidomics alterations lead to the accumulation of DGs in MCI subjects [319]. On the other hand, in the present study,phosphatidylglycerol (PG) and flavonoids showed lower plasma levels in the preclinical AD group. Flavonoid compounds could act against AD pathology by inhibiting microglia activation and Aβ aggregation. Therefore, a reduction in these compounds early in the disease may contribute to the development of AD pathways. However, a search of the literature failed to reveal any studies related to this finding. Studies have been reported that vitamin D showed higher levels in preclinical AD compared to healthy

participants, but we found that prior investigations reported reduced levels of these vitamins in AD and MIC- AD cases [325]. Since the cases examined here were classified as preclinical AD, it is possible that this group was exhibiting a compensatory response to the disease process. In addition,the discrimination between preclinical AD and healthy controls is characterized by the biomarkers 1-O-Palmitoyl-2-O-acetyl-sn-glycero-3-phosphorylcholine and pisumionoside, which were putatively annotated. Pisumionoside is an exogenous compound derived from vegetables, such as seedpods of garden peas, that could have a hepatoprotective function [326]. These levels are elevated in healthy subjects compared to preclinical AD subjects. Therefore, pisumionoside could have a protective effect against AD. Moreover,1-O-Palmitoyl-2-O-acetyl-sn-glycero-3-phosphorylcholine is a glycerophosphorylcholine that showed increased levels in AD, in concordance with previous studies [327]. Its oxidized products were considered biomarkers of neuroinflammation in other pathologies such as multiple sclerosis [328]. Moreover, other lipid families (glycosyldiacylglycerols, fatty acids, terpenoids, sesquiterpene mycotoxins, terpene lactones, phosphocholines, glucosylceramides, and fucopentanoses) were annotated by HMDB comparing MCI-AD and healthy groups. First, glycosyldiacylglycerols showed lower levels in the MCI-AD group. Previous studies found an increase in diacylglycerols in the frontal cortex in neurodegenerative diseases such as dementia with Lewy bodies or AD [329]. In addition, glycosylation showed a relationship with neurodegeneration and AD. Therefore, it could be an indicator of disease progression [330]. Moreover, fatty acids showed lower levels in the MCI-AD group, similar to previous reports [331,332], reflecting differences in intake and metabolism. Moreover, terpenoids and some vitamins showed higher levels in the MCI-AD group. In this sense, there is some controversy since previous studies showed protective effects for these compounds [333,334].

Regarding the targeted analysis, the developed analytical method was able to determine low plasma levels of some lipids that could be useful as potential AD biomarkers (18:1 LPE, 18:0 LPC, 16:1 SM (d18:1/16:1), and 16:0 SM (d18:1/16:0)). Accuracy was satisfactory for all of them. However, only 18:1 LPE showed statistically significant increased levels in preclinical and MCI-AD in comparison with healthy controls. Su et al. found this lipid increased in brain-derived extracellular vesicles from AD patients [335].

For LPC in plasma samples, a previous study showed an increase with aging, which is more evident under AD conditions [303]. Similarly, the present study found higher levels of LPC 18:1 and lower levels of L-α-phosphatidilcholine and PC in AD patients. However, Mulder et al. found a decrease in the ratio LysoPC/PC under MCI or dementia due to AD conditions [336]. In addition, the present study showed plasma 18:1 LPC correlations with CSF t-Tau and p-Tau, which are biomarkers currently employed in AD diagnosis. Specifically, Tau is considered a neurodegeneration biomarker [337]. In this sense, the correlation found between 18:1 LPC and Tau showed the potential utility of 18:1 LPC as a neurodegeneration biomarker. Similarly, previous studies showed the utility of the metabolites 18:0 LPC and 18:2 LPC as potential biomarkers for AD [90]. These discrepancies could be explained by the different types of samples used (plasma and CSF) as well as by the different isomers determined in these compounds' families. In addition, the ratio between LPC and PC in the plasma samples showed the capacity to differentiate between AD and non-AD participants [338].

The main limitation of this study is the small sample size. However, the participants were accurately classified into groups according to their amyloid status, cognitive state, and brain alterations with neuroimaging. Moreover, there is a lack of confirmation studies to identify the metabolites as reliable AD biomarkers. Nevertheless, this work provides a detailed lipidomic approach from untargeted and targeted analyses that identified potential biomarkers and pathways involved in early AD development. Although analyses of confounding variables, such as age, were not performed, correlations between age and lipids or lipid class were assessed.

4. Conclusions

A lipidomic approach was developed from untargeted and targeted analyses of plasma samples. It showed some differential expression of lipids between healthy participants and patients at the early stages of AD. Therefore, the plasma lipid profile could be useful in the early and minimally invasive detection of AD. Among lipid families, relevant results were obtained from DGs, LPEs, LPCs, MGs, and SMs. Specifically, MGs could be potentially useful in AD detection, while LPEs, LPCs, and SM are related more specifically to their preclinical stage and DGs are related to the MCI

stage. Among these families, 18:1 LPE showed potential utility as a biomarker for AD and neurodegeneration. In addition, other analyte families, such as phosphatidylglicerol, phosphocholine, glicerophosphocholine, glicerophosphoserine, glicoesphingolipid, vitamin E, terpenes, steroids, flavonoids, glycosyldiacylglycerols, fatty acids, glucosylceramides, and fucopentanoses, showed potential alterations in early AD stages. However, further analysis in a large number of samples is required to validate these preliminary results.

Chapter 11. Plasma microRNAs as potential biomarkers in early Alzheimer disease expresion

1. Summary

The aim of this chapter is to analyse the differential expression of a panel of miRNAs selected from sequencing analysis in plasma from early AD and control participants evaluating their potential usefulness as biomarkers and their implication in molecular pathways altered in early AD stages. For this, miRNAomic expression profiles were analysed by Next Generation Sequencing in plasma samples from MCI-AD (n = 19), preclinical AD (n = 8) and controls (n = 19). Then, the selected miRNAs were validated by quantitative PCR (q-PCR) and a Bayesian model was developed including them. Then the targets of the selected miRNAs and the pathways regulated by them were analyzed using miRDB.

2. Results

2.1. Participants characteristics

The participants' characteristics are summarized in Table 28. As can be seen, most of the variables showed no significant differences among participants' groups. In fact, only the clinical variables used in their diagnosis (CSF biomarkers levels, neuropsychological assessment) show statistically significant differences, as expected. In contrast, demographic variables (age, sex, educational level, medication use (statins, fibrates, benzodiazepines, antihypertensives), comorbidities (dyslipidemia, diabetes, hypertension)) are similar between the study groups.

Table 28. Participant's clinical and demographic variables.

Variable	Control (n = 19)	MCI-AD (n = 19)	Preclinical-AD (n=8)	*P* value
	Median (1st, 3rd Q.)			
Age (years)	69 (64.5, 70.5)	70 (67.5, 74)	68.5 (66.7, 70.5)	0.134
Sex, female, n (%)	8 (42.11%)	8 (42.11%)	5 (62.5%)	0.575
Educational level (n, %)				
Basic or primary	6 (31.58%)	7 (38.89%)	1 (12.5%)	0.094
Secondary	6 (31.58%)	10 (55.56%)	3 (37.5%)	
Uiversitary	7 (36.84%)	1 (5.56%)	4 (50%)	
Smoking Yes, n, (%)	3 (15.79%)	3 (15.79%)	2 (25%)	0.823
Alcohol Yes, n (%)	4 (21.05%)	2 (10.53%)	1 (12.5%)	0.647
Statins (n, %)	11 (57.89%)	10 (52.63%)	3 (37.5%)	0.625
Fibrates (n, %)	2 (10.53%)	2 (11.11%)	1 (14.29%)	0.690
Benzodiazepines (n, %)	3 (15.79%)	2 (10.53%)	1 (12.5%)	0.889
Antihipertensives (n, %)	8 (42.11%)	7 (38.89%)	1 (12.5%)	0.317
Dyslipidemia (n, %)	13 (68.42%)	10 (52.63%)	3 (37.5%)	0.303
Diabetes (n, %)	3 (15.79%)	1 (5.26%)	3 (37.5%)	0.103
Hypertenison (n, %)	9 (47.37%)	8 (42.11%)	1 (12.5%)	0.224
Aβ42 (pg mol-1)	1224 (967, 1429)	495 (456, 616)	671.5 (507.5, 714)	< 0.001
t-Tau (pg mol-1)	276 (227.5, 375)	578 (432.75, 785.75)	464 (337.5, 548.5)	0.001
p-Tau (pg mol-1)	40 (29, 44)	91 (58.75, 107.75)	67 (58.25, 99)	< 0.001
CDR	0 (0, 0)	0.5 (0.5, 0.5)	0 (0, 0)	< 0.001
MMSE	29 (27.5, 29.5)	24 (23, 25.75)	27 (26.75, 28.25)	< 0.001
FAQ	0 (0, 1)	7 (5, 10.5)	1 (0, 2)	< 0.001
RBANS.MR	101 (96.5, 106.5)	42 (40, 55)	86 (77.25, 98.75)	< 0.001

2.2. miRNAs validation

A panel of 11miRNAs was selected following the specified criteria (counts in at least 80% of the samples and previous findings in literature). The selected miRNAs were hsa-miR-92a-3p, hsa-miR-486-5p, hsa-miR-29a-3p, hsa-miR-486-3p, hsa-miR-150-5p, hsa-miR-142-5p, hsa-miR-320b, hsa-miR-483-3p, hsa-miR-1293, hsa-miR-342-3p, and hsa-miR-4259. Of these, 8 miRNAs were successfully quantified (has-miR-92a-3p, has-miR-486-5p, has-miR-29a-3p, miR-486-3p, miR-150-5p, miR-320b, miR-483-3p, miR-342-3p); while some miRNAs were not detected (hsa-miR-142-5p, miR-1293, hsa-miR-4259). The levels obtained for each miRNA are summarised in Table 29. As can be seen, small differences were obtained for each miRNA amongparticipants' groups.

Table 29. Median levels of miRNAs in plasma from participants' groups.

Variable (Total counts)	Control (n = 19) Median (IQR)	MCI-AD (n = 19) Median (IQR)	Preclinical AD (n = 8) Median (IQR)
hsa-miR-92a-3p	22.26 (21.12, 22.67)	21.51 (21.27, 22.72)	21.89 (21.37, 22.61)
hsa-miR-486-5p	22.72 (22.22, 23.43)	22.5 (22.13, 23.3)	23.33 (22.26, 24.21)
hsa-miR-29a-3p	26.86 (25.92, 27.55)	26.93 (26.4, 27.36)	27.62 (26.62, 27.99)
hsa-miR-486-3p	28.19 (27.47, 28.96)	28.07 (27.44, 29.35)	27.98 (27.4, 29.8)
hsa-miR-150-5p	24.18 (23.84, 24.9)	23.93 (23.38, 25.2)	23.93 (23.38, 24.49)
hsa-miR-320b	26.94 (26.26, 27.64)	26.73 (26.19, 27.1)	26.88 (25.94, 27.48)
hsa-miR-483-3p	31.53 (31.18, 32.32)	31.63 (30.97, 32.91)	31.5 (31.31, 31.74)
hsa-miR-342-3p	28.54 (28.07, 29.04)	28.48 (27.7, 29.46)	27.71 (27.05, 28.75)

Individually, the validated miRNAs showed no significant differences between groups. Therefore, two multivariate models, including the previously selected miRNAs, were developed to analyse the tendency of each miRNA in participants' groups. The first model included 3 participant groups (control, MCI-AD, preclinical AD); while the second model included 2 participant groups (AD (MCI-AD + preclinical-AD), control). In Table 30, the characteristics of the first model are summarised, showing that the miRNAS hsa-miR-92a-3p, hsa-miR-486-5p and hsa-miR-29a-3p had a high probability of direction (PD > 80%).

Specifically, hsa-miR-92a-3p showed a PD 85.40% of a negative estimate, so relatively reduced levels were found in AD. Similar results were obtained for hsa-miR-486-5p. In fact, it showed a high probability of a negative estimate with small Region of Practical Equivalence (ROPE) (< 15%), which defines the percentage of the area that is within the region of practical equivalence (equivalent to null effect)), showing an Odds Ratio (OR) lower than 1, and suggesting a protective effect for AD. By contrast, hsa-miR-29a-3p showed a positive estimate, so relatively increased levels were found in AD. Similarly, the characteristics of the model including 2 participants' groups (AD, control), showed that the miRNAS hsa-miR-92a-3p and hsa-miR-29a-3p had a PD > 90%, with negative and positive estimates, respectively.

These results are shown in Figure 32, which depicts the PD and ROPE for each miRNA. The miRNAs with a high PD (mir-92a-3p, miR-486-5p, miR-29a-3p), showed most of their area on one side of 0 (Figure 32a). In addition, mir-92a-3p and miR-486-5p showed a negative direction, while miR-29a-3p showed a positive direction. Figure 32b shows the ROPE region, being a small area in the first three miRNAs.

Table 30. Characteristics of the Bayesian model including 3 participants groups (control, preclinical-AD, MCI-AD).

Variables	Estimate	OR (CI 95%)	Inside Rope (%)	PD (%)
hsa-miR-92a-3p	−0.484	0.616 (0.241,1.455)	19.34%	85.40%
hsa-miR-486-5p	−0.649	0.522 (0.112,2.28)	14.15%	81.38%
hsa-miR-29a-3p	0.418	1.519 (0.662,3.626)	22.76%	82.88%
hsa-miR-486-3p	0.478	1.613 (0.462,5.929)	18.05%	77.88%
hsa-miR-150-5p	0.123	1.131 (0.243,5.574)	19.76%	55.27%
hsa-miR-320b	0.174	1.19 (0.373,4.02)	23.34%	60.68%
hsa-miR-483-3p	0.286	1.331 (0.624,2.968)	29.86%	77.15%
hsa-miR-342-3p	−0.458	0.632 (0.131,3.086)	16.47%	72.58%

The Probability of Direction (PD) is an index of effect existence, ranging from 50 to 100%, representing the certainty with which an effect goes in a particular direction. PD > 80% was considered significative. For each variable the direction depends on the estimate (negatives estimate < 0, and positives estimates > 0). Region of Practical Equivalence (ROPE) defines the percentage of the area that is within the region of practical equivalence (equivalent to null effect). OR odds ratio, CI confidence interval.

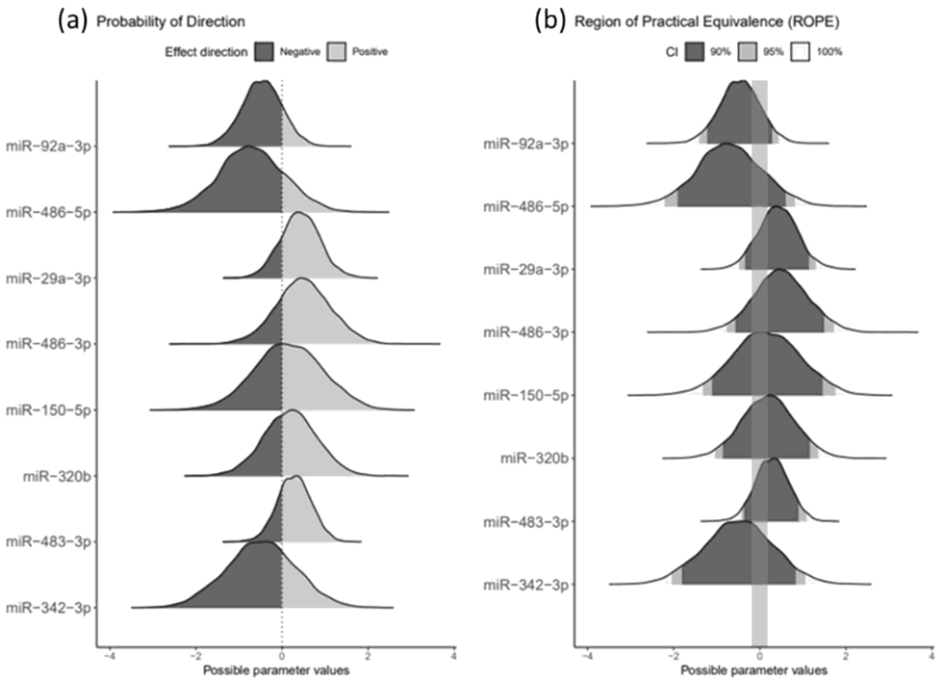

Figure 32. Probability of direction (PD) and Region of Practical Equivalence (ROPE) for each miRNA. (a) PD shows the estimation of direction for each biomarker, showing a protective AD effect for those with negative direction and risk AD effect for those with positive direction. Polygons show the density summary of the posterior draws and colored given the estimated direction (positive or negative) of the effect parameter. The proportion of the polygon that does not include zero is a statement about probability of the proposed direction of effect. (b) ROPE represents the area of null equivalence that is the percentage with none direction (positive or negative). Effects given a full ROPE based on a 100%, 95% and 90% highest posterior density interval. The proportion of the polygon that does not include zero is a statement about the significance of effect.

2.3. Pathway analysis

For the miRNAs with a high directional probability (hsa-92a-3p, hsa-486-5p, hsa- 29a-3p), their potential target genes were analysed in order to assess their involvement in the pathology development. Table 31 shows the potential target genes of the selected miRNAs related to AD mechanisms. As can be seen, 112 potential targets were obtained for miRNA hsa-92a-3p, 16 targets for hsa-486-5p, and 88 targets for hsa-29a-3p, with a target score of at least 95. In addition, each of the selected miRNAs regulated several

pathways. As can be seen in Figure 33, the most common pathways were cell signalling and transcription regulation, but also lipid metabolism, protein synthesis and modifications, and structural functions were regulatedby the selected miRNAs. First, the main pathways that could be regulated by the miRNA hsa-92a-3p are cell death or autophagy and cell proliferation pathways, and some pathways related to vesicle transport and synaptic transmission. Among the cell death targets, BCL2L11 (BCL2 like 11) is involved in neuronal and lymphocyte apoptosis and G3BP2 (G3BP stress granule assembly factor 2) is involved in stress response. In the cell proliferation pathway, the gene C21orf91 (chromosome 21 open reading frame 91) plays a role in the proliferation of neurons in the cortex. Among synaptic transmission targets, GLRA1 (glycine receptor alpha 1), SYN2 (synapsinII), SCN8A (sodium voltage-gated channel alpha subunit 8), CADM2 (cell adhesion molecule 2), CBLN4 (cerebellin 4 precursor), SYNJ1 (synaptojanin 1), SLC17A6 (solute carrier family 17 member 6), and NSF (N-ethyl-maleimide sensitive factor, vesicle fusing ATPase) are highlighted, being the last two targets involved in vesicle transport. Other important genes are REST (RE1 silencing transcription factor), which regulates neuronal genes transcription; and NEFH (neurofilament heavy), which contributes to the maintenance of neuronal structure. In addition, PPCS (phosphopantothenoylcysteine synthetase) could be relevant in the regulation and metabolism of CoenzymeA.

Secondly, the main pathways that could be regulated by the miRNA hsa-486-5p are cell signalling, lipid and protein pathways, structural functions and transcription.

Table 31. Potential target genes and related AD pathways. In this link it can be found the full name of each gene (*http://mirdb.org/mirdb/index.html*)

Pathway	**hsa-miR-92a-3p**	**hsa-miR-486-5p**	**hsa-miR-29a-3p**
Autophagy	TECPR2, EPG5		
Cell death	G3BP2, HIPK3, USP28, DNAJB9, BCL2L11,RNF38		TRIB2, XKR6, AKT3
proliferation	CD69, FNIP1, BTG2, MAP2K4, C21orf91, KLF4, FNIP2, GTF2A1, CDK16, ARID1B, CDCA7L, CCNJL, CUX1, MAP1B, RNF38		NAV1, NAV2, NAV3, IGF1, ZNF346, LIF, CDK6, SGMS2, PDIK1L, CHSY1, NEXMIF,AKT3, ADAMTS9
Cell signalling	PIKFYVE, DOCK9, ITGAV, EFR3A, RIC1, RNF38, GPR180, PLEKHA1, JMY, GNAQ, RGS17, PTEN, PCDH11X, GIT2, ADGRF2,CALN1, DPP10, LRCH1, HCN2	DCC, PTEN, SLC10A7, ARHGAP44, MARK1	NEXMIF, AKT3, DAAM2, PTEN, PGAP2,ROBO1, RAP1GDS1, RAB30, DGKH, CLDN1, TRAF3
Energetic metabolism and oxidative stress	NOX4, SESN3, PTEN, SLC12A5	PTEN	PTEN
Glucose metabolism	MAN2A1, FBN1, UGP2		FBN1
Immune response	TAGAP, CD69, KLF4, GLRA1, FOXN2, RAB23		TRAF3
lipid metabolism	PPCS, KIAA1109	FAHD1	OSBPL11
membrane transport	SLC12A5, SLC25A32, SGK3		SESTD1, ABCE1, SLC5A8
Nucleic acid metabolism and DNA organization	MORC3, RBM27, GID4, CPEB3, SLX4, AGO3, JMY, ANP32E, RSBN1		DOT1L, KMT5C, ERCC6, NASP, KDM5B,TDG
DNA and histones methylation			TET1. TET2, TET3, DOT1L, DNMT3A,

			DNMT3B, KDM5B
Protein degradation	FBXW7, SESN3, KLHL14, USP36, USP28, UBXN4		VPS37C, TRIM63
Protein synthesis and modifications			
	B3GALT2, PTAR1, GOLGA3, COG3, SGK3, ADAM10, EDEM1	COPS7B, MARK1, LMTK2, ABHD17B	ADAMTS9, ADAMTS6, DIO2, ABCE1
Structural function	ACTC1, ANP32E, NEFH, RSBN1, NCKAP5, NEFM, RHPN2, FBN1, MYO1B	SNRPD1, NCKAP5, LCE3E	COL5A3, COL5A1, COL3A1, FBN1, COL11A1, HAS3, TMEM169, COL19A1, COL4A1, COL1A1, COL7A1, SPARC, COL5A2, HMCN1, C1QTNF6, ADAMTS2,CEP68, PXDN, COL9A1, HAPLN3, RND3, TRAF3, RAB30, CLDN1
Synaptic transmission	GLRA1, SYN2, SCN8A, CADM2, CBLN4,SYNJ1, SLC17A6, NSF	ARHGAP44	
Transcription	MIER1, HAND2, TBL1XR1, LATS2, FOXN2, ZEB2, REST, GRHL1, TEAD1, HIVEP1	BTAF1, SNRPD1, FOXO1, ZNF331	HBP1, ATAD2B, BRWD3, NSD1, ZBTB34,NFIA, KDM5B, PURG, HIF3A, ZBTB5, ZNF282, AMER1, REST, TAF5, ZHX3, C16orf72
Vesicle transport	MYO1B, CDK16, PIKFYVE, SLC17A6, NSF, RAB23, DENND1B		ASAP2, VPS37C
Others	ZFC3H1, TTC9, ATXN1, DCAF6, LHFPL2,FAM160B1, ERGIC2, MAGEC2, SPRYD4, ANKRD28, TRIM36, FAM24A, BCL11B	TRIM36	ADAMTS17, PRR14L, FAM241A, LYSMD1,PXYLP1, SMS, ATAD2B

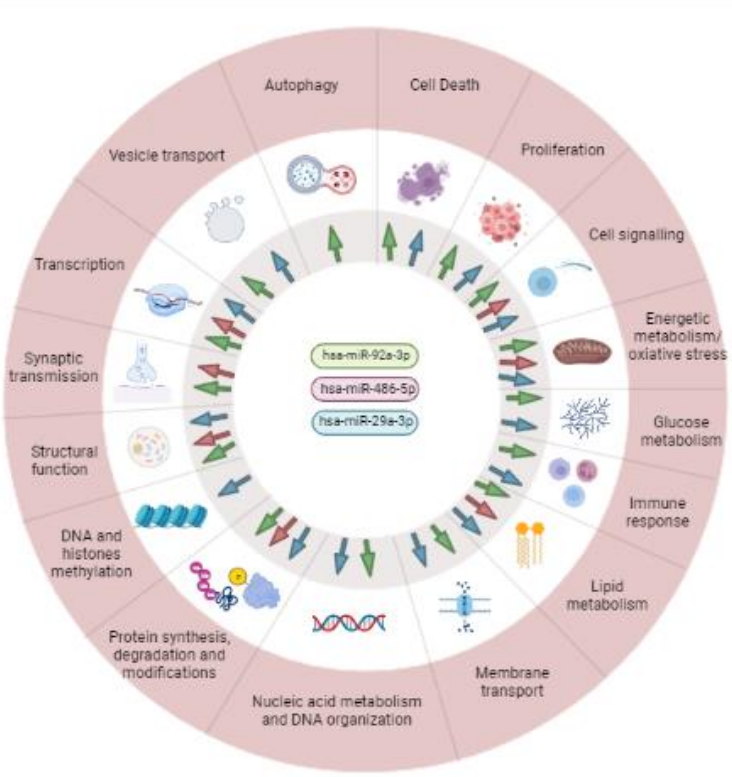

Figure 33. Pathways regulated by the three miRNAs that showed relationship with AD. The arrows indicate those miRNAs involved in each pathway. Each color represents a miRNA: green (hsa-miR-92a-3p), red (hsa- miR-486-5p) and blue (hsa-miR-29a-3p). *Created with BioRender.com.

Thirdly, the main pathway that could be regulated by the miRNA hsa-29a-3p is the cell proliferation pathway, which involves neurone regeneration and migration trough NAV3 (neuron navigator3), NAV1, and NAV2. Also, ZNF346 (zinc finger protein 346) could act to protect neurons and LIF (LIF, interleukin 6 family cytokine) is involved in neuronal differentiation. In cell signalling pathways, the targets DAAM2 (dishevelled associated activator of morphogenesis 2) and ROBO1 (roundabout guidance receptor 1) contribute to nervous system development and neuronal migration, respectively. Furthermore, miRNA hsa-29a-3p plays a role in structure regulation, specifically regulating the

synthesis of different collagen chains, and HMCN1 (hemicentin 1) is involved in macular degeneration and C1QTNF6 (C1q and TNF related 6) is involved in identical protein binding activity. Also, this miRNA could regulate REST in the transcription pathway.

3. Discussion

In this study, miRNA sequencing was carried out to identify potential early AD biomarkers. From these, a validation step was conducted, in which quantifiable miRNAs were identified, while some of them were not detected. In fact, the miRNAs not validated were hsa-miR-142-5p, hsa-miR-1293 and hsa-miR-4259. A previous study in cell line found a relationship between dysregulation of miR-142-5p expression and AD pathogenesis and synaptic dysfunction [339], and it was detected up-regulated in the blood of AD patients [340]. Also, hsa-miR-4259 was detected in saliva samples, but there is a lack of studies quantifying this biomarker in plasma samples [341]. In addition, has- miR-1293 was previously detected in platelets from hepatocellular carcinoma and lung adenocarcinoma cell line [342]. Nevertheless, there are no studies describing its association with AD.

Regarding the methodology, Haining et al., performed a similar study trying to find a miRNA profile in early AD. However, different cohorts for untargeted and targeted analysis were used [125]. Also, Dakterzada aimed to find miRNAs in plasma from AD participants, identifying a BACE1 related panel of biomarkers different from the miRNAs in the present work [343]. It could be due to the use of a different identification technique based on microarrays analysis [344]. The different methodologies employed could affect the miRNAs selection, so it shouldbe taken into account in comparisons with other studies [343].

Regarding the miRNAs that showed a trend with the pathology in the present study, they were hsa-miR- 92a-3p, has-miR-486-5p and hsa-miR-29a. First, hsa-miR-92a-3p showed a tendency for decreased levels in AD. A previous study showed dysregulation of 3 miRNAs related to synaptic proteins, including hsa-miR-92a-3p in MCI and AD [345]. Another study described the relationship between miR-92a-3p and Tau accumulation [346]. One of the most AD-relevant pathways that could be regulated by this miRNA is synaptic transmission [347]. Specifically, SYNJ1, a potential target for this miRNA, seemed to be involved in Aβ clearance [348,349], while synapsins could act on Aβ generation by

modulating BACE1 [350]. In addition, CBLN4 could regulate Aβ toxicity [351]. Regarding neuronal apoptosis, it could be regulated by this miRNA and the BCL2L2 target. In fact, a previous work showed that Aβ could regulate that pathway [352]. Other target genes (NEFH, REST), which are involved in neuronal structure and neuronal gene transcription, were described as potential AD diagnosis biomarkers [353,354].

Second, the present study showed a tendency towards reduced levels of hsa-miR-486-5p in AD. Similarly, Nagaraj et al. described a panel of 6 plasma miRNAs, including hsa-miR-486-5p, that differentiated between controls and MCI-AD [355]. This miRNA could regulate some genes involved in cell signalling, lipid and protein pathways, transcription and structural function.

Third, a trend towards higher levels for hsa-miR-29a-3p in AD plasma was found. Similarly, Shioya et al. described differential levels of this miRNA at brain level, suggesting its implication in neurodegeneration trough NAV3 (Neurone Navigator 3) regulation [356,357]. In addition, another miRNA from that family (hsa-miR-29c) has been related to AD pathology due to its involvement in the Aβ accumulation through the regulation of BACE1 [357,358]. Moreover, Müller et al. suggested that miR-29a could be a candidate biomarker for AD in CSF samples without cells [359]. In this regard, different types of collagenous chains and C1QTNF6 are targets of miRNA hsa-29a-3p. Previous studies described collagenous chains as a component from amyloid plaques [360]. The collagenous regulation may contribute to the assembly of amyloid fibres, enhancing the development of amyloid pathology. In addition, C1q complement protein co-localizes with the Aβ in brain [361,362]. Therefore, C1QTNF6, which is thought to play a role in identical protein binding, could help in the accumulation of C1q protein, triggering amyloid plaque formation (PubMed Gene). In addition, ROBO1 and DAAM2, which are involved in neuronal migration and nervous system development, are targets for this miRNA. In fact, ROBO1 could show a relationship with axon guidance dependent on presenilin, which helps in the proteolysis of Aβ precursor protein and triggers to AD pathology development [363,364]. Furthermore, DAAM2 was described by Ding et al. as a mediator in regenerative oligodendrocyte differentiation; while Sellers et al. demonstrated that Aβ synaptotoxicity is mediated by this protein [365,366].

The main limitations in this study are the small sample size, since it is quite difficult to have

a large number of biologically classified early AD patients (MCI, preclinical). Moreover, from the selected miRNAs, some of them were not validated as they were not correctly quantified, probably due to the fact that they were detected in few samples. In addition, the study design is cross-sectional. In order to obtain more accurate data from the different disease stages, it should be longitudinal. However, participants in this present study are perfectly characterized according to CSF biomarkers and their cognitive status, providing a reliable approach to the disease progression.

4. Conclusion

RNA sequencing analysis in plasma samples from participants with early AD and healthy controls allowed to identify some differentially expressed miRNAs. From them, 3 selected miRNAs (miRNA-92a-3p, miRNA-486-5p, miRNA-29a-3p) were slightly dysregulated in AD, being potential biomarkers of the pathology. In fact, they could be involved in the regulation of important pathways of the pathology, such as synaptic transmission, cell signalling, structure maintenance or cell metabolism, so they could be relevant therapeutic targets. However, further research with a larger sample is needed to verify these results, as well as to develop the potential mechanisms of action of these miRNAs.

Chapter 12. Epigenomics and lipidomics integration in Alzheimer Disease: pathways involved in early stages

1. Summary

The aim of this work was to carry out the integration of epigenomics and lipidomics analysis in plasma samples from patients with MCI-AD in order to advance the knowledge of early physiopathological mechanisms. For this, epigenomic and lipidomic analysis were carried out in plasma samples from patients with MCI-AD (n = 22) and controls (n = 5). Then, omics integration between microRNAs (miRNAs) and lipids was performed by PLS regression and target genes for the selected miRNAs were identified.

2. Results

2.1. Participants

Table 32. Demographic and clinical characteristics of the participants.

Variables	**Healthy Group (n = 5)**	**MCI-AD Group (n= 22)**
Age (years, median (IQR))	68 (68, 72)	72 (69, 74)
Gender (female, n (%))	2 (40%)	12 (54.5%)
CSF Aβ42 (pg mL^{-1}, median (IQR))	1346.74 (930, 1421)	517.16 (453.86, 634.45)
CSF Aβ42/ Aβ40 (median, IQR)	0.1 (0.09, 0.11)	0.05 (0.05, 0.05)
CSF t-Tau (pg mL^{-1}, median (IQR))	240 (238, 276)	566 (450, 780)
CSF p-Tau (pg mL^{-1}, median (IQR))	35 (35, 40)	81 (64.5, 107)
CSF NfL (pg mL^{-1}, median (IQR))	826.94 (791, 847.7)	1428.68 (1123.24, 1555.91)
CSF t-Tau/ Aβ42 (median (IQR))	0.2 (0.19, 0.25)	0.99 (0.79, 1.32)
CDR (score, median (IQR))	0 (0-0.5)	0.5 (0-1)
MMSE (score, median (IQR))	29 (29, 30)	24 (23, 26)
RBANS_DM (score, median (IQR))	100 (98, 110)	44 (40, 64)
FAQ (score, median (IQR))	1 (0, 2)	7 (4, 9)

CSF: cerebrospinal fluid; Aβ: amyloid β; IQR: inter-quartile range; CDR: Clinical Dementia Rating; MMSE: Mini-Mental State Examination; RBANS_DM: The Repeatable Battery for the Assessment of Neuropsychological Status_Delayed Memory; FAQ: Functional Activities Questionnaire.

Table 32 shows the demographic and clinical data for the participants. As expected, CSF biomarkers levels and neuropsychological tests were different between groups. In fact, the MCI-AD group showed lower levels for Aβ42, and higher levels for t-Tau and p-Tau; also, MCI-AD group showed lower scores for MMSE, and RBANS, and higher scores for CDR and FAQ.

2.2. Omics integration

The PLS model integrated two data matrices X (epigenomics) and Y (lipidomics). Additionally, PLS performed simultaneous variables selection in the two data sets, by means of LASSO penalization on the pair of loading vectors. In this sense, two components were chosen, and 25 variables were selected on each dimension and for each data set. The X-block represented miRNAs, and the Y-block represented lipids.

Samples from both sets were represented in the 'common' subspace spanned by the principal components (PC1, PC2). As can be seen in Figure 34, samples were differentiated in the plot according to the participants group, there was not observed a clear separation. Among the 25 selected variables for each data set, the miRNAs (block X) with higher loadings in the PLS regression were hsa-miR-494-3p, hsa-miR-6894-3p, hsa-miR-421 andhsa-let-7a-3p; and the lipids (block Y) with higher loadings were FA (20:3), FA (20:4), FA (16:0), FA (20:2), and FA (18:2) (see Figure 35).

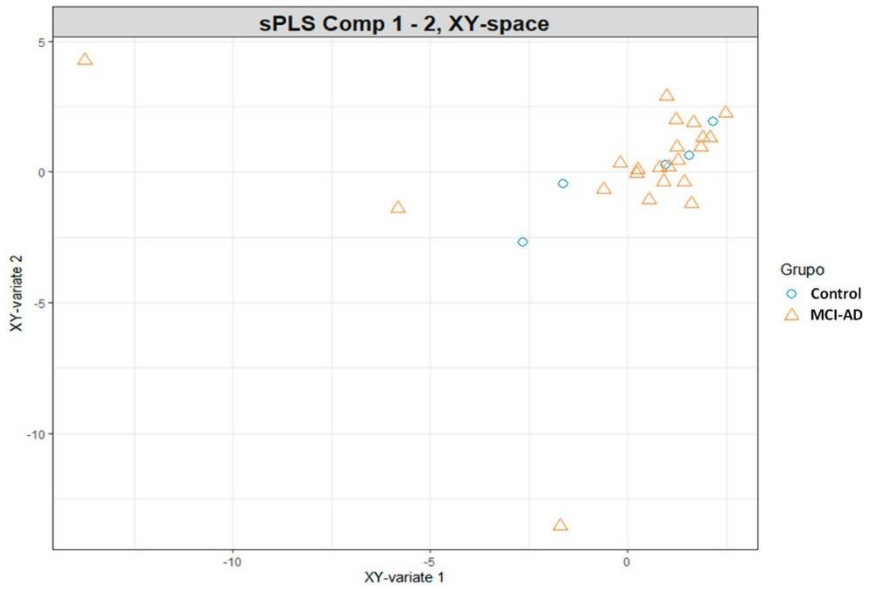

Figure 34. Scatter plot for participants samples in PLS analysis. Represent the samples distribution in the 'common' subspace between the two sets of components (epigenomics and lipidomics variables).

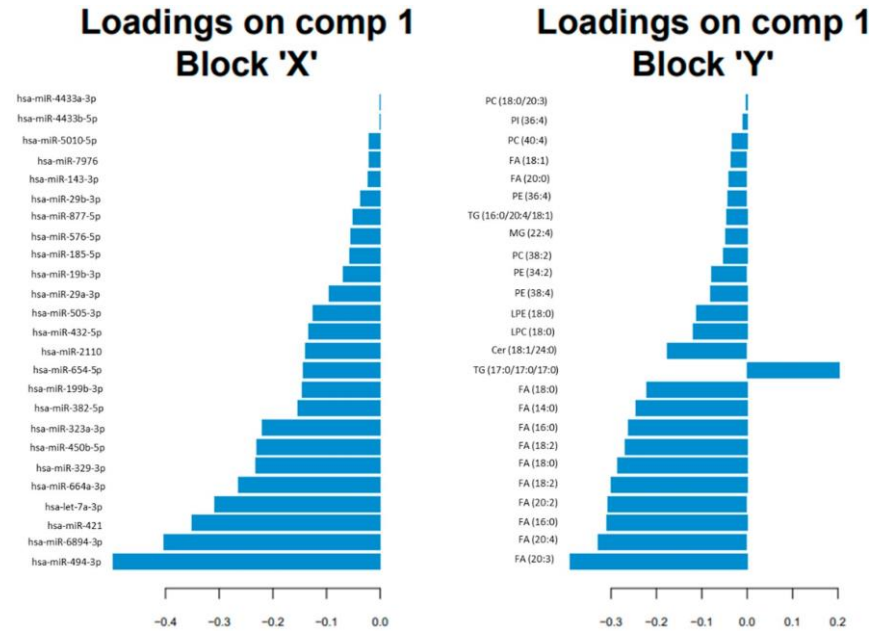

Figure 35. Horizontal barplot to visualise loading vector. The contribution of each variable for each component (comp) is represented in a barplot, where each bar length corresponds to the loading weight (importance) of the feature. The loading weight can be positive or negative.

The correlation circle plot depicted miRNAs and lipids selected on each component. Some subsets of variables were important to define each component. Actually, some miRNAs (hsa-miR-5010-5p, hsa- miR-421, hsa-miR-664a, hsa-miR-29b-3p, hsa-let-7a-3p, hsa-miR-19b-3p) and some lipids (FA (20:4), FA (20:3), FA (18:0)) mainly participated in defining the PLS component 2; and some miRNAs (hsa-miR-335-3p, hsa-miR-532-3p, hsa-miR-379-5p, hsa-miR-4646-3p, hsa-miR-425-3p) mainly participated in defining component 1. Additionally, miRNAs, such as hsa-miR-421 and hsa-miR-5010-5p, were positively correlated to the lipids FA (20:4) andFA (20:3); while these miRNAs were negatively correlated to the lipid TG (17:0/17:0/17:0).

The integration results were depicted by means of a heatmap. The similarity matrix was obtained from the PLS results [367] and agglomerative hierarchical clustering was derived using the Euclidean distance as the similarity measure, and the Ward

methodology [368]. In this sense, Figure 36 shows the heatmap for the correlations between miRNAs and lipids selected from PLS. The red color corresponded to positive correlation, while the blue color corresponded to negative correlation. Most of the correlations were positive.In general, Figure 37 showed a positive correlation between studied miRNAs and lipids. However, the lipid TG (17:0/17:0/17:0) showed a negative correlation with all the described miRNAs. In addition, similar miRNAs were grouped, showing clusters for miR-29a-3p, let-7a-3p, miR-576-5p, miR-185-5p, miR-6894-3p, miR-5010-5p; for miR-29b-3p, miR-877-5p, miR-494-3p, miR-4433a-3p, miR-4433b-5p; and for miR-421, miR-450b-5p, miR-664a-3p, miR-432-5p, miR-654-5p, miR-2110, miR-329-3p. In addition, similar lipids were grouped, showing clusters for FA (18:0)/FA (14:0)/FA (18:0)/FA (16:0)/FA (18:2) and FA (20:3)/FA (20:4)/FA (18:2)/FA (20:2)/FA (16:0).

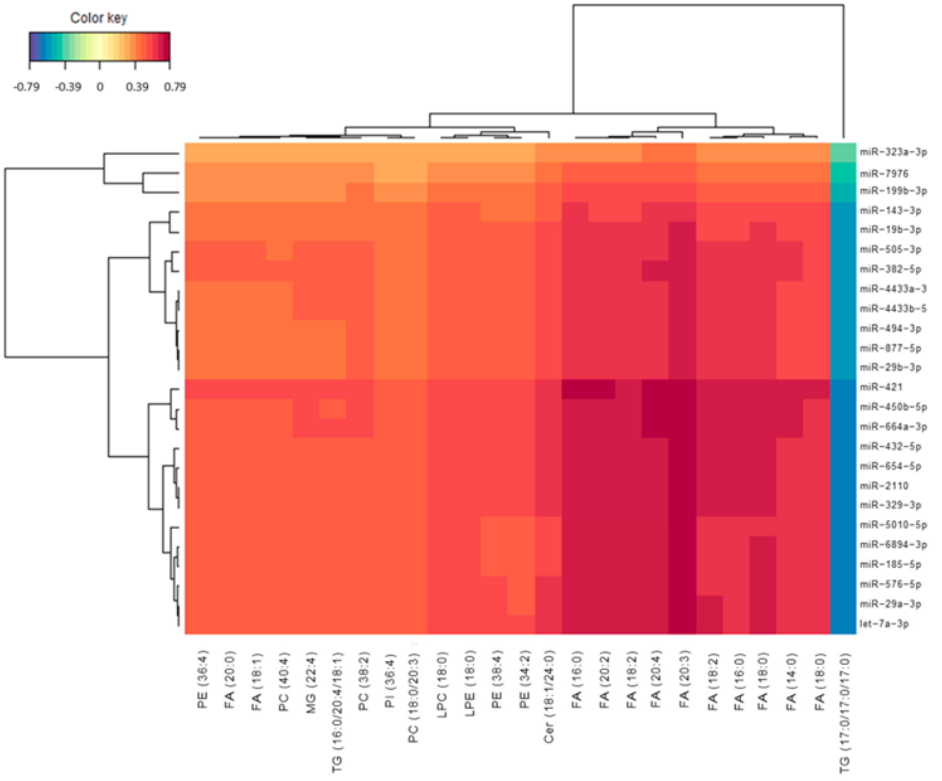

Figure 36. Heatmap representing correlations between miRNAs and lipid variables. Red colour represents positive correlations and blue colour represents negative correlations.

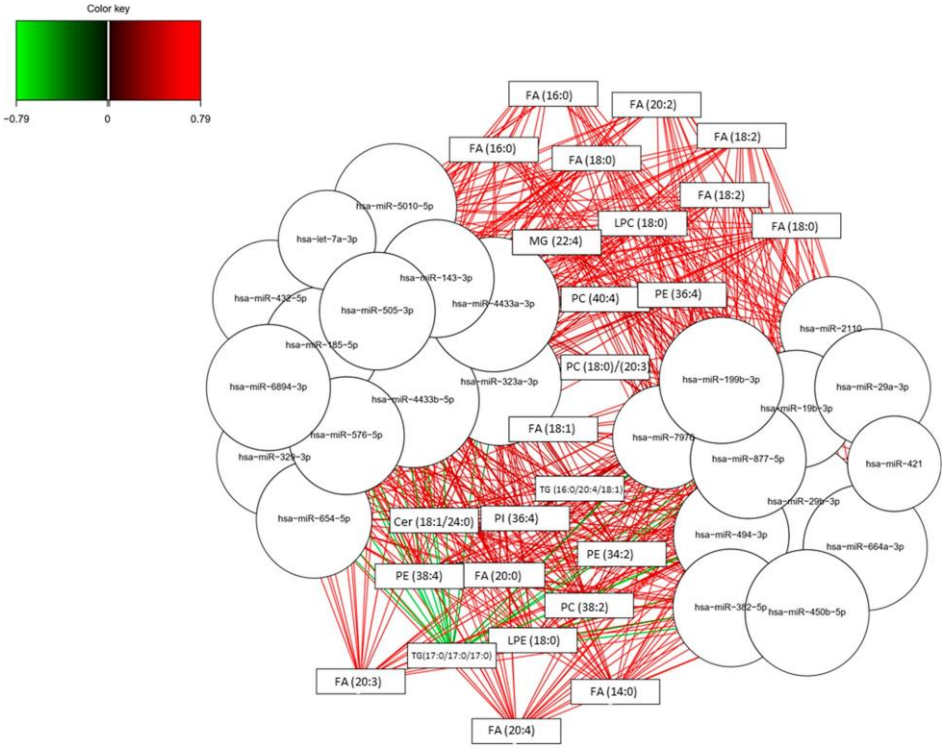

Figure 37. Relevance associations network for PLS. Pair-wise similarity matrix directly obtained from the latent components was calculated. The similarity value between a pair of variables is obtained by calculating the sum of the correlations between the original variables and each of the latent components of the model. The values in the similarity matrix can be seen as a robust approximation of the Pearson correlation.

2.3. Potential pathways involved in AD

In Table 33, the predicted target genes for the selected miRNAs were described paying special attention to the genes that are implied in lipid metabolism, specifically in fatty acids pathways, which showed correlation with the miRNAs. In fact, fatty acids family showed the strongest correlations with miRNAs (see Figure 37). Among the identified target genes, several enzymes, such as elongases (ELOVL1, ELOVL2, ELOVL3, ELOVL4, ELOVL5, ELOVL6, ELOVL7), fatty acid desaturase (FADS6), fatty acyl-CoA reductases (FAR 1, FAR 2), fatty acid binding protein (FABP7), and fatty acid 2-hydroxylase (FA2H) were highlighted.

Table 33. Predicted target genes related to fatty acids for the selected miRNAs (miRBase).

miRNA	Target Genes	
hsa−miR−494−3p	ELOVL3	(ELOVL fatty acid elongase 3)
	ELOVL5	(ELOVL fatty acid elongase 5)
hsa−miR−6894−3p	-	
hsa−miR−421	ARV1	(ARV1 homolog, fatty acid homeostasis modulator)
	FAR1	(fatty acyl-CoA reductase 1)
	ELOVL2	(ELOVL fatty acid elongase 2)
hsa−let−7a−3p	ELOVL2	(ELOVL fatty acid elongase 2)
	FA2H	(fatty acid 2-hydroxylase)
	ELOVL7	(ELOVL fatty acid elongase 7)
hsa−miR−664a−3p	FAR1	(fatty acyl-CoA reductase 1)
	ELOVL4	(ELOVL fatty acid elongase 4)
	ELOVL7	ELOVL fatty acid elongase 7
	ELOVL5	ELOVL fatty acid elongase 5
hsa−miR−329−3p	-	
hsa−miR−450b−5p	ELOVL6	(ELOVL fatty acid elongase 6)
hsa−miR−323a−3p	-	
hsa−miR−382−5p	-	
hsa−miR−199b−3p	-	
hsa−miR−654−5p	FADS6	(fatty acid desaturase 6)
	ELOVL1	(ELOVL fatty acid elongase 1)
hsa−miR−2110	ELOVL4	(ELOVL fatty acid elongase 4)
hsa−miR−432−5p	-	
hsa−miR−505−3p	ELOVL4	(ELOVL fatty acid elongase 4)
hsa−miR−29a−3p	ELOVL4	(ELOVL fatty acid elongase 4)
hsa−miR−19b−3p	ELOVL5	(ELOVL fatty acid elongase 5)
hsa−miR−185−5p	ELOVL4	(ELOVL fatty acid elongase 4)
	ELOVL2	(ELOVL fatty acid elongase 2)
	FAR1	(fatty acyl-CoA reductase 1)
hsa−miR−576−5p	FAR2	(fatty acyl-CoA reductase 2)
hsa−miR−877−5p	-	
hsa−miR−29b−3p	ELOVL4	(ELOVL fatty acid elongase 4)
hsa−miR−143−3p	FADS6	(fatty acid desaturase 6)
	FAR1	(fatty acyl-CoA reductase 1)
hsa−miR−7976	-	
hsa−miR−5010−5p	-	
hsa−miR−4433b−5p	-	
hsa−miR−4433a−3p	FABP7	(fatty acid binding protein 7)
	ELOVL4	(ELOVL fatty acid elongase 4)
	ELOVL2	(ELOVL fatty acid elongase 2)

Another representation for the integration results is based on relevance network for PLS regression, showing simultaneously positive and negative correlations between the two variable types (microRNAs, lipids). As can be seen in Figure 37, most of these correlations were positive. Specifically, the highest positive correlations corresponded to

these pairs of variables (FA (16:0) and FA (20:2) with hsa-miR-664, hsa-miR-432, hsa-miR-421, and hsa-miR-450b-5p; FA (18:0) and FA (18:2) with hsa-miR-664, hsa-miR-421 and hsa-miR-450b-5p; FA (20:3) and FA (20:4) with hsa-miR- 664, hsa-miR-211, hsa-miR-432, hsa-miR-329, hsa-miR-654, hsa-let-7a-3p, hsa-miR-29a-3p, hsa-miR-421, and hsa-miR-450b-5p). On the other hand, the highest negative correlations corresponded to the lipid TG (17:0/17:0/17:0) with some miRNAs (hsa-miR-664-3p, hsa- miR-2110, hsa-miR-432-5p, hsa-miR-329-3p, hsa-miR-654-5p, hsa-miR-185-5p, hsa-let-7a-3p, hsa-miR-576-5p, hsa-miR-29a-3p, hsa-miR-6894-3p, hsa-miR-421, hsa-miR-450b-5p).

2.4. Lipidomics and epigenomics in AD

From the univariate analysis, differences between groups were not obtained for miRNAs nor individual lipids. In addition, the analysis between age/gender and biomarkers levels showed no correlations for any miRNA or lipid analysed.

3. Discussion

Epigenomics and lipidomics analyses were carried out in plasma samples from early AD patients, identifying microRNAs and lipids, respectively. From these results, integration analysis was carried out in order to study associations between both compounds families; to evaluate their potential relationship with early AD development; and identify the potential pathways altered in early stages of the disease.

Some studies in literature are focused on multi-omics integration, mainly based on proteomics and miRNAs [369]. However, few studies are focused on lipidomic and miRNAs integration, which allow us to identify different biological activities involved in cell communication [370]. In general, the integration of omics results (lipidomics, metabolomics, proteomics, epigenomics) helps to give a global image of the mechanisms involved in complex diseases [371]. Nevertheless, this field of research is still underdeveloped in AD and few studies are based on this integration [59].

In the present study, integration and selection of variables from each dimension showed that some microRNAs (hsa-miR-494-3p, hsa-miR-6894-3p, hsa-miR-421 and hsa-let-7a-3p) and some lipids (FA (20:3), FA (20:4), FA (16:0), FA (20:2), FA (18:2))

had higher loadings in the regression model. Similarly, a previous study carried out in plasma from amyloid positive and amyloid negative participants obtained a signature of 71 miRNAs differentially expressed between groups, highlighting the hsa-miR-421 and hsa-let-7a- 3p [372]. In addition, a previous study from Hojati et al. revealed that hsa-miR-494-3p was slightly up-regulated in AD patients and that it was related to metabolic and cellular response to stress pathways [373]; while Lv et al., found that levels of hsa-let-7a-3p were elevated in patients with early onset familiar AD [374]. The up-regulation of hsa-let-7a-3p showed an increase in neurotoxicity in AD cell model [375]. On the other hand, previous studies found several fatty acids levels increased or decreased in AD [376,377]. Specifically, AD was related to lower levels of myristic 14:0, palmitic 16:0, stearic 18:0 and oleic 18:1 acid and a higher proportion of linoleic acid 18:2n - 6 [376]. However, this study was limited to FAs from 14:0 to 22:6 and did not determine all lipidic profiles. In addition, Conquer et al. described lower levels of phospholipid, PC 20:5n-3, DHA, total n-3 fatty acids, the n-3/n-6 ratio and phospholipid 24:0 compared to controls [377]. Moreover, Conquer et al. did not find differences for FA (20:3), FA (20:4), FA (20:2) and FA (18:2) in plasma samples from AD, cognitive impairment, and patients with other neurodegenerative diseases [377]. This discrepancy with the present results could be due to differences in AD diagnosis methods, since the previous study did not use CSF biomarkers to identify AD patients. In fact, these participants were classified by amyloid PET, and biomarkers were measured in erythrocytes. In addition, erythrocyte fatty acid composition varied according to disease development, showing differences between AD and non-AD participants for FA (20:4) but not for FA (20:3), FA (20:2) nor FA (18:2) [378].

Regarding correlations between microRNAs and lipids, and similarities among them in each omics data group, they showed that most of these correlations were positive. However, previous studies that correlated epigenomics (DNA hydroxymethylation) and metabolomics showed more variety between positive and negative correlations [379]. More specifically, several studies in neurodegeneration revealed the interaction between miRNAs expression and lipids regulation, mainly focussed on cholesterol metabolism [380]. Jauouen et al. described miR-33 function modulating ABCA1 and interfering with Aβ plaque formation through cholesterol metabolism regulation [381]. In the

present study, some miRNAs (miR-29a-3p, let-7a-3p, miR-576-5p, miR-185-5p, miR-6894-3p, miR-5010-5p; for miR-29b-3p, miR-877-5p, miR-494-3p, miR-4433a-3p, miR-4433b-5p; for miR-421, miR-450b-5p, miR-664a-3p, miR-432-5p, miR-654-5p, miR-2110, miR-329-3p) were grouped reflecting their similarity. Taking into account previous works, Kumar et al. found different miRNAs clustered expression, differentiating AD and control participants (hsa-miR-4741, hsa-miR-4668-5p, hsa-miR-3613-3p, hsa-miR-5001-5p, miR-4674) [382]. The discrepancies with present results may be due to the difference in the diagnosis of the patients, since the study from Kumar et al. was not based on CSF biomarkers. Moreover, Denk et al. showed clustered expression of miRNAs in control, AD and frontotemporal dementia participants, showing that some clusters included miRNAs from the same family, while others included different families in the same cluster, as in the present study [383]. However, the set of analysed miRNAs was limited. On the other hand, some lipids were grouped in the present paper (FA (18:0)/FA (14:0)/FA (18:0)/FA (16:0)/FA (18:2); FA (20:3)/FA (20:4)/FA (18:2)/FA (20:2)/FA (16:0)). In this sense, previous findings in an AD mice modelshowed different lipids expression clusters along the disease progression (two, three, seven months), showing mainly PEs in two months progression and a predomination of TG at seven months [384]. In addition, Kumar et al. described the co-regulation of different lipid sets, among which 17 were fatty acids [385].

Finally, the highest positive correlations between microRNAs and lipids were mainly for hsa-miR-664, hsa-miR-432, hsa-let-7a-3p, hsa-miR-29a-3p, hsa-miR-421 and has-miR-450b-5p with some fatty acids (FA (16:0), FA (18:0), FA (20:2), FA (20:3), FA (20:4)). In general, the described miRNAs showed a positive correlation with fatty acids. Of note, these miRNAs targeted sequences in genes implied in fatty acids metabolism. In this sense, previous studies showed a relationship between AD and fatty acids metabolism,demonstrating differential levels of fatty acids (FA (16:0), FA (18:0), FA (18:1), FA (18:2), FA (20:4), FA (20:5), FA (22:6)) similar to the present results [386]. Regarding hsa-miR-421, it showed a positive correlation with some detected lipids (FA (16:0), FA (20:2), FA (18:2), FA (20:4), FA (20:3), FA (18:0), FA (14:0)). Previous works identified the relationship between this miRNA and lipid metabolism regulation, specifically with triacylglycerol levels [387].On the other hand, the highest negative correlations corresponded to the triglyceride (TG (17:0/17:0/17:0)) with some miRNAs

(hsa-miR-664-3p, hsa-miR-432-5p, hsa-miR-329-3p, hsa-miR-654-5p, hsa-miR-185-5p, hsa-let-7a-3p, hsa-miR-576-5p, hsa-miR-29a-3p, hsa-miR-421, hsa-miR-450b-5p). Similarly, in literature it was shown that hsa-miR-29a could regulate the lipoprotein lipase (LPL) that catalyses hydrolysis of the triglycerides [388].

The main limitation of this study is the reduced number of healthy control patients. However, the availability of biologically identified (CSF biomarkers) patients with MCI due to AD provides a great potential in the identification of potential pathways involved in early AD. Other limitations in this study are: (i) the analytical method is a semiquantitative approach, (ii) the ApoE genotype has not been taken into account, although it is known that ApoE is involved in lipid homeostasis.

4. Conclusions

The present study highlights the potential of a multi-omics approach in the development of a signature of biomarkers of MCI-AD, as well as the description of potential metabolic pathways involved in AD since its early stages. Specifically, epigenomics and lipidomics integration allowed us to identify some associations between microRNAs and lipids, showing their relationship with early AD development. In fact, fatty acids impairment could be an important pathway involved in early AD. However, further work based on targeted analysis should be carried out in a larger cohort in order to validate these preliminary results, as well as to study the proposed pathways in detail.

GENERAL CONCLUSIONS AND OUTLOOK

1. OS and specifically lipid peroxidation seems to play a relevant role in AD from the earliest AD stages (preclinical and MCI). In addition, these pathways could provide biomarkers from minimally invasive samples (urine, plasma).

2. Some lipid peroxidation compounds (isoprostanes, neuroprostans, isofurantes, neurofurans and dihomo-isoprostanes) have been determined satisfactorily in urine, plasma and CSF samples employing newly validated analytical methods.

3. Multivariate linear and non-linear models developed including the levels of lipid peroxidation compounds in urine and plasma samples are promising screening tools to identify individuals with high risk of suffering from AD, especially the non-linear models such as ANN.

4. The levels of lipid peroxidation compounds determined in plasma show a better predictive capacity for AD compared to those in urine samples, despite the plasma levels do not correlate with the CSF levels.

5. Lipid peroxidation compounds could be potential diagnosis biomarkers for AD in preclinical stages, as well as potential differential diagnosis biomarkers, detecting patients with AD among individuals with other neurodegenerative diseases, showingsimilar clinical manifestations, or without cognitive impairment.

6. Plasma lipid peroxidation compounds levels are related to brain atrophy, cognitive status of patients and the CSF AD standard biomarker levels.

7. Omics techniques (metabolomics, lipidomics, epigenomics) are useful tools for the search of new biomarkers, as well as for advance in the knowledge of new pathological pathways altered in AD.

8. Metabolomic analysis revealed pathways altered in early AD stages (neurotransmitters, energy metabolism, lipids and amino acids). Also, other pathways with neuroprotective or antioxidant effects could be activated in the initial stages of the disease as compensatory mechanisms against the cellular damage.

9. The genotype ApoE is associated to lipid metabolomic profile and must be taken into account as a modifying variable in lipidomic and metabolomic studies.

10. Lipid metabolism is dysregulated in AD and plasma lipid profiling could help in AD diagnosis.

11. Epigenomics (miRNA) analysis revealed a potential dysregulation of pathways such as synaptic transmission, cell signalling, structure maintenance or cell metabolism in early AD stages.

12. The integrated study of biomarkers of different nature (lipids, miRNAa) may provide information about altered pathways in AD and thus provide new therapeutic targets.

Future work:

Lipid peroxidation compounds, metabolites, lipids and miRNAs in plasma samples have shown potential as early AD biomarkers. However, to assess the usefulness of the proposed biomarkers, a validation in an external cohort including general population should be performed.

On the other hand, the diagnostic capacity of lipids, miRNAs and lipid peroxidation compounds is not completely accurate due to the complexity of the disease. So, a wider characterization of different pathological pathways of the disease would be required. Therefore, one of the lines of future work would be a complete characterization of patients, including OS and lipid metabolism pathways but also different proteinopathies such as amyloid, Tau, neuroimaging patterns or omics profiles.

Moreover, the high degree of co-pathologies in neurodegenerative diseases, requires a complete characterization of all pathological pathways in order to develop therapies that could be applied specifically depending on the needs.

REFERENCES

1. Moya-Alvarado, G.; Gershoni-Emek, N.; Perlson, E.; Bronfman, F.C. Neurodegeneration and Alzheimer's Disease (AD). What Can Proteomics Tell Us About the Alzheimer's Brain? *Molecular & Cellular Proteomics* **2016**, *15*, 409–425, doi:10.1074/mcp.R115.053330.

2. Patterson, C. World Alzheimer Report 2018 The State of the Art of Dementia Research: New Frontiers. *Alzheimer's Disease International (ADI)* **2018**.

3. Pothen Skaria, A. The Economic and Societal Burden of Alzheimer Disease: Managed Care Considerations. *Am J Manag Care* **2022**, *28*, S188–S196, doi:10.37765/ajmc.2022.89236.

4. Breijyeh, Z.; Karaman, R. Comprehensive Review on Alzheimer's Disease: Causes and Treatment. *Molecules* **2020**, *25*, 5789, doi:10.3390/molecules25245789.

5. Aisen, P.S.; Cummings, J.; Jack, C.R.; Morris, J.C.; Sperling, R.; Frölich, L.; Jones, R.W.; Dowsett, S.A.; Matthews, B.R.; Raskin, J.; et al. On the Path to 2025: Understanding the Alzheimer's Disease Continuum. *Alzheimers Res Ther* **2017**, *9*, 60, doi:10.1186/s13195-017-0283-5.

6. Masters, C.L.; Bateman, R.; Blennow, K.; Rowe, C.C.; Sperling, R.A.; Cummings, J.L. Alzheimer's Disease. *Nat Rev Dis Primers* **2015**, *1*, 15056, doi:10.1038/nrdp.2015.56.

7. Knopman, D.S.; Amieva, H.; Petersen, R.C.; Chételat, G.; Holtzman, D.M.; Hyman, B.T.; Nixon, R.A.; Jones, D.T. Alzheimer Disease. *Nat Rev Dis Primers* **2021**, *7*, 33, doi:10.1038/s41572-021-00269-y.

8. Hardy, J.A.; Higgins, G.A. Alzheimer's Disease: The Amyloid Cascade Hypothesis. *Science (1979)* **1992**, *256*, 184–185, doi:10.1126/science.1566067.

9. Zhang, X.; Song, W. The Role of APP and BACE1 Trafficking in APP Processing and Amyloid-β Generation. *Alzheimers Res Ther* **2013**, *5*, 46, doi:10.1186/alzrt211.

10. Verghese, P.B.; Castellano, J.M.; Garai, K.; Wang, Y.; Jiang, H.; Shah, A.; Bu, G.; Frieden, C.; Holtzman, D.M. ApoE Influences Amyloid-β (Aβ) Clearance despite Minimal ApoE/Aβ Association in Physiological Conditions. *Proceedings of the National Academy of Sciences* **2013**, *110*, doi:10.1073/pnas.1220484110.

11. Barage, S.H.; Sonawane, K.D. Amyloid Cascade Hypothesis: Pathogenesis and Therapeutic Strategies in Alzheimer's Disease. *Neuropeptides* **2015**, *52*, 1–18, doi:10.1016/j.npep.2015.06.008.

12. Ferrari, C.; Sorbi, S. The Complexity of Alzheimer's Disease: An Evolving Puzzle. *Physiol Rev* **2021**, *101*, 1047–1081, doi:10.1152/physrev.00015.2020.

13. AVILA, J.; LUCAS, J.J.; PÉREZ, M.; HERNÁNDEZ, F. Role of Tau Protein in Both Physiological and Pathological Conditions. *Physiol Rev* **2004**, *84*, 361–384, doi:10.1152/physrev.00024.2003.

14. H. Ferreira-Vieira, T.; M. Guimaraes, I.; R. Silva, F.; M. Ribeiro, F. Alzheimer's Disease: Targeting the Cholinergic System. *Curr Neuropharmacol* **2016**, *14*, 101–115, doi:10.2174/1570159X13666150716165726.

15. Chen, Z.-R.; Huang, J.-B.; Yang, S.-L.; Hong, F.-F. Role of Cholinergic Signaling in Alzheimer's Disease. *Molecules* **2022**, *27*, 1816, doi:10.3390/molecules27061816.

16. Selkoe, D.J.; Hardy, J. The Amyloid Hypothesis of Alzheimer's Disease at 25 Years. *EMBO Mol Med* **2016**, *8*, 595–608, doi:10.15252/emmm.201606210.

17. Briggs, R.; Kennelly, S.P.; O'Neill, D. Drug Treatments in Alzheimer's Disease. *Clinical Medicine* **2016**, *16*, 247–253, doi:10.7861/clinmedicine.16-3-247.

18. Ionescu-Tucker, A.; Cotman, C.W. Emerging Roles of Oxidative Stress in Brain Aging and Alzheimer's Disease. *Neurobiol Aging* **2021**, *107*, 86–95, doi:10.1016/j.neurobiolaging.2021.07.014.

19. Akiyama, H. Inflammation and Alzheimer's Disease. *Neurobiol Aging* **2000**, *21*, 383–421, doi:10.1016/S0197-4580(00)00124-X.

20. Campos-Peña, V.; Pichardo-Rojas, P.; Sánchez-Barbosa, T.; Ortíz-Islas, E.; Rodríguez-Pérez, C.E.; Montes, P.; Ramos-Palacios, G.; Silva-Adaya, D.; Valencia-Quintana, R.; Cerna-Cortes, J.F.; et al. Amyloid β, Lipid Metabolism, Basal Cholinergic System, and Therapeutics in Alzheimer's Disease. *Int J Mol Sci* **2022**, *23*, 12092, doi:10.3390/ijms232012092.

21. Atri, A. The Alzheimer's Disease Clinical Spectrum. *Medical Clinics of North America* **2019**, *103*, 263–293, doi:10.1016/j.mcna.2018.10.009.

22. Scheltens, P.; De Strooper, B.; Kivipelto, M.; Holstege, H.; Chételat, G.; Teunissen, C.E.; Cummings, J.; van der Flier, W.M. Alzheimer's Disease. *The Lancet* **2021**, *397*, 1577–1590, doi:10.1016/S0140-6736(20)32205-4.

23. Albert, M.S.; DeKosky, S.T.; Dickson, D.; Dubois, B.; Feldman, H.H.; Fox, N.C.; Gamst, A.; Holtzman, D.M.; Jagust, W.J.; Petersen, R.C.; et al. The Diagnosis of Mild Cognitive Impairment Due to Alzheimer's Disease: Recommendations from the National Institute on Aging-Alzheimer's Association Workgroups on Diagnostic Guidelines for Alzheimer's Disease. *Alzheimer's & Dementia* **2011**, *7*, 270–279, doi:10.1016/j.jalz.2011.03.008.

24. McKhann, G.M.; Knopman, D.S.; Chertkow, H.; Hyman, B.T.; Jack, C.R.; Kawas, C.H.; Klunk, W.E.; Koroshetz, W.J.; Manly, J.J.; Mayeux, R.; et al. The Diagnosis of Dementia Due to Alzheimer's Disease: Recommendations from the National Institute on Aging-Alzheimer's Association Workgroups on Diagnostic Guidelines for Alzheimer's Disease. *Alzheimer's & Dementia* **2011**, *7*, 263–269, doi:10.1016/j.jalz.2011.03.005.

25. Jack, C.R.; Bennett, D.A.; Blennow, K.; Carrillo, M.C.; Dunn, B.; Haeberlein, S.B.; Holtzman, D.M.; Jagust, W.; Jessen, F.; Karlawish, J.; et al. NIA-AA Research Framework: Toward a Biological Definition of Alzheimer's Disease. *Alzheimer's & Dementia* **2018**, *14*, 535–562, doi:10.1016/j.jalz.2018.02.018.

26. Cummings, J.L.; Tong, G.; Ballard, C. Treatment Combinations for Alzheimer's Disease: Current and Future Pharmacotherapy Options. *Journal of Alzheimer's Disease* **2019**, *67*, 779–794, doi:10.3233/JAD-180766.

27. Kim, C.K.; Lee, Y.R.; Ong, L.; Gold, M.; Kalali, A.; Sarkar, J. Alzheimer's Disease: Key Insights from Two Decades of Clinical Trial Failures. *Journal of Alzheimer's Disease* **2022**, *87*, 83–100, doi:10.3233/JAD-215699.

28. van Dyck, C.H.; Swanson, C.J.; Aisen, P.; Bateman, R.J.; Chen, C.; Gee, M.; Kanekiyo, M.; Li, D.; Reyderman, L.; Cohen, S.; et al. Lecanemab in Early Alzheimer's Disease. *New England Journal of Medicine* **2023**, *388*, 9–21, doi:10.1056/NEJMoa2212948.

29. Liu, Z.; Zhou, T.; Ziegler, A.C.; Dimitrion, P.; Zuo, L. Oxidative Stress in Neurodegenerative Diseases: From Molecular Mechanisms to Clinical Applications. *Oxid Med Cell Longev* **2017**, *2017*, 1–11, doi:10.1155/2017/2525967.

30. Boutros, M.; Ray, S. Oxidative Stress. In *Reference Module in Biomedical Sciences*; Elsevier, 2023.

31. Fulda, S.; Gorman, A.M.; Hori, O.; Samali, A. Cellular Stress Responses: Cell Survival and Cell Death. *Int J Cell Biol* **2010**, *2010*, 1–23, doi:10.1155/2010/214074.

32. Bai, R.; Guo, J.; Ye, X.-Y.; Xie, Y.; Xie, T. Oxidative Stress: The Core Pathogenesis and Mechanism of Alzheimer's Disease. *Ageing Res Rev* **2022**, *77*, 101619, doi:10.1016/j.arr.2022.101619.

33. Cheignon, C.; Tomas, M.; Bonnefont-Rousselot, D.; Faller, P.; Hureau, C.; Collin, F. Oxidative Stress and the Amyloid Beta Peptide in Alzheimer's Disease. *Redox Biol* **2018**, *14*, 450–464, doi:10.1016/j.redox.2017.10.014.

34. Tönnies, E.; Trushina, E. Oxidative Stress, Synaptic Dysfunction, and Alzheimer's Disease. *Journal of Alzheimer's Disease* **2017**, *57*, 1105–1121, doi:10.3233/JAD-161088.

35. Frijhoff, J.; Winyard, P.G.; Zarkovic, N.; Davies, S.S.; Stocker, R.; Cheng, D.; Knight, A.R.; Taylor, E.L.; Oettrich, J.; Ruskovska, T.; et al. Clinical Relevance of Biomarkers of Oxidative Stress. *Antioxid Redox Signal* **2015**, *23*, 1144–1170, doi:10.1089/ars.2015.6317.

36. Marrocco, I.; Altieri, F.; Peluso, I. Measurement and Clinical Significance of Biomarkers of Oxidative Stress in Humans. *Oxid Med Cell Longev* **2017**, *2017*, 1–32, doi:10.1155/2017/6501046.

37. Cobley, J.N.; Fiorello, M.L.; Bailey, D.M. 13 Reasons Why the Brain Is Susceptible to Oxidative Stress. *Redox Biol* **2018**, *15*, 490–503, doi:10.1016/j.redox.2018.01.008.

38. Peña-Bautista, C.; Vento, M.; Baquero, M.; Cháfer-Pericás, C. Lipid Peroxidation in Neurodegeneration. *Clinica Chimica Acta* **2019**, *497*, 178–188, doi:10.1016/j.cca.2019.07.037.

39. Benseny-Cases, N.; Klementieva, O.; Cotte, M.; Ferrer, I.; Cladera, J. Microspectroscopy (MFTIR) Reveals Co-Localization of Lipid Oxidation and Amyloid Plaques in Human Alzheimer Disease Brains. *Anal Chem* **2014**, *86*, 12047–12054, doi:10.1021/ac502667b.

40. Sottero, B.; Leonarduzzi, G.; Testa, G.; Gargiulo, S.; Poli, G.; Biasi, F. Lipid Oxidation Derived Aldehydes and Oxysterols Between Health and Disease. *European Journal of Lipid Science and Technology* **2019**, *121*, 1700047, doi:10.1002/ejlt.201700047.

41. Milne, G.L.; Dai, Q.; Roberts, L.J. The Isoprostanes—25 Years Later. *Biochimica et Biophysica Acta (BBA) - Molecular and Cell Biology of Lipids* **2015**, *1851*, 433–445, doi:10.1016/j.bbalip.2014.10.007.

42. Tallima, H.; El Ridi, R. Arachidonic Acid: Physiological Roles and Potential Health Benefits – A Review. *J Adv Res* **2018**, *11*, 33–41, doi:10.1016/j.jare.2017.11.004.

43. Galano, J.-M.; Mas, E.; Barden, A.; Mori, T.A.; Signorini, C.; De Felice, C.; Barrett, A.; Opere, C.; Pinot, E.; Schwedhelm, E.; et al. Isoprostanes and Neuroprostanes: Total Synthesis, Biological Activity and Biomarkers of Oxidative Stress in Humans. *Prostaglandins Other Lipid Mediat* **2013**, *107*, 95–102, doi:10.1016/j.prostaglandins.2013.04.003.

44. Peña-Bautista, C.; Baquero, M.; Vento, M.; Cháfer-Pericás, C. Omics-Based Biomarkers for the Early Alzheimer Disease Diagnosis and Reliable Therapeutic Targets Development. *Curr Neuropharmacol* **2019**, *17*, 630–647, doi:10.2174/1570159X16666180926123722.

45. Mayo, S.; Benito-León, J.; Peña-Bautista, C.; Baquero, M.; Cháfer-Pericás, C. Recent Evidence in Epigenomics and Proteomics Biomarkers for Early and Minimally Invasive Diagnosis of Alzheimer's and Parkinson's Diseases. *Curr Neuropharmacol* **2021**, *19*, 1273–1303, doi:10.2174/1570159X19666201223154009.

46. Züllig, T.; Trötzmüller, M.; Köfeler, H.C. Lipidomics from Sample Preparation to Data Analysis: A Primer. *Anal Bioanal Chem* **2020**, *412*, 2191–2209, doi:10.1007/s00216-019-02241-y.

47. Johnson, C.H.; Ivanisevic, J.; Siuzdak, G. Metabolomics: Beyond Biomarkers and towards Mechanisms. *Nat Rev Mol Cell Biol* **2016**, *17*, 451–459, doi:10.1038/nrm.2016.25.

48. Schrimpe-Rutledge, A.C.; Codreanu, S.G.; Sherrod, S.D.; McLean, J.A. Untargeted Metabolomics Strategies—Challenges and Emerging Directions. *J Am Soc Mass Spectrom* **2016**, *27*, 1897–1905, doi:10.1007/s13361-016-1469-y.

49. Sun, T.; Wang, X.; Cong, P.; Xu, J.; Xue, C. Mass Spectrometry-based Lipidomics in Food Science and Nutritional Health: A Comprehensive Review. *Compr Rev Food Sci Food Saf* **2020**, *19*, 2530–2558, doi:10.1111/1541-4337.12603.

50. Varma, V.R.; Oommen, A.M.; Varma, S.; Casanova, R.; An, Y.; Andrews, R.M.; O'Brien, R.; Pletnikova, O.; Troncoso, J.C.; Toledo, J.; et al. Brain and Blood Metabolite Signatures of Pathology and Progression in Alzheimer Disease: A Targeted Metabolomics Study. *PLoS Med* **2018**, *15*, e1002482, doi:10.1371/journal.pmed.1002482.

51. He, Y.; Wang, Y.; Liu, S.; Pi, Z.; Liu, Z.; Xing, J.; Zhou, H. A Metabolomic Study of the Urine of Rats with Alzheimer's Disease and the Efficacy of Ding-Zhi-Xiao-Wan on the Afflicted Rats. *J Sep Sci* **2020**, *43*, 1458–1465, doi:10.1002/jssc.201900944.

52. Trushina, E.; Dutta, T.; Persson, X.-M.T.; Mielke, M.M.; Petersen, R.C. Identification of Altered Metabolic Pathways in Plasma and CSF in Mild Cognitive Impairment and Alzheimer's Disease Using Metabolomics. *PLoS One* **2013**, *8*, e63644, doi:10.1371/journal.pone.0063644.

53. Akyol, S.; Ugur, Z.; Yilmaz, A.; Ustun, I.; Gorti, S.K.K.; Oh, K.; McGuinness, B.; Passmore, P.; Kehoe, P.G.; Maddens, M.E.; et al. Lipid Profiling of Alzheimer's Disease Brain Highlights Enrichment in Glycerol(Phospho)Lipid, and Sphingolipid Metabolism. *Cells* **2021**, *10*, 2591, doi:10.3390/cells10102591.

54. Li, Y. Modern Epigenetics Methods in Biological Research. *Methods* **2021**, *187*, 104–113, doi:10.1016/j.ymeth.2020.06.022.

55. Lu, T.X.; Rothenberg, M.E. MicroRNA. *Journal of Allergy and Clinical Immunology* **2018**, *141*, 1202–1207, doi:10.1016/j.jaci.2017.08.034.

56. Moosavi, A.; Motevalizadeh Ardekani, A. Role of Epigenetics in Biology and Human Diseases. *Iran Biomed J* **2016**, *20*, 246–258, doi:10.22045/ibj.2016.01.

57. Takousis, P.; Sadlon, A.; Schulz, J.; Wohlers, I.; Dobricic, V.; Middleton, L.; Lill, C.M.; Perneczky, R.; Bertram, L. Differential Expression of MicroRNAs in Alzheimer's Disease Brain, Blood, and Cerebrospinal Fluid. *Alzheimer's & Dementia* **2019**, *15*, 1468–1477, doi:10.1016/j.jalz.2019.06.4952.

58. Sharma, V.K.; Mehta, V.; Singh, T.G. Alzheimer's Disorder: Epigenetic Connection and Associated Risk Factors. *Curr Neuropharmacol* **2020**, *18*, 740–753, doi:10.2174/1570159X18666200128125641.

59. Hampel, H.; Nisticò, R.; Seyfried, N.T.; Levey, A.I.; Modeste, E.; Lemercier, P.; Baldacci, F.; Toschi, N.; Garaci, F.; Perry, G.; et al. Omics Sciences for Systems Biology in Alzheimer's Disease: State-of-the-Art of the Evidence. *Ageing Res Rev* **2021**, *69*, 101346, doi:10.1016/j.arr.2021.101346.

60. Badhwar, A.; McFall, G.P.; Sapkota, S.; Black, S.E.; Chertkow, H.; Duchesne, S.; Masellis, M.; Li, L.; Dixon, R.A.; Bellec, P. A Multiomics Approach to Heterogeneity in Alzheimer's Disease: Focused Review and Roadmap. *Brain* **2020**, *143*, 1315–1331, doi:10.1093/brain/awz384.

61. Horgusluoglu, E.; Neff, R.; Song, W.; Wang, M.; Wang, Q.; Arnold, M.; Krumsiek, J.; Galindo-Prieto, B.; Ming, C.; Nho, K.; et al. Integrative Metabolomics-genomics Approach Reveals Key Metabolic Pathways and Regulators of Alzheimer's Disease. *Alzheimer's & Dementia* **2022**, *18*, 1260–1278, doi:10.1002/alz.12468.

62. Darst, B.F.; Lu, Q.; Johnson, S.C.; Engelman, C.D. Integrated Analysis of Genomics, Longitudinal Metabolomics, and Alzheimer's Risk Factors among 1,111 Cohort Participants. *Genet Epidemiol* **2019**, gepi.22211, doi:10.1002/gepi.22211.

63. Sepulcre, J.; Schultz, A.P.; Sabuncu, M.; Gomez-Isla, T.; Chhatwal, J.; Becker, A.; Sperling, R.; Johnson, K.A. In Vivo Tau, Amyloid, and Gray Matter Profiles in the Aging Brain. *Journal of Neuroscience* **2016**, *36*, 7364–7374, doi:10.1523/JNEUROSCI.0639-16.2016.

64. Gong, C.-X.; Liu, F.; Iqbal, K. Multifactorial Hypothesis and Multi-Targets for Alzheimer's Disease. *Journal of Alzheimer's Disease* **2018**, *64*, S107–S117, doi:10.3233/JAD-179921.

65. Peña-Bautista, C.; Baquero, M.; Vento, M.; Cháfer-Pericás, C. Free Radicals in Alzheimer's Disease: Lipid Peroxidation Biomarkers. *Clinica Chimica Acta* **2019**, *491*, 85–90, doi:10.1016/j.cca.2019.01.021.

66. Peña-Bautista, C.; Vento, M.; Baquero, M.; Cháfer-Pericás, C. Lipid Peroxidation in Neurodegeneration. *Clinica Chimica Acta* **2019**, *497*, 178–188, doi:10.1016/j.cca.2019.07.037.

67. Peña-Bautista, C.; Baquero, M.; Vento, M.; Cháfer-Pericás, C. Omics-Based Biomarkers for the Early Alzheimer Disease Diagnosis and Reliable Therapeutic Targets Development. *Curr Neuropharmacol* **2019**, *17*, 630–647, doi:10.2174/1570159X16666180926123722.

68. Sies, H. Oxidative Stress: A Concept in Redox Biology and Medicine. *Redox Biol* **2015**, *4*, 180–183, doi:10.1016/j.redox.2015.01.002.

69. Lushchak, V.I. Free Radicals, Reactive Oxygen Species, Oxidative Stress and Its Classification. *Chem Biol Interact* **2014**, *224*, 164–175, doi:10.1016/j.cbi.2014.10.016.

70. Turrens, J.F. Mitochondrial Formation of Reactive Oxygen Species. *J Physiol* **2003**, *552*, 335–344, doi:10.1113/jphysiol.2003.049478.

71. Mishra, V.; Banga, J.; Silveyra, P. Oxidative Stress and Cellular Pathways of Asthma and Inflammation: Therapeutic Strategies and Pharmacological Targets. *Pharmacol Ther* **2018**, *181*, 169–182, doi:10.1016/j.pharmthera.2017.08.011.

72. Dasuri, K.; Zhang, L.; Keller, J.N. Oxidative Stress, Neurodegeneration, and the Balance of Protein Degradation and Protein Synthesis. *Free Radic Biol Med* **2013**, *62*, 170–185, doi:10.1016/j.freeradbiomed.2012.09.016.

73. Cummings, J.; Zhou, Y.; Lee, G.; Zhong, K.; Fonseca, J.; Cheng, F. Alzheimer's Disease Drug Development Pipeline: 2023. *Alzheimer's & Dementia: Translational Research & Clinical Interventions* **2023**, *9*, doi:10.1002/trc2.12385.

74. Ayala, A.; Muñoz, M.F.; Argüelles, S. Lipid Peroxidation: Production, Metabolism, and Signaling Mechanisms of Malondialdehyde and 4-Hydroxy-2-Nonenal. *Oxid Med Cell Longev* **2014**, *2014*, 1–31, doi:10.1155/2014/360438.

75. Yin, H.; Xu, L.; Porter, N.A. Free Radical Lipid Peroxidation: Mechanisms and Analysis. *Chem Rev* **2011**, *111*, 5944–5972, doi:10.1021/cr200084z.

76. Scheff, S.W.; Ansari, M.A.; Mufson, E.J. Oxidative Stress and Hippocampal Synaptic Protein Levels in Elderly Cognitively Intact Individuals with Alzheimer's Disease Pathology. *Neurobiol Aging* **2016**, *42*, 1–12, doi:10.1016/j.neurobiolaging.2016.02.030.

77. Yadav, R.S.; Tiwari, N.K. Lipid Integration in Neurodegeneration: An Overview of Alzheimer's Disease. *Mol Neurobiol* **2014**, *50*, 168–176, doi:10.1007/s12035-014-8661-5.

78. Klosinski, L.P.; Yao, J.; Yin, F.; Fonteh, A.N.; Harrington, M.G.; Christensen, T.A.; Trushina, E.; Brinton, R.D. White Matter Lipids as a Ketogenic Fuel Supply in Aging Female Brain: Implications for Alzheimer's Disease. *EBioMedicine* **2015**, *2*, 1888–1904, doi:10.1016/j.ebiom.2015.11.002.

79. Ferreira, D.; Verhagen, C.; Hernández-Cabrera, J.A.; Cavallin, L.; Guo, C.-J.; Ekman, U.; Muehlboeck, J.-S.; Simmons, A.; Barroso, J.; Wahlund, L.-O.; et al. Distinct Subtypes of Alzheimer's Disease Based on Patterns of Brain Atrophy: Longitudinal Trajectories and Clinical Applications. *Sci Rep* **2017**, *7*, 46263, doi:10.1038/srep46263.

80. Sarria-Estrada, S.; Acevedo, C.; Mitjana, R.; Frascheri, L.; Siurana, S.; Auger, C.; Rovira, A. Reproducibilidad de La Valoración Cualitativa de La Atrofia Del Lóbulo Temporal Por RM. *Radiologia* **2015**, *57*, 225–228, doi:10.1016/j.rx.2014.04.002.

81. Peña-Bautista, C.; Baquero, M.; Vento, M.; Cháfer-Pericás, C. Free Radicals in Alzheimer's Disease: Lipid Peroxidation Biomarkers. *Clinica Chimica Acta* **2019**, *491*, 85–90, doi:10.1016/j.cca.2019.01.021.

82. Pimplikar, S.W. Multi-Omics and Alzheimer's Disease: A Slower but Surer Path to an Efficacious Therapy? *American Journal of Physiology-Cell Physiology* **2017**, *313*, C1–C2, doi:10.1152/ajpcell.00109.2017.

83. Zetterberg, H. Applying Fluid Biomarkers to Alzheimer's Disease. *American Journal of Physiology-Cell Physiology* **2017**, *313*, C3–C10, doi:10.1152/ajpcell.00007.2017.

84. Patti, G.J.; Yanes, O.; Siuzdak, G. Metabolomics: The Apogee of the Omics Trilogy. *Nat Rev Mol Cell Biol* **2012**, *13*, 263–269, doi:10.1038/nrm3314.

85. Wilkins, J.M.; Trushina, E. Application of Metabolomics in Alzheimer's Disease. *Front Neurol* **2018**, *8*, doi:10.3389/fneur.2017.00719.

86. Paglia, G.; Stocchero, M.; Cacciatore, S.; Lai, S.; Angel, P.; Alam, M.T.; Keller, M.; Ralser, M.; Astarita, G. Unbiased Metabolomic Investigation of Alzheimer's Disease Brain Points to Dysregulation of Mitochondrial Aspartate Metabolism. *J Proteome Res* **2016**, *15*, 608–618, doi:10.1021/acs.jproteome.5b01020.

87. Leeuw, F.A.; Peeters, C.F.W.; Kester, M.I.; Harms, A.C.; Struys, E.A.; Hankemeier, T.; Vlijmen, H.W.T.; Lee, S.J.; Duijn, C.M.; Scheltens, P.; et al. Blood-based Metabolic Signatures in Alzheimer's Disease. *Alzheimer's & Dementia: Diagnosis, Assessment & Disease Monitoring* **2017**, *8*, 196–207, doi:10.1016/j.dadm.2017.07.006.

88. Kaddurah-Daouk, R.; Zhu, H.; Sharma, S.; Bogdanov, M.; Rozen, S.G.; Matson, W.; Oki, N.O.; Motsinger-Reif, A.A.; Churchill, E.; Lei, Z.; et al. Alterations in Metabolic Pathways and Networks in Alzheimer's Disease. *Transl Psychiatry* **2013**, *3*, e244–e244, doi:10.1038/tp.2013.18.

89. Varma, V.R.; Oommen, A.M.; Varma, S.; Casanova, R.; An, Y.; Andrews, R.M.; O'Brien, R.; Pletnikova, O.; Troncoso, J.C.; Toledo, J.; et al. Brain and Blood Metabolite Signatures of Pathology and Progression in Alzheimer Disease: A Targeted Metabolomics Study. *PLoS Med* **2018**, *15*, e1002482, doi:10.1371/journal.pmed.1002482.

90. Cui, Y.; Liu, X.; Wang, M.; Liu, L.; Sun, X.; Ma, L.; Xie, W.; Wang, C.; Tang, S.; Wang, D.; et al. Lysophosphatidylcholine and Amide as Metabolites for Detecting Alzheimer Disease Using Ultrahigh-Performance Liquid Chromatography–Quadrupole Time-of-Flight Mass Spectrometry–Based Metabonomics. *J Neuropathol Exp Neurol* **2014**, *73*, 954–963, doi:10.1097/NEN.0000000000000116.

91. Koal, T.; Klavins, K.; Seppi, D.; Kemmler, G.; Humpel, C. Sphingomyelin SM(D18:1/18:0) Is Significantly Enhanced in Cerebrospinal Fluid Samples Dichotomized by Pathological Amyloid-B42, Tau, and Phospho-Tau-181 Levels. *Journal of Alzheimer's Disease* **2015**, *44*, 1193–1201, doi:10.3233/JAD-142319.

92. Pan, X.; Nasaruddin, M. Bin; Elliott, C.T.; McGuinness, B.; Passmore, A.P.; Kehoe, P.G.; Hölscher, C.; McClean, P.L.; Graham, S.F.; Green, B.D. Alzheimer's Disease–like Pathology Has Transient Effects on the Brain and Blood Metabolome. *Neurobiol Aging* **2016**, *38*, 151–163, doi:10.1016/j.neurobiolaging.2015.11.014.

93. Orešič, M.; Anderson, G.; Mattila, I.; Manoucheri, M.; Soininen, H.; Hyötyläinen, T.; Basignani, C. Targeted Serum Metabolite Profiling Identifies Metabolic Signatures in Patients with Alzheimer's Disease, Normal Pressure Hydrocephalus and Brain Tumor. *Front Neurosci* **2018**, *11*, doi:10.3389/fnins.2017.00747.

94. Wang, G.; Zhou, Y.; Huang, F.-J.; Tang, H.-D.; Xu, X.-H.; Liu, J.-J.; Wang, Y.; Deng, Y.-L.; Ren, R.-J.; Xu, W.; et al. Plasma Metabolite Profiles of Alzheimer's Disease and Mild Cognitive Impairment. *J Proteome Res* **2014**, *13*, 2649–2658, doi:10.1021/pr5000895.

95. Tang, Z.; Liu, L.; Li, Y.; Dong, J.; Li, M.; Huang, J.; Lin, S.; Cai, Z. Urinary Metabolomics Reveals Alterations of Aromatic Amino Acid Metabolism of Alzheimer's Disease in the Transgenic CRND8 Mice. *Curr Alzheimer Res* **2016**, *13*, 764–776, doi:10.2174/1567205013666160129095340.

96. Yilmaz, A.; Geddes, T.; Han, B.; Bahado-Singh, R.O.; Wilson, G.D.; Imam, K.; Maddens, M.; Graham, S.F. Diagnostic Biomarkers of Alzheimer's Disease as Identified in Saliva Using 1H NMR-Based Metabolomics. *Journal of Alzheimer's Disease* **2017**, *58*, 355–359, doi:10.3233/JAD-161226.

97. Graham, S.F.; Chevallier, O.P.; Elliott, C.T.; Hölscher, C.; Johnston, J.; McGuinness, B.; Kehoe, P.G.; Passmore, A.P.; Green, B.D. Untargeted Metabolomic Analysis of Human Plasma Indicates Differentially Affected Polyamine and L-Arginine Metabolism in Mild Cognitive Impairment Subjects Converting to Alzheimer's Disease. *PLoS One* **2015**, *10*, e0119452, doi:10.1371/journal.pone.0119452.

98. Mapstone, M.; Lin, F.; Nalls, M.A.; Cheema, A.K.; Singleton, A.B.; Fiandaca, M.S.; Federoff, H.J. What Success Can Teach Us about Failure: The Plasma Metabolome of Older Adults with Superior Memory and Lessons for Alzheimer's Disease. *Neurobiol Aging* **2017**, *51*, 148–155, doi:10.1016/j.neurobiolaging.2016.11.007.

99. Inoue, K.; Tsuchiya, H.; Takayama, T.; Akatsu, H.; Hashizume, Y.; Yamamoto, T.; Matsukawa, N.; Toyo'oka, T. Blood-Based Diagnosis of Alzheimer's Disease Using Fingerprinting Metabolomics Based on Hydrophilic Interaction Liquid Chromatography with Mass Spectrometry and Multivariate Statistical Analysis. *Journal of Chromatography B* **2015**, *974*, 24–34, doi:10.1016/j.jchromb.2014.10.022.

100. Voyle, N.; Kim, M.; Proitsi, P.; Ashton, N.J.; Baird, A.L.; Bazenet, C.; Hye, A.; Westwood, S.; Chung, R.; Ward, M.; et al. Blood Metabolite Markers of Neocortical Amyloid-β Burden: Discovery and Enrichment Using Candidate Proteins. *Transl Psychiatry* **2016**, *6*, e719–e719, doi:10.1038/tp.2015.205.

101. Lin, W.; Zhang, J.; Liu, Y.; Wu, R.; Yang, H.; Hu, X.; Ling, X. Studies on Diagnostic Biomarkers and Therapeutic Mechanism of Alzheimer's Disease through Metabolomics and Hippocampal Proteomics. *European Journal of Pharmaceutical Sciences* **2017**, *105*, 119–126, doi:10.1016/j.ejps.2017.05.003.

102. González-Domínguez, R.; García-Barrera, T.; Vitorica, J.; Gómez-Ariza, J.L. Application of Metabolomics Based on Direct Mass Spectrometry Analysis for the Elucidation of Altered Metabolic Pathways in Serum from the APP/PS1 Transgenic Model of Alzheimer's Disease. *J Pharm Biomed Anal* **2015**, *107*, 378–385, doi:10.1016/j.jpba.2015.01.025.

103. Olazarán, J.; Gil-de-Gómez, L.; Rodríguez-Martín, A.; Valentí-Soler, M.; Frades-Payo, B.; Marín-Muñoz, J.; Antúnez, C.; Frank-García, A.; Acedo-Jiménez, C.; Morlán-Gracia, L.; et al. A Blood-Based, 7-Metabolite Signature for the Early Diagnosis of Alzheimer's Disease. *Journal of Alzheimer's Disease* **2015**, *45*, 1157–1173, doi:10.3233/JAD-142925.

104. González-Domínguez, R.; García-Barrera, T.; Gómez-Ariza, J.L. Using Direct Infusion Mass Spectrometry for Serum Metabolomics in Alzheimer's Disease. *Anal Bioanal Chem* **2014**, *406*, 7137–7148, doi:10.1007/s00216-014-8102-3.

105. Marksteiner, J.; Blasko, I.; Kemmler, G.; Koal, T.; Humpel, C. Bile Acid Quantification of 20 Plasma Metabolites Identifies Lithocholic Acid as a Putative Biomarker in Alzheimer's Disease. *Metabolomics* **2018**, *14*, 1, doi:10.1007/s11306-017-1297-5.

106. Karjalainen, J.-P.; Mononen, N.; Hutri-Kähönen, N.; Lehtimäki, M.; Juonala, M.; Ala-Korpela, M.; Kähönen, M.; Raitakari, O.; Lehtimäki, T. The Effect of Apolipoprotein E Polymorphism on Serum Metabolome – a Population-Based 10-Year Follow-up Study. *Sci Rep* **2019**, *9*, 458, doi:10.1038/s41598-018-36450-9.

107. Wang, S.; Zhang, J.; Pan, T. APOE E4 Is Associated with Higher Levels of CSF SNAP-25 in Prodromal Alzheimer's Disease. *Neurosci Lett* **2018**, *685*, 109–113, doi:10.1016/j.neulet.2018.08.029.

108. Morris, J.K.; Uy, R.A.Z.; Vidoni, E.D.; Wilkins, H.M.; Archer, A.E.; Thyfault, J.P.; Miles, J.M.; Burns, J.M. Effect of APOE E4 Genotype on Metabolic Biomarkers in Aging and Alzheimer's Disease. *Journal of Alzheimer's Disease* **2017**, *58*, 1129–1135, doi:10.3233/JAD-170148.

109. Liao, F.; Yoon, H.; Kim, J. Apolipoprotein E Metabolism and Functions in Brain and Its Role in Alzheimer's Disease. *Curr Opin Lipidol* **2017**, *28*, 60–67, doi:10.1097/MOL.0000000000000383.

110. Bussy, A.; Snider, B.J.; Coble, D.; Xiong, C.; Fagan, A.M.; Cruchaga, C.; Benzinger, T.L.S.; Gordon, B.A.; Hassenstab, J.; Bateman, R.J.; et al. Effect of Apolipoprotein E4 on Clinical, Neuroimaging, and Biomarker Measures in Noncarrier Participants in the Dominantly Inherited Alzheimer Network. *Neurobiol Aging* **2019**, *75*, 42–50, doi:10.1016/j.neurobiolaging.2018.10.011.

111. Hanson, A.J.; Craft, S.; Banks, W.A. The APOE Genotype: Modification of Therapeutic Responses in Alzheimer's Disease. *Curr Pharm Des* **2015**, *21*, 114–120, doi:10.2174/1381612820666141020164222.

112. Kao, Y.-C.; Ho, P.-C.; Tu, Y.-K.; Jou, I.-M.; Tsai, K.-J. Lipids and Alzheimer's Disease. *Int J Mol Sci* **2020**, *21*, 1505, doi:10.3390/ijms21041505.

113. Liu, Y.; Thalamuthu, A.; Mather, K.A.; Crawford, J.; Ulanova, M.; Wong, M.W.K.; Pickford, R.; Sachdev, P.S.; Braidy, N. Plasma Lipidome Is Dysregulated in Alzheimer's Disease and Is Associated with Disease Risk Genes. *Transl Psychiatry* **2021**, *11*, 344, doi:10.1038/s41398-021-01362-2.

114. Zhang, X.; Liu, W.; Zan, J.; Wu, C.; Tan, W. Untargeted Lipidomics Reveals Progression of Early Alzheimer's Disease in APP/PS1 Transgenic Mice. *Sci Rep* **2020**, *10*, 14509, doi:10.1038/s41598-020-71510-z.

115. Llano, D.A.; Devanarayan, V. Serum Phosphatidylethanolamine and Lysophosphatidylethanolamine Levels Differentiate Alzheimer's Disease from Controls and Predict Progression from Mild Cognitive Impairment. *Journal of Alzheimer's Disease* **2021**, *80*, 311–319, doi:10.3233/JAD-201420.

116. Mielke, M.M.; Haughey, N.J.; Bandaru, V.V.R.; Weinberg, D.D.; Darby, E.; Zaidi, N.; Pavlik, V.; Doody, R.S.; Lyketsos, C.G. Plasma Sphingomyelins Are Associated with Cognitive Progression in Alzheimer's Disease. *Journal of Alzheimer's Disease* **2011**, *27*, 259–269, doi:10.3233/JAD-2011-110405.

117. Lim, W.L.F.; Martins, I.J.; Martins, R.N. The Involvement of Lipids in Alzheimer's Disease. *Journal of Genetics and Genomics* **2014**, *41*, 261–274, doi:10.1016/j.jgg.2014.04.003.

118. Proitsi, P.; Kim, M.; Whiley, L.; Simmons, A.; Sattlecker, M.; Velayudhan, L.; Lupton, M.K.; Soininen, H.; Kloszewska, I.; Mecocci, P.; et al. Association of Blood Lipids with Alzheimer's Disease: A Comprehensive Lipidomics Analysis. *Alzheimer's & Dementia* **2017**, *13*, 140–151, doi:10.1016/j.jalz.2016.08.003.

119. Zhang, L.; Li, L.; Meng, F.; Yu, J.; He, F.; Lin, Y.; Su, Y.; Hu, M.; Liu, X.; Liu, Y.; et al. Serum Metabolites Differentiate Amnestic Mild Cognitive Impairment From Healthy Controls and Predict Early Alzheimer's Disease via Untargeted Lipidomics Analysis. *Front Neurol* **2021**, *12*, doi:10.3389/fneur.2021.704582.

120. Fote, G.; Wu, J.; Mapstone, M.; Macciardi, F.; Fiandaca, M.S.; Federoff, H.J. Plasma Sphingomyelins in Late-Onset Alzheimer's Disease. *Journal of Alzheimer's Disease* **2021**, *83*, 1161–1171, doi:10.3233/JAD-200871.

121. Maes, O.; Chertkow, H.; Wang, E.; Schipper, H. MicroRNA: Implications for Alzheimer Disease and Other Human CNS Disorders. *Curr Genomics* **2009**, *10*, 154–168, doi:10.2174/138920209788185252.

122. Dong, H.; Li, J.; Huang, L.; Chen, X.; Li, D.; Wang, T.; Hu, C.; Xu, J.; Zhang, C.; Zen, K.; et al. Serum MicroRNA Profiles Serve as Novel Biomarkers for the Diagnosis of Alzheimer's Disease. *Dis Markers* **2015**, *2015*, 1–11, doi:10.1155/2015/625659.

123. Satoh, J.; Kino, Y.; Niida, S. MicroRNA-Seq Data Analysis Pipeline to Identify Blood Biomarkers for Alzheimer's Disease from Public Data. *Biomark Insights* **2015**, *10*, BMI.S25132, doi:10.4137/BMI.S25132.

124. Swarbrick, S.; Wragg, N.; Ghosh, S.; Stolzing, A. Systematic Review of MiRNA as Biomarkers in Alzheimer's Disease. *Mol Neurobiol* **2019**, *56*, 6156–6167, doi:10.1007/s12035-019-1500-y.

125. He, H.; Liu, A.; Zhang, W.; Yang, H.; Zhang, M.; Xu, H.; Liu, Y.; Hong, B.; Yan, F.; Yue, L.; et al. Novel Plasma MiRNAs as Biomarkers and Therapeutic Targets

of Alzheimer's Disease at the Prodromal Stage. *Journal of Alzheimer's Disease* **2021**, *83*, 779–790, doi:10.3233/JAD-210307.

126. Song, S.; Lee, J.U.; Jeon, M.J.; Kim, S.; Sim, S.J. Detection of Multiplex Exosomal MiRNAs for Clinically Accurate Diagnosis of Alzheimer's Disease Using Label-Free Plasmonic Biosensor Based on DNA-Assembled Advanced Plasmonic Architecture. *Biosens Bioelectron* **2022**, *199*, 113864, doi:10.1016/j.bios.2021.113864.

127. Cheng, L.; Doecke, J.D.; Sharples, R.A.; Villemagne, V.L.; Fowler, C.J.; Rembach, A.; Martins, R.N.; Rowe, C.C.; Macaulay, S.L.; Masters, C.L.; et al. Prognostic Serum MiRNA Biomarkers Associated with Alzheimer's Disease Shows Concordance with Neuropsychological and Neuroimaging Assessment. *Mol Psychiatry* **2015**, *20*, 1188–1196, doi:10.1038/mp.2014.127.

128. Hedman, Å.K.; Mendelson, M.M.; Marioni, R.E.; Gustafsson, S.; Joehanes, R.; Irvin, M.R.; Zhi, D.; Sandling, J.K.; Yao, C.; Liu, C.; et al. Epigenetic Patterns in Blood Associated With Lipid Traits Predict Incident Coronary Heart Disease Events and Are Enriched for Results From Genome-Wide Association Studies. *Circ Cardiovasc Genet* **2017**, *10*, doi:10.1161/CIRCGENETICS.116.001487.

129. Randolph, C.; Tierney, M.C.; Mohr, E.; Chase, T.N. The Repeatable Battery for the Assessment of Neuropsychological Status (RBANS): Preliminary Clinical Validity. *J Clin Exp Neuropsychol* **1998**, *20*, 310–319, doi:10.1076/jcen.20.3.310.823.

130. Pfeffer, R.I.; Kurosaki, T.T.; Harrah, C.H.; Chance, J.M.; Filos, S. Measurement of Functional Activities in Older Adults in the Community. *J Gerontol* **1982**, *37*, 323–329, doi:10.1093/geronj/37.3.323.

131. Hughes, C.P.; Berg, L.; Danziger, W.; Coben, L.A.; Martin, R.L. A New Clinical Scale for the Staging of Dementia. *British Journal of Psychiatry* **1982**, *140*, 566–572, doi:10.1192/bjp.140.6.566.

132. Folstein, M.F.; Folstein, S.E.; McHugh, P.R. "Mini-Mental State." *J Psychiatr Res* **1975**, *12*, 189–198, doi:10.1016/0022-3956(75)90026-6.

133. Frisoni, G.B.; Fox, N.C.; Jack, C.R.; Scheltens, P.; Thompson, P.M. The Clinical Use of Structural MRI in Alzheimer Disease. *Nat Rev Neurol* **2010**, *6*, 67–77, doi:10.1038/nrneurol.2009.215.

134. Anoop, A.; Singh, P.K.; Jacob, R.S.; Maji, S.K. CSF Biomarkers for Alzheimer's Disease Diagnosis. *Int J Alzheimers Dis* **2010**, *2010*, 1–12, doi:10.4061/2010/606802.

135. Blennow, K.; Dubois, B.; Fagan, A.M.; Lewczuk, P.; Leon, M.J.; Hampel, H. Clinical Utility of Cerebrospinal Fluid Biomarkers in the Diagnosis of Early Alzheimer's Disease. *Alzheimer's & Dementia* **2015**, *11*, 58–69, doi:10.1016/j.jalz.2014.02.004.

136. de la Torre, A.; Lee, Y.Y.; Mazzoni, A.; Guy, A.; Bultel-Poncé, V.; Durand, T.; Oger, C.; Lee, J.C.-Y.; Galano, J.-M. Total Syntheses and In Vivo Quantitation of

Novel Neurofuran and Dihomo-Isofuran Derived from Docosahexaenoic Acid and Adrenic Acid. *Chemistry - A European Journal* **2015**, *21*, 2442–2446, doi:10.1002/chem.201405497.

137. Oger, C.; Bultel-Poncé, V.; Guy, A.; Balas, L.; Rossi, J.-C.; Durand, T.; Galano, J.-M. The Handy Use of Brown's P2-Ni Catalyst for a Skipped Diyne Deuteration: Application to the Synthesis of a [D4]-Labeled F4t-Neuroprostane. *Chemistry - A European Journal* **2010**, *16*, 13976–13980, doi:10.1002/chem.201002304.

138. Oger, C.; Bultel-Poncé, V.; Guy, A.; Durand, T.; Galano, J.-M. Total Synthesis of Isoprostanes Derived from Adrenic Acid and EPA. *European J Org Chem* **2012**, *2012*, 2621–2634, doi:10.1002/ejoc.201200070.

139. Guy, A.; Oger, C.; Heppekausen, J.; Signorini, C.; De Felice, C.; Fürstner, A.; Durand, T.; Galano, J. Oxygenated Metabolites of N-3 Polyunsaturated Fatty Acids as Potential Oxidative Stress Biomarkers: Total Synthesis of 8-F3t -IsoP, 10-F4t-NeuroP and D4-10-F4t-NeuroP. *Chemistry – A European Journal* **2014**, *20*, 6374–6380, doi:10.1002/chem.201400380.

140. de La Torre, A.; Lee, Y.Y.; Oger, C.; Sangild, P.T.; Durand, T.; Lee, J.C.-Y.; Galano, J.-M. Synthesis, Discovery, and Quantitation of Dihomo-Isofurans: Biomarkers for In Vivo Adrenic Acid Peroxidation. *Angewandte Chemie International Edition* **2014**, *53*, 6249–6252, doi:10.1002/anie.201402440.

141. García-Blanco, A.; Peña-Bautista, C.; Oger, C.; Vigor, C.; Galano, J.-M.; Durand, T.; Martín-Ibáñez, N.; Baquero, M.; Vento, M.; Cháfer-Pericás, C. Reliable Determination of New Lipid Peroxidation Compounds as Potential Early Alzheimer Disease Biomarkers. *Talanta* **2018**, *184*, 193–201, doi:10.1016/j.talanta.2018.03.002.

142. Scheltens, P.; Leys, D.; Barkhof, F.; Huglo, D.; Weinstein, H.C.; Vermersch, P.; Kuiper, M.; Steinling, M.; Wolters, E.C.; Valk, J. Atrophy of Medial Temporal Lobes on MRI in "Probable" Alzheimer's Disease and Normal Ageing: Diagnostic Value and Neuropsychological Correlates. *J Neurol Neurosurg Psychiatry* **1992**, *55*, 967–972, doi:10.1136/jnnp.55.10.967.

143. Steyerberg, E.W.; Uno, H.; Ioannidis, J.P.A.; van Calster, B.; Ukaegbu, C.; Dhingra, T.; Syngal, S.; Kastrinos, F. Poor Performance of Clinical Prediction Models: The Harm of Commonly Applied Methods. *J Clin Epidemiol* **2018**, *98*, 133–143, doi:10.1016/j.jclinepi.2017.11.013.

144. Altmann, A.; Toloşi, L.; Sander, O.; Lengauer, T. Permutation Importance: A Corrected Feature Importance Measure. *Bioinformatics* **2010**, *26*, 1340–1347, doi:10.1093/bioinformatics/btq134.

145. Steyerberg, E.W.; Eijkemans, M.J.C.; Harrell, F.E.; Habbema, J.D.F. Prognostic Modelling with Logistic Regression Analysis: A Comparison of Selection and Estimation Methods in Small Data Sets. *Stat Med* **2000**, *19*, 1059–1079, doi:10.1002/(SICI)1097-0258(20000430)19:8<1059::AID-SIM412>3.0.CO;2-0.

146. Smith, G.C.S.; Seaman, S.R.; Wood, A.M.; Royston, P.; White, I.R. Correcting for Optimistic Prediction in Small Data Sets. *Am J Epidemiol* **2014**, *180*, 318–324, doi:10.1093/aje/kwu140.

147. Alibakshi, A. Strategies to Develop Robust Neural Network Models: Prediction of Flash Point as a Case Study. *Anal Chim Acta* **2018**, *1026*, 69–76, doi:10.1016/j.aca.2018.05.015.

148. Zhang, Z.; Lai, Z.; Xu, Y.; Shao, L.; Wu, J.; Xie, G.-S. Discriminative Elastic-Net Regularized Linear Regression. *IEEE Transactions on Image Processing* **2017**, *26*, 1466–1481, doi:10.1109/TIP.2017.2651396.

149. Friedman, J.; Hastie, T.; Tibshirani, R. Regularization Paths for Generalized Linear Models via Coordinate Descent. *J Stat Softw* **2010**, *33*, doi:10.18637/jss.v033.i01.

150. Smith, C.A.; Want, E.J.; O'Maille, G.; Abagyan, R.; Siuzdak, G. XCMS: Processing Mass Spectrometry Data for Metabolite Profiling Using Nonlinear Peak Alignment, Matching, and Identification. *Anal Chem* **2006**, *78*, 779–787, doi:10.1021/ac051437y.

151. Kuhl, C.; Tautenhahn, R.; Böttcher, C.; Larson, T.R.; Neumann, S. CAMERA: An Integrated Strategy for Compound Spectra Extraction and Annotation of Liquid Chromatography/Mass Spectrometry Data Sets. *Anal Chem* **2012**, *84*, 283–289, doi:10.1021/ac202450g.

152. Alcoriza-Balaguer, M.I.; García-Cañaveras, J.C.; López, A.; Conde, I.; Juan, O.; Carretero, J.; Lahoz, A. LipidMS: An R Package for Lipid Annotation in Untargeted Liquid Chromatography-Data Independent Acquisition-Mass Spectrometry Lipidomics. *Anal Chem* **2019**, *91*, 836–845, doi:10.1021/acs.analchem.8b03409.

153. Cordero, F.; Beccuti, M.; Arigoni, M.; Donatelli, S.; Calogero, R.A. Optimizing a Massive Parallel Sequencing Workflow for Quantitative MiRNA Expression Analysis. *PLoS One* **2012**, *7*, e31630, doi:10.1371/journal.pone.0031630.

154. Kulkarni, N.; Alessandrì, L.; Panero, R.; Arigoni, M.; Olivero, M.; Ferrero, G.; Cordero, F.; Beccuti, M.; Calogero, R.A. Reproducible Bioinformatics Project: A Community for Reproducible Bioinformatics Analysis Pipelines. *BMC Bioinformatics* **2018**, *19*, 349, doi:10.1186/s12859-018-2296-x.

155. A Language and Environment for Statistical Computing Available online: https://www.r-project.org/ (accessed on 6 June 2023).

156. Andrews, S. FastQC: A Quality Control Tool for High Throughtput Sequence Data. **2010**.

157. Martin, M. Cutadapt Removes Adapter Sequences from High-Throughput Sequencing Reads. *EMBnet J* **2011**, *17*, 10, doi:10.14806/ej.17.1.200.

158. Kozomara, A.; Griffiths-Jones, S. MiRBase: Integrating MicroRNA Annotation and Deep-Sequencing Data. *Nucleic Acids Res* **2011**, *39*, D152–D157, doi:10.1093/nar/gkq1027.

159. Rumble, S.M.; Lacroute, P.; Dalca, A. V.; Fiume, M.; Sidow, A.; Brudno, M. SHRiMP: Accurate Mapping of Short Color-Space Reads. *PLoS Comput Biol* **2009**, *5*, e1000386, doi:10.1371/journal.pcbi.1000386.

160. Lawrence, M.; Huber, W.; Pagès, H.; Aboyoun, P.; Carlson, M.; Gentleman, R.; Morgan, M.T.; Carey, V.J. Software for Computing and Annotating Genomic Ranges. *PLoS Comput Biol* **2013**, *9*, e1003118, doi:10.1371/journal.pcbi.1003118.

161. Schymanski, E.L.; Jeon, J.; Gulde, R.; Fenner, K.; Ruff, M.; Singer, H.P.; Hollender, J. Identifying Small Molecules via High Resolution Mass Spectrometry: Communicating Confidence. *Environ Sci Technol* **2014**, *48*, 2097–2098, doi:10.1021/es5002105.

162. Gil-de-la-Fuente, A.; Godzien, J.; Saugar, S.; Garcia-Carmona, R.; Badran, H.; Wishart, D.S.; Barbas, C.; Otero, A. CEU Mass Mediator 3.0: A Metabolite Annotation Tool. *J Proteome Res* **2019**, *18*, 797–802, doi:10.1021/acs.jproteome.8b00720.

163. Peña-Bautista, C.; Roca, M.; Hervás, D.; Cuevas, A.; López-Cuevas, R.; Vento, M.; Baquero, M.; García-Blanco, A.; Cháfer-Pericás, C. Plasma Metabolomics in Early Alzheimer's Disease Patients Diagnosed with Amyloid Biomarker. *J Proteomics* **2019**, *200*, 144–152, doi:10.1016/j.jprot.2019.04.008.

164. Https://Www.Roche-as.Es/Lightmix_global. Available online: https://www.roche-as.es/lightmix_global. (accessed on 6 June 2023).

165. Misra, B.B. New Tools and Resources in Metabolomics: 2016-2017. *Electrophoresis* **2018**, *39*, 909–923, doi:10.1002/elps.201700441.

166. Viant, M.R.; Kurland, I.J.; Jones, M.R.; Dunn, W.B. How Close Are We to Complete Annotation of Metabolomes? *Curr Opin Chem Biol* **2017**, *36*, 64–69, doi:10.1016/j.cbpa.2017.01.001.

167. Sultana, R.; Perluigi, M.; Butterfield, D.A. Lipid Peroxidation Triggers Neurodegeneration: A Redox Proteomics View into the Alzheimer Disease Brain. *Free Radic Biol Med* **2013**, *62*, 157–169, doi:10.1016/j.freeradbiomed.2012.09.027.

168. Peña-Bautista, C.; Vigor, C.; Galano, J.-M.; Oger, C.; Durand, T.; Ferrer, I.; Cuevas, A.; López-Cuevas, R.; Baquero, M.; López-Nogueroles, M.; et al. Plasma Lipid Peroxidation Biomarkers for Early and Non-Invasive Alzheimer Disease Detection. *Free Radic Biol Med* **2018**, *124*, 388–394, doi:10.1016/j.freeradbiomed.2018.06.038.

169. Bradley-Whitman, M.A.; Lovell, M.A. Biomarkers of Lipid Peroxidation in Alzheimer Disease (AD): An Update. *Arch Toxicol* **2015**, *89*, 1035–1044, doi:10.1007/s00204-015-1517-6.

170. Puertas, M.C.; Martínez-Martos, J.M.; Cobo, M.P.; Carrera, M.P.; Mayas, M.D.; Ramírez-Expósito, M.J. Plasma Oxidative Stress Parameters in Men and Women with Early Stage Alzheimer Type Dementia. *Exp Gerontol* **2012**, *47*, 625–630, doi:10.1016/j.exger.2012.05.019.

171. García-Blanco, A.; Baquero, M.; Vento, M.; Gil, E.; Bataller, L.; Cháfer-Pericás, C. Potential Oxidative Stress Biomarkers of Mild Cognitive Impairment Due to Alzheimer Disease. *J Neurol Sci* **2017**, *373*, 295–302, doi:10.1016/j.jns.2017.01.020.

172. Hartmann, S.; Ledur Kist, T.B. A Review of Biomarkers of Alzheimer's Disease in Noninvasive Samples. *Biomark Med* **2018**, *12*, 677–690, doi:10.2217/bmm-2017-0388.

173. Tuppo, E.E.; Forman, L.J.; Spur, B.W.; Chan-Ting, R.E.; Chopra, A.; Cavalieri, T.A. Sign of Lipid Peroxidation as Measured in the Urine of Patients with Probable Alzheimer's Disease. *Brain Res Bull* **2001**, *54*, 565–568, doi:10.1016/S0361-9230(01)00450-6.

174. Kim, K.M.; Jung, B.H.; Paeng, K.-J.; Kim, I.; Chung, B.C. Increased Urinary F2-Isoprostanes Levels in the Patients with Alzheimer's Disease. *Brain Res Bull* **2004**, *64*, 47–51, doi:10.1016/j.brainresbull.2004.04.016.

175. Praticò, D.; Clark, C.M.; Liun, F.; Lee, V.Y.-M.; Trojanowski, J.Q. Increase of Brain Oxidative Stress in Mild Cognitive Impairment. *Arch Neurol* **2002**, *59*, 972, doi:10.1001/archneur.59.6.972.

176. Sarica, A.; Cerasa, A.; Quattrone, A. Random Forest Algorithm for the Classification of Neuroimaging Data in Alzheimer's Disease: A Systematic Review. *Front Aging Neurosci* **2017**, *9*, doi:10.3389/fnagi.2017.00329.

177. Teipel, S.J.; Grothe, M.J.; Metzger, C.D.; Grimmer, T.; Sorg, C.; Ewers, M.; Franzmeier, N.; Meisenzahl, E.; Klöppel, S.; Borchardt, V.; et al. Robust Detection of Impaired Resting State Functional Connectivity Networks in Alzheimer's Disease Using Elastic Net Regularized Regression. *Front Aging Neurosci* **2017**, *8*, doi:10.3389/fnagi.2016.00318.

178. Lehallier, B.; Essioux, L.; Gayan, J.; Alexandridis, R.; Nikolcheva, T.; Wyss-Coray, T.; Britschgi, M. Combined Plasma and Cerebrospinal Fluid Signature for the Prediction of Midterm Progression From Mild Cognitive Impairment to Alzheimer Disease. *JAMA Neurol* **2016**, *73*, 203, doi:10.1001/jamaneurol.2015.3135.

179. Ramírez, J.; Górriz, J.M.; Ortiz, A.; Martínez-Murcia, F.J.; Segovia, F.; Salas-Gonzalez, D.; Castillo-Barnes, D.; Illán, I.A.; Puntonet, C.G. Ensemble of Random Forests One vs. Rest Classifiers for MCI and AD Prediction Using ANOVA Cortical and Subcortical Feature Selection and Partial Least Squares. *J Neurosci Methods* **2018**, *302*, 47–57, doi:10.1016/j.jneumeth.2017.12.005.

180. Dimitriadis, S.I.; Liparas, D.; Tsolaki, M.N. Random Forest Feature Selection, Fusion and Ensemble Strategy: Combining Multiple Morphological MRI

Measures to Discriminate among Healhy Elderly, MCI, CMCI and Alzheimer's Disease Patients: From the Alzheimer's Disease Neuroimaging Initiative (ADNI) Database. *J Neurosci Methods* **2018**, *302*, 14–23, doi:10.1016/j.jneumeth.2017.12.010.

181. ŞİRİN, F.B.; KUMBUL DOĞUÇ, D.; VURAL, H.; EREN, İ.; İNANLI, İ.; SÜTÇÜ, R.; DELİBAŞ, N. Plasma 8-IsoPGF2α and Serum Melatonin Levels in Patients with Minimal Cognitive Impairment and Alzheimer Disease. *Turk J Med Sci* **2015**, *45*, 1073–1077, doi:10.3906/sag-1406-134.

182. Praticò, D. The Neurobiology of Isoprostanes and Alzheimer's Disease. *Biochimica et Biophysica Acta (BBA) - Molecular and Cell Biology of Lipids* **2010**, *1801*, 930–933, doi:10.1016/j.bbalip.2010.01.009.

183. Casadesus, G.; Smith, M.A.; Basu, S.; Hua, J.; Capobianco, D.E.; Siedlak, S.L.; Zhu, X.; Perry, G. Increased Isoprostane and Prostaglandin Are Prominent in Neurons in Alzheimer Disease. *Mol Neurodegener* **2007**, *2*, 2, doi:10.1186/1750-1326-2-2.

184. Herbst-Robinson, K.J.; Liu, L.; James, M.; Yao, Y.; Xie, S.X.; Brunden, K.R. Inflammatory Eicosanoids Increase Amyloid Precursor Protein Expression via Activation of Multiple Neuronal Receptors. *Sci Rep* **2015**, *5*, 18286, doi:10.1038/srep18286.

185. Nazeri, A.; Ganjgahi, H.; Roostaei, T.; Nichols, T.; Zarei, M. Imaging Proteomics for Diagnosis, Monitoring and Prediction of Alzheimer's Disease. *Neuroimage* **2014**, *102*, 657–665, doi:10.1016/j.neuroimage.2014.08.041.

186. Marmarelis, V.Z.; Shin, D.C.; Orme, M.E.; Zhang, R. Model-Based Quantification of Cerebral Hemodynamics as a Physiomarker for Alzheimer's Disease? *Ann Biomed Eng* **2013**, *41*, 2296–2317, doi:10.1007/s10439-013-0837-z.

187. Ibáñez, C.; Simó, C.; Martín-Álvarez, P.J.; Kivipelto, M.; Winblad, B.; Cedazo-Mínguez, A.; Cifuentes, A. Toward a Predictive Model of Alzheimer's Disease Progression Using Capillary Electrophoresis–Mass Spectrometry Metabolomics. *Anal Chem* **2012**, *84*, 8532–8540, doi:10.1021/ac301243k.

188. Liao, W.; Long, X.; Jiang, C.; Diao, Y.; Liu, X.; Zheng, H.; Zhang, L. Discerning Mild Cognitive Impairment and Alzheimer Disease from Normal Aging. *Acad Radiol* **2014**, *21*, 597–604, doi:10.1016/j.acra.2013.12.001.

189. CHMATALOVA, Z.; VYHNALEK, M.; LACZO, J.; HORT, J.; POSPISILOVA, R.; PECHOVA, M.; SKOUMALOVA, A. Relation of Plasma Selenium and Lipid Peroxidation End Products in Patients With Alzheimer's Disease. *Physiol Res* **2017**, 1049–1056, doi:10.33549/physiolres.933601.

190. Tabaton, M.; Odetti, P.; Cammarata, S.; Borghi, R.; Monacelli, F.; Caltagirone, C.; Bossù, P.; Buscema, M.; Grossi, E. Artificial Neural Networks Identify the Predictive Values of Risk Factors on the Conversion of Amnestic Mild Cognitive

Impairment. *Journal of Alzheimer's Disease* **2010**, *19*, 1035–1040, doi:10.3233/JAD-2010-1300.

191. Lins, A.J.C.C.; Muniz, M.T.C.; Garcia, A.N.M.; Gomes, A.V.; Cabral, R.M.; Bastos-Filho, C.J.A. Using Artificial Neural Networks to Select the Parameters for the Prognostic of Mild Cognitive Impairment and Dementia in Elderly Individuals. *Comput Methods Programs Biomed* **2017**, *152*, 93–104, doi:10.1016/j.cmpb.2017.09.013.

192. Tang, J.; Wu, L.; Huang, H.; Feng, J.; Yuan, Y.; Zhou, Y.; Huang, P.; Xu, Y.; Yu, C. Back Propagation Artificial Neural Network for Community Alzheimer's Disease Screening in China. *Neural Regen Res* **2013**, *8*, 270–276, doi:10.3969/j.issn.1673-5374.2013.03.010.

193. Booij, B.B.; Lindahl, T.; Wetterberg, P.; Skaane, N.V.; Sæbø, S.; Feten, G.; Rye, P.D.; Kristiansen, L.I.; Hagen, N.; Jensen, M.; et al. A Gene Expression Pattern in Blood for the Early Detection of Alzheimer's Disease. *Journal of Alzheimer's Disease* **2011**, *23*, 109–119, doi:10.3233/JAD-2010-101518.

194. Konukoglu, E.; Coutu, J.-P.; Salat, D.H.; Fischl, B. Multivariate Statistical Analysis of Diffusion Imaging Parameters Using Partial Least Squares: Application to White Matter Variations in Alzheimer's Disease. *Neuroimage* **2016**, *134*, 573–586, doi:10.1016/j.neuroimage.2016.04.038.

195. Qi Zhou; Goryawala, M.; Cabrerizo, M.; Barker, W.; Loewenstein, D.; Duara, R.; Adjouadi, M. Multivariate Analysis of Structural MRI and PET (FDG and 18F-AV-45) for Alzheimer's Disease and Its Prodromal Stages. In Proceedings of the 2014 36th Annual International Conference of the IEEE Engineering in Medicine and Biology Society; IEEE, August 2014; pp. 1051–1054.

196. Wang, P.; Chen, K.; Yao, L.; Hu, B.; Wu, X.; Zhang, J.; Ye, Q.; Guo, X. Multimodal Classification of Mild Cognitive Impairment Based on Partial Least Squares. *Journal of Alzheimer's Disease* **2016**, *54*, 359–371, doi:10.3233/JAD-160102.

197. Toufan, M.; Namdar, H.; Abbasnezhad, M.; Habibzadeh, A.; Esmaeili, H.; Yaraghi, S.; Samani, Z. Diagnostic Values of Plasma, Fresh and Frozen Urine NT-ProBNP in Heart Failure Patients. *J Cardiovasc Thorac Res* **2014**, *6*, 111–115, doi:10.5681/jcvtr.2014.024.

198. Schley, G.; Köberle, C.; Manuilova, E.; Rutz, S.; Forster, C.; Weyand, M.; Formentini, I.; Kientsch-Engel, R.; Eckardt, K.-U.; Willam, C. Comparison of Plasma and Urine Biomarker Performance in Acute Kidney Injury. *PLoS One* **2015**, *10*, e0145042, doi:10.1371/journal.pone.0145042.

199. Quintana, M.; Guàrdia, J.; Sánchez-Benavides, G.; Aguilar, M.; Molinuevo, J.L.; Robles, A.; Barquero, M.S.; Antúnez, C.; Martínez-Parra, C.; Frank-García, A.; et al. Using Artificial Neural Networks in Clinical Neuropsychology: High Performance in Mild Cognitive Impairment and Alzheimer's Disease. *J Clin Exp Neuropsychol* **2012**, *34*, 195–208, doi:10.1080/13803395.2011.630651.

200. Peskind, E.R.; Riekse, R.; Quinn, J.F.; Kaye, J.; Clark, C.M.; Farlow, M.R.; DeCarli, C.; Chabal, C.; Vavrek, D.; Raskind, M.A.; et al. Safety and Acceptability of the Research Lumbar Puncture. *Alzheimer Dis Assoc Disord* **2005**, *19*, 220–225, doi:10.1097/01.wad.0000194014.43575.fd.

201. Spies, P.E. Reviewing Reasons for the Decreased CSF Abeta42 Concentration in Alzheimer. *Frontiers in Bioscience* **2012**, *17*, 2024, doi:10.2741/4035.

202. Quinn, J.F.; Montine, K.S.; Moore, M.; Morrow, J.D.; Kaye, J.A.; Montine, T.J. Suppression of Longitudinal Increase in CSF F2-Isoprostanes in Alzheimer's Disease. *Journal of Alzheimer's Disease* **2004**, *6*, 93–97, doi:10.3233/JAD-2004-6110.

203. Duits, F.H.; Kester, M.I.; Scheffer, P.G.; Blankenstein, M.A.; Scheltens, P.; Teunissen, C.E.; van der Flier, W.M. Increase in Cerebrospinal Fluid F2-Isoprostanes Is Related to Cognitive Decline in APOE E4 Carriers. *Journal of Alzheimer's Disease* **2013**, *36*, 563–570, doi:10.3233/JAD-122227.

204. Kuo, H.-C.; Yen, H.-C.; Huang, C.-C.; Hsu, W.-C.; Wei, H.-J.; Lin, C.-L. Cerebrospinal Fluid Biomarkers for Neuropsychological Symptoms in Early Stage of Late-Onset Alzheimer's Disease. *International Journal of Neuroscience* **2015**, *125*, 747–754, doi:10.3109/00207454.2014.971787.

205. Yao, Y.; Clark, C.M.; Trojanowski, J.Q.; Lee, V.M.-Y.; Praticò, D. Elevation of 12/15 Lipoxygenase Products in AD and Mild Cognitive Impairment. *Ann Neurol* **2005**, *58*, 623–626, doi:10.1002/ana.20558.

206. Kester, M.I.; Scheffer, P.G.; Koel-Simmelink, M.J.; Twaalfhoven, H.; Verwey, N.A.; Veerhuis, R.; Twisk, J.W.; Bouwman, F.H.; Blankenstein, M.A.; Scheltens, P.; et al. Serial CSF Sampling in Alzheimer's Disease: Specific versus Non-Specific Markers. *Neurobiol Aging* **2012**, *33*, 1591–1598, doi:10.1016/j.neurobiolaging.2011.05.013.

207. Leon, M.J.; Mosconi, L.; Li, J.; Santi, S.; Yao, Y.; Tsui, W.H.; Pirraglia, E.; Rich, K.; Javier, E.; Brys, M.; et al. Longitudinal CSF Isoprostane and MRI Atrophy in the Progression to AD. *J Neurol* **2007**, *254*, 1666–1675, doi:10.1007/s00415-007-0610-z.

208. De Vos, A.; Jacobs, D.; Struyfs, H.; Fransen, E.; Andersson, K.; Portelius, E.; Andreasson, U.; De Surgeloose, D.; Hernalsteen, D.; Sleegers, K.; et al. C-terminal Neurogranin Is Increased in Cerebrospinal Fluid but Unchanged in Plasma in Alzheimer's Disease. *Alzheimer's & Dementia* **2015**, *11*, 1461–1469, doi:10.1016/j.jalz.2015.05.012.

209. Le Bastard, N.; Aerts, L.; Leurs, J.; Blomme, W.; De Deyn, P.P.; Engelborghs, S. No Correlation between Time-Linked Plasma and CSF Aβ Levels. *Neurochem Int* **2009**, *55*, 820–825, doi:10.1016/j.neuint.2009.08.006.

210. Mehta, P.D.; Pirttila, T.; Patrick, B.A.; Barshatzky, M.; Mehta, S.P. Amyloid β Protein 1–40 and 1–42 Levels in Matched Cerebrospinal Fluid and Plasma from

Patients with Alzheimer Disease. *Neurosci Lett* **2001**, *304*, 102–106, doi:10.1016/S0304-3940(01)01754-2.

211. Sun, Y.-X.; Minthon, L.; Wallmark, A.; Warkentin, S.; Blennow, K.; Janciauskiene, S. Inflammatory Markers in Matched Plasma and Cerebrospinal Fluid from Patients with Alzheimer's Disease. *Dement Geriatr Cogn Disord* **2003**, *16*, 136–144, doi:10.1159/000071001.

212. Une, K.; Takei, Y.A.; Tomita, N.; Asamura, T.; Ohrui, T.; Furukawa, K.; Arai, H. Adiponectin in Plasma and Cerebrospinal Fluid in MCI and Alzheimer's Disease. *Eur J Neurol* **2011**, *18*, 1006–1009, doi:10.1111/j.1468-1331.2010.03194.x.

213. Jacobs, K.R.; Lim, C.K.; Blennow, K.; Zetterberg, H.; Chatterjee, P.; Martins, R.N.; Brew, B.J.; Guillemin, G.J.; Lovejoy, D.B. Correlation between Plasma and CSF Concentrations of Kynurenine Pathway Metabolites in Alzheimer's Disease and Relationship to Amyloid-β and Tau. *Neurobiol Aging* **2019**, *80*, 11–20, doi:10.1016/j.neurobiolaging.2019.03.015.

214. Janelidze, S.; Hertze, J.; Nägga, K.; Nilsson, K.; Nilsson, C.; Wennström, M.; van Westen, D.; Blennow, K.; Zetterberg, H.; Hansson, O. Increased Blood-Brain Barrier Permeability Is Associated with Dementia and Diabetes but Not Amyloid Pathology or APOE Genotype. *Neurobiol Aging* **2017**, *51*, 104–112, doi:10.1016/j.neurobiolaging.2016.11.017.

215. Algotsson, A.; Winblad, B. The Integrity of the Blood?Brain Barrier in Alzheimer?S Disease. *Acta Neurol Scand* **2007**, *115*, 403–408, doi:10.1111/j.1600-0404.2007.00823.x.

216. Takeda, S.; Sato, N.; Ikimura, K.; Nishino, H.; Rakugi, H.; Morishita, R. Increased Blood–Brain Barrier Vulnerability to Systemic Inflammation in an Alzheimer Disease Mouse Model. *Neurobiol Aging* **2013**, *34*, 2064–2070, doi:10.1016/j.neurobiolaging.2013.02.010.

217. Silveri, M.C. Frontotemporal Dementia to Alzheimer's Disease. *Dialogues Clin Neurosci* **2007**, *9*, 153–160, doi:10.31887/DCNS.2007.9.2/msilveri.

218. Torres, L.L.; Quaglio, N.B.; de Souza, G.T.; Garcia, R.T.; Dati, L.M.M.; Moreira, W.L.; de Melo Loureiro, A.P.; de souza-Talarico, J.N.; Smid, J.; Porto, C.S.; et al. Peripheral Oxidative Stress Biomarkers in Mild Cognitive Impairment and Alzheimer's Disease. *Journal of Alzheimer's Disease* **2011**, *26*, 59–68, doi:10.3233/JAD-2011-110284.

219. Gustaw-Rothenberg, K.; Kowalczuk, K.; Stryjecka-Zimmer, M. Lipids' Peroxidation Markers in Alzheimer's Disease and Vascular Dementia. *Geriatr Gerontol Int* **2009**, doi:10.1111/j.1447-0594.2009.00571.x.

220. Polidori, M.C.; Mattioli, P.; Aldred, S.; Cecchetti, R.; Stahl, W.; Griffiths, H.; Senin, U.; Sies, H.; Mecocci, P. Plasma Antioxidant Status, Immunoglobulin G Oxidation and Lipid Peroxidation in Demented Patients: Relevance to Alzheimer Disease and Vascular Dementia. *Dement Geriatr Cogn Disord* **2004**, *18*, 265–270, doi:10.1159/000080027.

221. McGrath, L.T. Increased Oxidative Stress in Alzheimer's Disease as Assessed with 4-Hydroxynonenal but Not Malondialdehyde. *QJM* **2001**, *94*, 485–490, doi:10.1093/qjmed/94.9.485.

222. Chmátalová, Z.; Vyhnálek, M.; Laczó, J.; Hort, J.; Skoumalová, A. Analysis of Lipophilic Fluorescent Products in Blood of Alzheimer's Disease Patients. *J Cell Mol Med* **2016**, *20*, 1367–1372, doi:10.1111/jcmm.12824.

223. Klaunig, J.E. Oxidative Stress and Cancer. *Curr Pharm Des* **2019**, *24*, 4771–4778, doi:10.2174/1381612825666190215121712.

224. Steven, S.; Frenis, K.; Oelze, M.; Kalinovic, S.; Kuntic, M.; Bayo Jimenez, M.T.; Vujacic-Mirski, K.; Helmstädter, J.; Kröller-Schön, S.; Münzel, T.; et al. Vascular Inflammation and Oxidative Stress: Major Triggers for Cardiovascular Disease. *Oxid Med Cell Longev* **2019**, *2019*, 1–26, doi:10.1155/2019/7092151.

225. Kim, G.H.; Kim, J.E.; Rhie, S.J.; Yoon, S. The Role of Oxidative Stress in Neurodegenerative Diseases. *Exp Neurobiol* **2015**, *24*, 325–340, doi:10.5607/en.2015.24.4.325.

226. Mufson, E.J.; Leurgans, S. Inability of Plasma and Urine F2A-Isoprostane Levels to Differentiate Mild Cognitive Impairment from Alzheimer's Disease. *Neurodegener Dis* **2010**, *7*, 139–142, doi:10.1159/000289224.

227. Feillet-Coudray, C.; Tourtauchaux, R.; Niculescu, M.; Rock, E.; Tauveron, I.; Alexandre-Gouabau, M.-C.; Rayssiguier, Y.; Jalenques, I.; Mazur, A. Plasma Levels of 8-EpiPGF2α, an in Vivo Marker of Oxidative Stress, Are Not Affected by Aging or Alzheimer's Disease. *Free Radic Biol Med* **1999**, *27*, 463–469, doi:10.1016/S0891-5849(99)00096-9.

228. Krishnan, S.; Rani, P. Evaluation of Selenium, Redox Status and Their Association with Plasma Amyloid/Tau in Alzheimer's Disease. *Biol Trace Elem Res* **2014**, *158*, 158–165, doi:10.1007/s12011-014-9930-x.

229. Hatanaka, H.; Hanyu, H.; Fukasawa, R.; Sato, T.; Shimizu, S.; Sakurai, H. Peripheral Oxidative Stress Markers in Diabetes-Related Dementia. *Geriatr Gerontol Int* **2016**, *16*, 1312–1318, doi:10.1111/ggi.12645.

230. Mc Ardle, R.; Galna, B.; Donaghy, P.; Thomas, A.; Rochester, L. Do Alzheimer's and Lewy Body Disease Have Discrete Pathological Signatures of Gait? *Alzheimer's & Dementia* **2019**, *15*, 1367–1377, doi:10.1016/j.jalz.2019.06.4953.

231. Leisman, G.; Moustafa, A.; Shafir, T. Thinking, Walking, Talking: Integratory Motor and Cognitive Brain Function. *Front Public Health* **2016**, *4*, doi:10.3389/fpubh.2016.00094.

232. Santangelo, R.; Dell'Edera, A.; Sala, A.; Cecchetti, G.; Masserini, F.; Caso, F.; Pinto, P.; Leocani, L.; Falautano, M.; Passerini, G.; et al. The CSF P-Tau181/Aβ42 Ratio Offers a Good Accuracy "In Vivo" in the Differential Diagnosis of Alzheimer's Dementia. *Curr Alzheimer Res* **2019**, *16*, 587–595, doi:10.2174/1567205016666190725150836.

233. Praticò, D.; Uryu, K.; Leight, S.; Trojanoswki, J.Q.; Lee, V.M.-Y. Increased Lipid Peroxidation Precedes Amyloid Plaque Formation in an Animal Model of Alzheimer Amyloidosis. *The Journal of Neuroscience* **2001**, *21*, 4183–4187, doi:10.1523/JNEUROSCI.21-12-04183.2001.

234. Lauretti, E.; Di Meco, A.; Chu, J.; Praticò, D. Modulation of AD Neuropathology and Memory Impairments by the Isoprostane F2α Is Mediated by the Thromboxane Receptor. *Neurobiol Aging* **2015**, *36*, 812–820, doi:10.1016/j.neurobiolaging.2014.10.005.

235. Soper, J.H.; Sugiyama, S.; Herbst-Robinson, K.; James, M.J.; Wang, X.; Trojanowski, J.Q.; Smith, A.B.; Lee, V.M.-Y.; Ballatore, C.; Brunden, K.R. Brain-Penetrant Tetrahydronaphthalene Thromboxane A2-Prostanoid (TP) Receptor Antagonists as Prototype Therapeutics for Alzheimer's Disease. *ACS Chem Neurosci* **2012**, *3*, 928–940, doi:10.1021/cn3000795.

236. Shineman, D.W.; Zhang, B.; Leight, S.N.; Pratico, D.; Lee, V.M.-Y. Thromboxane Receptor Activation Mediates Isoprostane-Induced Increases in Amyloid Pathology in Tg2576 Mice. *The Journal of Neuroscience* **2008**, *28*, 4785–4794, doi:10.1523/JNEUROSCI.0684-08.2008.

237. Peña-Bautista, C.; Baquero, M.; Ferrer, I.; Hervás, D.; Vento, M.; García-Blanco, A.; Cháfer-Pericás, C. Neuropsychological Assessment and Cortisol Levels in Biofluids from Early Alzheimer's Disease Patients. *Exp Gerontol* **2019**, *123*, 10–16, doi:10.1016/j.exger.2019.05.007.

238. Shi, L.; Westwood, S.; Baird, A.L.; Winchester, L.; Dobricic, V.; Kilpert, F.; Hong, S.; Franke, A.; Hye, A.; Ashton, N.J.; et al. Discovery and Validation of Plasma Proteomic Biomarkers Relating to Brain Amyloid Burden by SOMAscan Assay. *Alzheimer's & Dementia* **2019**, *15*, 1478–1488, doi:10.1016/j.jalz.2019.06.4951.

239. Li, H.; Habes, M.; Wolk, D.A.; Fan, Y. A Deep Learning Model for Early Prediction of Alzheimer's Disease Dementia Based on Hippocampal Magnetic Resonance Imaging Data. *Alzheimer's & Dementia* **2019**, *15*, 1059–1070, doi:10.1016/j.jalz.2019.02.007.

240. Jang, H.; Park, J.; Woo, S.; Kim, S.; Kim, H.J.; Na, D.L.; Lockhart, S.N.; Kim, Y.; Kim, K.W.; Cho, S.H.; et al. Prediction of Fast Decline in Amyloid Positive Mild Cognitive Impairment Patients Using Multimodal Biomarkers. *Neuroimage Clin* **2019**, *24*, 101941, doi:10.1016/j.nicl.2019.101941.

241. Vergallo, A.; Mégret, L.; Lista, S.; Cavedo, E.; Zetterberg, H.; Blennow, K.; Vanmechelen, E.; De Vos, A.; Habert, M.; Potier, M.; et al. Plasma Amyloid β 40/42 Ratio Predicts Cerebral Amyloidosis in Cognitively Normal Individuals at Risk for Alzheimer's Disease. *Alzheimer's & Dementia* **2019**, *15*, 764–775, doi:10.1016/j.jalz.2019.03.009.

242. Engelborghs, S.; Niemantsverdriet, E.; Struyfs, H.; Blennow, K.; Brouns, R.; Comabella, M.; Dujmovic, I.; Flier, W.; Frölich, L.; Galimberti, D.; et al. Consensus Guidelines for Lumbar Puncture in Patients with Neurological

Diseases. *Alzheimer's & Dementia: Diagnosis, Assessment & Disease Monitoring* **2017**, *8*, 111–126, doi:10.1016/j.dadm.2017.04.007.

243. Mapstone, M.; Cheema, A.K.; Fiandaca, M.S.; Zhong, X.; Mhyre, T.R.; MacArthur, L.H.; Hall, W.J.; Fisher, S.G.; Peterson, D.R.; Haley, J.M.; et al. Plasma Phospholipids Identify Antecedent Memory Impairment in Older Adults. *Nat Med* **2014**, *20*, 415–418, doi:10.1038/nm.3466.

244. Chatterjee, P.; Elmi, M.; Goozee, K.; Shah, T.; Sohrabi, H.R.; Dias, C.B.; Pedrini, S.; Shen, K.; Asih, P.R.; Dave, P.; et al. Ultrasensitive Detection of Plasma Amyloid-β as a Biomarker for Cognitively Normal Elderly Individuals at Risk of Alzheimer's Disease. *Journal of Alzheimer's Disease* **2019**, *71*, 775–783, doi:10.3233/JAD-190533.

245. Hilal, S.; Wolters, F.J.; Verbeek, M.M.; Vanderstichele, H.; Ikram, M.K.; Stoops, E.; Ikram, M.A.; Vernooij, M.W. Plasma Amyloid-β Levels, Cerebral Atrophy and Risk of Dementia: A Population-Based Study. *Alzheimers Res Ther* **2018**, *10*, 63, doi:10.1186/s13195-018-0395-6.

246. Lövheim, H.; Elgh, F.; Johansson, A.; Zetterberg, H.; Blennow, K.; Hallmans, G.; Eriksson, S. Plasma Concentrations of Free Amyloid β Cannot Predict the Development of Alzheimer's Disease. *Alzheimer's & Dementia* **2017**, *13*, 778–782, doi:10.1016/j.jalz.2016.12.004.

247. Karikari, T.K.; Benedet, A.L.; Ashton, N.J.; Lantero Rodriguez, J.; Snellman, A.; Suárez-Calvet, M.; Saha-Chaudhuri, P.; Lussier, F.; Kvartsberg, H.; Rial, A.M.; et al. Diagnostic Performance and Prediction of Clinical Progression of Plasma Phospho-Tau181 in the Alzheimer's Disease Neuroimaging Initiative. *Mol Psychiatry* **2021**, *26*, 429–442, doi:10.1038/s41380-020-00923-z.

248. Cheng, H.; Wang, M.; Li, J.-L.; Cairns, N.J.; Han, X. Specific Changes of Sulfatide Levels in Individuals with Pre-Clinical Alzheimer's Disease: An Early Event in Disease Pathogenesis. *J Neurochem* **2013**, *127*, 733–738, doi:10.1111/jnc.12368.

249. Fiandaca, M.S.; Zhong, X.; Cheema, A.K.; Orquiza, M.H.; Chidambaram, S.; Tan, M.T.; Gresenz, C.R.; FitzGerald, K.T.; Nalls, M.A.; Singleton, A.B.; et al. Plasma 24-Metabolite Panel Predicts Preclinical Transition to Clinical Stages of Alzheimer's Disease. *Front Neurol* **2015**, *6*, doi:10.3389/fneur.2015.00237.

250. Ma, Y.; Shen, X.; Xu, W.; Huang, Y.; Li, H.; Tan, L.; Tan, C.; Dong, Q.; Tan, L.; Yu, J. A Panel of Blood Lipids Associated with Cognitive Performance, Brain Atrophy, and Alzheimer's Diagnosis: A Longitudinal Study of Elders without Dementia. *Alzheimer's & Dementia: Diagnosis, Assessment & Disease Monitoring* **2020**, *12*, doi:10.1002/dad2.12041.

251. Kalaria, R.N.; Ihara, M. Medial Temporal Lobe Atrophy Is the Norm in Cerebrovascular Dementias. *Eur J Neurol* **2017**, *24*, 539–540, doi:10.1111/ene.13243.

252. Hsu, J.-L.; Lee, W.-J.; Liao, Y.-C.; Lirng, J.-F.; Wang, S.-J.; Fuh, J.-L. Posterior Atrophy and Medial Temporal Atrophy Scores Are Associated with Different Symptoms in Patients with Alzheimer's Disease and Mild Cognitive Impairment. *PLoS One* **2015**, *10*, e0137121, doi:10.1371/journal.pone.0137121.

253. Ferreira, D.; Cavallin, L.; Larsson, E.-M.; Muehlboeck, J.-S.; Mecocci, P.; Vellas, B.; Tsolaki, M.; Kłoszewska, I.; Soininen, H.; Lovestone, S.; et al. Practical Cut-Offs for Visual Rating Scales of Medial Temporal, Frontal and Posterior Atrophy in Alzheimer's Disease and Mild Cognitive Impairment. *J Intern Med* **2015**, *278*, 277–290, doi:10.1111/joim.12358.

254. Tagawa, R.; Hashimoto, H.; Nakanishi, A.; Kawarada, Y.; Muramatsu, T.; Matsuda, Y.; Kataoka, K.; Shimada, A.; Uchida, K.; Yoshida, A.; et al. The Relationship Between Medial Temporal Lobe Atrophy and Cognitive Impairment in Patients With Dementia With Lewy Bodies. *J Geriatr Psychiatry Neurol* **2015**, *28*, 249–254, doi:10.1177/0891988715590210.

255. Visser, P.J.; Scheltens, P.; Verhey, F.R.J.; Schmand, B.; Launer, L.J.; Jolles, J.; Jonker, C. Medial Temporal Lobe Atrophy and Memory Dysfunction as Predictors for Dementia in Subjects with Mild Cognitive Impairment. *J Neurol* **1999**, *246*, 477–485, doi:10.1007/s004150050387.

256. Granadillo, E.; Paholpak, P.; Mendez, M.F.; Teng, E. Visual Ratings of Medial Temporal Lobe Atrophy Correlate with CSF Tau Indices in Clinical Variants of Early-Onset Alzheimer Disease. *Dement Geriatr Cogn Disord* **2017**, *44*, 45–54, doi:10.1159/000477718.

257. Suk, H.-I.; Lee, S.-W.; Shen, D. Hierarchical Feature Representation and Multimodal Fusion with Deep Learning for AD/MCI Diagnosis. *Neuroimage* **2014**, *101*, 569–582, doi:10.1016/j.neuroimage.2014.06.077.

258. Canu, E.; Agosta, F.; Mandic-Stojmenovic, G.; Stojković, T.; Stefanova, E.; Inuggi, A.; Imperiale, F.; Copetti, M.; Kostic, V.S.; Filippi, M. Multiparametric MRI to Distinguish Early Onset Alzheimer's Disease and Behavioural Variant of Frontotemporal Dementia. *Neuroimage Clin* **2017**, *15*, 428–438, doi:10.1016/j.nicl.2017.05.018.

259. Miller, E.; Morel, A.; Saso, L.; Saluk, J. Isoprostanes and Neuroprostanes as Biomarkers of Oxidative Stress in Neurodegenerative Diseases. *Oxid Med Cell Longev* **2014**, *2014*, 1–10, doi:10.1155/2014/572491.

260. Fazekas, F.; Chawluk, J.; Alavi, A.; Hurtig, H.; Zimmerman, R. MR Signal Abnormalities at 1.5 T in Alzheimer's Dementia and Normal Aging. *American Journal of Roentgenology* **1987**, *149*, 351–356, doi:10.2214/ajr.149.2.351.

261. Elahi, F.M.; Marx, G.; Cobigo, Y.; Staffaroni, A.M.; Kornak, J.; Tosun, D.; Boxer, A.L.; Kramer, J.H.; Miller, B.L.; Rosen, H.J. Longitudinal White Matter Change in Frontotemporal Dementia Subtypes and Sporadic Late Onset Alzheimer's Disease. *Neuroimage Clin* **2017**, *16*, 595–603, doi:10.1016/j.nicl.2017.09.007.

262. Yen, H.-C.; Wei, H.-J.; Lin, C.-L. Unresolved Issues in the Analysis of F2-Isoprostanes, F4-Neuroprostanes, Isofurans, Neurofurans, and F2-Dihomo-Isoprostanes in Body Fluids and Tissue Using Gas Chromatography/Negative-Ion Chemical-Ionization Mass Spectrometry. *Free Radic Res* **2015**, *49*, 861–880, doi:10.3109/10715762.2015.1014812.

263. García-Flores, L.A.; Medina, S.; Oger, C.; Galano, J.-M.; Durand, T.; Cejuela, R.; Martínez-Sanz, J.M.; Ferreres, F.; Gil-Izquierdo, Á. Lipidomic Approach in Young Adult Triathletes: Effect of Supplementation with a Polyphenols-Rich Juice on Neuroprostane and F_2-Dihomo-Isoprostane Markers. *Food Funct* **2016**, *7*, 4343–4355, doi:10.1039/C6FO01000H.

264. Hatanaka, H.; Hanyu, H.; Fukasawa, R.; Hirao, K.; Shimizu, S.; Kanetaka, H.; Iwamoto, T. Differences in Peripheral Oxidative Stress Markers in Alzheimer's Disease, Vascular Dementia and Mixed Dementia Patients. *Geriatr Gerontol Int* **2015**, *15*, 53–58, doi:10.1111/ggi.12659.

265. Di Domenico, F.; Pupo, G.; Giraldo, E.; Badìa, M.-C.; Monllor, P.; Lloret, A.; Eugenia Schininà, M.; Giorgi, A.; Cini, C.; Tramutola, A.; et al. Oxidative Signature of Cerebrospinal Fluid from Mild Cognitive Impairment and Alzheimer Disease Patients. *Free Radic Biol Med* **2016**, *91*, 1–9, doi:10.1016/j.freeradbiomed.2015.12.004.

266. Vane, J.R.; Bakhle, Y.S.; Botting, R.M. CYCLOOXYGENASES 1 AND 2. *Annu Rev Pharmacol Toxicol* **1998**, *38*, 97–120, doi:10.1146/annurev.pharmtox.38.1.97.

267. Calsolaro, V.; Edison, P. Neuroinflammation in Alzheimer's Disease: Current Evidence and Future Directions. *Alzheimer's & Dementia* **2016**, *12*, 719–732, doi:10.1016/j.jalz.2016.02.010.

268. Johansson, J.U.; Woodling, N.S.; Wang, Q.; Panchal, M.; Liang, X.; Trueba-Saiz, A.; Brown, H.D.; Mhatre, S.D.; Loui, T.; Andreasson, K.I. Prostaglandin Signaling Suppresses Beneficial Microglial Function in Alzheimer's Disease Models. *Journal of Clinical Investigation* **2015**, *125*, 350–364, doi:10.1172/JCI77487.

269. Pohanka, M. Alzheimer´s Disease and Oxidative Stress: A Review. *Curr Med Chem* **2013**, *21*, 356–364, doi:10.2174/09298673113206660258.

270. Http://Www.Hmdb.ca/Metabolites/HMDB0041366.

271. Li, F.; Li, G.; Zhao, J.; Xiao, J.; Liu, Z.; Su, G. A Simple LC-MS Method for Determination of Cyasterone in Rat Plasma: Application to a Pilot Pharmacokinetic Study. *Biomedical Chromatography* **2016**, *30*, 867–871, doi:10.1002/bmc.3621.

272. Http://Www.Hmdb.ca/Metabolites/HMDB001151. Available online: http://www.hmdb.ca/metabolites/HMDB001151. (accessed on 6 June 2023).

273. Liu, W.; Li, Q. An Efficient Elastic Net with Regression Coefficients Method for Variable Selection of Spectrum Data. *PLoS One* **2017**, *12*, e0171122, doi:10.1371/journal.pone.0171122.

274. Liu, D.; Pitta, M.; Jiang, H.; Lee, J.-H.; Zhang, G.; Chen, X.; Kawamoto, E.M.; Mattson, M.P. Nicotinamide Forestalls Pathology and Cognitive Decline in Alzheimer Mice: Evidence for Improved Neuronal Bioenergetics and Autophagy Procession. *Neurobiol Aging* **2013**, *34*, 1564–1580, doi:10.1016/j.neurobiolaging.2012.11.020.

275. Gong, B.; Pan, Y.; Vempati, P.; Zhao, W.; Knable, L.; Ho, L.; Wang, J.; Sastre, M.; Ono, K.; Sauve, A.A.; et al. Nicotinamide Riboside Restores Cognition through an Upregulation of Proliferator-Activated Receptor-γ Coactivator 1α Regulated β-Secretase 1 Degradation and Mitochondrial Gene Expression in Alzheimer's Mouse Models. *Neurobiol Aging* **2013**, *34*, 1581–1588, doi:10.1016/j.neurobiolaging.2012.12.005.

276. Hou, Y.; Lautrup, S.; Cordonnier, S.; Wang, Y.; Croteau, D.L.; Zavala, E.; Zhang, Y.; Moritoh, K.; O'Connell, J.F.; Baptiste, B.A.; et al. NAD+ Supplementation Normalizes Key Alzheimer's Features and DNA Damage Responses in a New AD Mouse Model with Introduced DNA Repair Deficiency. *Proceedings of the National Academy of Sciences* **2018**, *115*, doi:10.1073/pnas.1718819115.

277. Chi, Y.; Sauve, A.A. Nicotinamide Riboside, a Trace Nutrient in Foods, Is a Vitamin B3 with Effects on Energy Metabolism and Neuroprotection. *Curr Opin Clin Nutr Metab Care* **2013**, *16*, 657–661, doi:10.1097/MCO.0b013e32836510c0.

278. Kurumatani, T.; Fastbom, J.; Bonkale, W.L.; Bogdanovic, N.; Winblad, B.; Ohm, T.G.; Cowburn, R.F. Loss of Inositol 1,4,5-Trisphosphate Receptor Sites and Decreased PKC Levels Correlate with Staging of Alzheimer's Disease Neurofibrillary Pathology. *Brain Res* **1998**, *796*, 209–221, doi:10.1016/S0006-8993(98)00347-3.

279. Frej, A.D.; Otto, G.P.; Williams, R.S.B. Tipping the Scales: Lessons from Simple Model Systems on Inositol Imbalance in Neurological Disorders. *Eur J Cell Biol* **2017**, *96*, 154–163, doi:10.1016/j.ejcb.2017.01.007.

280. Cristofano, A.; Sapere, N.; La Marca, G.; Angiolillo, A.; Vitale, M.; Corbi, G.; Scapagnini, G.; Intrieri, M.; Russo, C.; Corso, G.; et al. Serum Levels of Acyl-Carnitines along the Continuum from Normal to Alzheimer's Dementia. *PLoS One* **2016**, *11*, e0155694, doi:10.1371/journal.pone.0155694.

281. Thomas, S.C.; Alhasawi, A.; Appanna, V.P.; Auger, C.; Appanna, V.D. Brain Metabolism and Alzheimer's Disease: The Prospect of a Metabolite-Based Therapy. *J Nutr Health Aging* **2015**, *19*, 58–63, doi:10.1007/s12603-014-0511-7.

282. Lodeiro, M.; Ibáñez, C.; Cifuentes, A.; Simó, C.; Cedazo-Mínguez, Á. Decreased Cerebrospinal Fluid Levels of L-Carnitine in Non-Apolipoprotein E4 Carriers at Early Stages of Alzheimer's Disease. *Journal of Alzheimer's Disease* **2014**, *41*, 223–232, doi:10.3233/JAD-132063.

283. Mancuso, C.; Bates, T.E.; Butterfield, D.A.; Calafato, S.; Cornelius, C.; Lorenzo, A. De; Dinkova Kostova, A.T.; Calabrese, V. Natural Antioxidants in Alzheimer's Disease. *Expert Opin Investig Drugs* **2007**, *16*, 1921–1931, doi:10.1517/13543784.16.12.1921.

284. Kazak, F.; Yarim, G.F. Neuroprotective Effects of Acetyl- l -Carnitine on Lipopolysaccharide-Induced Neuroinflammation in Mice: Involvement of Brain-Derived Neurotrophic Factor. *Neurosci Lett* **2017**, *658*, 32–36, doi:10.1016/j.neulet.2017.07.059.

285. Jump, D.B.; Torres-Gonzalez, M.; Olson, L.K. Soraphen A, an Inhibitor of Acetyl CoA Carboxylase Activity, Interferes with Fatty Acid Elongation. *Biochem Pharmacol* **2011**, *81*, 649–660, doi:10.1016/j.bcp.2010.12.014.

286. Pisa, D.; Alonso, R.; Juarranz, A.; Rábano, A.; Carrasco, L. Direct Visualization of Fungal Infection in Brains from Patients with Alzheimer's Disease. *Journal of Alzheimer's Disease* **2014**, *43*, 613–624, doi:10.3233/JAD-141386.

287. Alonso, R.; Pisa, D.; Marina, A.I.; Morato, E.; Rábano, A.; Carrasco, L. Fungal Infection in Patients with Alzheimer's Disease. *Journal of Alzheimer's Disease* **2014**, *41*, 301–311, doi:10.3233/JAD-132681.

288. Pisa, D.; Alonso, R.; Rábano, A.; Rodal, I.; Carrasco, L. Different Brain Regions Are Infected with Fungi in Alzheimer's Disease. *Sci Rep* **2015**, *5*, 15015, doi:10.1038/srep15015.

289. Ibarguren, M.; López, D.J.; Escribá, P. V. The Effect of Natural and Synthetic Fatty Acids on Membrane Structure, Microdomain Organization, Cellular Functions and Human Health. *Biochimica et Biophysica Acta (BBA) - Biomembranes* **2014**, *1838*, 1518–1528, doi:10.1016/j.bbamem.2013.12.021.

290. Calzada, E.; Onguka, O.; Claypool, S.M. Phosphatidylethanolamine Metabolism in Health and Disease. In; 2016; pp. 29–88.

291. Tayebati, S.K.; Amenta, F. Choline-Containing Phospholipids: Relevance to Brain Functional Pathways. *Clin Chem Lab Med* **2013**, *51*, doi:10.1515/cclm-2012-0559.

292. Westman, E.; Spenger, C.; Öberg, J.; Reyer, H.; Pahnke, J.; Wahlund, L.-O. In Vivo 1H-Magnetic Resonance Spectroscopy Can Detect Metabolic Changes in APP/PS1 Mice after Donepezil Treatment. *BMC Neurosci* **2009**, *10*, 33, doi:10.1186/1471-2202-10-33.

293. Greenberg, N.; Grassano, A.; Thambisetty, M.; Lovestone, S.; Legido-Quigley, C. A Proposed Metabolic Strategy for Monitoring Disease Progression in Alzheimer's Disease. *Electrophoresis* **2009**, *30*, 1235–1239, doi:10.1002/elps.200800589.

294. Ibáñez, C.; Simó, C.; Martín-Álvarez, P.J.; Kivipelto, M.; Winblad, B.; Cedazo-Mínguez, A.; Cifuentes, A. Toward a Predictive Model of Alzheimer's Disease Progression Using Capillary Electrophoresis–Mass Spectrometry Metabolomics. *Anal Chem* **2012**, *84*, 8532–8540, doi:10.1021/ac301243k.

295. Klein, J. Membrane Breakdown in Acute and Chronic Neurodegeneration: Focus on Choline-Containing Phospholipids. *J Neural Transm* **2000**, *107*, 1027–1063, doi:10.1007/s007020070051.

296. de Wilde, M.C.; Vellas, B.; Girault, E.; Yavuz, A.C.; Sijben, J.W. Lower Brain and Blood Nutrient Status in Alzheimer's Disease: Results from Meta-Analyses. *Alzheimer's & Dementia: Translational Research & Clinical Interventions* **2017**, *3*, 416–431, doi:10.1016/j.trci.2017.06.002.

297. Matsuzaki, T.; Sasaki, K.; Hata, J.; Hirakawa, Y.; Fujimi, K.; Ninomiya, T.; Suzuki, S.O.; Kanba, S.; Kiyohara, Y.; Iwaki, T. Association of Alzheimer Disease Pathology with Abnormal Lipid Metabolism: The Hisayama Study. *Neurology* **2011**, *77*, 1068–1075, doi:10.1212/WNL.0b013e31822e145d.

298. Drolle, E.; Negoda, A.; Hammond, K.; Pavlov, E.; Leonenko, Z. Changes in Lipid Membranes May Trigger Amyloid Toxicity in Alzheimer's Disease. *PLoS One* **2017**, *12*, e0182194, doi:10.1371/journal.pone.0182194.

299. Liu, Y.; Li, N.; Zhou, L.; Li, Q.; Li, W. Plasma Metabolic Profiling of Mild Cognitive Impairment and Alzheimer's Disease Using Liquid Chromatography/Mass Spectrometry. *Cent Nerv Syst Agents Med Chem* **2015**, *14*, 113–120, doi:10.2174/1871524915666141216161246.

300. Lin, C.; Huang, C.; Huang, K.; Lin, K.; Yen, T.; Kuo, H. A Metabolomic Approach to Identifying Biomarkers in Blood of Alzheimer's Disease. *Ann Clin Transl Neurol* **2019**, *6*, 537–545, doi:10.1002/acn3.726.

301. Orešič, M.; Hyötyläinen, T.; Herukka, S.-K.; Sysi-Aho, M.; Mattila, I.; Seppänan-Laakso, T.; Julkunen, V.; Gopalacharyulu, P. V; Hallikainen, M.; Koikkalainen, J.; et al. Metabolome in Progression to Alzheimer's Disease. *Transl Psychiatry* **2011**, *1*, e57–e57, doi:10.1038/tp.2011.55.

302. Oberacher, H.; Arnhard, K.; Linhart, C.; Diwo, A.; Marksteiner, J.; Humpel, C. Targeted Metabolomic Analysis of Soluble Lysates from Platelets of Patients with Mild Cognitive Impairment and Alzheimer's Disease Compared to Healthy Controls: Is PC AeC40:4 a Promising Diagnostic Tool? *Journal of Alzheimer's Disease* **2017**, *57*, 493–504, doi:10.3233/JAD-160172.

303. Dorninger, F.; Moser, A.B.; Kou, J.; Wiesinger, C.; Forss-Petter, S.; Gleiss, A.; Hinterberger, M.; Jungwirth, S.; Fischer, P.; Berger, J. Alterations in the Plasma Levels of Specific Choline Phospholipids in Alzheimer's Disease Mimic Accelerated Aging. *Journal of Alzheimer's Disease* **2018**, *62*, 841–854, doi:10.3233/JAD-171036.

304. Penke, B.; Paragi, G.; Gera, J.; Berkecz, R.; Kovács, Z.; Crul, T.; VÍgh, L. The Role of Lipids and Membranes in the Pathogenesis of Alzheimer's Disease: A Comprehensive View. *Curr Alzheimer Res* **2018**, *15*, 1191–1212, doi:10.2174/1567205015666180911151716.

305. Li, N.; Liu, Y.; Li, W.; Zhou, L.; Li, Q.; Wang, X.; He, P. A UPLC/MS-Based Metabolomics Investigation of the Protective Effect of Ginsenosides Rg1 and

Rg2 in Mice with Alzheimer's Disease. *J Ginseng Res* **2016**, *40*, 9–17, doi:10.1016/j.jgr.2015.04.006.

306. Yamazaki, Y.; Zhao, N.; Caulfield, T.R.; Liu, C.-C.; Bu, G. Apolipoprotein E and Alzheimer Disease: Pathobiology and Targeting Strategies. *Nat Rev Neurol* **2019**, *15*, 501–518, doi:10.1038/s41582-019-0228-7.

307. Fonteh, A.N.; Chiang, J.; Cipolla, M.; Hale, J.; Diallo, F.; Chirino, A.; Arakaki, X.; Harrington, M.G. Alterations in Cerebrospinal Fluid Glycerophospholipids and Phospholipase A2 Activity in Alzheimer's Disease. *J Lipid Res* **2013**, *54*, 2884–2897, doi:10.1194/jlr.M037622.

308. Sharman, M.J.; Shui, G.; Fernandis, A.Z.; Lim, W.L.F.; Berger, T.; Hone, E.; Taddei, K.; Martins, I.J.; Ghiso, J.; Buxbaum, J.D.; et al. Profiling Brain and Plasma Lipids in Human APOE E2, E3, and E4 Knock-in Mice Using Electrospray Ionization Mass Spectrometry. *Journal of Alzheimer's Disease* **2010**, *20*, 105–111, doi:10.3233/JAD-2010-1348.

309. Igbavboa, U.; Eckert, G.P.; Malo, T.M.; Studniski, A.E.; Johnson, L.N.A.; Yamamoto, N.; Kobayashi, M.; Fujita, S.C.; Appel, T.R.; Müller, W.E.; et al. Murine Synaptosomal Lipid Raft Protein and Lipid Composition Are Altered by Expression of Human ApoE 3 and 4 and by Increasing Age. *J Neurol Sci* **2005**, *229–230*, 225–232, doi:10.1016/j.jns.2004.11.037.

310. Pointer, C.B.; Klegeris, A. Cardiolipin in Central Nervous System Physiology and Pathology. *Cell Mol Neurobiol* **2017**, *37*, 1161–1172, doi:10.1007/s10571-016-0458-9.

311. Monteiro-Cardoso, V.F.; Oliveira, M.M.; Melo, T.; Domingues, M.R.M.; Moreira, P.I.; Ferreiro, E.; Peixoto, F.; Videira, R.A. Cardiolipin Profile Changes Are Associated to the Early Synaptic Mitochondrial Dysfunction in Alzheimer's Disease. *Journal of Alzheimer's Disease* **2014**, *43*, 1375–1392, doi:10.3233/JAD-141002.

312. Kühn, T.; Floegel, A.; Sookthai, D.; Johnson, T.; Rolle-Kampczyk, U.; Otto, W.; von Bergen, M.; Boeing, H.; Kaaks, R. Higher Plasma Levels of Lysophosphatidylcholine 18:0 Are Related to a Lower Risk of Common Cancers in a Prospective Metabolomics Study. *BMC Med* **2016**, *14*, 13, doi:10.1186/s12916-016-0552-3.

313. Whiley, L.; Sen, A.; Heaton, J.; Proitsi, P.; García-Gómez, D.; Leung, R.; Smith, N.; Thambisetty, M.; Kloszewska, I.; Mecocci, P.; et al. Evidence of Altered Phosphatidylcholine Metabolism in Alzheimer's Disease. *Neurobiol Aging* **2014**, *35*, 271–278, doi:10.1016/j.neurobiolaging.2013.08.001.

314. Mielke, M.M.; Haughey, N.J.; Han, D.; An, Y.; Bandaru, V.V.R.; Lyketsos, C.G.; Ferrucci, L.; Resnick, S.M. The Association Between Plasma Ceramides and Sphingomyelins and Risk of Alzheimer's Disease Differs by Sex and APOE in the Baltimore Longitudinal Study of Aging. *Journal of Alzheimer's Disease* **2017**, *60*, 819–828, doi:10.3233/JAD-160925.

315. Jazvinšćak Jembrek, M.; Hof, P.R.; Šimić, G. Ceramides in Alzheimer's Disease: Key Mediators of Neuronal Apoptosis Induced by Oxidative Stress and A β Accumulation. *Oxid Med Cell Longev* **2015**, *2015*, 1–17, doi:10.1155/2015/346783.

316. Panchal, M.; Gaudin, M.; Lazar, A.N.; Salvati, E.; Rivals, I.; Ayciriex, S.; Dauphinot, L.; Dargère, D.; Auzeil, N.; Masserini, M.; et al. Ceramides and Sphingomyelinases in Senile Plaques. *Neurobiol Dis* **2014**, *65*, 193–201, doi:10.1016/j.nbd.2014.01.010.

317. Loft, L.M.I.; Moseholm, K.F.; Pedersen, K.K.W.; Jensen, M.K.; Koch, M.; Cronjé, H.T. Sphingomyelins and Ceramides: Possible Biomarkers for Dementia? *Curr Opin Lipidol* **2022**, *33*, 57–67, doi:10.1097/MOL.0000000000000804.

318. Semba, R.D. Perspective: The Potential Role of Circulating Lysophosphatidylcholine in Neuroprotection against Alzheimer Disease. *Advances in Nutrition* **2020**, *11*, 760–772, doi:10.1093/advances/nmaa024.

319. Wood, P.L.; Medicherla, S.; Sheikh, N.; Terry, B.; Phillipps, A.; Kaye, J.A.; Quinn, J.F.; Woltjer, R.L. Targeted Lipidomics of Fontal Cortex and Plasma Diacylglycerols (DAG) in Mild Cognitive Impairment and Alzheimer's Disease: Validation of DAG Accumulation Early in the Pathophysiology of Alzheimer's Disease. *Journal of Alzheimer's Disease* **2015**, *48*, 537–546, doi:10.3233/JAD-150336.

320. Blusztajn, J.K.; Gonzalez-Coviella, I.L.; Logue, M.; Growdon, J.H.; Wurtman, R.J. Levels of Phospholipid Catabolic Intermediates, Glycerophosphocholine and Glycerophosphoethanolamine, Are Elevated in Brains of Alzheimer's Disease but Not of Down's Syndrome Patients. *Brain Res* **1990**, *536*, 240–244, doi:10.1016/0006-8993(90)90030-F.

321. Walter, A.; Korth, U.; Hilgert, M.; Hartmann, J.; Weichel, O.; Hilgert, M.; Fassbender, K.; Schmitt, A.; Klein, J. Glycerophosphocholine Is Elevated in Cerebrospinal Fluid of Alzheimer Patients. *Neurobiol Aging* **2004**, *25*, 1299–1303, doi:10.1016/j.neurobiolaging.2004.02.016.

322. Ellison, D.W.; Beal, M.F.; Martin, J.B. Phosphoethanolamine and Ethanolamine Are Decreased in Alzheimer's Disease and Huntington's Disease. *Brain Res* **1987**, *417*, 389–392, doi:10.1016/0006-8993(87)90471-9.

323. Farber, S.A.; Slack, B.E.; Blusztajn, J.K. Role of Single-stranded DNA Regions and Y-box Proteins in Transcriptional Regulation of Viral and Cellular Genes. *The FASEB Journal* **2000**, *14*, 2198–2206, doi:10.1096/fj.99-0853.

324. Xing, Y.; Tang, Y.; Zhao, L.; Wang, Q.; Qin, W.; Zhang, J.-L.; Jia, J. Plasma Ceramides and Neuropsychiatric Symptoms of Alzheimer's Disease. *Journal of Alzheimer's Disease* **2016**, *52*, 1029–1035, doi:10.3233/JAD-151158.

325. Mavraki, E.; Ioannidis, P.; Tripsianis, G.; Gioka, T.; Kolousi, M.; Vadikolias, K. Vitamin D in Mild Cognitive Impairment and Alzheimer's Disease. A Study in Older Greek Adults. *Hippokratia* **2020**, *24*, 120–126.

326. MURAKAMI, T.; KOHNO, K.; NINOMIYA, K.; MATSUDA, H.; YOSHIKAWA, M. Medicinal Foodstuffs. XXV. Hepatoprotective Principle and Structures of Ionone Glucoside, Phenethyl Glycoside, and Flavonol Oligoglycosides from Young Seedpods of Garden Peas, Pisum Sativum L. *Chem Pharm Bull (Tokyo)* **2001**, *49*, 1003–1008, doi:10.1248/cpb.49.1003.

327. Ademowo, O.S.; Dias, H.K.I.; Milic, I.; Devitt, A.; Moran, R.; Mulcahy, R.; Howard, A.N.; Nolan, J.M.; Griffiths, H.R. Phospholipid Oxidation and Carotenoid Supplementation in Alzheimer's Disease Patients. *Free Radic Biol Med* **2017**, *108*, 77–85, doi:10.1016/j.freeradbiomed.2017.03.008.

328. Qin, J.; Goswami, R.; Balabanov, R.; Dawson, G. Oxidized Phosphatidylcholine Is a Marker for Neuroinflammation in Multiple Sclerosis Brain. *J Neurosci Res* **2007**, *85*, 977–984, doi:10.1002/jnr.21206.

329. Wood, P.L.; Tippireddy, S.; Feriante, J.; Woltjer, R.L. Augmented Frontal Cortex Diacylglycerol Levels in Parkinson's Disease and Lewy Body Disease. *PLoS One* **2018**, *13*, e0191815, doi:10.1371/journal.pone.0191815.

330. Haukedal, H.; Freude, K.K. Implications of Glycosylation in Alzheimer's Disease. *Front Neurosci* **2021**, *14*, doi:10.3389/fnins.2020.625348.

331. Cunnane, S.C.; Schneider, J.A.; Tangney, C.; Tremblay-Mercier, J.; Fortier, M.; Bennett, D.A.; Morris, M.C. Plasma and Brain Fatty Acid Profiles in Mild Cognitive Impairment and Alzheimer's Disease. *Journal of Alzheimer's Disease* **2012**, *29*, 691–697, doi:10.3233/JAD-2012-110629.

332. Marizzoni, M.; Cattaneo, A.; Mirabelli, P.; Festari, C.; Lopizzo, N.; Nicolosi, V.; Mombelli, E.; Mazzelli, M.; Luongo, D.; Naviglio, D.; et al. Short-Chain Fatty Acids and Lipopolysaccharide as Mediators Between Gut Dysbiosis and Amyloid Pathology in Alzheimer's Disease. *Journal of Alzheimer's Disease* **2020**, *78*, 683–697, doi:10.3233/JAD-200306.

333. Fanaee-Danesh, E.; Gali, C.C.; Tadic, J.; Zandl-Lang, M.; Carmen Kober, A.; Agujetas, V.R.; de Dios, C.; Tam-Amersdorfer, C.; Stracke, A.; Albrecher, N.M.; et al. Astaxanthin Exerts Protective Effects Similar to Bexarotene in Alzheimer's Disease by Modulating Amyloid-Beta and Cholesterol Homeostasis in Blood-Brain Barrier Endothelial Cells. *Biochimica et Biophysica Acta (BBA) - Molecular Basis of Disease* **2019**, *1865*, 2224–2245, doi:10.1016/j.bbadis.2019.04.019.

334. Grimm, M.; Mett, J.; Hartmann, T. The Impact of Vitamin E and Other Fat-Soluble Vitamins on Alzheimer´s Disease. *Int J Mol Sci* **2016**, *17*, 1785, doi:10.3390/ijms17111785.

335. Su, H.; Rustam, Y.H.; Masters, C.L.; Makalic, E.; McLean, C.A.; Hill, A.F.; Barnham, K.J.; Reid, G.E.; Vella, L.J. Characterization of Brain-derived Extracellular Vesicle Lipids in Alzheimer's Disease. *J Extracell Vesicles* **2021**, *10*, doi:10.1002/jev2.12089.

336. Mulder, C.; Wahlund, L.-O.; Teerlink, T.; Blomberg, M.; Veerhuis, R.; van Kamp, G.J.; Scheltens, P.; Scheffer, P.G. Decreased Lysophosphatidylcholine/Phosphatidylcholine Ratio in Cerebrospinal Fluid in Alzheimer?S Disease. *J Neural Transm* **2003**, *110*, 949–955, doi:10.1007/s00702-003-0007-9.

337. Jack, C.R.; Bennett, D.A.; Blennow, K.; Carrillo, M.C.; Feldman, H.H.; Frisoni, G.B.; Hampel, H.; Jagust, W.J.; Johnson, K.A.; Knopman, D.S.; et al. A/T/N: An Unbiased Descriptive Classification Scheme for Alzheimer Disease Biomarkers. *Neurology* **2016**, *87*, 539–547, doi:10.1212/WNL.0000000000002923.

338. Klavins, K.; Koal, T.; Dallmann, G.; Marksteiner, J.; Kemmler, G.; Humpel, C. The Ratio of Phosphatidylcholines to Lysophosphatidylcholines in Plasma Differentiates Healthy Controls from Patients with Alzheimer's Disease and Mild Cognitive Impairment. *Alzheimer's & Dementia: Diagnosis, Assessment & Disease Monitoring* **2015**, *1*, 295–302, doi:10.1016/j.dadm.2015.05.003.

339. Song, J.; Kim, Y.-K. Identification of the Role of MiR-142-5p in Alzheimer's Disease by Comparative Bioinformatics and Cellular Analysis. *Front Mol Neurosci* **2017**, *10*, doi:10.3389/fnmol.2017.00227.

340. Sørensen, S.S.; Nygaard, A.-B.; Christensen, T. MiRNA Expression Profiles in Cerebrospinal Fluid and Blood of Patients with Alzheimer's Disease and Other Types of Dementia – an Exploratory Study. *Transl Neurodegener* **2016**, *5*, 6, doi:10.1186/s40035-016-0053-5.

341. Wu, L.; Zheng, K.; Yan, C.; Pan, X.; Liu, Y.; Liu, J.; Wang, F.; Guo, W.; He, X.; Li, J.; et al. Genome-Wide Study of Salivary MicroRNAs as Potential Noninvasive Biomarkers for Detection of Nasopharyngeal Carcinoma. *BMC Cancer* **2019**, *19*, 843, doi:10.1186/s12885-019-6037-y.

342. Zhu, B.; Gu, S.; Wu, X.; He, W.; Zhou, H. Bioinformatics Analysis of Tumor-Educated Platelet MicroRNAs in Patients with Hepatocellular Carcinoma. *Biosci Rep* **2021**, *41*, doi:10.1042/BSR20211420.

343. Kloten, V.; Neumann, M.H.D.; Di Pasquale, F.; Sprenger-Haussels, M.; Shaffer, J.M.; Schlumpberger, M.; Herdean, A.; Betsou, F.; Ammerlaan, W.; af Hällström, T.; et al. Multicenter Evaluation of Circulating Plasma MicroRNA Extraction Technologies for the Development of Clinically Feasible Reverse Transcription Quantitative PCR and Next-Generation Sequencing Analytical Work Flows. *Clin Chem* **2019**, *65*, 1132–1140, doi:10.1373/clinchem.2019.303271.

344. Liu, H.; Xu, W.; Feng, J.; Ma, H.; Zhang, J.; Xie, X.; Zhuang, D.; Shen, W.; Liu, H.; Zhou, W. Increased Expression of Plasma MiRNA-320a and Let-7b-5p in Heroin-Dependent Patients and Its Clinical Significance. *Front Psychiatry* **2021**, *12*, doi:10.3389/fpsyt.2021.679206.

345. Siedlecki-Wullich, D.; Català-Solsona, J.; Fábregas, C.; Hernández, I.; Clarimon, J.; Lleó, A.; Boada, M.; Saura, C.A.; Rodríguez-Álvarez, J.; Miñano-Molina, A.J. Altered MicroRNAs Related to Synaptic Function as Potential Plasma

Biomarkers for Alzheimer's Disease. *Alzheimers Res Ther* **2019**, *11*, 46, doi:10.1186/s13195-019-0501-4.

346. Li, X.; Wang, Z.; Tan, L.; Wang, Y.; Lu, C.; Chen, R.; Zhang, S.; Gao, Y.; Liu, Y.; Yin, Y.; et al. Correcting MiR92a-VGAT-Mediated GABAergic Dysfunctions Rescues Human Tau-Induced Anxiety in Mice. *Molecular Therapy* **2017**, *25*, 140–152, doi:10.1016/j.ymthe.2016.10.010.

347. Kumar, S.; Reddy, P.H. The Role of Synaptic MicroRNAs in Alzheimer's Disease. *Biochimica et Biophysica Acta (BBA) - Molecular Basis of Disease* **2020**, *1866*, 165937, doi:10.1016/j.bbadis.2020.165937.

348. Zhu, L.; Zhong, M.; Zhao, J.; Rhee, H.; Caesar, I.; Knight, E.M.; Volpicelli-Daley, L.; Bustos, V.; Netzer, W.; Liu, L.; et al. Reduction of Synaptojanin 1 Accelerates Aβ Clearance and Attenuates Cognitive Deterioration in an Alzheimer Mouse Model. *Journal of Biological Chemistry* **2013**, *288*, 32050–32063, doi:10.1074/jbc.M113.504365.

349. Ando, K.; Ndjim, M.; Turbant, S.; Fontaine, G.; Pregoni, G.; Dauphinot, L.; Yilmaz, Z.; Suain, V.; Mansour, S.; Authelet, M.; et al. The Lipid Phosphatase Synaptojanin 1 Undergoes a Significant Alteration in Expression and Solubility and Is Associated with Brain Lesions in Alzheimer's Disease. *Acta Neuropathol Commun* **2020**, *8*, 79, doi:10.1186/s40478-020-00954-1.

350. Maesako, M.; Zoltowska, K.M.; Berezovska, O. Synapsin 1 Promotes Aβ Generation via BACE1 Modulation. *PLoS One* **2019**, *14*, e0226368, doi:10.1371/journal.pone.0226368.

351. Chacón, P.J.; del Marco, Á.; Arévalo, Á.; Domínguez-Giménez, P.; García-Segura, L.M.; Rodríguez-Tébar, A. Cerebellin 4, a Synaptic Protein, Enhances Inhibitory Activity and Resistance of Neurons to Amyloid-β Toxicity. *Neurobiol Aging* **2015**, *36*, 1057–1071, doi:10.1016/j.neurobiolaging.2014.11.006.

352. Yao, M.; Nguyen, T.-V. V.; Pike, C.J. β-Amyloid-Induced Neuronal Apoptosis Involves c-Jun N-Terminal Kinase-Dependent Downregulation of Bcl-w. *The Journal of Neuroscience* **2005**, *25*, 1149–1158, doi:10.1523/JNEUROSCI.4736-04.2005.

353. Brettschneider, J.; Petzold, A.; Schöttle, D.; Claus, A.; Riepe, M.; Tumani, H. The Neurofilament Heavy Chain (NfH^{SMI35}) in the Cerebrospinal Fluid Diagnosis of Alzheimer's Disease. *Dement Geriatr Cogn Disord* **2006**, *21*, 291–295, doi:10.1159/000091436.

354. Ashton, N.J.; Hye, A.; Leckey, C.A.; Jones, A.R.; Gardner, A.; Elliott, C.; Wetherell, J.L.; Lenze, E.J.; Killick, R.; Marchant, N.L. Plasma REST: A Novel Candidate Biomarker of Alzheimer's Disease Is Modified by Psychological Intervention in an at-Risk Population. *Transl Psychiatry* **2017**, *7*, e1148–e1148, doi:10.1038/tp.2017.113.

355. Nagaraj, S.; Laskowska-Kaszub, K.; Dębski, K.J.; Wojsiat, J.; Dąbrowski, M.; Gabryelewicz, T.; Kuźnicki, J.; Wojda, U. Profile of 6 MicroRNA in Blood

Plasma Distinguish Early Stage Alzheimer's Disease Patients from Non-Demented Subjects. *Oncotarget* **2017**, *8*, 16122–16143, doi:10.18632/oncotarget.15109.

356. Shioya, M.; Obayashi, S.; Tabunoki, H.; Arima, K.; Saito, Y.; Ishida, T.; Satoh, J. Aberrant MicroRNA Expression in the Brains of Neurodegenerative Diseases: MiR-29a Decreased in Alzheimer Disease Brains Targets Neurone Navigator 3. *Neuropathol Appl Neurobiol* **2010**, *36*, 320–330, doi:10.1111/j.1365-2990.2010.01076.x.

357. Lei, X.; Lei, L.; Zhang, Z.; Zhang, Z.; Cheng, Y. Downregulated MiR-29c Correlates with Increased BACE1 Expression in Sporadic Alzheimer's Disease. *Int J Clin Exp Pathol* **2015**, *8*, 1565–1574.

358. YANG, G.; SONG, Y.; ZHOU, X.; DENG, Y.; LIU, T.; WENG, G.; YU, D.; PAN, S. MicroRNA-29c Targets β-Site Amyloid Precursor Protein-Cleaving Enzyme 1 and Has a Neuroprotective Role in Vitro and in Vivo. *Mol Med Rep* **2015**, *12*, 3081–3088, doi:10.3892/mmr.2015.3728.

359. Müller, M.; Jäkel, L.; Bruinsma, I.B.; Claassen, J.A.; Kuiperij, H.B.; Verbeek, M.M. MicroRNA-29a Is a Candidate Biomarker for Alzheimer's Disease in Cell-Free Cerebrospinal Fluid. *Mol Neurobiol* **2016**, *53*, 2894–2899, doi:10.1007/s12035-015-9156-8.

360. Hashimoto, T. CLAC: A Novel Alzheimer Amyloid Plaque Component Derived from a Transmembrane Precursor, CLAC-P/Collagen Type XXV. *EMBO J* **2002**, *21*, 1524–1534, doi:10.1093/emboj/21.7.1524.

361. Afagh, A.; Cummings, B.J.; Cribbs, D.H.; Cotman, C.W.; Tenner, A.J. Localization and Cell Association of C1q in Alzheimer's Disease Brain. *Exp Neurol* **1996**, *138*, 22–32, doi:10.1006/exnr.1996.0043.

362. Söderberg, L.; Kakuyama, H.; Möller, A.; Ito, A.; Winblad, B.; Tjernberg, L.O.; Näslund, J. Characterization of the Alzheimer's Disease-Associated CLAC Protein and Identification of an Amyloid β-Peptide-Binding Site. *Journal of Biological Chemistry* **2005**, *280*, 1007–1015, doi:10.1074/jbc.M403628200.

363. Bai, G.; Chivatakarn, O.; Bonanomi, D.; Lettieri, K.; Franco, L.; Xia, C.; Stein, E.; Ma, L.; Lewcock, J.W.; Pfaff, S.L. Presenilin-Dependent Receptor Processing Is Required for Axon Guidance. *Cell* **2011**, *144*, 106–118, doi:10.1016/j.cell.2010.11.053.

364. Wang, B.; Li, H.; Mutlu, S.A.; Bowser, D.A.; Moore, M.J.; Wang, M.C.; Zheng, H. The Amyloid Precursor Protein Is a Conserved Receptor for Slit to Mediate Axon Guidance. *eNeuro* **2017**, *4*, ENEURO.0185-17.2017, doi:10.1523/ENEURO.0185-17.2017.

365. Ding, X.; Jo, J.; Wang, C.-Y.; Cristobal, C.D.; Zuo, Z.; Ye, Q.; Wirianto, M.; Lindeke-Myers, A.; Choi, J.M.; Mohila, C.A.; et al. The Daam2–VHL–Nedd4 Axis Governs Developmental and Regenerative Oligodendrocyte Differentiation. *Genes Dev* **2020**, *34*, 1177–1189, doi:10.1101/gad.338046.120.

366. Sellers, K.J.; Elliott, C.; Jackson, J.; Ghosh, A.; Ribe, E.; Rojo, A.I.; Jarosz-Griffiths, H.H.; Watson, I.A.; Xia, W.; Semenov, M.; et al. Amyloid β Synaptotoxicity Is Wnt-PCP Dependent and Blocked by Fasudil. *Alzheimer's & Dementia* **2018**, *14*, 306–317, doi:10.1016/j.jalz.2017.09.008.

367. González, I.; Cao, K.-A.L.; Davis, M.J.; Déjean, S. Visualising Associations between Paired 'Omics' Data Sets. *BioData Min* **2012**, *5*, 19, doi:10.1186/1756-0381-5-19.

368. Murtagh, F.; Legendre, P. Ward's Hierarchical Agglomerative Clustering Method: Which Algorithms Implement Ward's Criterion? *J Classif* **2014**, *31*, 274–295, doi:10.1007/s00357-014-9161-z.

369. Zhang, L.; Wu, K.; Bo, T.; Zhou, L.; Gao, L.; Zhou, X.; Chen, W. Integrated MicroRNA and Proteome Analysis Reveal a Regulatory Module in Hepatic Lipid Metabolism Disorders in Mice with Subclinical Hypothyroidism. *Exp Ther Med* **2019**, doi:10.3892/etm.2019.8281.

370. Hussey, G.S.; Pineda Molina, C.; Cramer, M.C.; Tyurina, Y.Y.; Tyurin, V.A.; Lee, Y.C.; El-Mossier, S.O.; Murdock, M.H.; Timashev, P.S.; Kagan, V.E.; et al. Lipidomics and RNA Sequencing Reveal a Novel Subpopulation of Nanovesicle within Extracellular Matrix Biomaterials. *Sci Adv* **2020**, *6*, doi:10.1126/sciadv.aay4361.

371. Alcazar, O.; Hernandez, L.F.; Nakayasu, E.S.; Nicora, C.D.; Ansong, C.; Muehlbauer, M.J.; Bain, J.R.; Myer, C.J.; Bhattacharya, S.K.; Buchwald, P.; et al. Parallel Multi-Omics in High-Risk Subjects for the Identification of Integrated Biomarker Signatures of Type 1 Diabetes. *Biomolecules* **2021**, *11*, 383, doi:10.3390/biom11030383.

372. Nair, P.S.; Raijas, P.; Ahvenainen, M.; Philips, A.K.; Ukkola-Vuoti, L.; Järvelä, I. Music-Listening Regulates Human MicroRNA Expression. *Epigenetics* **2021**, *16*, 554–566, doi:10.1080/15592294.2020.1809853.

373. Hojati, Z.; Omidi, F.; Dehbashi, M.; Mohammad Soltani, B. The Highlighted Roles of Metabolic and Cellular Response to Stress Pathways Engaged in Circulating Hsa-MiR-494-3p and Hsa-MiR-661 in Alzheimer's Disease. *Iran Biomed J* **2021**, *25*, 62–67, doi:10.29252/ibj.25.1.62.

374. Lv, Z.; Hu, L.; Yang, Y.; Zhang, K.; Sun, Z.; Zhang, J.; Zhang, L.; Hao, Y. Comparative Study of MicroRNA Profiling in One Chinese Family with PSEN1 G378E Mutation. *Metab Brain Dis* **2018**, *33*, 1711–1720, doi:10.1007/s11011-018-0279-2.

375. Gu, H.; Li, L.; Cui, C.; Zhao, Z.; Song, G. Overexpression of Let-7a Increases Neurotoxicity in a PC12 Cell Model of Alzheimer's Disease via Regulating Autophagy. *Exp Ther Med* **2017**, *14*, 3688–3698, doi:10.3892/etm.2017.4977.

376. Rönnemaa, E.; Zethelius, B.; Vessby, B.; Lannfelt, L.; Byberg, L.; Kilander, L. Serum Fatty-Acid Composition and the Risk of Alzheimer's Disease: A

Longitudinal Population-Based Study. *Eur J Clin Nutr* **2012**, *66*, 885–890, doi:10.1038/ejcn.2012.63.

377. Conquer, J.A.; Tierney, M.C.; Zecevic, J.; Bettger, W.J.; Fisher, R.H. Fatty Acid Analysis of Blood Plasma of Patients with Alzheimer's Disease, Other Types of Dementia, and Cognitive Impairment. *Lipids* **2000**, *35*, 1305–1312, doi:10.1007/s11745-000-0646-3.

378. Goozee, K.; Chatterjee, P.; James, I.; Shen, K.; Sohrabi, H.R.; Asih, P.R.; Dave, P.; Ball, B.; ManYan, C.; Taddei, K.; et al. Alterations in Erythrocyte Fatty Acid Composition in Preclinical Alzheimer's Disease. *Sci Rep* **2017**, *7*, 676, doi:10.1038/s41598-017-00751-2.

379. Johnson, L.A.; Torres, E.R.S.; Impey, S.; Stevens, J.F.; Raber, J. Apolipoprotein E4 and Insulin Resistance Interact to Impair Cognition and Alter the Epigenome and Metabolome. *Sci Rep* **2017**, *7*, 43701, doi:10.1038/srep43701.

380. Goedeke, L.; Fernández-Hernando, C. MicroRNAs: A Connection between Cholesterol Metabolism and Neurodegeneration. *Neurobiol Dis* **2014**, *72*, 48–53, doi:10.1016/j.nbd.2014.05.034.

381. Jaouen, F.; Gascon, E. Understanding the Role of MiR-33 in Brain Lipid Metabolism: Implications for Alzheimer's Disease. *The Journal of Neuroscience* **2016**, *36*, 2558–2560, doi:10.1523/JNEUROSCI.4571-15.2016.

382. Kumar, S.; Vijayan, M.; Reddy, P.H. MicroRNA-455-3p as a Potential Peripheral Biomarker for Alzheimer's Disease. *Hum Mol Genet* **2017**, *26*, 3808–3822, doi:10.1093/hmg/ddx267.

383. Denk, J.; Oberhauser, F.; Kornhuber, J.; Wiltfang, J.; Fassbender, K.; Schroeter, M.L.; Volk, A.E.; Diehl-Schmid, J.; Prudlo, J.; Danek, A.; et al. Specific Serum and CSF MicroRNA Profiles Distinguish Sporadic Behavioural Variant of Frontotemporal Dementia Compared with Alzheimer Patients and Cognitively Healthy Controls. *PLoS One* **2018**, *13*, e0197329, doi:10.1371/journal.pone.0197329.

384. Zhang, X.; Liu, W.; Zan, J.; Wu, C.; Tan, W. Untargeted Lipidomics Reveals Progression of Early Alzheimer's Disease in APP/PS1 Transgenic Mice. *Sci Rep* **2020**, *10*, 14509, doi:10.1038/s41598-020-71510-z.

385. Barupal, D.K.; Baillie, R.; Fan, S.; Saykin, A.J.; Meikle, P.J.; Arnold, M.; Nho, K.; Fiehn, O.; Kaddurah-Daouk, R. Sets of Coregulated Serum Lipids Are Associated with Alzheimer's Disease Pathophysiology. *Alzheimer's & Dementia: Diagnosis, Assessment & Disease Monitoring* **2019**, *11*, 619–627, doi:10.1016/j.dadm.2019.07.002.

386. Ooi, K.-L.M.; Vacy, K.; Boon, W.C. Fatty Acids and beyond: Age and Alzheimer's Disease Related Changes in Lipids Reveal the Neuro-Nutraceutical Potential of Lipids in Cognition. *Neurochem Int* **2021**, *149*, 105143, doi:10.1016/j.neuint.2021.105143.

387. Braga, A.A.; Bortolin, R.H.; Graciano-Saldarriaga, M.E.; Hirata, T.D.; Cerda, A.; de Freitas, R.C.; Lin-Wang, H.T.; Borges, J.B.; França, J.I.; Masi, L.N.; et al. High Serum MiR-421 Is Associated with Metabolic Dysregulation and Inflammation in Patients with Metabolic Syndrome. *Epigenomics* **2021**, *13*, 423–436, doi:10.2217/epi-2020-0247.

388. He, P.-P.; Jiang, T.; OuYang, X.-P.; Liang, Y.-Q.; Zou, J.-Q.; Wang, Y.; Shen, Q.-Q.; Liao, L.; Zheng, X.-L. Lipoprotein Lipase: Biosynthesis, Regulatory Factors, and Its Role in Atherosclerosis and Other Diseases. *Clinica Chimica Acta* **2018**, *480*, 126–137, doi:10.1016/j.cca.2018.02.006.

ANNEXES

8.1 Information of the articles included in the compendium

8.1.1. Chapter 1

New screening approach for Alzheimer's disease risk assessment from urine lipid peroxidation compounds. Peña-Bautista C, Vigor C, Galano JM, Oger C, Durand T, Ferrer I, Cuevas A, López-Cuevas R, Baquero M, López-Nogueroles M, Vento M, Hervás-Marín D, García-Blanco A, Cháfer-Pericás C. **Scientific Reports**. 2019 Oct 2;9(1):14244. doi: 10.1038/s41598-019-50837-2.

8.1.2. Chapter 2

Plasma lipid peroxidation biomarkers for early and non-invasive Alzheimer Disease detection. Peña-Bautista C, Vigor C, Galano JM, Oger C, Durand T, Ferrer I, Cuevas A, López-Cuevas R, Baquero M, López-Nogueroles M, Vento M, Hervás D, García-Blanco A, Cháfer-Pericás C. **Free Radical Biology and Medicine**. 2018 Aug 20;124:388-394. doi: 10.1016/j.freeradbiomed.2018.06.038.

8.1.3. Chapter 3

Assessment of lipid peroxidation and artificial neural network models in early Alzheimer Disease diagnosis. Peña-Bautista C, Durand T, Oger C, Baquero M, Vento M, Cháfer-Pericás C. **Clinical Biochemistry**. 2019 Oct;72:64-70. doi: 10.1016/j.clinbiochem.2019.07.008.

8.1.4. Chapter 4

Isoprostanoids Levels in Cerebrospinal Fluid Do Not Reflect Alzheimer's Disease. Peña-Bautista C, Baquero M, López-Nogueroles M, Vento M, Hervás D, Cháfer-Pericás C. **Antioxidants (Basel)**. 2020 May 10;9(5):407. doi: 10.3390/antiox9050407.

8.1.5. Chapter 5

Clinical Utility of Plasma Lipid Peroxidation Biomarkers in Alzheimer's Disease Differential Diagnosis. Peña-Bautista C, Álvarez L, Durand T, Vigor C, Cuevas A, Baquero M, Vento M, Hervás D, Cháfer-Pericás C. **Antioxidants (Basel)**. 2020 Jul 22;9(8):649. doi: 10.3390/antiox9080649.

8.1.6. Chapter 6

Lipid Peroxidation Assessment in Preclinical Alzheimer Disease Diagnosis. Peña-Bautista C, Álvarez-Sánchez L, Ferrer I, López-Nogueroles M, Cañada-Martínez AJ, Oger C, Galano JM, Durand T, Baquero M, Cháfer-Pericás C. **Antioxidants (Basel)**. 2021 Jun 29;10(7):1043. doi: 10.3390/antiox10071043.

8.1.7. Chapter 7

Lipid peroxidation biomarkers correlation with medial temporal atrophy in early Alzheimer Disease. Peña-Bautista C, López-Cuevas R, Cuevas A, Baquero M, Cháfer-Pericás C. **Neurochemistry International**. 2019 Oct;129:104519. doi: 10.1016/j.neuint.2019.104519.

8.1.8. Chapter 8

Plasma metabolomics in early Alzheimer's disease patients diagnosed with amyloid biomarker. Peña-Bautista C, Roca M, Hervás D, Cuevas A, López-Cuevas R, Vento M, Baquero M, García-Blanco A, Cháfer-Pericás C. **Journal of Proteomics**. 2019 May 30;200:144-152. doi: 10.1016/j.jprot.2019.04.008.

8.1.9. Chapter 9

Metabolomics study to identify plasma biomarkers in alzheimer disease: ApoE genotype effect. Peña-Bautista C, Roca M, López-Cuevas R, Baquero M, Vento M, Cháfer-Pericás C. **Journal of Pharmaceutical and Biomedical Analysis**. 2020 Feb 20;180:113088. doi: 10.1016/j.jpba.2019.113088

8.1.10. Chapter 10

Plasma Lipidomics Approach in Early and Specific Alzheimer's Disease Diagnosis. Peña-Bautista C, Álvarez-Sánchez L, Roca M, García-Vallés L, Baquero M, Cháfer-Pericás C. **Journal of Clinical Medicine**. 2022 Aug 27;11(17):5030. doi: 10.3390/jcm11175030.

8.1.11. Chapter 11

Plasma microRNAs as potential biomarkers in early Alzheimer disease expression. Peña-Bautista C, Tarazona-Sánchez A, Braza-Boils A, Balaguer A, Ferré-González L, Cañada-Martínez AJ, Baquero M, Cháfer-Pericás C. **Scientific Reports**. 2022 Sep 16;12(1):15589. doi: 10.1038/s41598-022-19862-6

8.1.12. Chapter 12

Epigenomics and Lipidomics Integration in Alzheimer Disease: Pathways Involved in Early Stages. Peña-Bautista C, Álvarez-Sánchez L, Cañada-Martínez AJ, Baquero M, Cháfer-Pericás C. **Biomedicines**. 2021 Dec 2;9(12):1812. doi: 10.3390/biomedicines9121812.

www.nature.com/scientificreports

SCIENTIFIC REPORTS
nature research

OPEN

New screening approach for Alzheimer's disease risk assessment from urine lipid peroxidation compounds

Received: 26 August 2018
Accepted: 20 September 2019
Published online: 02 October 2019

Carmen Peña-Bautista[1], Claire Vigor[2], Jean-Marie Galano[2], Camille Oger[2], Thierry Durand[2], Inés Ferrer[3], Ana Cuevas[3], Rogelio López-Cuevas[3], Miguel Baquero[3], Marina López-Nogueroles[4], Máximo Vento[1], David Hervás-Marin[5], Ana García-Blanco[1] & Consuelo Cháfer-Pericás[1]

Alzheimer Disease (AD) standard biological diagnosis is based on expensive or invasive procedures. Recent research has focused on some molecular mechanisms involved since early AD stages, such as lipid peroxidation. Therefore, a non-invasive screening approach based on new lipid peroxidation compounds determination would be very useful. Well-defined early AD patients and healthy participants were recruited. Lipid peroxidation compounds were determined in urine using a validated analytical method based on liquid chromatography coupled to tandem mass spectrometry. Statistical studies consisted of the evaluation of two different linear (Elastic Net) and non-linear (Random Forest) regression models to discriminate between groups of participants. The regression models fitted to the data from some lipid peroxidation biomarkers (isoprostanes, neuroprostanes, prostaglandines, dihomo-isoprostanes) in urine as potential predictors of early AD. These prediction models achieved fair validated area under the receiver operating characteristics (AUC-ROCs > 0.68) and their results corroborated each other since they are based on different analytical principles. A satisfactory early screening approach, using two complementary regression models, has been obtained from urine levels of some lipid peroxidation compounds, indicating the individual probability of suffering from early AD.

Alzheimer's disease (AD) is the main cause of dementia worldwide[1], and a continuous incidence increase is expected in the next few years with the corresponding great social and economic impact[2]. Nowadays, the standard diagnosis consists of specific neuroimaging procedures and biomarkers in cerebrospinal fluid (CSF)[3,4], with the corresponding disadvantages of high cost and invasive sampling. In addition, available treatments have proven to be more effective in early stages[5,6]. Therefore, it would be very useful to develop an early and non-invasive screening model based on the individual risk to develop the AD.

In recent years, there is an increase body research about the involvement of oxidative stress since early AD stages[7–9]. Specifically, lipid peroxidation plays an important role in the development of AD due to the high lipid composition of the brain, as well as its high oxygen consumption[10]. In fact, Benseny-Cases *et al.* observed co-localization of oxidized lipids with senile plaques[11], but also higher levels of oxidized lipids were found in plasma from AD patients than healthy individuals[12]. Among the lipid peroxidation products, isoprostanes (IsoPs) are considered important potential biomarkers of brain damage in AD[13]. Actually, high levels of F_2-IsoPs were found in CSF[14,15], as well as in plasma and serum from early AD patients[16,17]. However, few studies have been carried out in urine samples[18–20] and most of them did not develop any statistical models for predicting AD.

The regression models constitute an important tool to predict the individual risk of suffering from AD. In this sense, few AD predictive models using sophisticated statistical tools can be found in literature, and they are based on CSF biomarkers or not validated analytical methods[21–23]. In addition, most of them required expensive

[1]Neonatal Research Unit, Health Research Institute La Fe, Valencia, Spain. [2]Institut des Biomolécules Max Mousseron, IBMM, University of Montpellier, CNRS ENSCM, Montpellier, France. [3]Neurology Unit, University and Polytechnic Hospital La Fe, Valencia, Spain. [4]Analytical Unit Platform, Health Research Institute La Fe, Valencia, Spain. [5]Biostatistical Unit, Health Research Institute La Fe, Valencia, Spain. Correspondence and requests for materials should be addressed to A.G.-B. (email: Ana.garcia-blanco@uv.es) or C.C.-P. (email: m.consuelo.chafer@uv.es)

neuroimaging measures[24]. In this study we have developed regression models from lipid peroxidation biomarkers in urine in order to obtain a non-invasive and early AD screening approach.

Materials and Methods

Study design and participants. Participants were from the Neurology Unit (University and Polytechnic Hospital La Fe, Valencia, Spain). Their ages were between 50 and 75 years, and they were classified into early AD (case group) (n = 70) and healthy (control group) (n = 29) according to neuropsychological tests, neuroimaging (nuclear magnetic resonance, computerized axial tomography), and CSF biomarkers (β-amyloid, total tau (t-Tau), phosphorylated tau (p-Tau)).

The study protocol was approved by the Ethics Committee (CEIC) from Health Research Institute La Fe (Valencia, Spain), the methods were carried out in accordance with the relevant guidelines and regulations, and informed consent from all participants was obtained.

Lipid peroxidation compounds. The isoprostanes' standards 5-F_{2t}-IsoP, 2,3-dinor-15-*epi*-15-F_{2t}-IsoP, 15(*R*)-15-F_{2t}-IsoP, 15-F_{2t}-IsoP, 15-E_{2t}-IsoP, 15-keto-15-E_{2t}-IsoP, 15-keto-15-F_{2t}-IsoP, prostaglandins PGE_2, $PGF_{2\alpha}$, and 1a,1b-dihomo-$PGF_{2\alpha}$ and deuterated internal standard (IS) $PGF_{2\alpha}$-d_4 were from Cayman Chemical Company (Ann Arbor, Michigan, USA). The standards of 10-*epi*-10-F_{4t}-NeuroP, d_4-10-*epi*-10-F_{4t}-NeuroP, 4(*RS*)-4-F_{4t}-NeuroP, 14(*RS*)-14-F_{4t}-NeuroP, 7(*RS*)-*ST*-Δ^8-11-dihomo-IsoF, 17(*RS*)-10-*epi*-SC-Δ^{15}-11-dihomo-IsoF, 17-*epi*-17-F_{2t}-dihomo-IsoP, 17-F_{2t}-dihomo-IsoP, and *ent*-7(*RS*)-7-F_{2t}-dihomo-IsoP, were synthesized at the Institute of Biomolecules Max Mousseron (IBMM) (Montpellier, France) by Professor Durand's team[25].

The calibration curves were prepared by serial dilutions in H_2O (pH 3):CH_3OH (85:15 v/v) with CH_3COOH 0.01%, in concentrations from 300 nmol L^{-1} to 0.004 nmol L^{-1} of each analyte.

Urine samples analysis. Urine samples (n = 99) were collected in a sterile bottle and immediately stored at −80 °C until analysis (~6 months). As stated in a previous study, no deterioration was observed for the lipid peroxidation compounds at long-term, since samples were not subjected to freeze-thaw cycles[26]. Then, they were treated following the optimum procedure established in a previous work[26]. Briefly, samples were thawed on ice and 5 µL of the internal standard solution (PI) ($PGF_{2\alpha}$-d_4 10 µmol L^{-1} and d_4-10-*epi*-10-F_{4t}-NeuroP 6 µmol L^{-1}) were added to 1 mL of sample. Then, enzymatic hydrolysis was performed by adding the enzyme β-glucuronidase and sodium acetate buffer (100 mmol L^{-1}, pH 4.9) and incubated for 2 hours at 37 °C. Then, the reaction was stopped and the enzyme was precipitated with cold methanol and chlorhydric acid (37%, v/v) and centrifuged for 10 min (14000 g, 4 °C). The supernatant pH was adjusted to 6–7 with sodium hydroxide (2.5 mol L^{-1}). Then, a cleaning and pre-concentration step was carried out by solid-phase extraction (SPE). For this, the cartridges were first conditioned with methanol and H_2O, then the samples were loaded into the SPE cartridge and the cartridge was washed with ammonium acetate (100 mmol L^{-1}, pH 7) and heptane. Elution was carried out with 2 × 500 µL of methanol (5% v/v CH_3COOH). After that, the samples were evaporated in the vacuum evaporator and reconstituted in 100 µL of H_2O (pH 3):CH_3OH (85:15 v/v) containing 0.01% (v/v) CH_3COOH. Finally, the samples were injected into a chromatographic system (UPLC-MS/MS).

The results were standardized by the creatinine levels measured using a colorimetric kit (MicroVue creatinine EIA) and a spectrophotometer.

Chromatographic system. The chromatographic system consisted of a UPLC system (Waters Acquity) coupled to a Xevo TQD system mass spectrometry system (Waters, United Kingdom). The conditions used were: ionization in negative mode (ESI-), capillary tension 2.0 kV, source temperature of 150 °C, desolvation temperature of 395 °C, gas flow of the nitrogen cone of 150 L h^{-1}, and desolvation flow of 800 L h^{-1}.

The LC conditions were selected to achieve appropriate chromatographic retention and resolution by using a C_{18} column (2.1 × 100 mm, 1.7 µm) (Acquity UPLC BEH, Waters). Mobile phases consisted of water (0.01% v/v CH_3COOH as mobile phase A) and acetonitrile (0.01% v/v acetic acid as mobile phase B). The temperatures of the column and the autosampler were set at 55 °C and 4 °C, respectively. The injection volume was set at 8 µL and the flow rate was set to 0.45 mL min^{-1}. A total 8.5 min elution gradient was performed. It consisted of 0.5 min with eluent composition at 80% A and 20% B, which was gradually changed to 55% A and 45% B at 6 min; then B was increased to 95% along 0.2 min, and kept constant for 0.8 min. Finally, the mobile phase composition returned to the initial conditions, and it was maintained for 1.3 min for system conditioning.

The detection was performed by multiple reaction monitoring (MRM) using the acquisition parameters obtained in a previous work[26].

Statistical analysis. Data were summarized using median and interquartile range (IQR) in the case of continuous variables, and with relative and absolute frequencies in the case of categorical variables (Table 1). Prior to modelling, variables were log-transformed to avoid potential strongly influential outliers due to the highly skewed nature of some variables (Fig. S1 in Supplementary Material). Then, a logistic regression model based on elastic-net-penalized was developed including gender and age as covariates. The penalization parameter lambda was selected by performing 500 replications of ten-fold cross validation. The minimum cross-validated error was selected on each replication and the median from the selected lambda values was considered the consensus lambda. Since the minimum lambda value was used, an alternative variable selection method was performed as a sensitivity analysis. This alternative analysis consisted on a random forest using the Altmann *et al.* method[27]. The final elastic net model was validated using bootstrap validation. For this, the procedure of Steyerberg *et al.* was followed[28]. Statistical analyses were performed using the softwares R (version 3.5.0), the BootValidation R (version 0.1.3), glmnet R (version 2.0–16), and ranger (version 0.9.0).

Variable	Case (n = 70)	Control (n = 29)
Age (years) (median (IQR))	70.5 (68, 74)	66 (62, 72)
Gender (female) (n (%))	28 (40%)	18 (62%)
Secondary Studies (n (%))	10 (14%)	10 (34%)
Alcohol consumption (yes) (n (%))	6 (8%)	6 (21%)
Smoking status (yes) (n (%))	8 (11%)	1 (3%)
Medications (yes) (n (%))	54 (77%)	18 (62%)
Comorbidity (yes) (n (%))	53 (76%)	18 (62%)
[a]RBANS.DM (median (IQR))	44 (40, 49)	100 (91, 106)
[b]CDR (median (IQR))	0.5 (0.5,1)	0 (0,0)
[c]FAQ (median (IQR))	7 (3, 13)	0 (0, 0)
[d]MMSE (median (IQR))	22 (18, 26)	30 (28, 30)
CSF Amyloid β (pg mL^{-1}) (median (IQR))	568 (441, 668)	1227 (1143, 1144)
CSF t-Tau (pg mL^{-1}) (median (IQR))	553 (377, 790)	208 (141, 333)
CSF p-Tau (pg mL^{-1}) (median (IQR))	88 (71, 116)	51 (38, 70)
Temporal atrophy (yes) (n (%))	51 (72%)	2 (7%)
Depression (yes) (n (%))	9 (13%)	3 (10%)

Table 1. Demographic and clinical variables of the study participants. IQR: Interquartilic range. [a]RBANS-DM, Repeatable Battery for the Assessment of Neuropsychological Status- Delayed Memory (Standard Score; cut-off point < 85). [b]CDR, Clinical Dementia Rating, values: 0, 0.5, 1, 2. [c]FAQ, Functional Activities Questionnaire (Direct Score; cut-off point >9). [d]MMSE, Minimental State Examination.

Biomarkers	Case (n = 70) Median (IQR) (ng mg^{-1} creatinine)	Control (n = 29) Median (IQR) (ng mg^{-1} creatinine)
15(*R*)-15-F_{2t}-IsoP	0.72 (0.5, 1.56)	0.7 (0.48, 0.94)
PGE_2	1.98 (0.62, 3.5)	1.69 (0.93, 4.26)
15-keto-15-E_{2t}-IsoP	0.93 (0.53, 1.47)	1.02 (0.65, 1.54)
15-keto-15-F_{2t}-IsoP	0.84 (0.22, 1.94)	1.33 (0.58, 2)
2,3-dinor-15-epi-15-F_{2t}-IsoP	0.78 (0.53, 1.22)	0.65 (0.47, 1.09)
15-E_{2t}-IsoP	0.23 (0.06, 1.31)	0.16 (0.07, 0.58)
5-F_{2t}-IsoP	2.67 (1.68, 5.07)	2.37 (1.76, 3.37)
15-F_{2c}-IsoP	0.01 (0, 0.02)	0.01 (0, 0.02)
$PGF_{2\alpha}$	3.72 (2.79, 7.32)	3.38 (2.35, 5.17)
4(*RS*)-4-F_4-NeuroP	0.89 (0.67, 1.36)	0.72 (0.5, 1.01)
1a,1b-dihomo-$PGF_{2\alpha}$	1.33 (0.64, 2.48)	1.67 (1.05, 2.23)
10-*epi*-10-F_4-NeuroP	0.03 (0, 0.06)	0.01 (0, 0.05)
14(*RS*)-14-F_4-NeuroP	1.21 (0.76, 2.16)	1.27 (0.74, 1.94)
ent-7(*RS*)-7-F_{3t}-dihomo-IsoP	0.33 (0.14, 0.63)	0.28 (0.19, 0.36)
17-F_{3t}-dihomo-IsoP	0.09 (0, 0.38)	0.11 (0, 0.26)
17-*epi*-17-F_{3t}-dihomo-IsoP	0.01 (0, 0.07)	0 (0, 0)
17(*RS*)-10-*epi*-SC-Δ^{13}-11-dihomo-IsoF	0.03 (0, 0.1)	0.05 (0.03, 0.08)
7(*RS*)-ST-Δ^8-11-dihomo-IsoF	0 (0, 0.02)	0 (0, 0.03)

Table 2. Concentrations of lipid peroxidation biomarkers in urine samples. IQR, inter-quartile range; IsoP, isoprostane; dihomo-IsoP, dihomo-isoprostane; dihomo-IsoF, dihomo-isofuran, NeuroP, neuroprostane;

Results

Participants' characteristics. Table 1 shows the demographic and clinical data for both groups. Small differences were shown for age and gender between groups, so these variables were considered covariates. Regarding the neuropsychological variables (Clinical Dementia Rating (CDR), Repeatable Battery for the Assessment of Neuropsychological Status (RBANS), Functional Activities Questionnaire (FAQ), Minimental State Examination (MMSE) and biological measures (CSF β-amyloid, CSF t-Tau, CSF p-Tau, temporal atrophy) used in the standard diagnosis, they showed significant differences between groups. However, the demographic variables (age, gender, studies, alcohol, smoking status, medication and comorbidity) did not show statistical differences between groups.

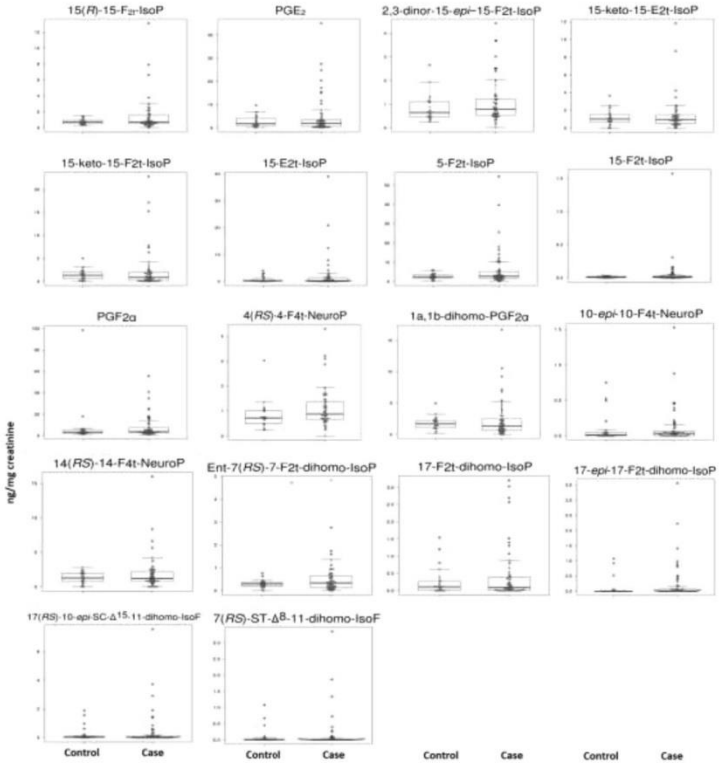

Figure 1. Box-Plot of the differences in different lipid peroxidation analytes levels between early AD (case) and healthy (control) groups.

Determination of urine lipid peroxidation biomarkers. Urine levels of lipid peroxidation compounds obtained for each group are shown in Table 2. Some of them (5-F_{2t}-IsoP, 2,3-dinor-15-epi-15-F_{2t}-IsoP, 15-E_{2t}-IsoP, PGE_2, $PGF_{2\alpha}$, 10-*epi*-10-F_{4t}-NeuroP, 4(*RS*)-4-F_{4t}-NeuroP, *ent*-7(*RS*)-7-F_{2t}-dihomo-IsoP) showed higher levels in early AD patients than in healthy controls, and some analytes (15-keto-15-E_{2t}-IsoP, 15-keto-15-F_{2t}-IsoP) showed lower values in the case group than in the control group. Figure 1 shows the box plots for each analyte.

Screening model from urine lipid peroxidation biomarkers. The elastic net model selected five variables corresponding to one isoprostane, one neuroprostane, one prostaglandin and two dihomo-isoprostanes shown in Table 3. The model also included gender and age, which were introduced as covariates. These predictor variables were combined as it is indicated in the formula below in order to estimate the individual probability (Pr) of suffering from AD.

$$\Pr(Y) = \frac{e^{-4.187+0.463*female+0.064*age-0.13*(A)+0.622*(B)-0.048*(C)+0.554*(D)+0.072*(E)}}{1+e^{-4.187+0.463*female+0.064*age-0.13*(A)+0.622*(B)-0.048*(C)+0.554*(D)+0.072*(E)}}$$

Variable	Coefficient (elastic net)	Importance (random forest)	p-value (random forest)
Gender (female)	0.463	0.17	0.08*
Age	0.064	1.09	0.012*
15-keto-15-F_{2t}-IsoP	−0.13	0.71	0.043*
4(*RS*)-F_{4t}-NeuroP	0.62	0.74	0.046*
1a,1b-dihomo-$PGF_{2\alpha}$	−0.048	0.73	0.035*
ent-7(*RS*)-7-F_{2t}-dihomo-IsoP	0.55	0.64	0.044*
17-*epi*-17-F_{2t}-dihomo-IsoP	0.072	0.58	0.029*
10-*epi*-10-F_{4t}-NeuroP	0	0.48	0.075
17-F_{2t}-dihomo-IsoP	0	0.35	0.133
17(*RS*)-10-*epi*-SC-Δ^{15}-11-dihomo-IsoF	0	0.21	0.219
15-E_{2t}-IsoP	0	0.17	0.293
5-F_{2t}-IsoP	0	0.14	0.325
2,3-dinor-15-*epi*-15-F_{2t}-IsoP	0	0.11	0.381
15(*R*)-15-F_{2t}-IsoP	0	0.10	0.379
PGE_2	0	0.08	0.405
15-keto-15-E_{2t}-IsoP	0	0.05	0.436
7(*RS*)-ST-Δ^4-11-dihomo-IsoF	0	−0.08	0.636
$PGF_{2\alpha}$	0	−0.09	0.603
14(*RS*)-14-F_{4t}-NeuroP	0	−0.25	0.755

Table 3. Results of the elastic net and random forest analyses. Coefficients of the elastic net model are interpreted as log-odds, so negative values indicate a negative association between higher concentration levels and risk of disease and positive values indicate a positive association between higher concentration levels and risk of disease. Importance values and p-values for random forest are derived from the gini index using Altman method.

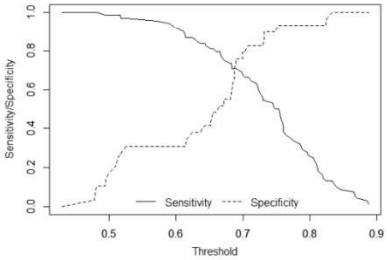

Figure 2. Sensitivity and specificity profile plot. The continuous line depicts the relationship between the probability threshold set in the model's prediction and its corresponding sensitivity and the dashed line represent the relationship between the probability threshold and the specificity.

A: 15-keto-15-F_{2t}-IsoP; B: 4(*RS*)-4-F_{4t}-NeuroP; C: 1a,1b-dihomo-$PGF_{2\alpha}$; D: *ent*-7(*RS*)-7-F_{2t}-dihomo-IsoP; E: 17-*epi*-17-F_{2t}-dihomo-IsoP

The alternative analysis using random forest selected the same five variables as the most important ones (Table 3), and they were also all considered statistically significant by the Altmann method[27]. Classification performance of the models was assessed using bootstrap in the case of elastic net and by the Out of Bag (OOB) estimate in the case of random forest. Bootstrap validated area under the receiver operating characteristics (AUC-ROC) for the elastic net model was 0.682 and OOB accuracy for the random forest model was 0.71, so their performance can be considered similar. Remarkably for the elastic net results, the sensitivity and specificity profile shows a sharp decrease of the sensitivity values as the specificity increases, forcing a decision between high sensitivity (0.97) at a cost of low specificity (0.31) or high specificity (0.93) at a cost of mediocre sensitivity (0.5) (Fig. 2).

Discussion

The reliable determination of lipid peroxidation products levels in urine samples from well-defined healthy and early AD participants, and the satisfactory classification performance of two complementary regression models allowed to develop an early and non-invasive screening model to identify individuals with high risk to develop the AD.

The role of lipid peroxidation in AD development has been largely studied[10], but few studies have been carried out determining isoprostanoids as target metabolites in AD[17,29]. In addition, the analytical methods used in most of these works were based on commercial kits or immunoassays what is associated to low specificity on isomers determinations[30]. Nevertheless, in the present study a previously validated analytical method based on mass spectrometry detection has been used, providing high selectivity and sensitivity, as well as high reliability to determine simultaneously several isoprostanoids isomers[26].

Regarding the development of early and non-invasive diagnosis, urine could be considered a promising matrix. However, few studies in literature have focused on this matrix[31,32]. Specifically, in the present work some compounds (PGE_2, 2,3-dinor-15-epi-15-F_{2t}-IsoP, 15-E_{2t}-IsoP, 5-F_{2t}-IsoP, $PGF_{2\alpha}$, 10-*epi*-10-F_{4t}-NeuroP, 4(*RS*)-4-F_{4t}-NeuroP and 17-*epi*-17-F_{3t}-dihomo-IsoP) showed higher concentrations in urine from AD patients than in healthy participants. Similarly, previous studies showed higher levels of some F_2-IsoPs in urine from patients with AD than in the control group[18–20]. However, further studies to clinically validate these potential biomarkers, using a larger number of samples from well-defined participants, and predictive models are required.

In this work, two alternative modeling methods with completely different characteristics were used. First, elastic net logistic regression is based on standard generalized linear regression models, thus assuming linearity of the relationship between predictors and the linear predictor, no interactions are assessed and the results are fully interpretable as in a standard logistic regression. On the other hand, random forest is a non-linear non-parametric model, that enable the assessment of higher order interactions between variables at a cost of lower statistical power compared to elastic net model when the relationship is linear[33,34]. Random forest does not provide an interpretable model, but provides a list of the most important variables in predicting the response. The fact that both methods obtained very similar results, provides robustness to our results.

In literature, few AD predictive models using these sophisticated statistical tools can be found[21–23,34], and most of them are based on neuroimaging measures[24]. However, none of them were based on non-invasive determination of lipid peroxidation biomarkers in early AD patients.

The diagnostic indexes obtained from both models indicated that the results could constitute a satisfactory screening approach from early AD stages with the consequent benefits for patients and health public system. In fact, the high sensitivity obtained would allow a reliable identification of high-risk patients in the early stages of AD, and they would be derived to a method with higher specificity to rule out false positives[17]. Nevertheless, further clinical validation using an external cohort of participants would be required in order to obtain a reliable diagnostic model.

Regarding the study limitations, the low number of controls compared to cases would be explained by the difficulty to obtain healthy participants with CSF biomarkers. Also, we did not include participants with other similar dementias, so differential AD diagnosis was not achieved. Further clinical validation work will be developed by including a higher number of controls, as well as patients with similar pathologies. In addition, a follow-up study will be carried out in order to evaluate the variation of these compounds levels along the time.

Conclusion

A set of new lipid peroxidation biomarkers has been determined in urine samples from well-defined participants (early AD, healthy) by means of a previously validated analytical method. So, reliable results have been obtained and used to develop a preliminary early and non-invasive screening model in order to identify potential individuals with high risk of suffering AD, although it could not be considered AD specific. For this, two different regression models (linear, elastic net; non-linear, random forest) were developed, obtaining similar performance in terms of variable selection and accuracy, in spite of being based on different analytical principles, and so providing robustness to the results.

Data Availability

The datasets generated during the current study are available from the corresponding author on reasonable request.

References

1. Prince, M., Albanese, E., Guerchet, M. & Prina, M. World Alzheimer Report 2014: Dementia and Risk Reduction an Analysis of Protective and Modifiable Factors (2014).
2. Wimo, A., Jönsson, L., Bond, J., Prince, M. & Winblad, B. Alzheimer Disease International. The worldwide economic impact of dementia 2010. *Alzheimers Dement.* **9**, 1–11 (2013).
3. Jack, C. R. *et al.* NIA-AA Research framework: Toward a biological definition of Alzheimer Disease. *Alzheimers Dement.* **14**, 535–562 (2018).
4. Albert, M. S. *et al.* The diagnosis of mild cognitive impairment due to Alzheimer's disease: recommendations from the National Institute on Aging-Alzheimer's Association workgroups on diagnostic guidelines for Alzheimer's disease. *Alzheimers Dement.* **7**, 270–279 (2011).
5. Briggs, R., Kennelly, S. P. & O'Neill, D. Drug treatments in Alzheimer's disease. *Clin. Med.* **16**, 247–253 (2016).
6. Bachurin, S. O., Gavrilova, S. I., Samsonova, A., Barreto, G. E. & Aliev, G. Corrigendum to "Mild cognitive impairment due to Alzheimer disease: Contemporary approaches to diagnostics and pharmacological intervention. *Pharmacol. Res.* **129**, 216–226 (2018).
7. Chen, Z. & Zhong, C. Oxidative stress in Alzheimer's disease. *Neurosci. Bull.* **30**, 271–281 (2014).
8. Sies, H. Oxidative stress: a concept in redox biology and medicine. *Redox Biol.* **4**, 180–183 (2015).
9. Moneim, A. E. Oxidant/Antioxidant imbalance and the risk of Alzheimer's disease. *Curr. Alzheimer Res.* **12**, 335–349 (2015).

10. Sultana, R., Perluigi, M. & Butterfield, A. D. Lipid peroxidation triggers neurodegeneration: a redox proteomics view into the Alzheimer disease brain. *Free Rad. Biol. Med.* **62**, 157–169 (2013).
11. Benseny-Cases, N., Klementieva, O., Cotte, M., Ferrer, I. & Cladera, J. Microspectroscopy (μFTIR) reveals co-localization of lipid oxidation and amyloid plaques in human Alzheimer disease brains. *Anal Chem.* **86**, 12047–12054 (2014).
12. Yoshida, Y. *et al.* Hydroxyoctadecadienoic acid and oxidatively modified peroxiredoxins in the blood of Alzheimer's disease patients and their potential as biomarkers. *Neurobiol.* **30**, 174–185 (2009).
13. Sultana, R., Perluigi, M. & Butterfield, D. A. Protein oxidation and lipid peroxidation in brain of subjects with Alzheimer's disease: insights into mechanism of neurodegeneration from redox proteomics. *Antioxid. Redox Signal.* **8**, 2021–2037 (2006).
14. Czerska, M., Zieliński, M. & Gromadzińska, J. Isoprostanes - A novel major group of oxidative stress markers. *Int. J. Occup. Med. Environ. Health.* **29**, 179–190 (2016).
15. Montine, T. J. *et al.* Increased cerebrospinal fluid F2-isoprostanes are associated with aging and latent Alzheimer's disease as identified by biomarkers. *Neuromolecular Med.* **13**, 37–43 (2011).
16. Sirin, F. B. *et al.* Plasma 8-isoPGF2α and serum melatonin levels in patients with minimal cognitive impairment and Alzheimer disease. *Turk. J. Med. Sci.* **45**, 1073–1077 (2015).
17. Peña-Bautista, C. *et al.* Plasma lipid peroxidation biomarkers for early and non-invasive Alzheimer Disease detection. *Free Rad. Biol. Med.* **124**, 388–394 (2018).
18. Tuppo, E. E. *et al.* Sign of lipid peroxidation as measured in the urine of patients with probable Alzheimer's disease. *Brain Res. Bull.* **54**, 565–568 (2001).
19. Kim, K. M., Jung, B. H., Paeng, K. J., Kim, I. & Chung, B. C. Increased urinary F(2)-isoprostanes levels in the patients with Alzheimer's disease. *Brain Res. Bull.* **64**, 47–51 (2004).
20. Praticò, D. *et al.* Increase in brain oxidative stress in mild cognitive impairment: a possible predictor of Alzheimer's disease. *Arch. Neurol.* **59**, 972–976 (2002).
21. Teipel, S. J. *et al.* Robust Detection of Impaired Resting State Functional Connectivity Networks in Alzheimer's Disease Using Elastic Net Regularized Regression. *Front. Aging Neurosci.* **8**, 318 (2017).
22. Lehallier, B. *et al.* Alzheimer's Disease Neuroimaging Initiative. Combined Plasma and Cerebrospinal Fluid Signature for the Prediction of Midterm Progression From Mild Cognitive Impairment to Alzheimer Disease. *JAMA Neurol.* **73**, 203–212 (2016).
23. Ramirez, J. *et al.* Alzheimer's Disease Neuroimaging Initiative. Ensemble of random forests One vs. Rest classifiers for MCI and AD prediction using ANOVA cortical and subcortical feature selection and partial least squares. *J. Neurosci. Methods.* **302**, 47–57 (2018).
24. Dimitriadis, S. I., Liparas, D. & Tsolaki, M. N. Alzheimer's Disease Neuroimaging Initiative. Random forest feature selection, fusion and ensemble strategy: Combining multiple morphological MRI measures to discriminate among healhy elderly, MCI, cMCI and alzheimer's disease patients: From the alzheimer's disease neuroimaging initiative (ADNI) database. *J. Neurosci. Methods.* **302**, 14–23 (2018).
25. de la Torre, A. *et al.* Total syntheses and *in vivo* quantitation of novel neurofuran and dihomo-isofuran derived from docosahexaenoic acid and adrenic acid. *Chemistry.* **21**, 2442–2446 (2015).
26. García-Blanco, A. *et al.* Reliable determination of new lipid peroxidation compounds as potential early Alzheimer Disease biomarkers. *Talanta.* **184**, 193–201 (2018).
27. Altmann, A., Toloşi, L., Sander, O. & Lengauer, T. Permutation importance: a corrected feature importance measure. *Bioinformatics.* **26**, 1340–1347 (2010).
28. Steyerberg, E. W., Eijkemans, M. J., Harrell, F. E. Jr. & Habbema, J. D. Prognostic modelling with logistic regression analysis: a comparison of selection and estimation methods in small data sets. *Stat. Med.* **19**, 1059–1079 (2000).
29. Bradley-Whitman, M. A. & Lovell, M. A. Biomarkers of lipid peroxidation in Alzheimer disease (AD): an update. *Arch. Toxicol.* **89**, 1035–1044 (2015).
30. Puertas, M. C. *et al.* Plasma oxidative stress parameters in men and women with early stage Alzheimer type dementia. *Exp. Gerontol.* **47**, 625–330 (2012).
31. García-Blanco, A. *et al.* Potential oxidative stress biomarkers of mild cognitive impairment due to Alzheimer disease. *J. Neurol. Sci.* **373**, 295–302 (2017).
32. Hartmann, S. & Ledur Kist, T. B. A review of biomarkers of Alzheimer's disease in noninvasive samples. *Biomark Med.* **12**, 677–690 (2018).
33. Sarica, A., Cerasa, A. & Quattrone, A. Random Forest Algorithm for the Classification of Neuroimaging Data in Alzheimer's Disease: A Systematic Review. *Front. Aging Neurosci.* **9**, 329 (2017).
34. Varma, V. R. *et al.* Brain and blood metabolite signatures of pathology and progression in Alzheimer disease: A targeted metabolomics study. *Plos One* **15**, e1002482 (2018).

Acknowledgements

CC-P acknowledges a "Miguel Servet I" Grant (CP16/00082) from the Instituto Carlos III (ISCIII, Spanish Ministry of Economy and Competitiveness). CP-B acknowledges a pre-doctoral Grant (associated to "Miguel Servet" project CP16/00082) from the Instituto Carlos III (Spanish Ministry of Economy, Industry and Competitiveness). AG-B acknowledges a Juan Rodés Grant (JR17/00003) from the ISCIII (Spanish Ministry of Economy, Industry and Competitiveness). This work was supported by the Instituto de Salud Carlos III (Miguel Servet I Project (CP16/00082) (Spanish Ministry of Economy and Competitiveness).

Author Contributions

C.C.-P. designed the study and wrote the main manuscript text. C.P.-B. and M.L.-N. carried out the experimental determinations. C.O., C.V., J.M.G. and T.D. synthesized the analytical standards. I.F. and A.G.-B. carried out the neuropsychological evaluations. D.H.-M. prepared the figures. M.B., R.L.-C., A.C. and M.V. reviewed the clinical aspects. All authors reviewed the manuscript.

Additional Information

Supplementary information accompanies this paper at https://doi.org/10.1038/s41598-019-50837-2.

Competing Interests: The authors declare no competing interests.

Publisher's note Springer Nature remains neutral with regard to jurisdictional claims in published maps and institutional affiliations.

Free Radical Biology and Medicine 124 (2018) 388–394

Contents lists available at ScienceDirect

Free Radical Biology and Medicine

journal homepage: www.elsevier.com/locate/freeradbiomed

Original article

Plasma lipid peroxidation biomarkers for early and non-invasive Alzheimer Disease detection

Carmen Peña-Bautista[a], Claire Vigor[b], Jean-Marie Galano[b], Camille Oger[b], Thierry Durand[b], Inés Ferrer[c], Ana Cuevas[c], Rogelio López-Cuevas[c], Miguel Baquero[c], Marina López-Nogueroles[d], Máximo Vento[a], David Hervás[e], Ana García-Blanco[a,*], Consuelo Cháfer-Pericás[a,*]

[a] Neonatal Research Unit, Health Research Institute La Fe, Valencia, Spain
[b] Institut des Biomolécules Max Mousseron, IBMM, University of Montpellier, CNRS ENSCM, Montpellier, France
[c] Neurology Unit, University and Polytechnic Hospital La Fe, Valencia, Spain
[d] Analytical Unit Platform, Health Research Institute La Fe, Valencia, Spain
[e] Biostatistical Unit, Health Research Institute La Fe, Valencia, Spain

ARTICLE INFO

Keywords:
Alzheimer disease
Mild-cognitive impairment
Plasma
Biomarker
Lipid peroxidation
Mass spectrometry
Diagnostic model

ABSTRACT

Introduction: Alzheimer Disease (AD) standard diagnosis is based on evaluations and biomarkers that are non-specific, expensive, or requires invasive sampling. Therefore, an early, and non-invasive diagnosis is required. As regards molecular mechanisms, recent research has shown that lipid peroxidation plays an important role.
Methods: Well-defined participants groups were recruited. Lipid peroxidation compounds were determined in plasma using a validated analytical method. Statistical studies consisted of an elastic-net-penalized logistic regression adjustment.
Results: The regression model fitted to the data included six variables (lipid peroxidation biomarkers) as potential predictors of early AD. This model achieved an apparent area under the receiver operating characteristics (AUC-ROCs) of 0.883 and a bootstrap-validated AUC-ROC of 0.817. Calibration of the model showed very low deviations from real probabilities.
Conclusion: A satisfactory early diagnostic model has been obtained from plasma levels of 6 lipid peroxidation compounds, indicating the individual probability of suffering from early AD.

1. Introduction

Alzheimer disease (AD), is a complex and clinically heterogeneous pathologic entity [1–3]. Structural and functional changes are already present in the early symptomatic phase of the disease, commonly known as Mild Cognitive Impairment (MCI), and even in preclinical phases. Diagnosis of AD is based on neurocognitive performance examination, mainly leading to clinical staging, and complementary explorations, as neuroimaging techniques, and cerebrospinal fluid (CSF) specific analysis. Neuroimaging features cannot be specific in nature, like brain atrophy or brain hypometabolism, when accessible. Specific hallmarks of disease can only be demonstrated by CSF analysis or amyloid positron emission tomography (PET). The determination of the 42-amino-acid variant of amyloid β (β-amyloid 1–42), total tau (t-tau), and phosphorylated-tau-181 (p-tau) proteins in CSF samples allows reliable, sensitive, and specific diagnosis of AD. However, CSF samples are obtained by lumbar puncture, an invasive procedure with several contraindications and secondary effects which is commonly not accepted by patients [4,5]. Besides, amyloid PET testing is a very expensive imaging procedure not suitable in most environments. Early diagnosis is a growing demand on common practice in order to achieve better management both in terms of treatment and prognosis. Therefore, an early, cost-effective and non-invasive diagnosis is required [6]. For these reasons, it would be advisable to determine specific and reliable AD biomarkers in common biological samples that allowed early AD diagnostic.

Regarding molecular mechanisms, oxidative stress (OS) plays an important role in neurodegenerative diseases [7,8]. In fact, OS is an important contributor to inflammation, neurotoxicity, and cell death in AD [9–11], and some oxidation products have been studied as possible early disease indicators [12]. In this sense, redox proteomics studies showed differences between AD and healthy groups for some metabolites like α-enolase and aldolase [13]. Also, Puertas et al. [14] found a decrease function in the antioxidant system, and higher levels of

* Corresponding authors.
E-mail addresses: ana.garcia-blanco@uv.es (A. García-Blanco), m.consuelo.chafer@uv.es (C. Cháfer-Pericás).

https://doi.org/10.1016/j.freeradbiomed.2018.06.038
Received 20 April 2018; Received in revised form 28 June 2018; Accepted 29 June 2018
Available online 30 June 2018

thiobarbituric acid reactive substances and carbonyl proteins in AD patients than in the control group. Similarly, Sliwinska et al. found an increased level of 8-oxoguanine in serum from AD patients [15]. Of note, lipid peroxidation shows a close relationship to AD since the brain is a susceptible organ due to its high lipid composition and high oxygen consumption [16].

According to lipid peroxidation studies, a relationship with AD was observed for compounds such as lipofuscin-like pigments and isoprostanes (IsoPs, products from araquidonic acid oxidation) [17,18]. Actually, significant correlation between F_2-IsoPs (13,14-dihydro-15-keto-$PGF_{2\alpha}$, 15-F_{2t}-IsoP) and β-amyloid was observed in CSF samples from MCI patients [19–21]. Nevertheless, taking into account the higher permeability of the blood-brain barrier since early AD stages [22], some lipid peroxidation compounds (15-F_{2t}-IsoP, 5-F_{2t}-IsoP, dinor TXB_2) have been determined in plasma and urine samples showing increased levels in AD and MCI patients versus healthy group [23–25]. Nevertheless, other studies did not find differences in the plasma and urine F_2-IsoPs levels between healthy, MCI and AD patients [26], as well between AD, Parkinson Disease (PD) and control group [27], or lower urinary levels were found in MCI group [28]. Therefore, more studies using well-defined groups (age, gender, comorbidity…), validated analytical methods and higher number of participants are required to draw conclusions.

The aim of this study is to evaluate the diagnostic performance of lipid peroxidation compounds as early AD biomarkers in plasma samples from a well-defined patient's group. To our knowledge this is the first potential diagnostic model obtained from the reliable determination of lipid peroxidation biomarkers employing a validated analytical method.

2. Materials and methods

2.1. Study design and participants

A prospective observational study was carried in the Neurology Unit of the University and Polytechnic Hospital La Fe, Valencia (Spain). The eligible participants were people between 50 and 80 years old who suffered from MCI due to AD (case group), and healthy individuals (control group). Patients were recruited from the out-patient Neurology Unit and healthy individuals from a community advertisement. For the case group, criteria eligibility included positive cognitive impairment, without impaired daily living activities, and with positive biomarkers (neuroimaging, CFS amyloid, CSF tau); and for the control group, people with absence of cognitive disturbances (negative cognitive impairment, and negative impaired functionality). The exclusion criteria included other known neurological impairments (stroke, brain tumour, severe head trauma, epilepsy, brain injury, multiple sclerosis…) or major psychiatric disorders (major depressive disorder, bipolar disorder, schizophrenia…), as well as patients with moderate to severe dementia, major sensory impairment or an invalidating previous pathology.

Current criteria employed to diagnose AD are based on recent revisions of the National Institute on Aging-Alzheimer's Association (NIA-AA) [29,30]. According to this, the standard clinical assessment used in this study is shown in Electronic Supplementary Material Table S1, and it was based on neuropsychological testing, structural neuroimaging by nuclear magnetic resonance (NMR) or computerized axial tomography (CAT), and CSF biomarkers. Neuropsychological testing included questionnaires addressing cognitive assessment (Repeatable Battery for Assessment of Neuropsychological Status, RBANS-MR) [31], daily function (Functionality Assessment Questionnaire, FAQ) [32] and global state (Clinical Dementia Rating, CDR) [33]. Neuroimaging, based on a 3-tesla NMR in the Radiology Service, addresses exclusion of structural causes of dementia such as tumours, vascular lesions and others, and they allow the detection of whole brain and hippocampal atrophy; medial temporal atrophy is a useful marker of progression to dementia of Alzheimer type among patients with MCI [34]. Biochemical determinations of CSF biomarkers (amyloid β, t-tau, p-tau) indicate the abnormal amyloid and tau proteins processing [35,36]. From 1–10 mL of CSF were collected under standardized procedure of lumbar puncture at 8 a.m. after overnight fasting. Amyloid β, t-tau and p-tau were measured by Innotest Elisa kit (Fujirebio Diagnostics, Ghent, Belgium) using a fully automated system (Lumipulse G, Fujirebio).

The Ethics Committee (CEIC) at the Health Research Institute La Fe (Valencia) approved the study protocol and informed consent was obtained from all the participants. They were recruited between January 2017 and July 2017, and classified into control (n = 26) and case (n = 68) groups. The characteristics of participants in this study are summarized in Table 1.

Table 1
Demographic and clinical characteristics, and biomarkers levels of the participants.

Variable		Case (n = 68)	Control (n = 26)
Age (years) (median (IQR))		71 (68, 74)	66 (62.25, 71.5)
Gender (female) (n (%))		39 (57.35%)	9 (34.62%)
Studies levels (n (%))	Primary	31 (45%)	14 (53%)
	Secondary	15 (22%)	5 (20%)
	Academic	22 (33%)	7 (27%)
Alcohol consumption (yes, n (%))		9 (13%)	6 (23%)
Smoking status (n (%))	Yes	10 (15%)	2 (8%)
	Former smoker (more than 10 years)	11 (16%)	8 (31%)
Medications (n (%))		54 (79%)	18 (69%)
Comorbidity (n (%))	None	15 (22%)	8 (31%)
	Dyslipemia	17 (25%)	6 (23%)
	Heart disease	1 (1%)	0 (0%)
	Arterial hypertension	8 (12%)	6 (23%)
	Two or more	23 (34%)	3 (11,5%)
	Others	4 (6%)	3 (11,5%)
Triglycerides (median (IQR))		90 (75.5, 120)	94.5 (83.75, 113.75)
Cholesterol (median (IQR))		195.5 (171.25, 220)	202.5 (193, 237)
CRP (median (IQR))		0 (0, 1.3)	0 (0, 0)
[a]RBANS.DM (median (IQR))		44 (40, 49)	100 (91.25, 105.25)
[b]CDR (median (IQR))		0.5 (0.5,1)	0 (0,0)
[c]FAQ (median (IQR))		8 (3, 13)	0 (0, 0)
CSF Amyloid β ($pg\,mL^{-1}$) (median (IQR))		565 (444.5, 673)	1197 (1150, 1423.5)
CSF total Tau ($pg\,mL^{-1}$) (median (IQR))		543 (386.5, 788.5)	208 (142, 326)
CSF phosphorylated Tau ($pg\,mL^{-1}$) (median (IQR))		87 (71.5, 108)	52 (41, 68.5)
Temporal atrophy (n (%))		51 (79.69%)	2 (8%)
Depression (n (%))		18 (28.57%)	4 (15.38%)

IQR: inter-quartile range.
CRP: C-reactive protein.
CSF: cerebrospinal fluid.
[a] RBANS-DM, Repeatable Battery for the Assessment of Neuropsychological Status- Delayed Memory (Standard Score; cut-off point < 85).
[b] CDR, Clinical Dementia Rating, values: 0, 0.5, 1, 2.
[c] FAQ, Functional Activities Questionnaire (Direct Score; cut-off point > 9).

2.2. Materials

As regards the lipid peroxidation products, standards of IsoPs and prostaglandins used for calibration include 15(*R*)− 15-F_{2t}-IsoP, 2,3-dinor-15-*epi*-15-F_{2t}-IsoP, 5-F_{2t}-IsoP, 15-keto-15-E_{2t}-IsoP, 15-keto-15-F_{2t}-IsoP, 15-E_{2t}-IsoP, 15-F_{2t}-IsoP, 1a,1b-dihomo-$PGF_{2\alpha}$, PGE_2, and $PGF_{2\alpha}$, as well as the deuterated internal standard (IS) $PGF_{2\alpha}$-D_4 and they were purchased from Cayman Chemical Company (Ann Arbor, Michigan, USA). The other standards corresponding to neuroprostanes (NeuroPs), dihomo-isoprostanes (dihomo-IsoPs) and dihomo-isofurans

(dihomo-IsoFs) (7(*RS*)-ST-Δ^8–11-dihomo-IsoF, 10-*epi*-10-F_{4t}-NeuroP, D_4–10-*epi*-10-F_{4t}-NeuroP, 4(*RS*)-F_{4t}-NeuroP, 17-*epi*-17-F_{2t}-dihomo-IsoP, 17-F_{2t}-dihomo-IsoP, 17(*RS*) − 10-*epi*-SC-Δ^{15}-11-dihomo-IsoF, *ent*-7(*RS*) − 7-F_{2t}-dihomo-IsoP, 14(*RS*) − 14-F_{4t}-NeuroP) were synthesized by Durand's team at the Institute des Biomolécules Max Mousseron (IBMM) (Montpellier, France) [37–41].

The centrifuge (multiSPIN) used was from Cleaver Scientific Ltd. (Warwickshire, United Kingdom) and the vortex mixer was from Velp Scientifica (Usmate, Italy). The speed vacuum concentrator (mi Vac) was from Genevac LTD (Ipswich, United Kingdom). The thermomixer HLC was from Ditabis (Pforzheim, Germany). The Strata X-AW (100 mg, 3 mL) solid phase extraction cartridges used for sample solid-phase extraction (SPE) and the SPE 12-position vacuum manifold were from Phenomenex (Madrid, Spain).

2.3. Sample collection and treatment

Plasma samples were collected from peripheral blood employing cryo-tubes with ethylenediaminetetraacetic acid. Then they were centrifuged for 10 min at 2000*g* and room temperature. Plasma was separated in a tube containing butylated hydroxytoluene (BHT) (0.25% (w/v) in ethanol) to avoid further oxidation of the sample. Afterward, samples were frozen at − 80 °C until analysis.

The sample treatment consisted of the addition of 5 μL of an internal standard solution ($PGF_{2\alpha}$-D_4 2 μmol L^{-1} and D_4–10-*epi*-10-F_{4t}-NeroP 1.2 μmol L^{-1}) and 400 μL of a potassium hydroxide solution (15% w/v) to 400 μL of plasma to carry out the hydrolysis (40 °C, 30 min). After that, the samples were placed on ice, diluted with 1 mL of H_2O (0.01% v/v acetic acid), acidified with hydrochloric acid (37%) and centrifuged for 10 min (5000*g*, 4 °C). Then, the supernatant final pH was adjusted to 7 by adding NaOH 2.5 mol L^{-1}. For clean-up and pre-concentration, a solid-phase extraction (SPE) procedure using Strata X-AW cartridges was carried out [28]. Briefly, SPE cartridges were conditioned (1 mL methanol, 1 mL H_2O), then the sample was loaded and it was washed (1 mL ammonium acetate buffer (0.1 mol L^{-1}, pH 7) and 1 mL heptane). Elution was carried out with 2 × 500 μL CH_3OH (5% (v/v) acetic acid). After that, eluted samples were evaporated in a speed vacuum concentrator and reconstituted in 100 μL of H_2O (0.01% acetic acid (v/v)):CH_3OH (85:15 v/v). Finally, they were injected in the chromatographic system.

2.4. Analytical method

The analytical method consisted of liquid chromatography coupled to tandem mass spectrometry (UPLC-MS/MS). The chromatographic system used was a Waters Acquity UPLC-Xevo TQD system (Milford, MA, USA). The optimum mass spectrometry (MS/MS) conditions were: negative electrospray ionization (ESI), capillary voltage 2.0 kV, source temperature 150 °C, desolvation temperature 395 °C, nitrogen cone and desolvation gas flows were 150 and 800 L h^{-1}, respectively, and dwell time was 10 ms. The MS/MS acquisition parameters are summarized in Electronic Supplementary Material Table S2. An Acquity UPLC BEH C_{18} column (2.1 × 100 mm, 1.7 μm) from Waters was used, and mobile phase consisted of water with 0.01% v/v acetic acid (A) and acetonitrile with 0.01% v/v acetic acid (B). The flow rate was 0.45 mL min^{-1}, the column temperature was 55 °C and the injection volume was 8 μL. A total 8.5 min elution gradient was performed as follows: during the first 0.5 min eluent composition was set at 80% A and 20% B, which was linearly changed to 55% A and 45% B from 0.5 to 6 min; then the proportion of B was increased to 95% in the next 0.2 min and kept constant for 0.8 min until minute 7. Finally, the initial conditions were recovered and maintained for 1.3 min for column conditioning.

2.5. Statistical analysis

As descriptive analysis, correlations among the different variables (18 lipid peroxidation compounds in plasma and 3 biomarkers in CSF) were assessed by constructing a correlation network based on the spearman correlation matrix of the variables. Correlations with an absolute value under 0.3 were excluded from the network to avoid spurious effects.

Prior to modelling, variables with near zero variance were excluded (1a,1b-dihomo-$PGF_{2\alpha}$ and 2,3-dinor-15-*epi*-15-F_{2t}-IsoP). With the remaining variables, an elastic-net-penalized logistic regression model was adjusted. Elastic net is able to perform variable selection at the same time of model fitting and produces parsimonious predictive models. This property improves generalization of the model to new data by avoiding overfitting. It is an adequate variable selection technique compared to other commonly used methods such as stepwise algorithms or univariate screening, which suffer from many consistency problems [42]. Age and gender were included in the models as covariates. Selection of the penalization parameter lambda, which controls the complexity of the model by decreasing the number of variables included in the model as it grows larger, was performed by estimating the bias-variance error curve of the population using 500 replications of ten-fold cross validation. The lambda value at one standard error from the minimum cross-validated error was selected on each replication and the median from the selected lambda values was chosen as the consensus lambda. The fitted elastic net model performance measured as optimism corrected AUC was validated using bootstrap, following the procedure of Smith et al. [43]. Statistical analyses were performed using R (version 3.4.3) and the BootValidation R (version 0.1.3) and glmnet (version 2.0–13) R packages.

3. Results

3.1. Patients' characteristics

Demographic, clinical and CSF biomarker data for both groups are summarized in Table 1. Age and gender showed small differences between groups, so they were included in the predictive model as covariates. As expected, RBANS, CDR, FAQ, β-amyloid, t-tau and p-tau were clearly different between both groups. C-reactive protein (CRP) was also different, with the AD patients displaying higher values. Depression was similar between both groups.

3.2. Analytical method validation

The analytical method showed an adequate linearity for all the analytes within the corresponding concentration ranges and coefficients of determination (R^2) ranged between 0.990 and 0.999. It also provided suitable precision, with intra-day and inter-day coefficients of variation of 2–11% (n = 3) and 5–13% (n = 6), respectively (at medium concentration level within the linearity interval). The limits of detection (signal to noise ratio of 3) obtained for each analyte ranged between 0.02 and 2 nmol L^{-1}, and the limits of quantification (signal to noise ratio of 10) were between 0.07 and 8 nmol L^{-1}.

The accuracy of the method was evaluated by analyzing standard solutions and spiked plasma samples containing the analytes at different concentration levels. In all the cases, the proposed method provided values close to the real concentrations, and matrix effect was considered negligible (see Table S3 in Electronic Supplementary Material), with the exemption of 15-keto-15-E_{2t}-IsoP, for which only a semi-quantitative determination was achieved.

3.3. Determination of plasma lipid peroxidation biomarkers and correlation analysis

Plasma levels of lipid peroxidation compounds are shown in Electronic Supplementary Material Table S4. Some of them (15(*R*) − 15-F_{2t}-IsoP, 15-keto-15-E_{2t}-IsoP, 15-keto-15-F_{2t}-IsoP, 15-E_{2t}-IsoP, 4(*RS*)-F_{4t}-NeuroP and *ent*-7(*RS*) − 7-F_{2t}-dihomo-IsoP) showed

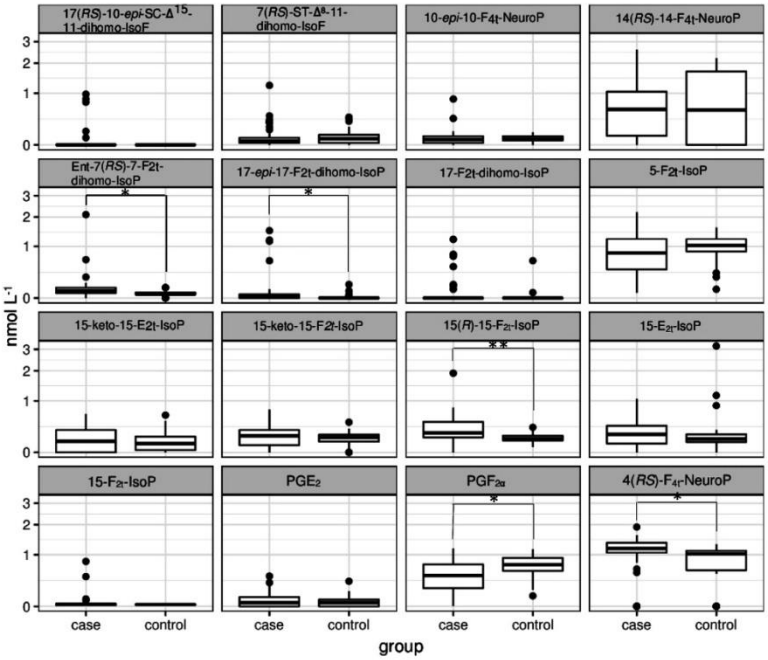

Fig. 1. Box plot graphs representing the concentration in plasma samples for each analyte in case and control groups. Boxes represent the 1st and 3rd quartiles, the black lines the median, and whiskers encompass from 1st quartile − 1.5 times the interquartile range to 3rd quartile + 1.5 times the interquartile range (* $p < 0.01$, ** $p < 0.001$).

higher levels in AD patients than in healthy controls. Fig. 1 shows the same results by means of box plots for each analyte, and some analytes showed lower values in the case group than in the control group ($PGF_{2\alpha}$, 5-F_{2t}-IsoP, 7(*RS*)-ST-Δ^8–11-dihomo-IsoF).

Correlation analysis among the plasma lipid peroxidation biomarkers and the CSF biomarkers (β-amyloid, t-tau and p-tau) was carried out by constructing a correlation network (Fig. 2). Red lines represent positive correlations while blue lines show negative correlations. Besides, the width of the line corresponds to the strength of the correlation. The figure shows an evident association between the CSF biomarkers (tau, p-tau, β-amyloid) and some plasma analytes, such as 15(*R*)-15-F_{2t}-IsoP formed from the arachidonic acid peroxidation, and *ent*-7(*RS*)-7-F_{2t}-dihomo-IsoP formed from the adrenic acid peroxidation. As observed in Fig. 1, these two plasma analytes showed higher levels in AD patients than in healthy participants, corroborating their high association with standard AD biomarkers. Other interesting associations were the correlation between *ent*-7(*RS*)-7-F_{2t}-dihomo-IsoP and PGE_2 which belongs to the prostaglandins family and may play an important role in the inflammatory response associated to AD; the correlation between the prostaglandin $PGF_{2\alpha}$, the isoprostane isomer 15-F_{2t}-IsoP that is studied in depth in a variety of biological systems, and 10-*epi*-10-F_{4t}-NeuroP formed from the docosahexanoic acid peroxidation; as well as the correlation between 15-E_{2t}-IsoP and 15-keto-15-F_{2t}-IsoP (Fig. 2). Also, some negative correlations were found between the prostaglandin $PGF_{2\alpha}$ and both 17-*epi*-17-F_{2t}-dihomo-IsoP and 4(*RS*)-F_{4t}-NeuroP. However, 14(*RS*)-14-F_{4t}-NeuroP does not show any correlation with the other compounds.

3.4. Diagnostic model from plasma lipid peroxidation biomarkers

The elastic-net logistic regression model fitted to the data selected six variables as potential predictors of AD. The model was also forced to include age and gender as covariates. These predictors were combined using the following formula in order to calculate the individual probability of suffering from AD (Pr):

$$\Pr(AD) = \frac{e^{LP}}{1+e^{LP}}$$

where LP = − 3.55 + 2.23 * 15(*R*)-15-F_{2t}-IsoP − 0.239 * 15-E_{2t}-IsoP − 1.424 * $PGF_{2\alpha}$ + 0.5098 * 4(*RS*)-F_{4t}-NeuroP − 0.08 * 14(*RS*)-14-F_{4t}-NeuroP + 0.154 * *Ent*-7(*RS*)-7-F_{2t}-dihomo-IsoP + 0.596 * gender + 0.059 * age

This model achieved an apparent area under the receiver operating characteristics (AUC-ROC) of 0.883 (95% Confidence Interval,

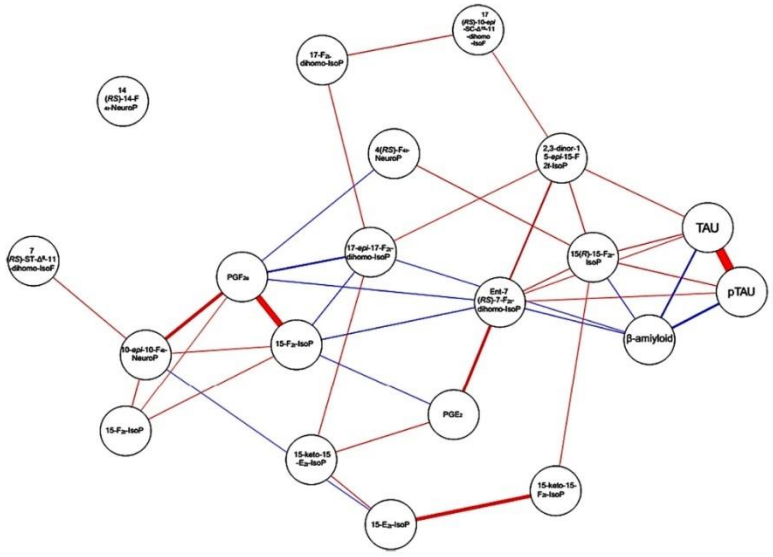

Fig. 2. Correlation network for all the lipid peroxidation products in plasma and CSF biomarkers (β-amyloid, t-tau and p-tau). The width of the line corresponds to the strength of the correlation, red lines represent positive correlations and blue lines represent negative correlations.

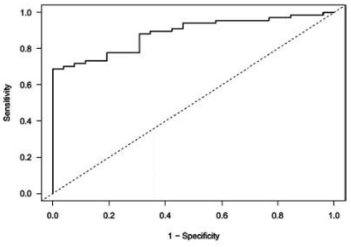

Fig. 3. Receiver operating characteristic curve for the diagnostic model. The AUC is 0.883 with a $p < 0.001$.

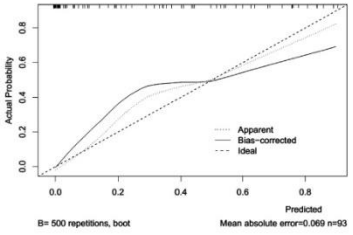

Fig. 4. Calibration plot of the model. The dotted line represents an empirical estimation of the in-sample observed probability versus the model-predicted probability. The continuous line represents the bias-corrected estimation of the observed probability versus the predicted probability. The dashed line represents the ideal 1:1 relationship between observed and predicted probabilities.

0.817–0.95, p-value < 0.001) (Fig. 3) and a bootstrap-validated AUC-ROC of 0.817. Calibration of the model was also assessed, obtaining very low deviations when comparing the fitted versus the real probabilities, except around the 30–40% mark, where the deviations toped at -10% (Fig. 4).

4. Discussion

In this study, we have used a validated analytical method to determine levels of 18 isoprostanoids in plasma from well-defined participants groups (early AD patients and healthy participants). Nowadays, the standard diagnosis criteria employed to classify the participants are based on the review from the NIA-AA [29,30]. However, since it shows some disadvantages, an early and reliable potential diagnosis method has been studied in this work.

The results obtained from the determination of 18 lipid peroxidation biomarkers in plasma samples indicate that higher concentrations of some compounds (15(*R*)-15-F_{2t}-IsoP, 15-keto-15-E_{2t}-IsoP, 15-keto-15-F_{2t}-IsoP, 15-E_{2t}-IsoP, 4(*RS*)-F_{4t}-NeuroP, *ent*-7(*RS*)-7-F_{2t}-dihomo-

IsoP) were found in early AD patients than in healthy participants. This finding corroborates the results obtained by Şirin et al. in which plasma levels of 15-F_{2t}-IsoP were higher in AD than in healthy individuals [23].

As regards the descriptive correlation analysis among plasma and CSF biomarkers, we considered that a correlation with an absolute value ≥ 0.3 may be relevant in the lipid peroxidation associated to early AD. Although it is not possible to explain the implications of all these correlations, some of these metabolites levels were altered in MCI-AD. Of note, 15(*R*)-15-F_{2t}-IsoP and *ent*-7(*RS*)-7-F_{2t}-dihomo-IsoP in plasma showed positive correlation with tau and p-tau in CSF, and negative correlation with β-amyloid in CSF. In this sense, a potential relationship between lipid peroxidation and the protein biology in brain was observed, confirming previous studies [18]. Actually, in a previous study it was found that the insert of β-amyloid aggregates into the lipid bilayer in cellular membrane, may lead to the formation of lipid peroxidation compounds [16]. On the other hand, some compounds in plasma were highly correlated, such as, $PGF_{2\alpha}$ and 15-F_{2t}-isoP, as well as $PGF_{2\alpha}$ and 10-*epi*-10-F_{4t}-NeuroP, and finally PGE_2 and *ent*-7(*RS*)-7-F_{2t}-dihomo-IsoP, indicating the presence of both enzymatic and non-enzymatic lipid oxidation since early AD, as well as inflammatory response also observed in previous studies [20,44]. Moreover, an important inverse relationship was observed between $PGF_{2\alpha}$ and 17-*epi*-17-F_{2t}-dihomoIsoP.

From these preliminary results, we elaborated a regression model showing good diagnostic accuracy from the biomarkers 15(*R*)-15-F_{2t}-IsoP, 15-E_{2t}-IsoP, $PGF_{2\alpha}$, 4(*RS*)-F_{4t}-NeuroP, 14(*RS*)-14-F_{4t}-NeuroP and *ent*-7(*RS*)-7-F_{2t}-dihomo-IsoP. Although these biomarkers are not able to discriminate between both groups when considered alone, they improve their discriminative ability when they are included in the diagnostic model with age and gender as covariates. Developing reliable diagnostic models in small data sets is difficult because the issue of overfitting is especially prominent in these cases. Common methods employed in medical literature include univariate screening, stepwise variable selection and, most recently, shrinkage or regularization methods such as lasso or elastic net. Of these, only regularization methods are able to produce stable estimates of the predictors and achieve good generalization of its predictive capacity [45]. In this study we used an elastic net penalized logistic regression model for AD diagnosis. Elastic net is a generalization of lasso and improves its prediction accuracy as it allows to deal with multicollinearity (high correlations between the different covariates) which was a property of our dataset. Our model achieved a promising validated AUC of 0.82 and has the advantage of providing an equation that can be used to obtain individualized estimates for each patient. The possibility to estimate the probability of AD opens the door to personalized decision making in the handling of potential AD patients. This would leave the use of CSF biomarkers, the gold standard for diagnosis, only for cases considered as high risk by our model.

Although the diagnostic accuracy of this model was not superior to the employment of CSF biomarkers this model has the advantage of being based on non-invasive sampling.

In literature, we can find some AD diagnosis models developed using different biomarkers. For instance, Nazeri et al. showed that different plasma proteins (interleukin-16, thyroxine-binding globulin, peptide tyrosine tyrosine, apolipoprotein E, eselectin, matrix metallopeptidase (10)) could be used to achieve the diagnosis and follow-up of the AD quite accurately against neuroimaging techniques, but these proteins are required to be clinically validated as possible AD indicators [46]. In addition, Marmarelis et al. proposed a diagnostic model based on cerebral hemodynamics through measures of pressure-changes and cerebral CO_2 vasomotor reactivity, but the specificity of this diagnosis has not been assessed and the number of participants is low [47]. Another model was based on the determination of CSF biomarkers by means of capillary electrophoresis coupled to mass spectrometry [48]. Also, a diagnostic model based on image techniques was described by Liao et al. in which age could explain some metabolic alterations, but the imaging techniques involve high economic costs [49].

To conclude, a satisfactory AD diagnostic model has been obtained from plasma lipid peroxidation biomarkers, indicating the individual probability of suffering from AD. To our knowledge, this is the first study evaluating the AD diagnostic accuracy of lipid peroxidation compounds in plasma from well-defined participants groups and using a validated analytical method. This is an important contribution in the study of an early and non-invasive AD diagnosis. In addition, the results from this work are relevant in the evaluation of OS as a molecular mechanism between amyloid deposition and neurodegeneration in AD. Prospective clinical validation of this potential diagnostic model will be carried out using an external group of patients.

Acknowledgement

We are greatly indebted to all participants, nursing, psychology and medical staff who voluntarily participated in the present study. Without their collaboration and enthusiasm this study could not have been completed.

CC-P acknowledges a "Miguel Servet I" Grant (CP16/00082) from the ISCIII (Spanish Ministry of Economy and Competitiveness). CP-B acknowledges a post-doctoral Grant (associated to "Miguel Servet" project CP16/00082) from the Instituto Carlos III (Spanish Ministry of Economy, Industry and Competitiveness).

Conflicts of interest

None of the authors of this manuscript declares having conflicts of interest.

Funding

This work was supported by the Instituto de Salud Carlos III (Miguel Servet I Project (CP16/00082)) (Spanish Ministry of Economy and Competitiveness).

Appendix A. Supporting information

Supplementary data associated with this article can be found in the online version at http://dx.doi.org/10.1016/j.freeradbiomed.2018.06.038.

References

[1] C.P. Ferri, M. Prince, C. Brayne, H. Brodaty, L. Fratiglioni, M. Ganguli, K. Hall, K. Hasegawa, H. Hendrie, Y. Huang, A. Jorm, C. Mathers, P.R. Menezes, E. Rimmer, M. Scazufca, Alzheimer's Disease International. Global prevalence of dementia: a Delphi consensus study, Lancet 366 (2005) 2112–2117.
[2] A. Wimo, L. JönssoN, J. Bond, M. Prince, B. Winblad, Alzheimer Disease International, The worldwide economic impact of dementia 2010, Alzheimers Dement. 9 (2013) 1–11.
[3] O. Serý, J. Povová, I. Míšek, L. Pešák, V. Janout, Molecular mechanisms of neuropathological changes in Alzheimer's disease: a review, Folia Neuropathol. 51 (2013) 1–9.
[4] G.M. McKhann, D.S. Knopman, H. Chertkow, B.T. Hyman, C.R. Jack, C.H. Kawas, W.E. Klunk, W.J. Koroshetz, J.J. Manly, R. Mayeux, R.C. Mohs, J.C. Morris, M.N. Rossor, P. Scheltens, M.C. Carrillo, B. Thies, S. Weintraub, The diagnosis of dementia due to Alzheimer's disease: recommendations from the National Institute on Aging-Alzheimer's Association workgroups on diagnostic guidelines for Alzheimer's disease, Alzheimers Dement. 7 (2011) 263–269.
[5] B. Dubois, H.H. Feldman, C. Jacova, S.T. DeKosky, P. Barberger-Gateau, J. Cummings, A. Delacourte, D. Galasko, S. Gauthier, G. Jicha, K. Meguro, K. O'Brien, F. Pasquier, P. Robert, M. Rossor, S. Salloway, Y. Stern, P.J. Visser, P. Scheltens, Research criteria for the diagnosis of Alzheimer's disease: revising the NINCDS-ADRDA criteria, Lancet Neurol. 6 (2007) 734–746.
[6] S.O. Bachurin, S.I. Gavrilova, A. Samsonova, G.E. Barreto, G. Aliev, Mild cognitive impairment due to Alzheimer disease: contemporary approaches to diagnostics and pharmacological intervention, Pharmacol. Res. 129 (2018) 216–226.
[7] A. Tramutola, C. Lanzillotta, M. Perluigi, D.A. Butterfield, Oxidative stress, protein modification and Alzheimer disease, Brain Res. Bull. 133 (2017) 88–96.
[8] M. Ramamoorthy, P. Sykora, M. Scheibye-Knudsen, C. Dunn, C. Kasmer, Y. Zhang, K.G. Becker, D.L. Croteau, V.A. Bohr, Sporadic Alzheimer disease fibroblasts display

an oxidative stress phenotype, Free Radic. Biol. Med. 53 (2012) 1371–1380.
[9] A. Gella, N. Durany, Oxidative stress in Alzheimer disease, Cell Adhes. Migr. 3 (2009) 88–93.
[10] F. Di Domenico, G. Pupo, E. Giraldo, M.C. Badia, P. Monllor, A. Lloret, M.E. Schininà, A. Giorgi, C. Cini, A. Tramutola, D.A. Butterfield, J. Viña, M. Perluigi, Oxidative signature of cerebrospinal fluid from mild cognitive impairment and Alzheimer disease patients, Free Radic. Biol. Med. 91 (2016) 1–9.
[11] P.I. Moreira, A. Nunomura, M. Nakamura, A. Takeda, J.C. Shenk, G. Aliev, M.A. Smith, G. Perry, Nucleic acid oxidation in Alzheimer disease, Free Radic. Biol. Med. 44 (2008) 1493–1505.
[12] M. Padurariu, A. Ciobica, R. Lefter, I.L. Serban, C. Stefanescu, R. Chirita, The oxidative stress hypothesis in Alzheimer's disease, Psychiatr. Danub. 25 (2013) 401–409.
[13] M. Perluigi, R. Sultana, G. Cenini, F. Di Domenico, M. Memo, W.M. Pierce, R. Coccia, D.A. Butterfield, Redox proteomics identification of 4-hydroxynonenal-modified brain proteins in Alzheimer's disease: role of lipid peroxidation in Alzheimer's disease pathogenesis, Proteom. Clin. Appl. 3 (2009) 682–693.
[14] M.C. Puertas, J.M. Martínez-Martos, M.P. Cobo, M.P. Carrera, M.D. Mayas, M.J. Ramírez-Expósito, Plasma oxidative stress parameters in men and women with early stage Alzheimer type dementia, Exp. Gerontol. 47 (2012) 625–630.
[15] A. Sliwinska, D. Kwiatkowski, P. Czarny, M. Toma, P. Wigner, J. Drzewoski, K. Fabianowska-Majewska, J. Szemraj, M. Maes, P. Galecki, T. Sliwinski, The levels of 7,8-dihydrodeoxyguanosine (8-oxoG) and 8-oxoguanine DNA glycosylase 1 (OGG1) - A potential diagnostic biomarkers of Alzheimer's disease, J. Neurol. Sci. 368 (2016) 155–159.
[16] R. Sultana, M. Perluigi, D.A. Butterfield, Lipid peroxidation triggers neurodegeneration: a redox proteomics view into the Alzheimer disease brain, Free Radic. Biol. Med. 62 (2013) 157–169.
[17] Z. Chmatalova, M. Vyhnalek, J. Laczo, J. Hort, R. Pospisilova, M. Pechova, A. Skoumalova, Relation of plasma selenium and lipid peroxidation end products in patients with Alzheimer's disease, Physiol. Res. 66 (2017) 1049–1056.
[18] D. Praticò, The neurobiology of isoprostanes and Alzheimer's disease, Biochim. Biophys. Acta 2010 (1801) 930–933.
[19] H.C. Kuo, H.C. Yen, C.C. Huang, W.C. Hsu, H.J. Wei, C.L. Lin, Cerebrospinal fluid biomarkers for neuropsychological symptoms in early stage of late-onset Alzheimer's disease, Int. J. Neurosci. 125 (2015) 747–754.
[20] G. Casadesus, M.A. Smith, S. Basu, J. Hua, D.E. Capobianco, S.L. Siedlak, X. Zhu, G. Perry, Increased isoprostane and prostaglandin are prominent in neurons in Alzheimer disease, Mol. Neurodegener. 2 (2007) 2.
[21] T.J. Montine, E.R. Peskind, J.F. Quinn, A.M. Wilson, K.S. Montine, D. Galasko, Increased cerebrospinal fluid F2-isoprostanes are associated with aging and latent Alzheimer's disease as identified by biomarkers, Neuromol. Med. 13 (2011) 37–43.
[22] A. Montagne, Z. Zhao, B.V. Zlokovic, Alzheimer's disease: a matter of blood–brain barrier dysfunction? J. Exp. Med. 214 (2017) 3151–3169.
[23] F.B. Sirin, D. Kumbul Doğuç, H. Vural, I. Eren, I. Inanli, R. Sütçü, N. Delibaş, Plasma 8-isoPGF2α and serum melatonin levels in patients with minimal cognitive impairment and Alzheimer disease, Turk. Med. Sci. 45 (2015) 1073–1077.
[24] D. Praticò, C.M. Clark, V.M. Lee, J.Q. Trojanowski, J. Rokach, G.A. FitzGerald, Increased 8,12-iso-iPF2alpha-VI in Alzheimer's disease: correlation of a noninvasive index of lipid peroxidation with disease severity, Ann. Neurol. 48 (2000) 809–812.
[25] E.E. Tuppo, L.J. Forman, B.W. Spur, R.E. Chan-Ting, A. Chopra, T.A. Cavalieri, Sign of lipid peroxidation as measured in the urine of patients with probable Alzheimer's disease, Brain Res. Bull. 54 (2001) 565–568.
[26] E.J. Mufson, S. Leurgans, Inability of plasma and urine F2A-isoprostane levels to differentiate mild cognitive impairment from Alzheimer's disease, Neurodegener. Dis. 7 (2010) 139–142.
[27] M.C. Irizarry, Y. Yao, B.T. Hyman, J.H. Growdon, D. Praticò, Plasma F2A isoprostane levels in Alzheimer's and Parkinson's disease, Neurodegener. Dis. 4 (2007) 403–405.
[28] A. García-Blanco, C. Peña-Bautista, C. Oger, C. Vigor, J.M. Galano, T. Durand, N. Martín-Ibáñez, M. Baquero, M. Vento, C. Chafer-Pericás, Reliable determination of new lipid peroxidation compounds as potential early Alzheimer Disease biomarkers, Talanta 184 (2018) 193–201.
[29] G.M. McKhann, D.S. Knopman, H. Chertkow, B.T. Hyman, C.R. Jack Jr., C.H. Kawas, W.E. Klunk, W.J. Koroshetz, J.J. Manly, R. Mayeux, R.C. Mohs, J.C. Morris, M.N. Rossor, P. Scheltens, M.C. Carrillo, B. Thies, S. Weintraub, C.H. Phelps, The diagnosis of dementia due to Alzheimer's disease: recommendations from the National Institute on Aging-Alzheimer's Association workgroups on diagnostic guidelines for Alzheimer's disease, Alzheimers Dement. 7 (2011) 263–269.
[30] M.S. Albert, S.T. DeKosky, D. Dickson, B. Dubois, H.H. Feldman, N.C. Fox, A. Gamst, D.M. Holtzman, W.J. Jagust, R.C. Petersen, P.J. Snyder, M.C. Carrillo, B. Thies, C.H. Phelps, The diagnosis of mild cognitive impairment due to Alzheimer's disease: recommendations from the National Institute on Aging-Alzheimer's Association workgroups on diagnostic guidelines for Alzheimer's disease, Alzheimers Dement. 7 (2011) 270–279.
[31] C. Randolph, M.C. Tierney, E. Mohr, T.N. Chase, The Repeatable Battery for the Assessment of Neuropsychological Status (RBANS): preliminary clinical validity, J. Clin. Exp. Neuropsychol. 20 (1998) 310–319.
[32] R.I. Pfeffer, T.T. Kurosaki, C.H. Harrah, J.M. Chance, S. Filos, Measurement of functional activities in older adults in the community, J. Gerontol. 37 (1982) 323–329.
[33] C.P. Hughes, L. Berg, W.L. Danziger, L.A. Coben, R.L. Martin, A new clinical scale for the staging of dementia, Br. J. Psychiatry 140 (1982) 566–572.
[34] G.B. Frisoni, N.C. Fox, C.R. Jack, P. Scheltens, P.M. Thompson, The clinical use of structural MRI in Alzheimer disease, Nat. Rev. Neurol. 6 (2010) 67–77.
[35] A. Anoop, P.K. Singh, R.S. Jacob, S.K. Maji, CSF biomarkers for Alzheimer's disease diagnosis, Int. J. Alz. Dis. 606802 (2010) 1–12.
[36] K. Blennow, B. Dubois, A.M. Fagan, P. Lewczuk, M.J. de Leon, H. Hampel, Clinical utility of cerebrospinal fluid biomarkers in the diagnosis of early Alzheimer's disease, Alzheimers Dement. 11 (2015) 58–69.
[37] A. de la Torre, Y.Y. Lee, A. Mazzoni, A. Guy, V. Bultel-Poncé, T. Durand, C. Oger, J.C. Lee, J.M. Galano, Total syntheses and in vivo quantitation of novel neurofuran and dihomo-isofuran derived from docosahexaenoic acid and adrenic acid, Chemistry 21 (2015) 2442–2446.
[38] C. Oger, V. Bultel-Poncé, A. Guy, L. Balas, J.C. Rossi, T. Durand, J.M. Galano, The handy use of Brown's catalyst for a skipped diyne deuteration: application to the synthesis of a d4-labeled-F4t-neuroprostane, Chem. Eur. J. 16 (2010) 13976–13980.
[39] C. Oger, V. Bultel-Poncé, A. Guy, T. Durand, J.M. Galano, Total synthesis of isoprostanes derived from Adrenic Acid and EPA, Eur. J. Org. Chem. 2012 (2012) 2621–2634.
[40] A. Guy, C. Oger, J. Hepekauzen, C. Signorini, T. Durand, C. De Felice, A. Fürstner, J.M. Galano, Oxygenated metabolites of n-3 polyunsaturated fatty acid as potential oxidative stress biomarkers: total synthesis of 8-F_{3t}-IsoP, 10-F_{4t}-NeuroP, and [D_4]-10-F_{4t}-NeuroP, Chem. Eur. J. 20 (2014) 6374–6380.
[41] A. de la Torre, Y.Y. Lee, C. Oger, P.T. Sangild, T. Durand, J.C.Y. Lee, J.M. Galano, Synthesis, discovery and quantitation of dihomo-Isofurans: novel biomarkers of in vivo adrenic acid peroxidation, Angew. Chem. Int. Ed. 24 (2014) 6249–6252.
[42] E.W. Steyerberg, H. Uno, J.P.A. Ioannidis, B. van Calster, Poor performance of clinical prediction models: the harm of commonly applied methods, J. Clin. Epidemiol. 4356 (2017) (30788-6).
[43] G.C. Smith, S.R. Seaman, A.M. Wood, P. Royston, I.R. White, Correcting for optimistic prediction in small data sets, Am. J. Epidemiol. 180 (2014) 318–324.
[44] K.J. Herbst-Robinson, L. Liu, M. James, Y. Yao, S.X. Xie, K.R. Brundena, Inflammatory eicosanoids increase amyloid precursor protein expression via activation of multiple neuronal receptors, Sci. Rep. 5 (2015) 18286.
[45] E.W. Steyerberg, M.J.C. Eijkemans, F.E. Harrell, J.D.F. Habbema, Prognostic modelling with logistic regression analysis: a comparison of selection and estimation methods in small data sets, Stat. Med. 19 (2000) 1059–1079.
[46] A. Nazeri, H. Ganjgahi, T. Roostaei, T. Nichols, M. Zarei, Alzheimer's disease neuroimaging Initiative, imaging proteomics for diagnosis, monitoring and prediction of Alzheimer's disease, Neuroimage 2 (2014) 657–665.
[47] V.Z. Marmarelis, D.C. Shin, M.E. Orme, R. Zhang, Model-based quantification of cerebral hemodynamics as a physiomarker for Alzheimer's disease? Ann. Biomed. Eng. 41 (2013) 2296–2317.
[48] C. Ibáñez, C. Simó, P.J. Martín-Álvarez, M. Kivipelto, B. Winblad, A. Cedazo-Mínguez, A. Cifuentes, Toward a predictive model of Alzheimer's disease progression using capillary electrophoresis-mass spectrometry metabolomics, Anal. Chem. 84 (2012) (8532-8340).
[49] W. Liao, X. Long, C. Jiang, Y. Diao, X. Liu, H. Zheng, L. Zhang, Alzheimer's Disease Neuroimaging Initiative, Discerning mild cognitive impairment and Alzheimer Disease from normal aging: morphologic characterization based on univariate and multivariate models, Acad. Radiol. 21 (2014) 597–604.

ARTICLE IN PRESS

Clinical Biochemistry xxx (xxxx) xxx–xxx

Contents lists available at ScienceDirect

Clinical Biochemistry

journal homepage: www.elsevier.com/locate/clinbiochem

Assessment of lipid peroxidation and artificial neural network models in early Alzheimer Disease diagnosis

Carmen Peña-Bautista[a], Thierry Durand[b], Camille Oger[b], Miguel Baquero[c], Máximo Vento[a], Consuelo Cháfer-Pericás[a,*]

[a] Neonatal Research Unit, Health Research Institute La Fe, Valencia, Spain
[b] Institut des Biomolécules Max Mousseron, IBMM, University of Montpellier, CNRS ENSCM, Montpellier, France
[c] Neurology Unit, University and Polytechnic Hospital La Fe, Valencia, Spain

ARTICLE INFO

Keywords:
Alzheimer Disease
Artificial neural network
Mass spectrometry
Partial least squares
Plasma
Lipid peroxidation
Urine

ABSTRACT

Objective: Lipid peroxidation constitutes a molecular mechanism involved in early Alzheimer Disease (AD) stages, and artificial neural network (ANN) analysis is a promising non-linear regression model, characterized by its high flexibility and utility in clinical diagnosis. ANN simulates neuron learning procedures and it could provide good diagnostic performances in this complex and heterogeneous disease compared with linear regression analysis. Design and Methods: In our study, a new set of lipid peroxidation compounds were determined in urine and plasma samples from patients diagnosed with early Alzheimer Disease (n = 70) and healthy controls (n = 26) by means of ultra-performance liquid chromatography coupled with tandem mass-spectrometry. Then, a model based on ANN was developed to classify groups of participants. Results: The diagnostic performances obtained using an ANN model for each biological matrix were compared with the corresponding linear regression model based on partial least squares (PLS), and with the non-linear (radial and polynomial) support vector machine (SVM) models. Better accuracy, in terms of receiver operating characteristic-area under curve (ROC-AUC), was obtained for the ANN models (ROC-AUC 0.882 in plasma and 0.839 in urine) than for PLS and SVM models. Conclusion: Lipid peroxidation and ANN constitute a useful approach to establish a reliable diagnosis when the prognosis is complex, multidimensional and non-linear.

1. Introduction

Alzheimer disease (AD) early diagnosis constitutes a subject of great concern, since AD is the main cause of dementia in the world, and it causes great burden on patients and families/care providers, as well as high social and economic impact [1]. In addition, there is a lack of effective therapeutic targets as well as non-invasive and cost-effective molecular diagnostic models, probably due to incomplete understanding of the AD pathophysiological mechanisms.

Nowadays, both the onset and development of AD have been linked to lipid peroxidation mechanisms given the high lipid composition, high metabolic activity and high oxygen consumption of the brain [2–4]. In fact, previous studies based on lipid peroxidation improved the understanding of pathophysiological mechanisms underlying AD, and also established new biomarkers for diagnosis, prognosis and therapeutic purposes [5]. Specifically, different isoprostanoids have been determined in cerebrospinal fluid samples (CSF) [6,7], plasma and serum [8], and in urine samples [9,10], showing correlation with early AD. These compounds can be classified depending on the modified lipid from which they derived. Thus, isoprostanes/isofurans are produced from arachidonic acid oxidation (all tissues), neuroprostanes/neurofurans from docosahexanoic acid oxidation (brain grey matter), and dihomo-isoprostanes/di-homo-isofurans from adrenic acid oxidation (brain white matter) [11]. In this sense, although some potential biomarkers have been identified, they have not been clinically validated [12,13]. In addition, some predictive models, mainly based on linear regression, have been developed [14,15], but the complexity of AD physiopathology could demand non-linear regression models to obtain satisfactory diagnostic results.

Artificial neural network (ANN) constitutes a promising statistical tool since it is flexible and can model highly non-linear systems, in which the relationships between variables are unknown or very complex [16–18]. The ANN models simulate the learning process carried out by the neurons, establishing connections among different variables, and allowing a complex data analysis through mathematical functions [17]. Neurons are placed in several layers (input, hidden, output) in the

* Corresponding author at: Health Research Institute La Fe, Avda de Fernando Abril Martorell, 106, 46026, Valencia, Spain.
E-mail address: m.consuelo.chafer@uv.es (C. Cháfer-Pericás).

https://doi.org/10.1016/j.clinbiochem.2019.07.008
Received 21 December 2018; Received in revised form 11 July 2019; Accepted 13 July 2019

Please cite this article as: Carmen Peña-Bautista, et al., Clinical Biochemistry, https://doi.org/10.1016/j.clinbiochem.2019.07.008

ANN. Specifically, the predictor variables are in the input layer, and the response variables are in the output layer. Then, some connections, similar to those in synapses, are established among the variables by means of different mathematical functions (hyperbolic, sigmoid…), and different coefficients are assigned to these interactions in order to improve the model's classification ability [19]. In this sense, ANN analysis is based on supervised learning which has the advantage of being tolerant with the highly complex and noisy data obtained from biological samples [17]. ANN analysis has also some disadvantages, namely the inability to exactly reproduce the same model due to the complex learning processes involved in the models' development [16], as well as the fact of being considered a "black box" by some authors [17].

Nowadays, there is an increasing body of research applying ANN analysis to clinical diagnosis, since it allows to establish complex interactions among variables involved in some multifactorial pathologies [20]. In fact, recent studies have provided satisfactory diagnostic results in different clinical areas [21–25]. However, few studies have compared the clinical predictive capacity of ANN models with linear regression models, and better results, in terms of accuracy, seem to be obtained from ANN analysis [26,27]. Among ANN studies focusing on early AD diagnosis, most of them were based on neurophysiological signals (electroencephalogram, neurofibrillary tangles) [28] or image tests [29–32], requiring high cost and highly specialized staff to interpret the results. Other ANN models based on neuropsychological tests and clinical variables predicted brain AD characteristic lesions (amyloid plaques, neurofibrillary tangles) [33], as well as mild cognitive impairment in elderly individuals [25,26]. Nevertheless, some neuropsychological tests are influenced by the patients' educational level, since high educational level could mask cognitive alteration and very low educational level (illiteracy) prevents the neuropsychological evaluation. An ANN model based on Raman spectroscopy in serum was employed to discriminate among AD patients, healthy individuals, and other types of dementias; however, this expensive equipment is not available in the clinical practice [34]. Moreover, some ANN models have also been developed using different biomarkers in blood, such as glucose and apolipoprotein E genotype as AD risk factors [35,36]. To our knowledge, ANN analysis has not ever been assessed as an early AD detection model from lipid peroxidation compounds, which are determined by validated analytical methods in plasma or urine samples.

The aim of this study was to develop and evaluate ANN models, in terms of complex disease diagnostic performance, comparing them with other linear and non-linear models. For this, a new set of lipid peroxidation biomarkers was determined in urine and plasma samples from well-defined mild cognitive-impairment due to AD patients and healthy participants.

2. Materials and methods

2.1. Patients and samples

Urine and plasma samples were collected from participants recruited in the University and Polytechnic Hospital La Fe (Valencia, Spain). They were classified as mild cognitive impairment due to Alzheimer's disease (MCI-AD, $n = 70$) and healthy control participants ($n = 26$) based on neuropsychological tests, structural neuroimaging, and CSF biomarkers (β-amyloid, total Tau, phosphorylated Tau) [37]. The study protocol was approved by the Ethics Committee (CEIC) of the Health Research Institute La Fe (Valencia, Spain), and informed consent was obtained from all the participants.

2.2. Analytical method

The samples were processed as indicated in previous studies, where the corresponding sample treatment procedures were optimized [9,38]. Thereafter, the samples were injected into the chromatographic system (UPLC-MS/MS) following previously validated analytical methods whose chromatographic and detection conditions were described in previous works [9,38]. Finally, the levels of a new set of lipid peroxidation biomarkers (isoprostanes, neuroprostanes, dihomoisoprostanes, isofurans, neurofurans, dihomoisofurans) were obtained.

2.3. Statistical analysis

Different regression models, based on linear discriminant analysis (partial least squares, PLS) and non-linear discriminant analysis (support vector machine, SVM; artificial neural networks, ANN), have been developed from lipid peroxidation compounds levels determined in urine and plasma samples from healthy and MCI-AD participants. Each model was trained and tested multiple times, and the diagnostic performance obtained for each model was evaluated.

The PLS analysis was carried out with the Unscrambler software version 7.6 (Camo, Woodbridge, USA), the SVM analysis with radial and polynomial kernel functions was carried out with IBM SPSS Modeler software version 1.0 (IBM, New York, USA) and the ANN analysis was carried out with SPSS software version 20.0 (SPSS, Inc., Chicago, IL, USA). These statistical multivariate models were developed for each sample matrix that was analyzed.

The PLS models were constructed from 24 independent variables (22 lipid peroxidation compounds, gender and age) as predictor variables, 1 dependent variable (participant group (MCI-AD/healthy control)) and 5 principal components. All variables were normalized, and a random cross validation (one left out) was carried out.

The SVM models with radial and polynomial kernel functions were developed from 24 independent variables (22 lipid peroxidation analytes, gender and age) and 1 dependent variable (participant group (MCI-AD/healthy control)). The dataset was randomly divided into training sample (70%), testing sample (15%) and validating sample (15%). The parameters utilized were detention criteria of $1.0E^{-3}$, regularization parameter (C) of 10, precision of regression of 0.1, and the kernel functions employed were radial basis function (gamma (γ) of 0.1) and polynomial function (γ of 1).

The ANN models were constructed from the 24 independent variables (gender and age as factors, 22 analytes as covariables), and 1 dependent variable (participant group (MCI-AD/healthy control)). In the first step, the dataset was randomly divided into training sample (70%), testing sample (15%) and validating sample (15%) [18], before model development. The training sample is used to train the network in several iterations improving the ANN performance. Then, the optimum values of weights and biases are determined, and the ANN performance is examined in the testing sample. The feedforward architecture was based on the predictors function Multilayer Perceptron (MPL), as training algorithm, that minimizes the prediction error of outputs, and the form of this function consists of input, hidden and output layers, but the number of neurons in each layer as well as the number of layers depend on the complexity of the studied system. The automatic architecture selection builds a network with one hidden layer, and the number of units in the hidden layer was tested between 1 and 50, 1 unit being the optimum number. The transfer functions for the hidden and output layers were hyperbolic tangent and normalized exponential function, respectively. These functions have the following forms:

$$\gamma(x) = \tanh(x) = (e^{x} - e^{-x})/(e^{x} + e^{-x})$$

$$\gamma(x_k) = \exp.(x_k)/\Sigma_j \exp(x_j), \text{ for } j = 1, \ldots, k \text{ (dimensions)}$$

In this sense, a three-layer 24-1-1-feed-forward propagation ANN model was trained and developed from 24 predictor variables (age, gender, lipid peroxidation compounds).

Regarding the training type, it was in batch, and the optimization algorithm to estimate the synaptic weights was based on scaled conjugate gradient including an initial lambda and an initial sigma values of 0.0000005 and 0.00005, respectively, as initial values for the weights and biases to optimize them in successive iterations.

2.4. Diagnostic performance evaluation

Under the previously indicated specifications, several ANN models were developed in each biological matrix, and the averages of them were considered as the most reliable corresponding models.

For diagnostic performance evaluation of the models PLS, SVM with polynomial and radial kernel functions, and ANN, receiver operating characteristic (ROC) curves were constructed from their corresponding validation results, indicating the area under the curve (AUC)-ROC as a parameter that represents the accuracy of each model. For the PLS model, it consisted of cross validation leaving one out, while for the SVM and ANN models, validation consisted of using data sets randomly divided. The corresponding area under the curve (AUC, 95% confidence interval (CI)), and the optimum cut-off value (the highest sum of sensitivity and specificity) were determined for each model in the prediction of AD. Finally, the diagnostic indices (sensitivity, specificity, positive likelihood ratio (LR+), negative likelihood ratio (LR−), diagnostic odds ratio (DOR)) were calculated. For all analysis, a $p < .05$ was considered to indicate a statistically significant difference.

3. Results

3.1. Demographic, clinical and analytical variables

The demographic and clinical variables for each group of participants are described in Table 1. All of them showed a non-normal distribution, so medians were compared between groups by means of Mann Whitney test for numerical variables, and Chi-square and Fisher exact tests for categorical variables. The clinical variables (Repeatable Battery for the Assessment of Neuropsychological Status (RBANS), Clinical Dementia Rating (CDR), Functional Activities Questionnaire (FAQ), Mini-Mental State Examination (MMSE), cerebrospinal fluid (CSF) β-amyloid, CSF total-Tau and CSF phosphorylated-Tau) showed statistically significant differences between MCI-AD and healthy control groups. On the other hand, demographic variables did not present statistically significant differences between both groups except of gender and age, so these variables were taken into account in the subsequent analyses.

The concentrations obtained for each analytical variable (22 analytes) in both matrices (urine, plasma) are summarized in Table 2. As we can see, statistically significant differences between groups were obtained for 17-*epi*-17-F_{2t}-dihomo-IsoP in urine samples, and for 15(*R*)-15-F_{2t}-IsoP, $PGF_{2\alpha}$, 4(*RS*)-4-F_{4t}-NeuroP, *ent*-7(*RS*)-7-F_{2t}-dihomo-IsoP, 17-*epi*-17-F_{2t}-dihomo-IsoP, isoprostanes, isofurans, neuroprostanes and neurofurans in plasma samples.

3.2. Multivariate statistical models

In this work we developed different multivariate models in order to improve the diagnostic utility of lipid peroxidation products from plasma and urine samples [9,38], since they do not have a high diagnostic capacity individually. For this, different multivariate models based on linear and non-linear regression were developed for each kind of biological sample and they were compared in terms of diagnostic performance.

First, PLS linear regression models were developed. For PLS in urine, in Fig. 1 we can see that the MCI-AD group showed higher levels for the compounds 15(*R*)-15-F_{2t}-IsoP, 2,3-dinor-15-*epi*-15-F_{2t}-IsoP, 4(*RS*)-4-F_{4t}-NeuroP, *ent*-7 (*RS*)-7-F_{2t}-dihomo-IsoP, 17-*epi*-17-F_{2t}-dihomo-IsoP, 10-*epi*-10-F_{4t}-NeuroP, 17-F_{2t}-dihomo-IsoP and neurofurans, as well as higher age and female proportion (Fig. 1a). However, the healthy participants are grouped on the left side of the score plot (Fig. 1b) because they showed lower levels for the previous compounds. Similarly, for PLS in plasma, in Fig. 2 we can see that the MCI-AD group showed higher levels for the compounds 15(*R*)-15-F_{2t}-IsoP, 4(*RS*)-4-F_{4t}-NeuroP, neuroprostanes, isoprostanes, *ent*-7(*RS*)-7-F_{2t}-dihomo-IsoP, neurofurans and isofurans, as well as higher age and female proportion (Fig. 2a). However, the healthy individuals are grouped in the left side of the score plot (Fig. 2b) due to their lower levels for the previous compounds.

Table 1
Demographic and clinical variables of the studied population.

Variable		MCI-AD ($n = 70$)	Healthy control ($n = 26$)	P-value
Gender (Female, n (%))		41 (58.6%)	9 (34.6%)	0.037*
Age (Median, (IQR))		70 (68–74)	66 (62–70)	0.044*
Depression (Yes, n (%))		9 (13%)	5 (19%)	0.566
Anxiety (Yes, n (%))		6 (9%)	2 (8%)	0.629
Studies levels (n (%))	Primary	28 (40%)	16 (61%)	0.173
	Secondary	20 (29%)	3 (12%)	
	Academic	22 (31%)	7 (27%)	
Smoking status (smoker or former smoker) (n (%))		50 (71%)	13 (50%)	0.124
Alcohol consumption (yes, n (%))		12 (17%)	2 (8%)	0.307
Medications (n, (%))	None	15 (22%)	8 (31%)	0.269
	psychotropic drugs	3 (4%)	2 (8%)	
	Antihypertensive	10 (14%)	7 (27%)	
	Statins	12 (17%)	3 (11%)	
	Two or more	30(43%)	6 (23%)	
Comorbidity (n, (%))	None	18 (26%)	10 (39%)	0.071
	Dyslipemia	18 (26%)	3 (11%)	
	Hypertension	10 (14%)	7 (27%)	
	Heart disease	0 (0%)	1 (4%)	
	Two or more	24 (34%)	5 (19%)	
RBANS-DM[1]		42 (40–49)	100 (90–106)	0.000*
CDR[2]		0.5 (0.5–1)	0 (0–0)	0.000*
FAQ[3]		7 (2 – 13)	0 (0–0)	0.000*
MMSE[4]		25 (19–29)	24 (21–27)	0.000*
CSF[5] β-amyloid (pg mL^{-1})		597 (445–687)	1186 (1033–1403)	0.000*
CSF t-Tau[6] (pg mL^{-1})		572 (396–857)	202 (139–320)	0.000*
CSF p-Tau[7] (pg mL^{-1})		88 (72–111)	49 (35–67)	0.000*

IQR: Interquartile range.
Data were expressed as median (interquartile range (IQR)) for non-parametric continuous variables, and number of cases (percentages) for categorical cases. The statistical calculations to compare between the two groups employed Mann-Whitney test, Chi-Square test and Fisher exact test, respectively.
[1] RBANS-DM, Repeatable Battery for the Assessment of Neuropsychological Status- Delayed Memory (Standard Score; cut-off point < 85).
[2] CDR, Clinical Dementia Rating, values: 0, 0.5, 1, 2.
[3] FAQ, Functional Activities Questionnaire (Direct Score; cut-off point > 9).
[4] MMSE, Minimental State Examination.
[5] CSF, Cerebrospinal fluid.
[6] t-Tau, total-Tau.
[7] p-Tau, phosphorylated-Tau.
* $p < .05$.

Secondly, SVM models with radial and polynomial kernel functions were developed from results in plasma and urine samples. Non linear functions were used in order to obtain a better classification of the participants.

Thirdly, non-linear regression models based on ANN were developed for urine and plasma samples in order to classify the two groups of participants. As shown in Fig. 3, 22 analytes, gender and age were included in the input layer. For the hidden and output layers, the transfer functions were hyperbolic tangent and normalized exponential functions, respectively.

3.3. Diagnostic performance for the statistical multivariate developed models

The diagnostic performance of each model was estimated from the corresponding ROC curves (Fig. 4). In urine samples, the ANN model provided an AUC of 0.839 (CI 95%, 0.746–0.933), while for the PLS model it was 0.653 (CI 95%, 0.526–0.780), and for the SVM models it

Table 2
Concentrations determined by UPLC-MS/MS for each analyte in plasma and urine samples from MCI-AD and healthy control participants.

Analyte	Plasma (nmol L^{-1})							Urine (ng mg creatinine $^{-1}$)						
	MCI-AD (n = 70)			Healthy control (n = 26)			*P*-value	MCI-AD (n = 70)			Healthy control (n = 26)			P-value
	Median	quartile		Median	quartile			Median	quartile		Median	quartile		
		1st	3rd		1st	3rd			1st	3rd		1st	3rd	
15(*R*)-15-F_{2t}-IsoP	0.30	0.23	0.46	0.20	0.15	0.26	0.000*	0.69	0.47	1.42	0.71	0.49	1.00	0.830
PGE_2	0.05	0.00	0.13	0.05	0.00	0.10	0.520	1.93	0.43	3.48	1.85	0.92	4.62	0.615
2,3-dinor-15-*epi*-15-F_{2t}-IsoP	0.00	0.00	0.03	0.00	0.00	0.00	0.067	0.73	0.49	1.22	0.65	0.47	1.12	0.458
15-keto-15-E_{2t}-IsoP	0.15	0.00	0.35	0.13	0.04	0.27	0.874	0.92	0.51	1.46	0.88	0.52	1.65	0.644
15-keto-15-F_{2t}-IsoP	0.23	0.09	0.35	0.23	0.14	0.28	0.599	0.79	0.16	1.85	1.52	0.60	2.20	0.094
15-E_{2t}-IsoP	0.26	0.12	0.43	0.19	0.09	0.28	0.320	0.18	0.05	1.29	0.19	0.06	0.76	0.830
5-F_{2t}-IsoP	0.78	0.40	1.26	0.99	0.73	1.23	0.362	2.66	1.61	4.85	2.70	1.77	3.85	0.817
15-F_{2t}-IsoP	0.02	0.01	0.04	0.02	0.02	0.03	0.638	0.01	0.00	0.02	0.01	0.00	0.02	0.113
$PGF_{2\alpha}$	0.51	0.24	0.76	0.74	0.48	0.94	0.008*	3.67	2.69	7.90	2.98	2.34	4.98	0.295
4(*RS*)-4-F_{4t}-NeuroP	1.14	0.96	1.33	1.03	0.00	1.13	0.003*	0.91	0.67	1.40	0.72	0.50	1.05	0.051
1a,1b-dihomo-$PGF_{2\alpha}$	0.00	0.00	0.00	0.00	0.00	0.00	0.784	1.26	0.61	2.35	1.63	1.01	2.32	0.232
10-*epi*-10-F_{4t}-NeuroP	0.08	0.03	0.15	0.09	0.03	0.14	0.731	0.03	0.00	0.06	0.01	0.00	0.04	0.094
14(*RS*)-14-F_{4t}-NeuroP	0.53	0.06	1.03	0.60	0.00	1.74	0.671	1.22	0.76	2.38	1.37	0.78	1.98	0.837
ent-7(*RS*)-7-F_{2t}-dihomo-IsoP	0.10	0.05	0.15	0.05	0.04	0.08	0.002*	0.32	0.13	0.60	0.29	0.21	0.39	1.000
17-F_{2t}-dihomo-IsoP	0.00	0.00	0.00	0.00	0.00	0.00	0.555	0.08	0.00	0.36	0.10	0.00	0.23	0.625
17-*epi*-17-F_{2t}-dihomo-IsoP	0.03	0.00	0.05	0.00	0.00	0.01	0.015*	0.01	0.00	0.06	0.00	0.00	0.00	0.019*
17(*RS*)-10-*epi*-SC-Δ^{15},11-dihomo-IsoF	0.00	0.00	0.00	0.00	0.00	0.00	0.164	0.03	0.00	0.11	0.05	0.02	0.08	0.330
7(*RS*)-ST-Δ^{8},11-dihomo-IsoF	0.04	0.03	0.08	0.09	0.02	0.16	0.067	0.00	0.00	0.02	0.00	0.00	0.03	0.849
Neurofurans[a]	0.09	−0.05	0.17	−0.10	−0.15	0.07	0.000*	3.13	1.76	6.62	4.15	2.51	5.95	0.356
Isofurans[a]	0.09	0.07	0.12	0.07	0.06	0.09	0.013*	4.36	2.53	7.25	4.29	3.37	9.64	0.343
Neuroprostanes[a]	−0.22	−0.70	0.19	−0.65	−0.76	−0.48	0.010*	3.52	2.25	4.97	3.77	2.02	6.17	0.650
Isoprostanes[a]	0.30	0.22	0.39	0.20	0.17	0.27	0.000*	6.20	3.82	12.37	7.30	4.67	11.45	0.491

* $p < .05$.
[a] Total parameters results expressed as intensity of signal units in plasma and as signal units mg^{-1} creatinine in urine.

was 0.644 (CI 95%, 0.539–0.749) with the polynomial function and 0.659 (CI 95%, 0.558–0.759) with the radial function. Similarly, in plasma samples, the ANN model provided an AUC of 0.882 (CI 95%, 0.814–0.949), while for PLS it was 0.765 (CI 95%, 0.633–0.868), and for SVM models it was 0.817 (CI 95%, 0.712–0.922) with the polynomial function and 0.827 (CI 95%, 0.739–0.915) with the radial function. Therefore, ANN models provided better diagnostic accuracy than PLS and SVM models in both matrices. Moreover, plasma matrix showed higher diagnostic accuracy than urine.

From the estimated optimal cut-off values, the diagnostic indices in the prediction of early AD were calculated for each developed model in plasma and urine samples (Table 3). For urine, the ANN model provided a sensitivity of 80.9%, while its specificity was 76.9%. In addition, DOR value for ANN model in urine revealed that there was strong association between the model results and the AD occurrence. Regarding the ANN model in plasma samples, it provided a sensitivity of 88.2%, while its specificity was 76.9%. This model also showed an elevated DOR value that supported its diagnostic value. DOR values were quite similar among plasma models, but ANN model showed better accuracy (AUC-ROC 0.882) than PLS (AUC-ROC 0.765) and SVM (AUC-ROC 0.827). Moreover, ANN model showed better sensitivity and a satisfactory balance between sensitivity and specificity. ANN model showed better balance, obtaining a higher number of participants correctly classified. By contrast, PLS model showed high specificity but low sensitivity, classifying the AD participants as healthy subjects; while SVM model showed high sensitivity but low specificity, classifying the healthy subjects as AD patients. In general, for both matrices, the PLS model was the most specific, the SVM model was the most sensitive, and the ANN model showed the best balance of sensitivity/specificity.

4. Discussion

Some of the analytes studied in this work showed statistically significant differences, such as 17-*epi*-17-F_{2t}-dihomo-IsoP in urine samples, and 15(*R*)-15-F_{2t}-IsoP, $PGF_{2\alpha}$, 4(*RS*)-4-F_{4t}-NeuroP, *ent*-7(*RS*)-7-F_{2t}-dihomo-IsoP, 17-*epi*-17-F_{2t}-dihomo-IsoP, isoprostanes, isofurans, neuroprostanes and neurofurans in plasma samples. Nevertheless, each analyte individually did not provide a reliable AD diagnosis. In contrast, a multivariate model based on ANN showed better accuracy than PLS and SVM models, and analytes from plasma samples were more useful than those in urine samples to achieve a reliable AD diagnosis.

Some studies found lipid peroxidation products as biomarkers for AD diagnosis, and most of them were based on individual biomarkers, such as lipid peroxidation end products [39] or TBARS [40]. However, multivariate models could reflect the oxidative stress status of patients better, showing superior diagnostic indices and higher accuracy. Specifically, a previous work developed an ANN model based on different AD risk factors studied the predictive value of these factors [35]. It showed high capacity to integrate different data and achieve a general evaluation. Other developed ANN models to diagnose AD or MCI were based on image, genetics, neuropsychology or other biomarkers [25,41], but the present study is the first one using lipid peroxidation compounds as biomarkers. In general, previous studies based on ANN showed model accuracies around 90%, similar to our results. Also, PLS models have been developed for AD diagnosis. They were mainly based on gene expression and neuroimaging [42–44], but none of them was based on our set of lipid peroxidation products. In addition, a previous study for MCI diagnosis compared PLS model to other statistical tests, such as Random Forest showing the higher PLS diagnostic power [45].

The diagnostic indices obtained for each model in the present study indicated that the ANN model in both matrices showed a satisfactory accuracy (> 80%). In addition, the plasma ANN model showed, in general, better diagnostic indices than the urine model, corroborating previous studies in the literature [46,47]. Specifically, the ANN model based on the plasma levels of lipid peroxidation products showed high DOR value, sensitivity, and accuracy, as well as, satisfactory specificity, so it is considered a reliable diagnostic model. In this sense, Quintana et al. also found that ANN models showed better discriminant capacity than linear models in AD diagnosis [26]. AD is a complex disease process in which multiple factors are involved and that could be the

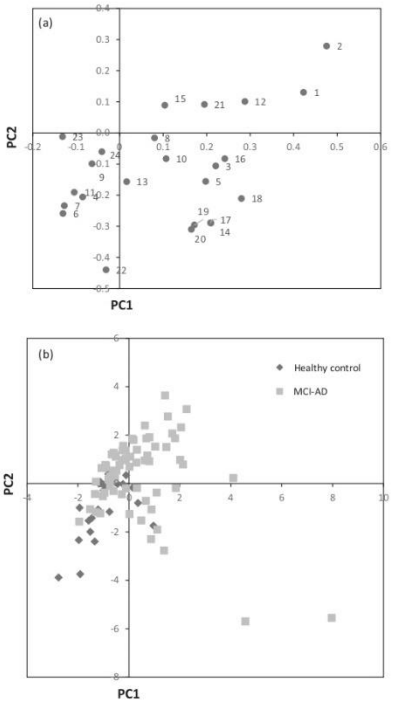

Fig. 1. Plots representing results of the partial least squares regression model in urine samples. (a) Loadings plot. 1: Gender; 2: Age; 3: 15(*R*)-15-F_{2t}-IsoP; 4: PGE_2; 5: 2,3-dinor-15-*epi*-15-F_{2t}-IsoP; 6: 15-keto-15-E_{2t}-IsoP; 7: 15-keto-15-F_{2t}-IsoP; 8: 15-E_{2t}-IsoP; 9: 5-F_{2t}-IsoP; 10: 15-F_{2t}-IsoP; 11: $PGF_{2\alpha}$; 12: 4(*RS*)-F_{4t}-NeuroP; 13: 1a,1b-dihomo-$PGF_{2\alpha}$; 14: 10-*epi*-10-F_{4t}-NeuroP; 15: 14(*RS*)-14-F_{4t}-NeuroP; 16: *ent*-7(*RS*)-7-F_{2t}-dihomo-IsoP; 17: 17-F_{2t}-dihomo-IsoP; 18: 17-epi-17-F_{2t}-dihomo-IsoP; 19: 17(*RS*)-10-epi-SC-Δ^{15}-11-dihomo-IsoF; 20: 7(*RS*)-ST-Δ^{8}-11-dihomo-IsoF; 21: neurofurans; 22: isofurans; 23: neuroprostanes; 24: isoprostanes. (b) Scores plot.

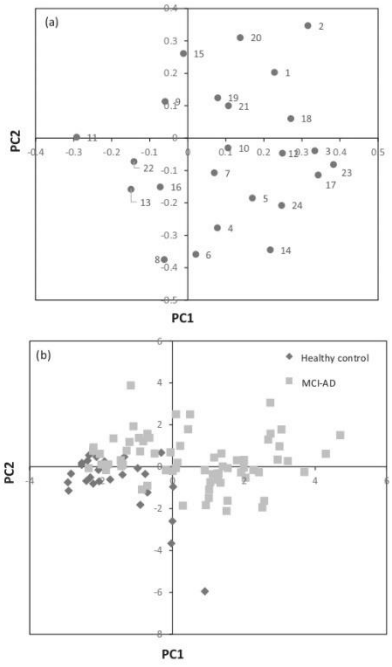

Fig. 2. Plots representing results of the partial least squares regression model in plasma samples. (a) Loadings plot. 1: Gender; 2: Age; 3: 15(*R*)-15-F_{2t}-IsoP; 4: PGE_2; 5: 2,3-dinor-15-epi-15-F_{2t}-IsoP; 6: 15-keto-15-E_{2t}-IsoP; 7: 15-keto-15-F_{2t}-IsoP; 8: 15-E_{2t}-IsoP; 9: 5-F_{2t}-IsoP; 10: 15-F_{2t}-IsoP; 11: $PGF_{2\alpha}$; 12: 4(*RS*)-4-F_{4t}-NeuroP; 13: 1a,1b-dihomo-$PGF_{2\alpha}$; 14: neuroprostanes; 15: 10-*epi*-10-F_{4t}-NeuroP; 16: 14(*RS*)-14-F_{4t}-NeuroP; 17: isoprostanes; 18: *ent*-7(*RS*)-7-F_{2t}-dihomo-IsoP; 19: 17-F_{2t}-dihomo-IsoP; 20: 17-*epi*-17-F_{2t}-dihomo-IsoP; 21: 17(*RS*)-10-*epi*-SC-Δ^{15}-11-dihomo-IsoF; 22: 7(*RS*)-*ST*-Δ^{8}-11-dihomo-IsoF; 23: neurofurans; 24: isofurans. (b) Scores plot.

reason why non-linear regression models showed a better predictive capacity than those models based on linear regression [35].

Regarding the biological matrix, the proposed ANN diagnostic model in plasma samples constitutes a promising minimally invasive approach that could avoid, in some cases, the current diagnostic methods, which involve invasive sampling and expensive techniques [48]. In this sense, the ANN models have a satisfactory diagnostic capacity, and they are able to classify the participants into healthy and MCI-AD with high accuracy in both matrices as an early screening tool.

5. Conclusion

The non-linear regression model based on ANN explained the non-

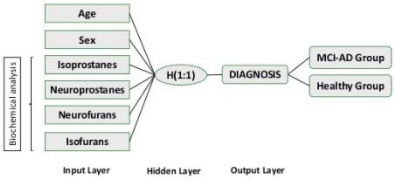

Fig. 3. General structure of the developed neural network for the prediction of early AD consisting of 24 input variables, 1 hidden layer with 1 node, and 1 output variable.

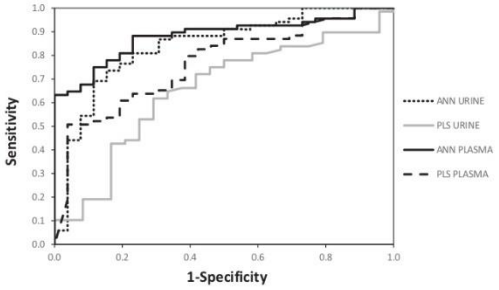

Fig. 4. Receiver operating Characteristic curves for PLS and ANN models in plasma and urine samples.

Table 3
Diagnostic indices for each developed statistical model in the prediction of MCI-AD from lipid peroxidation compounds determined in urine and plasma samples.

	Urine				Plasma			
	PLS	ANN	SVM		PLS	ANN	SVM	
			Radial	Polynomial			Radial	Polynomial
AUC (CI 95%)	0.653 (0.526–0.780)	0.839 (0.746–0.933)	0.659 (0.558–0.759)	0.644 (0.539–0.749)	0.765 (0.663–0.868)	0.882 (0.814–0.949)	0.827 (0.739–0.915)	0.817 (0.712–0.922)
Sensitivity (%, CI 95%)	63.2 (51.4–73.7)	80.9 (70.0–88.5)	92.9 (68.5–98.7)	92.3 (66.7–98.6)	50.7 (39.2–62.2)	88.2 (78.5–93.9)	92.3 (66.7–98.6)	100.0 (77.2–100)
Specificity (%, CI 95%)	70.8 (50.8–85.1)	76.9 (57.9–89.0)	11.1 (2.0–43.5)	37.5 (13.7–69.4)	96.2 (81.1–99.3)	76.9 (57.9–89.0)	50.0 (21.5–78.5)	25.0 (7.1–59.1)
LR + (CI 95%)	2.17 (1.13–4.15)	3.50 (1.72–7.14)	1.04 (0.80–1.37)	1.48 (0.84–2.58)	13.19 (1.90–91.40)	3.82 (1.89–7.75)	1.85 (0.91–3.76)	1.33 (0.89–1.99)
LR- (CI 95%)	0.52 (0.36–0.74)	0.25 (0.15–0.41)	0.64 (0.07–6.06)	0.21 (0.03–1.49)	0.51 (0.40–0.66)	0.15 (0.08–0.30)	0.15 (0.02–1.08)	–
DOR (CI 95%)	4.18 (1.52–11.46)	14.10 (4.72–42.13)	1.63 (0.09–29.78)	7.20 (0.60–87.02)	25.74 (3.30–200.67)	25.00 (7.73–80.81)	12.0 (1.02–141.34)	–

PLS, partial least squares; ANN, artificial neural network; SVM, support vector machine; AUC, area under the curve; LR+, positive likelihood ratio; LR-, negative likelihood ratio; CI, confidence interval; DOR, diagnostic odds ratio.

linear relationship between the levels of lipid peroxidation compounds and the diagnosis of a complex pathophysiological process, such as AD, constituting a promising screening approach. Specifically, the developed ANN model in plasma samples showed high accuracy and suitable diagnostic indices in early AD prediction. Nevertheless, further research will need to be carried out to clinically validate this diagnostic model. This approach constitutes a significant advance in early AD diagnosis, using minimally invasive sampling techniques, and offers important economic cost reduction for the public health system.

Funding

This work was supported by the Instituto de Salud Carlos III (Miguel Servet I Project (CP16/00082)) (Spanish Ministry of Economy and Competitiveness, and European Regional Development Fund).

Declaration of Competing Interest

None.

Acknowledgement

CC-P acknowledges a "Miguel Servet I" Grant (CP16/00082) from the Instituto Carlos III (ISCIII, Spanish Ministry of Economy and Competitiveness). CP-B acknowledges a pre-doctoral Grant (associated to "Miguel Servet" project CP16/00082) from the ISCIII (Spanish Ministry of Economy, Industry and Competitiveness).

The authors are grateful for the professional English language editing to Mr. Arash Javadinejad, English Instructor and Publication Editor at the Instituto de Investigación Sanitaria La Fe, Valencia, Spain.

References

[1] M. Prince, E. Albanese, M. Guerchet, M. Prina, World Alzheimer Report 2014: Dementia and Risk Reduction an Analysis of Protective and Modifiable Factors, (2014).
[2] W. Huang, X. Zhang, W.W. Chen, Role of oxidative stress in Alzheimer's disease, Biomed. Rep. 4 (2016) 519–522.
[3] R. Sultana, M. Perluigi, D. Allan Butterfield, Lipid peroxidation triggers neurodegeneration: a redox proteomics view into the Alzheimer disease brain, Free Radic. Biol. Med. 62 (2013) 157–169.
[4] Z. Chen, C. Zhong, Oxidative stress in Alzheimer's disease, Neurosci. Bull. 30 (2014) 271–281.
[5] C. Peña-Bautista, M. Baquero, M. Vento, C. Cháfer-Pericás, Free radicals in Alzheimer's disease: lipid peroxidation biomarkers, Clin. Chim. Acta 491 (2019) 85–90.
[6] M. Czerska, M. Zieliński, J. Gromadzińska, Isoprostanes - a novel major group of oxidative stress markers, Int. J. Occup. Med. Environ. Health 29 (2016) 179–190.
[7] T.J. Montine, E.R. Peskind, J.F. Quinn, A.M. Wilson, K.S. Montine, D. Galasko, Increased cerebrospinal fluid F2-isoprostanes are associated with aging and latent Alzheimer's disease as identified by biomarkers, NeuroMolecular Med. 13 (2011) 37–43.
[8] F.B. Sirin, D. Kumbul Doğuç, H. Vural, I. Eren, I. Inanli, R. Sütçü, N. Delibaş, Plasma 8-isoPGF2α and serum melatonin levels in patients with minimal cognitive impairment and Alzheimer disease, Turk. J. Med. Sci. 45 (2015) 1073–1077.

[9] A. García-Blanco, C. Peña-Bautista, C. Oger, C. Vigor, J.M. Galano, T. Durand, N. Martín-Ibáñez, M. Baquero, M. Vento, C. Cháfer-Pericás, Reliable determination of new lipid peroxidation compounds as potential early Alzheimer Disease biomarkers, Talanta. 184 (2018) 193–201.

[10] S. Hartmann, T.B. Ledur Kist, A review of biomarkers of Alzheimer's disease in noninvasive samples, Biomark. Med 12 (2018) 677–690.

[11] L. Roberts, J.P. Fessel, The biochemistry of the isoprostane, neuroprostane, and isofuran pathways of lipid peroxidation, Chem. Phys. Lipids 128 (2004) 173–186.

[12] B. Olsson, R. Lautner, U. Andreasson, A. Öhrfelt, E. Portelius, M. Bjerke, M.H.C. er Rosén, C. Olsson, G. Strobel, E. Wu, K. Dakin, M. Petzold, K. Blennow, H. Zetterberg, CSF and blood biomarkers for the diagnosis of Alzheimer's disease: a systematic review and meta-analysis, Lancet 15 (2016) 673–684.

[13] R. Wurtman, Biomarkers in the diagnosis and management of Alzheimer's disease, Metabolism 64 (2015) S47–S50.

[14] C. Ibáñez, C. Simó, P.J. Martín-Álvarez, M. Kivipelto, B. Winblad, A. Cedazo-Mínguez, A. Cifuentes, Toward a predictive model of Alzheimer's disease progression using capillary electrophoresis-mass spectrometry metabolomics, Anal. Chem. 84 (2012) 8532–8540.

[15] A. Alexiou, V.D. Mantzavinos, N.H. Greig, M.A. Kamal, A Bayesian model for the prediction and early diagnosis of Alzheimer's disease, Front. Aging Neurosci. 31 (2017) 69–77.

[16] B. Dębska, B. Guzowska-Świder, Application of artificial neural network in food classification, Anal. Chim. Acta 705 (2011) 283–291.

[17] D. Zafeiris, S. Rutella, G.R. Ball, An artificial neural network integrated pipeline for biomarker discovery using Alzheimer's disease as a case study, Comput. Struct. Biotech. J. 16 (2018) 77–87.

[18] A. Alibakshi, Strategies to develop robust neural network models: prediction of flash point as a case study, Anal. Chim. Acta 1026 (2018) 69–76.

[19] L.A. Berrueta, R.M. Alonso-Salces, K. Héberger, Supervised pattern recognition in food analysis, J. Chromatogr. A 1158 (2007) 196–214.

[20] W.D. Hong, X.R. Chen, S.Q. Jin, Q.K. Huang, Q.H. Zhu, J.Y. Pan, Use of an artificial neural network to predict persistent organ failure in patients with acute pancreatitis, Clinics (Sao Paulo) 68 (2013) 27–31.

[21] J. Yazdani Charati, G. Janbabaei, N. Alipour, S. Mohammadi, S. Ghorbani Gholiabad, A. Fendereski, Survival prediction of gastric cancer patients by Artificial Neural Network model, Gastroenterol. Hepatol. Bed. Bench. 11 (2018) 110–117.

[22] L. He, H. Li, S.K. Holland, W. Yuan, M. Altaye, N.A. Parikh, Early prediction of cognitive deficits in very preterm infants using functional connectome data in an artificial neural network framework, Neuroimage Clin. 18 (2018) 290–297.

[23] D. Devikanniga, R. Joshua Samuel Raj, Classification of osteoporosis by artificial neural network based on monarch butterfly optimisation algorithm, Healthc. Technol. Lett. 5 (2018) 70–75.

[24] A. Catic, L. Gurbeta, A. Kurtovic-Kozaric, S. Mehmedbasic, A. Badnjevic, Application of Neural Networks for classification of Patau, Edwards, Down, Turner and Klinefelter Syndrome based on first trimester maternal serum screening data, ultrasonographic findings and patient demographics, BMC Med. Genet. 11 (2018) 19.

[25] A.J.C.C. Lins, M.T.C. Muniz, A.N.M. Garcia, A.V. Gomes, R.M. Cabral, C.J.A. Bastos-Filho, Using artificial neural networks to select the parameters for the prognostic of mild cognitive impairment and dementia in elderly individuals, Comput. Methods Prog. Biomed. 152 (2017) 93–104.

[26] M. Quintana, J. Guàrdia, G. Sánchez-Benavides, M. Aguilar, J.L. Molinuevo, A. Robles, M.S. Barquero, C. Antúnez, C. Martínez-Parra, A. Frank-García, M. Fernández, R. Blesa, J. Peña-Casanova, Neuronorma Study Team, Using artificial neural networks in clinical neuropsychology: high performance in mild cognitive impairment and Alzheimer's disease, J. Clin. Exp. Neuropsychol. 34 (2012) 195–208.

[27] G. Li, X. Zhou, J. Liu, Y. Chen, H. Zhang, Y. Chen, J. Liu, H. Jiang, J. Yang, S. Nie, Comparison of three data mining models for prediction of advanced schistosomiasis prognosis in the Hubei provine, cPLoS Negl. Trop. Dis. 12 (2018) e0006262.

[28] E. Grossi, M.P. Buscema, D. Snowdon, P. Antuono, Neuropathological findings processed by artificial neural networks (ANNs) can perfectly distinguish Alzheimer's patients from controls in the Nun Study, BMC Neurol. 7 (2007) 15.

[29] F. Bertè, G. Lamponi, R.S. Calabrò, P. Bramanti, Elman neural network for the early identification of cognitive impairment in Alzheimer's disease, Funct. Neurol. 29 (2014) 57–65.

[30] X. Deng, K. Li, S. Liu, Preliminary study on application of artificial neural network to the diagnosis of Alzheimer's disease with magnetic resonance imaging, Chin. Med. J. 112 (1999) 232–237.

[31] H.F. da Silva Lopes, J.M. Abe, R. Anghinah, Application of paraconsistent artificial neural networks as a method of aid in the diagnosis of Alzheimer disease, J. Med. Syst. 34 (2010) 1073–1081.

[32] J.M. Abe, H.F.D.S. Lopes, R. Anghinah, Paraconsistent artificial neural networks and Alzheimer disease: a preliminary study, Dement. Neuropsychol. 1 (2007) 241–247.

[33] M. Buscema, E. Grossi, D. Snowdon, P. Antuono, M. Intraligi, G. Maurelli, R. Savarè, Artificial neural networks and artificial organisms can predict Alzheimer pathology in individual patients only on the basis of cognitive and functional status, Neuroinformatics. 2 (2004) 399–416.

[34] E. Ryzhikova, O. Kazakov, L. Halamkova, D. Celmins, P. Malone, E. Molho, E.A. Zimmerman, I.K. Lednev, Raman spectroscopy of blood serum for Alzheimer's disease diagnostics: specificity relative to other types of dementia, J. Biophotonics 8 (2015) 584–596.

[35] M. Tabaton, P. Odetti, S. Cammarata, R. Borghi, F. Monacelli, C. Caltagirone, P. Bossù, M. Buscema, E. Grossi, Artificial neural networks identify the predictive values of risk factors on the conversion of amnestic mild cognitive impairment, J. Alzheimers Dis. 19 (2010) 1035–1040.

[36] E. Grossi, A. Stoccoro, P. Tannorella, L. Migliore, F. Coppedè, Artificial neural networks link one-carbon metabolism to gene-promoter methylation in Alzheimer's disease, J. Alzheimers Dis. 53 (2016) 1517–1522.

[37] C.R. Jack, D.A. Bennett, K. Blennow, M.C. Carrillo, B. Dunn, S.B. Haeberlein, D.M. Holtzman, W. Jagust, F. Jessen, J. Karlawish, E. Liu, J.L. Molinuevo, T. Montine, C. Phelps, K.P. Rankin, C.C. Rowe, P. Scheltens, E. Siemers, H.M. Snyder, R. Sperling, NIA-AA Research Framework: toward a biological definition of Alzheimer's disease, Alzheimers Dement. 14 (2018) 535–562.

[38] C. Peña-Bautista, C. Vigor, J.M. Galano, C. Oger, T. Durand, I. Ferrer, A. Cuevas, R. López-Cuevas, M. Baquero, M. López-Nogueroles, M. Vento, D. Hervás, A. García-Blanco, C. Cháfer-Pericás, Plasma lipid peroxidation biomarkers for early and non-invasive Alzheimer Disease detection, Free Radic. Biol. Med. 124 (2018) 388–394.

[39] Z. Chmatalova, M. Vyhnalek, J. Laczo, J. Hort, R. Pospisilova, M. Pechova, A. Skoumalova, Relation of plasma selenium and lipid peroxidation end products in patients with Alzheimer's disease, Physiol. Res. 66 (2017) 1049–1056.

[40] M.C. Puertas, J.M. Martínez-Martos, M.P. Cobo, M.P. Carrera, M.D. Mayas, M.J. Ramírez-Expósito, Plasma oxidative stress parameters in men and women with early stage Alzheimer type dementia, Exp. Gerontol. 47 (2012) 625–630.

[41] J. Tang, L. Wu, H. Huang, J. Feng, Y. Yuan, Y. Zhou, P. Huang, Y. Xu, C. Yu, Back propagation artificial neural network for community Alzheimer's disease screening in China, Neural Regen. Res. 8 (2013) 270–276.

[42] B.B. Booij, T. Lindahl, P. Wetterberg, N.V. Skaane, S. Sæbø, G. Feten, P.D. Rye, L.I. Kristiansen, N. Hagen, M. Jensen, K. Bårdsen, B. Winblad, P. Sharma, A. Lönneborg, A gene expression pattern in blood for the early detection of Alzheimer's disease, J. Alzheimers Dis. 23 (2011) 109–119.

[43] E. Konukoglu, J.P. Coutu, D.H. Salat, B. Fischl, Alzheimer's Disease Neuroimaging Initiative (ADNI), Multivariate statistical analysis of diffusion imaging parameters using partial least squares: application to white matter variations in Alzheimer's disease, Neuroimage 134 (2016) 573–586.

[44] Q. Zhou, M. Goryawala, M. Cabrerizo, W. Barker, D. Loewenstein, R. Duara, M. Adjouadi, Multivariate analysis of structural MRI and PET (FDG and 18F-AV-45) for Alzheimer's disease and its prodromal stages, Conf. Proc. IEEE. Eng. Med. Biol. Soc. 2014 (2014) 1051–1054.

[45] P. Wang, K. Chen, L. Yao, B. Hu, X. Wu, J. Zhang, Q. Ye, X. Guo, Alzheimer's disease neuroimaging initiative. Multimodal classification of mild cognitive impairment based on partial least squares, J. Alzheimers Dis. 54 (2016) 359–371.

[46] M. Toufan, H. Namdar, M. Abbasnezhad, A. Habibzadeh, H. Esmaeili, S. Yaraghi, Z. Samani, Diagnostic values of plasma, fresh and frozen urine NT-proBNP in heart failure patients, J. Cardiovasc. Thorac. Res. 6 (2014) 111–115.

[47] G. Schley, C. Köberle, E. Manuilova, S. Rutz, C. Forster, M. Weyand, I. Formentini, R. Kientsch-Engel, K.U. Eckardt, C. Willam, Comparison of plasma and urine biomarker performance in acute kidney injury, PLoS One 10 (2015) e0145042.

[48] E.R. Peskind, R. Riekse, J.F. Quinn, J. Kaye, C.M. Clark, M.R. Farlow, C. Decarli, C. Chabal, D. Vavrek, M.A. Raskind, D. Galasko, Safety and acceptability of the research lumbar puncture, Alzheimer Dis. Assoc. Disord. 19 (2005) 220–225.

antioxidants

MDPI

Article

Isoprostanoids Levels in Cerebrospinal Fluid Do Not Reflect Alzheimer's Disease

Carmen Peña-Bautista [1], Miguel Baquero [2], Marina López-Nogueroles [3], Máximo Vento [1], David Hervás [4] and Consuelo Cháfer-Pericás [1,*]

1 Neonatal Research Unit, Health Research Institute La Fe, 46026 Valencia, Spain; carpebau93@gmail.com (C.P.-B.); maximo.vento@uv.es (M.V.)
2 Neurology Unit, University and Polytechnic Hospital La Fe, 46026 Valencia, Spain; miquelbaquero@gmail.com
3 Analytical Unit Platform, Health Research Institute La Fe, 46026 Valencia, Spain; marina_lopez@iislafe.es
4 Biostatistical Unit, Health Research Institute La Fe, 46026 Valencia, Spain; bioestadistica@iislafe.es
* Correspondence: m.consuelo.chafer@uv.es; Tel.: +34-96-124-67-21

Received: 16 April 2020; Accepted: 7 May 2020; Published: 10 May 2020

check for updates

Abstract: Previous studies showed a relationship between lipid oxidation biomarkers from plasma samples and Alzheimer's Disease (AD), constituting a promising diagnostic tool. In this work we analyzed whether these plasma biomarkers could reflect specific brain oxidation in AD. In this work lipid peroxidation compounds were determined in plasma and cerebrospinal fluid (CSF) samples from AD and non-AD (including other neurological pathologies) participants, by means of an analytical method based on liquid chromatography coupled with mass spectrometry. Statistical analysis evaluated correlations between biological matrices. The results did not show satisfactory correlations between plasma and CSF samples for any of the studied lipid peroxidation biomarkers (isoprostanes, neuroprostanes, prostaglandines, dihomo-isoprostanes). However, some of the analytes showed correlations with specific CSF biomarkers for AD and with neuropsychological tests (Mini-Mental State Examination (MMSE), Repeatable Battery for the Assessment of Neuropsychological Status (RBANS)). In conclusion, lipid peroxidation biomarkers in CSF samples do not reflect their levels in plasma samples, and no significant differences were observed between participant groups. However, some of the analytes could be useful as cognitive decline biomarkers.

Keywords: Alzheimer's disease; cerebrospinal fluid; biomarker; lipid peroxidation; mass spectrometry; blood-brain barrier

1. Introduction

Alzheimer's Disease (AD) is the main cause of dementia worldwide and one of the most important causes of death in elderly people [1]. The demographic change in population highlights a possible increase in the impact of this pathology on society and the economy [2]. AD is characterized mainly by memory loss and progressive cognitive impairments that ends up incapacitating patients and prevent them from participating in the activities of daily life [3]. Histologically, AD is characterized by an intracellular and extracellular accumulation of phosphorylated tau (p-Tau) and β-amyloid proteins in neurons that leads to synapse loss [4]. However, the complete physiopathological mechanisms of the pathology are not completely understand.

Different metabolites from cerebrospinal fluid (CSF) samples have been studied as potential AD diagnosis biomarkers in order to improve the diagnosis accuracy of amyloid, total Tau (t-Tau) and p-Tau levels. In fact, α-synuclein determination complements actual AD biomarkers and allows to distinguish between mild cognitive impairment (MCI) due to AD and other MCI causes with better

accuracy [5]. Furthermore, synaptosomal-associated protein-25 (SNAP-25), visinin-like protein 1 (VILIP-1), and chitinase3-like protein 1 (YKL-40) were altered at very early stages of the pathology [6], and cholecystokinin was related to a lower likelihood of MCI and better neuropsychological status [7]. However, CSF is obtained by means of a painful procedure that is not advisable for some individuals and it is not considered a population screening test. Nowadays, there is a growing field that is trying to find biomarkers in other biological fluids that could reflect brain damage from the disease [8]. Moreover, different authors found a correlation between biomarkers from CSF and plasma samples [9]. However, the correlation between these two biofluids for analytes (e.g., amyloid-β) is not clear and could depend on the analytical techniques used, as well as the effects of transportation through the brain-blood barrier (BBB) [10].

Neurodegenerative disorders show an important relationship with some oxidative stress mechanisms, especially lipid peroxidation [11]. In this sense, products originating from damage to lipid components of cellular membranes have been detected in the AD brain [12]. In addition, impaired lipid peroxidation levels have been found in peripheral fluids [13,14], offering an important step forward in non-invasive diagnosis [15]. Nevertheless, the interaction between the release of lipid peroxidation compounds by the central nervous system (CNS) and peripheral levels has not been evaluated.

The aim of this study was to measure a new set of lipid peroxidation products in CSF samples, and to evaluate their capacity to reflect neurodegeneration (correlation with amyloid and tau biomarker levels) and neuropsychological status (correlation with neuropsychological tests). In addition, we tried to establish a correlation between CSF and plasma lipid peroxidation biomarker levels in order to evaluate the latter as minimally invasive diagnosis biomarkers.

2. Materials and Methods

2.1. Study Design and Participants

The study protocol was approved by the Ethics Committee (CEIC) of the Health Research Institute La Fe (Valencia, Spain), (project reference number 2016/0257), and informed consent was obtained from all participants. Participants were recruited from the Neurology Unit at the University and Polytechnic Hospital La Fe (Valencia, Spain). Seventy-six patients aged between 50 and 75 years were included in the study. They were classified as AD (including mild cognitive impairment due to AD (MCI) and mild to moderate dementia due to AD) and non-AD (healthy controls and other dementias and cognitive impairments not caused by AD) groups. For this, they were subjected to neuropsychological tests (Repeatable Battery for the Assessment of Neuropsychological Status (RBANS), Clinical Dementia Rating (CDR), Mini-Mental State Examination (MMSE), Functional Activities Questionnaire (FAQ)) [16–19], structural neuroimaging by means of magnetic resonance imaging (MRI) or computerized axial tomography (CAT) [20], and CSF biomarkers (β-amyloid peptide (Aβ), t-Tau, p-Tau) [21,22]. The AD group was characterized by positive levels of Aβ, t-Tau and p-Tau and altered levels for neuropsychological evaluation by RBANS scale. In the non-AD group, participants with negative CSF biomarkers (Aβ, t-Tau and p-Tau) were included.

2.2. Samples Analysis

CSF samples (n = 76) were obtained by lumbar puncture as part of the diagnostic protocol in the Polytechnic University Hospital La Fe (Valencia, Spain), and they were kept at –80 °C. The analysis consisted of samples thawing on ice and adding 5 µL of the internal standard solution (IS) (d_4-10-*epi*-10-F_{4t}-NeuroP at 6 µmol L^{-1}, and PGF2α-d_4 at 10 µmol L^{-1}) to 600 µL CSF, and they were diluted with 1300 µL of water. Then, a cleaning and pre-concentration step was carried out by solid-phase extraction (SPE) as described previously [14,15]. Briefly, the cartridges were conditioned (1 mL methanol and 1 mL H_2O), then the samples were loaded, after that cartridges were washed (1 mL ammonium acetate (100 mmol L^{-1}, pH 7) and 1 mL heptane). Finally, analytes were eluted (2 × 500 µL of methanol (5% v/v CH_3COOH)). Then, samples were evaporated to dryness (vacuum evaporator)

and reconstituted (100 µL of H_2O (pH 3):CH_3OH (85:15 *v/v*) with 0.01% (*v/v*) CH_3COOH) to be injected into ultra-performance liquid chromatography coupled to tandem mass spectrometry (UPLC-MS/MS) (Waters Acquity UPLC-Xevo TQD system (Milford, MA, USA)).

Plasma samples from the same participants were analyzed by the method previously described by Peña-Bautista et al. [15].

2.3. Chromatographic System

The chromatographic system used consists of a Waters Acquity UPLC system coupled to a Xevo TQD system mass spectrometry system (Waters, United Kingdom). The HPLC conditions used were described in previous works [14,15].

2.4. Statistical Analysis

Differences between groups for numerical variables were analyzed by the Mann-Whitney test using SPSS version 20.0 software (SPSS, Inc., Chicago, IL, USA) and the values were expressed as median and interquartile range (IQR). Categorical variables were analyzed by the chi-square test. Finally, correlations among the biomarkers, as well as between the biofluids were analyzed by Pearson Correlation.

3. Results

3.1. Participants' Characteristics

The clinical and demographic characteristics of the population are summarized in Table 1. There were no differences between groups for age and gender. By contrast, CSF biomarkers (Aβ, t-Tau and p-Tau) showed statistically significant differences between participant groups as was expected. The CSF Aβ levels were lower in the AD than in the non-AD patients. It could be explained by the aggregation of Aβ in the brain, hindering its transport to the CSF [23]. Similarly, the neuropsychological status (RBANS, MMSE, FAQ) showed differences between the groups while CDR did not show differences.

3.2. Correlation between CSF Isoprostanoids and Standard CSF Biomarkers

We analyzed possible correlations between the different isoprostanoids families (isoprostanes, neuroprotanes, dihomo-isoprostanes) (Figure S1), and CSF AD-specific biomarkers (Aβ, t-Tau, p-Tau) in order to establish a possible relationship between oxidative stress (brain grey and white matter damage) and amyloid pathology. Table 2 shows that Aβ correlates negatively with 7(*RS*)-ST-Δ^8-11-dihomo-IsoF, 5-F_{2t}-IsoP, total neurofurans and isofurans. In addition, p-Tau showed negative correlation with PGE_2.

3.3. Correlations between CSF Isoprostanoids and Neuropsychological Evaluation

Regarding correlations between the isoprostanoids biomarkers and neuropsychological evaluation of the participants, Table 2 shows that RBANS and especially its visuospatial/constructional domain showed correlations with 15-F_{2t}-IsoP, Ent-7(*RS*)-F_{2t}-dihomo-IsoP and 15-keto-15-F_{2t}-IsoP. The latter also showed correlation with the RBANS attention domain and with MMSE. Moreover, 15-keto-15-E_{2t}-IsoP correlated with FAQ and CDR scores.

Table 1. Demographic and clinical variables of the study participants.

Variables	Non-AD (n = 34) [$]	AD (n = 42)	p-Value (Mann-Whitney)
Age (years) Median (IQR)	66 (63, 72)	70 (68, 73)	0.102
Gender (Female) (n, %))	17 (50%)	28 (67%)	0.142
CSF β-amyloid (pg mL^{-1}) Median (IQR)	1236.50 (950, 1435)	630 (535, 735)	0.000 *
CSF t-Tau (pg mL^{-1}) Median (IQR)	230 (159, 347)	573 (436, 1005)	0.000 *
CSF p-Tau (pg mL^{-1}) Median (IQR)	47 (32, 61)	86 (71, 122)	0.000 *
CDR Median (IQR)	0.5 (0, 0.5)	0.5 (0.5, 1)	0.071
MMSE Median (IQR)	27 (21, 28)	24 (18, 25)	0.004 *
RBANS.IM Median (IQR)	73 (69, 90)	57 (40, 67)	0.000 *
RBANS.V/C Median (IQR)	87 (75, 100)	75 (57, 87)	0.016 *
RBANS.L Median (IQR)	85 (60, 92)	60 (51, 82)	0.031 *
RBANS.A Median (IQR)	79 (60, 88)	60 (49, 79)	0.004 *
RBANS.DM Median (IQR)	68 (56, 88)	40 (40, 53)	0.000 *
FAQ Median (IQR)	3 (0, 8)	7 (3, 13)	0.015 *

* $p < 0.05$; IQR: inter-quartile range; RBANS.IM: Repeatable Battery for the Assessment of Neuropsychological Status–Immediate Memory; RBANS.V/C: RBANS–Visuospatial/Constructional; RBANS.L: RBANS–Language; RBANS.A: RBANS–Attention; RBANS.DM: RBANS–Delayed Memory; CDR: Clinical Dementia Rating values; FAQ: Functional Activities Questionnaire; CSF: cerebrospinal fluid. [$] The non-AD group is composed of healthy controls (n = 4) and other dementias and cognitive impairments not caused by AD (n = 30).

Table 2. Correlations between CSF isoprostanoids and clinical variables (standard CSF biomarkers, neuropsychological evaluation).

Correlations		CSF Aβ	CSF t-Tau	CSF p-Tau	CDR	MMSE	RBANS.IM	RBANS.V/C	RBANS.L	RBANS.A	RBANS.DM	FAQ
15(*R*)-15-F_{2t}-IsoP	PCC	0.196	0.094	0.032	0.038	0.159	0.030	0.124	0.031	0.147	0.022	0.076
	p-value	0.089	0.419	0.783	0.770	0.226	0.818	0.341	0.811	0.262	0.865	0.561
PGE_2	PCC	0.013	−0.205	−0.267	−0.031	0.095	0.136	0.043	0.219	0.106	0.061	−0.044
	p-value	0.908	0.076	0.020 *	0.811	0.471	0.298	0.743	0.092	0.418	0.643	0.738
2,3-dinor-15-epi-15-F_{2t}-IsoP	PCC	−0.107	0.128	0.100	−0.047	0.081	0.010	0.021	0.019	0.074	−0.122	−0.025
	p-value	0.358	0.272	0.391	0.724	0.538	0.939	0.873	0.887	0.574	0.352	0.852
15-keto-15-E_2-IsoP	PCC	−0.088	−0.074	−0.015	0.297	−0.181	−0.113	−0.054	−0.037	−0.101	−0.120	0.275
	p-value	0.449	0.524	0.897	0.021 *	0.167	0.391	0.709	0.782	0.442	0.361	0.034 *
15-keto-15-F_{2t}-IsoP	PCC	−0.109	−0.107	−0.101	−0.117	0.259	0.149	0.344	0.216	0.280	0.019	−0.230
	p-value	0.350	0.359	0.385	0.374	0.045 *	0.254	0.007 *	0.097	0.030 *	0.884	0.077
15-E_2-IsoP	PCC	−0.106	0.039	0.108	−0.137	0.072	0.088	−0.017	−0.047	0.146	0.051	−0.085
	p value	0.360	0.741	0.353	0.296	0.587	0.514	0.893	0.724	0.265	0.697	0.517
8-F_{2t}-IsoP	PCC	−0.242	−0.031	0.020	−0.005	0.103	−0.175	−0.029	−0.101	−0.032	−0.067	−0.050
	p value	0.033 *	0.789	0.866	0.967	0.435	0.181	0.850	0.444	0.808	0.613	0.703
15-F_{2t}-IsoP	PCC	−0.011	−0.068	−0.024	0.038	0.120	−0.022	0.263	−0.051	0.178	−0.007	−0.058
	p-value	0.903	0.562	0.834	0.775	0.360	0.870	0.041 *	0.699	0.173	0.959	0.659
$PGF_{2\alpha}$	PCC	−0.171	0.022	0.051	−0.075	0.031	−0.113	−0.138	−0.066	−0.070	−0.127	−0.097
	p-value	0.140	0.849	0.660	0.569	0.814	0.390	0.292	0.615	0.595	0.332	0.459
4(*RS*)-F_4t-NeuroP	PCC	−0.018	−0.167	−0.130	−0.175	−0.019	0.109	−0.078	0.052	−0.123	−0.060	−0.119
	p-value	0.877	0.150	0.263	0.181	0.709	0.406	0.554	0.532	0.348	0.647	0.356
10-epi-10-F_4t-NeuroP	PCC	−0.106	−0.045	−0.017	0.103	0.048	−0.077	0.068	−0.108	0.098	−0.047	0.013
	p-value	0.361	0.699	0.895	0.434	0.717	0.557	0.606	0.417	0.455	0.720	0.912
14(*RS*)-14-F_4t-NeuroP	PCC	0.017	−0.167	−0.124	−0.074	0.071	0.029	−0.006	−0.006	0.135	0.105	−0.150
	p-value	0.886	0.150	0.284	0.574	0.591	0.824	0.965	0.962	0.304	0.423	0.252
Ent-7(*RS*)-7-F_{2t}-dihomo-IsoP	PCC	−0.004	−0.081	−0.086	−0.030	0.186	0.053	0.349	0.011	0.240	−0.066	−0.173
	p-value	0.974	0.487	0.462	0.797	0.156	0.679	0.006 *	0.931	0.065	0.615	0.186
17-F_{2t}-dihomo-IsoP	PCC	0.010	0.086	0.056	0.009	0.026	0.099	0.153	0.139	0.017	0.102	0.053
	p-value	0.935	0.460	0.760	0.947	0.842	0.451	0.242	0.290	0.899	0.440	0.688
17-epi-17-F_{2t}-dihomo-IsoP	PCC	0.003	0.079	0.073	0.006	0.012	0.129	0.076	0.180	0.034	0.014	0.018
	p-value	0.982	0.497	0.530	0.963	0.928	0.326	0.561	0.168	0.797	0.914	0.893

Table 2. *Cont.*

Correlations		CSF Aβ	CSF t-Tau	CSF p-Tau	CDR	MMSE	RBANS.IM	RBANS.V/C	RBANS.L	RBANS.A	RBANS.DM	FAQ
17(RS)-10-epi-SC-A^{15}-11-dihomo-IsoF	PCC	0.093	0.014	0.012	0.055	0.226	0.026	0.170	0.054	0.242	0.156	0.014
	p-value	0.422	0.901	0.916	0.675	0.083	0.847	0.191	0.653	0.062	0.233	0.913
7(RS)-ST-A^{9}-11-dihomo-IsoF	PCC	−0.262	0.030	0.035	0.048	−0.030	−0.155	−0.041	−0.230	−0.110	−0.029	0.131
	p-value	0.022 *	0.797	0.765	0.715	0.821	0.238	0.761	0.077	0.405	0.825	0.318
Isoprostanes [$]	PCC	−0.196	−0.022	−0.010	−0.085	0.004	−0.150	−0.238	−0.193	−0.141	−0.040	0.070
	p-value	0.089	0.852	0.863	0.520	0.976	0.253	0.067	0.139	0.284	0.761	0.940
Neuroprostanes [$]	PCC	−0.001	−0.011	−0.005	0.102	−0.019	−0.077	0.207	−0.029	0.055	0.028	−0.026
	p-value	0.995	0.924	0.775	0.437	0.883	0.556	0.113	0.823	0.678	0.851	0.841
Neurofurans [$]	PCC	−0.246	−0.032	0.019	−0.159	0.142	0.122	−0.008	−0.013	0.093	0.135	−0.057
	p-value	0.032 *	0.784	0.871	0.224	0.278	0.353	0.953	0.920	0.481	0.304	0.667
Isofurans [$]	PCC	−0.309	0.013	0.062	−0.098	−0.051	−0.120	−0.084	−0.083	−0.085	−0.132	0.040
	p-value	0.007 *	0.914	0.595	0.458	0.698	0.359	0.523	0.530	0.527	0.315	0.760

PCC: Pearson correlation coefficient; * $p < 0.05$; [$] Total parameters.

3.4. CSF and Plasma Lipid Peroxidation Biomarkers

A previous study described a diagnosis model for early AD based on the quantification of these isoprostanoid compounds in plasma samples. In the present study it was evaluated if these plasma levels reflected brain damage by means of the determination of the corresponding levels in CSF samples. In this sense, only 17(*RS*)-10-epi-SC-Δ^{15}-11-dihomo-IsoF showed correlation between both matrices (PCC = 0.248, $p = 0.031$). In addition, when we analysed the results separately for AD and non-AD groups, we found that the non-AD group showed correlations between the two matrices for 15(*R*)-15-F_{2t}-IsoP (PCC = 0.388, $p = 0.024$), 15-keto-15-F_{2t}-IsoP (PCC = 0.360, $p = 0.037$) and 5-F_{2t}-IsoP (PCC = 0.345, $p = 0.046$). However, these analytes did not show correlation between plasma and CSF samples in AD patients. In this AD group, 17-F_{2t}-dihomo-IsoP (PCC = 0.399, $p = 0.009$) and 17(*RS*)-10-epi-SC-Δ^{15}-11-dihomo-IsoF (PCC = 0.345, $p = 0.045$) showed correlation between CSF and plasma samples.

Table 3 shows the plasma levels of isoprostanoids biomarkers. Some metabolites showed statistically significant differences between the groups for 15(*R*)-15-F_{2t}-IsoP ($p < 0.001$), 2,3-dinor-15-epi-15-F_{2t}-IsoP ($p = 0.028$), 5-F_{2t}-IsoP ($p = 0.021$), 15-F_{2t}-IsoP ($p < 0.001$), $PGF_{2\alpha}$ ($p = 0.011$), neuroprostanes ($p = 0.029$), 10-epi-10-F_{4t}-NeuroP ($p < 0.001$), isoprostanes ($p < 0.001$), Ent-7(*RS*)-7-F_{2t}-dihomo-IsoP ($p < 0.001$), and 17-epi-17-F_{2t}-dihomo-IsoP ($p < 0.001$). However, none of the CSF compounds showed statistically significant differences between the AD and non-AD groups.

Table 3. Concentrations of lipid peroxidation biomarkers in plasma samples.

Concentration (nmol L^{-1})	Non-AD ($n = 34$)	AD ($n = 42$)	p-Value Mann-Whitney
15(*R*)-15-F_{2t}-IsoP Median (IQR)	0.075 (0, 0.231)	0.300 (0.188, 0.394)	<0.001 *
PGE_2 Median (IQR)	0.050 (0, 0.100)	0.038 (0, 0.125)	0.590
2,3-dinor-15-epi-15-F_{2t}-IsoP Median (IQR)	0 (0, 0)	0 (0, 0.006)	0.028 *
15-keto-15-E_{2t}-IsoP Median (IQR)	0.150 (0, 0.250)	0.163 (0, 0.325)	0.541
15-keto-15-F_{2t}-IsoP Median (IQR)	0.113 (0.044, 0.181)	0.225 (0.069, 0.331)	0.065
15-E_{2t}-IsoP Median (IQR)	0.200 (0.100, 0.325)	0.213 (0.019, 0.525)	0.900
5-F_{2t}-IsoP Median (IQR)	0.263 (0.056, 0.831)	0.700 (0.350, 1.125)	0.021 *
15-F_{2t}-IsoP Median (IQR)	0 (0, 0)	0.020 (0.009, 0.035)	<0.001 *
$PGF_{2\alpha}$ Median (IQR)	0.238 (0.044, 0.363)	0.413 (0.194, 0.706)	0.011 *
4(*RS*)-F_{4t}-NeuroP Median (IQR)	0 (0, 1.475)	1.100 (0.763, 1.425)	0.119
1a,1b-dihomo-$PGF_{2\alpha}$ Median (IQR)	0 (0, 0)	0 (0, 0)	0.219
10-epi-10-F_{4t}-NeuroP Median (IQR)	0.225 (0.175, 0.281)	0.079 (0.025, 0.175)	<0.001 *
14(*RS*)-14-F_{4t}-NeuroP Median (IQR)	0.300 (0.019, 0.850)	0.563 (0.131, 1.044)	0.316
Ent-7(*RS*)-7-F_{2t}-dihomo-IsoP Median (IQR)	0 (0, 0.050)	0.075 (0.050, 0.150)	<0.001 *
17-F_{2t}-dihomo-IsoP Median (IQR)	0 (0, 0)	0 (0, 0)	0.096
17-epi-17-F_{2t}-dihomo-IsoP Median (IQR)	0 (0, 0)	0 (0, 0.025)	<0.001 *
17(*RS*)-10-epi-SC-Δ^{15}-11-dihomo-IsoF Median (IQR)	0 (0, 0)	0 (0, 0)	0.066
7(*RS*)-ST-Δ^{8}-11-dihomo-IsoF Median (IQR)	0.013 (0, 0.050)	0.025 (0, 0.075)	0.098
Isoprostanes [$] Median (IQR)	0.449 (0.396, 0.488)	0.345 (0.234, 0.409)	<0.001 *
Neuroprostanes [$] Median (IQR)	0.142 (0.050, 0.207)	0 (0, 0.268)	0.029 *
Isofurans [$] Median (IQR)	0.073 (0.058, 0.105)	0.085 (0.069, 0.115)	0.202
Neurofurans [$] Median (IQR)	0.114 (0.082, 0.173)	0.093 (0, 0.169)	0.111

[$] Arbitrary units: intensity of signal units x (internal standard concentration, mg L^{-1}); * p-value < 0.05.

4. Discussion

The reliable determination of lipid peroxidation product levels in CSF samples from biologically defined groups (AD and non-AD), based on specific AD biomarkers, was carried out. A previous study showed that these biomarkers were useful to diagnose AD with high accuracy when they were measured in plasma samples [15]. Previous studies also showed an increase of CSF isoprostanes in AD patients when their levels were corrected by ventricular volume, and these levels correlated with other clinical variables [24]; although Dutis et al. did not find any differences for CSF isoprostanes between AD, MCI and healthy control groups [25]. Therefore, ventricular volume could affect the concentration measured in CSF samples and that could be the reason why no differences were found between participant groups with or without AD.

In the present work, although isoprostanoids did not show differences between AD and non-AD groups, some lipid peroxidation products determined in CSF correlated with CSF Aβ and p-Tau levels. These results are consistent with those obtained by Kuo et al. who did not find differences between AD and non-AD groups for CSF levels of F2-isoprostanes and F4-neuroprostanes, but showed correlations with these metabolites and CSF Aβ levels [26]. By contrast, Yao et al. found that 12(S)-hydroxyeicosatetraenoic (HETE) acid and 15(S)-HETE correlated with CSF tau but not with CSF β-amyloid [27]. As amyloid biomarkers are specific for AD, isoprostanes seem to be more specific for amyloid pathology and AD than other biomarkers, such as HETE.

In our study, there is a correlation between isoprostanoids, such as 15-keto-15-F_{2t}-IsoP, and cognitive impairments identified through MMSE scale examination. Similar results were obtained by Duits et al. that found a correlation between MMSE and F_2-isoprostanes in ApoE ε4 carriers [25]. Moreover, Kester et al. did not find differences for CSF isoprostanes levels between non-demented, MCI and AD patients, but these analytes showed an increase in the follow up of these participants showing an association with cognitive decline and MMSE examination [28]. In fact, CSF isoprostanes were described by de Leon et al. as good, not only in diagnosis, but also in AD progression study [29]. However, Yao et al. did not find any correlation between MMSE score and 12(S)-HETE and 15(S)-HETE, while in the present study 8-iso-15-keto-$PGF_{2\alpha}$ correlated with this neuropsychological status evaluation [27]. Therefore, ApoE ε4 could be another important variable that affects isoprostanes levels in CSF.

In this study, correlations between lipid peroxidation levels in CSF and plasma samples were not found. Similarly, plasma and CSF levels of other metabolites, such as neurogranin, did not show any correlation [30]. Moreover, Aβ42 measured in plasma and CSF samples did not show any correlation [31], while Mehta et al. did not find correlation for Aβ40 and Aβ42 between these two biofluids [32]. However, Sun et al. studied correlations between different analytes such as α(1)-antichymotrypsin (ACT), α(1)-antitrypsin (AAT), interleukin-6 (IL-6), monocyte chemoattractant protein-1 (MCP-1) and oxidised low-density lipoprotein (oxLDL) between plasma and CSF samples. They found correlations for ACT, IL-6, MCP-1 and oxLDL, the latter showing a weaker correlation [33]. In addition, other analytes, such as adiponectin showed a correlation between these two matrices [34]. Moreover, different metabolites from the kyneurine pathway showed correlation between plasma and CSF samples, some showing a relationship with other CSF biomarkers (t-Tau, p-Tau) [9]. Therefore, metabolites exchange between BBB is not always equal, and concentrations between both biofluids could show differential distribution depending on the metabolite characteristics. As a hypothesis, CSF is continuously filtrating, so isoprotanes are not accumulated in this fluid, and the analyte concentrations in CSF are dependent on ventricular volume. By contrast, metabolites accumulating in the blood system for longer could be more easily measured. Previous studies showed that BBB permeability is increased under pathologic conditions, such as AD [35,36], and this permeability depends on inflammatory processes [37]. BBB alteration in AD could be responsible for the differences in correlation between plasma and CSF levels of different analytes in AD and non-AD. In addition, ventricular volume could influence the concentration of different metabolites in CSF, so corrections to this volume could result in a better correlation between plasma and CSF levels.

5. Conclusions

New lipid peroxidation biomarkers were satisfactorily measured in CSF samples from participants with AD and without AD (including healthy controls and other neurological pathologies) by an analytical method based on HPLC-MS/MS. These CSF metabolites are not able to discriminate between AD and non-AD groups, although some of them correlate with neuropsychological evaluations, as well as standard AD CSF biomarkers (β-amyloid, p-Tau). On the other hand, the levels of each isoprostanoid in plasma and CSF did not show correlation. It could be that changes in the transportation of substances through the BBB, the clearance of these compounds did not allow their accumulation and quantification in CSF, due to the necessity to correct CSF biomarker levels with ventricular volume. However, the CSF isoprostanoids levels could be useful in the evaluation of cognitive capacity.

Supplementary Materials: The following are available online at http://www.mdpi.com/2076-3921/9/5/407/s1, Figure S1: Chemical structures of isoprostanes, dihomo-isoprostanes, and neuroprostanes.

Author Contributions: Conceptualization, C.C.-P.; data curation, C.P.-B., M.B. and C.C.-P.; formal analysis, C.P.-B. and M.L.-N.; funding acquisition, C.C.-P.; investigation, C.P.-B., M.B., M.L.-N. and C.C.-P.; methodology, C.P.-B. and M.B.; project administration, C.C.-P.; resources, C.C.-P.; software, D.H.; supervision, M.B., M.V. and C.C.-P.; validation, D.H. and C.C.-P.; visualization, C.P.-B., M.B. and M.V.; writing—original draft, C.P.-B. and M.B.; writing—review and editing, C.P.-B., M.B., M.V. and C.C.-P. All authors have read and agreed to the published version of the manuscript.

Funding: This work was supported by the Instituto de Salud Carlos III (Miguel Servet I Project (CP16/00082) (Spanish Ministry of Economy and Competitiveness).

Acknowledgments: We are greatly indebted to all participants, nursing, psychology, and medical staff who voluntarily participated in the present study. Authors acknowledge Durand's team for the synthesis of the standards employed in the analysis. C.C.-P. acknowledges a "Miguel Servet I" Grant (CP16/00082) from the Instituto Carlos III (ISCIII, Spanish Ministry of Economy and Competitiveness). C.P.-B. acknowledges a pre-doctoral Grant (associated to "Miguel Servet" project CP16/00082) from the Instituto Carlos III (Spanish Ministry of Economy, Industry and Competitiveness).

Conflicts of Interest: The authors declare no conflict of interest.

References

1. Kramarow, E.A.; Tejada-Vera, B. Dementia Mortality in the United States, 2000–2017. *Natl. Vital Stat. Rep.* **2019**, *68*, 1–29. [PubMed]
2. Alzheimer's Association. 2016 Alzheimer's disease facts and figures. *Alzheimers. Dement.* **2016**, *12*, 459–509. [CrossRef] [PubMed]
3. WHO. *Dementia*; WHO: Geneva, Switzerland, 2019.
4. Bloom, G.S. Amyloid-β and Tau. *JAMA Neurol.* **2014**, *71*, 505. [CrossRef] [PubMed]
5. García-Ayllón, M.S.; Monge-Argilés, J.A.; Monge-García, V.; Navarrete, F.; Cortés-Gómez, M.A.; Sánchez-Payá, J.; Manzanares, J.; Gasparini-Berenguer, R.; Leiva-Santana, C.; Sáez-Valero, J. Measurement of CSF α-synuclein improves early differential diagnosis of mild cognitive impairment due to Alzheimer's disease. *J. Neurochem.* **2019**, *150*, 218–230. [CrossRef]
6. Schindler, S.E.; Li, Y.; Todd, K.W.; Herries, E.M.; Henson, R.L.; Gray, J.D.; Wang, G.; Graham, D.L.; Shaw, L.M.; Trojanowski, J.Q.; et al. Emerging cerebrospinal fluid biomarkers in autosomal dominant Alzheimer's disease. *Alzheimer's Dement.* **2019**, *15*, 655–665. [CrossRef]
7. Plagman, A.; Hoscheidt, S.; McLimans, K.E.; Klinedinst, B.; Pappas, C.; Anantharam, V.; Kanthasamy, A.; Willette, A.A. Cholecystokinin and Alzheimer's disease: A biomarker of metabolic function, neural integrity, and cognitive performance. *Neurobiol. Aging* **2019**, *76*, 201–207. [CrossRef]
8. Kim, M.; Snowden, S.; Suvitaival, T.; Ali, A.; Merkler, D.J.; Ahmad, T.; Westwood, S.; Baird, A.; Proitsi, P.; Nevado-Holgado, A.; et al. Primary fatty amides in plasma associated with brain amyloid burden, hippocampal volume, and memory in the European Medical Information Framework for Alzheimer's Disease biomarker discovery cohort. *Alzheimer's Dement.* **2019**, *15*, 817–827. [CrossRef]
9. Jacobs, K.R.; Lim, C.K.; Blennow, K.; Zetterberg, H.; Chatterjee, P.; Martins, R.N.; Brew, B.J.; Guillemin, G.J.; Lovejoy, D.B. Correlation between plasma and CSF concentrations of kynurenine pathway metabolites in Alzheimer's disease and relationship to amyloid-β and tau. *Neurobiol. Aging* **2019**, *80*, 11–20. [CrossRef]

10. Teunissen, C.E.; Chiu, M.-J.; Yang, C.-C.; Yang, S.-Y.; Scheltens, P.; Zetterberg, H.; Blennow, K. Plasma Amyloid-β (Aβ42) Correlates with Cerebrospinal Fluid Aβ42 in Alzheimer's Disease. *J. Alzheimer's Dis.* **2018**, *62*, 1857–1863. [CrossRef]
11. Shamoto-Nagai, M.; Hisaka, S.; Naoi, M.; Maruyama, W. Modification of α-synuclein by lipid peroxidation products derived from polyunsaturated fatty acids promotes toxic oligomerization: Its relevance to Parkinson disease. *J. Clin. Biochem. Nutr.* **2018**, *62*, 207–212. [CrossRef]
12. Sultana, R.; Perluigi, M.; Butterfield, D.A. Lipid peroxidation triggers neurodegeneration: A redox proteomics view into the Alzheimer disease brain. *Free Radic. Biol. Med.* **2013**, *62*, 157–169. [CrossRef] [PubMed]
13. Tsou, H.-H.; Hsu, W.-C.; Fuh, J.-L.; Chen, S.-P.; Liu, T.-Y.; Wang, H.-T. Alterations in Acrolein Metabolism Contribute to Alzheimer's Disease. *J. Alzheimer's Dis.* **2017**, *61*, 571–580. [CrossRef] [PubMed]
14. García-Blanco, A.; Peña-Bautista, C.; Oger, C.; Vigor, C.; Galano, J.-M.; Durand, T.; Martín-Ibáñez, N.; Baquero, M.; Vento, M.; Cháfer-Pericás, C. Reliable determination of new lipid peroxidation compounds as potential early Alzheimer Disease biomarkers. *Talanta* **2018**, *184*, 193–201. [CrossRef]
15. Peña-Bautista, C.; Vigor, C.; Galano, J.-M.; Oger, C.; Durand, T.; Ferrer, I.; Cuevas, A.; López-Cuevas, R.; Baquero, M.; López-Nogueroles, M.; et al. Plasma lipid peroxidation biomarkers for early and non-invasive Alzheimer Disease detection. *Free Radic. Biol. Med.* **2018**, *124*, 388–394. [CrossRef] [PubMed]
16. Randolph, C.; Tierney, M.C.; Mohr, E.; Chase, T.N. The Repeatable Battery for the Assessment of Neuropsychological Status (RBANS): Preliminary clinical validity. *J. Clin. Exp. Neuropsychol.* **1998**, *20*, 310–319. [CrossRef] [PubMed]
17. Pfeffer, R.I.; Kurosaki, T.T.; Harrah, C.H.; Chance, J.M.; Filos, S. Measurement of functional activities in older adults in the community. *J. Gerontol.* **1982**, *37*, 323–329. [CrossRef]
18. Hughes, C.P.; Berg, L.; Danziger, W.; Coben, L.A.; Martin, R.L. A new clinical scale for the staging of dementia. *Br. J. Psychiatry* **1982**, *140*, 566–572. [CrossRef]
19. Folstein, M.F.; Folstein, S.E.; McHugh, P.R. Mini-mental state. *J. Psychiatr. Res.* **1975**, *12*, 189–198. [CrossRef]
20. Frisoni, G.B.; Fox, N.C.; Jack, C.R.; Scheltens, P.; Thompson, P.M. The clinical use of structural MRI in Alzheimer disease. *Nat. Rev. Neurol.* **2010**, *6*, 67–77. [CrossRef]
21. Anoop, A.; Singh, P.K.; Jacob, R.S.; Maji, S.K. CSF Biomarkers for Alzheimer's Disease Diagnosis. *Int. J. Alzheimers. Dis.* **2010**, *2010*, 1–12. [CrossRef]
22. Blennow, K.; Dubois, B.; Fagan, A.M.; Lewczuk, P.; de Leon, M.J.; Hampel, H. Clinical utility of cerebrospinal fluid biomarkers in the diagnosis of early Alzheimer's disease. *Alzheimer's Dement.* **2015**, *11*, 58–69. [CrossRef] [PubMed]
23. Spies, P.E.; Verbeek, M.M.; van Groen, T.; Classeen, J.A. Reviewing reasons for the decreased CSF Abeta42 concentration in Alzheimer disease. *Front Biosci (Landmark Ed).* **2012**, *17*, 2024–2034. [CrossRef] [PubMed]
24. Quinn, J.F.; Montine, K.S.; Moore, M.; Morrow, J.D.; Kaye, J.A.; Montine, T.J. Suppression of longitudinal increase in CSF F2-isoprostanes in Alzheimer's disease. *J. Alzheimer's Dis.* **2004**, *6*, 93–97. [CrossRef] [PubMed]
25. Duits, F.H.; Kester, M.I.; Scheffer, P.G.; Blankenstein, M.A.; Scheltens, P.; Teunissen, C.E.; van der Flier, W.M. Increase in Cerebrospinal Fluid F2-Isoprostanes is Related to Cognitive Decline in APOE ε4 Carriers. *J. Alzheimer's Dis.* **2013**, *36*, 563–570. [CrossRef]
26. Kuo, H.-C.; Yen, H.-C.; Huang, C.-C.; Hsu, W.-C.; Wei, H.-J.; Lin, C.-L. Cerebrospinal fluid biomarkers for neuropsychological symptoms in early stage of late-onset Alzheimer's disease. *Int. J. Neurosci.* **2015**, *125*, 747–754. [CrossRef]
27. Yao, Y.; Clark, C.M.; Trojanowski, J.Q.; Lee, V.M.-Y.; Praticò, D. Elevation of 12/15 lipoxygenase products in AD and mild cognitive impairment. *Ann. Neurol.* **2005**, *58*, 623–626. [CrossRef]
28. Kester, M.I.; Scheffer, P.G.; Koel-Simmelink, M.J.; Twaalfhoven, H.; Verwey, N.A.; Veerhuis, R.; Twisk, J.W.; Bouwman, F.H.; Blankenstein, M.A.; Scheltens, P.; et al. Serial CSF sampling in Alzheimer's disease: Specific versus non-specific markers. *Neurobiol. Aging* **2012**, *33*, 1591–1598. [CrossRef]
29. Leon, M.J.; Mosconi, L.; Li, J.; Santi, S.; Yao, Y.; Tsui, W.H.; Pirraglia, E.; Rich, K.; Javier, E.; Brys, M.; et al. Longitudinal CSF isoprostane and MRI atrophy in the progression to AD. *J. Neurol.* **2007**, *254*, 1666–1675. [CrossRef]
30. De Vos, A.; Jacobs, D.; Struyfs, H.; Fransen, E.; Andersson, K.; Portelius, E.; Andreasson, U.; De Surgeloose, D.; Hernalsteen, D.; Sleegers, K.; et al. C-terminal neurogranin is increased in cerebrospinal fluid but unchanged in plasma in Alzheimer's disease. *Alzheimer's Dement.* **2015**, *11*, 1461–1469. [CrossRef]

31. Le Bastard, N.; Aerts, L.; Leurs, J.; Blomme, W.; De Deyn, P.P.; Engelborghs, S. No correlation between time-linked plasma and CSF Aβ levels. *Neurochem. Int.* **2009**, *55*, 820–825. [CrossRef]
32. Mehta, P.; Pirttila, T.; Patrick, B.; Barshatzky, M.; Mehta, S. Amyloid β protein 1–40 and 1–42 levels in matched cerebrospinal fluid and plasma from patients with Alzheimer disease. *Neurosci. Lett.* **2001**, *304*, 102–106. [CrossRef]
33. Sun, Y.-X.; Minthon, L.; Wallmark, A.; Warkentin, S.; Blennow, K.; Janciauskiene, S. Inflammatory Markers in Matched Plasma and Cerebrospinal Fluid from Patients with Alzheimer's Disease. *Dement. Geriatr. Cogn. Disord.* **2003**, *16*, 136–144. [CrossRef] [PubMed]
34. Une, K.; Takei, Y.A.; Tomita, N.; Asamura, T.; Ohrui, T.; Furukawa, K.; Arai, H. Adiponectin in plasma and cerebrospinal fluid in MCI and Alzheimer's disease. *Eur. J. Neurol.* **2011**, *18*, 1006–1009. [CrossRef] [PubMed]
35. Janelidze, S.; Hertze, J.; Nägga, K.; Nilsson, K.; Nilsson, C.; Wennström, M.; van Westen, D.; Blennow, K.; Zetterberg, H.; Hansson, O. Increased blood-brain barrier permeability is associated with dementia and diabetes but not amyloid pathology or APOE genotype. *Neurobiol. Aging* **2017**, *51*, 104–112. [CrossRef]
36. Algotsson, A.; Winblad, B. The integrity of the blood-brain barrier in Alzheimer's disease. *Acta Neurol. Scand.* **2007**, *115*, 403–408. [CrossRef] [PubMed]
37. Takeda, S.; Sato, N.; Ikimura, K.; Nishino, H.; Rakugi, H.; Morishita, R. Increased blood–brain barrier vulnerability to systemic inflammation in an Alzheimer disease mouse model. *Neurobiol. Aging* **2013**, *34*, 2064–2070. [CrossRef]

antioxidants

MDPI

Article

Clinical Utility of Plasma Lipid Peroxidation Biomarkers in Alzheimer's Disease Differential Diagnosis

Carmen Peña-Bautista [1], Lourdes Álvarez [2], Thierry Durand [3], Claire Vigor [3], Ana Cuevas [2], Miguel Baquero [2], Máximo Vento [1], David Hervás [4] and Consuelo Cháfer-Pericás [1,*]

1 Neonatal Research Unit, Health Research Institute La Fe, 46026 Valencia, Spain; carpebau@alumni.uv.es (C.P.-B.); maximo.vento@uv.es (M.V.)
2 Neurology Unit, University and Polytechnic Hospital La Fe, 46026 Valencia, Spain; lourdes.alvsa@gmail.com (L.A.); anais85@gmail.com (A.C.); miquelbaquero@gmail.com (M.B.)
3 Institut des Biomolécules Max Mousseron, IBMM, University of Montpellier, CNRS ENSCM, 34093 Montpellier, France; thierry.durand@umontpellier.fr (T.D.); claire.vigor@umontpellier.fr (C.V.)
4 Biostatistical Unit, Health Research Institute La Fe, 46026 Valencia, Spain; bioestadistica@iislafe.es
* Correspondence: m.consuelo.chafer@uv.es; Tel.: +34-961-246-721; Fax: +34-961-246-620

Received: 26 June 2020; Accepted: 21 July 2020; Published: 22 July 2020

Abstract: Background: Differential diagnosis of Alzheimer's disease (AD) is a complex task due to the clinical similarity among neurodegenerative diseases. Previous studies showed the role of lipid peroxidation in early AD development. However, the clinical validation of potential specific biomarkers in minimally invasive samples constitutes a great challenge in early AD diagnosis. Methods: Plasma samples from participants classified into AD (n = 138), non-AD (including MCI and other dementias not due to AD) (n = 70) and healthy (n = 50) were analysed. Lipid peroxidation compounds (isoprostanes, isofurans, neuroprostanes, neurofurans) were determined by ultra-performance liquid chromatography coupled with tandem mass spectrometry. Statistical analysis for biomarkers' clinical validation was based on Elastic Net. Results: A two-step diagnosis model was developed from plasma lipid peroxidation products to diagnose early AD specifically, and a bootstrap validated AUC of 0.74 was obtained. Conclusion: A promising AD differential diagnosis model was developed. It was clinically validated as a screening test. However, further external validation is required before clinical application.

Keywords: plasma; lipid peroxidation; Alzheimer's disease; differential diagnosis; clinical validation

1. Introduction

Alzheimer's disease (AD) is the dementia type with the highest incidence worldwide [1]. Its physiopathology is incompletely known and, although it has some specific features, it shares common clinical aspects and metabolic pathways with other neurodegenerative disorders [2]. So, finding specific AD biochemical features is not an easy task. The available therapeutic methods only achieve remarkable symptomatic relief when applied at an early stage. Therefore, clinical validation of potential, early, and specific AD biomarkers in minimally invasive samples is crucial to improve the disease prognosis.

Currently, standard specific AD diagnosis is based on the determination of protein peptides (β-amyloid42, tau), by immunoassay (ELISA technique), in invasively obtained cerebrospinal fluid sampling (CSF) and the expensive brain amyloid PET exams [3]. Recent research has focused on the identification of potential early biomarkers in minimally invasive samples. In general, these new methods show low AD specificity, and they have not been clinically validated [4–6]. In fact, a previous study in plasma samples showed high capacity discriminating between AD and healthy participants, but it did not evaluate other similar pathologies [4]. Moreover, few studies have focused on the preclinical

AD stage, asymptomatic step detected from CSF biomarkers. For instance, Eruysal et al. discriminated between preclinical AD and healthy participants [5]. In the AD mild cognitive impairment (MCI) stage, patients show cognitive impairment not altering their daily activities, while in mild dementia stage they show an inability to lead a normal life [7]. In this sense, Gao et al. demonstrated that a sensible detection of amyloid 42 peptide is able to differentiate between AD, MCI and healthy participants [8]. Inflammatory biomarkers also could differentiate between AD, MCI and healthy controls [9]. However, other pathologies were not assessed in order to establish the specificity in AD diagnosis.

The main AD histological hallmarks are extracellular senile plaques and neurofibrillary tangles [10]. The former is originated by the extracellular deposition of the accumulated amyloid-beta peptide (i.e., forty-two amino acid long amyloid-beta peptide [Aβ42]). At the same time, the latter is a consequence of intracellular accumulation of tau protein hyperphosphorylated [11]. In fact, it should be reported that cerebrospinal fluid (CSF) concentrations of Aβ42, total tau (t-tau), and hyperphosphorylated tau (p-tau) proteins have been validated as "core" biomarkers of AD pathophysiology. They are pathophysiological biomarkers of amyloid pathology, cortical axonal degeneration, and tangle pathology, respectively [12,13]. In addition, other mechanisms as inflammation or oxidative stress have been related to AD [14]. Specifically, previous studies have shown that lipid peroxidation is involved in the development of neurodegeneration [15]. In this sense, different products derived from lipid peroxidation (e.g., isoprostanes, thiobarbituric acid-reactive substances, fluorescent lipofuscin-like pigments) have been evaluated in different human samples for early AD diagnosis [16–18] and results have reflected the difficulty to develop an AD differential diagnosis with this kind of determinations [4].

Nowadays, substantial research has focused on the development of a specific and reliable biochemical AD diagnosis and significant efforts are currently ongoing aimed to enhancing the landscape of blood-based biomarkers for AD [19]. In this regard, some studies have aimed to a diagnosis looking for specific profiles in AD using a combination of several blood biomarkers [20]. Nevertheless, limited specificity was obtained over other neurodegenerative diseases, such as frontotemporal dementia [21,22], Parkinson's disease [23], or dementia with Lewy bodies (DLB) [24]. Moreover, most of the studies for differential diagnosis are based on CSF samples [25,26]. On the other hand, few studies have clinically validated the potential biomarkers [27]. However, no satisfactory results have been obtained, so further work is required in this line in order to establish new biomarkers which can be validated and applied to the clinical routine.

Therefore, the aim of this work is to develop an early AD diagnosis model, using minimally invasive samples such as plasma that allow a differential diagnosis from other similar neurological and neurodegenerative diseases with similar clinical symptoms. Moreover, we have carried out an internal validation that shows the potential clinical utility of some lipid peroxidation biomarkers in plasma for differential diagnosis of AD.

2. Materials and Methods

2.1. Study Design and Participants

Participants were aged between 50 and 75 years, and admitted to the Neurology Unit of the University and Polytechnic Hospital La Fe (Valencia, Spain). They were classified into AD group ($n = 138$), non-AD group ($n = 70$) and the healthy group ($n = 50$). The AD group included patients with MCI-AD and mild dementia due to AD who showed cognitive complaints without daily living activities impairment or with minor daily living activities impairment. The non-AD group included patients with MCI not due to AD, frontotemporal dementia, vascular dementia, or DLB. This classification was carried out according to a protocol described in Table 1 based on neuropsychological evaluation (clinical dementia rating (CDR), Repeatable Battery for the Assessment of Neuropsychological Status-Delayed Memory (RBANS.DM)), CSF biomarkers (ß-amyloid, Tau and phosphorylate Tau (p-Tau)), and neuroimaging (amyloid PET), following the National Institute on Aging-Alzheimer's Association (NIA-AA) recommendations [3].

Regarding exclusion criteria, patients with a history of structural brain disease (tumor, stroke, etc.), major head trauma, epilepsy, multiple sclerosis and major psychiatric disorders were excluded, as well as patients that were not able to undergo neuropsychological evaluations.

The study protocol (project reference number 2016/0257) was approved by the Ethics Committee (CEIC) from Health Research Institute La Fe (Valencia, Spain). The methods were carried out in accordance with relevant guidelines and regulations, and informed consent from all participants was obtained.

2.2. Lipid Peroxidation Componuds

Isoprostanes' standards were from Cayman Chemical Company (Ann Arbor, Michigan, USA) (15(*R*)-15-F_{2t}-IsoP, PGE_2, 2,3-dinor-iPF2 αIII, 15-keto-15-E_{2t}-IsoP, 15-keto-15-F_{2t}-IsoP, 15-E_{2t}-IsoP, 15-F_{2t}-IsoP, 5-F_{2t}-IsoP, $PGF_{2\alpha}$, 1a,1b-dihomo-$PGF_{2\alpha}$, or synthesized at the Institute of Biomolecules Max Mousseron (IBMM) (Montpellier, France) by Dr Durand's team (4(*RS*)-F_{4t}-NeuroP, 10-*epi*-10-F_{4t}-NeuroP, 14(*RS*)-14-F_{4t}-NeuroP, Ent-7(*RS*)-F_{2t}-dihomo-IsoP, 17-F_{2t}-dihomo-IsoP, 17-*epi*-17-F_{2t}-dihomo-IsoP, 17(*RS*)-10-*epi*-SC-Δ^{15}-11-dihomo-IsoF, 7(*RS*)-ST-Δ^{8}-11-dihomo-IsoF) [28].

2.3. Sample Treatment

Blood samples were centrifuged for 10 min at 2000 g and plasma samples were stored at −80 °C until the analysis. Samples were thawed on ice and 5 µL of the internal standard solution ($PGF_{2\alpha}$-D_4 2 µmol L^{-1} and D_4–10-epi-10-F_{4t}-NeroP 1.2 µmol L^{-1}) were added. Then, a basic hydrolysis with potassium hydroxide and a clean-up step with solid phase extraction (SPE) were carried out. Briefly, SPE was carried out using Strata X-AW cartridges, the procedure consisted on a cartridge conditioning step with methanol and H_2O, a sample loading, washing steps with ammonium acetate buffer (0.1 mol L^{-1}, pH 7) and heptane, and an elution step with 2 × 500 µL CH3OH (5% (*v*/*v*) acetic acid). Then samples were evaporated and reconstituted in 100 µL of H2O (0.01% acetic acid (*v*/*v*)):CH3OH (85:15 *v*/*v*). Finally, samples were injected in a chromatographic system, and they were analyzed by ultra-performance liquid chromatography coupled with tandem mass spectrometry (UPLC-MS/MS) [4].

2.4. UPLC-MS/MS

The analytical method consists of ultra-performance liquid chromatography coupled to tandem mass spectrometry (UPLC-MS/MS) described in a previous study [4]. Briefly, a Waters Acquity UPLC-Xevo TQD system (Milford, MA USA) and negative electrospray ionization (ESI) were used. The column employed was an Acquity UPLC BEH C18 (2.1 × 100 MM, 1.7 µm). The mobile phase was (A) water (0.01% *v*/*v* acetic acid) and (B) acetonitrile (0.01% acetic acid) [4]. The analytical method was validated in a previous study [4], showing linearity with confidence intervals of 0.990–0.99. In addition, inter-day and intra-day coefficients of variation were 5–13% and 2–11%, respectively.

2.5. Statistical Analysis

Variables distribution was studied using a Kolmogorov–Smirnov test. Data were summarized using median (1st, 3rd quartile) in the case of continuous variables and with relative and absolute frequencies in the case of categorical variables. A two-stage model for Alzheimer's disease diagnosis was developed by adjusting two nested logistic regression models. The first model was based on the discrimination capacity of the neuropsychological evaluation to differentiate between control and case (including AD and non-AD groups) participants. Specifically, the clinical variables RBANS.DM (Repeatable Battery for the Assessment of Neuropsychological Status. Delayed Memory) and CDR (Clinical Dementia Rating) were used as predictors in this first model. The second model was based on the discrimination capacity of lipid peroxidation products from plasma samples to differentiate between AD and non-AD patients in the case group. Specifically, the potential predictors in this second model were 15(*R*)-15-F_{2t}-IsoP, PGE_2, 2,3-dinor-i$PF_{2\alpha}$-III, 15-keto-15-E_{2t}-IsoP, 15-keto-15-F_{2t}-IsoP, 15-E_{2t}-IsoP, 5-F_{2t}-IsoP, 15-F_{2t}-IsoP, $PGF_{2\alpha}$, 1a,1b-dihomo-$PGF_{2\alpha}$, 4(*RS*)-F_{4t}-NeuroP, 10-*epi*-10-F_{4t}-NeuroP,

14(*RS*)-14-F_{4t}-NeuroP, Ent-7(*RS*)-F_{2t}-dihomo-IsoP, 17-F_{2t}-dihomo-IsoP, 17-*epi*-17-F_{2t}-dihomo-IsoP, 17(*RS*)-10-*epi*-SC-Δ^{15}-11-dihomo-IsoF, 7(*RS*)-ST-Δ^{8}-11-dihomo-IsoF, as well as the total parameters IsoP, IsoF and NeuroF. Selection of the final predictors in the model was performed using Elastic Net [29]. Performance of the model was assessed by estimating optimism-corrected AUC using 200 bootstrap replications. All statistical analyses were performed using R (version 3.6) and R packages pROC (version 1.14.0) and brms (version 2.8.0).

Table 1. Participants' classification attending to neuropsychological evaluation, neuroimage and cerebrospinal fluid biomarkers.

Tests	AD Group	Non-AD Group	Healthy Group
Neuropsychological tests			
CDR [30]	0.5–1	0.5–1	0
RBANS.DM [31]	≤85	≤85	>85
Neuroimage tests			
Amyloid PET	Positive	Negative	Negative
CSF biomarkers [32,33]			
β-amyloid (pg mL^{-1})	≤725	≥725	≥725
t-tau (pg mL^{-1})	≥85	≤85	≤85
p-tau (pg mL^{-1})	≥350	≤350	≤350

CDR: Clinical dementia rating; RBANS.DM: Repeatable Battery for the Assessment of Neuropsychological Status-Delayed Memory; CSF: cerebrospinal fluid; t-tau: total tau; p-tau: phosphorylated tau.

3. Results

The demographic and clinical data from the participants are summarized in Table 2. The clinical variables allowed to differentiate among participants groups. Specifically, the CSF biomarkers (ß-amyloid42, Tau, p-Tau) levels identify AD patients from control and non-AD participants. Moreover, the neuropsychological evaluation (RBANS.DM, CDR) identifies control participants.

Table 2. Clinical and demographic variables for the participants.

Variables	AD Group (*n* = 138)	Healthy Group (*n* = 50)	Non-AD Group (*n* = 70)
Age (years, median (IQR))	71 (68, 74)	67 (62, 69)	66 (62, 71)
Gender (female, *n* (%))	80 (59.7%)	19 (38.78%)	31 (48.44%)
RBANS.DM (median (IQR))	44 (40, 56)	100 (92, 106)	64 (52, 81)
CDR (median (IQR))	0.5 (0.5–1)	0 (0–0)	0.5 (0.5–1)
β-amyloid (pg mL^{-1}, median (IQR))	580 (464, 694)	1085 (924, 1308)	1049 (850, 1264)
t-Tau (pg mL^{-1}, median (IQR))	707 (428, 830)	255 (144, 313)	322 (190, 395)
p-Tau (pg mL^{-1}, median (IQR))	99 (71, 110)	47 (32, 60)	52 (34, 61)

The analytes concentrations found in plasma samples from participants groups are summarized in Table 3. All these variables showed non-normal distribution, so the non-parametric test (Kruskal–Wallis) was applied showing statistically significant differences among groups for some lipid peroxidation compounds (15-E2t-IsoP, PGF2α, 4(RS)-F4t-NeuroP, 10-epi-10-F4t-NeuroP, IsoP).

The first model, using these neuropsychological variables, was able to discriminate between control and patients. It achieved a very high accuracy, with an AUC of 0.99 and a bootstrap validated AUC of 0.99. These results show that separating control participants from case patients (AD, non-AD) is straightforward using standard neuropsychological evaluation tests. In Figure 1a, it can be seen that participants without any neurological or neurodegenerative disease (healthy participants) are grouped in the left and upper side, indicating higher RBANS.DM and lower CDR punctuations. The formula for this first prediction step is the following:

$$\Pr(Case/Control) = \frac{e^{9.25-0.13\times RBANS+22.71\times CDR}}{1+e^{9.25-0.13\times RBANS+22.71\times CDR}} \quad (1)$$

The second model, for discriminating between AD and non-AD patients in the case group included the variables 10-epi-10-F4t-NeuroP and IsoPs (Figure 1b), and it achieved an AUC of 0.79 and a bootstrap validated AUC of 0.74. Calibration of the model was satisfactory. It was assessed using bootstrapping and comparing predicted vs. obtained values, observing very low deviations. The formula for this final prediction step, to be applied only to the individuals predicted as patients (case) by the first step, is the following:

$$\Pr(AD/non-AD) = \frac{e^{-0.14+1.15\times log(IsoP_s)+2.24\times 10-epi-10-F4t-NeuroP}}{1+e^{-0.14+1.15\times log(IsoP_s)+2.24\times 10-epi-10-F4t-NeuroP}} \quad (2)$$

Table 3. Analytes concentrations in plasma samples from participants groups.

Variable Median (IQR) (nmol L^{-1})	AD Group (n = 138)	Healthy Group (n = 50)	Non-AD Group (n = 70)	P-Value (Kruskal–Wallis)
	Median (IQR)	Median (IQR)	Median (IQR)	
15(R)-15-F_{2t}-IsoP	0.21 (0.12, 0.32)	0.19 (0.13, 0.29)	0.19 (0.09, 0.33)	0.361
PGE_2	0.08 (0, 0.38)	0.08 (0.02, 0.36)	0.12 (0.03, 0.36)	0.913
2,3-dinor-i$PF_{2\alpha}$-III	0 (0, 0)	0 (0, 0)	0 (0, 0)	0.418
15-keto-15-F_{2t}-IsoP	0.04 (0, 0.13)	0.03 (0, 0.14)	0 (0, 0.2)	0.924
15-keto-15-F_{2t}-IsoP	0.14 (0.06, 0.37)	0.14 (0.09, 0.23)	0.16 (0.1, 0.33)	0.872
15-E_{2t}-IsoP	0.2 (0.09, 0.93)	0.2 (0.12, 0.64)	0.48 (0.18, 1.05)	0.041 *
5-F_{2t}-IsoP	0.77 (0.37, 1.45)	1.12 (0.54, 1.46)	1.08 (0.45, 1.55)	0.542
15-F_{2t}-IsoP	0.03 (0.01, 0.06)	0.02 (0.01, 0.04)	0.01 (0, 0.07)	0.129
$PGF_{2\alpha}$	0.43 (0.17, 0.91)	0.78 (0.4, 1.08)	0.62 (0.3, 1.13)	0.005 *
4(RS)-F_{4t}-NeuroP	1.2 (0.59, 1.44)	1.22 (0.7, 1.43)	0.5 (0, 1.43)	0.006 *
1a,1b-dihomo-$PGF_{2\alpha}$	0 (0, 0)	0 (0, 0)	0 (0, 0)	0.178
10-*epi*-10-F_{4t}-NeuroP	0.13 (0.05, 0.2)	0.13 (0.07, 0.18)	0.22 (0.17, 0.31)	<0.001 *
14(RS)-14-F_{4t}-NeuroP	0.56 (0.1, 1.2)	0.62 (0, 1.33)	0.52 (0.1, 1.48)	0.891
IsoP[$]	0.36 (0.26, 0.55)	0.31 (0.19, 0.45)	0.54 (0.42, 0.93)	<0.001 *
Ent-7(RS)-F_{2t}-dihomo-IsoP	0.12 (0.08, 0.17)	0.11 (0.07, 0.15)	0.13 (0, 0.45)	0.181
17-F_{2t}-dihomo-IsoP	0 (0, 0)	0 (0, 0)	0 (0, 0)	0.989
17-*epi*-17-F_{2t}-dihomo-IsoP	0 (0, 0.02)	0 (0, 0)	0 (0, 0.18)	0.168
17(RS)-10-*epi*-SC-Δ^{15}-11-dihomo-IsoF	0 (0, 0)	0 (0, 0)	0 (0, 0)	0.536
7(RS)-ST-Δ^{8}-11-dihomo-IsoF	0.06 (0, 0.12)	0.11 (0, 0.18)	0.02 (0, 0.1)	0.155
NeuroF[$]	0.13 (0.06, 0.25)	0.07 (−0.1, 0.25)	0.14 (0.08, 0.2)	0.022 *
IsoF[$]	0.14 (0.08, 0.29)	0.11 (0.07, 0.3)	0.2 (0.08, 0.39)	0.336

[$] Arbitrary units: (intensity of signal units × (internal standard concentration, nmol L^{-1}); * $P < 0.05$; IQR: Inter-quartile range.

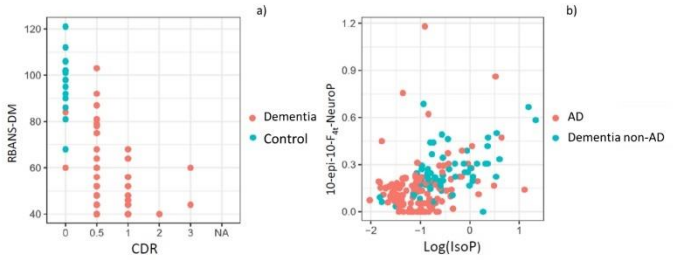

Figure 1. (**a**) Representation of control and dementia patients by using standard neuropsychological evaluation tests (RBANS-DM, CDR); (**b**) Representation of AD and non-AD patients by using the variables 10-*epi*-10-F_{4t}-NeuroP and IsoP.

4. Discussion

In this work it is described a new diagnosis model based on plasma lipid peroxidation biomarkers and neuropsychological scores, which evaluate memory, cognition and functional performance.

This model could be able to differentiate AD from healthy subjects and participants with other pathologies, such as MCI not due to AD, frontotemporal dementia, vascular dementia, or DLB. Differential diagnosis between AD and non-AD pathologies are commonly a challenge in neurology units especially in early stages [34], since some pathologies show similar clinical symptoms. Therefore, a reliable early diagnosis model is required to be applied to clinical practice.

Recent research has shown an increasing interest in the clinical validation of potential biomarkers to early and specific diagnose AD using minimally invasive biological samples [35]. Among the physiological mechanisms that are already impaired in early disease stages, lipid peroxidation has shown some promising results, and plasma samples constitute an interesting matrix in the search for the corresponding biomarkers [16,36–42].

Among lipid peroxidation biomarkers evaluated in plasma, some AD studies found altered levels for malondialdehyde [36–38,42], 4-hydroxynonenal [39], lipophilic fluorescent products [40,41], and isoprostanes [4]. In general, these potential biomarkers showed elevated levels in AD in comparison with healthy participants, reflecting high oxidative stress at systemic level. However, oxidative stress is common in many pathologies, such as cancer [43] or vascular diseases [44], as well as in other neurodegenerative diseases [45]. For that reason, the present work focused on the need to develop a specific diagnosis model for AD. In fact, AD shows similar clinical symptoms to other pathologies, and the differential AD diagnosis constitutes the real diagnostic challenge. In this sense, lipid peroxidation biomarkers were evaluated as potential specific AD biomarkers, as the brain has a high lipid composition (polyunsaturated fatty acids . . .) [46]. For this, a previously developed and validated analytical method was applied [4]. This method showed adequate linearity for all the analytes within the corresponding concentration ranges, and suitable precision. The limits of detection and accuracy were satisfactory, and matrix effect was considered negligible. Among studied compounds, statistically significant results were obtained for two prostaglandins (derived from araquidonic acid), two neuroprostanes (derived from docosahexanoic acid), and isoprostanes as total parameter (15-E2t-IsoP, PGF2α, 4(RS)-F4t-NeuroP, 10-epi-10-F4t-NeuroP, IsoP). In contrast to the results in this work, some studies determining isoprostanoids did not obtain satisfactory results [47,48]. It could be explained by the limited list of compounds assessed in literature. However, in the present study a set of 18 compounds were evaluated simultaneously, and it could provide more information about the oxidative state of each individual.

In addition, the present study shows the strengths of using standard diagnosis based on biological definition (CSF biomarkers) to identify accurately the participants (early AD patients, healthy controls, non-AD patients). Furthermore, it is important to highlight the relevant discrimination capacity of the neuropsychological evaluation to identify accurately the healthy controls. From this accurate participant's classification, a further AD specific and minimally invasive diagnosis was developed. For this, a two-step model was required using the advantages of the neuropsychological evaluation (first step), and the plasma lipid peroxidation determinations (second step). In the developed model, the first step identified the healthy participants, while the second step increased the diagnosis specificity, differentiating AD patients from other patients with other pathologies with similar symptoms. In this sense, a one-step model would not be able to distinguish accurately among AD, non-AD and healthy patients. Therefore, the two-step developed model was required to achieve the minimally invasive and differential AD diagnosis.

Regarding AD differential diagnosis, our study achieved high discriminative power. Albeit not outstanding, it serves as a first approach for developing a differential diagnosis model based on lipid peroxidation compounds. Some studies can be found in literature identifying different biomarkers that differentiate AD from vascular dementia [49], and diabetes-related dementia [50]. However, there is a lack of preliminary studies with clinical validation. A recent study focused on differentiating AD and DLB by means of different pathological signatures of gait [51] supported the theory of interacting cognitive-motor networks [52]. In addition, a previous study found that the CSF p-tau181/Aβ42 ratio might reliably detect AD pathology in patients suffering from different types of dementia [26]. In the present work the non-AD group included a large variety of pathologies, such as MCI not

due to AD, frontotemporal dementia, vascular dementia, and DLB. The different lipid peroxidation pattern observed between AD and non-AD subjects could be corroborated by a previous study, which suggested that high lipid peroxidation levels preceded β-amyloid accumulation in brain [53]. Among the physiological mechanisms that could explain the different lipid peroxidation levels between AD and non-AD pathologies, it is important to highlight the role of potential mediators between lipid peroxidation products and AD pathology [54]. Specifically, thromboxane A2 receptor is activated by isoprostanes and promotes amyloid aggregation [55,56]. In fact, previous studies have shown that agonists for this receptor reduced this amyloid increase and they could be potential treatments for AD [55]. On the other hand, another study found co-localization of lipid oxidation and amyloid plaques in brain [57]. From the clinical point of view, the specificity described in the developed diagnosis model could have a great value due to the high clinical similarity among pathological symptoms.

As regards biomarkers and neuropsychological tests, they were selected from our previous experience. In fact, a study carried out with the same lipid peroxidation compounds in plasma samples from AD and healthy participants showed the capacity of these analytes as potential biomarkers for AD [4]. In that work, a one-step diagnosis model was developed from the levels obtained for six lipid peroxidation compounds. The corresponding diagnosis model could differentiate early AD patients from healthy participants with satisfactory accuracy (AUC-ROC 0.817). Nevertheless, it showed the disadvantage of low sample size. Moreover, the differential diagnosis power from non-AD pathologies, which constitutes an important diagnostic problem in clinical practice, was not evaluated [4]. On the other hand, a previous model for early AD diagnosis was developed from the RBANS.DM test. It showed a high discriminative power between AD and non-AD participants [58]. For that reason, RBANS.DM was included in the first step of the present model, improving biomarkers diagnosis power. In this sense, the present developed diagnosis model is based on two steps, the sample size has been suitable to carry out an internal clinical validation, and the differential diagnosis has been included.

Finally, few studies have carried out an external clinical validation of potential biomarkers (plasma proteins, magnetic resonance imaging scans) differentiating two groups of participants (discovery group, validation group) [59,60]. In order to improve the statistical power, other studies developed an internal clinical validation [61,62]. Similarly, in this work, an internal clinical validation was carried out obtaining a satisfactory diagnostic power, since a large sample size was available. Most of previous works were based on CSF biomarkers or neuroimaging biomarkers, so the internal clinical validation based on plasma lipid peroxidation biomarkers constitutes a promising new approach.

The two-step diagnosis model developed in the present work provides the probability of suffering AD from early stages. In the first step, in a given population, it is possible to discriminate the control patients of case patients and thus putative AD patients. In the second step, AD diagnosis can be differentiated from other neurodegenerative diseases also involving cognitive impairment. These results combined with other factors (e.g., age, gender, familiar background, risk factors . . .) could decide upon the further need of using invasive techniques to establish the patient's diagnosis [63]. Therefore, the present diagnosis model could be considered a relevant approach in the clinical practice field.

5. Conclusions

A two-step early and differential diagnostic model has been developed indicating the individual probability of suffering from early AD, using low cost and minimally invasive procedures for the potential diagnosis. It consisted of a simultaneous approach from neuropsychological and biochemical fields. Lipid peroxidation has been assayed as a physiological mechanism which is impaired at early stages in AD. In this sense, a large set of related biomarkers were determined in plasma samples, selecting two compounds in the development of an AD differential diagnosis model. The corresponding internal validation was satisfactory, and further external validation of the developed model will be carried out as a fundamental stage before being applied in the clinical routine use. This is a promising screening test that could avoid the current invasive diagnosis method and could be useful in diagnosis and investigation.

Author Contributions: C.C.-P., M.V. and M.B. designed the experimental approach, directed the project. C.C.-P., C.P.-B. and M.B. wrote the manuscript. C.C.P., C.P.-B. performed the experimental work. T.D. and C.V. synthetized the standards employed in the analysis. A.C., L.Á., M.B. evaluate participants and made a specific diagnosis for all participants. D.H. performed the statistical analysis. All authors have read and agreed to the published version of the manuscript

Funding: The work was supported by a CC-P post-doctoral "Miguel Servet I" Grant (CP16/00082) from the Health Research Institute Carlos III (Spanish Ministry of Economy and Competitiveness), and the European Regional Development Fund (FEDER) and CP-B was supported by a research Grant (associated to "Miguel Servet" project CP16/00082) from the Health Research Institute Carlos III (Spanish Ministry of Economy, Industry and Competitiveness).

Acknowledgments: We are greatly indebted to all participants, nursing, psychology and medical staff who voluntarily participated in the present study. Without their collaboration and enthusiasm this study could not have been completed. The work was supported by a post-doctoral "Miguel Servet I" Grant (CP16/00082) from the Health Research Institute Carlos III (Spanish Ministry of Economy and Competitiveness), and the European Regional Development Fund (FEDER) and CP-B was supported by a research Grant (associated to "Miguel Servet" project CP16/00082) from the Health Research Institute Carlos III (Spanish Ministry of Economy, Industry and Competitiveness). The authors are grateful for the professional English language editing to Arash Javadinejad, English Instructor and Publication Editor at the Instituto de Investigación Sanitaria La Fe, Valencia, Spain.

Conflicts of Interest: The authors declare no conflict of interest.

References

1. Kukull, W.A.; Higdon, R.; Bowen, J.D.; McCormick, W.C.; Teri, L.; Schellenberg, G.D.; van Belle, G.; Jolley, L.; Larson, E.B. Dementia and Alzheimer Disease Incidence. *Arch. Neurol.* **2002**, *59*, 1737–1746. [CrossRef] [PubMed]
2. Kalaria, R. Similarities between Alzheimer's disease and vascular dementia. *J. Neurol. Sci.* **2002**, *203–204*, 29–34. [CrossRef]
3. Jack, C.R.; Bennett, D.A.; Blennow, K.; Carrillo, M.C.; Dunn, B.; Haeberlein, S.B.; Holtzman, D.M.; Jagust, W.; Jessen, F.; Karlawish, J.; et al. NIA-AA Research Framework: Toward a biological definition of Alzheimer's disease. *Alzheimer's Dement.* **2018**, *14*, 535–562. [CrossRef]
4. Peña-Bautista, C.; Vigor, C.; Galano, J.-M.; Oger, C.; Durand, T.; Ferrer, I.; Cuevas, A.; López-Cuevas, R.; Baquero, M.; López-Nogueroles, M.; et al. Plasma lipid peroxidation biomarkers for early and non-invasive Alzheimer Disease detection. *Free Radic. Biol. Med.* **2018**, *124*, 388–394. [CrossRef]
5. Eruysal, E.; Ravdin, L.; Kamel, H.; Iadecola, C.; Ishii, M. Plasma lipocalin-2 levels in the preclinical stage of Alzheimer's disease. *Alzheimer's Dement. Diagn. Assess. Dis. Monit.* **2019**, *11*, 646–653. [CrossRef]
6. Guzman-Martinez, L.; Maccioni, R.B.; Farías, G.A.; Fuentes, P.; Navarrete, L.P. Biomarkers for Alzheimer's Disease. *Curr. Alzheimer Res.* **2019**, *16*, 518–528. [CrossRef]
7. Alzheimer's Association. 2014 Alzheimer's disease facts and figures. *Alzheimer's Dement.* **2014**, *10*, e47–e92. [CrossRef]
8. Gao, H.; Liu, M.; Zhao, Z.; Yang, C.; Zhu, L.; Cai, Y.; Yang, Y.; Hu, Z. Diagnosis of Mild Cognitive Impairment and Alzheimer's Disease by the Plasma and Serum Amyloid-beta 42 Assay through Highly Sensitive Peptoid Nanosheet Sensor. *ACS Appl. Mater. Interfaces* **2020**, *12*, 9693–9700. [CrossRef]
9. Morgan, A.R.; Touchard, S.; Leckey, C.; O'Hagan, C.; Nevado-Holgado, A.J.; Barkhof, F.; Bertram, L.; Blin, O.; Bos, I.; Dobricic, V.; et al. Inflammatory biomarkers in Alzheimer's disease plasma. *Alzheimer's Dement.* **2019**, *15*, 776–787. [CrossRef]
10. Kamat, P.K.; Kalani, A.; Rai, S.; Swarnkar, S.; Tota, S.; Nath, C.; Tyagi, N. Mechanism of Oxidative Stress and Synapse Dysfunction in the Pathogenesis of Alzheimer's Disease: Understanding the Therapeutics Strategies. *Mol. Neurobiol.* **2016**, *53*, 648–661. [CrossRef]
11. Hampel, H.; Frank, R.; Broich, K.; Teipel, S.J.; Katz, R.G.; Hardy, J.; Herholz, K.; Bokde, A.L.W.; Jessen, F.; Hoessler, Y.C.; et al. Biomarkers for Alzheimer's disease: Academic, industry and regulatory perspectives. *Nat. Rev. Druş Discov.* **2010**, *9*, 560–574. [CrossRef] [PubMed]
12. Molinuevo, J.L.; Ayton, S.; Batrla, R.; Bednar, M.M.; Bittner, T.; Cummings, J.; Fagan, A.M.; Hampel, H.; Mielke, M.M.; Mikulskis, A.; et al. Current state of Alzheimer's fluid biomarkers. *Acta Neuropathol.* **2018**, *136*, 821–853. [CrossRef]

13. Blennow, K.; Hampel, H.; Weiner, M.; Zetterberg, H. Cerebrospinal fluid and plasma biomarkers in Alzheimer disease. *Nat. Rev. Neurol.* **2010**, *6*, 131–144. [CrossRef] [PubMed]
14. Candore, G.; Bulati, M.; Caruso, C.; Castiglia, L.; Colonna-Romano, G.; Di Bona, D.; Duro, G.; Lio, D.; Matranga, D.; Pellicanò, M.; et al. Inflammation, Cytokines, Immune Response, Apolipoprotein E, Cholesterol, and Oxidative Stress in Alzheimer Disease: Therapeutic Implications. *Rejuvenation Res.* **2010**, *13*, 301–313. [CrossRef] [PubMed]
15. Peña-Bautista, C.; Baquero, M.; Vento, M.; Cháfer-Pericás, C. Free radicals in Alzheimer's disease: Lipid peroxidation biomarkers. *Clin. Chim. Acta* **2019**, *491*, 85–90. [CrossRef]
16. García-Blanco, A.; Peña-Bautista, C.; Oger, C.; Vigor, C.; Galano, J.-M.; Durand, T.; Martín-Ibáñez, N.; Baquero, M.; Vento, M.; Cháfer-Pericás, C. Reliable determination of new lipid peroxidation compounds as potential early Alzheimer Disease biomarkers. *Talanta* **2018**, *184*, 193–201. [CrossRef]
17. Yuan, L.; Liu, J.; Ma, W.; Dong, L.; Wang, W.; Che, R.; Xiao, R. Dietary pattern and antioxidants in plasma and erythrocyte in patients with mild cognitive impairment from China. *Nutrition* **2016**, *32*, 193–198. [CrossRef]
18. Balmuș, I.-M.; Strungaru, S.-A.; Ciobica, A.; Nicoara, M.-N.; Dobrin, R.; Plavan, G.; Ștefănescu, C. Preliminary Data on the Interaction between Some Biometals and Oxidative Stress Status in Mild Cognitive Impairment and Alzheimer's Disease Patients. *Oxidative Med. Cell. Longev.* **2017**, *2017*. [CrossRef]
19. Hampel, H.; O'Bryant, S.E.; Molinuevo, J.L.; Zetterberg, H.; Masters, C.L.; Lista, S.; Kiddle, S.J.; Batrla, R.; Blennow, K. Blood-based biomarkers for Alzheimer disease: Mapping the road to the clinic. *Nat. Rev. Neurol.* **2018**, *14*, 639–652. [CrossRef]
20. Nagele, E.; Han, M.; DeMarshall, C.; Belinka, B.; Nagele, R. Diagnosis of Alzheimer's Disease Based on Disease-Specific Autoantibody Profiles in Human Sera. *PLoS ONE* **2011**, *6*, e23112. [CrossRef]
21. Denk, J.; Oberhauser, F.; Kornhuber, J.; Wiltfang, J.; Fassbender, K.; Schroeter, M.L.; Volk, A.E.; Diehl-Schmid, J.; Prudlo, J.; Danek, A.; et al. Specific serum and CSF microRNA profiles distinguish sporadic behavioural variant of frontotemporal dementia compared with Alzheimer patients and cognitively healthy controls. *PLoS ONE* **2018**, *13*, e0197329. [CrossRef] [PubMed]
22. Vogelgsang, J.; Shahpasand-Kroner, H.; Vogelgsang, R.; Streit, F.; Vukovich, R.; Wiltfang, J. Multiplex immunoassay measurement of amyloid-β42 to amyloid-β40 ratio in plasma discriminates between dementia due to Alzheimer's disease and dementia not due to Alzheimer's disease. *Exp. Brain Res.* **2018**, *236*, 1241–1250. [CrossRef] [PubMed]
23. Delvaux, E.; Mastroeni, D.; Nolz, J.; Chow, N.; Sabbagh, M.; Caselli, R.J.; Reiman, E.M.; Marshall, F.J.; Coleman, P.D. Multivariate analyses of peripheral blood leukocyte transcripts distinguish Alzheimer's, Parkinson's, control, and those at risk for developing Alzheimer's. *Neurobiol. Aging* **2017**, *58*, 225–237. [CrossRef] [PubMed]
24. Josviak, N.D.; Batistela, M.S.; Souza, R.K.M.; Wegner, N.R.; Bono, G.F.; Sulzbach, C.D.; Simão-Silva, D.P.; Piovezan, M.R.; Souza, R.L.R.; Furtado-Alle, L. Plasma butyrylcholinesterase activity: A possible biomarker for differential diagnosis between Alzheimer's disease and dementia with Lewy bodies? *Int. J. Neurosci.* **2017**, *127*, 1082–1086. [CrossRef] [PubMed]
25. García-Ayllón, M.S.; Monge-Argilés, J.A.; Monge-García, V.; Navarrete, F.; Cortés-Gómez, M.A.; Sánchez-Payá, J.; Manzanares, J.; Gasparini-Berenguer, R.; Leiva-Santana, C.; Sáez-Valero, J. Measurement of CSF α-synuclein improves early differential diagnosis of mild cognitive impairment due to Alzheimer's disease. *J. Neurochem.* **2019**, *150*, 218–230. [CrossRef]
26. Santangelo, R.; Dell'Edera, A.; Sala, A.; Cecchetti, G.; Masserini, F.; Caso, F.; Pinto, P.; Leocani, L.; Falautano, M.; Passerini, G.; et al. The CSF p-tau181/Aβ42 Ratio Offers a Good Accuracy "In Vivo" in the Differential Diagnosis of Alzheimer's Dementia. *Curr. Alzheimer Res.* **2019**, *16*, 587–595. [CrossRef]
27. Casanova, R.; Varma, S.; Simpson, B.; Kim, M.; An, Y.; Saldana, S.; Riveros, C.; Moscato, P.; Griswold, M.; Sonntag, D.; et al. Blood metabolite markers of preclinical Alzheimer's disease in two longitudinally followed cohorts of older individuals. *Alzheimer's Dement.* **2016**, *12*, 815–822. [CrossRef]
28. de la Torre, A.; Lee, Y.Y.; Mazzoni, A.; Guy, A.; Bultel-Poncé, V.; Durand, T.; Oger, C.; Lee, J.C.-Y.; Galano, J.-M. Total Syntheses and In Vivo Quantitation of Novel Neurofuran and Dihomo-isofuran Derived from Docosahexaenoic Acid and Adrenic Acid. *Chem. A Eur. J.* **2015**, *21*, 2442–2446. [CrossRef]
29. Zhang, Z.; Lai, Z.; Xu, Y.; Shao, L.; Wu, J.; Xie, G.-S. Discriminative Elastic-Net Regularized Linear Regression. *IEEE Trans. Image Process.* **2017**, *26*, 1466–1481. [CrossRef]

30. Hughes, C.P.; Berg, L.; Danziger, W.L.; Coben, L.A.; Martin, R.L. A new clinical scale for the staging of dementia. *Br. J. Psychiatry* **1982**, *140*, 566–572. [CrossRef]
31. Randolph, C.; Tierney, M.C.; Mohr, E.; Chase, T.N. The Repeatable Battery for the Assessment of Neuropsychological Status (RBANS): Preliminary Clinical Validity. *J. Clin. Exp. Neuropsychol.* **1998**, *20*, 310–319. [CrossRef] [PubMed]
32. Anoop, A.; Singh, P.K.; Jacob, R.S.; Maji, S.K. CSF Biomarkers for Alzheimer's Disease Diagnosis. *Int. J. Alzheimers. Dis.* **2010**, *2010*. [CrossRef] [PubMed]
33. Blennow, K.; Dubois, B.; Fagan, A.M.; Lewczuk, P.; de Leon, M.J.; Hampel, H. Clinical utility of cerebrospinal fluid biomarkers in the diagnosis of early Alzheimer's disease. *Alzheimer's Dement.* **2015**, *11*, 58–69. [CrossRef] [PubMed]
34. Silveri, M.C. Frontotemporal dementia to Alzheimer's disease. *Dialogues Clin. Neurosci.* **2007**, *9*, 153–160. [PubMed]
35. Peña-Bautista, C.; Baquero, M.; Vento, M.; Cháfer-Pericás, C. Omics-based Biomarkers for the Early Alzheimer Disease Diagnosis and Reliable Therapeutic Targets Development. *Curr. Neuropharmacol.* **2019**, *17*, 630–647. [CrossRef]
36. Torres, L.L.; Quaglio, N.B.; de Souza, G.T.; Garcia, R.T.; Dati, L.M.M.; Moreira, W.L.; de Melo Loureiro, A.P.; de souza-Talarico, J.N.; Smid, J.; Porto, C.S.; et al. Peripheral Oxidative Stress Biomarkers in Mild Cognitive Impairment and Alzheimer's Disease. *J. Alzheimer's Dis.* **2011**, *26*, 59–68. [CrossRef]
37. Gustaw-Rothenberg, K.; Kowalczuk, K.; Stryjecka-Zimmer, M. Lipids' peroxidation markers in Alzheimer's disease and vascular dementia. *Geriatr. Gerontol. Int.* **2010**, *10*, 161–166. [CrossRef]
38. Polidori, M.C.; Mattioli, P.; Aldred, S.; Cecchetti, R.; Stahl, W.; Griffiths, H.; Senin, U.; Sies, H.; Mecocci, P. Plasma Antioxidant Status, Immunoglobulin G Oxidation and Lipid Peroxidation in Demented Patients: Relevance to Alzheimer Disease and Vascular Dementia. *Dement. Geriatr. Cogn. Disord.* **2004**, *18*, 265–270. [CrossRef]
39. McGrath, L.T. Increased oxidative stress in Alzheimer's disease as assessed with 4-hydroxynonenal but not malondialdehyde. *QJM* **2001**, *94*, 485–490. [CrossRef]
40. Chmatalova, Z.; Vyhnalek, M.; Laczo, J.; Hort, J.; Pospisilova, R.; Pechova, M.; Skoumalova, A. Relation of plasma selenium and lipid peroxidation end products in patients with Alzheimer's disease. *Physiol. Res.* **2017**, *66*, 1049–1056. [CrossRef]
41. Chmátalová, Z.; Vyhnálek, M.; Laczó, J.; Hort, J.; Skoumalová, A. Analysis of lipophilic fluorescent products in blood of Alzheimer's disease patients. *J. Cell. Mol. Med.* **2016**, *20*, 1367–1372. [CrossRef] [PubMed]
42. Puertas, M.C.; Martínez-Martos, J.M.; Cobo, M.P.; Carrera, M.P.; Mayas, M.D.; Ramírez-Expósito, M.J. Plasma oxidative stress parameters in men and women with early stage Alzheimer type dementia. *Exp. Gerontol.* **2012**, *47*, 625–630. [CrossRef] [PubMed]
43. Klaunig, J.E. Oxidative Stress and Cancer. *Curr. Pharm. Des.* **2019**, *24*, 4771–4778. [CrossRef]
44. Steven, S.; Frenis, K.; Oelze, M.; Kalinovic, S.; Kuntic, M.; Bayo Jimenez, M.T.; Vujacic-Mirski, K.; Helmstädter, J.; Kröller-Schön, S.; Münzel, T.; et al. Vascular Inflammation and Oxidative Stress: Major Triggers for Cardiovascular Disease. *Oxidative Med. Cell. Longev.* **2019**, *2019*, 1–26. [CrossRef] [PubMed]
45. Kim, G.H.; Kim, J.E.; Rhie, S.J.; Yoon, S. The Role of Oxidative Stress in Neurodegenerative Diseases. *Exp. Neurobiol.* **2015**, *24*, 325–340. [CrossRef]
46. Sultana, R.; Perluigi, M.; Butterfield, D.A. Lipid peroxidation triggers neurodegeneration: A redox proteomics view into the Alzheimer disease brain. *Free Radic. Biol. Med.* **2013**, *62*, 157–169. [CrossRef]
47. Mufson, E.J.; Leurgans, S. Inability of Plasma and Urine F2A-Isoprostane Levels to Differentiate Mild Cognitive Impairment from Alzheimer's Disease. *Neurodegener. Dis.* **2010**, *7*, 139–142. [CrossRef]
48. Feillet-Coudray, C.; Tourtauchaux, R.; Niculescu, M.; Rock, E.; Tauveron, I.; Alexandre-Gouabau, M.-C.; Rayssiguier, Y.; Jalenques, I.; Mazur, A. Plasma levels of 8-epiPGF2α, an in vivo marker of oxidative stress, are not affected by aging or Alzheimer's disease. *Free Radic. Biol. Med.* **1999**, *27*, 463–469. [CrossRef]
49. Krishnan, S.; Rani, P. Evaluation of Selenium, Redox Status and Their Association with Plasma Amyloid/Tau in Alzheimer's Disease. *Biol. Trace Elem. Res.* **2014**, *158*, 158–165. [CrossRef]
50. Hatanaka, H.; Hanyu, H.; Fukasawa, R.; Sato, T.; Shimizu, S.; Sakurai, H. Peripheral oxidative stress markers in diabetes-related dementia. *Geriatr. Gerontol. Int.* **2016**, *16*, 1312–1318. [CrossRef]
51. Mc Ardle, R.; Galna, B.; Donaghy, P.; Thomas, A.; Rochester, L. Do Alzheimer's and Lewy body disease have discrete pathological signatures of gait? *Alzheimer's Dement.* **2019**, *15*, 1367–1377. [CrossRef] [PubMed]

52. Leisman, G.; Moustafa, A.; Shafir, T. Thinking, Walking, Talking: Integratory Motor and Cognitive Brain Function. *Front. Public Health* **2016**, *4*, 94. [CrossRef] [PubMed]
53. Praticò, D.; Uryu, K.; Leight, S.; Trojanoswki, J.Q.; Lee, V.M.Y. Increased lipid peroxidation precedes amyloid plaque formation in an animal model of Alzheimer amyloidosis. *J. Neurosci.* **2001**, *21*, 4183–4187. [CrossRef] [PubMed]
54. Lauretti, E.; Di Meco, A.; Chu, J.; Praticò, D. Modulation of AD neuropathology and memory impairments by the isoprostane F2α is mediated by the thromboxane receptor. *Neurobiol. Aging* **2015**, *36*, 812–820. [CrossRef] [PubMed]
55. Soper, J.H.; Sugiyama, S.; Herbst-Robinson, K.; James, M.J.; Wang, X.; Trojanowski, J.Q.; Smith, A.B.; Lee, V.M.-Y.; Ballatore, C.; Brunden, K.R. Brain-Penetrant Tetrahydronaphthalene Thromboxane A2-Prostanoid (TP) Receptor Antagonists as Prototype Therapeutics for Alzheimer's Disease. *ACS Chem. Neurosci.* **2012**, *3*, 928–940. [CrossRef]
56. Shineman, D.W.; Zhang, B.; Leight, S.N.; Pratico, D.; Lee, V.M.-Y. Thromboxane Receptor Activation Mediates Isoprostane-Induced Increases in Amyloid Pathology in Tg2576 Mice. *J. Neurosci.* **2008**, *28*, 4785–4794. [CrossRef]
57. Benseny-Cases, N.; Klementieva, O.; Cotte, M.; Ferrer, I.; Cladera, J. Microspectroscopy (μFTIR) Reveals Co-localization of Lipid Oxidation and Amyloid Plaques in Human Alzheimer Disease Brains. *Anal. Chem.* **2014**, *86*, 12047–12054. [CrossRef]
58. Peña-Bautista, C.; Baquero, M.; Ferrer, I.; Hervás, D.; Vento, M.; García-Blanco, A.; Cháfer-Pericás, C. Neuropsychological assessment and cortisol levels in biofluids from early Alzheimer's disease patients. *Exp. Gerontol.* **2019**, *123*, 10–16. [CrossRef]
59. Shi, L.; Westwood, S.; Baird, A.L.; Winchester, L.; Dobricic, V.; Kilpert, F.; Hong, S.; Franke, A.; Hye, A.; Ashton, N.J.; et al. Discovery and validation of plasma proteomic biomarkers relating to brain amyloid burden by SOMAscan assay. *Alzheimer's Dement.* **2019**, *15*, 1478–1488. [CrossRef]
60. Li, H.; Habes, M.; Wolk, D.A.; Fan, Y. A deep learning model for early prediction of Alzheimer's disease dementia based on hippocampal magnetic resonance imaging data. *Alzheimer's Dement.* **2019**, *15*, 1059–1070. [CrossRef] [PubMed]
61. Jang, H.; Park, J.; Woo, S.; Kim, S.; Kim, H.J.; Na, D.L.; Lockhart, S.N.; Kim, Y.; Kim, K.W.; Cho, S.H.; et al. Prediction of fast decline in amyloid positive mild cognitive impairment patients using multimodal biomarkers. *NeuroImage Clin.* **2019**, *24*, 101941. [CrossRef] [PubMed]
62. Vergallo, A.; Mégret, L.; Lista, S.; Cavedo, E.; Zetterberg, H.; Blennow, K.; Vanmechelen, E.; De Vos, A.; Habert, M.-O.; Potier, M.-C.; et al. Plasma amyloid β 40/42 ratio predicts cerebral amyloidosis in cognitively normal individuals at risk for Alzheimer's disease. *Alzheimer's Dement.* **2019**, *15*, 764–775. [CrossRef] [PubMed]
63. Engelborghs, S.; Niemantsverdriet, E.; Struyfs, H.; Blennow, K.; Brouns, R.; Comabella, M.; Dujmovic, I.; van der Flier, W.; Frölich, L.; Galimberti, D.; et al. Consensus guidelines for lumbar puncture in patients with neurological diseases. *Alzheimer's Dement. Diagn. Assess. Dis. Monit.* **2017**, *8*, 111–126. [CrossRef] [PubMed]

antioxidants

MDPI

Article

Lipid Peroxidation Assessment in Preclinical Alzheimer Disease Diagnosis

Carmen Peña-Bautista [1], Lourdes Álvarez-Sánchez [1,2], Inés Ferrer [1,2], Marina López-Nogueroles [3], Antonio José Cañada-Martínez [4], Camille Oger [5], Jean-Marie Galano [5], Thierry Durand [5], Miguel Baquero [1,2] and Consuelo Cháfer-Pericás [1,*]

[1] Alzheimer's Disease Research Group, Health Research Institute La Fe, 46026 Valencia, Spain; carpebau93@gmail.com (C.P.-B.); lourdes_alvarez@iislafe.es (L.Á.-S.); ines_ferrer@iislafe.es (I.F.); miquelbaquero@gmail.com (M.B.)
[2] Division of Neurology, University and Polytechnic Hospital La Fe, 46026 Valencia, Spain
[3] Analytical Unit Platform, Health Research Institute La Fe, 46026 Valencia, Spain; marina_lopez@iislafe.es
[4] Data Science Unit, Health Research Institute La Fe (IIS La Fe), 46026 Valencia, Spain; bioestadistica@iislafe.es
[5] Institut des Biomolécules Max Mousseron, IBMM, University of Montpellier, CNRS, ENSCM, 34093 Montpellier, France; camille.oger@umontpellier.fr (C.O.); jeangalano@yahoo.co.uk (J.-M.G.); thierry.durand@umontpellier.fr (T.D.)
* Correspondence: m.consuelo.chafer@uv.es; Tel.: +34-96-124-66-61; Fax: +34-96-124-57-46

check for updates

Citation: Peña-Bautista, C.; Álvarez-Sánchez, L.; Ferrer, I.; López-Nogueroles, M.; Cañada-Martínez, A.J.; Oger, C.; Galano, J.-M.; Durand, T.; Baquero, M.; Cháfer-Pericás, C. Lipid Peroxidation Assessment in Preclinical Alzheimer Disease Diagnosis. *Antioxidants* **2021**, *10*, 1043. https://doi.org/10.3390/antiox10071043

Academic Editors: C. Henrique Alves, Peter M. J. Quinn and António Francisco Ambrósio

Received: 31 May 2021
Accepted: 24 June 2021
Published: 29 June 2021

Publisher's Note: MDPI stays neutral with regard to jurisdictional claims in published maps and institutional affiliations.

Abstract: Alzheimer disease (AD) is an increasingly common neurodegenerative disease, especially in countries with aging populations. Its diagnosis is complex and is usually carried out in advanced stages of the disease. In addition, lipids and oxidative stress have been related to AD since the earliest stages. A diagnosis in the initial or preclinical stages of the disease could help in a more effective action of the treatments. Isoprostanoid biomarkers were determined in plasma samples from preclinical AD participants (n = 12) and healthy controls (n = 31) by chromatography and mass spectrometry (UPLC-MS/MS). Participants were accurately classified according to cerebrospinal fluid (CSF) biomarkers and neuropsychological examination. Isoprostanoid levels did not show differences between groups. However, some of them correlated with CSF biomarkers (t-tau, p-tau) and with cognitive decline. In addition, a panel including 10 biomarkers showed an area under curve (AUC) of 0.96 (0.903–1) and a validation AUC of 0.90 in preclinical AD prediction. Plasma isoprostanoids could be useful biomarkers in preclinical diagnosis for AD. However, these results would require a further validation with an external cohort.

Keywords: Alzheimer disease; plasma; biomarker; lipid peroxidation; mass spectrometry; preclinical

1. Introduction

Alzheimer disease (AD), the most prevalent cause of dementia, is characterized in terms of histopathology by its histological markers. Specifically, an intracellular accumulation of phosphorylated tau (p-tau) protein leads to the formation of neurofibrillary tangles, while an extracellular accumulation of β-amyloid peptide leads to the formation of senile plaques. These markers lead to a synapse loss that causes neuron dysfunction and neurodegeneration. Additionally, tau accumulation is a mechanism shared with other neurodegenerative diseases, while β-amyloid accumulation is supposed to be specific for AD [1]. These histopathological findings are present in the brain before AD symptoms appear. In fact, impairment in amyloid β-42 (Aβ42), and tau proteins in cerebrospinal fluid (CSF) samples are detectable some years before clinical symptoms appear. In this sense, preclinical AD could be defined as biomarker evidence of AD's pathological changes in cognitively healthy individuals [2]; evidence that can be obtained from cerebrospinal fluid (CSF) biomarkers and amyloid brain Positron Emission Tomography (PET) scan. Therefore, positivity in amyloid brain status identifies preclinical AD in asymptomatic cases. Research

focusing on this preclinical AD stage is required in order to advance in the knowledge of AD physiopathological mechanisms, as well as to identify new, early and minimally invasive AD biomarkers, which could be determined in the general population, providing data for a better individual prognosis, new therapeutic targets or other benefits.

Blood samples (plasma, serum) are a promising matrix for identifying potential AD biomarkers [3]. A recent study focused on plasma samples from preclinical AD patients, determining different proteins and peptides (p-tau 181, amyloid-β40, amyloid-β42), showed some evidence that plasma analysis could guide the selection of candidates to receive a diagnosis of their amyloid status, and so reduce the number of amyloid PET scans required to identify amyloid-β-positive individuals [4]. Similarly, Janelidze et al. found that impaired plasma p-tau 217 levels correlated with positivity in the brain before tau-PET in AD cases [5]. In the same way, Suárez-Calvet et al. observed that plasma p-tau 181 was significantly increased in the preclinical stage [6], showing early changes in neuronal tau metabolism. Another study focused on the relationship between plasma amyloid-β and cognitive decline in preclinical AD, revealed specific associations with the decline in episodic memory and executive function [7].

Reviewing non-specific AD biomarkers related to other aspects of preclinical AD, plasma lipocalin-2 was associated with some impairment of executive function, at least in preclinical AD [8]. Additionally, some lipids were identified as potential plasma biomarkers [9]. Moreover, exosomes are an emerging sample matrix [10]. In fact, a recent work showed an early neuronal lysosomal dysfunction [11]. Nevertheless, no conclusive results have been obtained, especially in relation to differential AD diagnosis, as well as in longitudinal studies evaluating clinical progression [12].

Regarding potential physiopathological mechanisms involved in early AD, an increasing number of studies highlight the involvement of oxidative stress, determining several parameters such as oxidatively damaged lipids, proteins and nucleic acids [13,14]. Specifically, lipid peroxidation plays an important role since brain is a susceptible organ characterized by both high lipid content and oxygen consumption. Thus, lipid peroxidation is an important factor in the development of neurodegenerative diseases, especially involving ferroptosis and mitochondrial dysfunction as pathological mechanisms [15]. In this sense, the impairment of lipid peroxidation biomarkers in the brain was found together with histological lesions produced in neurodegenerative diseases, such as brain β-amyloid plaques. In addition, previous studies observed an AD relationship with impaired levels of some plasma lipid peroxidation compounds [16]. It could be explained by the high permeability of the blood-brain barrier since early AD stages [17]. However, a previous study in CSF samples did not show correlations between plasma and CSF samples for any of the studied lipid peroxidation compounds (isoprostanes, neuroprostanes . . .); also, lipid peroxidation biomarkers in CSF samples did not show significant differences between participant groups [18]. In general, previous studies found that some plasma isoprostanes and neuroprostanes isomers could be useful, to some extent, in clinical or research fields as their levels are different between early symptomatic AD stages (patients with mild cognitive impairment (MCI) due to AD) and healthy controls [19,20].

The aim of the present work is to evaluate the possibility of using these lipid peroxidation compounds as minimally invasive biomarkers of preclinical AD, as well as to evaluate whether its use could be beneficial in the development of a potential prevention approach to be applied to the general asymptomatic population.

2. Materials and Methods

2.1. Study Design and Participants

In this study involving people with unimpaired cognition, participants with detected preclinical AD (n = 12) and a control group with elderly participants without AD pathology (n = 31) were included. The preclinical AD group included participants with positive CSF AD biomarkers (β-amyloid-42 < 725 pg·mL^{-1}, total tau (t-tau > 485 pg·mL^{-1}), phosphorylated tau (p-tau > 56 pg·mL^{-1})), and normal cognitive evaluation test scores (clinical

dementia rating (CDR) ≤ 0.5 [21], mini-mental state examination (MMSE) ≥ 27 [22], repeatable battery for the assessment of neuropsychological status delayed memory domain (RBANS.DM) ≥ 85 [23]). The control group included participants with negative levels for CSF AD biomarkers (β-amyloid-42 > 725 pg·mL^{-1}, t-tau < 485 pg·mL^{-1}, p-tau < 56 pg·mL^{-1}) and normal cognitive tests (CDR ≤ 0.5 [21], MMSE ≥ 27 [22], RBANS.DM ≥ 85 [23]) (see Table 1). Participants with major brain disorders, traumatic brain injuries and psychiatric disorders were excluded, as well as participants that were not able to complete the neuropsychological evaluations.

Table 1. Clinical assessment to classify the study participants.

Clinical Assessment	Classification of Participants	
	Control	Preclinical AD
RBANS.DM [1]	≥85	≥85
FAQ [2]	<9	<9
CDR [3]	0-0.5	0–0.5
MMSE [4]	≥27	≥27
CSF t-tau (pg mL^{-1})	<485	>485
CSF p-tau (pg mL^{-1})	<56	>56
CSF β-amyloid42 (pg mL^{-1})	>725	<725
CSF t-tau/β-amyloid42	<0.51	>0.51

[1] RBANS.DM, repeatable battery for the assessment of neuropsychological status-delayed memory (standard score; cut-off point < 85). [2] FAQ, functional activities questionnaire (direct score; cut-off point > 9). [3] CDR, clinical dementia rating, values: 0, 0.5, 1, 2. [4] MMSE, mini-mental state (cut off point < 27). CSF, cerebrospinal fluid.

The Ethics Committee from Health Research Institute La Fe (Valencia) approved the protocol (ethical protocol code: 2019/0105) and all included participants signed the informed consent before the study procedures.

2.2. *Sample Collection and Treatment*

Blood samples were collected, employing cryo-tubes with ethylenediaminetetraacetic acid, for all participants. They were centrifuged for 15 min at 1500× *g*. Plasma fraction (approximately 4 mL) was separated in a tube containing butylated 8-hydroxytoluene (BHT) (0.25 % (*w*/*v*) in ethanol) to avoid further oxidation of the sample. Then, samples were stored at −80 °C until the analysis.

Sample treatment was previously described by Peña-Bautista et al. [19]. Briefly, 5 µL of an internal standard solution (PGF2α-D4 2 µmol L-1 and D4-10-epi-10-F4t-NeuroP 1.2 µmol L-1) and 400 µL of a potassium hydroxide solution (15% *w*/*v*) were added to 400 µL of plasma to carry out the hydrolysis (40 °C, 30 min). Then, proteins were precipitated with HCl. After that, the supernatant pH was adjusted to 7. Then, samples were purified by solid phase extraction in order to preconcentrate analytes and minimize interferences. Finally, the extract was evaporated and reconstituted to be analyzed by ultra-performance liquid chromatography coupled to tandem mass spectrometry (UPLC-MS/MS) [24].

2.3. *Statistical Analysis*

Median differences between participant groups were analyzed using the chi-square test for categorical variables and the Mann–Whitney test for numerical variables. Bivariate correlations were established using the Pearson correlation. For all the analysis, significance value was p value < 0.05. Box-plots were used to represent the levels of isoprostanoids biomarkers.

In order to discriminate between participants groups, the elastic net logistic regression model was used to select "variables" with the glmnet package [25], due to the collinear nature and high dimensionality of the data. The elastic net regularization method of the

estimated beta coefficients improves upon ordinary least squares. It linearly combines the L1 and L2 penalties of the lasso and ridge methods. Regularization parameter λ determines the amount of regularization. An optimal value for λ was determined performing a 5-fold cross-validation, which yielded the minimum cross-validated mean-squared error (CVM). A median of 500 repetitions of the cross validation was calculated in order to improve lambda´s robustness.

3. Results

3.1. Patients' Characteristics

Demographic characteristics of the participants are described in Table 2. Participants showed median ages between 62 and 70 years old and they showed comparable normal cognitive status, with similar median RBANS.DM and CDR scores. As expected, the control group showed higher median levels of β-amyloid-42 than the preclinical group, and the control group showed lower levels of t-tau and p-tau than the preclinical group. Additionally, both groups showed similar use of medications, comorbidities and educational levels.

Table 2. Participants' clinical and demographic description.

Variable		Control Group (n = 31) Median (1st, 3rd Quartile)	Preclinical Group (n = 12) Median (1st, 3rd Quartile)
Age (years)		62 (58.5, 67)	70 (60.75, 74)
Gender (Female, n (%))		19 (61.29%)	6 (50%)
Smoke (Yes, n (%))		6 (27.27%)	1 (14.29%)
Alcohol (Yes, n (%))		6 (27.27%)	0 (0%)
RBANS.DM (score)		98 (94, 102)	94.5 (87, 100.25)
RBANS.A (score)		91 (82, 98.5)	85 (78, 91)
RBANS.L (score)		90 (83, 94)	88.5 (82.5, 94.25)
RBANS.VC (score)		92 (84, 105)	87 (75, 105)
RBANS.IM (score)		87 (83, 98.5)	85 (81.75, 94)
CDR (score)		0.5 (0, 0.5)	0.5 (0, 0.5)
CSF β-amyloid-42 (pg mL $^{-1}$)		1224 (975.5, 1409.5)	571.5 (407, 683.29)
CSF t-tau (pg mL^{-1})		212 (181.5, 259)	443.5 (256.75, 607.75)
CSF p-tau (pg mL^{-1})		34 (26.5, 38.5)	74 (40.75, 86)
CSF t-tau/β-amyloid-42		0.18 (0.16–0.21)	0.70 (0.51–0.97)
FAQ (score)		1 (0, 3.5)	1 (0, 3)
GDS (score)		11 (5.5, 13)	5 (3.75, 9)
Educational level	Basic/primary	10 (32.26%)	4 (33.33%)
	Secondary	7 (22.58%)	2 (16.67%)
	Universitary	14 (45.16%)	6 (50%)
Medication (n, (%))			
Statins		9 (40.91%)	3 (42.86%)
Fibrates		0 (0%)	1 (14.29%)
Morphics		0 (0%)	0 (0%)
ACEI		1 (4.55%)	0 (0%)
Neuroleptics		2 (9.09%)	0 (0%)
Benzodiazepines		6 (27.27%)	2 (28.57%)

Table 2. *Cont.*

Variable	Control Group (n = 31) Median (1st, 3rd Quartile)	Preclinical Group (n = 12) Median (1st, 3rd Quartile)
Antiepileptics	1 (4.55%)	0 (0%)
Anticoagulants	0 (0%)	0 (0%)
Antihipertensives	7 (31.82%)	2 (28.57%)
Corticoids	1 (4.55%)	0 (0%)
Anti-inflammatory	3 (13.64%)	0 (0%)
Comorbidity (n, (%))		
Dyslipidemia	11 (50%)	3 (42.86%)
Diabetes	9 (40.91%)	1 (14.29%)
Hypertension	8 (36.36%)	2 (28.57%)
Heart Disease	1 (4.55%)	0 (0%)
Cerebrovascular	1 (4.55%)	0 (0%)
Depression	4 (18.18%)	2 (28.57%)
Anxiety	3 (13.64%)	2 (28.57%)

RBANS, Repeatable Battery for the Assessment of Neuropsychological Status (DM, delayed memory; A, attention; L, learning; VC, visuospatial/constructional; IM, immediate memory); CDR, clinical dementia rating; CSF cerebrospinal fluid; FAQ, functional activities questionnaire; GDS, geriatric depression scale; ACEI, acetylcholinesterase inhibitors.

3.2. Plasma Levels of Lipid Peroxidation Lipid Compounds

The plasma levels obtained for the determined lipid peroxidation compounds are summarized in Table 3 for each participant group. As can be seen, these potential biomarkers did not show statistically significant differences between preclinical AD patients and healthy participants (Table 3). Figure 1 shows the corresponding boxplots, observing slight differences in median values between groups. In general, lower levels were obtained for the preclinical AD group.

Table 3. Plasma levels of lipid peroxidation compounds.

Variable (nmol L^{-1})	Control (n = 31)	Preclinical (n = 12)	p Value
	Median (1st, 3rd Quartile)	Median (1st, 3rd Quartile)	
15-*epi*-15-F_{2t}-IsoP	0.62 (0.48, 0.82)	0.51 (0.34, 0.74)	0.414
PGE_2	0.3 (0.26, 0.38)	0.29 (0.27, 0.36)	0.738
2,3-dinor-15-*epi*-15-F_{2t}-IsoP	0.03 (0, 0.03)	0.03 (0.02, 0.03)	0.602
15-keto-15-E_{2t}-IsoP	1.02 (0.72, 1.35)	0.94 (0.69, 1.27)	0.384
15-keto-15-F_{2t}-IsoP	0.65 (0.45, 0.85)	0.66 (0.34, 0.89)	0.926
15-E_{2t}-IsoP	1.05 (0.8, 1.39)	1.26 (0.89, 1.46)	0.478
5-F_{2t}-IsoP	2.75 (2.16, 3.19)	2.35 (1.63, 2.9)	0.414
15-F_{2t}-IsoP	0.05 (0.05, 0.05)	0.05 (0.05, 0.07)	0.430
$PGF_{2\alpha}$	0.32 (0.25, 0.51)	0.34 (0.22, 0.65)	0.968
4(*RS*)-4-F_{4t}-NeuroP	3.62 (2.72, 4.9)	3.45 (2.36, 4.58)	0.800
1a,1b-dihomo-$PGF_{2\alpha}$	3.67 (3.06, 4.43)	3.14 (2.31, 4.34)	0.478
10-*epi*-10-F_{4t}-NeuroP	0.17 (0.11, 0.26)	0.15 (0.07, 0.25)	0.698
14(*RS*)-14-F_{4t}-NeuroP	1.77 (1.29, 2.31)	1.35 (1.03, 2.08)	0.355
ent-7(*RS*)-7-F_{2t}-dihomo-IsoP	0 (0, 0)	0 (0, 0.01)	0.414

Table 3. *Cont.*

Variable (nmol L^{-1})	Control (n = 31)	Preclinical (n = 12)	p Value
	Median (1st, 3rd Quartile)	Median (1st, 3rd Quartile)	
17-F_{2t}-dihomo-IsoP	0 (0, 0)	0 (0, 0)	1.000
17-*epi*-17-F_{2t}-dihomo-IsoP	0 (0, 0)	0 (0, 0)	1.000
17(*RS*)-10-*epi*-SC-Δ^{15}-11-dihomo-IsoF	0 (0, 0)	0 (0, 0)	0.679
7(*RS*)-ST-Δ^{8}-11-dihomo-IsoF	0 (0, 0.22)	0 (0, 0)	0.165
Neurofurans	0.27 (0.19, 0.37)	0.24 (0.21, 0.41)	0.679
Isofurans	0.52 (0.4, 0.65)	0.5 (0.41, 0.69)	0.718
Dihomo-isoprostanes	0.15 (0.14, 0.17)	0.15 (0.13, 0.17)	0.883
Dihomo-isofurans	0.01 (0.01, 0.02)	0.01 (0.01, 0.02)	0.883
Neuroprostanes	0.64 (0.49, 0.76)	0.59 (0.45, 0.77)	0.679
Isoprostanes	1.5 (1.25, 1.84)	1.32 (1.14, 1.67)	0.328

Correlations were computed between CSF biomarkers (β-amyloid-42, tau and p-tau) and plasma lipid peroxidation biomarkers (see Figure 2). Results showed that t-tau correlated with 15-F_{2t}-IsoP (r = 0.397, p = 0.008), and PGF2α (r = 0.339, p = 0.026); and p-tau correlated with 15-F_{2t}-IsoP (0.401, p = 0.008), and PGF2α (r = 0.329, p = 0.031). In addition, correlations were assayed between neuropsychological status and plasma biomarkers. Specifically, RBANS.DM correlated with 2,3-dinor-15-*epi*-15-F_{2t}-IsoP (r = −0.314, p = 0.040), 15-E_{2t}-IsoP (r = −0.432, p = 0.025), 5-F_{2t}-IsoP (r = −0.335, p = 0.028), 15-F_{2t}-IsoP (r = −0.390, p = 0.10), and PGF2α (r = −0.342, p = 0.025). Additionally, CDR showed correlation with 15-*epi*-15-F_{2t}-IsoP (r = 0.329, p = 0.031), PGE2 (r = 0.329, p = 0.031), 2,3-dinor-15-*epi*-15-F_{2t}-IsoP (r = 0.316, p = 0.039), 15-keto-15-E_{2t}-IsoP (r = 0.333, p = 0.029), 15-keto-15-F_{2t}-IsoP (r = 0.319, p = 0.037), 15-E_{2t}-IsoP (r = 0.363, p = 0.017), and 4(*RS*)-4-F_{4t}-NeuroP (r = 0.332, p = 0.030).

3.3. Potential Diagnosis Model

The developed model included 10 analytical variables (15-*epi*-15-F_{2t}-IsoP, PGE2, 15-keto-15-E_{2t}-IsoP, 15-keto-15-F_{2t}-IsoP, 15-E_{2t}-IsoP, PGF2α, 4(*RS*)-4-F4t-NeuroP, 1a,1b-dihomo-PGF2α, 10-*epi*-10-F_{4t}-NeuroP, 14(*RS*)-14-F_{4t}-NeuroP), as well as age and gender. Table 4 shows the model characteristics and the tendency of the different selected biomarkers. The conditional effect for each variable is represented in Figure 3, showing the increase or decrease in preclinical-AD probability according to the levels for each variable. This model showed an AUC of 0.96 (CI 95%, 0.903–1) (Figure 4), and a validation AUC of 0.90. The sensitivity and specificity profile shows a satisfactory compromise, with high sensitivity (0.91) at a high specificity (0.93), constituting the optimum cut-off point (0.44) (Figure 5). The equation of the developed model determining the probability of suffering from preclinical-AD status is shown.

$$\Pr(preclinical\text{-AD}) = \frac{e^{LP}}{1 + e^{LP}}$$

where LP = −6.566–0.153 * Female + 0.164 *Age—11.622 * A − 28.241 * B − 3.277 * C + 2.457 * D + 6.391 * E + 8.988 * F − 0.174 * G + 0.315 * H + 9.298 * I − 0.323 * J

A: 15-*epi*-15-F_{2t}-IsoP
B: PGE_2
C: 15-keto-15-E_{2t}-IsoP
D: 15-keto-15-F_{2t}-IsoP
E: 15-E_{2t}-IsoP
F: $PGF_{2\alpha}$

G: 4(RS)-4-F_{4t}-NeuroP
H: 1a,1b-dihomo-$PGF_{2\alpha}$
I: 10-*epi*-10-F_{4t}-NeuroP
J: 14(*RS*)-14-F_{4t}-NeuroP

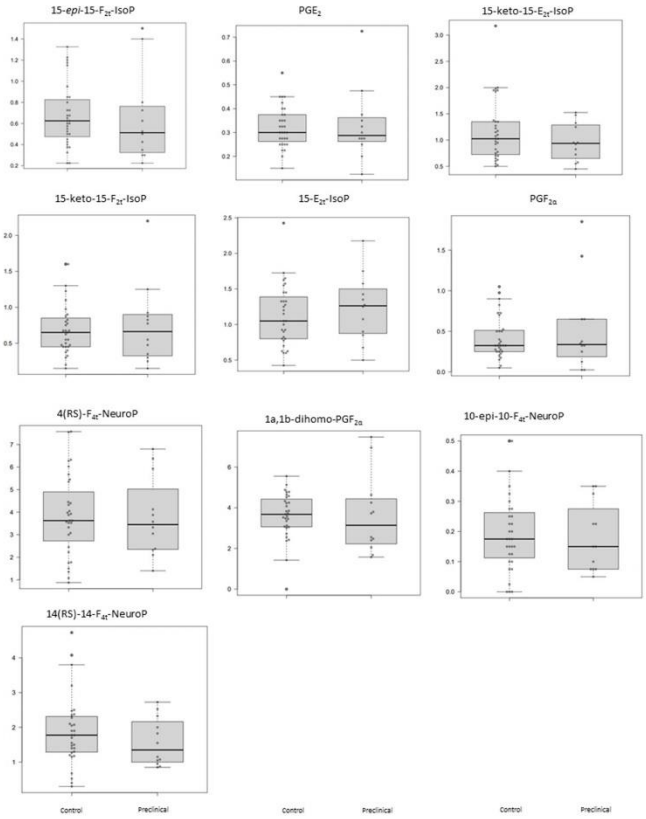

Figure 1. Box plots representing the concentrations in plasma samples for each analyte in control and preclinical-AD groups. Boxes represent the 1st and 3rd quartiles, and the black lines, the median.

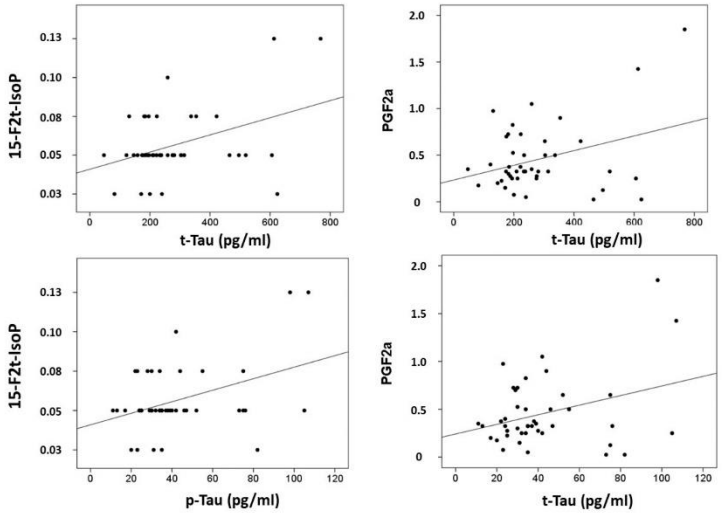

Figure 2. Correlation plots between plasma metabolites and CSF biomarkers.

Table 4. Model parameters.

Variables	Estimate	Exponential Estimate. ($e^{Estimate}$)
(Intercept)	−6.566	0.001
Gender (Females)	−0.153	0.858
Age	0.164	1.178
15-epi-15-F_{2t}-IsoP	−11.622	0
PGE_2	−28.241	0
15-keto-15-E_{2t}-IsoP	−3.277	0.038
15-keto-15-F_{2t}-IsoP	2.457	11.671
15-E_{2t}-IsoP	6.391	596.158
$PGF_{2\alpha}$	8.988	8003.721
4(RS)-4-F_{4t}-NeuroP	−0.174	0.841
1a,1b-dihomo-$PGF_{2\alpha}$	0.315	1.371
10-*epi*-10-F_{4t}-NeuroP	9.289	10,823.421
14(*RS*)-14-F_{4t}-NeuroP	−0.323	0.724
Lambda	0.004	

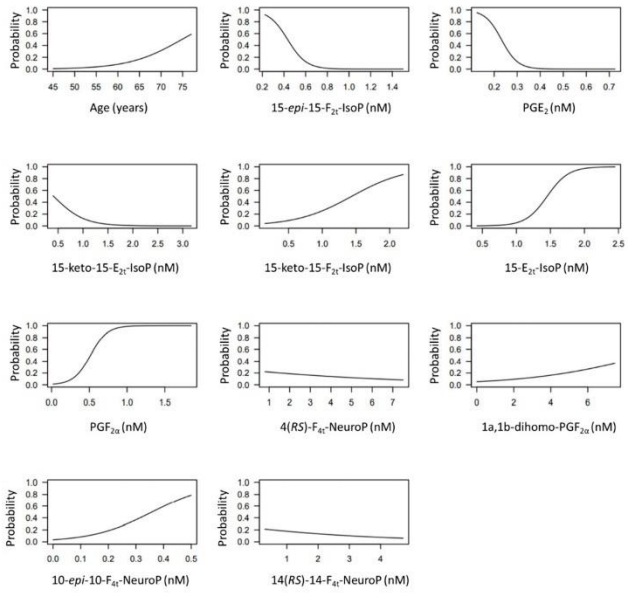

Figure 3. Conditional effect plots for each variable included in the model to predict the probability of preclinical-AD.

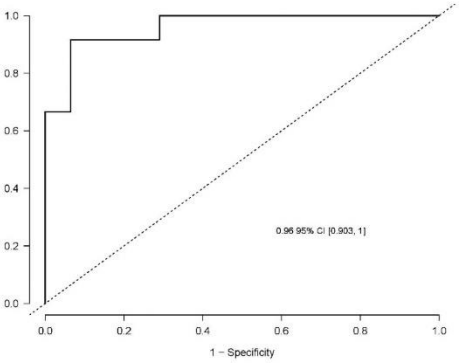

Figure 4. Receiver operating characteristic curve for the diagnostic model. The area under curve (AUC) is 0.96 (95% Confidence interval (CI), 0.903–1).

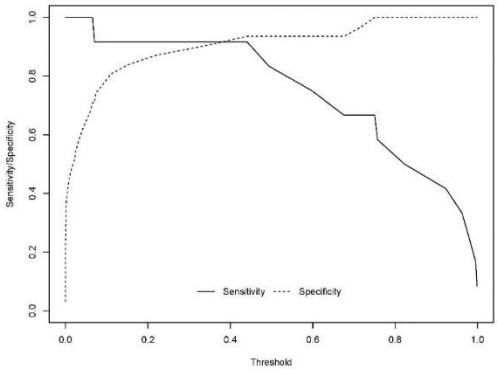

Figure 5. Sensitivity and specificity profile plot. The continuous line represents the relationship between the probability threshold set in the model's prediction and the sensitivity. The dashed line represents the relationship between the probability threshold and the specificity.

4. Discussion

In this work, some lipid peroxidation compounds were measured simultaneously in plasma samples from preclinical AD and healthy elderly participants, using UPLC-MS/MS as an analytical technique. These biomarkers did not show statistically significant different levels between both groups, although small differences could be observed for each metabolite. In addition, some of them showed a correlation with specific CSF biomarkers for AD (t-tau, p-tau) and with neuropsychological tests (RBANS.DM, CDR), showing a certain relationship with early AD development. Thus, a multivariate model was developed including some of these lipid peroxidation compounds, and showing their potential utility in discrimination between preclinical AD patients and healthy participants. In fact, the multivariate model takes into account the effect of each individual predictor, which could change in the presence of other variables, generating a composed algorithm, and it provides accurate predictions. These compounds were studied because they can reflect specific impairment of brain white matter or grey matter. However, their specificity would be determined in further studies, because there is no clear evidence that potentially detectable changes would be AD-specific, or if they would be general biomarkers of impairment of brain lipid metabolism.

In the literature, in some studies focused on searching for AD plasma biomarkers, mainly lipidic molecules were assayed [19,26]. However, most of them were based on participants with MCI and AD, all of them were patients with clinical symptoms (memory loss, cognitive decline), but none of them evaluated the group of well-characterized preclinical participants [19,27,28]. In fact, a previous work from our group was focused on the determination of lipid peroxidation compounds (isoP, NeuroP, isoF, NeuroF) in plasma samples from MCI-AD patients, developing a diagnosis model [19]. In that model, the selected compounds were 15-*epi*-15-F_{2t}-IsoP, 15-E_{2t}-IsoP, $PGF_{2\alpha}$, 4(*RS*)-F_{4t}-NeuroP, 14(*RS*)-14-F_{4t}-NeuroP, and Ent-7(*RS*)-7-F_{2t}-dihomo-IsoP. All of them, except Ent-7(*RS*)-7-F_{2t} dihomo-IsoP, were included in the present diagnosis model to predict AD in presymptomatic stage (preclinical AD). However, higher concentrations for these compounds were found in MCI-AD patients than in healthy participants; while lower concentrations were obtained for 15-*epi*-15-F_{2t}-IsoP and 4(*RS*)-F_{4t}-NeuroP in preclinical AD patients. These differences could be explained by the disease progression. In addition, the new developed model included

more variables (PGE_2, 15-keto-15-E_{2t}-IsoP, 15-keto-15-F_{2t}-IsoP, 1a,1b-dihomo-$PGF_{2\alpha}$, 10-*epi*-10-F_{4t}-NeuroP) in order to improve the accuracy (AUC validated = 0.90) in comparison with the previous model (AUC validated = 0.82) [19].

Recent research has focused on earlier AD stages, before the appearance of the first clinical manifestations of the disease. In general, these studies were about plasma β-amyloid-42/β-amyloid-40 ratio, showing an AUC of 0.78 in the discrimination between normal cognitive individuals with PET β-amyloid positivity and negativity [29]. In addition, plasma β-amyloid levels showed an association with dementia (determined by Mini Mental State Examination (MMSE) and the Geriatric Mental State Schedule (GMS)) and AD [30]. However, other study showed that plasma β-amyloid levels could not predict AD in preclinical participants [31]. A further study focused on plasma p-tau revealed its utility in AD diagnosis and prognosis, showing increased values since preclinical stages and an accuracy of 85% in AD dementia diagnosis [32]. However, the present work is the first study evaluating lipid peroxidation compounds in preclinical AD patients accurately diagnosed by CSF biomarkers.

Similarly, some of the studied biomarkers were lipidic compounds in plasma from preclinical AD participants [33]. In fact, the study carried out by Mapstone et al. analyzed lipids (phosphatidylcholine, Lysophosphatidylcholine, acylcarnitines, etc.), and it was carried out following the progression along 5 years, showing their potential utility as progression AD biomarkers [28].

The model developed in the present work was based on the plasma levels of 10 lipid peroxidation compounds. It is shown that an increase in the levels of these biomarkers (15-keto-15-F_{2t}-IsoP, 15-E_{2t}-IsoP, $PGF_{2\alpha}$, 10-*epi*-10-F_{4t}-NeuroP) could increase the probability of suffering from AD. Previous studies showed the utility of models based on plasma lipids as predictor approach of conversion amnestic MCI to AD or AD progression since preclinical stages [9,28]. The biomarkers determined in these studies are mainly related to membrane integrity, while ours are derived from oxidative stress. Another panel including 17 lipids can predict cognitive decline and brain atrophy in AD and it is related to clinical diagnosis in AD and t-tau CSF levels [34].

Early AD diagnosis remains a big challenge for human sciences. There is a high need for easily available biomarkers now that specific biomarkers have been described. These specific biomarkers are invasive and expensive; so minimally invasive biomarkers are in demand. The utility of these putative biomarkers can be found in the diagnostic paradigm, identifying people at risk for developing cognitive impairment, with a biological suspicion of specific or non-specific neurodegeneration, or other pre-diagnostic characteristics. In addition, these biomarkers could be useful in identifying subgroups with different disease evolution, different therapeutic response, and different neuropsychological dysfunction.

Among the study limitations, it is important to highlight the small sample used. This limitation is an evident issue and the results of a study with a higher number of cases cannot be anticipated. However, the present study could be considered exploratory. It is important to remark that the participants were selected in an asymptomatic stage, and highlight the difficulties of realizing CSF studies in asymptomatic cases. Another limitation is the exclusion of cases with other similar neurodegenerative diseases. Different patterns of biomarkers are expected in other neurodegenerative diseases, but in the present study, they were not evaluated. Therefore, these are preliminary results and further analysis in a large external cohort is required.

5. Conclusions

Lipid peroxidation biomarkers were determined in plasma from participants with preclinical AD and healthy elderly participants, showing no differences individually. However, these biomarkers showed a correlation with other specific AD CSF biomarkers and neuropsychological status. The multivariate model including 10 of these biomarkers constitutes a promising diagnostic tool to be applied to the general population in early AD

detection. However, further validation studies are necessary to confirm the utility of this potential model for preclinical AD diagnosis.

Author Contributions: Conceptualization, C.C.-P. and M.B.; methodology, C.P.-B. and L.Á.-S.; software, A.J.C.-M.; formal analysis, C.P.-B., M.L.-N. and I.F.; resources, T.D., C.O. and J.-M.G. writing—original draft preparation, C.C.-P. and C.P.-B.; writing—review and editing, C.C.-P. and M.B.; supervision, C.C.-P.; funding acquisition, C.C.-P. All authors have read and agreed to the published version of the manuscript.

Funding: This work was supported by the Instituto de Salud Carlos III (Miguel Servet I Project (CP16/00082)) and PI19/00570 (Spanish Ministry of Economy and Competitiveness, and Fondo Europeo Desarrollo Regional). CCP acknowledges MS16/00082. CPB acknowledges PFIS FI20/00022. LA acknowledges RH CM20/00140.

Institutional Review Board Statement: The study was conducted according to the guidelines of the Declaration of Helsinki, and approved by the Ethics Committee) of Health Research Institute La Fe (protocol code 2019/0105, 03/06/2019).

Informed Consent Statement: Informed consent was obtained from all subjects involved in the study.

Data Availability Statement: The data presented in this study are available on request from the corresponding author.

Conflicts of Interest: None of the authors of this manuscript declares having conflicts of interest.

References

1. Niedowicz, D.M.; Nelson, P.T.; Paul Murphy, M. Alzheimers Disease: Pathological Mechanisms and Recent Insights. *Curr. Neuropharmacol.* **2011**, *9*, 674–684. [CrossRef] [PubMed]
2. Scheltens, P.; Blennow, K.; Breteler, M.M.B.; de Strooper, B.; Frisoni, G.B.; Salloway, S.; Van de Flier, W.M. Alzheimer's disease. *Lancet* **2016**, *388*, 505–517. [CrossRef]
3. Hu, H.; Tan, L.; Bi, Y.-L.; Xu, W.; Tan, L.; Shen, X.-N.; Hou, X.-H.; Ma, Y.-H.; Dong, Q.; Yu, J.-T. Association between methylation of BIN1 promoter in peripheral blood and preclinical Alzheimer's disease. *Transl. Psychiatry* **2021**, *11*, 89. [CrossRef]
4. Keshavan, A.; Pannee, J.; Karikari, T.K.; Lantero Rodriguez, J.; Ashton, N.J.; Nicholas, J.M.; Cash, D.M.; Coath, W.; Lane, C.A.; Parker, T.D.; et al. Population-based blood screening for preclinical Alzheimer's disease in a British birth cohort at age 70. *Brain* **2020**, *144*, 434–449. [CrossRef]
5. Janelidze, S.; Berron, D.; Smith, R.; Strandberg, O.; Proctor, N.K.; Dage, J.L.; Stomrud, E.; Palmqvist, S.; Mattsson-Carlgren, N.; Hansson, O. Associations of Plasma Phospho-Tau217 Levels With Tau Positron Emission Tomography in Early Alzheimer Disease. *JAMA Neurol.* **2021**, *78*, 149. [CrossRef]
6. Suárez-Calvet, M.; Karikari, T.K.; Ashton, N.J.; Gispert, J.D.; Salvado, G.; Fauria, K.; Shekari, M.; Grau-Rivera, O.; Stoops, E.; Blennow, K.; et al. Novel tau biomarkers phosphorylated at T181, T217 or T231 rise in the initial stages of the preclinical Alzheimer's continuum when only subtle changes in Aβ pathology are detected. *EMBO Mol. Med.* **2020**, *12*, e12921. [CrossRef] [PubMed]
7. Lim, Y.Y.; Maruff, P.; Kaneko, N.; Doecke, J.; Fowler, C.; Kato, T.; Rowe, C.C.; Arahata, Y.; Ito, K.; Masters, C.L.; et al. Plasma Amyloid-β Biomarker Associated with Cognitive Decline in Preclinical Alzheimer's Disease. *J. Alzheimer's Dis.* **2020**, *77*, 1057–1065. [CrossRef]
8. Eruysal, E.; Ravdin, L.; Kamel, H.; Iadecola, C.; Ishii, M. Plasma lipocalin-2 levels in the preclinical stage of Alzheimer's disease. *Alzheimer's Dement. Diagn. Assess. Dis. Monit.* **2019**, *11*, 646–653. [CrossRef]
9. Fiandaca, M.S.; Zhong, X.; Cheema, A.K.; Orquiza, M.H.; Taan, M.T.; Gresenz, C.R.; Nalls, M.A.; Singleton, A.B.; Mapstone, M.; Chidambaram, S.; et al. Plasma 24-metabolite Panel Predicts Preclinical Transition to Clinical Stages of Alzheimer's Disease. *Front. Neurol.* **2015**, *6*, 237. [CrossRef] [PubMed]
10. Jia, L.; Zhu, M.; Kong, C.; Pang, Y.; Zhang, H.; Qiu, Q.; Wei, C.; Tang, Y.; Wang, Q.; Li, Y.; et al. Blood neuro-exosomal synaptic proteins predict Alzheimer's disease at the asymptomatic stage. *Alzheimer's Dement.* **2021**, *17*, 49–60. [CrossRef] [PubMed]
11. Goetzl, E.J.; Boxer, A.; Schwartz, J.B.; Abner, E.L.; Petersen, R.C.; Miller, B.L.; Kapogiannis, D. Altered lysosomal proteins in neural-derived plasma exosomes in preclinical Alzheimer disease. *Neurology* **2015**, *85*, 40–47. [CrossRef] [PubMed]
12. Gross, A.L.; Walker, K.A.; Moghekar, A.R.; Pettigrew, C.; Soldan, A.; Albert, M.S.; Walston, J.D. Plasma Markers of Inflammation Linked to Clinical Progression and Decline During Preclinical AD. *Front. Aging Neurosci.* **2019**, *11*, 229. [CrossRef] [PubMed]
13. Plascencia-Villa, G.; Perry, G. Preventive and Therapeutic Strategies in Alzheimer's Disease: Focus on Oxidative Stress, Redox Metals, and Ferroptosis. *Antioxid. Redox Signal.* **2021**, *34*, 591–610. [CrossRef] [PubMed]
14. García-Blanco, A.; Baquero, M.; Vento, M.; Gil, E.; Bataller, L.; Cháfer-Pericás, C. Potential oxidative stress biomarkers of mild cognitive impairment due to Alzheimer disease. *J. Neurol. Sci.* **2017**, *373*, 295–302. [CrossRef]

15. Peña-Bautista, C.; Vento, M.; Baquero, M.; Cháfer-Pericás, C. Lipid peroxidation in neurodegeneration. *Clin. Chim. Acta* **2019**, *497*, 178–188. [CrossRef] [PubMed]
16. Chmatalova, Z.; Vyhnalek, M.; Laczo, J.; Hort, J.; Pospisilova, R.; Pechova, M.; Skoumalova, A. Relation of Plasma Selenium and Lipid Peroxidation End Products in Patients with Alzheimer's Disease. *Physiol. Res.* **2017**, *66*, 1049–1056. [CrossRef]
17. Montagne, A.; Zhao, Z.; Zlokovic, B.V. Alzheimer's disease: A matter of blood-brain barrier dysfunction? *J. Exp. Med.* **2017**, *214*, 3151–3169. [CrossRef]
18. Peña-Bautista, C.; Baquero, M.; Lopez-Nogueores, M.; Vento, M.; Hervas, D.; Cháfer-Pericás, C. Isoprostanoids Levels in Cerebrospinal Fluid Do Not Reflect Alzheimer's Disease. *Antioxidants* **2020**, *9*, 407. [CrossRef]
19. Peña-Bautista, C.; Vigor, C.; Galano, J.-M.; Oger, C.; Durand, T.; Ferrer, I.; Cuevas, A.; Vento, M.; Baquero, M.; Cháfer-Pericás, C.; et al. Plasma lipid peroxidation biomarkers for early and non-invasive Alzheimer Disease detection. *Free Radic. Biol. Med.* **2018**, *124*, 388–394. [CrossRef]
20. Peña-Bautista, C.; Alvarez, L.; Baquero, M.; Ferrer, I.; Garcia, L.; Hervas-Marin, D.; Cháfer-Pericás, C. Plasma isoprostanoids assessment as Alzheimer's disease progression biomarkers. *J. Neurochem.* **2020**, *157*, 2187–2194. [CrossRef]
21. Hughes, C.P.; Berg, L.; Danziger, W.; Coben, L.A.; Martin, R.L. A New Clinical Scale for the Staging of Dementia. *Br. J. Psychiatry* **1982**, *140*, 566–572. [CrossRef]
22. Folstein, M.F.; Folstein, S.E.; McHugh, P.R. "Mini-mental state": A practical method for grading the cognitive state of patients for the clinician. *J. Psychiatr. Res.* **1975**, *12*, 189–198. [CrossRef]
23. Randolph, C.; Tierney, M.C.; Mohr, E.; Chase, T.N. The Repeatable Battery for the Assessment of Neuropsychological Status (RBANS): Preliminary Clinical Validity. *J. Clin. Exp. Neuropsychol.* **1998**, *20*, 310–319. [CrossRef]
24. Peña-Bautista, C.; Avarez, L.; Durand, T.; Vigor, C.; Cuevas, A.; Baquero, M.; Vento, M.; Hervas, D.; Cháfer-Pericás, C. Clinical Utility of Plasma Lipid Peroxidation Biomarkers in Alzheimer's Disease Differential Diagnosis. *Antioxidants* **2020**, *9*, 649. [CrossRef]
25. Friedman, J.; Hastie, T.; Tibshirani, R. Regularization Paths for Generalized Linear Models via Coordinate Descent. *J. Stat. Softw.* **2010**, *33*, 1–22. [CrossRef]
26. Peña-Bautista, C.; Roca, M.; Hervas, D.; Cuevas, A.; Lopez-Cuevas, R.; Vento, M.; Baquero, M.; Garcia-Blanco, A.; Cháfer-Pericás, C. Plasma metabolomics in early Alzheimer's disease patients diagnosed with amyloid biomarker. *J. Proteom.* **2019**, *200*, 144–152. [CrossRef] [PubMed]
27. Proitsi, P.; Kim, M.; Whiley, L.; Simmons, A.; Lupton, M.K.; Soininen, H.; Tsolaki, M.; Vellas, B.; Lovestone, S.; Powell, J.F.; et al. Association of blood lipids with Alzheimer's disease: A comprehensive lipidomics analysis. *Alzheimer's Dement.* **2017**, *13*, 140–151. [CrossRef] [PubMed]
28. Mapstone, M.; Cheema, A.K.; Fiandaca, M.S.; Zhong, X.; Mhyre, T.R.; Hall, W.J.; Fisher, S.G.; Peterson, D.R.; Haley, J.M.; Tan, M.T.; et al. Plasma phospholipids identify antecedent memory impairment in older adults. *Nat. Med.* **2014**, *20*, 415–418. [CrossRef] [PubMed]
29. Chatterjee, P.; Elmi, M.; Goozee, K.; Shah, T.; Sohrabi, H.R.; Dias, C.B.; Pedrini, S.; Shen, K.; Asih, P.R.; Dave, P.; et al. Ultrasensitive Detection of Plasma Amyloid-β as a Biomarker for Cognitively Normal Elderly Individuals at Risk of Alzheimer's Disease. *J. Alzheimer's Dis.* **2019**, *71*, 775–783. [CrossRef]
30. Hilal, S.; Wolters, F.J.; Verbeek, M.M.; Vanderstichele, H.; Ikram, M.K.; Stoopes, E.; Ikram, M.A.; Vernooij, M.W. Plasma amyloid-β levels, cerebral atrophy and risk of dementia: A population-based study. *Alzheimer's Res. Ther.* **2018**, *10*, 63. [CrossRef]
31. Lövheim, H.; Elgh, F.; Johansson, A.; Zetterberg, H.; Blennow, K.; Hallmans, G.; Eriksson, S. Plasma concentrations of free amyloid β cannot predict the development of Alzheimer's disease. *Alzheimer's Dement.* **2017**, *13*, 778–782. [CrossRef] [PubMed]
32. Karikari, T.K.; Benedet, A.L.; Ashton, N.J.; Rodriguez, J.L.; Snellman, A.; Lussier, F.; Rial, A.M.; Pascoal, T.A.; Andeasson, U.; Blennow, K.; et al. Diagnostic performance and prediction of clinical progression of plasma phospho-tau181 in the Alzheimer's Disease Neuroimaging Initiative. *Mol. Psychiatry* **2021**, *26*, 429–442. [CrossRef] [PubMed]
33. Cheng, H.; Wang, M.; Li, J.-L.; Cairns, N.J.; Han, X. Specific changes of sulfatide levels in individuals with pre-clinical Alzheimer's disease: An early event in disease pathogenesis. *J. Neurochem.* **2013**, *127*, 733–738. [CrossRef] [PubMed]
34. Ma, Y.; Shen, X.N.; Xu, W.; Huang, Y.-Y.; Li, H.-Q.; Tan, L.; Dong, Q.; Tan, L.; Yu, Y.-T. A panel of blood lipids associated with cognitive performance, brain atrophy, and Alzheimer's diagnosis: A longitudinal study of elders without dementia. *Alzheimer's Dement. Diagn. Assess. Dis. Monit.* **2020**, *12*, e12041. [CrossRef]

Neurochemistry International 129 (2019) 104519

Contents lists available at ScienceDirect

Neurochemistry International

journal homepage: www.elsevier.com/locate/neuint

Lipid peroxidation biomarkers correlation with medial temporal atrophy in early Alzheimer Disease

Carmen Peña-Bautista[a], Rogelio López-Cuevas[b], Ana Cuevas[b], Miguel Baquero[b], Consuelo Cháfer-Pericás[a,*]

[a] Neonatal Research Unit, Health Research Institute La Fe, Valencia, Spain
[b] Neurology Unit, University and Polytechnic Hospital La Fe, Valencia, Spain

ARTICLE INFO

Keywords:
Alzheimer disease
Plasma biomarkers
Neurodegeneration
Neuroimage
Oxidative stress

ABSTRACT

Alzheimer Disease (AD) is a pathology that causes millions of deaths every year and it also generates severe economic consequences for families and public health systems. Oxidative stress is related to neurodegenerative diseases damage. In fact, brain lipid oxidation could produce brain atrophy. The main objective of this study is the evaluation of atrophy and lipid peroxidation damage in AD patients. We studied medial temporal brain atrophy by magnetic resonance imaging (MRI) and a set of lipid peroxidation biomarkers from plasma samples, respectively. The participants were AD patients in early stages (n = 80) and healthy controls (n = 32). Some lipid peroxidation compounds (neuroprostanes, isoprostanes, neurofurans, isofurans, 17-*epi*-17-F_{2t}-dihomo-IsoP, $PGF_{2\alpha}$) in plasma showed statistically significant correlation with medial temporal atrophy. So, they were selected to generate an AD diagnosis model, showing an AUC-ROC of 0.900, close to accuracy achieved by the model based on neuroimaging analysis (AUC-ROC 0.929). In addition, the new model showed suitable specificity, so it could be used as screening test. The developed model based on plasma biomarkers could reflect white and grey matter lipid peroxidation, which occurs in medial temporal lobe in early AD patients. Nevertheless, more studies are needed in this field in order to evaluate specificity against other dementias or neurodegenerative diseases.

1. Introduction

Alzheimer disease (AD) is the fifth global cause of death according to the World Health Organization (WHO), coming to the third position in high-income countries. In fact, the growing number of death caused by this disease in last years, constitutes a great concern ("World Health Organisation, 2018"). This long progressive pathology involves high costs for families and governments, and the development of new early diagnostic methods and effective treatments are necessary (Alzheimer's Association, 2016).

Clinically, AD is characterized by a cognitive impairment, being memory loss the main symptom. These progressive symptoms are consequences of anatomical alterations in AD patients' brain. The main hallmarks are accumulation of β-amyloid peptides and hyperphosphorylated tau protein, which lead to synapsis loss and degeneration in different brain areas (Kamat et al., 2016). Nowadays, AD diagnosis relies on clinical judgment and exclusion of secondary causes. Diagnosis specificity and certainty, especially in early stages (e.g. mild cognitive impairment (MCI)), can be improved by means of disease biomarkers, such as β-amyloid and tau proteins levels in cerebrospinal fluid (CSF) (Nordberg, 2015). Paying more attention to neuroimaging is useful in AD diagnosis and progression prediction (Rathore et al., 2017) (Sørensen et al., 2017), but sometimes the employment of different image techniques is required to improve their diagnostic capacity (Mi et al., 2017), which increases diagnosis costs (Ramos Bernardes da Silva Filho et al., 2017). Throughout the AD course, different brain areas could be affected (Ferreira et al., 2017). One area with a remarkable atrophy grade during AD progression is the medial temporal lobe, where the hippocampus is located, and this alteration has been used to develop diagnosis models with high reproducibility (Sarria-Estrada et al., 2015). The hippocampus study is even useful in MCI progression prediction (Persson et al., 2017).

Regarding oxidative stress, it is related to AD progression (Pohanka, 2014) and its characteristic synapsis loss since early stages of the disease (Kamat et al., 2016). Actually, it could modify brain proteins and lipids levels, and give place to morphological brain changes (Scheff et al., 2016) (Yadav and Tiwari, 2014) (Klosinski et al., 2015). In this sense, the main objective of this study is to evaluate the correlation

* Corresponding author. Health Research Institute La Fe, Avda de Fernando Abril Martorell, 106; 46026, Valencia, Spain.
E-mail address: m.consuelo.chafer@uv.es (C. Cháfer-Pericás).

https://doi.org/10.1016/j.neuint.2019.104519
Received 3 June 2019; Received in revised form 10 July 2019; Accepted 5 August 2019
Available online 06 August 2019
0197-0186/

Abbreviations

AD	Alzheimer Disease
AdA	adrenic acid
AA	arachidonic acid
BBB	blood brain barrier
CDR	Clinical Dementia Rating
CSF	cerebrospinal fluid
DHA	docosahexaenoic acid
DT	difusion tensor
EOAD	Early Onset Alzheimer DIsease
FAQ	Functional Activities Questionnaire
EDTA	ethylenediaminetetraacetic acid
MCI	mild cognitive impairment
MRI	magnetic resonance imaging
MTA	medial temporal atrophy
NIA-AA	National Institute on Aging- NIA-AA - Alzheimer's Association
PET	positron emission tomography
PLS	partial least squares
p-Tau	phosphorylated Tau
RBANS-DM	Repeatable Battery for the Assessment of Neuropsychological Status-Delayed Memory
RLC	relative light changes
ROC	receiver operating characteristic curve
SPE	solid phase extraction
UPLC-MS/MS	ultra-performance liquid chromatography coupled with tandem mass spectrometry
WHO	World Health Organization

between plasma lipid peroxidation biomarkers and anatomical brain changes, specifically medial temporal atrophy.

2. Material and methods

2.1. Participants

Participants between 50 and 80 years old were recruited from de Neurology Unit of the University and Polytechnic Hospital La Fe, Valencia (Spain). Informed consent was approved by the Ethics Committee of the Health Research Institute La Fe (Valencia). Participants were classified in case and control groups according to National Institute on Aging-Alzheimer's Association (NIA-AA) criteria including CSF biomarkers (β-amyloid, Tau and phosphorylate Tau (p-Tau)) and neurophsycological tests (clinical dementia rating (CDR), Functional Activities Questionnaire (FAQ), Repeatable Battery for the Assessment of Neuropsychological Status-Delayed Memory (RBANS-DM), Mini-mental state examination (MMSE)) (McKhann et al., 2011) (Albert et al., 2011). We excluded patients with history of brain structural disease (tumor, stroke, etc), Fazekas score greater than 2, major head trauma, epilepsy, multiple sclerosis and major psychiatric disorders, as well as patients with advanced dementia and patients that were not able to undergo neuropsychological evaluations because of their educational level.

2.2. Sample collection, storage and treatment

Blood samples were taken from all participants using cryo-tubes with ethylenediaminetetraacetic acid (EDTA). They were centrifuged for 10 min at 2000 g and supernatant (plasma) was stored at −80 °C until the analysis. Sample treatment was described in a previous work (Peña-Bautista et al., 2018). Briefly, samples were thawed on ice after adding the internal standard, a basic hydrolysis with potassium hidroxyde and a clean-up step with solid phase extraction (SPE) were carried out. Finally, samples were injected in a chromatographic system and were analyzed by ultra-performance liquid chromatography coupled with tandem mass spectrometry (UPLC-MS/MS) (Peña-Bautista et al., 2018).

CSF samples were obtained as part of the diagnostic protocol in the Polytechnic University Hospital La Fe (Valencia). From 1 to 10 mL of CSF were collected under standardized procedure of lumbar puncture at 8 a.m. after overnight fasting, and they were stored at −80 °C until analysis. Biochemical determinations (β-amyloid, t-Tau, p-Tau) were carried out by Innotest Elisa kit (Fujirebio Diagnostics, Ghent, Belgium) using a fully automated system (Lumipulse G, Fujirebio).

2.3. Neuroimaging data acquisition

Magnetic resonance imaging (MRI) was performed as part of the routine clinical assessment. Images were obtained using three MRI scanners (Siemens): two 1.5 T and one 3T machines were used. Imaging protocol included axial, sagittal and coronal views of the brain using T1, T2, gradient echo and fluid attenuation inversion recovery (FLAIR) sequences. Medial temporal atrophy (MTA) was assessed visually by a single rater relative light changes (RLC) using FLAIR or T1 coronal images at the level of the hippocampus. The visual assessment of MTA was ranged from 0 (no atrophy) to 4 (severe atrophy) and was based on criteria and score system proposed by Scheltens et al. (1992).

2.4. Statistical analysis

First, univariate statistical analysis was carried out using SPSS software version 20.0 (SPSS, Inc., Chicago, IL, USA). The differences between the variables medians of case group and control group were analyzed using the non-parametric Mann Whitney test for numerical variables, and Chi-Square test for nominal variables. Correlations between plasma biomarkers and image data were evaluated by Pearson correlation coefficient (r).

The multivariate statistical analysis was carried out using the Minitab software version 18 (USA). Discriminant analysis was performed by partial least squares regression (PLS). Then, the Receiver operating characteristic curve (ROC) of the discriminant model was obtained. Two models were constructed, the first included plasma biomarkers (isoprostanes, neuroprostanes, isofurans, neurofurans, 17-*epi*-17-F_{2t}-dihomo-IsoP, $PGF_{2\alpha}$), gender and age as predictor variables, and the second included image data (MTA-R (right), MTA-L (left) and MTA-S (sum)), gender and age as predictor variables. The response variable used was group (control-case). All the variables were standardized and cross-validation of the models was carried out. Then diagnosis indices (sensitivity, specificity, positive predictive value, negative predictive value) were calculated for both models.

2.5. Declaration of sources of funding

This work was supported by the Instituto de Salud Carlos III (Miguel Servet I Project [grant number CP16/00082]) (Spanish Ministry of Economy and Competitiveness, and European Regional Development Fund).

3. Results

3.1. Participants' description

In Table 1, demographic and clinical characteristics from the study

Table 1
Demographic and clinical variables for the participants.

Variables	Control (n = 32)	Case (n = 80)	P value
Age (years, median (IQR))	66 (62–69)	71 (68–74)	0.000*
Gender (female, n (%))	11 (34%)	47 (59%)	0.020*
β-amyloid (pg mL^{-1}, median (IQR))	1192 (1051–1444)	588 (441–676)	0.000*
t-Tau (pg mL^{-1}, median (IQR))	171 (108–284)	523 (361–775)	0.000*
p-Tau (pg mL^{-1}, median (IQR))	44 (27–57)	82 (66–116)	0.000*
CDR (median (IQR))	0 (0–0)	0.5 (0.5–1)	0.000*
MMSE (median (IQR))	30 (28–30)	22 (18–26)	0.000*
RBANS.DM (median (IQR))	100 (92–106)	44 (40–52)	0.000*
FAQ (median (IQR))	0 (0–0)	7 (3–13)	0.000*
GDS (median (IQR))	3 (1–7)	7 (4–11)	0.021*
Fazekas (median (IQR))	0 (0–1)	1 (0–1)	0.018*
ATM-RIGHT (median (IQR))	0 (0–0)	2 (1–2)	0.000*
ATM-LEFT (median (IQR))	0 (0–0)	1 (1–2)	0.000*
ATM (R + L) (median (IQR))	0 (0–0)	3 (2–4)	0.000*

population are summarized. Age and gender showed statistically significant differences between both groups, so they were included as covariates in the multivariate models. As expected, clinical variables (CSF β-amyloid, CSF Tau, CSF p-Tau, RBANS-DM, CDR, FAQ, MMSE) showed statistically significant differences between case and control groups.

3.2. Image measurement data

Using neuroimaging techniques, the variables determined were MTA-R, MTA-L, MTA-S and Fazekas. As can be seen in Table 2, the three MTA indices showed statistically significant differences between groups, as well as Fazekas.

3.3. Analyte determination

In Table 2 medians of analytes levels determined in plasma from case and control groups are summarized. 8-iso-15(*R*)-$PGF_{2\alpha}$, 2,3-dinor-$iPF_{2\alpha}$-III, 8-iso-15-keto-PGE_2, 4(*RS*)-F_{4t}-NeuroP, neuroprostanes, isoprostanes, Ent-7(*RS*)-F_{2t}-dihomo-IsoP and 17-*epi*-17-F_{2t}-dihomo-IsoP, showed higher levels in the case group than in the control group. Inversely, $PGF_{2\alpha}$, 14(*RS*)-14-F_{4t}-NeuroP, 5-$iPF_{2\alpha}$-VI and 7(*RS*)-*ST*-Δ^8-11-dihomo-IsoF showed higher levels in the control group. Nevertheless, only 8-iso-15(*R*)-$PGF_{2\alpha}$ ($p = 0.042$), $PGF_{2\alpha}$ ($p = 0.001$), 4(*RS*)-F_{4t}-NeuroP ($p = 0.030$), neuroprostanes ($p = 0.001$), isoprostanes ($p = 0.006$) and 17-*epi*-17-F_{2t}-dihomo-IsoP ($p = 0.008$) showed statistically significant differences between groups.

3.4. Correlation between plasma lipid peroxidation biomarkers levels and image indices

Relationship between neuroimaging indices and plasma biomarker levels was analyzed, and some statistically significant correlation was observed. In fact, MTA in right brain lobe showed positive correlation with neuroprostanes ($r = 0.242$, $p = 0.010$), and 17-*epi*-17-F_{2t}-dihomo-IsoP ($r = 0.223$, $p = 0.018$), while it showed negative correlation with $PGF_{2\alpha}$ ($r = -0.259$, $p = 0.006$). Similar results were obtained with MTA in the left side, positive correlation was observed with neuroprostanes ($r = 0.213$, $p = 0.024$), and 17-*epi*-17-F_{2t}-dihomo-IsoP ($r = 0.214$, $p = 0.024$), while it showed negative correlation with $PGF_{2\alpha}$ ($r = -0.305$, $p = 0.001$). In the same sense, the sum of MTA in both brain lobes showed correlation with neuroprostanes ($r = 0.234$, $p = 0.013$), 17-*epi*-17-F_{2t}-dihomo-IsoP ($r = 0.224$, $p = 0.018$) and $PGF_{2\alpha}$ (PCC = −0.288, $p = 0.002$). In addition, Fazekas, index related to vascular brain disease, showed correlation with 17-F_{2t}-dihomo-IsoP ($r = 0.215$, $p = 0.023$) (see Fig. 1).

3.5. Multivariate analysis

Two statistical models were carried out, the first based on neuroimaging analysis and the second based on plasma lipid peroxidation biomarkers levels. As it is shown in Fig. 2a, the model based on neuroimaging analysis showed a correlation between the different MTA measures (right and left lobe and total MTA), but age and gender did not correlate with them. Also, the scatter plot (Fig. 2b) showed a satisfactory separation between participants groups. In this sense, the case group is characterized by higher levels of MTA. For this model, the Area under Curve-Receiver Operating Characteristic AUC-ROC is 0.929 (CI 95%, 0.882–0.977). Besides, this model has a sensitivity of 90.00%, a specificity of 84.38% and its positive and negative predictive values are 93.51% and 77.14, respectively.

Regarding the model constructed by plasma biomarkers (neuroprostanes, isoprostanes, neurofurans, isofurans, 17-*epi*-17-F_{2t}-dihomo-IsoP, $PGF_{2\alpha}$), a negative correlation between PGF2α and isoprostanes and isofurans was observed, but age and gender did not correlate with biomarkers (Fig. 2c). Also, Fig. 2d shows a satisfactory discrimination between case and control groups. This model could diagnose AD or not-AD with an accuracy of AUC-ROC = 0.900 (0.845–0.956). The diagnosis indices for this model were sensitivity 72.5%, specificity 100%, negative predictive value 59.26% and positive predictive value 100%.

4. Discussion

The parameter MTA is commonly related to cerebrovascular dementias (Kalaria and Ihara, 2017). Previous works showed that this morphological alteration is associated with MCI and AD, showing higher damage grade in AD than in MCI patients, as well as a correlation with neuropsychological evaluation tests (e.g. MMSE, CDR) (Hsu et al., 2015). In this sense, some cut-off values for MTA to be used as AD diagnosis and MCI prognosis were established (Ferreira et al., 2015). In addition, MTA is related to cognitive impairment in patients with Dementia with Lewy Bodies (Tagawa et al., 2015). Medial temporal lobe atrophy evaluation contributes to a better diagnosis accuracy (Visser et al., 1999). Moreover, correlations between MTA and CSF biomarkers t-tau and p-tau for different variants of Early-Onset Alzheimer Disease (EOAD) were described (Granadillo et al., 2017). Nowadays, neuropsychological tests and CSF biomarkers are employed as AD diagnosis, these two parameters could be related to MTA, so the evaluation

Table 2
Concentrations of analytes in plasma samples from participants groups.

	Control (n = 32)	Case (n = 80)	P value
8-iso-15(R)-$PGF_{2\alpha}$	0.25 (0.20–0.35)	0.30 (0.23–0.49)	0.042*
PGE_2	0.06 (0.01–0.75)	0.09 (0.00–0.28)	0.693
2,3-dinor-$iPF_{2\alpha}$-III	0.00 (0.00–0.00)	0.00 (0.00–0.03)	0.950
8-iso-15-keto-PGE_2	0.06 (0.00–0.17)	0.13 (0.00–0.34)	0.425
8-iso-15-keto- $PGF_{2\alpha}$	0.25 (0.18–0.33)	0.26 (0.13–0.35)	0.754
8-iso-PGE_2	0.28 (0.15–1.98)	0.39 (0.18–0.78)	0.689
5-$iPF_{2\alpha}$-VI	0.94 (0.67–1.22)	0.71 (0.35–1.22)	0.123
8-iso-$PGF_{2\alpha}$	0.02 (0.01–0.03)	0.02 (0.01–0.03)	0.841
$PGF_{2\alpha}$	0.74 (0.60–0.94)	0.48 (0.25–0.78)	0.001*
4(RS)-F_{4t}-NeuroP	1.03 (0.71–1.24)	1.15 (0.96–1.33)	0.030*
1a,1b-dihomo-$PGF_{2\alpha}$	0.00 (0.00–0.00)	0.00 (0.00–0.00)	0.326
Neuroprostanes	0.29 (0.22–0.38)	0.83 (0.26–1.52)	0.001*
10-epi-10-F_{4t}-NeuroP	0.11 (0.07–0.18)	0.09 (0.03–0.18)	0.390
14(RS)-14-F_{4t}-NeuroP	0.90 (0.00–1.51)	0.80 (0.29–1.27)	0.930
Isoprostanes	0.22 (0.18–0.34)	0.32 (0.23–0.40)	0.006*
Ent-7(RS)-F_{2t}-dihomo-IsoP	0.08 (0.05–0.17)	0.13 (0.08–0.18)	0.145
17-F_{2t}-dihomo-IsoP	0.00 (0.00–0.00)	0.00 (0.00–0.00)	0.302
17-epi-17-F_{2t}-dihomo-IsoP	0.00 (0.00–0.00)	0.00 (0.00–0.03)	0.008*
7(RS)-10-epi-*SC*–Δ^{15}-11-dihomo-IsoF	0.00 (0.00–0.00)	0.00 (0.00–0.00)	0.150
7(RS)-*ST*-Δ^8-11-dihomo-IsoF	0.10 (0.01–0.25)	0.05 (0.01–0.19)	0.199
Neurofurans	0.18 (0.11–0.26)	0.18 (0.13–0.27)	0.762
Isofurans	0.09 (0.06–0.22)	0.10 (0.08–0.16)	0.399

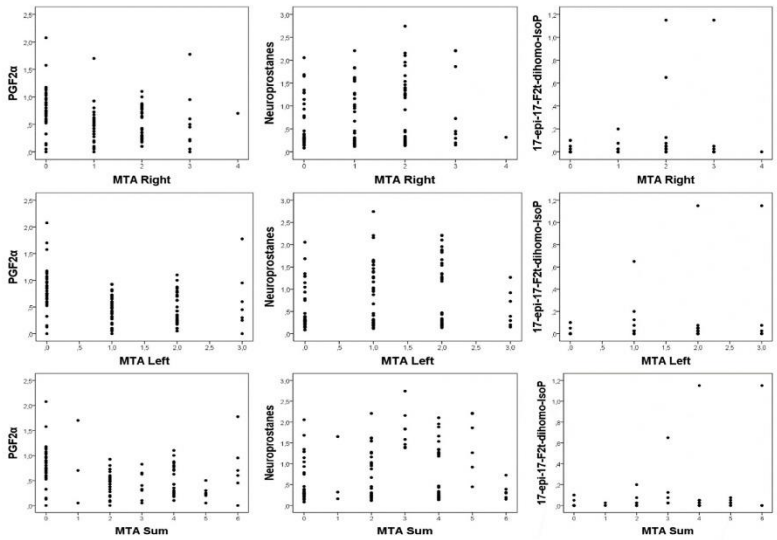

Fig. 1. Correlations between neuroimaging variables and plasma biomarkers levels.

of atrophy could be useful in AD diagnosis, as well as the lipid peroxidation study as a possible pathway implied in AD. Our results showed that a diagnosis model based only on this atrophy evaluation could diagnose AD with an accuracy of 0.929. It could avoid actual lumbar puncture used in AD diagnosis nowadays, as well as neuropsycological evaluations that require a considerable amount of time on part of specialized staff and is tiresome for patients. In this sense, other diagnosis models for AD based on neuroimaging techniques have been developed. Specifically, a model based on Magnetic Resonance Imaging (MRI) and Positron Emission Tomography (PET) was able to differentiated between AD, MCI and healthy control groups with accuracies between 0.75 and 0.95 (Suk et al., 2014). The model developed by Canu et al. (2017) was able to distinguish between EOAD and behavioral variant of frontotemporal dementia with an accuracy of 0.82 based on cortical thickness and DT (diffusion tensor) MRI measures (Canu et al., 2017). Our model shows better accuracy, but its specificity is required to be evaluated employing other dementias or neurodegenerative diseases. This model shows good diagnosis indices, especially its high specificity that could allow the application of this model as a preliminary screening test although it probably needs other tests to give a reliable diagnosis.

Regarding the evaluation of possible correlations between neuroimaging results (MTA) and different lipid peroxidation products in plasma samples form AD and healthy participants, the highest correlations were between brain MTA and neuroprostanes. Therefore, specific brain alterations could be measured in plasma samples by means of these lipid peroxidation products (Miller et al., 2014). As MTA scale is based mainly in grey matter atrophy, neuroprostanes could explain this alteration evaluation (Scheltens et al., 1992). In addition, neuroprostanes levels were statistically significant different between AD and healthy participants. Therefore, they are satisfactory AD biomarkers. In addition, the dihomo-isoprostanes could be obtained from brain white matter oxidation. The correlation found between MTA and these compounds could be explained as some white matter atrophy that occurs together with the grey matter alterations in medial temporal lobe mainly in the hipocampus from AD patients. We also analyzed correlations between our biomarkers and Fazekas, which is a scale based on brain white matter lesions and it is usually related to vascular pathologies. This scale is not AD specific but it could help to discard AD as a cause of vascular dementia (Fazekas et al., 1987). Punctuation for this scale showed statistically significant correlation with 17-F_{2t}-dihomo-IsoP that is a white matter lipid peroxidation product. So, this biomarker could be useful in the study of white matter lesions present in different neudegenerative diseases, not only in AD, and sometimes it could serve to discard AD diagnosis or to differentiate it from frontotemporal dementia whose symptoms could be confused (Elahi et al., 2017).

Regarding plasma biomarkers, neuroprostanes and neurofurans are derived from docosahexaenoic acid (DHA) oxidation, while isoprostanes and isofurans come from the arachidonic acid (AA) oxidation (Yen et al., 2015), and dihomo isoprostanes (e.g. 17-*epi*-17-F_{2t}-dihomo-IsoP) come from adrenic acid (AdA) oxidation (García-Flores et al., 2016). DHA is the major polyunsaturated fatty acid in the brain (Galano et al., 2013) so, the presence of neuroprostanes and neurofurans in different human biofluids is highly brain specific. For the quantification of these lipid peroxidation biomarkers in plasma samples, the analytical method was previously described (Peña-Bautista et al., 2018), and the developed model could distinguish between AD and healthy patients with an accuracy of 0.90. Therefore, it could reflect brain lipid peroxidation damage (neuroprostanes, neurofurans, 17-*epi*-17-F_{2t}-dihomo-

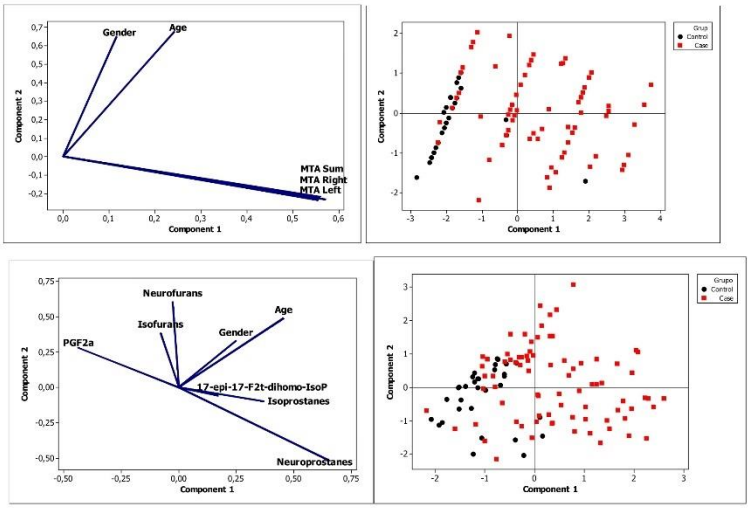

Fig. 2. PLS models. First, model based on neuroimaging techniques (a) loading graph and (b) score plot. Second, model based on plasma biomarkers (c) loading plot and (d) score plot.

IsoP), and oxidative stress at systemic level in AD patients. In fact, it was shown in previous works (Hatanaka et al., 2015) (Di Domenico et al., 2016). Also, the presence of a negative correlation between $PGF_{2\alpha}$ and MTA, and its capacity to discriminate between AD and control groups ($p = 0.001$) are remarkable. This analyte is an inflammatory mediator and it is derived from arachidonic acid oxidation by an enzymatic pathway (Vane et al., 1998). Previous studies showed that inflammation is related to AD progression (Calsolaro and Edison, 2016), and inhibition of cyclooxygenases that are implied in prostaglandin pathway in AD models, showed beneficial effects. So, probably in very early stages of the disease these mechanisms try to avoid the disease progression (Johansson et al., 2015). In addition, it is known that in neurodegenerative diseases the brain blood barrier (BBB) is altered (Janelidze et al., 2017). Specifically in AD, previous works showed an increase on BBB permeability (Algotsson and Winblad, 2007), allowing that different lipid peroxidation products generated in brain could pass through the BBB, and being found at peripheral level. For this reason, we constructed a model based on plasma biomarkers levels that could reflect brain MTA including damage to white matter, grey matter and also inflammatory mediators. That model shows really satisfactory diagnosis indices. Its specificity of 100% is especially remarkable. In our study, all patients diagnosed as positive with our model were AD patients. By contrast, its weak point is the sensitivity (72.5%). For that reason, the new model could serve as a screening test. Only when the test result is negative, patients will have to undergo additional tests to confirm the diagnosis. It would improve the diagnosis based on only image tests because biomarkers reflecting specific brain atrophy in AD patients would constitute an integrative vision of oxidative status (Pohanka, 2014). In any case, more studies are required to confirm this diagnosis capacity, and other dementias or neurodegenerative diseases have to be included in the study to evaluate the model specificity.

5. Conclusion

Correlation between plasma neuroprostanes and dihomoisoprostanes with neuroimaging data could indicate that the neurodegeneration occurred in different brain areas is related to oxidative stress damage and brain lipid peroxidation. Lipid peroxidation biomarkers could reflect brain damage that accompanied neurodegenerative diseases. However, their specificity should be studied comparing the results with other neurodegenerative and brain pathologies. AD diagnosis model based on lipid peroxidation biomarkers shows similar accuracy as the neuroimaging model, and it reflects the implication of this pathway in the pathology since its early stages. The model based on lipid peroxidation biomarkers (neuroprostanes, neurofurans, isoprostanes, isofurans, 17-*epi*-17-F_{2t}-dihomo-IsoP, $PGF_{2\alpha}$) could be used as a screening test for AD diagnosis avoiding in many cases invasive and expensive diagnosis techniques.

Conflicts of interest

The authors report no conflict of interest.

Funding

This work was supported by the Instituto de Salud Carlos III (Miguel Servet I Project (CP16/00082)) (Spanish Ministry of Economy and Competitiveness, and European Regional Development Fund).

Acknowledgements

CC-P acknowledges a post-doctoral "Miguel Servet I" Grant (CP16/00082) from the Health Research Institute Carlos III (Spanish Ministry of Economy and Competitiveness), and the European Regional

Development Fund (FEDER). CP-B acknowledges a pre-doctoral Grant (associated to "Miguel Servet" project CP16/00082) from the Health Research Institute Carlos III (Spanish Ministry of Economy, Industry and Competitiveness). The authors are grateful for the synthesis of the lipid peroxidation compounds by Professor Durand's team at the Institute des Biomolécules Max Mousseron (IBMM) (Montpellier, France).

References

Albert, M.S., DeKosky, S.T., Dickson, D., Dubois, B., Feldman, H.H., Fox, N.C., Gamst, A., Holtzman, D.M., Jagust, W.J., Petersen, R.C., Snyder, P.J., Carrillo, M.C., Thies, B., Phelps, C.H., 2011. The diagnosis of mild cognitive impairment due to Alzheimer's disease: recommendations from the National Institute on Aging-Alzheimer's Association workgroups on diagnostic guidelines for Alzheimer's disease. Alzheimer's Dementia 7, 270–279. https://doi.org/10.1016/j.jalz.2011.03.008.

Algotsson, A., Winblad, B., 2007. The integrity of the blood?brain barrier in Alzheimer?s disease. Acta Neurol. Scand. 115, 403–408. https://doi.org/10.1111/j.1600-0404.2007.00823.x.

Alzheimer's Association, 2016. 2016 Alzheimer's disease facts and figures. Alzheimers. Dement. 12, 459–509.

Calsolaro, V., Edison, P., 2016. Neuroinflammation in Alzheimer's disease: current evidence and future directions. Alzheimer's Dementia 12, 719–732. https://doi.org/10.1016/j.jalz.2016.02.010.

Canu, E., Agosta, F., Mandic-Stojmenovic, G., Stojković, T., Stefanova, E., Inuggi, A., Imperiale, F., Copetti, M., Kostic, V.S., Filippi, M., 2017. Multiparametric MRI to distinguish early onset Alzheimer's disease and behavioural variant of frontotemporal dementia. NeuroImage Clin 15, 428–438. https://doi.org/10.1016/j.nicl.2017.05.018.

Di Domenico, F., Pupo, G., Giraldo, E., Badia, M.-C., Monllor, P., Lloret, A., Eugenia Schinina, M., Giorgi, A., Cini, C., Tramutola, A., Butterfield, D.A., Viña, J., Perluigi, M., 2016. Oxidative signature of cerebrospinal fluid from mild cognitive impairment and Alzheimer disease patients. Free Radic. Biol. Med. 91, 1–9. https://doi.org/10.1016/j.freeradbiomed.2015.12.004.

Elahi, F.M., Marx, G., Cobigo, Y., Staffaroni, A.M., Kornak, J., Tosun, D., Boxer, A.L., Kramer, J.H., Miller, B.L., Rosen, H.J., 2017. Longitudinal white matter change in frontotemporal dementia subtypes and sporadic late onset Alzheimer's disease. NeuroImage Clin 16, 595–603. https://doi.org/10.1016/j.nicl.2017.09.007.

Fazekas, F., Chawluk, J., Alavi, A., Hurtig, H., Zimmerman, R., 1987. MR signal abnormalities at 1.5 T in Alzheimer's dementia and normal aging. Am. J. Roentgenol. 149, 351–356. https://doi.org/10.2214/ajr.149.2.351.

Ferreira, D., Cavallin, L., Larsson, E.-M., Muehlboeck, J.-S., Mecocci, P., Vellas, B., Tsolaki, M., Kloszewska, I., Soininen, H., Lovestone, S., Simmons, A., Wahlund, L.-O., Westman, E., 2015. Practical cut-offs for visual rating scales of medial temporal, frontal and posterior atrophy in Alzheimer's disease and mild cognitive impairment. J. Intern. Med. 278, 277–290. https://doi.org/10.1111/joim.12358.

Ferreira, D., Verhagen, C., Hernández-Cabrera, J.A., Cavallin, L., Guo, C.-J., Ekman, U., Muehlboeck, J.-S., Simmons, A., Barroso, J., Wahlund, L.-O., Westman, E., 2017. Distinct subtypes of Alzheimer's disease based on patterns of brain atrophy: longitudinal trajectories and clinical applications. Sci. Rep. 7, 46263. https://doi.org/10.1038/srep46263.

Galano, J.-M., Mas, E., Barden, A., Mori, T.A., Signorini, C., De Felice, C., Barrett, A., Opere, G., Pinot, E., Schwedhelm, E., Benndorf, R., Roy, J., Le Guennec, J.-Y., Oger, C., Durand, T., 2013. Isoprostanes and neuroprostanes: total synthesis, biological activity and biomarkers of oxidative stress in humans. Prostaglandins Other Lipid Mediat. 107, 95–102. https://doi.org/10.1016/j.prostaglandins.2013.04.003.

García-Flores, L.A., Medina, S., Oger, C., Galano, J.-M., Durand, T., Cejuela, R., Martínez-Sanz, J.M., Ferreres, F., Gil-Izquierdo, Á., 2016. Lipidomic approach in young adult triathletes: effect of supplementation with a polyphenols-rich juice on neuroprostane and F 2 -dihomo-isoprostane markers. Food Funct 7, 4343–4355. https://doi.org/10.1039/C6FO01000H.

Granadillo, E., Paholpak, P., Mendez, M.F., Teng, E., 2017. Visual ratings of medial temporal lobe atrophy correlate with CSF tau indices in clinical variants of early-onset alzheimer disease. Dement. Geriatr. Cognit. Disord. 44, 45–54. https://doi.org/10.1159/000477718.

Hatanaka, H., Hanyu, H., Fukuzawa, R., Hirao, K., Shimizu, S., Kanetaka, H., Iwamoto, T., 2015. Differences in peripheral oxidative stress markers in Alzheimer's disease, vascular dementia and mixed dementia patients. Geriatr. Gerontol. Int. 15, 53–58. https://doi.org/10.1111/ggi.12659.

Hsu, J.-L., Lee, W.-J., Liao, Y.-C., Lirng, J.-F., Wang, S.-J., Fuh, J.-L., 2015. Posterior atrophy and medial temporal atrophy scores are associated with different symptoms in patients with alzheimer's disease and mild cognitive impairment. PLoS One 10, e0137121. https://doi.org/10.1371/journal.pone.0137121.

Janelidze, S., Hertze, J., Nägga, K., Nilsson, K., Nilsson, C., Wennström, M., van Westen, D., Blennow, K., Zetterberg, H., Hansson, O., 2017. Increased blood-brain barrier permeability is associated with dementia and diabetes but not amyloid pathology or APOE genotype. Neurobiol. Aging 51, 104–112. https://doi.org/10.1016/j.neurobiolaging.2016.11.017.

Johansson, J.U., Woodling, N.S., Wang, Q., Panchal, M., Liang, X., Trueba-Saiz, A., Brown, H.D., Mhatre, S.D., Loui, T., Andreasson, K.I., 2015. Prostaglandin signaling suppresses beneficial microglial function in Alzheimer's disease models. J. Clin. Investig. 125, 350–364. https://doi.org/10.1172/JCI77487.

Kalaria, R.N., Ihara, M., 2017. Medial temporal lobe atrophy is the norm in cerebrovascular dementias. Eur. J. Neurol. 24, 539–540. https://doi.org/10.1111/ene.13243.

Kamat, P.K., Kalani, A., Rai, S., Swarnkar, S., Tota, S., Nath, C., Tyagi, N., 2016. Mechanism of oxidative stress and synapse dysfunction in the pathogenesis of alzheimer's disease: understanding the therapeutics strategies. Mol. Neurobiol. 53, 648–661. https://doi.org/10.1007/s12035-014-9053-6.

Klosinski, L.P., Yao, J., Yin, F., Fonteh, A.N., Harrington, M.G., Christensen, T.A., Trushina, E., Brinton, R.D., 2015. White matter lipids as a ketogenic fuel supply in aging female brain: implications for alzheimer's disease. EBioMedicine 2 1888–904. https://doi.org/10.1016/j.ebiom.2015.11.002.

McKhann, G.M., Knopman, D.S., Chertkow, H., Hyman, B.T., Jack, C.R., Kawas, C.H., Klunk, W.E., Koroshetz, W.J., Manly, J.J., Mayeux, R., Mohs, R.C., Morris, J.C., Rossor, M.N., Scheltens, P., Carrillo, M.C., Thies, B., Weintraub, S., Phelps, C.H., 2011. The diagnosis of dementia due to Alzheimer's disease: recommendations from the National Institute on Aging-Alzheimer's Association workgroups on diagnostic guidelines for Alzheimer's disease. Alzheimer's Dementia 7, 263–269. https://doi.org/10.1016/j.jalz.2011.03.005.

Mi, L., Zhang, W., Zhang, J., Fan, Y., Goradia, D., Chen, K., Reiman, E.M., Gu, X., Wang, Y., 2017. An optimal transportation based univariate neuroimaging index. Proceedings. IEEE Int. Conf. Comput. Vis. 182–191 2017.

Miller, E., Morel, A., Saso, L., Saluk, J., 2014. Isoprostanes and neuroprostanes as biomarkers of oxidative stress in neurodegenerative diseases. Oxid. Med. Cell. Longev. 1–10. 2014. https://doi.org/10.1155/2014/572491.

Nordberg, A., 2015. Towards early diagnosis in Alzheimer disease. Nat. Rev. Neurol. 11, 69–70. https://doi.org/10.1038/nrneurol.2014.257.

Peña-Bautista, C., Vigor, C., Galano, J.-M., Oger, C., Durand, T., Ferrer, I., Cuevas, A., López-Cuevas, R., Baquero, M., López-Nogueroles, M., Vento, M., Hervás, D., García-Blanco, A., Cháfer-Pericás, C., 2018. Plasma lipid peroxidation biomarkers for early and non-invasive Alzheimer Disease detection. Free Radic. Biol. Med. 124, 388–394. https://doi.org/10.1016/j.freeradbiomed.2018.06.038.

Persson, K., Barca, M.L., Eldholm, R.S., Cavallin, L., Šaltytė Benth, J., Selbæk, G., Braekhus, A., Saltvedt, I., Engedal, K., 2017. Visual evaluation of medial temporal lobe atrophy as a clinical marker of conversion from mild cognitive impairment to dementia and for predicting progression in patients with mild cognitive impairment and mild alzheimer's disease. Dement. Geriatr. Cognit. Disord. 44, 12–24. https://doi.org/10.1159/000477342.

Pohanka, M., 2014. Alzheimer's disease and oxidative stress: a review. Curr. Med. Chem. 21, 356–364.

Ramos Bernardes da Silva Filho, S., Oliveira Barbosa, J.H., Rondinoni, C., dos Santos, A.C., Garrido Salmon, C.E., da Costa Lima, N.K., Ferriolli, E., Moriguti, J.C., 2017. Neuro-degeneration profile of Alzheimer's patients: a brain morphometry study. NeuroImage Clin 15, 15–24. https://doi.org/10.1016/j.nicl.2017.04.001.

Rathore, S., Habes, M., Iftikhar, M.A., Shacklett, A., Davatzikos, C., 2017. A review on neuroimaging-based classification studies and associated feature extraction methods for Alzheimer's disease and its prodromal stages. NeuroImage 155, 530–548. https://doi.org/10.1016/j.neuroimage.2017.03.057.

Sarria-Estrada, S., Acevedo, C., Mitjana, R., Frascheri, L., Sitrana, S., Auger, C., Rovira, A., 2015. Reproducibility of qualitative assessments of temporal lobe atrophy in MRI studies. Radiologia 57, 225–228. https://doi.org/10.1016/j.rx.2014.04.002.

Scheff, S.W., Ansari, M.A., Mufson, E.J., 2016. Oxidative stress and hippocampal synaptic protein levels in elderly cognitively intact individuals with Alzheimer's disease pathology. Neurobiol. Aging 42, 1–12. https://doi.org/10.1016/j.neurobiolaging.2016.02.030.

Scheltens, P., Leys, D., Barkhof, F., Huglo, D., Weinstein, H.C., Vermersch, P., Kuiper, M., Steinling, M., Wolters, E.C., Valk, J., 1992. Atrophy of medial temporal lobes on MRI in "probable" Alzheimer's disease and normal ageing: diagnostic value and neuropsychological correlates. J. Neurol. Neurosurg. Psychiatry 55, 967–972. https://doi.org/10.1136/jnnp.55.10.967.

Sørensen, L., Igel, C., Pai, A., Balas, I., Anker, C., Lillholm, M., Nielsen, M., 2017. Differential diagnosis of mild cognitive impairment and Alzheimer's disease using structural MRI cortical thickness, hippocampal shape, hippocampal texture, and volumetry. Alzheimer's Disease Neuroimaging Initiative and the Australian Imaging Biomarkers and Lifestyle flagship study of ageing. NeuroImage. Clin. 13, 470–482. https://doi.org/10.1016/j.nicl.2016.11.025.

Suk, H.-I., Lee, S.-W., Shen, D., 2014. Hierarchical feature representation and multimodal fusion with deep learning for AD/MCI diagnosis. Neuroimage 101, 569–582. https://doi.org/10.1016/j.neuroimage.2014.06.077.

Tagawa, K., Hashimoto, H., Nakanishi, A., Kawarada, Y., Muramatsu, T., Matsuda, Y., Kataoka, K., Shimada, A., Uchida, K., Yoshida, A., Higashiyama, S., Kawabe, J., Kai, T., Shiomi, S., Mori, H., Inoue, K., 2015. The relationship between medial temporal lobe atrophy and cognitive impairment in patients with dementia with Lewy Bodies. J. Geriatr. Psychiatry Neurol. 28, 249–254. https://doi.org/10.1177/0891988715590210.

Vane, J.R., Bakhle, Y.S., Botting, R.M., 1998. CYCLOOXYGENASES 1 AND 2. Annu. Rev. Pharmacol. Toxicol. 38, 97–120. https://doi.org/10.1146/annurev.pharmtox.38.1.97.

Visser, P.J., Scheltens, P., Verhey, F.R., Schmand, B., Launer, L.J., Jolles, J., Jonker, C., 1999. Medial temporal lobe atrophy and memory dysfunction as predictors for dementia in subjects with mild cognitive impairment. J. Neurol. 246, 477–485.

[WWW document] World health organisation, 2018. n.d. URL. http://www.who.int/en/news-room/fact-sheets/detail/the-top-10-causes-of-death.

Yadav, R.S., Tiwari, N.K., 2014. Lipid integration in neurodegeneration: an overview of alzheimer's disease. Mol. Neurobiol. 50, 168–176. https://doi.org/10.1007/s12035-014-8661-5.

Yen, H.-C., Wei, H.-J., Lin, C.-L., 2015. Unresolved issues in the analysis of F 2 -isoprostanes, F 4 -neuroprostanes, isofurans, neurofurans, and F 2 -dihomo-isoprostanes in body fluids and tissue using gas chromatography/negative-ion chemical-ionization mass spectrometry. Free Radic. Res. 49, 861–880. https://doi.org/10.3109/10715762.2015.1014812.

Journal of Proteomics 200 (2019) 144–152

Contents lists available at ScienceDirect

Journal of Proteomics

journal homepage: www.elsevier.com/locate/jprot

Plasma metabolomics in early Alzheimer's disease patients diagnosed with amyloid biomarker

Carmen Peña-Bautista[a], Marta Roca[b], David Hervás[c], Ana Cuevas[d], Rogelio López-Cuevas[d], Máximo Vento[a], Miguel Baquero[d], Ana García-Blanco[a,*], Consuelo Cháfer-Pericás[a,*]

[a] Neonatal Research Unit, Health Research Institute La Fe, Valencia, Spain
[b] Analytical Unit Platform, Health Research Institute La Fe, Valencia, Spain
[c] Biostatistical Unit, Health Research Institute La Fe, Valencia, Spain
[d] Neurology Unit, University and Polytechnic Hospital La Fe, Valencia, Spain

ARTICLE INFO

Keywords:
Mild cognitive impairment
Alzheimer's disease
Plasma
Metabolomics
Biomarker

ABSTRACT

An untargeted metabolomics study has been carried out using plasma samples from patients with Mild Cognitive Impairment due to Alzheimer's disease patients (MCI-AD, $n = 29$) and healthy people (n = 29)). They have been classified following the National Institute on Aging and Alzheimer's Association (NIA-AA) recommendations and cerebrospinal fluid biomarkers. The analytical method was based on liquid chromatography coupled to high resolution mass spectrometry. The data process from the corresponding metabolic profiles retained 1158 molecular features in positive and 424 in negative ionization mode. Differences between metabolomic profiles from MCI-AD patients and healthy participants were investigated using a penalized logistic regression analysis (ElasticNet), and being able to select automatically the most informative variables (53 molecular features).

From the molecular features selected for the elastic net models, 16 variables were preliminarily identified by The Human Metabolome Database (amino acids, lipids…). However, only 4 of these variables were tentatively identified by MS/MS and all ions fragmentation modes, being choline the only confirmed metabolite. Regarding their metabolic pathways, they could be involved in cholinergic system, energy metabolism, amino acids and lipids pathways. To conclude, this is a reliable approach to early AD mechanisms, and choline has been identified as a promising AD diagnosis metabolite.

Significance: The untargeted analysis carried out in human plasma samples from early Alzheimer's disease patients and healthy individuals, and the use of sophisticated statistical tools, identified some metabolic pathways and plasma biomarkers. Preliminarily, cholinergic system, energy metabolism, and aminoacids and lipids pathways may be involved in early Alzheimer's disease development.

1. Introduction

Alzheimer's disease (AD) is based on a complex physiopathology and there is a lack of early and non-invasive biomarkers. In fact, the standard diagnosis consists of invasive cerebrospinal fluid (CSF) (β-amyloid biomarker) or expensive evaluations based on criteria established on recent revisions of the National Institute on Aging-Alzheimer's Association (NIA-AA) [1–3]. Nevertheless, molecular perturbations may occur at systemic level in early stages, before the appearance of characteristic symptoms, and plasma constitutes a promising minimally invasive sample in the development of new biomarkers. Therefore, further research is required in order to advance in the AD physiopathological knowledge, which could enhance the identification and clinical validation of new biomarkers, as well as the development of effective therapeutic targets.

The omics technologies address the pathological mechanisms underlying complex diseases, such as AD [4]. Specifically, metabolomics is a useful approach to the phenotype of the organism in health and AD status [5]. Actually, recent metabolomics studies have identified some metabolic pathways altered in AD, such as polyamine pathway, lysine metabolism, tricarboxylic acid cycle, lipid metabolism, neurotransmission and inflammation [6], as well as the impairment of some metabolite levels (tyrosine, glycylglycine, glutamine, lysophosphatic acid, platelet-activating factor, organic acids, isoprostanes, prostaglandines) [7].

In general, metabolomics studies in AD have been applied to

* Corresponding authors at: Health Research Institute La Fe, Avda de Fernando Abril Martorell, 106, 46026 Valencia, Spain.
E-mail addresses: ana.garcia-blanco@uv.es (A. García-Blanco), m.consuelo.chafer@uv.es (C. Cháfer-Pericás).

https://doi.org/10.1016/j.jprot.2019.04.008
Received 7 January 2019; Received in revised form 1 April 2019; Accepted 7 April 2019
Available online 09 April 2019
1874-3919/

different biological samples [8,9]. Nevertheless, there is an increasing interest on improving the early AD diagnosis by means of minimally invasive samples, such as serum [10,11], plasma [7,12], urine [13], and saliva [14]. Specifically, plasma is a promising matrix since some biochemical pathways have showed disturbances in patients with AD, such as amino acids, amines and polyamines metabolisms [12,15–17], as well as lipid metabolism [9,10,18–21], even in mild-cognitive impairment (MCI) phase [12]. Also, a previous study developed a model based on 7-metabolite signature with satisfactory accuracy to distinguish between amnestic MCI and healthy people [22]. Nevertheless, most of metabolomics studies in plasma have been developed from animal models [9,21,23], and among human studies few of them defined MCI-AD participants from the standard CSF biomarkers [7]. In this sense, the ambiguity in dementia type diagnosis is considered an important limitation in the development of AD reliable diagnostic models [12,15,16,22,24,25].

The aim of this work is to identify reliable plasma biomarkers associated to MCI due to Alzheimer's disease by means of untargeted metabolomics and sophisticated statistical tools. To our knowledge this is the first metabolomics study carried out in human plasma samples from MCI-AD patients with CSF biomarkers-based diagnosis.

2. Experimental section

2.1. Study design and participants

A prospective observational study was carried out in the Neurology Unit (University and Polytechnic Hospital La Fe, Valencia (Spain)). The Ethics Committee (CEIC) at the Health Research Institute La Fe (Valencia) approved the study protocol and informed consent was obtained from all the participants. The participants were people with MCI due to AD (case group, $n = 29$), and healthy individuals (control group, n = 29). The inclusion criteria were age between 50 and 80 years old. The MCI-AD group was defined according to NIA-AA recommendations on diagnostic guidelines [2]. Therefore, the core clinical criteria for the MCI diagnosis were considered (criteria for the clinical and cognitive syndrome, cognitive characteristics of MCI…), as well as the CSF biomarkers indicating a high likelihood that the MCI syndrome is due to AD (positive β-amyloid biomarker and positive biomarker of neural injury). In this sense, the MCI-AD participants group showed cognitive complaints and some degree of cognitive impairment in neuropsychological evaluation without daily living activities impairment, and positive biomarkers as defined by current criteria (amyloid PET imaging or CSF amyloid/tau). The healthy group showed absence of cognitive disturbances and negative AD biomarkers. The exclusion criteria were other neurological impairments (stroke, severe head trauma, Parkinson's disease, epilepsy, multiple sclerosis brain injury, brain tumour…), major psychiatric disorders (major depressive disorder, schizophrenia, bipolar disorder…), or a previous invalidating pathology. The standard clinical assessment used in this study was based on neuropsychological and functional assessment (Repeatable Battery for the Assessment of Neuropsychological Status (RBANS) with scores according to five domains (immediate memory-RBANS.IM, visuospatial/constructional-RBANS·V/C, language-RBANS.L, attention-RBANS.A, delayed memory-RBANS.DM), Functionality Assessment Questionnaire (FAQ), Clinical Dementia Rating (CDR), Mini-Mental State Examination (MMSE)) [26–29], structural neuroimaging by means of nuclear magnetic resonance (NMR) or computed tomography scan (CTS) [30], and CSF biomarkers [31,32], or amyloid PET imaging.

2.2. Reagents and chemicals

All reagents used were of analytical grade. Acetonitrile, formic acid (99%) and ultrapure water were obtained from Merck (Darmstadt, Germany), and ethanol from LabKem (Ireland). The internal standards reserpine, leucine enkephaline and phenylalanine-d5, as well as butylated hydroxytoluene (BHT), were purchased from Sigma-Aldrich (St. Louis, MO, USA).

2.3. Sample collection and treatment

Plasma samples were collected from peripheral blood in cryo-tubes containing EDTA. They were centrifuged (10 min, 2000 *g*, room temperature), and plasma was separated using a tube with BHT (0.25% (w/v) in ethanol) as antioxidant. Then, samples were frozen at −80 °C until analysis.

Samples were thawed on ice, 150 μL of cold acetonitrile (0.1%, v/v) were added to 50 μL of plasma, vortexed and kept at −20 °C for 30 min, for protein precipitation. After centrifugation at 13000 *g* (10 min, 4 °C), 20 μL of the supernatant were transferred to a 96-wells plate for liquid chromatography coupled to mass spectrometry (LC-MS) analysis. Then, 70 μL of H_2O (0.1% HCOOH, v/v), and 10 μL of internal standard mix solution (reserpine, leucine enkephaline, phenylalanine-d5, 20 μM each one) were added to each sample. Quality control (QC) was prepared by mixing 10 μL from each plasma sample. Blank was prepared replacing plasma by ultrapure water in order to identify potential artefacts from the tube, reagents and other materials. Finally, plasma samples, QCs and blanks were injected in the chromatographic system. In order to avoid intra-batch variability, as well as to enhance quality and reproducibility, the scheme analysis consisted of random injection order and analysis of QC every 6 plasma samples. Blank analysis was performed at the end of the sequence. Sample stability and analytical drift were investigated through the internal standard intensities.

2.4. UPLC-Q-ToF-MS instrumentation

Metabolomic analysis was performed on an Ultra-Performance Liquid Chromatography (UPLC) system coupled to an iFunnel quadrupole time of flight (Q-ToF) Agilent 6550 mass spectrometer (Agilent Technologies, CA, USA). Chromatographic separation was performed by using an UPLC BEH C_{18} (100 × 2.1 mm, 1.7 μm, Waters, Wexford, Ireland) column from Waters (Wexford, Ireland). Autosampler and column temperatures were set to 4 °C and 40 °C, respectively. The injection volume was 5 μL. A gradient elution with a total run time of 14 min was performed at a flow rate of 400 μL min^{-1} as follows: 98% of mobile phase A (H_2O, 0.1% v/v HCOOH) for 1 min, a linear gradient from 2% to 15% of mobile phase B (CH3CN, 0.1% v/v HCOOH) for 2 min, from 15% to 50% B for 3 min and from 50% to 95% for 3 min. Finally, 95% B was held for 3 min and a 0.55 min gradient was used to return to the initial conditions, which were held for 2.5 min to totally column recovery. Full scan MS data from 50 to 1700 m/z with a scan frequency of 6 Hz was collected. Both positive and negative electrospray ionization modes (ESI +, ESI −) were used and the conditions were set as follows: gas temperature, 200 °C; drying gas, 14 L min^{-1}; nebulizer, 60 psi; sheath gas temperature, 350 °C; sheath gas flow, 11 L min^{-1}. Automatic MS spectra recalibration was carried out introducing a reference standard into the source via a reference sprayer valve during the analysis. Q-ToF-MS was also used under auto MS/MS and all-ions (MS^E) fragmentation modes for the simultaneous acquisition at low and high collision energies, which provide useful information about the (de)protonated molecules and main fragment ions for the identification of discovered metabolites.

2.5. Data processing

In the first place, pre-processing of acquired data from the full scan analysis by UPLC-Q-ToF-MS is required to detect molecular features. Data processing was done by using the XCMS package in R [33], for peak detection, noise filtering, peak alignment, grouping, and normalization of data; and the CAMERA package [34], for identification of isotopes and most probable adducts. Finally, a data matrix was generated including molecular features (m/z-retention time), sample ID

(observations) and peak intensities. Before the statistical analysis, data quality (reproducibility, stability) was evaluated by means of the internal standards stability and the QC's coefficients of variation (CV). Those molecular features with CV > 30% were removed from the data matrix, and a normalization method (fold change) was also used to eliminate intra-batch variability due to technical differences. Finally, the obtained peaks table was used for statistical analysis.

2.6. Statistical analysis and molecular features identification

Demographic and clinical data from participants were summarized using median and inter-quartile range for continuous variables, and relative and absolute frequencies for categorical variables. Univariate analysis was carried comparing medians between both participants groups by Mann Whitney test for each metabolite. In addition, the fold change ratio of mean in MCI-AD/mean in control group was calculated for each metabolite. All these analysis were carried out with SPSS software version 20.0 (SPSS, Inc., Chicago, IL, USA).

Multivariate analysis was based on an Elastic Net penalized logistic regression [35], it was adjusted to identify the most influential variables in the differentiation between healthy individuals and MCI-AD patients using R (version 3.5), R packages glmnet (version 2.0-16), and BootValidation (version 0.1.5). Penalized regression methods consist on fitting a regression model subject to a specific restriction (a bound on the value of the coefficients). This method forces the shrinkage of the parameters to zero, potentially performing variable selection at the model-fitting step. Penalization factor for the Elastic Net was selected using 500 repetitions of 10-fold cross-validation. From each repetition the highest lambda at one standard error from the minimum was selected (one-standard-error rule) and the median of the 500 lambda values was used as the final penalization factor. With the selected features, the Elastic net models obtained for each ionization mode were evaluated by estimating its optimism corrected area under curve-receiver operating characteristics (AUC-ROC) by bootstrapping, following the procedure of Gordon et al. [36].

Molecular features selected by Elastic Net analysis were preliminarily identified by querying their exact mass against those presented in the online Human Metabolome Database (HMDB) (http://www.hmdb.ca/) and the Metlin database (https://metlin.scripps.edu) within a mass range of ± 10 ppm. The identities of the selected features were verified by comparing the MS/MS and all-ions spectra with those of the proposed metabolites in the cited online databases, as well as by using authentic standards whenever available.

3. Results

3.1. Participants demographic and clinical characteristics

The demographic and clinical characteristics of participants in this study are summarized in Table 1. As we can see, age and gender showed differences between groups and for that reason they were included in the multivariate model as co-variables. As expected from participants' classification, temporal atrophy was higher in MCI-AD, and the CSF biomarkers showed significant differences between groups. Regarding the neuropsychological evaluations, the RBANS (IM, V/C, L, A, DM) and MMSE scores were lower in MCI-AD patients than in control subjects, while the FAQ and CDR scores were higher in the MCI-AD group.

3.2. Multivariable analysis and selection of discriminant variables

Elastic net models were used to select discriminant variables. Outcomes of these models identified 24 and 29 discriminant variables between MCI-AD and control subjects in positive and negative ionization mode, respectively (see Supplementary Material Table S1). The different levels of these variables between participants groups were represented in heat map visualizations of the variables' values (Fig. 1).

Table 1
Demographic and clinical characteristics of study participants.

Variable		Control (n = 29)	MCI-AD (n = 29)
Age (years) (median (IQR))		65 (63, 70)	72 (69, 75)
Gender (female) (n (%))		9 (31.03%)	19 (65.52%)
Studies levels (n (%))	Basics	6 (20%)	17 (59%)
	University	11 (38%)	5 (17%)
Medications (n (%))	Statins	10 (34%)	17 (59%)
	Fibrates	3 (10%)	2 (7%)
	Benzodiazepines	2 (7%)	4 (13.79%)
	Opiates	0 (0%)	0 (0%)
	Anticipileptics	1 (3.45%)	0 (0%)
	Antihipertensives	10 (35.71%)	14 (48.28%)
	Corticoids	0 (0%)	2 (6.9%)
Comorbidity (n (%))	Dyslipidemia	10 (35.71%)	16 (55.17%)
	Diabetes	3 (10%)	3 (10.34%)
	Hypertension	11 (38%)	13 (44.83%)
	Heart Disease	1 (3.45%)	0 (0%)
Smoking status (n (%))	Yes	1 (3.45%)	2 (6.9%)
	Former smoker (> 10 years)	9 (31%)	7 (24.14%)
Alcohol or drugs consumption (n (%))		6 (21.43%)	3 (10.34%)
Presenile family background (n (%))	None	22 (76%)	22 (88%)
	First grade	5 (17%)	5 (17%)
	Second grade	2 (7%)	0 (0%)
Depression (n (%))		3 (10.34%)	4 (14%)
Anxiety (n (%))		1 (3.45%)	3 (10.34%)
Temporal atrophy (n (%))		2 (7.14%)	20 (69%)
CSF Amyloid β (pg mL^{-1}) (median (IQR))		1256 (1164, 1464)	600 (496, 687)
CSF total Tau (pg mL^{-1}) (median (IQR))		196 (141, 298)	590 (465, 782)
CSF phosphorylated Tau (pg mL^{-1}) (median (IQR))		48 (37, 60)	84 (73, 104)
RBANS.IM (median (IQR))		93 (84,107)	61 (51,75)
RBANS.V/C (median (IQR))		101 (86,112)	81 (75,92)
RBANS.L (median (IQR))		92 (86,97)	71 (59,85)
RBANS.A (median (IQR))		100 (82,112)	68 (56,81)
RBANS.DM (median (IQR))		100 (92, 106)	48 (40, 66)
MMSE (median (IQR))		30 (28,30)	25 (24,28)
FAQ (median (IQR))		0 (0, 0)	5 (0, 8.5)
CDR (n (%))	0	29 (100%)	5 (17%)
	0.5	0 (0%)	18 (62%)
	1	0 (0%)	6 (21%)

IQR: Inter-quartile range.

As we can see, the levels of relative increase were depicted in green, while the levels of relative decrease were depicted in red. In this sense, most of the metabolites showed higher levels in MCI-AD group than in control group. The discrimination power of these selected variables was measured as bootstrap validated AUC, being 0.993 and 0.990 in negative and positive ionization mode, respectively.

3.3. Metabolites identification

From the 53 variables selected by the elastic net models, 16 variables were preliminarily identified as potential metabolites, only 4 of these variables were tentatively identified with their MS fragments pattern (MS/MS and/or all-ions fragmentation), being only 1 variable finally confirmed with its pure standard (Table 2).

Among the tentatively identified metabolites, first the variable m/z 635.2954 was identified as rescinnamine, a drug used for hypertension treatment. It is important to note that the incidence of hypertension did not show differences between control and MCI-AD groups (Table 1), so it is unlikely to be this compound. Second, the variable m/z 538.3073 was identified with three potential metabolites (24,25-diacetylvulgaroside, cyasterone, soraphen A), 24,25-diacetylvulgaroside and cyasterone were exogenous products derived from fruits and plants [37,38], while soraphen A was a myxobacterium product that may be related to some infection in AD. So, we hypothesize that the metabolite

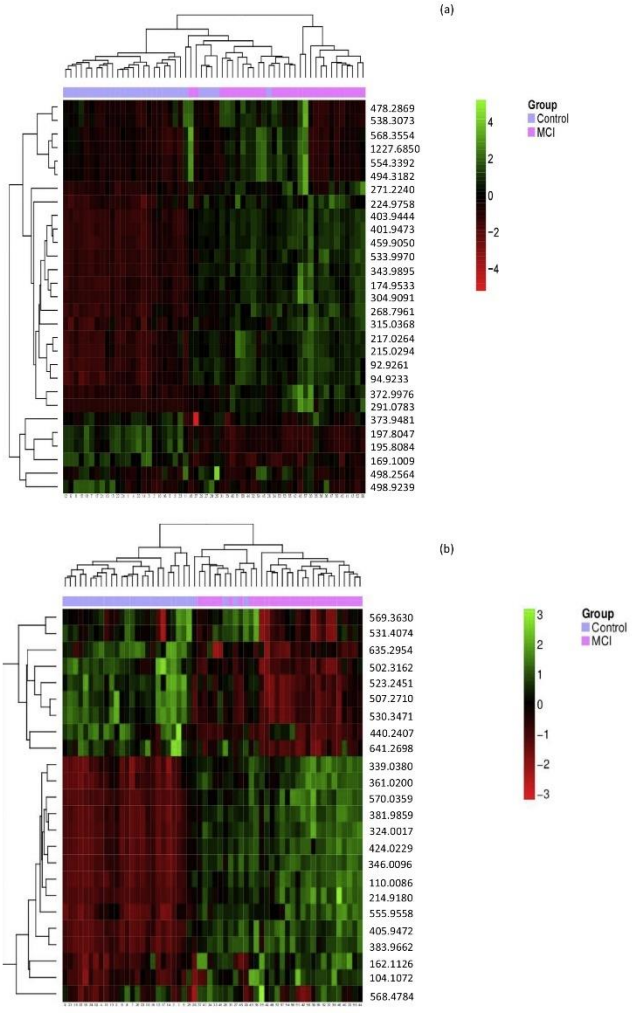

Fig. 1. Heatmap including the selected variables by the elastic net logistic regression model. Z-scores for each variable are represented in a color-coded scale were values at the mean are black, values under the mean are red and values over the mean are green. Ordering of rows and columns of the heatmap is performed by hierarchical clustering of the observations (columns) and of the variables (rows). a) for the negative ionization mode, and b) for the positive ionization mode. (For interpretation of the references to color in this figure legend, the reader is referred to the web version of this article.)

Table 2
Metabolomic variables selected by Elastic Net statistical models and preliminarily identified by The Human Metabolome Database.

Mass (m/z)	Retention time (min)	Addact	Formula	Identification of variables		Compound class/Metabolism	Fold change[a]
				Metabolite annotation	Verification mode		
104.1072	0.60	$[M + H]^+$	C5H14NO	Choline	MS fragmentation pattern and chemical standard (confirmed)	Quaternary ammonium/Cholinergic system	1.582
162.1126	0.60	$[M + H]^+$	C7H15NO3	L-carnitine; Malonyl-Carnitin		Amines/Energy metabolism and fatty acid oxidation	1.750
		$[M + H]^+$	C7H16NO3	S-Carnitinium		Quaternary ammonium (Carnitines)/fatty acid oxidation	
324.0917	0.68	M^+		Unknown			3.211
339.0380	0.65	$[M + H]^+$	C14H10O10	2,3,4-trihydroxy-5-[(3,4,5-trihydroxybenzoyl)oxy]benzoic acid; 2,4,5-trihydroxy-3-[(3,4,5-trihydroxybenzoyl)oxy]benzoic acid; 3,4-dihydroxy-5-[(2,3,4,5-tetrahydroxybenzoyl)oxy]benzoic acid; 4,4',5,5,6,6'-hexahydroxy-[1,1'-biphenyl]-2,2'-dicarboxylic acid	Organic compound (depsides and depsidones)/Benzene hydroxylation	1.696
361.0200	0.65	$[M + Na]^+$					1.834
346.0096	0.68	M^+		Unknown			2.529
381.9859	0.66	M^+		Unknown			2.703
383.9662	0.70	M^+		Unknown			2.897
405.9472	0.67	M^+		Unknown			3.292
424.0229	0.73	$[M + H]^+$	C16H13NO7S2	5-Amino-4-hydroxy-3-(phenylazo)-2,7-naphthalenedisulfonic acid		Food dye	2.542
485.2893	9.38	M^+		Unknown			0.628
502.3162	9.37	M^+		Unknown			0.633
507.2710	9.37	M^+		Unknown			0.580
523.2451	9.37	$[M + H]^+$	C28H39ClO7	4-Deoxyphysalolactone		Withanolides/Inflammation pathways	0.564
	0.00	$[M + H]^+$	C29H34N2O7	Bargustanine		Benzylisoquinolines/Neuromuscular-blocking drugs	
530.3471	9.37	$[M + H]^+$		Unknown			0.563
531.4074	12.79	$[M + H]^+$	C33H54O5	alpha-Tocopherol succinate		Vitamin E/Antioxidant activity	0.764
555.9557	0.76	$[M + H]^+$		Unknown			1.865
568.4784	10.48	$[M + H]^+$		Unknown			1.045
569.3630	12.79	$[M + Na]^+$	C30H58O4S2	Dilauryl 3,3'-thiodipropionate		Dicarboxylic acids/Membrane formation	0.762
570.0358	0.66	M^+		Unknown			4.656
635.2954	6.72	$[M + H]^+$	C35H42N2O9	Rescinnamine	MS fragmentation pattern (tentatively identified)	Antihypertensive drug	0.903
92.9260	0.62	M		Unknown			1.425
94.9233	0.62	M		Unknown			1.400
169.1009	1.03	M		Unknown			0.780
174.9533	0.54	M^-		Unknown			1.731
195.8083	0.65	M^-		Unknown			0.515
197.8046	0.65	M^-		Unknown			0.484
215.0294	0.62	$[M-H]^-$	C31H7ClO2	Chlorobydrin		Halohydrins/Cell membrane	1.648
217.0264	0.62	$[M-H_2O-H]^-$	C11H12N2S2	Brassitin		3-allylindole (exogenous)	1.663
		$[M + HCOO]^-$	C7H9O3P	Monomethyl phenylphosphonate		Exogenous	
		$[M-H_2O-H]^-$	C7H12N2O3S	Cysteinyl-Aspartate		Dipeptide/Protein catabolism	
		$[M-H_2O-H]^-$	C7H12N2O3S	Aspartyl-Cysteine		Dipeptide/Protein catabolism	
224.9758	0.72	M^-		Unknown			1.578
268.7960	0.61	M^-		Unknown			1.514
271.2240	9.61	M^-		Unknown			1.565
291.0783	0.70	M^-		Unknown			1.594
294.9990	0.53	M^-		Unknown			2.562
315.0368	0.64	$[M-H_2O]^-$	C11H15N3O6P	Nicotinamide riboside		Amide/Cellular energy maintenance	1.337
		$[M-H_2O]^-$	C11H16N2O8P	Beta-nicotinamide D-ribonucleotide			
343.9895	0.67	M^-		Unknown			2.713
372.9974	0.65	M^-		Unknown			1.835
373.9481	6.98	M^-		Unknown			0.929
401.9472	0.66	M^-		Unknown			2.427

(continued on next page)

Table 2 (*continued*)

Mass (m/z)	Retention time (min)	Adduct	Formula	Identification of variables		Compound class/Metabolism	Fold change[a]
				Metabolite annotation	Verification mode		
403.9443	0.66	M^-		Unknown			3.314
459.9050	0.66	M		Unknown			2.854
478.2869	8.19	M^-		Unknown			1.174
494.3182	9.05						1.541
498.2564	8.02	$[M-H]^-$	$C25H42NO7P$	Lyso PE(20:5/0:0); Lyso PE(0:0/20:5)		Lysophospholipid/Lipid metabolism	0.748
498.9239	8.16	$[M-H]^-$	$C6H16O18P4$	Inositol 1,3,4,5-tetraphosphate; 1D-Myo-inositol 1,3,4,6-tetrakisphosphate; D-Myo-inositol 3,4,5,6-tetrakisphosphate; 1D-Myo-inositol 1,4,5,6-tetrakisphosphate		Second messengers in Ca2+ and Cl- regulation through membrane/Inositol metabolism	0.649
533.9969	0.72			Unknown			2.925
538.3073	8.19	$[M-H_2O]^-$	$C29H44O8$	24,25-diacetylvulgaroside	MS fragmentation pattern (tentatively identified)	Exogenous	1.186
				Cysteetone		Exogenous	
				Soraphen A		Macrolide/Lipid metabolism	
554.3392	9.05	$[M + HCOO]^-$	$C25H52NO7P$	Lyso PE(20:0/0:0) or Lyso PE(0:0/20:0)	MS fragmentation pattern (tentatively identified)	Lysophospholipid/Lipid metabolism	1.534
568.3554	9.39	M^-		Unknown			1.351
1227.6849	9.39	M^-		Unknown			1.491

[a] Fold change is calculated by the average value of the MCI-AD group compared to the control group.

with mass 538.3073 could be soraphen A. Third, the variable m/z 498.2564 was identified as lysophosphatidylethanolamines (Lyso PE (20:0/0:0) or Lyso PE (0:0/20:0)), breakdown products of phosphatidylethanolamine, present in cells of all organisms [39]. Finally, the variable m/z 104.1072 was also confirmed with its pure standard and identified as choline.

The relative levels of these variables in each group of participants are depicted in Fig. 1. In general, the MCI-AD group showed increased levels for Lyso PE (m/z 498.2564), soraphen A (m/z 538.3073), and choline (m/z 104.1072). However, there is a small group of MCI-AD participants with decreased levels for Lyso PE (m/z 498.2564) and soraphen A (m/z 538.3073) (Fig. 1). In Fig. 2, the differences between MCI-AD and control groups are depicted for the metabolites verified by MS fragmentation patterns, showing statistically significant differences for choline ($p < .001$), rescinamine ($p < .001$) and Lyso PE ($p < .05$).

4. Discussion

An untargeted metabolomics study has been carried out in plasma samples to identify potential early AD biomarkers. For this, plasma samples from participants with CSF biomarker-confirmed diagnosis (healthy and MCI-AD), as well as a reliable and robust analytical method based on minimal sample treatment and UPLC-Q-ToF-MS chromatographic system were used. Specifically, the valuable samples from healthy and MCI-AD participants classified by specific AD biomarkers in CSF [3], together with the high quality, reproducibility and stability of the analytical method, provided high reliability to the experimental results. In fact, few studies in literature employed specific CSF biomarkers to identify clearly AD patients [7]. Also, few works have focused on AD patients at early stage [7,10–12,22], and few of them employed simple and robust untargeted analytical methods [12,22].

From the metabolomics results obtained in both mass spectrometry ionization modes, a multivariate statistical analysis was carried out to select the most discriminant variables between healthy individuals and MCI-AD patients. It was based on Elastic net penalized logistic regression, and the corresponding models obtained for each ionization mode provided high accuracy (AUC 0.990 and 0.993, respectively). However, most of previous works developed partial least squares (PLS) discriminant models [9,12,15,16,21], adding all the studied variables into the model because PLS is not able to assign zero coefficients. Therefore, PLS has the consequent limitations in metabolites selection and accuracy assessment. Nevertheless, elastic net is able to shrink the coefficients of uninformative variables exactly to zero, selecting automatically the most informative variables. This entails that the coefficients of elastic net model are more stable and reliable compared with those of PLS. Another difference between both statistical models is related to the selection of relevant variables. For elastic net, the variable selection is performed at the model-fitting step; while for PLS it relies on ranking methods, such as variable importance in projection (VIP) scores, which are affected by variable correlation, and they are sensitive to tuning parameters [40].

Among the discriminant molecular features selected for the elastic net models, some variables were preliminarily identified (choline, carnitine and nicotinamide derivatives, depsides, tocopherols, dipeptides, Lyso PEs, inositol derivatives). They are involved to cholinergic system, energy metabolism, amino acids and lipids metabolism, as well as nicotinamide pathways. These results agree with previous works in which lipids and amines biochemical pathways were altered in AD [15–21]. In addition, the nicotinamide pathway is involved in the mitochondrial transport chain that is related to the progression of AD through oxidative stress generation [41], so it could explain the higher levels found for nicotinamide ribotide or beta-nicotinamide D-ribonucleotide in the MCI group. Previous studies proposed nicotinamide riboside as a potential AD treatment since it showed beneficial effects on

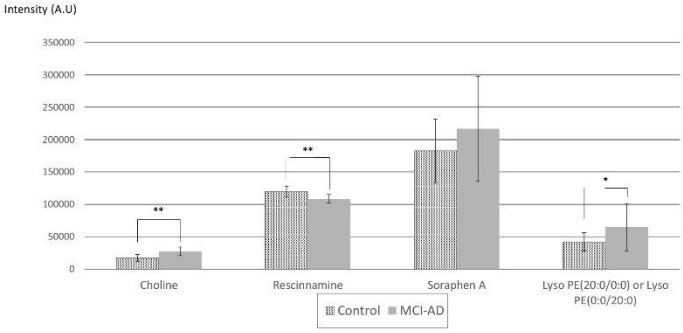

Fig. 2. Bar graph representing the tentatively identified metabolites levels for each participants group (MCI-AD, control). (* $p < .05$, ** $p < .001$).

cognition and β-amyloid toxicity in AD mouse model [42], and in DNA repair [43]. This metabolite also showed beneficial effects on neuroprotection and energy metabolism that is directly implied in AD pathology [44]. Regarding inositol pathway, some metabolites were down-regulated in MCI-AD (inositol-1,3,4,5-tetraphosphate or 1D-myo-inositol-1,3,4,6-tetrakisphosphate or D-myo-inositol-3,4,5,6-tetrakisphosphate or 1D-myo-inositol-1,4,5,6-tetrakisphosphate). Similarly, inositol-1,4,5-trisphosphate receptor levels were lower in AD and it could be important in the neurofibrillary pathology [45]. In general, inositol is an important membrane component. Its brain derivates are implied in synaptic transport, and neurotransmitter secretion, and they regulate autophagy [46]. According to carnitine pathway, higher levels were found for MCI-AD group. Nevertheless, studies from literature found that serum acetyl-L-carnitine and other acyl-L-carnitine levels decreased in MCI and AD subjects [47,48], as well as in CSF samples [49]. A possible explanation to the higher levels obtained for acetylcarnitine in the MCI-AD group may be that these compounds have antioxidant function [50], so natural mechanisms could be activated at early AD stages in order to face into the oxidative stress associated to further disease development. In addition, a mice model study demonstrated that acetyl-L-carnitine protects against neuroinflammation [51]. Therefore, the high levels found in early AD stages could be a compensatory mechanism, activating the protective mechanisms against the development of the disease.

The tentatively identified discriminant variables in this study were Lyso PE (20:0/0:0)/Lyso PE (0:0/20:0), choline and probably soraphen A. In spite of soraphen A was not confirmed by its standard, we discarded the other two possible compounds with the same mass (24,25-diacetylvulgaroside and cyasterone) as they are fruit and vegetables products, while soraphen A could show a possible relationship with fungal infection. So, Lyso PE (20:0/0:0)/Lyso PE (0:0/20:0), choline and soraphen A could be considered potential early AD biomarkers in plasma. In general, the MCI-AD group showed increased levels for soraphen A, Lyso PE and choline. First, soraphen A is produced by myxobacteria, and it can act as acetyl-CoA carboxylase inhibitor, which would alter the lipid synthesis pathways, avoiding the fatty acids elongation [52]. In the present study, most of MCI-AD patients showed increased levels of this metabolite. It may be indirectly related to the also higher levels of choline. Probably, the impairment in fatty acid elongation would lead to an increase in short-chain fatty acids levels, such as, choline. On the other hand, this potential myxobacteria infection is a controversial result that should be studied in depth, as well as other unexplained findings in literature relative to microscopic evidence of fungal infections in brain tissue from AD patients [53–55]. Second, Lyso PEs usually show low circulating levels, and they are considered biomarkers of the progression of AD [56]. In general, previous studies found that an alteration in lipid metabolism correlates with AD development [57]. However, a few participants from MCI-AD group showed decreased levels for soraphen A and Lyso PE, and further research is required to differentiate patients' subgroups. Third, choline was the only confirmed metabolite, constituting a promising biomarker in early AD diagnosis. It is a precursor metabolite in acetylcholine synthesis, so it plays an important role in this neurotransmitter function. In addition, it is a key component in some lipids with relevant brain functions, such as phosphatydilcholine [58], corroborating the impairment observed in early AD stage. However, the choline levels found in AD patients from different metabolomics studies showed some discrepancy [52,59–61], probably due to the heterogeneous experimental conditions used (animal or human model, AD stage, sample matrix, analytical technique). In the present study, MCI-AD patients showed increased levels of this metabolite, as it was observed by Lin et al. 2017 [21]. It could be explained by the fact that in early AD stages the cholinergic transmission is reduced, and as compensatory response choline production would be increased. In addition, the pathology development involves a cellular integrity impairment, allowing the release of compounds out of the cell, such as choline [62]. Nevertheless, a recent study showed lower levels of choline in AD patients compared to healthy subjects [63]. Probably, the different disease phases show different biochemical profiles [17].

5. Conclusions

An untargeted metabolomics study has been carried out in plasma samples from patients with MCI due to AD and healthy participants, achieving the identification of some metabolites that could be involved in early AD development. They have important roles in some metabolic pathways related to neurotransmitters, energy metabolism, and lipids and amino acids pathways. However, only choline was confirmed, and further work will be carried out using a targeted analytical method based on UPLC-MS/MS in order to clinically validate this promising early AD biomarker. In addition, some tentatively identified compounds with neuroprotective or antioxidant effects were found elevated in MCI-AD patients. This may be explained by the activation of compensatory mechanisms to prevent AD development since its early stages.

Conflicts of interest

None of the authors of this manuscript declares having conflicts of interest.

Funding

This work was supported by the Instituto de Salud Carlos III (Miguel Servet I Project (CP16/00082)) (Spanish Ministry of Economy and Competitiveness and European Regional Development Fund).

Acknowledgement

We are greatly indebted to all participants, nursing, psychology and medical staff who voluntarily participated in the present study. Without their collaboration and enthusiasm this study could not have been completed.

CC-P acknowledges a "Miguel Servet I" Grant (CP16/00082) from the Instituto de Salud Carlos III (Spanish Ministry of Economy and Competitiveness). CP-B acknowledges a post-doctoral Grant (associated to "Miguel Servet" project CP16/00082) from the ISCIII (Spanish Ministry of Economy, Industry and Competitiveness). AG-B acknowledges a post-doctoral Grant (associated to "Juan Rodés" project CP17/00003) from the ISCIII (Spanish Ministry of Economy, Industry and Competitiveness).

Appendix A. Supplementary data

Supplementary data to this article can be found online at https://doi.org/10.1016/j.jprot.2019.04.008.

References

[1] G.M. McKhann, D.S. Knopman, H. Chertkow, B.T. Hyman, C.R. Jack Jr., C.H. Kawas, W.E. Klunk, W.J. Koroshetz, J.J. Manly, R. Mayeux, R.C. Mohs, J.C. Morris, M.N. Rossor, P. Scheltens, M.C. Carrillo, B. Thies, S. Weintraub, C.H. Phelps, The diagnosis of dementia due to Alzheimer's disease: recommendations from the National Institute on Aging-Alzheimer's Association workgroups on diagnostic guidelines for Alzheimer's disease, Alzheimers Dement. 7 (2011) 263–269.

[2] M.S. Albert, S.T. DeKosky, D. Dickson, B. Dubois, H.H. Feldman, N.C. Fox, A. Gamst, D.M. Holtzman, W.J. Jagust, R.C. Petersen, P.J. Snyder, M.C. Carrillo, B. Thies, C.H. Phelps, The diagnosis of mild cognitive impairment due to Alzheimer's disease: recommendations from the National Institute on Aging-Alzheimer's Association workgroups on diagnostic guidelines for Alzheimer's disease, Alzheimers Dement. 7 (2011) 270–279.

[3] C.R. Jack Jr., D.A. Bennett, K. Blennow, M.C. Carrillo, B. Dunn, S.B. Haeberlein, D.M. Holtzman, W. Jagust, F. Jessen, J. Karlawish, E. Liu, J.L. Molinuevo, T. Montine, C. Phelps, K.P. Rankin, C.C. Rowe, P. Scheltens, E. Siemers, H.M. Snyder, R. Sperling, NIA-AA research framework: toward a biological definition of Alzheimer's disease, Alzheimers Dement. 14 (2018) 535–562.

[4] H. Zetterberg, Applying fluid biomarkers to Alzheimer's disease, Am. J. Physiol. Cell Physiol. 313 (2017) C3–C10.

[5] C.N.A. Enche Ady, S.M. Lim, L.K. Teh, M.Z. Salleh, A.V. Chin, M.P. Tan, P.J.H. Poi, S.B. Kamaruzzaman, A.B. Abdul Majeed, K. Ramasamy, Metabolomic-guided discovery of Alzheimer's disease biomarkers from body fluid, J. Neurosci. Res. 95 (2017) 2005–2024.

[6] J.M. Wilkins, E. Trushina, Application of metabolomics in Alzheimer's disease, Front. Neurol. 8 (2018) 719.

[7] F.A. de Leeuw, C.F.W. Peeters, M.I. Kester, A.C. Harms, E.A. Struys, T. Hankemeier, H.W.T. van Vlijmen, S.J. van der Lee, C.M. van Duijn, P. Scheltens, A. Demirkan, M.A. van de Wiel, W.M. van der Flier, C.E. Teunissen, Blood-based metabolic signatures in Alzheimer's disease, Alzheimers. Dement. (Amst). 8 (2017) 196–207.

[8] T. Koal, K. Klavins, D. Seppi, G. Kemmler, C. Humpel, Sphingomyelin SM(d18:1/18:0) is significantly enhanced in cerebrospinal fluid samples dichotomized by pathological amyloid-beta42, tau, and phospho-tau-181 levels, J. Alzheimers Dis. 44 (2015) 1193–1201.

[9] X. Pan, M.B. Nasaruddin, C.T. Elliott, B. McGuinness, A.P. Passmore, P.G. Kehoe, C. Hölscher, P.L. McClean, S.F. Graham, B.D. Green, Alzheimer's disease-like pathology has transient effects on the brain and blood metabolome, Neurobiol. Aging 38 (2016) 151–163.

[10] V.R. Varma, A.M. Oommen, S. Varma, R. Casanova, Y. An, R.M. Andrews, R. O'Brien, O. Pletnikova, J.C. Troncoso, J. Toledo, R. Baillie, M. Arnold, G. Kastenmueller, K. Nho, P.M. Doraiswamy, A.J. Saykin, R. Kaddurah-Daouk, C. Legido-Quigley, M. Thambisetty, Brain and blood metabolite signatures of pathology and progression in Alzheimer disease: a targeted metabolomics study, PLoS Med. 15 (2018) e1002482.

[11] M. Orešič, G. Anderson, I. Mattila, M. Manoucheri, H. Soininen, T. Hyötyläinen, C. Basignani, Targeted serum metabolite profiling identifies metabolic signatures in patients with Alzheimer's disease, normal pressure hydrocephalus and brain tumor, Front. Neurosci. 11 (2018) 747.

[12] G. Wang, Y. Zhou, F.J. Huang, H.D. Tang, X.H. Xu, J.J. Liu, Y. Wang, Y.L. Deng, R.J. Ren, W. Xu, J.F. Ma, Y.N. Zhang, A.H. Zhao, S.D. Chen, W. Jia, Plasma metabolite profiles of Alzheimer's disease and mild cognitive impairment, J. Proteome Res. 13 (2014) 2649–2658.

[13] Z. Tang, L. Liu, Y. Li, J. Dong, M. Li, J. Huang, S. Lin, Z. Cai, Urinary metabolomics reveals alterations of aromatic amino acid metabolism of Alzheimer's disease in the transgenic CRND8 mice, Curr. Alzheimer Res. 13 (2016) 764–776.

[14] A. Yilmaz, T. Geddes, B. Han, R.O. Bahado-Singh, G.D. Wilson, K. Imam, M. Maddens, S.F. Graham, Diagnostic biomarkers of Alzheimer's disease as identified in saliva using 1H NMR-based metabolomics, J. Alzheimers Dis. 58 (2017) 355–359.

[15] E. Trushina, T. Dutta, X.M. Persson, M.M. Mielke, R.C. Petersen, Identification of altered metabolic pathways in plasma and CSF in mild cognitive impairment and Alzheimer's disease using metabolomics, PLoS One 8 (2013) e63644.

[16] S.F. Graham, O.P. Chevallier, C.T. Elliott, C. Hölscher, J. Johnston, B. McGuinness, P.G. Kehoe, A.P. Passmore, B.D. Green, Untargeted metabolomic analysis of human plasma indicates differentially affected polyamine and L-arginine metabolism in mild cognitive impairment subjects converting to Alzheimer's disease, PLoS One 10 (2015) e0119452.

[17] M. Mapstone, F. Lin, M.A. Nalls, A.K. Cheema, A.B. Singleton, M.S. Fiandaca, H.J. Federoff, What success can teach us about failure: the plasma metabolome of older adults with superior memory and lessons for Alzheimer's disease, Neurobiol. Aging 51 (2017) 148–155.

[18] K. Inoue, H. Tsuchiya, T. Takayama, H. Akatsu, Y. Hashizume, T. Yamamoto, N. Matsukawa, T. Toyo'oka, Blood-based diagnosis of Alzheimer's disease using fingerprinting metabolomics based on hydrophilic interaction liquid chromatography with mass spectrometry and multivariate statistical analysis, J. Chromatogr. B Analyt. Technol. Biomed. Life Sci. 974 (2015) 24–34.

[19] N. Voyle, M. Kim, P. Proitsi, N.J. Ashton, A.L. Baird, C. Bazenet, A. Hye, S. Westwood, R. Chung, M. Ward, G.D. Rabinovici, S. Lovestone, G. Breen, C. Legido-Quigley, R.J. Dobson, S.J. Kiddle, Alzheimer's disease neuroimaging initiative. Blood metabolite markers of neocortical amyloid-β burden: discovery and enrichment using candidate proteins, Transl. Psychiatry 6 (2016) e719.

[20] F.A. de Leeuw, C.F.W. Peeters, M.I. Kester, A.C. Harms, E.A. Struys, T. Hankemeier, H.W.T. van Vlijmen, S.J. van der Lee, C.M. van Duijn, P. Scheltens, A. Demirkan, M.A. van de Wiel, W.M. van der Flier, C.E. Teunissen, Blood-based metabolic signatures in Alzheimer's disease, Alzheimers. Dement. (Amst). 8 (2017) 196–207.

[21] W. Lin, J. Zhang, Y. Liu, R. Wu, H. Yang, X. Hu, X. Ling, Studies on diagnostic biomarkers and therapeutic mechanism of Alzheimer's disease through metabolomics and hippocampal proteomics, Eur. J. Pharm. Sci. 105 (2017) 119–126.

[22] J. Olazarán, L. Gil-de-Gómez, A. Rodríguez-Martín, M. Valentí-Soler, B. Frades-Payo, J. Marín-Muñoz, C. Antúnez, A. Frank-García, C. Acedo-Jiménez, L. Morlán-Gracia, R. Petidier-Torregrossa, M.C. Guisasola, F. Bermejo-Pareja, Á. Sánchez-Ferro, D.A. Pérez-Martínez, S. Manzano-Palomo, R. Farquhar, A. Rábano, M.A. Calero, A blood-based, 7-metabolite signature for the early diagnosis of Alzheimer's disease, J. Alzheimers Dis. 45 (2015) 1157–1173.

[23] R. González-Domínguez, T. García-Barrera, J. Vitorica, J.L. Gómez-Ariza, Application of metabolomics based on direct mass spectrometry analysis for the elucidation of altered metabolic pathways in serum from the APP/PS1 transgenic model of Alzheimer's disease, J. Pharm. Biomed. Anal. 107 (2015) 378–385.

[24] R. González-Domínguez, T. García-Barrera, J.L. Gómez-Ariza, Using direct infusion mass spectrometry for serum metabolomics in Alzheimer's disease, Anal. Bioanal. Chem. 406 (2014) 7137–7148.

[25] J. Marksteiner, I. Blasko, G. Kemmler, T. Koal, C. Humpel, Bile acid quantification of 20 plasma metabolites identifies lithocholic acid as a putative biomarker in Alzheimer's disease, Metabolomics. 14 (1) (2018).

[26] C. Randolph, M.C. Tierney, E. Mohr, T.N. Chase, The repeatable battery for the assessment of neuropsychological status (RBANS): preliminary clinical validity, J. Clin. Exp. Neuropsychol. 20 (1998) 310–319.

[27] R.I. Pfeffer, T.T. Kurosaki, C.H. Harrah Jr., J.M. Chance, S. Filos, Measurement of functional activities in older adults in the community, J. Gerontol. 37 (1982) 323–329.

[28] C.P. Hughes, L. Berg, W.L. Danziger, L.A. Coben, R.L. Martin, A new clinical scale for the staging of dementia, Br. J. Psychiatry 140 (1982) 566–572.

[29] M.F. Folstein, S.E. Folstein, P.R. McHugh, Mini-mental state. A practical method for grading the cognitive state of patients for the clinician, J. Psychiatr. Res. 12 (1975) 189–198.

[30] G.B. Frisoni, N.C. Fox, C.R. Jack Jr., P. Scheltens, P.M. Thompson, The clinical use of structural MRI in Alzheimer disease, Nat. Rev. Neurol. 6 (2010) 67–77.

[31] A. Anoop, P.K. Singh, R.S. Jacob, S.K. Maji, CSF biomarkers for Alzheimer's disease diagnosis, Int. J. Alzheimers Dis. 606802 (2010) 1–12.

[32] K. Blennow, B. Dubois, A.M. Fagan, P. Lewczuk, M.J. de Leon, H. Hampel, Clinical utility of cerebrospinal fluid biomarkers in the diagnosis of early Alzheimer's disease, Alzheimers Dement. 11 (2015) 58–69.

[33] C.A. Smith, E.J. Want, G. O'Maille, R. Abagyan, G. Siuzdak, XCMS: processing mass spectrometry data for metabolite profiling using nonlinear peak alignment, matching and identification, Anal. Chem. 78 (2006) 779–787.

[34] C. Kuhl, R. Tautenhahn, C. Boettcher, T.R. Larson, S. Neumann, CAMERA: an integrated strategy for compound spectra extraction and annotation of liquid chromatography/mass spectrometry data sets, Anal. Chem. 84 (2012) 283–289.

[35] J. Friedman, T. Hastie, R. Tibshirani, Regularization paths for generalized linear models via coordinate descent, J. Stat. Softw. 33 (1) (2010).
[36] G.C. Smith, S.R. Seaman, A.M. Wood, P. Royston, I.R. White, Correcting for optimistic prediction in small data sets, Am. J. Epidemiol. 180 (2014) 318–324.
[37] http://www.hmdb.ca/metabolites/HMDB0041366.
[38] F. Li, G. Li, J. Zhao, J. Xiao, Z. Liu, G. Su, A simple LC-MS method for determination of cyasterone in rat plasma: application to a pilot pharmacokinetic study, Biomed. Chromatogr. 30 (2016) 867–871.
[39] http://www.hmdb.ca/metabolites/HMDB001151.
[40] W. Liu, Q. Li, An efficient elastic net with regression coefficients method for variable selection of spectrum data, PLoS One 12 (2017) e0171122.
[41] D. Liu, M. Pitta, H. Jiang, J.H. Lee, G. Zhang, X. Chen, E.M. Kawamoto, M.P. Mattson, Nicotinamide forestalls pathology and cognitive decline in Alzheimer mice: evidence for improved neuronal bioenergetics and autophagy procession, Neurobiol. Aging 34 (2013) 1564–1580.
[42] B. Gong, Y. Pan, P. Vempati, W. Zhao, L. Knable, L. Ho, J. Wang, M. Sastre, K. Ono, A.A. Sauve, G.M. Pasinetti, Nicotinamide riboside restores cognition through an upregulation of proliferator-activated receptor-γ coactivator 1α regulated β-secretase 1 degradation and mitochondrial gene expression in Alzheimer's mouse models, Neurobiol. Aging 34 (2013) 1581–1588.
[43] Y. Hou, S. Lautrup, S. Cordonnier, Y. Wang, D.L. Croteau, E. Zavala, Y. Zhang, K. Moritoh, J.F. O'Connell, B.A. Baptiste, T.V. Stevnsner, M.P. Mattson, V.A. Bohr, NAD+ supplementation normalizes key Alzheimer's features and DNA damage responses in a new AD mouse model with introduced DNA repair deficiency, Proc. Natl. Acad. Sci. U. S. A. 115 (2018) E1876–E1885.
[44] Y. Chi, A.A. Sauve, Nicotinamide riboside, a trace nutrient in foods, is a vitamin B3 with effects on energy metabolism and neuroprotection, Curr. Opin. Clin. Nutr. Metab. Care 16 (2013) 657–661.
[45] T. Kurumatani, J. Fastbom, W.L. Bonkale, N. Bogdanovic, B. Winblad, T.G. Ohm, R.F. Cowburn, Loss of inositol 1,4,5-trisphosphate receptor sites and decreased PKC levels correlate with staging of Alzheimer's disease neurofibrillary pathology, Brain Res. 796 (1998) 209–221.
[46] A.D. Frej, G.P. Otto, R.S. Williams, Tipping the scales: lessons from simple model systems on inositol imbalance in neurological disorders, Eur. J. Cell Biol. 96 (2017) 154–163.
[47] A. Cristofano, N. Sapere, G. La Marca, A. Angiolillo, M. Vitale, G. Corbi, G. Scapagnini, M. Intrieri, C. Russo, G. Corso, A. Di Costanzo, Serum levels of acylcarnitines along the continuum from Normal to Alzheimer's dementia, PLoS One 11 (2016) e0155694.
[48] S.C. Thomas, A. Alhasawi, V.P. Appanna, C. Auger, V.D. Appanna, Brain metabolism and Alzheimer's disease: the prospect of a metabolite-based therapy, J. Nutr. Health Aging 19 (2015) 58–63.
[49] M. Ledeiro, C. Ibáñez, A. Cifuentes, C. Simó, Á. Cedazo-Mínguez, Decreased cerebrospinal fluid levels of L-carnitine in non-apolipoprotein E4 carriers at early stages of Alzheimer's disease, J. Alzheimers Dis. 41 (2014) 223–232.
[50] C. Mancuso, T.E. Bates, D.A. Butterfield, S. Calafato, C. Cornelius, A. De Lorenzo, A.T. Dinkova Kostova, V. Calabrese, Natural antioxidants in Alzheimer's disease, Expert Opin. Investig. Drugs 16 (2007) 1921–1931.
[51] F. Kazak, G.F. Yarim, Neuroprotective effects of acetyl-l-carnitine on lipopolysaccharide-induced neuroinflammation in mice: involvement of brain-derived neurotrophic factor, Neurosci. Lett. 658 (2017) 32–36.
[52] D.B. Jump, M. Torres-Gonzalez, L.K. Olson, Soraphen a, an inhibitor of acetyl CoA carboxylase activity, interferes with fatty acid elongation, Biochem. Pharmacol. 81 (2011) 649–660.
[53] D. Pisa, R. Alonso, A. Juarranz, A. Rábano, L. Carrasco, Direct visualization of fungal infection in brains from patients with Alzheimer's disease, J. Alzheimers Dis. 43 (2015) 613–624.
[54] R. Alonso, D. Pisa, A.I. Marina, E. Morato, A. Rábano, L. Carrasco, Fungal infection in patients with Alzheimer's disease, J. Alzheimers Dis. 41 (2014) 301–311.
[55] D. Pisa, R. Alonso, A. Rábano, I. Rodal, L. Carrasco, Different brain regions are infected with Fungi in Alzheimer's disease, Sci. Rep. 5 (2015) 15015.
[56] M. Ibarguren, D.J. López, P.V. Escribá, The effect of natural and synthetic fatty acids on membrane structure, microdomain organization, cellular functions and human health, Biochim. Biophys. Acta 1838 (2014) 1680–1692.
[57] F. Calzada, O. Onguka, S.M. Claypool, Phosphatidylethanolamine metabolism in health and disease, Int. Rev. Cell Mol. Biol. 321 (2016) 29–88.
[58] S.K. Tayebati, F. Amenta, Choline-containing phospholipids: relevance to brain functional pathways, Clin. Chem. Lab. Med. 51 (2013) 513–521.
[59] E. Westman, C. Spenger, J. Oberg, H. Reyer, J. Pahnke, L.O. Wahlund, In vivo 1H-magnetic resonance spectroscopy can detect metabolic changes in APP/PS1 mice after donepezil treatment, BMC Neurosci. 10 (2009) 33.
[60] N. Greenberg, A. Grassano, M. Thambisetty, S. Lovestone, C. Legido-Quigley, A proposed metabolic strategy for monitoring disease progression in Alzheimer's disease, Electrophoresis 30 (2009) 1235–1239.
[61] C. Ibáñez, C. Simó, P.J. Martin-Álvarez, M. Kivipelto, B. Winblad, A. Cedazo-Mínguez, A. Cifuentes, Toward a predictive model of Alzheimer's disease progression using capillary electrophoresis-mass spectrometry metabolomics, Anal. Chem. 84 (2012) 8532–8540.
[62] J. Klein, Membrane breakdown in acute and chronic neurodegeneration: focus on choline-containing phospholipids, J. Neural Transm. (Vienna) 107 (2000) 1027–1063.
[63] M.C. de Wilde, B. Vellas, E. Girault, A.C. Yavuz, J.W. Sijben, Lower brain and blood nutrient status in Alzheimer's disease: results from meta-analyses, Alzheimers. Dement. (N Y). 3 (2017) 416–431.

Journal of Pharmaceutical and Biomedical Analysis 180 (2020) 113088

Contents lists available at ScienceDirect

Journal of Pharmaceutical and Biomedical Analysis

journal homepage: www.elsevier.com/locate/jpba

Metabolomics study to identify plasma biomarkers in alzheimer disease: ApoE genotype effect

carmen peña-bautista[a], marta roca[b], rogelio lópez-cuevas[c], miguel baquero[c], máximo vento[a], consuelo cháfer-pericás[a,*]

[a] Neonatal Research Unit, Health Research Institute La Fe, Valencia, Spain
[b] Analytical Unit Platform, Health Research Institute La Fe, Valencia, Spain
[c] Neurology Unit, University and Polytechnic Hospital La Fe, Valencia, Spain

ARTICLE INFO

Article history:
Received 24 October 2019
Received in revised form 3 December 2019
Accepted 24 December 2019
Available online 26 December 2019

Keywords:
Alzheimer disease
Metabolomics
Plasma
Biomarker
Lipid
Apolipoprotein E

ABSTRACT

Alzheimer Disease (AD) is the main cause of dementia, and it has a great social and economic impact worldwide. It is a complex multifactorial disease, and we still do not know enough about its causes. For this reason, omics studies could be a useful tool for the search for new biomarkers and for enhancing the knowledge of different metabolic pathways that may be altered in the initial stages of the disease. Metabolomic analysis was carried out for plasma samples from early AD patients and healthy controls. Obtained data were normalized and analyzed by volcano plot and supervised orthogonal-least-squares-discriminant analysis. Fifteen variables were selected as the most important variables for the groups' discrimination, and the different levels of 6 identified metabolites could discriminate between patients with different ApoE4 genotypes (ε4-carriers and non ε4-carriers). In conclusion, ApoE4 genotype is associated with changes in lipid metabolomics profile in AD patients, and it could be relevant for the development of AD since early stages.

1. Introduction

Dementia constitutes a public priority for World Health Organization (WHO) due to the high associated mortality and its great impact in the society since its incidence is growing year by year [1,2]. Among the dementia causes, it is important to highlight Alzheimer Disease (AD), a multifactorial disease with some risk factors (*e.g.*, genetics, life-style, metabolism, vascular characteristics) and high social and economic impact worldwide [3]. This entity is characterized histologically by the brain accumulation of β-amyloid peptide and hyperphosphorylated tau protein, brain atrophy and neuronal loss. Its symptoms, among which the loss of memory stands out [4], are mainly related to synaptic dysfunction. AD can be diagnosed or detected by the changes in the level of β-amyloid peptide and tau species in cerebrospinal fluid (CSF), even before the first symptoms begin. The AD natural history is divided in three stages, pre-clinical, where biological changes are present but without clinical manifestations [5]; mild cognitive impairment, when symptoms appear and cognitive deficiencies are detectable but no impairment in daily functioning exists [6]; and dementia, when symptoms are severe enough to disrupt patient's activities of daily living [7]. However, few studies have focused on the progression of CSF biomarkers along the course of the disease [8]. For that reason, it is important to develop new strategies that allow a reliable AD diagnosis based on non-invasive samples.

Metabolomics is postulated as a promising tool in the search for non-invasive biomarkers for diagnosis, prognosis, or treatment monitoring [9]. In fact, it could reflect all metabolomics changes occurring in the organism in the case of multifactorial diseases, such as AD, in which several molecular pathways are involved [10]. Metabolomics studies in AD showed some altered pathways, such as oxidative stress or neurotransmission [11], mitochondrial [12], tryptophan and purines metabolisms [13] and altered metabolite levels for some lipids, such as, sphingolipids [14], amino acids and phospholipids [15]. In these studies, the CSF samples were the most used biological fluid [16], but also plasma [17], serum [18] or saliva samples [19] were analyzed. However, there is a lack of reproducible results, probably due to the differences in participants' clinical characteristics and operational definitions among studies [16–19]. In few studies, AD standard biomarkers (amyloid β-42, total tau, p-tau) were determined in CSF as key determinants of patients' biological status, as recommended by the National Insti-

* Corresponding author at: Health Research Institute La Fe, Avda de Fernando Abril Martorell, 106 46026, Valencia, Spain.
E-mail address: m.consuelo.chafer@uv.es (c. cháfer-pericás).

https://doi.org/10.1016/j.jpba.2019.113088
0731-7085/

tute of Aging and the Alzheimer association (NIA-AA) guidelines [20].

Regarding AD risk factors which would be interesting to include in metabolomics studies, Apolipoprotein E4 (ApoE4) genotype is one of the most important, although the mechanisms that relate it to the disease are still unknown [21]. ApoE4 genotype is associated with earlier amyloid deposition [22]. In this sense, some patients showed different responses against therapies according to their ApoE genotype [23]. Also, previous studies found a relationship between different metabolite networks and the ApoE genotype [24], as well as between ApoE polymorphisms and metabolomic changes [25]. Moreover, targeted studies found differences in biomarkers such as CSF SNAP-25, or blood metabolic biomarkers between ApoE4 carriers and non-carriers [26] [27].

The aim of this work is to identify metabolites altered in first AD stages using well-defined participants groups to find new potential diagnosis biomarkers, as well as to evaluate the effect of ApoE4 genotype on the metabolomic profile of individuals with early AD.

2. Material and methods

2.1. Participants and samples collection

Blood samples from patients with defined Alzheimer disease in preclinic, prodromic, or mild dementia stages (early AD, n = 29) and healthy controls (n = 29) were obtained. Participants in both groups were recruited consecutively from the Neurology Unit of the University and Polytechnic Hospital La Fe, Valencia (Spain). They were aged between 50 and 80 years old. The diagnostic criteria included a comprehensive neuropsychological evaluation that included the Repeatable Battery for Assessment of Neuropsychological Status (RBANS) [28], Functionality Assessment Questionnaire (FAQ) [29] and Clinical Dementia Rating (CDR) [30]. Assessment also included image analysis by means of NMR-TAC and cerebrospinal fluid (CSF) levels of amyloid β–42 peptide, total tau and p-tau. In this sense, preclinical cases did not show any symptoms; prodromal cases showed the core criteria for mild cognitive impairment (MCI), with clinical symptoms and typical neuropsychological alterations without achieving dementia diagnosis; and mild dementia cases showed cognitive impairment with impaired functionality. All the patients showed typical CSF AD biomarker pattern. The control group showed normal neuropsychology, normal CDR, and normal CSF biomarker pattern. Participants not accomplishing all the conditions defined for each group or showing other neuropsychological, psychiatric, relevant systemic comorbidities, or those unable to undergo the evaluations were excluded.

Samples were centrifuged and stored at -80 °C until the analysis. Plasma samples treatment was previously described by Peña-Bautista et al. [31]. The informed consent was obtained from all participants, and the Ethics Committee of the Health Research Institute of La Fe (Valencia) approved the study protocol. CSF biochemical determinations (β-amyloid, t-Tau, p-Tau) were carried out by Innotest Elisa kit (Fujirebio Diagnostics, Ghent, Belgium) using a fully automated system (Lumipulse G, Fujirebio).

2.2. Apolipoprotein e genotype

ApoE genotype was determined by PCR using LightMix® Kit ApoE C112R R158C from Roche Diagnostics [32], in blood samples from early AD participants following the manufacturer protocol.

2.3. Data pre-processing

Samples were analysed by means of ultra-performance liquid chromatography coupled to time-of-flight mass spectrometry (UPLC-Q-ToF MS), as it was described in a previous work [31]. Data processing was carried out in the Analytical Unit of the Health Research Institute of La Fe (Valencia) using an in-house R processing script with XCMS and CAMERA packages for peak detection, noise filtering, and peak alignment. The aligned dataset was then filtered according to the quality assurance (QA) criteria of coefficient of variation (CV) <30 % in quality control samples (QC) and the presence of the variable in 60 % of the samples in at least one of the compared groups. Prior to statistical analysis, four normalization methods were performed in order to find the most appropriate method for this study. They were two approaches based on multiple internal standard (IS), a median fold change normalization, and a QC-based robust locally weighted scatter plot smoothing (LOESS) for signal correction. After evaluation, LOESS data normalization was selected for statistical analysis.

2.4. Statistical analysis

Participants' descriptive statistical analysis was carried out using median and inter-quartile range for continuous variables, and relative and absolute frequencies for categorical variables. Differences between healthy and early AD groups were evaluated by means of Mann-Whitney test for numerical variables and Chi-square test for categorical variables. The software used was IBM® SPSS® Statistics version 20.0 (SPSS, Inc., Chicago, IL, USA). Statistically significant differences were considered from p value < 0.05.

For multivariate statistical analysis, data from positive and negative ionization modes were treated simultaneously. First, the normalized variables obtained from data processing were visualized in a Volcano Plot to show which variables present a stronger combination of fold change (FC) and statistical significance (p-value) from a *t*-test. Significant variables (*p* value *t*-test <0.05 and abs (log2 FC)> 1) were selected for a supervised orthogonal-least-squares discriminant analysis (OPLS-DA) validated by an iterative 7-fold cross-validation (CV) approach. The validity and robustness of the models were evaluated by $R^2(Y)$ (model fit) and $Q^2(Y)$ (predictive ability) diagnostic parameters. Quality of CV $Q^2(Y)$ was assessed by using the p-value from CV-anova analysis. R^2Y-intercepts and Q^2Y-intercepts from 1000 times permutation test in the OPLS-DA model was also used to evaluate the overfitting risk. Most discriminant variables were selected according to their Variance Importance in Projection plot values (VIP > 1.0), and a jack-knife confidence interval that did not include zero. Finally, the potential metabolites were submitted to identification process. Volcano plots were carried out using the R platform, while the multivariate analysis was carried out using Simca 14.1 software (Sartorius Stedim Biotech, Aubagne, France).

2.5. Metabolites' annotation

Variables selected by OPLS-DA analysis were identified by using the online CEU Mass Mediator (CMM 3.0, Gil de la Fuente et al., 2019) [33] which combines the results of several online databases, among which Human Metabolome Database (HMDB) (http://hmdb.ca/), Metlin (https://metlin.scripps.edu/), LipidMaps (http://www.lipidmaps.org) and Kegg (http://www.kegg.jp) are used. Annotation of variables (*m/z*) was carried by querying their accurate mass (AM) against those presented in these sources within a mass range of ±5 ppm. Only those metabolites that appeared at least in the HMDB were finally selected. The adducts included were $[M^+H]$, $[M^+Na]$, $[2M^+H]$, and $[2M^+Na]$ for positive ionization mode, and $[M^-H]$, $[M^+HCOOH^-H]$, $[2M^-H]$ for negative ionization mode. Neutral water loss was also taken into account for both ionization modes. A scoring of annotation was calculated by the CMM based on the probability to form specific adducts, as well as their retention time (T_R), and lipid elution order based in T_R and the number of carbons and double bonds. Metabolites' annotation was also sup-

ported by comparing the obtained MS/MS fragmentation spectra with those experimental spectra proposed in databases. Annotation confidence levels were determined according to the categorical scoring system proposed by the Metabolomics Community. They were level 1, identification of molecular feature through AM and T_R, matching with its chemical standard; level 2, putatively annotation through AM and MS/MS spectra matching with online databases; level 3, putatively characterization of compounds by AM matching with online databases; and level 4, feature without annotation (unknown compound) [31,32].

3. Results and discussion

3.1. Demographic and clinical data of participants

Clinical and demographic characteristics from participants are summarized in Table 1. There were no differences between control and early AD groups for demographic variables except for gender and age. However, clinical variables (neuroimaging, CSF biomarkers (amyloid β, total tau, p-tau), and neuropsychological evaluation tests (RBANS, CDR, FAQ)) showed differences between groups as it was expected.

3.2. Metabolomic differences between healthy and early AD subjects

The Volcano Plot analysis, carried out for the healthy control and early AD groups, showed 36 significant variables (Fig. 1a). The supervised OPLS-DA analysis was carried out with those variables in order to find the most powerful discriminant metabolites between groups. As shown in Fig. 1b, the OPLS-DA model revealed a clear separation between early AD cases and healthy controls (except for some misclassified controls), with good R^2Y (0.738) and Q^2Y (0.679) parameters, indicating biochemical changes between groups. The model was satisfactorily validated with a 7-fold cross validation method (p CV-anova <0.001) and 1000 permutation tests (R^2Y- intercept = 0.074, Q^2Y-intercept=-0.253).

Potential metabolites contributing to early AD and healthy controls separation were subjected to identification and confirmation based on a threshold of VIP value >1. Finally, 15 variables were studied and tentatively identified by using CMM tool and mass fragmentation strategies (see Table S1 in Supplementary Material). Metabolite annotation based on AM, retention time and MS/MS spectra from chemical standard lead to the confirmation of m/z 1043.7008 as Lysophosphatidylcholine (18:1) (Lyso PC (18:1)) (Fig. S1). This metabolite showed levels with differences statistically significant between early AD and healthy control participants (Fig. 1c). In addition, the variable m/z 1047.7345 was putatively characterized as NeuAcalpha2-3Galbeta-Cer(d18:1/20:0), LysoPE(21:0), LysoPC(18:0) or PC(O-16:0/2:0), all of them were glycerophospholipids. On the other hand, m/z 570.0359, and m/z 335.0450 were putatively characterized as chemical compound, and phenols, organic sulphuric acids, or fatty acyls classes, respectively. The other variables could not be identified by any of the databases.

As previous works described, it seems that lipid metabolism plays an important role in AD physiopathology [35], and it could be useful in the discrimination between early AD and healthy controls. In this sense, previous studies showed that membrane lipid composition could be involved in the activity of gamma secretase, an enzyme acting in the appearance of β-amyloid peptide, the most characteristic hallmark of AD [33,34]. In addition, structural changes in lipid membrane could change the interaction with β-amyloid protein [37].

Regarding lipid metabolites, lysophosphatidylcholine is postulated as a potential plasma biomarker. Similarly, Liu et al. and

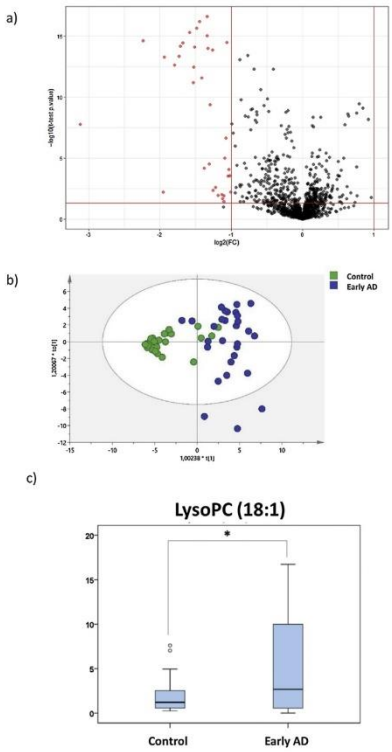

Fig. 1. a) Volcano Plot representing the significant variables in the discrimination between early AD and healthy control groups. The non-significant variables are represented in grey, the significant variables are represented in red (p value t-test> 0.05 and FC > 2); b) OPLS-DA represents differential distribution between early AD and healthy control groups; c) Boxplot of plasma analytical responses of LysoPC(18:1). (For interpretation of the references to colour in this figure legend, the reader is referred to the web version of this article).
*p value < 0.05.

Lin et al. found that lysophosphatidilcholines and phosphatidilcholines showed differential levels between AD and healthy elderly in plasma samples [38,39]. In fact, most of metabolomics studies carried out in plasma for AD biomarkers identification showed lipids as important potential biomarkers [40]. Oberacher et al. 2017 found similar results using soluble lysates from platelets where different phosphocholines seemed to discriminate between early AD and healthy controls [41]. Also, Dorninger et al. 2018 found that although lphosphatidylysocholine levels increased in normal aging, this increase is more remarkable in probable AD patients [42]. In addition, it was demonstrated that lysophosphatidylcholines increased the *in vitro* formation of Aβ1–42 oligomer [36,37]. On the

Table 1
Demographic and clinical variables for the participants groups.

Variable		Control (n = 29)	First AD stages (n = 29)
Age (years) (median (IQR))		65 (63, 70)	72 (69, 75)
Gender (female) (n (%))		9 (31.03 %)	19 (65.52 %)
Education level (n (%))	Basics	6 (20 %)	17 (59 %)
	University	11 (38 %)	5 (17 %)
Medications (n (%))	Statins	10 (34 %)	17 (59 %)
	Fibrates	3 (10 %)	2 (7 %)
	Benzodiazepines	2 (7 %)	4 (13.79 %)
	Opiates	0 (0 %)	0 (0 %)
	Antiepileptics	1 (3.45 %)	0 (0 %)
	Antihipertensives	10 (35.71 %)	14 (48.28 %)
	Corticoids	0 (0 %)	2 (6.9 %)
Comorbidity (n (%))	Dyslipidemia	10 (35.71 %)	16 (55.17 %)
	Diabetes	3 (10 %)	3 (10.34 %)
	Hypertension	11 (38 %)	13 (44.83 %)
	Heart Disease	1 (3.45 %)	0 (0 %)
Smoking status (n (%))	Yes	1 (3.45 %)	2 (6.9 %)
	Former smoker (more than 10 years)	9 (31 %)	7 (24.14 %)
Alcohol or drugs consumption (n (%))		6 (21.43 %)	3 (10.34 %)
Presenile family background (n (%))	None	22 (76 %)	22 (88 %)
	First grade	5 (17 %)	5 (17 %)
	Second grade	2 (7 %)	0 (0 %)
Depression (n (%))		3 (10.34 %)	4 (14 %)
Anxiety (n (%))		1 (3.45 %)	3 (10.34 %)
Temporal atrophy (n (%))		2 (7.14 %)	20 (69 %)
CSF amyloid β (pg mL^{-1}) (median (IQR))		1256 (1164, 1464)	600 (496, 687)
CSF total tau (pg mL^{-1}) (median (IQR))		196 (141, 298)	590 (465, 782)
CSF phosphorylated tau (pg mL^{-1}) (median (IQR))		48 (37, 60)	84 (73, 104)
RBANS.DM (median (IQR))		100 (92, 106)	48 (40, 66)
FAQ (median (IQR))		0 (0, 0)	5 (0, 8.5)
CDR (n (%))	0	29 (100 %)	5 (17 %)
	0.5	0 (0 %)	18 (62 %)
	1	0 (0 %)	6 (21 %)

Table 2
Metabolitesánnotation from ApoE classification.

AM (m/z)	t_R (min)	Adduct Ion	Formula	Identification of variables		Compound class / Metabolism	FC[c]
				Metabolite annotation	Level #		
1087.6829	8.86	M-H	C6 H102O12P2	alpha-D-galactosyl undecaprenyl diphosphate	2	Prenol lipids/Lipid metabolism	0.46
1043.7008	8.85	2M + H	C26H52NO7P	LysoPC(18:1)	1	Glycerophospholipids / Lipid metabolism	0.26
508.3746	9.02	M + H	C26H54NO6P	LysoPC(P-18:0)	3[a]	Glycerophospholipids	0.48
530.3563	9.02	M + Na	C26H54NO6P	LysoPC(P-18:0)	3[b]	Glycerophospholipids	0.48
536.3696	9.16	M + H	C27H54NO7P	LysoPE(0:0/22:1(13Z)) LysoPE(22:1(13Z)/0:0)	3[a]	Glycerophospholipids	0.50
1261.8213	8.69	M + H	C67H122O17P2	CL(8:0/14:0/18:2(9Z,11Z)/18:2(9Z,11Z) CL(8:0/i14:0/18:2(9Z,11Z)/18:2(9Z,11Z))	3	Glycerophospholipids	0.50
1018.6680	8.70	+		Unknown	4		0.50
548.8109	8.85	+		Unknown	4		0.46

1: confirmed; 2: putative annotated; 3: putative characterized; 4: unknown.
LysoPC: Lysophosphatidylcholine.
LysoPE: lysophosphatidylethanolamine.
CL: cardiolipin.
[a] Score 1 for ionization rules (particular adducts formation depending on the lipid class, ionisation mode and mobile phase modifier used) based on CMM is very likely right (score range between 1.5–2).
[b] Score 1 for ionization rules (particular adducts formation depending on the lipid class, ionisation mode and mobile phase modifier used) based on CMM is likely right (score range between 1–1.5).
[c] FC: Fold Change was calculated as median signal of carriers divided to non-carriers.

contrary, Li et al. found decreased levels of lysophosphocholines in brain tissue from AD mice model [43].

3.3. Metabolomic differences between ApoE4 genotypes

In Fig. 1b, we appreciate a clear clustering in the control group, while the early AD case group showed high scattering, indicating a within class variation. In order to explain this variability, we proposed the ApoE4 genotype as a potential variable since it is considered an important risk factor in AD development. Specifically, ApoE genotype is related to AD pathogenesis as the ε4 allele is involved in cholesterol brain metabolism and in the maintenance of membrane integrity [44]. In addition, it is related to other pathways such as lipid metabolism, synaptic function, glucose metabolism microglial response, or tau pathology, among others [45]. Therefore, ApoE genotype could generate differences in metabolomic profile. Previously, Karjalainen et al. indicated that ApoE-ε4 carriers and non-carriers showed differential serum metabolomics profile, it could be associated to different pathological status [25]. Therefore, in the present study, different metabolic profiles in plasma from early AD patients, as well as the ApoE genotype, influence were evaluated.

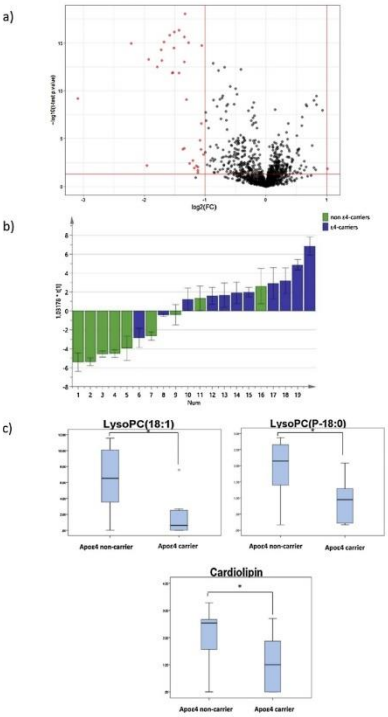

Fig. 2. a) Volcano Plot representing the significant variables in the discrimination between early AD ε4-carrier and non ε4-carrier groups. The non-significant variables are represented in grey, the significant variables are represented in red (p value *t*-test> 0.05 and FC > 2); b) OPLS-DA represents differential distribution between ε4-carrier and non ε4-carrier groups; c) Boxplot of plasma analytical responses of LysoPC(18:1), LysoPC (P-18:0) and cardiolipin. (For interpretation of the references to colour in this figure legend, the reader is referred to the web version of this article).
*p value < 0.05.

The metabolomics differences were evaluated using the same statistical procedure described above. It was applied in early AD cases previously classified as ε4-carriers and non ε4-carriers according to the PCR analysis results. In this sense, 20 significant variables were selected in the Volcano Plot (Fig. 2a) for the following OPLS-DA analysis. As it is shown in the score plot (Fig. 2b), few samples were misclassified and the model presented R^2Y (0.437) and Q^2Y (0.394) diagnostic parameters. Nevertheless, the model was reliable with a CV-anova p-value <0.05 and acceptable permutation test (R^2Y-intercept = 0.04, Q^2Y-intercept = −0.206). In order to find out the metabolites whose concentrations were altered in ε4-carriers, compared to non ε4-carriers, we selected those variables in the Variance Important Projection Plot VIP value >1 and which their jack-knife confidence interval did not include zero.

Finally, 8 variables were tentatively identified by using the CMM tool (see Table 2). All these analytes showed lower values for ε4-carriers. Specifically, *m/z* 1043.7008 with a fold-change ratio of 0.26 was confirmed as LysoPC(18:1) by using a chemical standard, and it showed statistically significant differences between groups. This variable was previously confirmed in the metabolome comparison between healthy and early AD groups. Other variables were putatively characterized as LysoPC(P-18:0), LysoPE(0:0/22:1(13Z)), and cardiolipins. As can be seen in Fig. 2c, some of these metabolites showed statistically significant differences between ε4-carriers and non ε4-carriers.

Regarding the identified compounds class, most of them are glycerophospholipids (Table 2). Fonteh et al. previously described differences for different glycerophospholipids in CSF from AD patients and healthy controls [46]. However, Sharman did not find differences for glycerophospholipids levels in brain tissue nor plasma samples from knock-in mice with different human ApoE subtypes expression [47]. On the other hand, Igbavboa et al. found differential composition in synaptosomal lipid rafts depending on ApoE genotype [48]. In general, lipid metabolites are the most relevant compounds, since cardiolipins, lysophosphatidylcholines and lysophosphatidylethanolamines are discriminant variables between early AD and healthy control groups, as well as between ε4-carriers and non ε4-carriers.

Regarding cardiolipins, they are phospholipids highly present in the mitochondrial membrane, and they have been related to brain disorders and neurodegenerative diseases, such as AD [49]. In this study, cardiolipins showed lower signals in ε4-carriers than non ε4-carriers. This dysregulation could be associated with mitochondrial dysfunction in AD synapsis [50].

Among lysophosphatidylcholines, LysoPC(18:1) is one of the most important discriminant variables between ε4-carriers and non ε4-carriers in this study, and its plasmatic levels were previously related to a lower risk of different cancer kinds [51]. In addition, Whiley et al. found that the determination of 3 different phosphatidylcholines combined with ApoE genotype, provided a satisfactory discriminant capacity between AD and non-AD participants [52]. Nevertheless, the present study showed lower levels for this compound in the healthy and ε4-carrier groups in comparison with the non ε4-carrier group. This finding reinforces the idea that the ApoE genotype plays an important role in the development of AD. In this sense, LysoPC (18:1) levels and ApoE genotype could be a useful tool for early AD diagnosis.

Regarding the limitations of the present study, it is important to highlight the low number of participants, since it is very difficult to achieve early AD patients and healthy people identified from CSF biomarkers levels.

4. Conclusions

Different levels for plasma metabolites are found in early AD patients compared to healthy controls, reflecting the different metabolic pathways that are affected in this disease. Among these analytes, different lipid compounds stand out, so lipid metabolism is an important pathway that seems to fail since early stages of the pathology. Therefore, it could constitute a source of biomarkers for the early AD diagnosis, as well as further therapeutic targets. In addition, in the early AD patients, different metabolic profiles were obtained depending on their ApoE genotype (ε4-carriers, non ε4-carriers). Actually, different glycerophospholipids were altered between these groups. It could involve an important advancement in the knowledge of the different impaired mechanisms, as well as the improvement in precision medicine for diagnosis and treat-

ment. Nevertheless, further work based on target analysis would be required for the quantification of these potential biomarkers in a larger number of participants in order to validate the diagnostic performance of these metabolites.

Funding

This work was supported by the Instituto de Salud Carlos III (Miguel Servet I Project (CP16/00082)) (Spanish Ministry of Economy and Competitiveness).

CRediT authorship contribution statement

carmen peña-bautista: Methodology, Writing - original draft. **marta roca:** Methodology, Data curation. **rogelio lópez-cuevas:** Conceptualization. **miguel baquero:** Investigation, Supervision. **máximo vento:** Supervision. **consuelo cháfer-pericás:** Conceptualization, Investigation, Writing - review & editing.

Acknowledgement

We are greatly indebted to all participants, nursing, psychology and medical staff who voluntarily participated in the present study. Without their collaboration and enthusiasm this study could not have been completed.

CC-P acknowledges a "Miguel Servet I" Grant (CP16/00082) from the ISCIII (Spanish Ministry of Economy and Competitiveness). CP-B acknowledges a pre-doctoral Grant (associated to "Miguel Servet" project CP16/00082) from the Instituto Carlos III (Spanish Ministry of Economy, Industry and Competitiveness).

The authors are grateful for the professional English language editing to Mr. Arash Javadinejad, English Instructor and Publication Editor at the Instituto de Investigación Sanitaria La Fe, Valencia, Spain.

Declaration of Competing Interest

None.

Appendix A. Supplementary data

Supplementary material related to this article can be found, in the online version, at doi:https://doi.org/10.1016/j.jpba.2019.113088.

References

[1] M. Wortmann, Dementia: a global health priority - Highlights from an ADI and World Health Organization report, Alzheimers Res. Ther. (2012), http://dx.doi.org/10.1186/alzrt143.

[2] H. Niu, I. Alvarez-Alvarez, F. Guillen-Grima, M.J. Al-Rahamneh, I. Aguinaga-Ontoso, Trends of mortality from Alzheimer's disease in the European Union, 1994-2013, Eur. J. Neurol. 24 (2017) 858–866, http://dx.doi.org/10.1111/ene.13302.

[3] S. Sindi, F. Mangialasche, M. Kivipelto, Advances in the prevention of alzheimer's disease, F1000Prime Rep. 7 (2015), http://dx.doi.org/10.12703/P7-50.

[4] A.L. Calderon-Garcidueñas, C. Duyckaerts, Alzheimer Disease, 2018, pp. 325–337, http://dx.doi.org/10.1016/B978-0-12-802395-2.00023-7.

[5] R.A. Sperling, P.S. Aisen, L.A. Beckett, D.A. Bennett, S. Craft, A.M. Fagan, T. Iwatsubo, C.R. Jack, J. Kaye, T.J. Montine, D.C. Park, E.M. Reiman, C.C. Rowe, E. Siemers, Y. Stern, K. Yaffe, M.C. Carrillo, B. Thies, M. Morrison-Bogorad, M.V. Wagster, C.H. Phelps, Toward defining the preclinical stages of Alzheimer's disease: recommendations from the National Institute on Aging-Alzheimer's Association workgroups on diagnostic guidelines for Alzheimer's disease, Alzheimer's Dement. 7 (2011) 280–292, http://dx.doi.org/10.1016/j.jalz.2011.03.003.

[6] M.S. Albert, S.T. DeKosky, D. Dickson, B. Dubois, H.H. Feldman, N.C. Fox, A. Gamst, D.M. Holtzman, W.J. Jagust, R.C. Petersen, P.J. Snyder, M.C. Carrillo, B. Thies, C.H. Phelps, The diagnosis of mild cognitive impairment due to Alzheimer's disease: recommendations from the National Institute on Aging-Alzheimer's Association workgroups on diagnostic guidelines for Alzheimer's disease, Alzheimer's Dement. 7 (2011) 270–279, http://dx.doi.org/10.1016/j.jalz.2011.03.008.

[7] G.M. McKhann, D.S. Knopman, H. Chertkow, B.T. Hyman, C.R. Jack, C.H. Kawas, W.E. Klunk, W.J. Koroshetz, J.J. Manly, R. Mayeux, R.C. Mohs, J.C. Morris, M.N. Rossor, P. Scheltens, M.C. Carrillo, B. Thies, S. Weintraub, C.H. Phelps, The diagnosis of dementia due to Alzheimer's disease: recommendations from the National Institute on Aging-Alzheimer's Association workgroups on diagnostic guidelines for Alzheimer's disease, Alzheimer's Dement. 7 (2011) 263–269, http://dx.doi.org/10.1016/j.jalz.2011.03.005.

[8] M.D. Garrett, R. Valle, A methodological critique of the National Institute of Aging and Alzheimer's Association Guidelines for Alzheimer's disease, dementia, and mild cognitive impairments, Dementia. 15 (2016) 239–254, http://dx.doi.org/10.1177/1471301214525166.

[9] A. Klupczyńska, P. Dereziński, Z.J. Kokot, Metabolomics in medical sciences--trends, challenges and perspectives., Acta Pol. Pharm. 72 (n.d.) 629–641. http://www.ncbi.nlm.nih.gov/pubmed/26647618.

[10] W. Lin, J. Zhang, Y. Liu, R. Wu, H. Yang, X. Hu, X. Ling, Studies on diagnostic biomarkers and therapeutic mechanism of Alzheimer's disease through metabolomics and hippocampal proteomics, Eur. J. Pharm. Sci. 105 (2017) 119–126, http://dx.doi.org/10.1016/j.ejps.2017.05.003.

[11] R. González-Domínguez, T. García-Barrera, J.L. Gómez-Ariza, Using direct infusion mass spectrometry for serum metabolomics in Alzheimer's disease, Anal. Bioanal. Chem. 406 (2014) 7137–7148, http://dx.doi.org/10.1007/s00216-014-8102-3.

[12] G. Paglia, M. Stocchero, S. Cacciatore, S. Lai, P. Angel, M.T. Alam, M. Keller, M. Ralser, G. Astarita, Unbiased metabolomic investigation of alzheimer's disease brain points to dysregulation of mitochondrial aspartate metabolism, J. Proteome Res. 15 (2016) 608–618, http://dx.doi.org/10.1021/acs.jproteome.5b01020.

[13] R. Kaddurah-Daouk, H. Zhu, S. Sharma, M. Bogdanov, S.G. Rozen, W. Matson, N.O. Oki, A.A. Motsinger-Reif, E. Churchill, Z. Lei, D. Appleby, M.A. Kling, J.Q. Trojanowski, P.M. Doraiswamy, S.E. Arnold, Alterations in metabolic pathways and networks in Alzheimer's disease, Transl. Psychiatry 3 (2013) e244, http://dx.doi.org/10.1038/tp.2013.18.

[14] V.R. Varma, A.M. Oommen, S. Varma, R. Casanova, Y. An, R.M. Andrews, R. O'Brien, O. Pletnikova, J.C. Troncoso, J. Toledo, R. Baillie, M. Arnold, G. Kastenmueller, K. Nho, P.M. Doraiswamy, A.J. Saykin, R. Kaddurah-Daouk, C. Legido-Quigley, M. Thambisetty, Brain and blood metabolite signatures of pathology and progression in Alzheimer disease: a targeted metabolomics study, PLoS Med. 15 (2018), e1002482, http://dx.doi.org/10.1371/journal.pmed.1002482.

[15] Y. Cui, X. Liu, M. Wang, L. Liu, X. Sun, L. Ma, W. Xie, C. Wang, S. Tang, D. Wang, Q. Wu, Lysophosphatidylcholine and Amide as metabolites for detecting alzheimer disease using ultrahigh-performance liquid chromatography–Quadrupole time-of-Flight mass spectrometry–Based metabonomics, J. Neuropathol. Exp. Neurol. 73 (2014) 954–963, http://dx.doi.org/10.1097/NEN.0000000000000116.

[16] E. Trushina, T. Dutta, X.-M.T. Persson, M.M. Mielke, R.C. Petersen, Identification of altered metabolic pathways in plasma and CSF in mild cognitive impairment and alzheimer's disease using metabolomics, PLoS One 8 (2013), e63644, http://dx.doi.org/10.1371/journal.pone.0063644.

[17] G. Wang, Y. Zhou, F.-J. Huang, H.-D. Tang, X.-H. Xu, J.-J. Liu, Y. Wang, Y.-L. Deng, R.-J. Ren, W. Xu, J.-F. Ma, Y.-N. Zhang, A.-H. Zhao, S.-D. Chen, W. Jia, Plasma metabolite profiles of alzheimer's disease and mild cognitive impairment, J. Proteome Res. 13 (2014) 2649–2658, http://dx.doi.org/10.1021/pr5000895.

[18] J.B. Toledo, M. Arnold, G. Kastenmüller, R. Chang, R.A. Baillie, X. Han, M. Thambisetty, J.D. Tenenbaum, K. Suhre, J.W. Thompson, L.St. John-Williams, S. MahmoudianDehkordi, D.M. Rotroff, J.R. Jack, A. Motsinger-Reif, S.L. Risacher, C. Blach, J.E. Lucas, T. Massaro, G. Louie, H. Zhu, G. Dallmann, K. Klavins, T. Koal, S. Kim, K. Nho, L. Shen, R. Casanova, S. Varma, C. Legido-Quigley, M.A. Moseley, K. Zhu, M.Y.R. Henrion, S.J. van der Lee, A.C. Harms, A. Demirkan, T. Hankemeier, C.M. van Duijn, J.Q. Trojanowski, L.M. Shaw, A.J. Saykin, M.W. Weiner, P.M. Doraiswamy, R. Kaddurah-Daouk, Metabolic network failures in Alzheimer's disease: a biochemical road map, Alzheimer's Dement. 13 (2017) 965–984, http://dx.doi.org/10.1016/j.jalz.2017.01.020.

[19] A. Yilmaz, T. Geddes, B. Han, R.O. Bahado-Singh, G.D. Wilson, K. Imam, M. Maddens, S.F. Graham, Diagnostic biomarkers of alzheimer's disease as identified in saliva using 1H NMR-Based metabolomics, J. Alzheimers Dis. 58 (2017) 355–359, http://dx.doi.org/10.3233/JAD-161226.

[20] C.R. Jack, D.A. Bennett, K. Blennow, M.C. Carrillo, B. Dunn, S.B. Haeberlein, D.M. Holtzman, W. Jagust, F. Jessen, J. Karlawish, E. Liu, J.L. Molinuevo, T. Montine, C. Phelps, K.P. Rankin, C.C. Rowe, P. Scheltens, E. Siemers, H.M. Snyder, R. Sperling, C. Elliott, E. Masliah, L. Ryan, N. Silverberg, NIA-AA Research Framework: toward a biological definition of alzheimer's disease, Alzheimer's Dement. 14 (2018) 535–562, http://dx.doi.org/10.1016/j.jalz.2018.02.018.

[21] F. Liao, H. Yoon, J. Kim, Apolipoprotein E metabolism and functions in brain and its role in Alzheimer's disease, Curr. Opin. Lipidol. (1) (2016), http://dx.doi.org/10.1097/MOL.0000000000000383.

[22] A. Bussy, B.J. Snider, D. Coble, C. Xiong, A.M. Fagan, C. Cruchaga, T.L.S. Benzinger, B.A. Gordon, J. Hassenstab, R.J. Bateman, J.C. Morris, Effect of apolipoprotein E4 on clinical, neuroimaging, and biomarker measures in noncarrier participants in the Dominantly Inherited Alzheimer Network, Neurobiol. Aging 75 (2019) 42–50, http://dx.doi.org/10.1016/j.neurobiolaging.2018.10.011.

[23] A.J. Hanson, S. Craft, W.A. Banks, The APOE genotype: modification of therapeutic responses in Alzheimer's disease, Curr. Pharm. Des. 21 (2015) 114–120 http://www.ncbi.nlm.nih.gov/pubmed/25330331.

[24] F.A. de Leeuw, C.F.W. Peeters, M.I. Kester, A.C. Harms, E.A. Struys, T. Hankemeier, H.W.T. van Vlijmen, S.J. van der Lee, C.M. van Duijn, P. Scheltens, A. Demirkan, M.A. van de Wiel, W.M. van der Flier, C.E. Teunissen, Blood-based metabolic signatures in alzheimer's disease, alzheimer's dement, Diagnosis, Assess. Dis. Monit. 8 (2017) 196–207, http://dx.doi.org/10.1016/j.dadm.2017.07.006.

[25] J.-P. Karjalainen, N. Mononen, N. Hutri-Kähönen, M. Lehtimäki, M. Juonala, M. Ala-Korpela, M. Kähönen, O. Raitakari, T. Lehtimäki, The effect of apolipoprotein E polymorphism on serum metabolome – a population-based 10-year follow-up study, Sci. Rep. 9 (2019) 458, http://dx.doi.org/10.1038/s41598-018-36450-9.

[26] S. Wang, J. Zhang, T. Pan, APOE ε4 is associated with higher levels of CSF SNAP-25 in prodromal Alzheimer's disease, Neurosci. Lett. 685 (2018) 109–113, http://dx.doi.org/10.1016/j.neulet.2018.08.029.

[27] J.K. Morris, R.A.Z. Uy, E.D. Vidoni, H.M. Wilkins, A.E. Archer, J.P. Thyfault, J.M. Miles, J.M. Burns, Effect of APOE ε4 genotype on metabolic biomarkers in aging and alzheimer's disease, J. Alzheimers Dis. 58 (2017) 1129–1135, http://dx.doi.org/10.3233/JAD-170148.

[28] C. Randolph, M.C. Tierney, E. Mohr, T.N. Chase, The Repeatable Battery for the Assessment of Neuropsychological Status (RBANS): preliminary clinical validity, J. Clin. Exp. Neuropsychol. 20 (1998) 310–319, http://dx.doi.org/10.1076/jcen.20.3.310.823.

[29] R.I. Pfeffer, T.T. Kurosaki, C.H. Harrah, J.M. Chance, S. Filos, Measurement of functional activities in older adults in the community, J. Gerontol. 37 (1982) 323–329 http://www.ncbi.nlm.nih.gov/pubmed/7069156.

[30] R.L. Martin, C.P. Hughes, L. Berg, W.L. Danziger, L.A. Coben, A new clinical scale for the staging of dementia, Br. J. Psychiatry 140 (1982) 566–572, 7104545.

[31] C. Peña-Bautista, M. Roca, D. Hervás, A. Cuevas, R. López-Cuevas, M. Vento, M. Baquero, A. García-Blanco, C. Cháfer-Pericás, Plasma metabolomics in early Alzheimer's disease patients diagnosed with amyloid biomarker, J. Proteomics 200 (2019) 144–152, http://dx.doi.org/10.1016/j.jprot.2019.04.008.

[32] No Title, (n.d.), https://www.roche-as.es/lightmix.global.

[33] A. Gil-de-la-Fuente, J. Godzien, S. Saugar, R. Garcia-Carmona, H. Badran, D.S. Wishart, C. Barbas, A. Otero, CEU mass mediator 3.0: a metabolite annotation tool, J. Proteome Res. 18 (2019) 797–802, http://dx.doi.org/10.1021/acs.jproteome.8b00720.

[34] B.B. Misra, New tools and resources in metabolomics: 2016-2017, Electrophoresis. 39 (2018) 909–923, http://dx.doi.org/10.1002/elps.201700441.

[35] T. Matsuzaki, K. Sasaki, J. Hata, Y. Hirakawa, K. Fujimi, T. Ninomiya, S.O. Suzuki, S. Kanba, Y. Kiyohara, T. Iwaki, Association of Alzheimer disease pathology with abnormal lipid metabolism: the Hisayama Study, Neurology. 77 (2011) 1068–1075, http://dx.doi.org/10.1212/WNL.0b013e31822e145d.

[36] B. Penke, G. Paragi, J. Gera, R. Berkecz, Z. Kovács, T. Crul, L. Vígh, The role of lipids and membranes in the pathogenesis of alzheimer's disease: a comprehensive view, Curr. Alzheimer Res. 15 (2018) 1191–1212, http://dx.doi.org/10.2174/1567205015666180911151716.

[37] E. Drolle, A. Negoda, K. Hammond, E. Pavlov, Z. Leonenko, Changes in lipid membranes may trigger amyloid toxicity in Alzheimer's disease, PLoS One 12 (2017), e0182194, http://dx.doi.org/10.1371/journal.pone.0182194.

[38] Y. Liu, N. Li, L. Zhou, Q. Li, W. Li, Plasma metabolic profiling of mild cognitive impairment and alzheimer's disease using liquid Chromatography/Mass spectrometry, Cent. Nerv. Syst. Agents Med. Chem. 14 (2015) 113–120, http://dx.doi.org/10.2174/1871524915666141216161246.

[39] C. Lin, C. Huang, K. Huang, K. Lin, T. Yen, H. Kuo, A metabolomic approach to identifying biomarkers in blood of Alzheimer's disease, Ann. Clin. Transl. Neurol. 6 (2019) 537–545, http://dx.doi.org/10.1002/acn3.726.

[40] M. Orešič, T. Hyötyläinen, S.-K. Herukka, M. Sysi-Aho, I. Mattila, T. Seppänan-Laakso, V. Julkunen, P.V. Gopalacharyulu, M. Hallikainen, J. Koikkalainen, M. Kivipelto, S. Helisalmi, J. Lötjönen, H. Soininen, Metabolome in progression to Alzheimer's disease, Transl. Psychiatry 1 (2011) e57, http://dx.doi.org/10.1038/tp.2011.55.

[41] H. Oberacher, K. Arnhard, C. Linhart, A. Diwo, J. Marksteiner, C. Humpel, Targeted metabolomic analysis of soluble lysates from platelets of patients with mild cognitive impairment and alzheimer's disease compared to healthy controls: is PC aeC40:4 a promising diagnostic tool? J. Alzheimers Dis. 57 (2017) 493–504, http://dx.doi.org/10.3233/JAD-160172.

[42] F. Dorninger, A.B. Moser, J. Kou, C. Wiesinger, S. Forss-Petter, A. Gleiss, M. Hinterberger, S. Jungwirth, P. Fischer, J. Berger, Alterations in the plasma levels of specific choline phospholipids in alzheimer's disease mimic accelerated aging, J. Alzheimers Dis. 62 (2018) 841–854, http://dx.doi.org/10.3233/JAD-171036.

[43] N. Li, Y. Liu, W. Li, L. Zhou, Q. Li, X. Wang, P. He, A UPLC/MS-based metabolomics investigation of the protective effect of ginsenosides Rg1 and Rg2 in mice with Alzheimer's disease, J. Ginseng Res. 40 (2016) 9–17, http://dx.doi.org/10.1016/j.jgr.2015.04.006.

[44] G. Operto, R. Cacciaglia, O. Grau-Rivera, C. Falcon, A. Brugulat-Serrat, P. Ródenas, R. Ramos, S. Morán, M. Esteller, N. Bargalló, J.L. Molinuevo, J.D. Gispert, White matter microstructure is altered in cognitively normal middle-aged APOE-ε4 homozygotes, Alzheimers Res. Ther. 10 (2018) 48, http://dx.doi.org/10.1186/s13195-018-0375-x.

[45] Y. Yamazaki, N. Zhao, T.R. Caulfield, C.-C. Liu, G. Bu, Apolipoprotein E and Alzheimer disease: pathobiology and targeting strategies, Nat. Rev. Neurol. 15 (2019) 501–518, http://dx.doi.org/10.1038/s41582-019-0228-7.

[46] A.N. Fonteh, J. Chiang, M. Cipolla, J. Hale, F. Diallo, A. Chirino, X. Arakaki, M.G. Harrington, Alterations in cerebrospinal fluid glycerophospholipids and phospholipase A 2 activity in Alzheimer's disease, J. Lipid Res. 54 (2013) 2884–2897, http://dx.doi.org/10.1194/jlr.M037622.

[47] M.J. Sharman, G. Shui, A.Z. Fernandis, W.L.F. Lim, T. Berger, E. Hone, K. Taddei, I.J. Martins, J. Ghiso, J.D. Buxbaum, S. Gandy, M.R. Wenk, R.N. Martins, Profiling brain and plasma lipids in human APOE ε2, ε3, and ε4 knock-in mice using electrospray ionization mass spectrometry, J. Alzheimers Dis. 20 (2010) 105–111, http://dx.doi.org/10.3233/JAD-2010-1348.

[48] U. Igbavboa, G.P. Eckert, T.M. Malo, A.E. Studniski, L.N.A. Johnson, N. Yamamoto, M. Kobayashi, S.C. Fujita, T.R. Appel, W.E. Müller, W.G. Wood, K. Yanagisawa, Murine synaptosomal lipid raft protein and lipid composition are altered by expression of human apoE 3 and 4 and by increasing age, J. Neurol. Sci. 229–230 (2005) 225–232, http://dx.doi.org/10.1016/j.jns.2004.11.037.

[49] C.B. Pointer, A. Klegeris, Cardiolipin in central nervous system physiology and pathology, Cell. Mol. Neurobiol. 37 (2017) 1161–1172, http://dx.doi.org/10.1007/s10571-016-0458-9.

[50] V.F. Monteiro-Cardoso, M.M. Oliveira, T. Melo, M.R.M. Domingues, P.I. Moreira, E. Ferreiro, F. Peixoto, R.A. Videira, Cardiolipin profile changes are associated to the early synaptic mitochondrial dysfunction in alzheimer's disease, J. Alzheimers Dis. 43 (2014) 1375–1392, http://dx.doi.org/10.3233/JAD-141002.

[51] T. Kühn, A. Floegel, D. Sookthai, T. Johnson, U. Rolle-Kampczyk, W. Otto, M. von Bergen, H. Boeing, R. Kaaks, Higher plasma levels of lysophosphatidylcholine 18:0 are related to a lower risk of common cancers in a prospective metabolomics study, BMC Med. 14 (2016) 13, http://dx.doi.org/10.1186/s12916-016-0552-3.

[52] L. Whiley, A. Sen, J. Heaton, P. Proitsi, D. García-Gómez, R. Leung, N. Smith, M. Thambisetty, I. Kloszewska, P. Mecocci, H. Soininen, M. Tsolaki, B. Vellas, S. Lovestone, C. Legido-Quigley, Evidence of altered phosphatidylcholine metabolism in Alzheimer's disease, Neurobiol. Aging 35 (2014) 271–278, http://dx.doi.org/10.1016/j.neurobiolaging.2013.08.001.

Journal of Clinical Medicine

MDPI

Article

Plasma Lipidomics Approach in Early and Specific Alzheimer's Disease Diagnosis

Carmen Peña-Bautista [1], Lourdes Álvarez-Sánchez [1,2], Marta Roca [3], Lorena García-Vallés [2], Miguel Baquero [1,2] and Consuelo Cháfer-Pericás [1,*]

[1] Alzheimer's Disease Research Group, Health Research Institute La Fe, 46026 Valencia, Spain
[2] Division of Neurology, University and Polytechnic Hospital La Fe, 46026 Valencia, Spain
[3] Analytical Unit, Health Research Institute La Fe, 46026 Valencia, Spain
* Correspondence: m.consuelo.chafer@uv.es

Abstract: Background: The brain is rich in lipid content, so a physiopathological pathway in Alzheimer's disease (AD) could be related to lipid metabolism impairment. The study of lipid profiles in plasma samples could help in the identification of early AD changes and new potential biomarkers. Methods: An untargeted lipidomic analysis was carried out in plasma samples from preclinical AD (n = 11), mild cognitive impairment-AD (MCI-AD) (n = 31), and healthy (n = 20) participants. Variables were identified by means of two complementary methods, and lipid families' profiles were studied. Then, a targeted analysis was carried out for some identified lipids. Results: Statistically significant differences were obtained for the diglycerol (DG), lysophosphatidylethanolamine (LPE), lysophosphatidylcholine (LPC), monoglyceride (MG), and sphingomyelin (SM) families as well as for monounsaturated (MUFAs) lipids, among the participant groups. In addition, statistically significant differences in the levels of lipid families (ceramides (Cer), LPE, LPC, MG, and SM) were observed between the preclinical AD and healthy groups, while statistically significant differences in the levels of DG, MG, and PE were observed between the MCI-AD and healthy groups. In addition, 18:1 LPE showed statistically significant differences in the targeted analysis between early AD (preclinical and MCI) and healthy participants. Conclusion: The different plasma lipid profiles could be useful in the early and minimally invasive detection of AD. Among the lipid families, relevant results were obtained from DGs, LPEs, LPCs, MGs, and SMs. Specifically, MGs could be potentially useful in AD detection; while LPEs, LPCs, and SM seem to be more related to the preclinical stage, while DGs are more related to the MCI stage. Specifically, 18:1 LPE showed a potential utility as an AD biomarker.

Keywords: Alzheimer's disease; plasma; lipids; diagnosis

Citation: Peña-Bautista, C.; Álvarez-Sánchez, L.; Roca, M.; García-Vallés, L.; Baquero, M.; Cháfer-Pericás, C. Plasma Lipidomics Approach in Early and Specific Alzheimer's Disease Diagnosis. *J. Clin. Med.* **2022**, *11*, 5030. https://doi.org/10.3390/jcm11175030

Academic Editors: Stephen D. Ginsberg and Elliott J. Mufson

Received: 27 June 2022
Accepted: 23 August 2022
Published: 27 August 2022

1. Introduction

Alzheimer's disease (AD) is a complex and multifactorial disease, whose mechanisms of action are currently not fully understood [1]. The most accepted hypotheses describe the accumulation of amyloid-β peptide and phosphorylated Tau (p-Tau) protein in the brain as the cause of the disease [2]. These histological alterations produce neuronal loss, leading to clinical manifestations (memory loss and cognitive decline) [2]. However, when the clinical manifestations are visible, the brain damage is already too great, and current treatments do not show great effectiveness [3]. Currently, the diagnosis of AD is based on cerebrospinal fluid (CSF) biomarkers, neuropsychological evaluations, and neuroimaging [4]. Therefore, there is a need to identify early physiopathological pathways and minimally invasive AD biomarkers.

Lipid metabolism could be related to AD early development since the brain is rich in lipid content, and aging could produce a dysregulation in lipid homeostasis [5]. Therefore, several lipids have been described as potential biomarkers for the disease in different types of biological samples [5]. In fact, the implication of lipids from the cell membrane has

been described in APP processing and in amyloid pathology [6]. Several lipid families, such as sphingomyelins (SM), cholesterol esters (CE), phosphatidylcholines (PC), phosphatidylethanolamines (PE), phosphatidylinositols (PI), ceramides (Cer), and triglycerides (TG), have been related to AD [7,8]. These biomarkers could be useful not only for diagnosis but also for disease progression prediction. In fact, LysoPE (LPE) and PE are useful biomarkers for monitoring the conversion of MCI to AD [9], and plasma sphingomyelins have been related to cognitive decline in probable AD patients [10]. In fact, lipidomic analyses have been carried out in order to study the involvement of lipids in AD pathology and progression [11]. Brain tissue from elderly healthy participants and patients with different stages of AD showed differential expression of lipids such as glycerolipids, glycerophospholipids, and sphingolipids [12]. In addition, this research field focusing on these compounds as potential biomarkers in peripheral biofluids (e.g., plasma and serum) is gaining attention [13–15].

The aim of this work is to evaluate plasma lipid profiles from untargeted and targeted approaches, identifying lipid families and single lipids involved in early AD as potential biomarkers.

2. Material and Methods

2.1. Participants and Sample Collection

The participants were between 50 and 80 years old. They were classified into patients with preclinical AD (n = 12), patients with mild cognitive impairment (MCI) due to AD (MCI-AD, n = 31), and healthy controls (n = 20). The clinical assessment consisted of a neuropsychological evaluation based on the Repeatable Battery for Assessment of Neuropsychological Status Delayed Memory (RBANS.DM) [16], Functionality Assessment Questionnaire (FAQ) [17], Mini-Mental State Examination (MMSE) [18], and Clinical Dementia Rating (CDR) [19]. Moreover, NMR-TAC and cerebrospinal fluid (CSF) (β-amyloid-42 peptide, total Tau, and phosphorylated Tau) analyses were carried out. In this sense, patients with preclinical AD show normal cognitive assessments and positive AD biomarkers (CSF and neuroimaging); patients with MCI-AD show impaired cognitive assessments (cutoff for mild cognitive impairment from the scales mentioned above) and positive AD biomarkers; and control participants do not show cognitive impairment and show negative AD biomarkers. Patients with known major neurological or psychiatric conditions were excluded. Informed consent was obtained from all participants, and the Ethics Committee of the Health Research Institute of La Fe (Valencia, Spain) approved the study protocol (2019/0105).

Blood samples were collected from the participants, centrifuged to separate the plasma fractions, and stored at −80 °C until the analysis.

2.2. Liquid Chromatography and Mass Spectrometry Analysis

2.2.1. Sample Preparation

The plasma sample treatment was previously described by Peña-Bautista et al. [20]. Briefly, 150 µL of cold isopropanol (IPA) was added to 50 µL of plasma, vortexed, and kept at −20 °C for 30 min. Then, it was centrifuged (13,000× g, 10 min, 4 °C), and 90 µL of supernatant was transferred to a 96-well plate. After that, 10 µL of an internal standard (IS) mix solution (17:0 LPC, d18:1/17:0 SM, and 17:0 PE) (100 µg/mL, each compound) was added to each sample. Quality control (QC) was prepared by mixing 10 µL from each plasma sample. A blank was prepared with ultrapure water using the same extraction tube used for blood collection.

2.2.2. Liquid Chromatography

Samples were analyzed by ultra-performance liquid chromatography coupled to time-of-flight mass spectrometry (UPLC-TOF/MS-Orbitrap QExactive Plus MS) following the normalized protocol from the Analytical Unit in Health Research Unit La Fe (Valencia, Spain).

Briefly, the chromatographic conditions consisted of using an Acquity UPLC CSH C18 column (100 × 2.1 mm, 1.7 µm) from Waters. The mobile phase in the positive ionization mode was acetonitrile/water (60:40) with formic acid (10 mM) (A) and isopropyl alcohol/acetonitrile (90:10) with formic acid (10 mM) (B); in the negative ionization mode, it was acetonitrile/water (60:40) with acetic acid (10 mM) (A) and isopropyl alcohol/acetonitrile (90:10) with acetic acid (10 mM) (B). The flow rate was 0.40 mL min^{-1}, the column temperature was 65 °C, and the injection volume was 5 µL.

2.2.3. Untargeted Analysis

In the untargeted analysis, the mass spectrometry conditions consisted of positive and negative ionization, an *m/z* range of 70–1700 Da, a resolution full scan of 70,000, a capillary voltage of 2.5 kV, a sheath gas flow rate of 35, an auxiliary gas flow rate of 15, a sweep gas flow rate of 0, a capillary temperature of 250 °C, an s-lens RF level of 65, and an auxiliary gas heater temperature of 200 °C. Samples were randomly injected in the chromatographic system in order to avoid intrabatch variability. Regarding the QC sample, it was analyzed every seven injections to monitor and correct changes in the instrument response. Moreover, it was repeatedly analyzed under the auto MS/MS and all-ion (MSE) fragmentation modes to provide useful information of fragment ions for identification purposes. The stability of the analytical system during the analysis was investigated through the trends and drifts of IS intensities over the course of the batch analysis. A blank analysis was performed at the end of the sequence and was used to identify artefacts from sampling, the preparation of samples, and analysis.

Then, some variables were annotated, with a mass error <5 ppm, and some of them were selected for a subsequent targeted analysis.

2.2.4. Targeted Analysis

Some of previous variables were selected for a targeted analysis through the analysis of chemical standards, attending to the following criteria. First, lipid families that showed statistically significant differences among the participant groups were selected. Then, individual compounds from these families that showed statistically significant differences between groups were selected. In the case of no commercially available standards, similar lipid compounds from the same family were selected.

The sample treatment and the MS/MS method were developed for the simultaneous targeted analysis of seven lipid compounds (18:1 LPE, 18:0 LPC, 16:1 SM (d18:1/16:1), 16:0 SM (d18:1/16:0), 18:0 SM (d18:1/d18:0), 18:1 (9-Cis) PE (DOPE), and 24:0 SM). In addition, 17:0 LPC, 17:0 SM (d18:1/17:0), and 17:0 PE were used as internal standards. Metabolite concentrations were calculated by an internal calibration using a reaction and multiple monitoring (MRM) method. The employed mass spectrometry conditions consisted of positive ionization, a capillary voltage of 3 kV, a sheath gas flow rate of 35, an auxiliary gas flow rate of 15, a sweep gas flow rate, a capillary temperature of 250 °C, an s-lens RF level, and an auxiliary gas heater temperature of 200 °C. The normalized collision energy was 25 for all compounds. The multiple reaction monitoring (MRM) method parameters are summarized in Table 1.

Analytical Method Validation

The analytical characteristics assayed during the validation procedure were the linearity range, precision, accuracy, limit of detection (LOD), and limit of quantification (LOQ). The accuracy was evaluated by means of the recovery test. For this, standards were spiked at three concentration levels, and they were analyzed in triplicate. The precision was estimated from the analysis of standards and spiked samples at three concentration levels (i.e., low, medium, and high) in triplicate. The LOD and LOQ were established experimentally as the concentrations required to generate signal-to-noise ratios of 3 and 10, respectively.

Table 1. Acquisition parameters for targeted lipid analysis.

Compound	Mass to Charge (*m*/*z*) Precursor Ion	Chemical Formula (M)	Product Ion (*m*/*z*) (Quantitative)	Product Ion (*m*/*z*) (Qualitative)
18:1 LPE	480.30847	C23H46NO7P	308.294	
18:0 LPC	524.37107	C26H54NO7P	184.073	104.107
16:1 SM (d18:1/16:1)	701.5592	C39H77N2O6P	184.073	104.107
16:0 SM (d18:1/16:0)	703.57485	C39H79N2O6P	184.073	104.107
18:0 SM (d18:1/18:0)	731.60615	C41H83N2O6P	184.073	104.107
18:1 (9-Cis) PE (DOPE)	744.55378	C41H78NO8P	308.294	
24:0 SM	815.70005	C47H95N2O6P	184.073	86.0963
17:0 LPC	568.3626	C25H52NO7P	184.073	
17:0 SM (d18:1/17:0)	717.5905	C40H81N2O6P	184.073	
17:0 PE	720.22537	C39H78NO8P	184.073	

LPE: lysophosphatidylethanolamine; LPC: lysophosphatidylcholine; SM: sphingomyelin; PE: phosphatidylethanolamine; DOPE: dioleoyl phosphatidylethanolamine.

2.3. Preprocessing and Data Analysis

The results from the untargeted analytical method were converted to the mzXML file format, and the data were processed (peak detection, noise filtering, and peak alignment) using an *in-house* R processing script based in the LipidMS package published by Alcoriza-Balaguer et al. and developed in the Analytical Unit of the Health Research Institute of La Fe (Valencia) [21]. Then, the obtained dataset was filtered, considering the criteria of the coefficient of variation (CV) <30% in the QC samples, the presence of the feature in 60% of the samples in at least one group, and the blank (water processed as a sample). In fact, a fold-change cutoff (biological sample signal/blank signal < 5) was used to remove features that were not sufficiently abundant in the biological samples. After that, a drift correction from QC-based robust locally weighted scatter plot smoothing (LOESS) for data normalization was performed (excluding potential artefacts). Finally, the obtained normalized dataset was annotated and statistically analyzed.

In order to increase the metabolic coverage, two data analysis strategies were used. The variables were identified by two complementary methods in order to identify more metabolites with different polarity ranges. As a first method, annotation using the LipidMS package and statistical analysis was carried out with the variables. As a second method, annotation by means of the variable accurate mass (AM), using the CEU mass mediator database (including the Kegg, LipidMaps, Metlin, and Human Metabolome databases), a mass range of ±5 ppm, and some adducts ([M+H], [M+Na], [2M+NH4], [M+NH4], and [M+H-2O] for the positive ionization mode and [M-H], [M+HCOOH-H], [2M-H], and [M+Na-2H] for the negative ionization mode), was carried out. In this second approach, the identity of the metabolites was confirmed by comparing the obtained MS/MS fragmentation spectra with those predicted and proposed in the databases. In this sense, four annotation confidence levels were evaluated, as proposed by E. Schymanski et al. (2014) [22]. They were level 1 (identified compounds with structures confirmed by AM, MS/MS spectra, retention time (rt), and reference standards); level 2 (compounds putatively annotated through AM and experimental or predicted MS/MS spectra matched with online libraries); level 3 (compounds putatively characterized by AM matched with online databases); and level 4 (unknown compounds) [23,24].

The results from the targeted analytical method were the signal intensities (arbitrary units) obtained for each lipid compound in plasma samples, and their concentrations were determined from the corresponding calibration curves.

2.4. Statistical Analysis

Participant's characteristics (demographic and clinical) were analyzed using the median and interquartile range (IQR) for continuous variables and relative and absolute frequencies for categorical variables. Differences between participant groups (age controls

and early AD) were evaluated by means of the Mann–Whitney test for numerical variables and the Chi-square test for categorical variables.

The variables identified by the LipidMS package [21] were grouped into lipid families (CE, Cer, diglycerol (DG), fatty acid (FA), lysophosphatidylethanolamine (LPE), lysophosphatidylcholine (LPC), monoglyceride (MG), PC, PE, PI, SM, and TG). In addition, we calculated the variables monounsaturated (MUFAS), polyunsaturated (PUFAS), and saturated (SFAS) as the sum of levels (MUFAS, PUFAS, and SFAS, respectively), including all previous lipid families. Then, a univariate statistical analysis was carried out for each lipid class (the sum of signals from the individual lipids in each family). Specifically, the Kruskal–Wallis and Mann–Whitney tests were used to compare the lipid levels among the participant groups. From these lipid families, some compounds were selected for the targeted analysis. Similarly, the univariate analysis was based on the Kruskal–Wallis and Mann–Whitney tests for quantitative variables and the Chi-square test for categorical variables. Correlation analyses were carried out by Pearson correlation test. Analyses were carried out with the software IBM® SPSS® Statistics version 20.0 (SPSS, Inc., Chicago, IL, USA). Statistically significant differences were considered from p value <0.05 for all analyses.

On the other hand, a multivariate statistical analysis was carried out with the variables detected in the untargeted analysis in order to identify other potential biomarkers (not identified by the LipidMS package). For this, data from the positive and negative ionization modes were considered simultaneously. First, the normalized variables were visualized in a volcano plot carried out using an *in-house* script in R platform. From this, variables with a stronger combination of fold change (FC) (abs (log2 FC) > 1) and statistical significance (p value of t-test < 0.05) in each comparison (MCI-AD vs. control and preclinical AD vs. control) were FDR-adjusted and selected for a supervised orthogonal least squares discriminant analysis (OPLS-DA). The OPLS-DA was carried out using Simca 14.1 software (Sartorius Stedim Biotech, Aubagne, France), and it was validated by a seven cross-validation procedure (CV, dataset split into seven subsets). The corresponding models were evaluated by $R^2(Y)$ (model fit) and $Q^2(Y)$ (predictive ability) diagnostic indexes, the p-value of the CV-ANOVA model, and a permutation test. The most discriminant variables were selected according to their variance importance in projection plot values (VIP > 1.0). Once selected, these features were annotated as potential metabolites by the CEU mass mediator database according to the Schymanski levels of identification [22]. In summary, Figure 1 shows the workflow of these analyses.

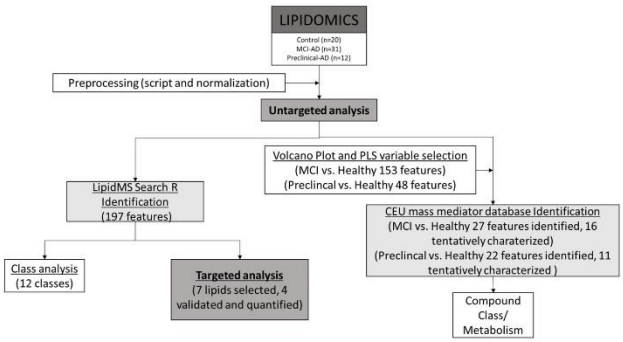

Figure 1. Workflow of the analyses.

3. Results

3.1. Participant Demographic and Clinical Data

In Table 2, the clinical and demographic characteristics of the participants are summarized. As was expected, neuropsychological variables (CDR, RBANS, FAQ, and MMSE) and CSF biomarkers (amyloid β42, t-Tau, and p-Tau) showed statistically significant differences among the participant groups. In addition, age showed statistically significant differences among the groups. In this sense, the correlations between age and all lipids (from the untargeted and targeted analyses) were assessed, without obtaining significant results for any lipids (see Table S1 in the Supplementary Material).

Table 2. Clinical and demographic participant characteristics.

		Healthy (n = 31)	MCI-AD (n = 20)	Preclinical AD (n = 11)	p Value (Kruskal–Wallis)
Median Age (years) (IQR)		62 (58, 68)	72 (69, 74)	70 (60, 74)	0.000
Gender (Female, n (%))		19 (61%)	10 (53%)	6 (50%)	0.737
Educational Level	Primary (n (%))	10 (32%)	7 (39%)	4 (33%)	0.023
	Secondary (n (%))	7 (23%)	10 (56%)	2 (17%)	
	University (n (%))	14 (45%)	2 (18%)	6 (50%)	
Concomitant Medication	Statins (n (%))	9 (41%)	12 (63%)	3 (25%)	0.335
	Fibrates (n (%))	0 (0%)	3 (17%)	1 (8%)	0.143
	Benzodiazepines (n (%))	6 (27%)	3 (16%)	2 (17%)	0.635
	Antidepressants (n (%))	7 (32%)	2 (11%)	0 (0%)	0.085
	Antiepileptics (n (%))	1 (5%)	0 (0%)	0 (0%)	0.547
	Antihypertensives (n (%))	7 (32%)	9 (50%)	2 (29%)	0.424
	Corticoids (n (%))	1 (5%)	0 (0%)	0 (0%)	0.547
	Anti-inflammatories (n (%))	3 (14%)	0 (0%)	0 (0%)	0.151
Comorbidities	Dyslipidemia (n (%))	11 (50%)	11 (58%)	3 (43%)	0.766
	Diabetes (n (%))	3 (14%)	2 (11%)	0 (0%)	0.589
	Hypertension (n (%))	8 (36%)	9 (47%)	2 (29%)	0.628
	Heart Disease (n (%))	1 (5%)	0 (0%)	0 (0%)	0.547
	Cerebrovascular (n (%))	1 (5%)	0 (0%)	0 (0%)	0.547
Smoke (Yes, n (%))		6 (27%)	3 (16%)	1 (14%)	0.598
Alcohol (Yes, n (%))		6 (27%)	2 (11%)	0 (0%)	0.157
Depression (Yes, n (%))		5 (23%)	5 (26%)	2 (29%)	0.939
Anxiety (Yes, n (%))		4 (18%)	3 (16%)	2 (29%)	0.757
Amyloid β42 (pg mL $^{-1}$) Median (IQR)		1224 (964, 1421)	495 (452, 622)	572 (383, 694)	0.000
t-Tau (pg mL^{-1}) Median (IQR)		212 (181, 259)	578 (449, 793)	444 (208, 611)	0.000
p-Tau (pg mL^{-1}) Median (IQR)		34 (25, 39)	91 (62, 109)	74 (28, 94)	0.000
CDR Median (IQR)		0.5 (0, 0.5)	0.5 (0.5, 0.5)	0.5 (0, 0.5)	0.001
MMSE Median (IQR)		29 (28, 29)	24 (22, 25)	29 (27, 30)	0.000
RBANS.DM Median (IQR)		98 (94, 103)	42 (40, 53)	95 (87, 101)	0.000
FAQ Median (IQR)		1 (0, 4)	7 (5, 10)	1 (0, 3)	0.000

IQR: Inter-quartile range; AD: Alzheimer Disease; MCI-AD: mils cognitive impairment due to Alzheimer Disease; CDR: Clinical Dementia Rating; MMSE: Mini-Mental State Examination; FAQ: Functionality Assessment Questionnaire; RBANS: Repeatable Battery for Assessment of Neuropsychological Status; DM: Delayed memory.

3.2. Lipids Identified by LipidMS Package

From the untargeted analysis, 197 features were annotated by the LipidMS package. They were grouped into some lipid families (4 CE, 16 Cer, 2 DG, 20 FA, 3 LPE, 16 LPC, 2 MG, 73 PC, 9 PE, 5 PI, 12 SM, and 35 TG). As can be seen in Figure 2, the main families were PC (37%), TG (18%), and FA (10%). In Table 3, the DG, LPE, LPC, MG, and SM

families and monounsaturated lipids showed statistically significant differences among the three participant groups (preclinical AD, MCI-AD, and healthy). Moreover, the healthy and preclinical AD groups showed statistically significant differences in the levels of the Cer, LPE, LPC, MG, and SM families, while the MCI-AD and healthy groups showed statistically significant differences in the levels of DG, MG, and PE. In addition, Figure 3 shows the boxplots representing the levels of the lipid families in the participant groups (preclinical AD, MCI-AD, and healthy). In general, higher levels were obtained for the preclinical AD group, and lower levels were obtained for the MCI-AD group. A similar tendency was observed for monounsaturated, polyunsaturated, and saturated lipids, although only monounsaturated compounds showed statistically significant differences. In general, a trend was not found for any of the lipid families between the preclinical and MCI groups.

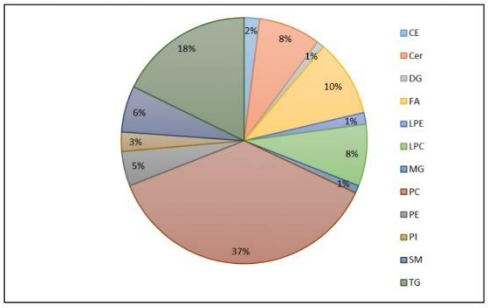

Figure 2. Lipid families identified from untargeted lipidomic analysis and identification by LipidMS package. CE: Cholesterol esters; Cer: Ceramides; DG: Diglycerols; FA: Fatty acids; LPC: Lys phosphatidylcholines; LPE: Lysophosphatidylethanolamines; MG: Monoglycerides; PC: Phosphatidylcholines; PE: Phosphatidylethanolamines; PI: Phosphatidylinositols; SM: Sphingomyelins; TG: Triglycerides.

Table 3. Average sum of the different lipid families' levels in the participant groups (preclinical AD, MCI-AD, and healthy).

Lipid Family	Healthy Controls (HC) (n = 31)	MCI-AD (n = 20)	Preclinical AD (n = 11)	p Value (Kruskal–Wallis)	Healthy vs. Preclinical AD (Mann–Whitney, p Value)	Healthy vs. MCI-AD (Mann–Whitney, p Value)
CE (a.u.)	4.15 (2.86, 4.83)	3.60 (3.03, 5.04)	4.47 (3.86, 4.96)	0.416	0.350	0.685
Cer (a.u.)	4.39 (3.52, 4.39)	3.94 (2.42, 5.75)	5.67 (5.09, 6.87)	0.070	0.038 *	0.452
DG (a.u.)	2.05 (1.56, 2.22)	1.51 (1.25, 1.98)	2.20 (1.94, 2.73)	0.007 *	0.155	0.023 *
FA (a.u.)	15.04 (9.29, 22.21)	13.42 (9.44, 18.38)	22.32 (11.48, 26.24)	0.299	0.201	0.685
LPE (a.u.)	8.68 (7.16, 11.41)	7.61 (4.77, 12.73)	13.86 (10.32, 17.10)	0.006 *	0.002 *	0.418
LPC (a.u.)	18.48 (13.62, 12.39)	15.75 (8.93, 24.98)	27.37 (22.68, 35.24)	0.006 *	0.001 *	0.396
MG (a.u.)	1.48 (1.02, 2.83)	0.81 (0.48, 1.10)	2.52 (1.77, 3.56)	<0.001 *	0.017 *	0.002 *
PC (a.u.)	46.66 (35.34, 56.80)	41.08 (27.78, 55.27)	53.13 (43.75, 59.73)	0.202	0.257	0.316
PE (a.u.)	7.04 (5.09, 8.78)	4.76 (3.05, 9.53)	6.85 (6.13, 10.46)	0.061	0.572	0.034 *
PI (a.u.)	3.50 (2.86, 4.99)	3.08 (2.09, 5.00)	3.77 (2.70, 6.13)	0.366	0.553	0.307
SM (a.u.)	8.63 (6.13, 10.48)	5.79 (3.13, 10.02)	11.21 (9.65, 12.90)	0.001 *	0.003 *	0.061
TG (a.u.)	24.05 (19.40, 28.94)	21.00 (18.36, 29.71)	22.21 (17.83, 27.27)	0.625	0.381	0.537
Monounsaturated (a.u.)	39.78 (31.30, 47.49)	33.35 (22.55, 46.09)	47.79 (45.98, 60.65)	0.011 *	0.009 *	0.232
Polyunsaturated (a.u.)	93.13 (74.29, 113.90)	78.75 (58.62, 106.44)	104.67 (88.91, 111.74)	0.170	0.233	0.307
Saturated (a.u.)	156.73 (132.57, 189.15)	138.36 (99.15, 168.83)	191.35 (155.78, 203.83)	0.100	0.054	0.452

a.u.: arbitrary units. * $p < 0.05$. HC: healthy control.

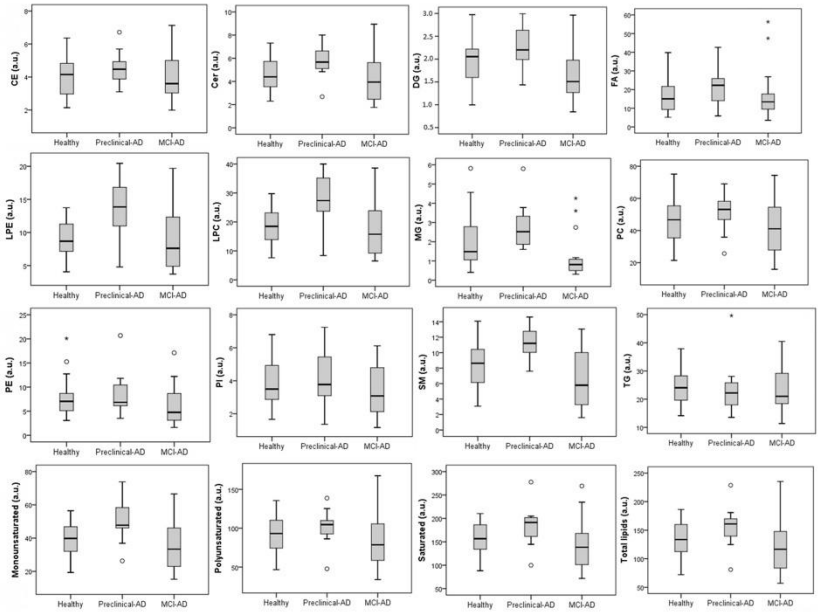

Figure 3. Boxplots representing the levels of lipid families for each participant group (healthy, preclinical AD, and MCI-AD. There were 4 CEs, 4 Cers, 2 DGs, 14 FAs, 3 LPEs, 8 LPCs, 2 MGs, 44 PCs, 7 PEs, 3 PIs, 9 SMs, and 25 TGs included in the analysis (a.u.: arbitrary units)). o: outlayer. *: Extreme outlayer.

3.2.1. Targeted Analysis

From previous results, the selected lipids were 18:1 LPE, 18:0 LPC, 16:1 SM (d18:1/16:1), 16:0 SM (d18:1/16:0), 18:0 SM (d18:1/d18:0), 18:1 (9-Cis) PE (DOPE), and 24:0 SM. The corresponding analytical method was developed and validated, obtaining satisfactory analytical performance for 18:1 LPE, 18:0 LPC, 16:1 SM (d18:1/16:1), and 16:0 SM (d18:1/16:0) (see Table 4). In fact, the accuracy was satisfactory, with recoveries around 100%, except for 18:0 LPC with recoveries >130%, probably due to the matrix effect. Moreover, a suitable sensitivity was obtained, with LODs between 0.548 and 4.185 nmol L^{-1} and LOQs between 1.83 and 13.95 nmol L^{-1}. The other analytes did not show suitable analytical performance (18:0 SM (d18:1/d18:0), 18:1 (9-Cis) PE (DOPE), and 24:0 SM), and they were not determined in plasma samples.

Table 4. Analytical method validation.

Analyte	Standard Concentration (nmol L^{-1})	Recovery (%)	LOD (nmol L^{-1})	LOQ (nmol L^{-1})	Linearity Range (nmol L^{-1})	Equation (y = a + bx) $a \pm s_a$ $b \pm s_b$ R^2
18:1 LPE	6.25	108 ± 14	0.548	1.83	1.83–26.30	0.0019 ± 0.0008
	9.38	109 ± 15				0.0027 ± 0.000063
	12.5	104 ± 17				0.998
18:0 LPC	50	153 ± 15	4.185	13.95	13.95–209.38	0.012 ± 0.024
	75	147 ± 15				0.0072 ± 0.00022
	100	134 ± 21				0.997
16:1 SM (d18:1/16:1)	50	101 ± 11	2.857	9.52	9.52–208.11	0.0774 ± 0.021
	75	101 ± 11				0.0064 ± 0.00019
	100	96 ± 16				0.997
16:0 SM (d18:1/16:0)	12.5	108 ± 58	1.240	4.13	4.13–52.51	−0.0041 ± 0.0063
	18.75	102 ± 6				0.012 ± 0.00024
	25	82 ± 5				0.999
18:0 SM (d18:1/d18:0)	3.13	100 ± 26	0.289	0.96	0.96–13.23	0.0014 ± 0.0011
	4.69					0.0047 ± 0.00017
	6.25	119 ± 59				0.996
18:1 (9-Cis) PE (DOPE)	0.78	103 ± 65	0.069	0.23	0.23–3.30	0.00019 ± 0.00015
	1.17					0.0024 ± 0.000089
	1.56	62 ± 62				0.996
24:0 SM	6.25		0.306	1.02	1.02–26.02	0.24 ± 0.03
	9.38					0.044 ± 0.003
	12.50					0.990

3.2.2. Sample Analysis

A panel of four lipids (previously selected) was determined in plasma samples from healthy participants (n = 20) and patients with preclinical AD (n = 11) and MCI-AD (n = 31). The concentrations of each lipid in the participant groups are summarized in Table 5. As can be seen, statistically significant differences were observed for 18:1 LPE among the three groups (p = 0.010) and between the AD (preclinical + MCI) and healthy groups (p = 0.003). In addition, this potential AD biomarker showed a correlation with some CSF biomarkers (t-Tau (0.299, p = 0.022) and p-Tau (0.290, p = 0.026)). It should be mentioned that no correlation was observed between the lipids levels and age (see Table S1 in the Supplementary Material).

Table 5. Lipid concentrations in plasma from participant groups (healthy, MCI-AD, and preclinical AD).

Lipids	Healthy Control (HC) (n = 31) Median (IQR) (nmol L^{-1})	MCI-AD (n = 20) Median (IQR) (nmol L^{-1})	Preclinical AD (n = 11) Median (IQR) (nmol L^{-1})	Kruskal-Wallis p Value (Three Groups)	Mann–Whitney p Value (AD vs. Non-AD)
18:1 LPE	1.37 (0.38, 1.83)	1.8 (1.2, 4.2)	1.8 (0.9, 3.7)	0.010 *	0.003 *
18:0 LPC	67 (61, 80)	65 (56, 96)	81 (60, 105)	0.504	0.569
16:1 SM	15 (7, 27)	13 (8, 24)	19 (15, 25)	0.501	0.647
16:0 SM	177 (137, 206)	168 (132, 213)	209 (159, 239)	0.374	0.371

* p value < 0.05.

In addition, LPE 18:1 showed an AUC-ROC of 0.722 (95% CI, 0.595–0.848), discriminating between early AD (preclinical + MCI) and healthy participants.

3.3. Compounds Identified by CEU Mass Mediator Database

3.3.1. Preclinical AD vs. Healthy Subjects

The volcano plot analysis from the preclinical AD and healthy groups showed 48 significant variables (Figure 4a). The OPLS-DA analysis was carried out with these

variables in order to identify the most discriminant variables between the groups. This model showed a p value <0.001 and a clear separation between preclinical AD cases and healthy participants (Figure 4b), with good R2Y (0.637) and Q2Y (0.566) parameters. The model was satisfactorily validated (1000 iterations) with R2Y = 0.202 and Q2Y = −0.373.

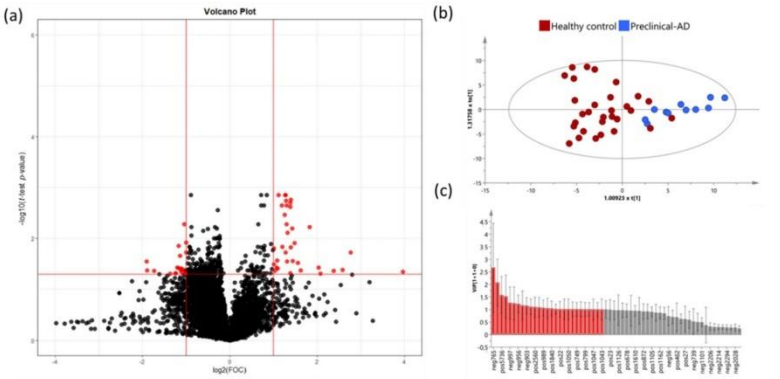

Figure 4. (**a**) Volcano Plot representing the significant variables in the discrimination between healthy controls and preclinical AD participants. Statistically significant variables are represented in red ($p < 0.05$, FC > 2); (**b**) OPLS-DA plot represents differential distribution between healthy controls and preclinical AD; (**c**) Threshold VIP plot value > 1 (red variables).

Potential compounds were subjected to identification and confirmation based on a threshold of VIP value >1 (27 variables) (Figure 4c). Finally, 16 variables were tentatively characterized by querying our experimental MS data with those provided in the commercial databases (see Table S2 in the Supplementary Material). From them, some variables showed more weight over the model (m/z 1484.140079, 508.3767054, 494.3609278, and 770.6063157). In addition, two variables were putatively annotated through AM and MS/MS mass spectra with online databases. These variables were pisumionoside (m/z 405.2102471) and 1-O-Palmitoyl-2-O-acetyl-sn-glycero-3-phosphorylcholine (m/z 520.3404329).

3.3.2. Mild Cognitive Impairment-AD vs. Healthy Controls

The volcano plot analysis from the MCI-AD and healthy groups showed 153 significant variables (Figure 5a). The OPLS-DA analysis was carried out with these variables in order to identify the most discriminant lipids between the groups. This model showed a CV p-value <0.001 and a clear separation between MCI-AD and healthy control participants (Figure 5b), with good R2Y (0.926) and Q2Y (0.785) parameters. The model was satisfactorily validated (1000 iterations) with R2Y = 0.572 and Q2Y = −0.686.

Potential metabolites were subjected to identification and confirmation based on a threshold of VIP value > 1 (22 variables) (Figure 5c). Finally, 11 variables were tentatively characterized by using the corresponding databases (see Table S3 in the Supplementary Material). From them, some variables showed more weight over the model (m/z 409.3113, 362.2550, 350.3417, and 518.351396). In addition, the variable m/z 766.573457 was putatively annotated trough AM and MS/MS mass spectra with online databases, and it was identified as a phosphocholine.

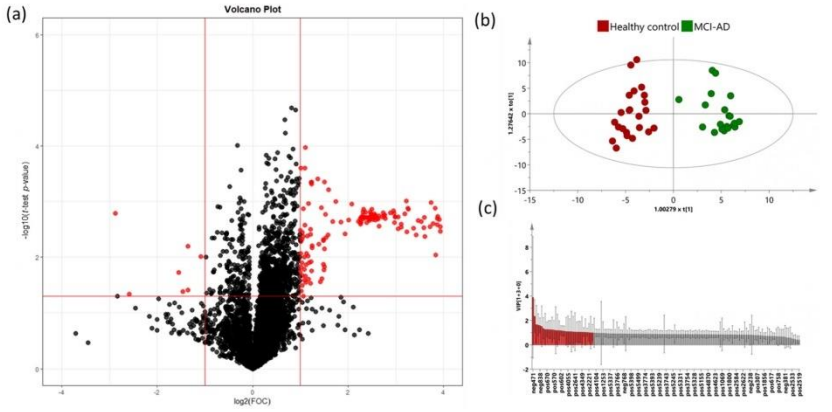

Figure 5. (**a**) Volcano plot representing the significant variables in the discrimination between healthy controls and MCI-AD. Statistically significant variables are represented in red ($p < 0.05$, FC > 2); (**b**) OPLS-DA plot represents differential distribution between healthy controls and MCI-AD. (**c**) Threshold VIP plot value > 1 (red variables).

4. Discussion

A lipidomic approach was developed in plasma samples from participants classified according to their amyloid status (CSF biomarkers) to identify lipid alterations involved in the onset of AD. For this, an untargeted analysis was carried out, and comparisons between early AD (preclinical or MCI) and healthy participants were evaluated. Some significant variables were identified in early AD deregulation, and lipid families were evaluated. Finally, a complementary multivariate analysis was carried out in order to identify other potential discriminative variables.

Lipid families identified by the LipidMS database revealed the potential implication of DG, LPE, LPC, MG, and SM in early AD. In the comparison between preclinical AD and healthy groups, some lipid families were identified as potential biomarkers (Cer, LPEs, LPCs, MGs, and SMs), as they were differentially expressed, especially the monounsaturated species. Similarly, Mielke et al. found an association between Cer and SMs with the risk of AD, although they described differential risks between men and women [25]. In addition, Jazvinšćak Jembrek et al. described the role of ceramides as mediators of neuronal apoptosis related to oxidative stress and Aβ accumulation [26]. Therefore, this deregulation of ceramides in the preclinical stages of the disease could contribute to the advancement of clinical manifestations contributing to neuronal loss. Moreover, Panchal et al. described ceramide accumulation in AD plaques [27]. In addition, SM/ceramide has been related to AD cognitive decline [10]. However, the utility of ceramides as biomarkers for dementias requires further investigation [28]. LPE was described as a biomarker for progression to AD [9], although our results suggest that it could be a potential biomarker for preclinical stages. Similarly, LPCs could be a potential biomarker for the first stages of AD. In this sense, LPCs play a role in polyunsaturated fatty acid (PUFAs) transport across the blood brain barrier, perhaps controlling the availability of these essential compounds for the proper functioning of the brain [29]. In the comparison between MCI-AD and healthy controls, different lipid families were identified as potential biomarkers (DGs, MGs, and PEs). Similarly, Wood et al. found increased levels of DGs and MGs in early AD [30]. PEs

could be involved in the physiopathology of AD due to their involvement in cell processes such as oxidative phosphorylation, mitochondrial biogenesis, and autophagy [31]. Our results show that MGs could be potential biomarkers of early AD, including both the preclinical and MCI-AD stages. In addition, LPE, LPC, and SM seem to be more specifically altered in the preclinical stage, while DGs could be useful as biomarkers for the MCI stage.

On the other hand, the annotation of variables by means of other databases (HMDB, Kegg, and Metlin) reported other important annotated variables and metabolite classes. In the discrimination between preclinical AD and healthy subjects, some lipid families were found, such as phosphatidylglicerol, glicerophosphocholine, glicerophosphoserine, phosphoethanolamine, phosphocholine, glicoesphingolipid, diacilglicerol, terpenes, steroids, flavonoid classes, and vitamin E. Specifically, plasma glycerophosphocholine compounds were observed at higher levels in the preclinical AD group. Similarly, other studies showed elevated levels of this lipid in AD brains [32] as well as in cerebrospinal fluid samples from AD patients [33,34], indicating that abnormal phospholipid metabolism in the brain is characteristic of AD. In addition, the present study found that plasma phosphoethanolamine levels were lower in the preclinical AD group, and a previous work found lower levels for PE in AD brain samples [35]. In fact, PE is a precursor for phosphatidylcholine and a substrate for important posttranslational modifications [31]. Moreover, phosphocholine is a precursor of phosphatidylcholine, and higher levels were obtained for the preclinical AD group, indicating a potential membrane impairment in the early disease process [36]. Moreover, glycosphingolipids could be involved in preclinical AD since higher levels were obtained in plasma samples from these participants. In this regard, ceramides, which are involved in sphingolipid metabolism, showed an association with neuropsychiatric symptoms [37]. Moreover, we found higher levels of DGs in the preclinical AD group, similar to the increased plasma levels in early AD, suggesting that lipidomics alterations lead to the accumulation of DGs in MCI subjects [30]. On the other hand, in the present study, phosphatidylglycerol (PG) and flavonoids showed lower plasma levels in the preclinical AD group. Flavonoid compounds could act against AD pathology by inhibiting microglia activation and Aβ aggregation. Therefore, a reduction in these compounds early in the disease may contribute to the development of AD pathways. However, a search of the literature failed to reveal any studies related to this finding. Studies have been reported that vitamin D showed higher levels in preclinical AD compared to healthy participants, but we found that prior investigations reported reduced levels of these vitamins in AD and MIC-AD cases [38]. Since the cases examined here were classified as preclinical AD, it is possible that this group was exhibiting a compensatory response to the disease process. In addition, the discrimination between preclinical AD and healthy controls is characterized by the biomarkers 1-O-Palmitoyl-2-O-acetyl-sn-glycero-3-phosphorylcholine and pisumionoside, which were putatively annotated. Pisumionoside is an exogenous compound derived from vegetables, such as seedpods of garden peas, that could have a hepatoprotective function [39]. These levels are elevated in healthy subjects compared to preclinical AD subjects. Therefore, pisumionoside could have a protective effect against AD. Moreover, 1-O-Palmitoyl-2-O-acetyl-sn-glycero-3-phosphorylcholine is a glycerophosphorylcholine that showed increased levels in AD, in concordance with previous studies [40]. Its oxidized products were considered biomarkers of neuroinflammation in other pathologies such as multiple sclerosis [41]. Moreover, other lipid families (glycosyldiacylglycerols, fatty acids, terpenoids, sesquiterpene mycotoxins, terpene lactones, phosphocholines, glucosylceramides, and fucopentanoses) were annotated by HMDB comparing MCI-AD and healthy groups. First, glycosyldiacylglycerols showed lower levels in the MCI-AD group. Previous studies found an increase in diacylglycerols in the frontal cortex in neurodegenerative diseases such as dementia with Lewy bodies or AD [42]. In addition, glycosylation showed a relationship with neurodegeneration and AD. Therefore, it could be an indicator of disease progression [43]. Moreover, fatty acids showed lower levels in the MCI-AD group, similar to previous reports [44,45], reflecting differences in intake and metabolism. Moreover, terpenoids and some vitamins showed higher levels in the MCI-AD group. In

this sense, there is some controversy since previous studies showed protective effects for these compounds [46,47].

Regarding the targeted analysis, the developed analytical method was able to determine low plasma levels of some lipids that could be useful as potential AD biomarkers (18:1 LPE, 18:0 LPC, 16:1 SM (d18:1/16:1), and 16:0 SM (d18:1/16:0)). Accuracy was satisfactory for all of them. However, only 18:1 LPE showed statistically significant increased levels in preclinical and MCI-AD in comparison with healthy controls. Su et al. found this lipid increased in brain-derived extracellular vesicles from AD patients [48]. For LPC in plasma samples, a previous study showed an increase with aging, which is more evident under AD conditions [49]. Similarly, the present study found higher levels of LPC 18:1 and lower levels of L-α-phosphatidilcholine and PC in AD patients. However, Mulder et al. found a decrease in the ratio LysoPC/PC under MCI or dementia due to AD conditions [50]. In addition, the present study showed plasma 18:1 LPC correlations with CSF Tau and p-Tau, which are biomarkers currently employed in AD diagnosis. Specifically, Tau is considered a neurodegeneration biomarker [51]. In this sense, the correlation found between 18:1 LPC and Tau showed the potential utility of 18:1 LPC as a neurodegeneration biomarker. Similarly, previous studies showed the utility of the metabolites 18:0 LPC and 18:2 LPC as potential biomarkers for AD [52]. These discrepancies could be explained by the different types of samples used (plasma and CSF) as well as by the different isomers determined in these compounds' families. In addition, the ratio between LPC and PC in the plasma samples showed the capacity to differentiate between AD and non-AD participants [53].

The main limitation of this study is the small sample size. However, the participants were accurately classified into groups according to their amyloid status, cognitive state, and brain alterations with neuroimaging. Moreover, there is a lack of confirmation studies to identify the metabolites as reliable AD biomarkers. Nevertheless, this work provides a detailed lipidomic approach from untargeted and targeted analyses that identified potential biomarkers and pathways involved in early AD development. Although analyses of confounding variables, such as age, were not performed, correlations between age and lipids or lipid class were assessed.

5. Conclusions

A lipidomic approach was developed from untargeted and targeted analyses of plasma samples. It showed some differential expression of lipids between healthy participants and patients at the early stages of AD. Therefore, the plasma lipid profile could be useful in the early and minimally invasive detection of AD. Among lipid families, relevant results were obtained from DGs, LPEs, LPCs, MGs, and SMs. Specifically, MGs could be potentially useful in AD detection, while LPEs, LPCs, and SM are related more specifically to their preclinical stage and DGs are related to the MCI stage. Among these families, 18:1 LPE showed potential utility as a biomarker for AD and neurodegeneration. In addition, other analyte families, such as phosphatidylglicerol, phosphocholine, glicerophosphocholine, glicerophosphoserine, glicoesphingolipid, vitamin E, terpenes, steroids, flavonoids, glycosyldiacylglycerols, fatty acids, glucosylceramides, and fucopentanoses, showed potential alterations in early AD stages. However, further analysis in a large number of samples is required to validate these preliminary results.

Supplementary Materials: The following supporting information can be downloaded at: https://www.mdpi.com/article/10.3390/jcm11175030/s1, Table S1: Correlation analysis between age and lipid class or targeted lipids.; Table S2: Metabolites' annotation from metabolome comparison of preclinical-AD vs. healthy subjects; Table S3: Metabolites' annotation from metabolome comparison of MCI-AD vs. healthy subjects.

Author Contributions: Conceptualization, C.C.-P. and M.B.; methodology, C.P.-B., L.Á.-S. and L.G.-V.; validation, C.P.-B. and M.R.; formal analysis, M.R. and C.C.-P.; data curation, M.R.; writing—original draft preparation, C.P.-B.; writing—review and editing, C.C.-P.; supervision, M.B.; funding acquisition, C.C.-P. All authors have read and agreed to the published version of the manuscript.

Funding: This work was supported by the Instituto de Salud Carlos III Project PI19/00570 (Spanish Ministry of Economy and Competitiveness, cofunded by European Union). CCP acknowledges CPII21/00006. CPB acknowledges PFIS FI20/00022. LAS acknowledges Río Hortega CM20/00140. Part of the equipment used in this work was cofunded by the Generalitat Valenciana and European Regional Development Fund (FEDER) funds (PO FEDER of Comunitat Valenciana 2014–2020).

Institutional Review Board Statement: The study was conducted in accordance with the Declaration of Helsinki, and approved by the Institutional Review Board (or Ethics Committee) of Instituto de Investigación Sanitaria La Fe (protocol code 2019/0105 and date of approval 22 May 2019).

Informed Consent Statement: Informed consent was obtained from all subjects involved in the study.

Data Availability Statement: Data are available in the BioStudies public repository with the accession number S-BSST877.

Acknowledgments: CC-P acknowledges a postdoctoral "Miguel Servet" grant CPII21/00006 and an FIS PI19/00570 grant from the Health Institute Carlos III (Spanish Ministry of Economy, Industry and Innovation). LA-S acknowledges an "RH" grant CM16/00174 from the Health Institute Carlos III. CP-B acknowledges a predoctoral "PFIS" grant FI20/00022 from the Health Institute Carlos III.

Conflicts of Interest: The authors report no conflict of interest.

Abbreviations

AM	Accurate Mass
AD	Alzheimer's Disease
CDR	Clinical Dementia Rating
CE	Cholesterol Esters
Cer	Ceramides
CSF	Cerebrospinal Fluid
DG	Diglycerols
FA	Fatty Acids
FAQ	Functionality Assessment Questionnaire
IPA	Isopropanol
IQR	Interquartile Range
LOD	Limit of Detection
LOQ	Limit of Quantification
LPC	Lysophosphatidylcholines
LPE	Lysophosphatidylethanolamines
MCI	Mild Cognitive Impairment
MG	Monoglycerides
MMSE	Mini-Mental State Examination
OPLS-DA	Orthogonal Partial Least-Squares Discriminant Analysis
PC	Phosphatidylcholines
PE	Phosphatidylethanolamines
PI	Phosphatidylinositols
QC	Quality Control
RBANS	Repeatable Battery for Assessment of Neuropsychological Status Delayed Memory
SM	Sphingomyelins
TG	Triglycerides
TOF-MS	Time-of-Flight Mass Spectrometry
UPLC	Ultra-Performance Liquid Chromatography
VIP	Variance Importance in Projection

References

1. Gong, C.-X.; Liu, F.; Iqbal, K. Multifactorial Hypothesis and Multi-Targets for Alzheimer's Disease. *J. Alzheimer's Dis.* **2018**, *64*, S107–S117. [CrossRef] [PubMed]
2. Bloom, G.S. Amyloid-β and Tau. *JAMA Neurol.* **2014**, *71*, 505. [CrossRef] [PubMed]

3. Pais, M.; Martinez, L.; Ribeiro, O.; Loureiro, J.; Fernandez, R.; Valiengo, L.; Canineu, P.; Stella, F.; Talib, L.; Radanovic, M.; et al. Early Diagnosis and Treatment of Alzheimer's Disease: New Definitions and Challenges. *Braz. J. Psychiatry* **2020**, *42*, 431–441. [CrossRef] [PubMed]
4. Weller, J.; Budson, A. Current Understanding of Alzheimer's Disease Diagnosis and Treatment. *F1000Research* **2018**, *7*, 1161. [CrossRef]
5. Kao, Y.-C.; Ho, P.-C.; Tu, Y.-K.; Jou, I.-M.; Tsai, K.-J. Lipids and Alzheimer's Disease. *Int. J. Mol. Sci.* **2020**, *21*, 1505. [CrossRef]
6. Chew, H.; Solomon, V.A.; Fonteh, A.N. Involvement of Lipids in Alzheimer's Disease Pathology and Potential Therapies. *Front. Physiol.* **2020**, *11*, 598. [CrossRef]
7. Liu, Y.; Thalamuthu, A.; Mather, K.A.; Crawford, J.; Ulanova, M.; Wong, M.W.K.; Pickford, R.; Sachdev, P.S.; Braidy, N. Plasma Lipidome Is Dysregulated in Alzheimer's Disease and Is Associated with Disease Risk Genes. *Transl. Psychiatry* **2021**, *11*, 344. [CrossRef]
8. Zhang, X.; Liu, W.; Zan, J.; Wu, C.; Tan, W. Untargeted Lipidomics Reveals Progression of Early Alzheimer's Disease in APP/PS1 Transgenic Mice. *Sci. Rep.* **2020**, *10*, 14509. [CrossRef]
9. Llano, D.A.; Devanarayan, V. Serum Phosphatidylethanolamine and Lysophosphatidylethanolamine Levels Differentiate Alzheimer's Disease from Controls and Predict Progression from Mild Cognitive Impairment. *J. Alzheimer's Dis.* **2021**, *80*, 311–319. [CrossRef]
10. Mielke, M.M.; Haughey, N.J.; Bandaru, V.V.R.; Weinberg, D.D.; Darby, E.; Zaidi, N.; Pavlik, V.; Doody, R.S.; Lyketsos, C.G. Plasma Sphingomyelins Are Associated with Cognitive Progression in Alzheimer's Disease. *J. Alzheimer's Dis.* **2011**, *27*, 259–269. [CrossRef]
11. Lim, W.L.F.; Martins, I.J.; Martins, R.N. The Involvement of Lipids in Alzheimer's Disease. *J. Genet. Genom.* **2014**, *41*, 261–274. [CrossRef] [PubMed]
12. Akyol, S.; Ugur, Z.; Yilmaz, A.; Ustun, I.; Gorti, S.K.K.; Oh, K.; McGuinness, B.; Passmore, P.; Kehoe, P.G.; Maddens, M.E.; et al. Lipid Profiling of Alzheimer's Disease Brain Highlights Enrichment in Glycerol(Phospho)Lipid, and Sphingolipid Metabolism. *Cells* **2021**, *10*, 2591. [CrossRef] [PubMed]
13. Proitsi, P.; Kim, M.; Whiley, L.; Simmons, A.; Sattlecker, M.; Velayudhan, L.; Lupton, M.K.; Soininen, H.; Kloszewska, I.; Mecocci, P.; et al. Association of Blood Lipids with Alzheimer's Disease: A Comprehensive Lipidomics Analysis. *Alzheimer's Dement.* **2017**, *13*, 140–151. [CrossRef] [PubMed]
14. Zhang, L.; Li, L.; Meng, F.; Yu, J.; He, F.; Lin, Y.; Su, Y.; Hu, M.; Liu, X.; Liu, Y.; et al. Serum Metabolites Differentiate Amnestic Mild Cognitive Impairment From Healthy Controls and Predict Early Alzheimer's Disease via Untargeted Lipidomics Analysis. *Front. Neurol.* **2021**, *12*, 1305. [CrossRef]
15. Fote, G.; Wu, J.; Mapstone, M.; Macciardi, F.; Fiandaca, M.S.; Federoff, H.J. Plasma Sphingomyelins in Late-Onset Alzheimer's Disease. *J. Alzheimer's Dis.* **2021**, *83*, 1161–1171. [CrossRef]
16. Randolph, C.; Tierney, M.C.; Mohr, E.; Chase, T.N. The Repeatable Battery for the Assessment of Neuropsychological Status (RBANS): Preliminary Clinical Validity. *J. Clin. Exp. Neuropsychol.* **1998**, *20*, 310–319. [CrossRef]
17. Pfeffer, R.I.; Kurosaki, T.T.; Harrah, C.H.; Chance, J.M.; Filos, S. Measurement of Functional Activities in Older Adults in the Community. *J. Gerontol.* **1982**, *37*, 323–329. [CrossRef]
18. Folstein, M.F.; Folstein, S.E.; McHugh, P.R. Mini-Mental State. *J. Psychiatric Res.* **1975**, *12*, 189–198. [CrossRef]
19. Hughes, C.P.; Berg, L.; Danziger, W.; Coben, L.A.; Martin, R.L. A New Clinical Scale for the Staging of Dementia. *Br. J. Psychiatry* **1982**, *140*, 566–572. [CrossRef]
20. Peña-Bautista, C.; Roca, M.; Hervás, D.; Cuevas, A.; López-Cuevas, R.; Vento, M.; Baquero, M.; García-Blanco, A.; Cháfer-Pericás, C. Plasma Metabolomics in Early Alzheimer's Disease Patients Diagnosed with Amyloid Biomarker. *J. Proteom.* **2019**, *200*, 144–152. [CrossRef]
21. Alcoriza-Balaguer, M.I.; García-Cañaveras, J.C.; López, A.; Conde, I.; Juan, O.; Carretero, J.; Lahoz, A. LipidMS: An R Package for Lipid Annotation in Untargeted Liquid Chromatography-Data Independent Acquisition-Mass Spectrometry Lipidomics. *Anal. Chem.* **2019**, *91*, 836–845. [CrossRef] [PubMed]
22. Schymanski, E.L.; Jeon, J.; Gulde, R.; Fenner, K.; Ruff, M.; Singer, H.P.; Hollender, J. Identifying Small Molecules via High Resolution Mass Spectrometry: Communicating Confidence. *Environ. Sci. Technol.* **2014**, *48*, 2097–2098. [CrossRef] [PubMed]
23. Misra, B.B. New Tools and Resources in Metabolomics: 2016–2017. *Electrophoresis* **2018**, *39*, 909–923. [CrossRef] [PubMed]
24. Viant, M.R.; Kurland, I.J.; Jones, M.R.; Dunn, W.B. How Close Are We to Complete Annotation of Metabolomes? *Curr. Opin. Chem. Biol.* **2017**, *36*, 64–69. [CrossRef]
25. Mielke, M.M.; Haughey, N.J.; Han, D.; An, Y.; Bandaru, V.V.R.; Lyketsos, C.G.; Ferrucci, L.; Resnick, S.M. The Association Between Plasma Ceramides and Sphingomyelins and Risk of Alzheimer's Disease Differs by Sex and APOE in the Baltimore Longitudinal Study of Aging. *J. Alzheimer's Dis.* **2017**, *60*, 819–828. [CrossRef]
26. Jazvinščak Jembrek, M.; Hof, P.R.; Šimić, G. Ceramides in Alzheimer's Disease: Key Mediators of Neuronal Apoptosis Induced by Oxidative Stress and A β Accumulation. *Oxidative Med. Cell. Longev.* **2015**, *2015*, 346783. [CrossRef]
27. Panchal, M.; Gaudin, M.; Lazar, A.N.; Salvati, E.; Rivals, I.; Ayciriex, S.; Dauphinot, L.; Dargère, D.; Auzeil, N.; Masserini, M.; et al. Ceramides and Sphingomyelinases in Senile Plaques. *Neurobiol. Dis.* **2014**, *65*, 193–201. [CrossRef]
28. Loft, L.M.I.; Mosholm, K.F.; Pedersen, K.K.W.; Jensen, M.K.; Koch, M.; Cronjé, H.T. Sphingomyelins and Ceramides: Possible Biomarkers for Dementia? *Curr. Opin. Lipidol.* **2022**, *33*, 57–67. [CrossRef]

29. Semba, R.D. Perspective: The Potential Role of Circulating Lysophosphatidylcholine in Neuroprotection against Alzheimer Disease. *Adv. Nutr.* **2020**, *11*, 760–772. [CrossRef]
30. Wood, P.L.; Medicherla, S.; Sheikh, N.; Terry, B.; Phillipps, A.; Kaye, J.A.; Quinn, J.F.; Woltjer, R.L. Targeted Lipidomics of Fontal Cortex and Plasma Diacylglycerols (DAG) in Mild Cognitive Impairment and Alzheimer's Disease: Validation of DAG Accumulation Early in the Pathophysiology of Alzheimer's Disease. *J. Alzheimer's Dis.* **2015**, *48*, 537–546. [CrossRef]
31. Calzada, E.; Onguka, O.; Claypool, S.M. Phosphatidylethanolamine Metabolism in Health and Disease. *Int. Rev. Cell. Mol. Biol.* **2016**, *321*, 29–88. [CrossRef] [PubMed]
32. Blusztajn, J.K.; Gonzalez-Coviella, I.L.; Logue, M.; Growdon, J.H.; Wurtman, R.J. Levels of Phospholipid Catabolic Intermediates, Glycerophosphocholine and Glycerophosphoethanolamine, Are Elevated in Brains of Alzheimer's Disease but Not of Down's Syndrome Patients. *Brain Res.* **1990**, *536*, 240–244. [CrossRef]
33. Walter, A.; Korth, U.; Hilgert, M.; Hartmann, J.; Weichel, O.; Hilgert, M.; Fassbender, K.; Schmitt, A.; Klein, J. Glycerophosphocholine Is Elevated in Cerebrospinal Fluid of Alzheimer Patients. *Neurobiol. Aging* **2004**, *25*, 1299–1303. [CrossRef] [PubMed]
34. Fonteh, A.N.; Chiang, J.; Cipolla, M.; Hale, J.; Diallo, F.; Chirino, A.; Arakaki, X.; Harrington, M.G. Alterations in Cerebrospinal Fluid Glycerophospholipids and Phospholipase A2 Activity in Alzheimer's Disease. *J. Lipid Res.* **2013**, *54*, 2884–2897. [CrossRef] [PubMed]
35. Ellison, D.W.; Beal, M.F.; Martin, J.B. Phosphoethanolamine and Ethanolamine Are Decreased in Alzheimer's Disease and Huntington's Disease. *Brain Res.* **1987**, *417*, 389–392. [CrossRef]
36. Farber, S.A.; Slack, B.E.; Blusztajn, J.K. Role of Single-stranded DNA Regions and Y-box Proteins in Transcriptional Regulation of Viral and Cellular Genes. *FASEB J.* **2000**, *14*, 2198–2206. [CrossRef]
37. Xing, Y.; Tang, Y.; Zhao, L.; Wang, Q.; Qin, W.; Zhang, J.-L.; Jia, J. Plasma Ceramides and Neuropsychiatric Symptoms of Alzheimer's Disease. *J. Alzheimer's Dis.* **2016**, *52*, 1029–1035. [CrossRef]
38. Mavraki, E.; Ioannidis, P.; Tripsianis, G.; Gioka, T.; Kolousi, M.; Vadikolias, K. Vitamin D in Mild Cognitive Impairment and Alzheimer's Disease. A Study in Older Greek Adults. *Hippokratia* **2020**, *24*, 120–126.
39. Murakami, T.; Kohno, K.; Ninomiya, K.; Matsuda, H.; Yoshikawa, M. Medicinal Foodstuffs. XXV. Hepatoprotective Principle and Structures of Ionone Glucoside, Phenethyl Glycoside, and Flavonol Oligoglycosides from Young Seedpods of Garden Peas, *Pisum sativum* L. *Chem. Pharm. Bull.* **2001**, *49*, 1003–1008. [CrossRef]
40. Ademowo, O.S.; Dias, H.K.I.; Milic, I.; Devitt, A.; Moran, R.; Mulcahy, R.; Howard, A.N.; Nolan, J.M.; Griffiths, H.R. Phospholipid Oxidation and Carotenoid Supplementation in Alzheimer's Disease Patients. *Free Radic. Biol. Med.* **2017**, *108*, 77–85. [CrossRef]
41. Qin, J.; Goswami, R.; Balabanov, R.; Dawson, G. Oxidized Phosphatidylcholine Is a Marker for Neuroinflammation in Multiple Sclerosis Brain. *J. Neurosci. Res.* **2007**, *85*, 977–984. [CrossRef] [PubMed]
42. Wood, P.L.; Tippireddy, S.; Feriante, J.; Woltjer, R.L. Augmented Frontal Cortex Diacylglycerol Levels in Parkinson's Disease and Lewy Body Disease. *PLoS ONE* **2018**, *13*, e0191815. [CrossRef]
43. Haukedal, H.; Freude, K.K. Implications of Glycosylation in Alzheimer's Disease. *Front. Neurosci.* **2021**, *14*, 625348. [CrossRef] [PubMed]
44. Cunnane, S.C.; Schneider, J.A.; Tangney, C.; Tremblay-Mercier, J.; Fortier, M.; Bennett, D.A.; Morris, M.C. Plasma and Brain Fatty Acid Profiles in Mild Cognitive Impairment and Alzheimer's Disease. *J. Alzheimer's Dis.* **2012**, *29*, 691–697. [CrossRef]
45. Marizzoni, M.; Cattaneo, A.; Mirabelli, P.; Festari, C.; Lopizzo, N.; Nicolosi, V.; Mombelli, E.; Mazzelli, M.; Luongo, D.; Naviglio, D.; et al. Short-Chain Fatty Acids and Lipopolysaccharide as Mediators Between Gut Dysbiosis and Amyloid Pathology in Alzheimer's Disease. *J. Alzheimer's Dis.* **2020**, *78*, 683–697. [CrossRef]
46. Fanaee-Danesh, E.; Gali, C.C.; Tadic, J.; Zandl-Lang, M.; Carmen Kober, A.; Agujetas, V.R.; de Dios, C.; Tam-Amersdorfer, C.; Stracke, A.; Albrecher, N.M.; et al. Astaxanthin Exerts Protective Effects Similar to Bexarotene in Alzheimer's Disease by Modulating Amyloid-Beta and Cholesterol Homeostasis in Blood-Brain Barrier Endothelial Cells. *Biochim. Biophys. Acta (BBA)—Mol. Basis Dis.* **2019**, *1865*, 2224–2245. [CrossRef]
47. Grimm, M.; Mett, J.; Hartmann, T. The Impact of Vitamin E and Other Fat-Soluble Vitamins on Alzheimer´s Disease. *Int. J. Mol. Sci.* **2016**, *17*, 1785. [CrossRef]
48. Su, H.; Rustam, Y.H.; Masters, C.L.; Makalic, E.; McLean, C.A.; Hill, A.F.; Barnham, K.J.; Reid, G.E.; Vella, L.J. Characterization of Brain-derived Extracellular Vesicle Lipids in Alzheimer's Disease. *J. Extracell. Vesicles* **2021**, *10*, e12089. [CrossRef]
49. Dorninger, F.; Moser, A.B.; Kou, J.; Wiesinger, C.; Forss-Petter, S.; Gleiss, A.; Hinterberger, M.; Jungwirth, S.; Fischer, P.; Berger, J. Alterations in the Plasma Levels of Specific Choline Phospholipids in Alzheimer's Disease Mimic Accelerated Aging. *J. Alzheimer's Dis.* **2018**, *62*, 841–854. [CrossRef]
50. Mulder, C.; Wahlund, L.-O.; Teerlink, T.; Blomberg, M.; Veerhuis, R.; van Kamp, G.J.; Scheltens, P.; Scheffer, P.G. Decreased Lysophosphatidylcholine/Phosphatidylcholine Ratio in Cerebrospinal Fluid in Alzheimer?S Disease. *J. Neural Transm.* **2003**, *110*, 949–955. [CrossRef]
51. Jack, C.R.; Bennett, D.A.; Blennow, K.; Carrillo, M.C.; Feldman, H.H.; Frisoni, G.B.; Hampel, H.; Jagust, W.J.; Johnson, K.A.; Knopman, D.S.; et al. A/T/N: An Unbiased Descriptive Classification Scheme for Alzheimer Disease Biomarkers. *Neurology* **2016**, *87*, 539–547. [CrossRef] [PubMed]

52. Cui, Y.; Liu, X.; Wang, M.; Liu, L.; Sun, X.; Ma, L.; Xie, W.; Wang, C.; Tang, S.; Wang, D.; et al. Lysophosphatidylcholine and Amide as Metabolites for Detecting Alzheimer Disease Using Ultrahigh-Performance Liquid Chromatography–Quadrupole Time-of-Flight Mass Spectrometry–Based Metabonomics. *J. Neuropathol. Exp. Neurol.* **2014**, *73*, 954–963. [CrossRef] [PubMed]
53. Klavins, K.; Koal, T.; Dallmann, G.; Marksteiner, J.; Kemmler, G.; Humpel, C. The Ratio of Phosphatidylcholines to Lysophosphatidylcholines in Plasma Differentiates Healthy Controls from Patients with Alzheimer's Disease and Mild Cognitive Impairment. *Alzheimer's Dement. Diagn. Assess. Dis. Monit.* **2015**, *1*, 295–302. [CrossRef] [PubMed]

www.nature.com/scientificreports

scientific reports

Check for updates

OPEN

Plasma microRNAs as potential biomarkers in early Alzheimer disease expression

Carmen Peña-Bautista[1], Adrián Tarazona-Sánchez[1], Aitana Braza-Boils[2], Angel Balaguer[1], Laura Ferré-González[1], Antonio J. Cañada-Martínez[1], Miguel Baquero[1,3] & Consuelo Cháfer-Pericás[1]✉

The microRNAs (miRNAs) are potential biomarkers for complex pathologies due to their involvement in the regulation of several pathways. Alzheimer Disease (AD) requires new biomarkers in minimally invasive samples that allow an early diagnosis. The aim of this work is to study miRNAS as potential AD biomarkers and their role in the pathology development. In this study, participants (n = 46) were classified into mild cognitive impairment due to AD (MCI-AD, n = 19), preclinical AD (n = 8) and healthy elderly controls (n = 19), according to CSF biomarkers levels (amyloid β42, total tau, phosphorylated tau) and neuropsychological assessment. Then, plasma miRNAomic expression profiles were analysed by Next Generation Sequencing. Finally, the selected miRNAs were validated by quantitative PCR (q-PCR). A panel of 11 miRNAs was selected from omics expression analysis, and 8 of them were validated by q-PCR. Individually, they did not show statistically significant differences among participant groups. However, a multivariate model including these 8 miRNAs revealed a potential association with AD for three of them. Specifically, relatively lower expression levels of miR-92a-3p and miR-486-5p are observed in AD patients, and relatively higher levels of miR-29a-3p are observed in AD patients. These biomarkers could be involved in the regulation of pathways such as synaptic transmission, structural functions, cell signalling and metabolism or transcription regulation. Some plasma miRNAs (miRNA-92a-3p, miRNA-486-5p, miRNA-29a-3p) are slightly dysregulated in AD, being potential biomarkers of the pathology. However, more studies with a large sample size should be carried out to verify these results, as well as to further investigate the mechanisms of action of these miRNAs.

MicroRNAs (miRNAs) have been postulated in recent years as good biomarkers for the diagnosis, prognosis and therapies of different pathologies[1]. They are non-coding 19–25 nucleotides RNA molecules, which are involved in the regulation of gene expression[2].

Alzheimer's disease (AD) is the most common dementia in developed countries, being one of the leading causes of death, disability and dependency in older populations[3]. However, despite the efforts and economic investments made in research into this pathology, it is a complex pathology in which several factors are involved and whose mechanisms are not fully understood[4]. Specifically, the most consolidated mechanisms are those involved in the accumulation of amyloid-β42 peptide and phosphorylated Tau (p-Tau) in brain[5]. Nevertheless, other mechanisms such as oxidative stress, neuroinflammation or lipid metabolism could contribute to the pathology[5–8]. Nowadays, the diagnosis of AD is complex and relies on cerebrospinal fluid (CSF) biomarkers (amyloid-β42, t-Tau, p-Tau) levels, neuroimaging (NMR, PET), and neuropsychological assessment[9–12]. Thus, further research focused on minimally invasive biomarkers is required[13].

Regarding physiopathological mechanisms involved in AD development, miRNAs have been postulated as mediators. Each miRNA could be involved in different pathways as it can have different target genes. In fact, a miRNA could recognize a regulatory region in different genes, regulating, activating or inactivating their expression. Specifically, some miRNAs have been related to the regulation of amyloid protein precursor (APP) cleavage, presenilin-1 (PSEN1) and beta-site amyloid precursor protein cleaving enzyme 1 (BACE1), as well as in oxidative stress and other AD risk factors[14]. In addition, differential expression of miRNAs in AD could be useful in the

[1]Alzheimer Disease Research Group, Instituto de Investigación Sanitaria La Fe, Avda de Fernando Abril Martorell, 106, 46026 Valencia, Spain. [2]Inherited Cardiomyopathies and Sudden Death Unit, Instituto de Investigación Sanitaria La Fe, Valencia, Spain. [3]Neurology Unit, Hospital Universitario y Politécnico La Fe, Valencia, Spain. ✉email: m.consuelo.chafer@uv.es

diagnosis of the pathology, and some miRNAs have been described as potential biomarkers for AD diagnosis and prognosis[15]. Some miRNAs showed good performance as biomarkers, mainly panels including different miRNAs might be dysregulated several years before the onset of disease symptoms[16]. Several panels were developed from plasma, serum or exosomes, showing their potential for a minimally invasive disease diagnosis[17–19]. In general, different results have been found in the literature, probably due to the lack of diagnostic biomarkers used in the classification of participants or due to the differential methodologies applied in sequencing or data processing.

The aim of this work is to analyse the differential expression of a panel of miRNAs selected from sequencing analysis in plasma from AD and non-AD patients, evaluating their potential usefulness as biomarkers or in the development of therapeutic targets, as well as to study their potential implications in the course of the AD.

Material And Methods

Participants and samples collection. In this study, participants (n = 46) were aged between 50 and 80 years old and were classified into mild cognitive impairment due to AD (MCI-AD, n = 19), preclinical-AD (n = 8) and healthy controls (n = 19), according to the National Institute on Aging and Alzheimer's Association (NIA-AA) criteria. Briefly, the control group showed negative CSF biomarkers or amyloid PET, and normal neuropsychological assessment; the MCI-AD group showed positive CSF biomarkers or amyloid PET, and impaired neuropsychological assessment; the preclinical-AD group showed positive CSF biomarkers or amyloid PET, and normal neuropsychological assessment. Participants with other major disorders and those unable to complete the assessment were excluded. All participants were recruited at the Neurology Unit of the University and Polytechnic Hospital La Fe (Valencia, Spain) after signing informed consent, and plasma samples were obtained at the same time the lumbar puncture. The study protocol (2019/0105) was approved by the Ethics Committee (CEIC) of the Instituto de Investigación Sanitaria La Fe (Valencia, Spain). No randomisation was performed to allocate subjects in the study. No pre-registration was performed. The study is blinded as the classification of participants was performed by a person other than the experimenter. No sample calculation was performed. All methods were carried out in accordance with relevant guidelines and regulations.

RNA extraction. RNA was isolated for RNA sequencing using the miRNeasy plasma kit (Qiagen, Germany) following the manufacturer's protocol. Briefly, 200 µL of plasma and 700 µL of QIAzol lysis reagent were incubated for 5 min at room temperature (RT). Then, 140 µL of chloroform were added and incubated at RT for 3 min and centrifuged at 1200 g (15 min, 4 °C). The aqueous phase was mixed in a new tube with 525 µL of ethanol and transferred to a RNeasy MinElute spin column followed by a centrifugation step at 10000 g (30 s, RT). The column was then washed with RWT buffer (700 µL) and RPE buffer (500 µL) and dried for 90 s at 10000 g. Finally, the elution step was performed with 15 µL of RNase-free water (13000 g, 1 min).

For PCR validation, RNA extraction was carried out in a similar way but including a previous step, which consisted on the addition of RNS spike-in before the protocol.

RNA sequencing method. *Construction of RNA libraries.* The miRNA libraries were prepared from total RNA using the NEXTFLEX® Small RNA-Seq v3 Kit for Illumina Platforms (Bioo Scientific Corporation, Texas, USA). Briefly, the small RNA molecules were first ligated to the 3'-4 N adenylated adapters, taking advantage of the phosphate group at their terminal end, which allows the exclusive targeting of these molecules. Secondly, the 5'-4 N adapters were ligated. Later, reverse transcription of the molecule into cDNA was carried out. The generated cDNA fragments were then amplified and indexed by PCR using different barcode primers for each sample. Finally, a size-selective purification was carried out.

The quality control and concentration of the libraries were verified with the Agilent Technologies 2100 bioanalyser using highly sensitivity DNA chips (Central Unit for Research in Medicine (Universitat de València)). Subsequently, an equimolecular pool of each library was prepared for sequencing.

Sequencing on an Illumina equipment. Sequencing was carried out on the NGS NextSeq 550 platform (Illumina, San Diego, CA, USA) by single read sequencing of 50 cycles (1 × 50 bp).

Data analysis. *Pre-processing, quality control and normalization.* NGS data (raw fastq files from sRNA sequencing) were processed following the standard protocol proposed by Cordero et al.[20] implemented in the function mirnaCounts from docker4seq package[21] with default parameters in R[22]. First, a sequence quality control check was generated using FastQC[23] and then cutadapt[24] program was used for the adapter trimming. Specifically, adapters and low-quality reads (Phred Score < 10) were trimmed and removed (44.014.980 reads). Once adapters were removed, sequence reads (219.207.246 good quality reads) were mapped against miRNA precursors from miRBase (v.21)[25], using SHRIMP[26,27], filtering out a total of 95,03% reads. Finally, miRNA quantification from the resulting 4,97% of mapped reads were generated using the function count Overleaps from GenomicRanges package[28], resulting in a total of 9.799.858 miRNA counts in a total of 2.386 miRNAs.

miRNAs selection. From the miRNAs identified in the pre-processing, quality control and normalization process, some of them were selected. Specifically, those miRNAs which showed a number of counts different from zero in at least 80% of the samples and that were corroborated in literature. Finally, the selected miRNAs were validated by means of qPCR in the same plasma samples.

miRNAs validation by quantitative PCR. *Quantitative PCR procedure.* From the extracted RNA, retrotranscription and amplification steps were carried out following the manufacturer's recommendation

('TaqMan Advanced miRNA Assays) [https://tools.thermofisher.com/content/sfs/manuals/100027897_TaqManAdv_miRNA_Assays_UG.pdf]. Briefly, the protocol consisted of four steps. First, the addition of a polyA tail, after the adapter ligation, followed by the retrotranscription step, and then the specific miRNA amplification. Finally, samples were diluted, and real time PCR (RT-PCR) was carried out in duplicate using the thermocycler (ViiA7, Applied Biosystems, California, USA).

Statistical analysis. The number of counts obtained from RT-PCR were averaged for duplicates, discarding replicates with values within ±2 counts from mean. Then, samples were normalized using the mean and standard deviation. The miRNAs detected in at least 80% of the samples and with a difference between replicates < 1 count were considered satisfactorily quantified. The effect of each biomarker on pathology was then analyzed by Bayesian models: the first model discriminates among control, MCI-AD and preclinical AD groups; and the second model discriminates between AD (preclinical AD, MCI-AD) and control groups. For these models, some parameters were calculated (estimate, which indicates the direction of the miRNAs levels; Odds Ratio; Percentage Inside Rope, which defines the percentage of the area that is within the region of practical equivalence (equivalent to null effect); probability of direction (PD), which indicates the probability that the effect has in a particular direction (indicated by the estimate). PD > 80% was considered significative).

Pathway analysis. The target genes of the differentially expressed miRNAs were studied using the miR data base (miRDB). The selected target genes were those with a target score ≥95. Then, the targets were classified according to cellular pathways and functions in order to analyze the implication in AD.

Ethics approval. The study protocol (2019/0105) was approved by the Ethics Committee (CEIC) from Health Research Institute La Fe (Valencia, Spain).

Consent to participate. Informed consent was obtained from all individual participants included in the study.

Research involving Human Participants and/or Animals. Yes, human participants.

Informed consent. All the participants were recruited in the Neurology Unit from University and Polytechnic Hospital La Fe (Valencia, Spain) after signing the informed consent.

Results

Participants characteristics. The participants' characteristics are summarized in Table 1. As can be seen, most of the variables showed no significant differences among participants' groups. In fact, only the clinical variables used in their diagnosis (CSF biomarkers levels, neuropsychological assessment) show statistically significant differences, as expected. In contrast, demographic variables (age, sex, educational level, medication use (statins, fibrates, benzodiazepines, antihypertensives), comorbidities (dyslipidemia, diabetes, hypertension)) are similar between the study groups.

miRNAs validation. A panel of 11miRNAs was selected following the specified criteria (counts in at least 80% of the samples and previous findings in literature). The selected miRNAs were hsa-miR-92a-3p, hsa-miR-486-5p, hsa-miR-29a-3p, hsa-miR-486-3p, hsa-miR-150-5p, hsa-miR-142-5p, hsa-miR-320b, hsa-miR-483-3p, hsa-miR-1293, hsa-miR-342-3p, and hsa-miR-4259. Of these, 8 miRNAs were successfully quantified (has-miR-92a-3p, has-miR-486-5p, has-miR-29a-3p, miR-486-3p, miR-150-5p, miR-320b, miR-483-3p, miR-342-3p); while some miRNAs were not detected (hsa-miR-142-5p, miR-1293, hsa-miR-4259). The levels obtained for each miRNA are summarised in Table 2. As can be seen, small differences were obtained for each miRNA among participants' groups.

Individually, the validated miRNAs showed no significant differences between groups. Therefore, two multivariate models, including the previously selected miRNAs, were developed to analyse the tendency of each miRNA in participants' groups. The first model included 3 participant groups (control, MCI-AD, preclinical AD); while the second model included 2 participant groups (AD (MCI-AD + preclinical-AD), control). In Table 3, the characteristics of the first model are summarised, showing that the miRNAS hsa-miR-92a-3p, hsa-miR-486-5p and hsa-miR-29a-3p had a high probability of direction (PD > 80%). Specifically, hsa-miR-92a-3p showed a PD 85.40% of a negative estimate, so relatively reduced levels were found in AD. Similar results were obtained for hsa-miR-486-5p. In fact, it showed a high probability of a negative estimate with small Region of Practical Equivalence (ROPE) (< 15%), which defines the percentage of the area that is within the region of practical equivalence (equivalent to null effect)), showing an Odds Ratio (OR) lower than 1, and suggesting a protective effect for AD. By contrast, hsa-miR-29a-3p showed a positive estimate, so relatively increased levels were found in AD. Similarly, the characteristics of the model including 2 participants' groups (AD, control), showed that the miRNAS hsa-miR-92a-3p and hsa-miR-29a-3p had a PD > 90%, with negative and positive estimates, respectively.

These results are shown in Fig. 1, which depicts the PD and ROPE for each miRNA. The miRNAs with a high PD (mir-92a-3p, miR-486-5p, miR-29a-3p), showed most of their area on one side of 0 (Fig. 1a). In addition, mir-92a-3p and miR-486-5p showed a negative direction, while miR-29a-3p showed a positive direction. Figure 1b shows the ROPE region, being a small area in the first three miRNAs.

Variable	Control (n = 19)	MCI-AD (n = 19)	Preclinical-AD (n = 8)	*P* value
	Median (1st, 3rd Q.)			
Age (years)	69 (64.5, 70.5)	70 (67.5, 74)	68.5 (66.7, 70.5)	0.134
Sex, female, n (%)	8 (42.11%)	8 (42.11%)	5 (62.5%)	0.575
Educational level (n, %)				
Basic or primary	6 (31.58%)	7 (38.89%)	1 (12.5%)	0.094
Secondary	6 (31.58%)	10 (55.56%)	3 (37.5%)	
Uiversitary	7 (36.84%)	1 (5.56%)	4 (50%)	
Smoking Yes, n, (%)	3 (15.79%)	3 (15.79%)	2 (25%)	0.823
Alcohol Yes, n (%)	4 (21.05%)	2 (10.53%)	1 (12.5%)	0.647
Statins (n, %)	11 (57.89%)	10 (52.63%)	3 (37.5%)	0.625
Fibrates (n, %)	2 (10.53%)	2 (11.11%)	1 (14.29%)	0.690
Benzodiazepines (n, %)	3 (15.79%)	2 (10.53%)	1 (12.5%)	0.889
Antihipertensives (n, %)	8 (42.11%)	7 (38.89%)	1 (12.5%)	0.317
Dyslipidemia (n, %)	13 (68.42%)	10 (52.63%)	3 (37.5%)	0.303
Diabetes (n, %)	3 (15.79%)	1 (5.26%)	3 (37.5%)	0.103
Hypertenison (n, %)	9 (47.37%)	8 (42.11%)	1 (12.5%)	0.224
Amyloid-β42 (pg mol-1)	1224 (967, 1429)	495 (456, 616)	671.5 (507.5, 714)	< 0.001
t-Tau (pg mol-1)	276 (227.5, 375)	578 (432.75, 785.75)	464 (337.5, 548.5)	0.001
p-Tau (pg mol-1)	40 (29, 44)	91 (58.75, 107.75)	67 (58.25, 99)	< 0.001
CDR	0 (0, 0)	0.5 (0.5, 0.5)	0 (0, 0)	< 0.001
MMSE	29 (27.5, 29.5)	24 (23, 25.75)	27 (26.75, 28.25)	< 0.001
FAQ	0 (0, 1)	7 (5, 10.5)	1 (0, 2)	< 0.001
RBANS.MR	101 (96.5, 106.5)	42 (40, 55)	86 (77.25, 98.75)	< 0.001

Table 1. Participant's clinical and demographic variables.

Variable (Total counts)	Control (n = 19)	MCI-AD (n = 19)	Preclinical AD (n = 8)
	Median (1st, 3rd Q.)		
hsa-miR-92a-3p	22.26 (21.12, 22.67)	21.51 (21.27, 22.72)	21.89 (21.37, 22.61)
hsa-miR-486-5p	22.72 (22.22, 23.43)	22.5 (22.13, 23.3)	23.33 (22.26, 24.21)
hsa-miR-29a-3p	26.86 (25.92, 27.55)	26.93 (26.4, 27.36)	27.62 (26.62, 27.99)
hsa-miR-486-3p	28.19 (27.47, 28.96)	28.07 (27.44, 29.35)	27.98 (27.4, 29.8)
hsa-miR-150-5p	24.18 (23.84, 24.9)	23.93 (23.38, 25.2)	23.93 (23.38, 24.49)
hsa-miR-320b	26.94 (26.26, 27.64)	26.73 (26.19, 27.1)	26.88 (25.94, 27.48)
hsa-miR-483-3p	31.53 (31.18, 32.32)	31.63 (30.97, 32.91)	31.5 (31.31, 31.74)
hsa-miR-342-3p	28.54 (28.07, 29.04)	28.48 (27.7, 29.46)	27.71 (27.05, 28.75)

Table 2. Median levels of miRNAs in plasma from participants' groups.

Pathway analysis. For the miRNAs with a high directional probability (has-92a-3p, has-486-5p, has-29a-3p), their potential target genes were analysed in order to assess their involvement in the pathology development. Table 4 shows the potential target genes of the selected miRNAs related to AD mechanisms. As can be seen, 112 potential targets were obtained for miRNA hsa-92a-3p, 16 targets for hsa-486-5p, and 88 targets for hsa-29a-3p, with a target score of at least 95. In addition, each of the selected miRNAs regulated several pathways. As can be seen in Fig. 2, the most common pathways were cell signalling and transcription regulation, but also lipid metabolism, protein synthesis and modifications, and structural functions were regulated by the selected miRNAs. First, the main pathways that could be regulated by the miRNA hsa-92a-3p are cell death or autophagy and cell proliferation pathways, and some pathways related to vesicle transport and synaptic transmission. Among the cell death targets, BCL2L11 (BCL2 like 11) is involved in neuronal and lymphocyte apoptosis and G3BP2 (G3BP stress granule assembly factor 2) is involved in stress response. In the cell proliferation pathway, the gene C21orf91 (chromosome 21 open reading frame 91) plays a role in the proliferation of neurons in the cortex. Among synaptic transmission targets, GLRA1 (glycine receptor alpha 1), SYN2 (synapsin II), SCN8A (sodium voltage-gated channel alpha subunit 8), CADM2 (cell adhesion molecule 2), CBLN4 (cerebellin 4 precursor), SYNJ1 (synaptojanin 1), SLC17A6 (solute carrier family 17 member 6), and NSF (N-ethylmaleimide sensitive factor, vesicle fusing ATPase) are highlighted, being the last two targets involved in vesicle transport. Other important genes are REST (RE1 silencing transcription factor), which regulates neuronal genes

Variables	Estimate	OR (CI 95%)	Inside Rope (%)	PD (%)
hsa-miR-92a-3p	−0.484	0.616 (0.241,1.455)	19.34%	85.40%
hsa-miR-486-5p	−0.649	0.522 (0.112,2.28)	14.15%	81.38%
hsa-miR-29a-3p	0.418	1.519 (0.662,3.626)	22.76%	82.88%
hsa-miR-486-3p	0.478	1.613 (0.462,5.929)	18.05%	77.88%
hsa-miR-150-5p	0.123	1.131 (0.243,5.574)	19.76%	55.27%
hsa-miR-320b	0.174	1.19 (0.373,4.02)	23.34%	60.68%
hsa-miR-483-3p	0.286	1.331 (0.624,2.968)	29.86%	77.15%
hsa-miR-342-3p	−0.458	0.632 (0.131,3.086)	16.47%	72.58%

Table 3. Characteristics of the Bayesian model including 3 participants groups (control, preclinical-AD, MCI-AD). The Probability of Direction (PD) is an index of effect existence, ranging from 50 to 100%, representing the certainty with which an effect goes in a particular direction. PD > 80% was considered significative. For each variable the direction depends on the estimate (negatives estimate < 0, and positives estimates > 0). Region of Practical Equivalence (ROPE) defines the percentage of the area that is within the region of practical equivalence (equivalent to null effect). *OR* odds ratio, *CI* confidence interval.

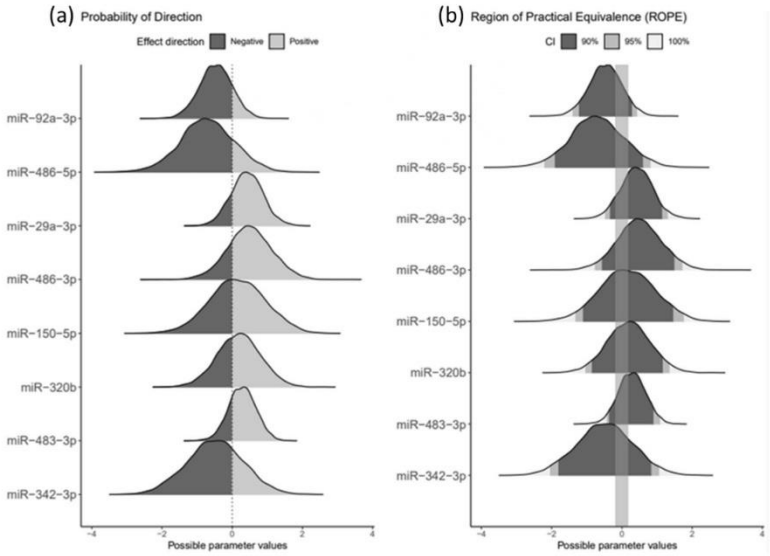

Figure 1. Probability of direction (PD) and Region of Practical Equivalence (ROPE) for each miRNA. (**a**) PD shows the estimation of direction for each biomarker, showing a protective AD effect for those with negative direction and risk AD effect for those with positive direction. Polygons show the density summary of the posterior draws and coloured given the estimated direction (positive or negative) of the effect parameter. The proportion of the polygon that does not include zero is a statement about probability of the proposed direction of effect. (**b**) ROPE represents the area of null equivalence that is the percentage with none direction (positive or negative). Effects given a full ROPE based on a 100%, 95% and 90% highest posterior density interval. The proportion of the polygon that does not include zero is a statement about the significance of effect.

Pathway	hsa-miR-92a-3p	hsa-miR-486-5p	hsa-miR-29a-3p
Autophagy	TECPR2, EPG5		
Cell death	G3BP2, HIPK3, USP28, DNAJB9, BCL2L11, RNF38		TRIB2, XKR6, AKT3
proliferation	CD69, FNIP1, BTG2, MAP2K4, C21orf91, KLF4, FNIP2, GTF2A1, CDK16, ARID1B, CDCA7L, CCNJL, CUX1, MAP1B, RNF38		NAV1, NAV2, NAV3, IGF1, ZNF346, LIF, CDK6, SGMS2, PDIK1L, CHSY1, NEXMIF, AKT3, ADAMTS9
Cell signalling	PIKFYVE, DOCK9, ITGAV, EFR3A, RIC1, RNF38, GPR180, PLEKHA1, JMY, GNAQ, RGS17, PTEN, PCDH11X, GIT2, ADGRF2, CALN1, DPP10, LRCH1, HCN2	DCC, PTEN, SLC10A7, ARHGAP44, MARK1	NEXMIF, AKT3, DAAM2, PTEN, PGAP2, ROBO1, RAP1GDS1, RAB30, DGKH, CLDN1, TRAF3
Energetic metabolism and oxidative stress	NOX4, SESN3, PTEN, SLC12A5	PTEN	PTEN
Glucose metabolism	MAN2A1, FBN1, UGP2		FBN1
Immune response	TAGAP, CD69, KLF4, GLRA1, FOXN2, RAB23		TRAF3
lipid metabolism	PPCS, KIAA1109	FAHD1	OSBPL11
membrane transport	SLC12A5, SLC25A32, SGK3		SESTD1, ABCE1, SLC5A8
Nucleic acid metabolism and DNA organization	MORC3, RBM27, GID4, CPEB3, SLX4, AGO3, JMY, ANP32E, RSBN1		DOT1L, KMT5C, ERCC6, NASP, KDM5B, TDG
DNA and histones methylation			TET1, TET2, TET3, DOT1L, DNMT3A, DNMT3B, KDM5B
Protein degradation	FBXW7, SESN3, KLHL14, USP36, USP28, UBXN4		VPS37C, TRIM63
Protein synthesis and modifications			
	B3GALT2, PTAR1, GOLGA3, COG3, SGK3, ADAM10, EDEM1	COPS7B, MARK1, LMTK2, ABHD17B	ADAMTS9, ADAMTS6, DIO2, ABCE1
Structural function	ACTC1, ANP32E, NEFH, RSBN1, NCKAP5, NEFM, RHPN2, FBN1, MYO1B	SNRPD1, NCKAP5, LCE3E	COL5A3, COL5A1, COL3A1, FBN1, COL11A1, HAS3, TMEM169, COL19A1, COL4A1, COL1A1, COL7A1, SPARC, COL5A2, HMCN1, C1QTNF6, ADAMTS2, CEP68, PXDN, COL9A1, HAPLN3, RND3, TRAF3, RAB30, CLDN1
Synaptic transmission	GLRA1, SYN2, SCN8A, CADM2, CBLN4, SYNJ1, SLC17A6, NSF	ARHGAP44	
Transcription	MIER1, HAND2, TBL1XR1, LATS2, FOXN2, ZEB2, REST, GRHL1, TEAD1, HIVEP1	BTAF1, SNRPD1, FOXO1, ZNF331	HBP1, ATAD2B, BRWD3, NSD1, ZBTB34, NFIA, KDM5B, PURG, HIF3A, ZBTB5, ZNF282, AMER1, REST, TAF5, ZHX3, C16orf72
Vesicle transport	MYO1B, CDK16, PIKFYVE, SLC17A6, NSF, RAB23, DENND1B		ASAP2, VPS37C
Others	ZFC3H1, TTC9, ATXN1, DCAF6, LHFPL2, FAM160B1, ERGIC2, MAGEC2, SPRYD4, ANKRD28, TRIM36, FAM24A, BCL11B	TRIM36	ADAMTS17, PRR14L, FAM241A, LYSMD1, PXYLP1, SMS, ATAD2B

Table 4. Potential target genes and related AD pathways. In this link it can be found the full name of each gene (http://mirdb.org/mirdb/index.html).

transcription; and NEFH (neurofilament heavy), which contributes to the maintenance of neuronal structure. In addition, PPCS (phosphopantothenoylcysteine synthetase) could be relevant in the regulation and metabolism of CoenzymeA.

Secondly, the main pathways that could be regulated by the miRNA hsa-486-5p are cell signalling, lipid and protein pathways, structural functions and transcription.

Thirdly, the main pathway that could be regulated by the miRNA hsa-29a-3p is the cell proliferation pathway, which involves neurone regeneration and migration trough NAV3 (neuron navigator3), NAV1, and NAV2. Also, ZNF346 (zinc finger protein 346) could act to protect neurons and LIF (LIF, interleukin 6 family cytokine) is involved in neuronal differentiation. In cell signalling pathways, the targets DAAM2 (dishevelled associated activator of morphogenesis 2) and ROBO1 (roundabout guidance receptor 1) contribute to nervous system development and neuronal migration, respectively. Furthermore, miRNA hsa-29a-3p plays a role in structure regulation, specifically regulating the synthesis of different collagen chains, and HMCN1 (hemicentin 1) is involved in macular degeneration and C1QTNF6 (C1q and TNF related 6) is involved in identical protein binding activity. Also, this miRNA could regulate REST in the transcription pathway.

Discussion

In this study, miRNA sequencing was carried out to identify potential early AD biomarkers. From these, a validation step was conducted, in which quantifiable miRNAs were identified, while some of them were not detected. In fact, the miRNAs not validated were hsa-miR-142-5p, hsa-miR-1293 and hsa-miR-4259. A previous study in cell line found a relationship between dysregulation of miR-142-5p expression and AD pathogenesis and synaptic dysfunction[29], and it was detected up-regulated in the blood of AD patients[30]. Also, hsa-miR-4259 was detected

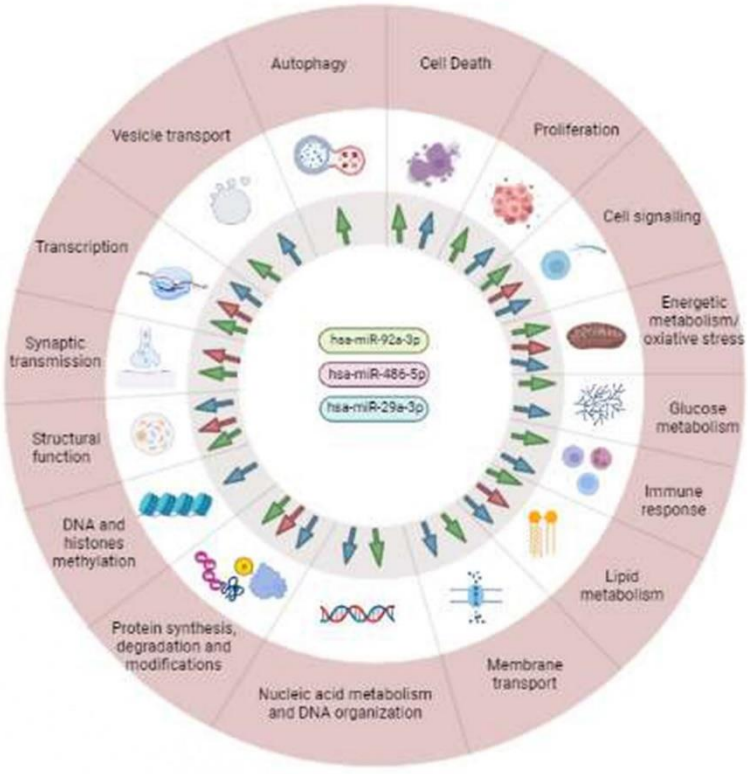

Figure 2. Pathways regulated by the three miRNAs that showed relationship with AD. The arrows indicate those miRNAs involved in each pathway. Each color represents a miRNA: green (hsa-miR-92a-3p), red (hsa-miR-486-5p) and blue (hsa-miR-29a-3p). *Created with BioRender.com.

in saliva samples, but there is a lack of studies quantifying this biomarker in plasma samples[31]. In addition, has-miR-1293 was previously detected in platelets from hepatocellular carcinoma and lung adenocarcinoma cell line[32]. Nevertheless, there are no studies describing its association with AD.

Regarding the methodology, Haining et al., performed a similar study trying to find a miRNA profile in early AD. However, different cohorts for untargeted and targeted analysis were used[17]. Also, Dakterzada aimed to find miRNAs in plasma from AD participants, identifying a BACE-1 related panel of biomarkers different from the miRNAs in the present work[33]. It could be due to the use of a different identification technique based on microarrays analysis[34]. The different methodologies employed could affect the miRNAs selection, so it should be taken into account in comparisons with other studies[33].

Regarding the miRNAs that showed a trend with the pathology in the present study, they were hsa-miR-92a-3p, has-miR-486-5p and hsa-miR-29a. First, hsa-miR-92a-3p showed a tendency for decreased levels in AD. A previous study showed dysregulation of 3 miRNAs related to synaptic proteins, including hsa-miR-92a-3p in MCI and AD[35]. Another study described the relationship between miR-92a-3p and tau accumulation[36]. One of the most AD-relevant pathways that could be regulated by this miRNA is synaptic transmission[37]. Specifically,

SYNJ1, a potential target for this miRNA, seemed to be involved in amyloid beta clearance[38,39], while synapsins could act on amyloid beta generation by modulating BACE1[40]. In addition, CBLN4 could regulate amyloid beta toxicity[41]. Regarding neuronal apoptosis, it could be regulated by this miRNA and the BCL2L2 target. In fact, a previous work showed that amyloid beta could regulate that pathway[42]. Other target genes (NEFH, REST), which are involved in neuronal structure and neuronal gene transcription, were described as potential AD diagnosis biomarkers[13,41].

Second, the present study showed a tendency towards reduced levels of hsa-miR-486-5p in AD. Similarly, Nagaraj et al. described a panel of 6 plasma miRNAs, including hsa-miR-486-5p, that differentiated between controls and MCI-AD[45]. This miRNA could regulate some genes involved in cell signalling, lipid and protein pathways, transcription and structural function.

Third, a trend towards higher levels for hsa-miR-29a-3p in AD plasma was found. Similarly, Shioya et al. described differential levels of this miRNA at brain levels, suggesting its implication in neurodegeneration trough NAV3 (Neurone Navigator 3) regulation[46]. In addition, another miRNA from that family (hsa-miR-29c) has been related to AD pathology due to its involvement in the amyloid beta accumulation through the regulation of BACE1[47,48]. Moreover, Müller et al. suggested that miR-29a could be a candidate biomarker for AD in CSF samples without cells[49]. In this regard, different types of collagenous chains and C1QTNF6 are targets of miRNA hsa-29a-3p. Previous studies described collagenous chains as a component from amyloid plaques[50]. The collagenous regulation may contribute to the assembly of amyloid fibres, enhancing the development of amyloid pathology. In addition, C1q complement protein co-localizes with the amyloid beta in brain[51,52]. Therefore, C1QTNF6, which is thought to play a role in identical protein binding, could help in the accumulation of C1q protein, triggering amyloid plaque formation (PubMed Gene). In addition, ROBO1 and DAAM2, which are involved in neuronal migration and nervous system development, are targets for this miRNA. In fact, ROBO1 could show a relationship with axon guidance dependent on presenilin, which helps in the proteolysis of amyloid-β precursor protein and triggers to AD pathology development[53,54]. Furthermore, DAAM2 was described by Ding et al. as a mediator in regenerative oligodendrocyte differentiation; while Sellers et al. demonstrated that Aβ synaptotoxicity is mediated by this protein[55,56].

The main limitations in this study are the small sample size, since it is quite difficult to have a large number of biologically classified early AD patients (MCI, preclinical). Moreover, from the selected miRNAs, some of them were not validated as they were not correctly quantified, probably due to the fact that they were detected in few samples. In addition, the study design is cross-sectional. In order to obtain more accurate data from the different disease stages, it should be longitudinal. However, participants in this present study are perfectly characterized according to CSF biomarkers and their cognitive status, providing a reliable approach to the disease progression.

Conclusions

RNA sequencing analysis in plasma samples from participants with early AD and healthy controls allowed to identify some differentially expressed miRNAs. From them, 3 selected miRNAs (miRNA-92a-3p, miRNA-486-5p, miRNA-29a-3p) were slightly dysregulated in AD, being potential biomarkers of the pathology. In fact, they could be involved in the regulations of important pathways of the pathology, such as synaptic transmission, cell signalling, structure maintenance or cell metabolism, so they could be relevant therapeutic targets. However, further research with a larger sample is needed to verify these results, as well as to develop the potential mechanisms of action of these miRNAs.

Data availability

The datasets generated during the current study are available in the ArrayExpress repository, accession number E-MTAB-11103.

Received: 23 May 2022; Accepted: 6 September 2022
Published online: 16 September 2022

References

1. Hammond, S. M. An overview of microRNAs. *Adv. Drug Deliv. Rev.* **87**, 3–14. https://doi.org/10.1016/j.addr.2015.05.001 (2015).
2. Lu, T. X. & Rothenberg, M. E. MicroRNA. *J. Allergy Clin. Immunol.* **141**, 1202–1207. https://doi.org/10.1016/j.jaci.2017.08.034 (2018).
3. W.H. Organization, Dementia, (2021). https://www.who.int/news-room/fact-sheets/detail/dementia
4. Niedowicz, D. M., Nelson, P. T. & Paul Murphy, M. Alzheimers Disease: Pathological Mechanisms and Recent Insights. *Curr. Neuropharmacol.* **9**, 674–684. https://doi.org/10.2174/157015911798376181 (2011).
5. Lloret, A., Fuchsberger, T., Giraldo, E. & Viña, J. Molecular mechanisms linking amyloid β toxicity and Tau hyperphosphorylation in Alzheimer's disease. *Free Radic. Biol. Med.* **83**, 186–191. https://doi.org/10.1016/j.freeradbiomed.2015.02.028 (2015).
6. Yang, S.-H. Cellular and molecular mediators of neuroinflammation in Alzheimer disease. *Int. Neurourol. J.* **23**, S54-62. https://doi.org/10.5213/inj.1938184.092 (2019).
7. Berr, C., Balansard, B., Arnaud, J., Roussel, A.-M. & Alpérovitch, A. Cognitive decline is associated with systemic oxidative stress: The EVA Study. *J. Am. Geriatr. Soc.* **48**, 1285–1291. https://doi.org/10.1111/j.1532-5415.2000.tb02603.x (2000).
8. Bowman, G. L. *et al.* Blood-brain barrier breakdown, neuroinflammation, and cognitive decline in older adults. *Alzheimer's Dement.* **14**, 1640–1650. https://doi.org/10.1016/j.jalz.2018.06.2857 (2018).
9. Weller, J. & Budson, A. Current understanding of Alzheimer's disease diagnosis and treatment. *F1000Res* https://doi.org/10.12688/f1000research.14506.1 (2018).
10. McKhann, G. M. *et al.* The diagnosis of dementia due to Alzheimer's disease: Recommendations from the National Institute on Aging-Alzheimer's association workgroups on diagnostic guidelines for Alzheimer's disease. *Alzheimer's Dement.* **7**, 263–269. https://doi.org/10.1016/j.jalz.2011.03.005 (2011).

11. Albert, M. S. *et al.* The diagnosis of mild cognitive impairment due to Alzheimer's disease: Recommendations from the national institute on aging-Alzheimer's association workgroups on diagnostic guidelines for Alzheimer's disease. *Alzheimer's Dement.* 7, 270–279. https://doi.org/10.1016/j.jalz.2011.03.008 (2011).
12. Sperling, R. A. *et al.* Toward defining the preclinical stages of Alzheimer's disease: Recommendations from the national institute on aging-Alzheimer's association workgroups on diagnostic guidelines for Alzheimer's disease. *Alzheimer's Dement.* 7, 280–292. https://doi.org/10.1016/j.jalz.2011.03.003 (2011).
13. Hampel, H. *et al.* Blood-based biomarkers for Alzheimer disease: Mapping the road to the clinic. *Nat. Rev. Neurol.* **14**, 639–652. https://doi.org/10.1038/s41582-018-0079-7 (2018).
14. Maes, O., Chertkow, H., Wang, E. & Schipper, H. MicroRNA: Implications for Alzheimer disease and other human CNS disorders. *Curr. Genomics* **10**, 154–168. https://doi.org/10.2174/138920209788185252 (2009).
15. Angelucci, F. *et al.* MicroRNAs in Alzheimer's disease: Diagnostic markers or therapeutic agents?. *Front Pharmacol.* https://doi.org/10.3389/fphar.2019.00665 (2019).
16. Swarbrick, S., Wragg, N., Ghosh, S. & Stolzing, A. Systematic review of miRNA as biomarkers in Alzheimer's disease. *Mol. Neurobiol.* **56**, 6156–6167. https://doi.org/10.1007/s12035-019-1500-y (2019).
17. He, H. *et al.* Novel plasma miRNAs as biomarkers and therapeutic targets of Alzheimer's disease at the prodromal stage. *J. Alzheimer's Dis.* **83**, 779–790. https://doi.org/10.3233/JAD-210307 (2021).
18. Song, S., Lee, J. U., Jeon, M. J., Kim, S. & Sim, S. J. Detection of multiplex exosomal miRNAs for clinically accurate diagnosis of Alzheimer's disease using label-free plasmonic biosensor based on DNA-Assembled advanced plasmonic architecture. *Biosens. Bioelectron.* **199**, 113864. https://doi.org/10.1016/j.bios.2021.113864 (2022).
19. Cheng, L. *et al.* Prognostic serum miRNA biomarkers associated with Alzheimer's disease shows concordance with neuropsychological and neuroimaging assessment. *Mol. Psychiatry* **20**, 1188–1196. https://doi.org/10.1038/mp.2014.127 (2015).
20. Cordero, F., Beccuti, M., Arigoni, M., Donatelli, S. & Calogero, R. A. Optimizing a massive parallel sequencing workflow for quantitative miRNA expression analysis. *PLoS ONE* **7**, e31630. https://doi.org/10.1371/journal.pone.0031630 (2012).
21. Kulkarni, N. *et al.* Reproducible bioinformatics project: A community for reproducible bioinformatics analysis pipelines. *BMC Bioinform.* **19**, 349. https://doi.org/10.1186/s12859-018-2296-x (2018).
22. R.C. Team., R: A language and environment for statistical computing, (2018). https://www.r-project.org/
23. S. Andrews, FastQC: A quality control tool for high throughtput sequence data 2010, (n.d.). www.bioinformatics.babraham.ac.uk/projects/fastqc/
24. Martin, M. Cutadapt removes adapter sequences from high-throughput sequencing reads. *EMBnet J.* https://doi.org/10.14806/ej.17.1.200 (2011).
25. Kozomara, A. & Griffiths-Jones, S. miRBase: Integrating microRNA annotation and deep-sequencing data. *Nucleic Acids Res.* **39**, D152–D157. https://doi.org/10.1093/nar/gkq1027 (2011).
26. Rumble, S. M. *et al.* SHRiMP: Accurate mapping of short color-space reads. *PLoS Comput. Biol.* 5, e1000386. https://doi.org/10.1371/journal.pcbi.1000386 (2009).
27. David, M., Dzamba, M., Lister, D., Ilie, L. & Brudno, M. SHRiMP2: Sensitive yet practical short read mapping. *Bioinformatics* **27**, 1011–1012. https://doi.org/10.1093/bioinformatics/btr046 (2011).
28. Lawrence, M. *et al.* Software for computing and annotating genomic ranges. *PLoS Comput. Biol.* **9**, e1003118. https://doi.org/10.1371/journal.pcbi.1003118 (2013).
29. Song, J. & Kim, Y.-K. Identification of the role of miR-142–5p in Alzheimer's disease by comparative bioinformatics and cellular analysis. *Front Mol. Neurosci.* https://doi.org/10.3389/fnmol.2017.00227 (2017).
30. Sorensen, S. S., Nygaard, A.-B. & Christensen, T. miRNA expression profiles in cerebrospinal fluid and blood of patients with Alzheimer's disease and other types of dementia–an exploratory study. *Transl. Neurodegener.* https://doi.org/10.1186/s40035-016-0053-5 (2016).
31. Wu, L. *et al.* Genome-wide study of salivary microRNAs as potential noninvasive biomarkers for detection of nasopharyngeal carcinoma. *BMC Cancer* **19**, 843. https://doi.org/10.1186/s12885-019-6037-y (2019).
32. Zhu, B., Gu, S., Wu, X., He, W. & Zhou, H. Bioinformatics analysis of tumor-educated platelet microRNAs in patients with hepatocellular carcinoma. Biosci. Rep. https://doi.org/10.1042/BSR20211420 (2021).
33. Kloten, V. *et al.* Multicenter evaluation of circulating plasma MicroRNA extraction technologies for the development of clinically feasible reverse transcription quantitative PCR and next-generation sequencing analytical work flows. *Clin. Chem.* **65**, 1132–1140. https://doi.org/10.1373/clinchem.2019.303271 (2019).
34. Liu, H. *et al.* Increased expression of plasma miRNA-320a and let-7b-5p in heroin-dependent patients and its clinical significance. *Front Psychiatry* https://doi.org/10.3389/fpsyt.2021.679206 (2021).
35. Siedlecki-Wullich, D. *et al.* Altered microRNAs related to synaptic function as potential plasma biomarkers for Alzheimer's disease. *Alzheimers Res. Ther.* **11**, 46. https://doi.org/10.1186/s13195-019-0501-4 (2019).
36. Li, X. *et al.* Correcting miR92a-vGAT-mediated GAB aergic Dysfunctions rescues human tau-induced anxiety in mice. *Mol. Ther.* **25**, 140–152. https://doi.org/10.1016/j.ymthe.2016.10.010 (2017).
37. Kumar, S. & Reddy, P. H. The role of synaptic microRNAs in Alzheimer's disease. *Biochim. Biophys. Acta (BBA) Mol. Basis Dis.* https://doi.org/10.1016/j.bbadis.2020.165937 (2020).
38. Zhu, L. *et al.* Reduction of synaptojanin 1 accelerates Aβ clearance and attenuates cognitive deterioration in an Alzheimer mouse model. *J. Biol. Chem.* **288**, 32050–32063. https://doi.org/10.1074/jbc.M113.504365 (2013).
39. Ando, K. *et al.* The lipid phosphatase synaptojanin 1 undergoes a significant alteration in expression and solubility and is associated with brain lesions in Alzheimer's disease. *Acta Neuropathol. Commun.* **8**, 79. https://doi.org/10.1186/s40478-020-00954-1 (2020).
40. Maesako, M., Zoltowska, K. M. & Berezovska, O. Synapsin 1 promotes Aβ generation via BACE1 modulation. *PLoS ONE* **14**, e0226368. https://doi.org/10.1371/journal.pone.0226368 (2019).
41. Chacón, P. J. *et al.* Cerebellin 4, a synaptic protein, enhances inhibitory activity and resistance of neurons to amyloid-β toxicity. *Neurobiol. Aging.* **36**, 1057–1071. https://doi.org/10.1016/j.neurobiolaging.2014.11.006 (2015).
42. Yao, M. Amyloid-induced neuronal apoptosis involves c-Jun N-terminal kinase-dependent downregulation of Bcl-w. *J. Neurosci.* **25**, 1149–1158. https://doi.org/10.1523/JNEUROSCI.4736-04.2005 (2005).
43. Brettschneider, J. *et al.* The neurofilament heavy chain (NfHSMI35) in the cerebrospinal fluid diagnosis of Alzheimer's disease. *Dement. Geriatr. Cogn. Disord.* **21**, 291–295. https://doi.org/10.1159/000091436 (2006).
44. Ashton, N. J. *et al.* Plasma REST: A novel candidate biomarker of Alzheimer's disease is modified by psychological intervention in an at-risk population. *Transl. Psychiatry* **7**, e1148–e1148. https://doi.org/10.1038/tp.2017.113 (2017).
45. Nagaraj, S. *et al.* Profile of 6 microRNA in blood plasma distinguish early stage Alzheimer's disease patients from non-demented subjects. *Oncotarget* **8**, 16122–16143. https://doi.org/10.18632/oncotarget.15109 (2017).
46. Shioya, M. *et al.* Aberrant microRNA expression in the brains of neurodegenerative diseases: miR-29a decreased in Alzheimer disease brains targets neurone navigator 3. *Neuropathol. Appl. Neurobiol.* **36**, 320–330. https://doi.org/10.1111/j.1365-2990.2010.01076.x (2010).
47. Lei, X., Lei, L., Zhang, Z., Zhang, Z. & Cheng, Y. Downregulated miR-29c correlates with increased BACE1 expression in sporadic Alzheimer's disease. *Int. J. Clin. Exp. Pathol.* **8**, 1565–1574 (2015).
48. Yang, G. *et al.* MicroRNA-29c targets β-site amyloid precursor protein-cleaving enzyme 1 and has a neuroprotective role in vitro and in vivo. *Mol. Med. Rep.* **12**, 3081–3088. https://doi.org/10.3892/mmr.2015.3728 (2015).

49. Müller, M. *et al.* MicroRNA-29a Is a candidate biomarker for Alzheimer's disease in cell-free cerebrospinal fluid. *Mol. Neurobiol.* **53**, 2894–2899. https://doi.org/10.1007/s12035-015-9156-8 (2016).
50. Hashimoto, T. CLAC: A novel Alzheimer amyloid plaque component derived from a transmembrane precursor, CLAC-P/collagen type XXV. *EMBO J.* **21**, 1524–1534. https://doi.org/10.1093/emboj/21.7.1524 (2002).
51. Afagh, A., Cummings, B. J., Cribbs, D. H., Cotman, C. W. & Tenner, A. J. Localization and cell association of C1q in Alzheimer's disease Brain. *Exp. Neurol.* **138**, 22–32. https://doi.org/10.1006/exnr.1996.0043 (1996).
52. Söderberg, L. *et al.* Characterization of the Alzheimer's disease-associated CLAC protein and identification of an amyloid β-peptide-binding site. *J. Biol. Chem.* **280**, 1007–1015. https://doi.org/10.1074/jbc.M403628200 (2005).
53. Bai, G. *et al.* Presenilin-dependent receptor processing is required for axon guidance. *Cell* **144**, 106–118. https://doi.org/10.1016/j.cell.2010.11.053 (2011).
54. Wang, B. *et al.* The amyloid precursor protein is a conserved receptor for slit to mediate axon guidance. *ENeuro* https://doi.org/10.1523/ENEURO.0185-17.2017 (2017).
55. Ding, X. *et al.* The daam2–VHL–Nedd4 axis governs developmental and regenerative oligodendrocyte differentiation. *Genes Dev.* **34**, 1177–1189. https://doi.org/10.1101/gad.338046.120 (2020).
56. Sellers, K. J. *et al.* Amyloid β synaptotoxicity is Wnt-PCP dependent and blocked by fasudil. *Alzheimer's Dement.* **14**, 306–317. https://doi.org/10.1016/j.jalz.2017.09.008 (2018).

Acknowledgements
This study has been funded by Instituto de Salud Carlos III through the project "PI19/00570" (Co-funded by European Regional Development Fund, "A way to make Europe"). CC-P acknowledges a postdoctoral "Miguel Servet" grant CPII21/00006 from the Health Institute Carlos III (Spanish Ministry of Economy, Industry and Innovation). CP-B acknowledges a predoctoral "PFIS" grant FI20/00022 from the Health Institute Carlos III.

Author contributions
Conceptualization: C.C.P., A.B.B.; Methodology: C.P.B., A.T.S., A.B.B., L.F.G.; Formal analysis and investigation: C.C.P., A.B., A.J.C.M.; Writing—original draft preparation: C.P.B., A.T.S.; Writing—review and editing: C.C.P., M.B.; Funding acquisition: C.C.P.; Supervision: C.C.P., M.B.

Funding
This study has been funded by Instituto de Salud Carlos III through the project "PI19/00570" (Co-funded by European Regional Development Fund, "A way to make Europe").

Competing interests
The authors declare no competing interests.

Additional information
Correspondence and requests for materials should be addressed to C.C.-P.

Reprints and permissions information is available at www.nature.com/reprints.

Publisher's note Springer Nature remains neutral with regard to jurisdictional claims in published maps and institutional affiliations.

biomedicines

MDPI

Communication

Epigenomics and Lipidomics Integration in Alzheimer Disease: Pathways Involved in Early Stages

Carmen Peña-Bautista [1], Lourdes Álvarez-Sánchez [1,2], Antonio José Cañada-Martínez [3], Miguel Baquero [1,2] and Consuelo Cháfer-Pericás [1,*]

[1] Alzheimer's Disease Research Group, Health Research Institute La Fe, 46026 Valencia, Spain; mariadelcarmen_pena@iislafe.es (C.P.-B.); lourdes_alvarez@iislafe.es (L.Á.-S.); baquero_miq@gva.es (M.B.)
[2] Division of Neurology, University and Polytechnic Hospital La Fe, 46026 Valencia, Spain
[3] Data Science Unit, Health Research Institute La Fe (IIS La Fe), 46026 Valencia, Spain; bioestadistica@iislafe.es
* Correspondence: m.consuelo.chafer@uv.es; Tel.: +34-96-124-67-21; Fax: +34-96-124-57-46

Abstract: Background: Alzheimer Disease (AD) is the most prevalent dementia. However, the physiopathological mechanisms involved in its development are unclear. In this sense, a multi-omics approach could provide some progress. Methods: Epigenomic and lipidomic analysis were carried out in plasma samples from patients with mild cognitive impairment (MCI) due to AD (n = 22), and healthy controls (n = 5). Then, omics integration between microRNAs (miRNAs) and lipids was performed by Sparse Partial Least Squares (s-PLS) regression and target genes for the selected miRNAs were identified. Results: 25 miRNAs and 25 lipids with higher loadings in the sPLS regression were selected. Lipids from phosphatidylethanolamines (PE), lysophosphatidylcholines (LPC), ceramides, phosphatidylcholines (PC), triglycerides (TG) and several long chain fatty acids families were identified as differentially expressed in AD. Among them, several fatty acids showed strong positive correlations with miRNAs studied. In fact, these miRNAs regulated genes implied in fatty acids metabolism, as elongation of very long-chain fatty acids (ELOVL), and fatty acid desaturases (FADs). Conclusions: The lipidomic–epigenomic integration showed that several lipids and miRNAs were differentially expressed in AD, being the fatty acids mechanisms potentially involved in the disease development. However, further work about targeted analysis should be carried out in a larger cohort, in order to validate these preliminary results and study the proposed pathways in detail.

Keywords: Alzheimer disease; plasma; biomarker; lipids; microRNAs; integration

Citation: Peña-Bautista, C.; Álvarez-Sánchez, L.; Cañada-Martínez, A.J.; Baquero, M.; Cháfer-Pericás, C. Epigenomics and Lipidomics Integration in Alzheimer Disease: Pathways Involved in Early Stages. *Biomedicines* **2021**, *9*, 1812. https://doi.org/10.3390/biomedicines9121812

Academic Editor: Atsushi Iwata

Received: 29 October 2021
Accepted: 29 November 2021
Published: 2 December 2021

1. Introduction

Alzheimer disease (AD) is the most prevalent dementia [1]. Some hallmarks are clearly related to AD; accumulation of extracellular β-amyloid plaques and intracellular Tau neurofibrillary tangles. Nevertheless, the physiopathological mechanisms involved in the complex and multifactorial AD development remain unclear [2]. Therefore, a multi-omics approach could provide some progress in this field.

AD development could involve the reconfiguration of the epigenome and the modification of some genes expression have an impact in different disease pathways [3]. Specifically, differential expression of microRNAs have been found in recent AD studies [4,5]. These miRNAs could act as an epigenetic mechanism modifying the expression of different proteins post-transcriptionally [6]. Therefore, an increase or decrease in the levels of miRNAs could influence the expression of different proteins or enzymes. In this context, Hébert et al. described different miRNAs related to Amyloid precursor protein (APP) expression [7]. Therefore, epigenomics could be implicated in this pathology.

Lipidomics could also play an important role in AD development. In fact, lipids, the main component of cell membranes, are strongly related to brain function and neurodegenerative diseases [8]. Specifically, the lipids from phospholipids, triglycerides, sphingolipids

and cholesteryl esters correlated with clinical AD diagnosis, brain atrophy and disease progression [9]. A previous study developed a combination of 24 molecules to classify patients with high accuracy (>70%), and identified some metabolic features (triglycerides, phosphatidylcholines) [10].

Integrative network analysis of multi-omics results allowed us to identify molecular mechanisms in AD. A previous study based on RNA and Whole Genome Sequencing (WGS) observed signaling circuits of complex molecular interactions in key brain regions [11]. In another multi-omics study, Xicota et al. 2019 studied RNAseq, metabolomics and lipidomics, they found a signature of some blood metabolites and transcripts, which identified asymptomatic AD patients [12]. Additionally, a study from the literature showed the integration of genome-wide association studies with expression data, identifying some genes related to AD physiopathology. Specifically, the pathways were involved in calcium homeostasis [13]. In addition, a recent study was based on an integrative analysis of blood microRNAs expression and genomic data to develop an AD prognosis model, including 24 single nucleotide polymorphism-microRNA (miR-eQTLs), as well as age, sex, and APOE4 genotype [14]. From these miR-eQTLs, four genes related to AD (SHC1, FOXO1, GSK3B, and PTEN) were identified. Similarly, a genomics and metabolomics study demonstrated the utility of these data integration with AD risk factors to understand the mechanisms involved, revealing the importance of glycine as a mediator in cardiovascular and diabetes risk [15]. Epigenomic–lipidomic integration would allow the global study of the regulatory mechanisms involved in AD such as lipid homeostasis, oxidative stress, synaptic vesicle trafficking, inflammation, etc. [16]. These omics data were analysed together to develop an understanding of lipid regulation by epigenomics. Previous works based on the analysis of genome-wide DNA methylation showed that an epigenetic pattern was associated with cholesterol regulation [17]. In addition, in Parkinson Disease (PD), an epigenetic (DNA methylation) regulation was involved in the inactivation of the autophagy system, contributing to protein accumulation [18]. Thus, the study of the integration between epigenomics and lipidomics could show lipid regulation mechanisms involved in AD.

The aim of this work was to carry out the integration of epigenomics and lipidomics analysis in plasma samples from patients with mild cognitive impairment (MCI) due to AD, in order to advance the knowledge of early physiopathological mechanisms.

2. Materials and Methods

2.1. Participants and Samples Collection

All the participants were aged between 50 and 80 years old. Patients with known major neurological or psychiatric conditions were excluded. Assessment included a neuropsychological evaluation (Repeatable Battery for Assessment of Neuropsychological Status (RBANS) [19], Functionality Assessment Questionnaire (FAQ) [20], Clinical Dementia Rating (CDR) [21], MMSE [22]), analysis by means of NMR-TAC and cerebrospinal fluid (CSF) levels of amyloid β-42 peptide, *t*-Tau and *p*-Tau (Table 1). According to this, participants were classified into patients with MCI-AD (n = 22), and healthy controls (n = 5).

Blood samples from participants were collected into EDTA-tubes, and plasma was separated. Then, plasma samples were stored at −80 °C until the analysis.

Table 1. Clinical and neuropsychological criteria for participants' classification.

Test or Biomarker	Participant Group	
	Control	MCI-AD
CDR *	0–0.5	0.5–1
MMSE *	≥27	<27
RBANS.DM *	≥85	<85

Table 1. *Cont.*

Test or Biomarker	Participant Group	
	Control	MCI-AD
FAQ	<9	>9
Neuroimaging Structural (NMR-TAC)	Normal	Altered
CSF amyloid β42 (pg mL^{-1})	≥700	<700
CSF *t*-Tau (pg mL^{-1})	<350	≥350
CSF *p*-Tau (pg mL^{-1})	<85	≥85

* In MCI-AD group minimum 2 of the 3 cognitive status test (CDR, MMSE, RBANS.DM) should be altered.

2.2. *Omics Analysis*

2.2.1. Epigenomics

Epigenomic analysis was carried out by means of NGS NextSeq 550 platform (Illumina, San Diego, CA, USA) by single read sequencing of 50 cycles (1 × 50 bp). Data were processed and normalised to quantify and generate miRNA counts. The miRbase (v.21) allowed us to identify the miRNAs. Then, the identification of potential target genes for the selected miRNAs were carried out by miRbase (v.21, Manchester, UK).

2.2.2. Lipidomics

Lipidomic analysis was carried out by means of ultra-performance liquid chromatography coupled to time-of-flight mass spectrometry (MS). The internal standard consisted of a mix of: MG(17:0), LPC(17:0), Cer(d18:1/17:0), DG(17:0/17:0), SM(d18:1/17:0), PE(17:0/17:0), PC(17:0/17:0), TG(17:0/17:0/17:0), CE(17:0), PG(17:0/17:0) and PS(17:0/17:0). The chromatographic and mass spectrometry conditions were those established in the standard procedures of the Analytical Unit from Health Research Unit from Health Research Institute La Fe. Briefly, data were processed for peak detection, noise filtering, and peak alignment. The procedure was conducted to reduce the intra-batch variability, as well as to ensure the quality and reproducibility of the analysis. It consisted of a random injection order, at the beginning of the sequence 5 quality control (QC) samples were analysed in order to condition column and equipment, and every 5–7 samples a QC was analysed in Full MS mode. Additionally, at the beginning, middle, and end of the sequence, some QCs were analysed in Fragmentation in Data Independent mode and in Fragmentation in Data Dependent mode to proceed to the annotations of lipid species with the LipidMS annotations package. Then, data were filtered to exclude variables whose coefficients of variation in the QCs were higher than 30%, and variables with zeros in more than 60% of samples. Then, data were normalised. Finally, the library LipidMSid was used to identify the lipids.

2.3. *Statistical Analysis and Lipidomics-Epigenomics Integration*

Data were summarised using median (1st, 3rd quartiles) for quantitative variables and absolute frequency (%) for qualitative variables.

Sparse Partial Least Squares (sPLS) regression was applied to the previous data sets to select variables (miRNAs, lipids) and integrate them. The sPLS approach combines both integration and variable selection on two data sets in a one-step strategy [23].

Then, the graphical representations (correlation circle plots, heatmaps, relevance networks) resulting from the statistical approach were plotted.

Individual differences between groups were carried out by Mann–Whitney test, and correlations by Pearson Correlation. In all the cases, statistical significance was fixed in a p value of 0.05.

Statistical analyses were performed using R software (v 4.0.3, Auckland, CA, USA) and mixOmics (v 6.16.2) and clickR (v 0.7.35) packages and SPSS software version 20.0 (SPSS, Inc., Chicago, IL, USA).

3. Results

3.1. Participants

Table 2 shows the demographic and clinical data for the participants. As expected, CSF biomarkers levels and neuropsychological tests were different between groups. In fact, the MCI-AD group showed lower levels for amyloid β-42, and higher levels for *t*-Tau and *p*-Tau; also, MCI-AD group showed lower scores for MMSE, and RBANS, and higher scores for CDR and FAQ.

Table 2. Demographic and clinical characteristics of the participants.

Variables	Healthy Group (n = 5)	MCI-AD Group (n = 22)
Age (years, median (IQR))	68 (68, 72)	72 (69, 74)
Gender (female, n (%))	2 (40%)	12 (54.5%)
CSF amyloid β-42 (pg mL^{-1}, median (IQR))	1346.74 (930, 1421)	517.16 (453.86, 634.45)
CSF amyloid β-42/amyloid β-40 (median, IQR)	0.1 (0.09, 0.11)	0.05 (0.05, 0.05)
CSF *t*-Tau (pg mL^{-1}, median (IQR))	240 (238, 276)	566 (450, 780)
CSF *p*-Tau (pg mL^{-1}, median (IQR))	35 (35, 40)	81 (64.5, 107)
CSF NfL (pg mL^{-1}, median (IQR))	826.94 (791, 847.7)	1428.68 (1123.24, 1555.91)
CSF *t*-Tau/amyloid β-42 (median (IQR))	0.2 (0.19, 0.25)	0.99 (0.79, 1.32)
CDR (score, median (IQR))	0 (0–0.5)	0.5 (0–1)
MMSE (score, median (IQR))	29 (29, 30)	24 (23, 26)
RBANS_DM (score, median (IQR))	100 (98, 110)	44 (40, 64)
FAQ (score, median (IQR))	1 (0, 2)	7 (4, 9)

CSF: cerebrospinal fluid; IQR: inter-quartile range; CDR: Clinical Dementia Rating; MMSE: Mini-Mental State Examination; RBANS_DM: The Repeatable Battery for the Assessment of Neuropsychological Status_Delayed Memory; FAQ: Functional Activities Questionnaire.

3.2. Omics Integration

The sPLS model integrated two data matrices X (epigenomics) and Y (lipidomics). Additionally, sPLS performed simultaneous variables selection in the two data sets, by means of LASSO penalization on the pair of loading vectors. In this sense, two components were chosen, and 25 variables were selected on each dimension and for each data set. The X-block represented miRNAs, and the Y-block represented lipids.

Samples from both sets were represented in the 'common' subspace spanned by the principal components (PC1, PC2). As can be seen in Figure 1, samples were differentiated in the plot according to the participants group, there was not observed a clear separation.

Among the 25 selected variables for each data set, the miRNAs (block X) with higher loadings in the sPLS regression were hsa-miR-494-3p, hsa-miR-6894-3p, hsa-miR-421 and hsa-let-7a-3p; and the lipids (block Y) with higher loadings were FA (20:3), FA (20:4), FA (16:0), FA (20:2), and FA (18:2) (see Figure 2).

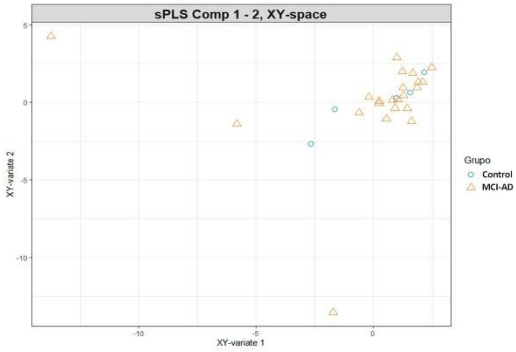

Figure 1. Scatter plot for participants samples in sPLS analysis. Represent the samples distribution in the 'common' subspace between the two sets of components (epigenomics and lipidomics variables).

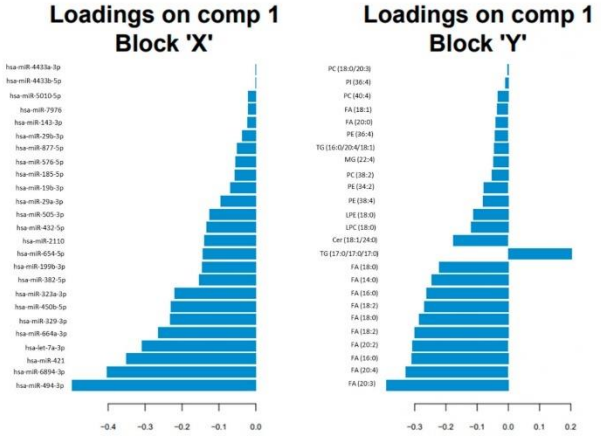

Figure 2. Horizontal barplot to visualise loading vector. The contribution of each variable for each component (comp) is represented in a barplot, where each bar length corresponds to the loading weight (importance) of the feature. The loading weight can be positive or negative.

The correlation circle plot depicted microRNAs and lipids selected on each component. As can be seen in the Supplementary Material (Figure S1), some subsets of variables were important to define each component. Actually, some miRNAs (hsa-miR-5010-5p, hsa-miR-421, hsa-miR-664a, hsa-miR-29b-3p, hsa-let-7a-3p, hsa-miR-19b-3p) and some lipids (FA (20:4), FA (20:3), FA (18:0)) mainly participated in defining the sPLS component 2; and some miRNAs (hsa-miR-335-3p, hsa-miR-532-3p, hsa-miR-379-5p, hsa-miR-4646-3p, hsa-miR-425-3p) mainly participated in defining component 1. Additionally, miRNAs, such

as hsa-miR-421 and hsa-miR-5010-5p, were positively correlated to the lipids FA (20:4) and FA (20:3); while these miRNAs were negatively correlated to the lipid TG (17:0/17:0/17:0).

The integration results were depicted by means of a heatmap. The similarity matrix was obtained from the sPLS results [24], and agglomerative hierarchical clustering was derived using the Euclidean distance as the similarity measure, and the Ward methodology [25]. In this sense, Figure 3 shows the heatmap for the correlations between miRNAs and lipids selected from sPLS. The red colour corresponded to positive correlation, while the blue colour corresponded to negative correlation. Most of the correlations were positive. In general, Figure 4 showed a positive correlation between studied miRNAs and lipids. However, the lipid TG (17:0/17:0/17:0) showed a negative correlation with all the described miRNAs. In addition, similar miRNAs were grouped, showing clusters for miR-29a-3p, let-7a-3p, miR-576-5p, miR-185-5p, miR-6894-3p, miR-5010-5p; for miR-29b-3p, miR-877-5p, miR-494-3p, miR-4433a-3p, miR-4433b-5p; and for miR-421, miR-450b-5p, miR-664a-3p, miR-432-5p, miR-654-5p, miR-2110, miR-329-3p. In addition, similar lipids were grouped, showing clusters for FA (18:0)/FA (14:0)/FA (18:0)/FA (16:0)/FA (18:2) and FA (20:3)/FA (20:4)/FA (18:2)/FA (20:2)/FA (16:0).

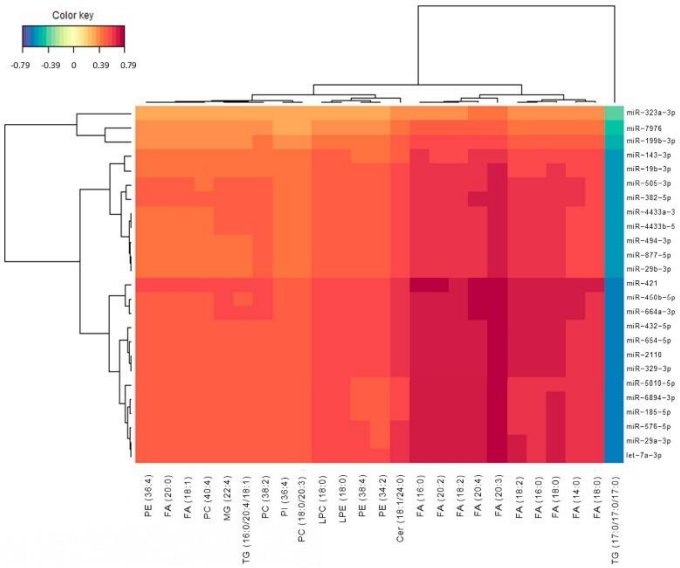

Figure 3. Heatmap representing correlations between miRNAs and lipid variables. Red colour represents positive correlations and blue colour represents negative correlations.

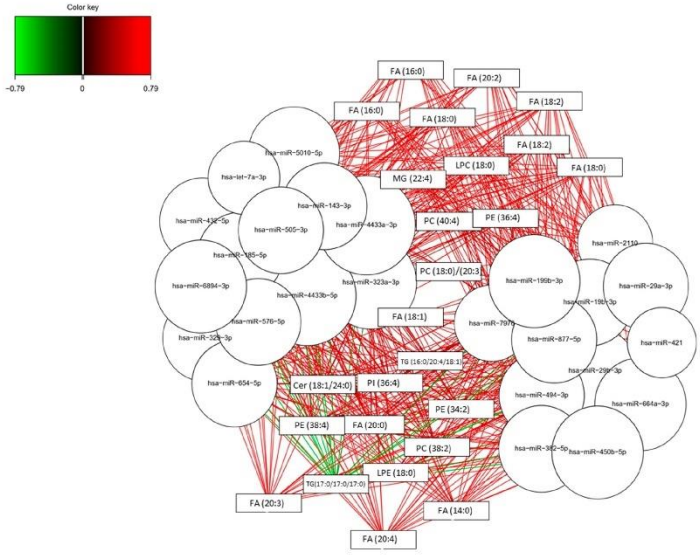

Figure 4. Relevance associations network for sPLS. Pair-wise similarity matrix directly obtained from the latent components was calculated. The similarity value between a pair of variables is obtained by calculating the sum of the correlations between the original variables and each of the latent components of the model. The values in the similarity matrix can be seen as a robust approximation of the Pearson correlation.

3.3. *Potential Pathways Involved in AD*

In Table 3, the predicted target genes for the selected miRNAs were described paying special attention to the genes that are implied in lipid metabolism, specifically in fatty acids pathways, which showed correlation with the miRNAs. In fact, fatty acids family showed the strongest correlations with miRNAs (see Figure 4). Among the identified target genes, several enzymes, such as elongases (ELOVL1, ELOVL2, ELOVL3, ELOVL4, ELOVL5, ELOVL6, ELOVL7), fatty acid desaturase (FADS6), fatty acyl-CoA reductases (FAR 1, FAR 2), fatty acid binding protein (FABP7), and fatty acid 2-hydroxylase (FA2H) were highlighted.

Another representation for the integration results is based on relevance network for sPLS regression, showing simultaneously positive and negative correlations between the two variable types (microRNAs, lipids). As can be seen in Figure 4 and the Supplementary Material in Table S1, most of these correlations were positive. Specifically, the highest positive correlations corresponded to these pairs of variables (FA (16:0) and FA (20:2) with hsa-miR-664, hsa-miR-432, hsa-miR-421, and hsa-miR-450b-5p; FA (18:0) and FA (18:2) with hsa-miR-664, hsa-miR-421 and hsa-miR-450b-5p; FA (20:3) and FA (20:4) with hsa-miR-664, hsa-miR-211, hsa-miR-432, hsa-miR-329, hsa-miR-654, hsa-let-7a-3p, hsa-miR-29a-3p, hsa-miR-421, and hsa-miR-450b-5p). On the other hand, the highest negative correlations corresponded to the lipid TG (17:0/17:0/17:0) with some miRNAs (hsa-miR-664-3p, hsa-miR-2110, hsa-miR-432-5p, hsa-miR-329-3p, hsa-miR-654-5p, hsa-miR-185-5p, hsa-let-7a-3p, hsa-miR-576-5p, hsa-miR-29a-3p, hsa-miR-6894-3p, hsa-miR-421, hsa-miR-450b-5p).

Table 3. Predicted target genes related to fatty acids for the selected miRNAs (miRBase).

miRNA	Target Genes
hsa-miR-494-3p	ELOVL3 (ELOVL fatty acid elongase 3)
	ELOVL5 (ELOVL fatty acid elongase 5)
hsa-miR-6894-3p	
hsa-miR-421	ARV1 (ARV1 homolog, fatty acid homeostasis modulator)
	FAR1 (fatty acyl-CoA reductase 1)
	ELOVL2 (ELOVL fatty acid elongase 2)
hsa-let-7a-3p	ELOVL2 (ELOVL fatty acid elongase 2)
	FA2H (fatty acid 2-hydroxylase)
	ELOVL7 (ELOVL fatty acid elongase 7)
hsa-miR-664a-3p	FAR1 (fatty acyl-CoA reductase 1)
	ELOVL4 (ELOVL fatty acid elongase 4)
	ELOVL7 ELOVL fatty acid elongase 7
	ELOVL5 ELOVL fatty acid elongase 5
hsa-miR-329-3p	
hsa-miR-450b-5p	ELOVL6 (ELOVL fatty acid elongase 6)
hsa-miR-323a-3p	
hsa-miR-382-5p	
hsa-miR-199b-3p	
hsa-miR-654-5p	FADS6 (fatty acid desaturase 6)
	ELOVL1 (ELOVL fatty acid elongase 1)
hsa-miR-2110	ELOVL4 (ELOVL fatty acid elongase 4)
hsa-miR-432-5p	
hsa-miR-505-3p	ELOVL4 (ELOVL fatty acid elongase 4)
hsa-miR-29a-3p	ELOVL4 (ELOVL fatty acid elongase 4)
hsa-miR-19b-3p	ELOVL5 (ELOVL fatty acid elongase 5)
hsa-miR-185-5p	ELOVL4 (ELOVL fatty acid elongase 4)
	ELOVL2 (ELOVL fatty acid elongase 2)
	FAR1 (fatty acyl-CoA reductase 1)
hsa-miR-576-5p	FAR2 (fatty acyl-CoA reductase 2)
hsa-miR-877-5p	
hsa-miR-29b-3p	ELOVL4 (ELOVL fatty acid elongase 4)
hsa-miR-143-3p	FADS6 (fatty acid desaturase 6)
	FAR1 (fatty acyl-CoA reductase 1)
hsa-miR-7976	
hsa-miR-5010-5p	
hsa-miR-4433b-5p	
hsa-miR-4433a-3p	FABP7 (fatty acid binding protein 7)
	ELOVL4 (ELOVL fatty acid elongase 4)
	ELOVL2 (ELOVL fatty acid elongase 2)

3.4. Lipidomics and Epigenomics in AD

From the univariate analysis, differences between groups were not obtained for miRNAs nor individual lipids. Median values are summarised as Supplementary Material (Table S2). In addition, boxplots representing the lipid levels for each participants group were also depicted in the Supplementary Material (Figure S2).

In addition, the analysis between age/gender and biomarkers levels showed no correlations for any miRNA or lipid analysed.

4. Discussion

Epigenomics and lipidomics analyses were carried out in plasma samples from early AD patients, identifying microRNAs and lipids, respectively. From these results, integration analysis was carried out in order to study associations between both compounds families; to evaluate their potential relationship with early AD development; and identify the potential pathways altered in early stages of the disease.

Some studies in literature are focused on multi-omics integration, mainly based on proteomics and miRNAs [26]. However, few studies are focused on lipidomic and miRNAs integration, which allow us to identify different biological activities involved in cell communication [27]. In general, the integration of omics results (lipidomics, metabolomics, proteomics, epigenomics) helps to give a global image of the mechanisms involved in complex diseases [28]. Nevertheless, this field of research is still underdeveloped in AD and few studies are based on this integration [16].

In the present study, integration and selection of variables from each dimension showed that some microRNAs (hsa-miR-494-3p, hsa-miR-6894-3p, hsa-miR-421 and hsa-let-7a-3p) and some lipids (FA (20:3), FA (20:4), FA (16:0), FA (20:2), FA (18:2)) had higher loadings in the regression model. Similarly, a previous study carried out in plasma from amyloid positive and amyloid negative participants obtained a signature of 71 miRNAs differentially expressed between groups, highlighting the hsa-miR-421 and hsa-let-7a-3p [29]. In addition, a previous study from Hojati et al. revealed that hsa-miR-494-3p was slightly up-regulated in AD patients and that it was related to metabolic and cellular response to stress pathways [30]; while Lv et al., found that levels of hsa-let-7a-3p were elevated in patients with early onset familiar AD [31]. The up-regulation of hsa-let-7a-3p showed an increase in neurotoxicity in AD cell model [32]. On the other hand, previous studies found several fatty acids levels increased or decreased in AD [33,34]. Specifically, AD was related to lower levels of myristic 14:0, palmitic 16:0, stearic 18:0 and oleic 18:1 acid and a higher proportion of linoleic acid 18:2n−6 [33]. However, this study was limited to FAs from 14:0 to 22:6 and did not determine all lipidic profiles. In addition, Conquer et al. described lower levels of phospholipid, PC 20:5n-3, DHA, total n−3 fatty acids, the n−3/n−6 ratio and phospholipid 24:0 compared to controls [34]. Moreover, Conquer et al. did not find differences for FA (20:3), FA (20:4), FA (20:2) and FA (18:2) in plasma samples from AD, cognitive impairment, and patients with other neurodegenerative diseases [34]. This discrepancy with the present results could be due to differences in AD diagnosis methods, since the previous study did not use CSF biomarkers to identify AD patients. In fact, these participants were classified by amyloid PET, and biomarkers were measured in erythrocytes. In addition, erythrocyte fatty acid composition varied according to disease development, showing differences between AD and non-AD participants for FA (20:4) but not for FA (20:3), FA (20:2) nor FA (18:2) [35].

Regarding correlations between microRNAs and lipids, and similarities among them in each omics data group, they showed that most of these correlations were positive. However, previous studies that correlated epigenomics (DNA hydroxymethylation) and metabolomics showed more variety between positive and negative correlations [36]. More specifically, several studies in neurodegeneration revealed the interaction between miRNAs expression and lipids regulation, mainly focussed on cholesterol metabolism [37]. Jauouen et al. described miR-33 function modulating ABCA1 and interfering with Aβ plaque formation through cholesterol metabolism regulation [38]. In the present study, some

miRNAs (miR-29a-3p, let-7a-3p, miR-576-5p, miR-185-5p, miR-6894-3p, miR-5010-5p; for miR-29b-3p, miR-877-5p, miR-494-3p, miR-4433a-3p, miR-4433b-5p; for miR-421, miR-450b-5p, miR-664a-3p, miR-432-5p, miR-654-5p, miR-2110, miR-329-3p) were grouped reflecting their similarity. Taking into account previous works, Kumar et al. found different miRNAs clustered expression, differentiating AD and control participants (hsa-miR-4741, hsa-miR-4668-5p, hsa-miR-3613-3p, hsa-miR-5001-5p, miR-4674) [39]. The discrepancies with present results may be due to the difference in the diagnosis of the patients, since the study from Kumar et al. was not based on CSF biomarkers. Moreover, Denk et al. showed clustered expression of miRNAs in control, AD and frontotemporal dementia participants, showing that some clusters included miRNAs from the same family, while others included different families in the same cluster, as in the present study [40]. However, the set of analysed miRNAs was limited. On the other hand, some lipids were grouped in the present paper (FA (18:0)/FA (14:0)/FA (18:0)/FA (16:0)/FA (18:2); FA (20:3)/FA (20:4)/FA (18:2)/FA (20:2)/FA (16:0)). In this sense, previous findings in an AD mice model showed different lipids expression clusters along the disease progression (two, three, seven months), showing mainly PEs in two months progression and a predomination of TG at seven months [41]. In addition, Kumar et al. described the co-regulation of different lipid sets, among which 17 were fatty acids [42].

Finally, the highest positive correlations between microRNAs and lipids were mainly for hsa-miR-664, hsa-miR-432, hsa-let-7a-3p, hsa-miR-29a-3p, hsa-miR-421 and hsa-miR-450b-5p with some fatty acids (FA (16:0), FA (18:0), FA (20:2), FA (20:3), FA (20:4)). In general, the described miRNAs showed a positive correlation with fatty acids. Of note, these miRNAs targeted sequences in genes implied in fatty acids metabolism. In this sense, previous studies showed a relationship between AD and fatty acids metabolism, demonstrating differential levels of fatty acids (FA (16:0), FA (18:0), FA (18:1), FA (18:2), FA(20:4), FA (20:5), FA (22:6)) similar to the present results [43]. Regarding hsa-miR-421, it showed a positive correlation with some detected lipids (FA (16:0), FA (20:2), FA (18:2), FA (20:4), FA (20:3), FA (18:0), FA (14:0)). Previous works identified the relationship between this miRNA and lipid metabolism regulation, specifically with triacylglycerol levels [44].On the other hand, the highest negative correlations corresponded to the triglyceride (TG (17:0/17:0/17:0)) with some miRNAs (hsa-miR-664-3p, hsa-miR-432-5p, hsa-miR-329-3p, hsa-miR-654-5p, hsa-miR-185-5p, hsa-let-7a-3p, hsa-miR-576-5p, hsa-miR-29a-3p, hsa-miR-421, hsa-miR-450b-5p). Similarly, in literature it was shown that hsa-miR-29a could regulate the lipoprotein lipase (LPL) that catalyses hydrolysis of the triglycerides [45].

The main limitation of this study is the reduced number of healthy control patients. However, the availability of biologically identified (CSF biomarkers) patients with MCI due to AD provides a great potential in the identification of potential pathways involved in early AD. Other limitations in this study are: (i) the analytical method is a semiquantitative approach, (ii) the ApoE genotype has not been taken into account, although it is known that ApoE is involved in lipid homeostasis.

5. Conclusions

The present study highlights the potential of a multi-omics approach in the development of a signature of biomarkers of MCI-AD, as well as the description of potential metabolic pathways involved in AD since its early stages. Specifically, epigenomics and lipidomics integration allowed us to identify some associations between microRNAs and lipids, showing their relationship with early AD development. In fact, fatty acids impairment could be an important pathway involved in early AD. However, further work based on targeted analysis should be carried out in a larger cohort in order to validate these preliminary results, as well as to study the proposed pathways in detail.

Supplementary Materials: The following are available online at https://www.mdpi.com/article/10.3390/biomedicines9121812/s1, Figure S1: Correlation circle plot between miRNAs and lipids selected on each component, Figure S2: Boxplots representing lipid levels in participants' groups, Table S1: Correlation matrix representing the individual correlation between miRNAs and lipids, Table S2: Median values for individual miRNAs and lipids in control and MCI-AD participants.

Author Contributions: Conceptualization, C.C.-P.; methodology, C.P.-B. and L.Á.-S.; software, A.J.C.-M.; formal analysis, C.P.-B. and A.J.C.-M.; investigation, C.C.-P. and M.B.; data curation, L.Á.-S.; writing—original draft preparation, C.C.-P. and C.P.-B.; writing—review and editing, C.C.-P.; supervision, M.B.; funding acquisition, C.C.-P. All authors have read and agreed to the published version of the manuscript.

Funding: This study has been funded by Instituto de Salud Carlos III through the project PI19/00570 (Co-funded by European Regional Development Fund, "A way to make Europe"). CCP acknowledges MS16/00082. CPB acknowledges PFIS FI20/00022. LAS acknowledges Río Hortega CM20/00140.

Institutional Review Board Statement: The study was approved by the Ethics Committee Health at the Research Institute La Fe (Valencia) (protocol code 2019/0105, 22 May 2019).

Informed Consent Statement: Informed consent was obtained from all subjects involved in the study.

Data Availability Statement: The data that support the findings of this study are available on request from the corresponding author (C.C.-P.).

Acknowledgments: This work was supported by the Instituto de Salud Carlos III Project PI19/00570 (Spanish Ministry of Economy and Competitiveness, and Fondo Europeo Desarrollo Regional). CCP acknowledges MS16/00082. CPB acknowledges PFIS FI20/00022. LAS acknowledges RH CM20/00140.

Conflicts of Interest: None of the authors of this manuscript declare having any conflict of interest.

References

1. Alzheimer's Association. 2020 Alzheimer's disease facts and figures. *Alzheimer's Dement.* **2020**, *16*, 391–460. [CrossRef]
2. Gong, C.-X.; Liu, F.; Iqbal, K. Multifactorial hypothesis and multi-targets for Alzheimer's disease. *J. Alzheimer's Dis.* **2018**, *64*, S107–S117. [CrossRef]
3. Nativio, R.; Lan, Y.; Donahue, G.; Sidoli, S.; Berson, A.; Srinivasan, A.R.; Shcherbakova, O.; Amlie-Wolf, A.; Nie, J.; Cui, X.; et al. An integrated multi-omics approach identifies epigenetic alterations associated with Alzheimer's disease. *Nat. Genet.* **2020**, *52*, 1024–1035. [CrossRef] [PubMed]
4. Takousis, P.; Sadlon, A.; Schulz, J.; Wohlers, I.; Dobricic, V.; Middleton, L.; Lill, C.M.; Perneczky, R.; Bertram, L. Differential expression of microRNAs in Alzheimer's disease brain, blood, and cerebrospinal fluid. *Alzheimer's Dement.* **2019**, *15*, 1468–1477. [CrossRef] [PubMed]
5. Mayo, S.; Benito-León, J.; Peña-Bautista, C.; Baquero, M.; Cháfer-Pericás, C. Recent evidence in epigenomics and proteomics biomarkers for early and minimally invasive diagnosis of Alzheimer's and Parkinson's diseases. *Curr. Neuropharmacol.* **2021**, *19*, 1273–1303. [CrossRef]
6. Cannell, I.G.; Kong, Y.W.; Bushell, M. How do microRNAs regulate gene expression? *Biochem. Soc. Trans.* **2008**, *36*, 1224–1231. [CrossRef]
7. Hébert, S.S.; Horré, K.; Nicolaï, L.; Bergmans, B.; Papadopoulou, A.S.; Delacourte, A.; De Strooper, B. MicroRNA regulation of Alzheimer's Amyloid precursor protein expression. *Neurobiol. Dis.* **2009**, *33*, 422–428. [CrossRef] [PubMed]
8. Kao, Y.-C.; Ho, P.-C.; Tu, Y.-K.; Jou, I.-M.; Tsai, K.-J. Lipids and Alzheimer's disease. *Int. J. Mol. Sci.* **2020**, *21*, 1505. [CrossRef] [PubMed]
9. Xu, J.; Bankov, G.; Kim, M.; Wretlind, A.; Lord, J.; Green, R.; Hodges, A.; Hye, A.; Aarsland, D.; Velayudhan, L.; et al. Integrated lipidomics and proteomics network analysis highlights lipid and immunity pathways associated with Alzheimer's disease. *Transl. Neurodegener.* **2020**, *9*, 36. [CrossRef]
10. Proitsi, P.; Kim, M.; Whiley, L.; Simmons, A.; Sattlecker, M.; Velayudhan, L.; Lupton, M.K.; Soininen, H.; Kloszewska, I.; Mecocci, P.; et al. Association of blood lipids with Alzheimer's disease: A comprehensive lipidomics analysis. *Alzheimer's Dement.* **2017**, *13*, 140–151. [CrossRef]
11. Wang, M.; Li, A.; Sekiya, M.; Beckmann, N.D.; Quan, X.; Schrode, N.; Fernando, M.B.; Yu, A.; Zhu, L.; Cao, J.; et al. Transformative network modeling of multi-omics data reveals detailed circuits, key regulators, and potential therapeutics for Alzheimer's disease. *Neuron* **2021**, *109*, 257–272.e14. [CrossRef] [PubMed]
12. Xicota, L.; Ichou, F.; Lejeune, F.-X.; Colsch, B.; Tenenhaus, A.; Leroy, I.; Fontaine, G.; Lhomme, M.; Bertin, H.; Habert, M.-O.; et al. Multi-omics signature of brain amyloid deposition in asymptomatic individuals at-risk for Alzheimer's disease: The INSIGHT-preAD study. *EBioMedicine* **2019**, *47*, 518–528. [CrossRef]

13. Bihlmeyer, N.A.; Merrill, E.; Lambert, Y.; Srivastava, G.P.; Clark, T.W.; Hyman, B.T.; Das, S. Novel methods for integration and visualization of genomics and genetics data in Alzheimer's disease. *Alzheimer's Dement.* **2019**, *15*, 788–798. [CrossRef] [PubMed]
14. Shigemizu, D.; Akiyama, S.; Higaki, S.; Sugimoto, T.; Sakurai, T.; Boroevich, K.A.; Sharma, A.; Tsunoda, T.; Ochiya, T.; Niida, S.; et al. Prognosis prediction model for conversion from mild cognitive impairment to Alzheimer's disease created by integrative analysis of multi-omics data. *Alzheimers. Res. Ther.* **2020**, *12*, 145. [CrossRef] [PubMed]
15. Darst, B.F.; Lu, Q.; Johnson, S.C.; Engelman, C.D. Integrated analysis of genomics, longitudinal metabolomics, and Alzheimer's risk factors among 1,111 cohort participants. *Genet. Epidemiol.* **2019**, *43*, 657–674. [CrossRef]
16. Hampel, H.; Nisticò, R.; Seyfried, N.T.; Levey, A.I.; Modeste, E.; Lemercier, P.; Baldacci, F.; Toschi, N.; Garaci, F.; Perry, G.; et al. Omics sciences for systems biology in Alzheimer's disease: State-of-the-art of the evidence. *Ageing Res. Rev.* **2021**, *69*, 101346. [CrossRef]
17. Hedman, Å.K.; Mendelson, M.M.; Marioni, R.E.; Gustafsson, S.; Joehanes, R.; Irvin, M.R.; Zhi, D.; Sandling, J.K.; Yao, C.; Liu, C.; et al. Epigenetic patterns in blood associated with lipid traits predict incident coronary heart disease events and are enriched for results from genome-wide association studies. *Circ. Cardiovasc. Genet.* **2017**, *10*, e001487. [CrossRef] [PubMed]
18. Gordevicius, J.; Li, P.; Marshall, L.L.; Killinger, B.A.; Lang, S.; Ensink, E.; Kuhn, N.C.; Cui, W.; Maroof, N.; Lauria, R.; et al. Epigenetic inactivation of the autophagy–lysosomal system in appendix in Parkinson's disease. *Nat. Commun.* **2021**, *12*, 5134. [CrossRef] [PubMed]
19. Randolph, C.; Tierney, M.C.; Mohr, E.; Chase, T.N. The Repeatable Battery for the Assessment of Neuropsychological Status (RBANS): Preliminary clinical validity. *J. Clin. Exp. Neuropsychol.* **1998**, *20*, 310–319. [CrossRef]
20. Pfeffer, R.I.; Kurosaki, T.T.; Harrah, C.H.; Chance, J.M.; Filos, S. Measurement of functional activities in older adults in the community. *J. Gerontol.* **1982**, *37*, 323–329. [CrossRef]
21. Hughes, C.P.; Berg, L.; Danziger, W.L.; Coben, L.A.; Martin, R.L. A new clinical scale for the staging of dementia. *Br. J. Psychiatry* **1982**, *140*, 566–572. [CrossRef] [PubMed]
22. Kurlowicz, L.; Wallace, M. The mini-mental state examination (MMSE). *J. Gerontol. Nurs.* **1999**, *25*, 8–9. [CrossRef]
23. Kulkarni, N.; Alessandrì, L.; Panero, R.; Arigoni, M.; Olivero, M.; Ferrero, G.; Cordero, F.; Beccuti, M.; Calogero, R.A. Reproducible bioinformatics project: A community for reproducible bioinformatics analysis pipelines. *BMC Bioinform.* **2018**, *19*, 349. [CrossRef] [PubMed]
24. González, I.; Cao, K.-A.L.; Davis, M.J.; Déjean, S. Visualising associations between paired 'omics' data sets. *BioData Min.* **2012**, *5*, 19. [CrossRef]
25. Murtagh, F.; Legendre, P. Ward's hierarchical agglomerative clustering method: Which algorithms implement Ward's criterion? *J. Classif.* **2014**, *31*, 274–295. [CrossRef]
26. Zhang, L.; Wu, K.; Bo, T.; Zhou, L.; Gao, L.; Zhou, X.; Chen, W. Integrated microRNA and proteome analysis reveal a regulatory module in hepatic lipid metabolism disorders in mice with subclinical hypothyroidism. *Exp. Ther. Med.* **2020**, *19*, 897–906. [CrossRef] [PubMed]
27. Hussey, G.S.; Molina, C.P.; Cramer, M.C.; Tyurina, Y.Y.; Tyurin, V.A.; Lee, Y.C.; El-Mossier, S.O.; Murdock, M.H.; Timashev, P.S.; Kagan, V.E.; et al. Lipidomics and RNA sequencing reveal a novel subpopulation of nanovesicle within extracellular matrix biomaterials. *Sci. Adv.* **2020**, *6*, eaay4361. [CrossRef]
28. Alcazar, O.; Hernandez, L.F.; Nakayasu, E.S.; Nicora, C.D.; Ansong, C.; Muehlbauer, M.J.; Bain, J.R.; Myer, C.J.; Bhattacharya, S.K.; Buchwald, P.; et al. Parallel multi-omics in high-risk subjects for the identification of integrated biomarker signatures of type 1 diabetes. *Biomolecules* **2021**, *11*, 383. [CrossRef] [PubMed]
29. Nair, P.S.; Raijas, P.; Ahvenainen, M.; Philips, A.K.; Ukkola-Vuoti, L.; Järvelä, I. Music-listening regulates human microRNA expression. *Epigenetics* **2021**, *16*, 554–566. [CrossRef]
30. Hojati, Z.; Omidi, F.; Dehbashi, M.; Mohammad Soltani, B. The highlighted roles of metabolic and cellular response to stress pathways engaged in circulating hsa-miR-494-3p and hsa-miR-661 in Alzheimer's disease. *Iran. Biomed. J.* **2021**, *25*, 62–67. [CrossRef]
31. Lv, Z.; Hu, L.; Yang, Y.; Zhang, K.; Sun, Z.; Zhang, J.; Zhang, L.; Hao, Y. Comparative study of microRNA profiling in one Chinese Family with PSEN1 G378E mutation. *Metab. Brain Dis.* **2018**, *33*, 1711–1720. [CrossRef]
32. Gu, H.; Li, L.; Cui, C.; Zhao, Z.; Song, G. Overexpression of let-7a increases neurotoxicity in a PC12 cell model of Alzheimer's disease via regulating autophagy. *Exp. Ther. Med.* **2017**, *14*, 3688–3698. [CrossRef]
33. Rönnemaa, E.; Zethelius, B.; Vessby, B.; Lannfelt, L.; Byberg, L.; Kilander, L. Serum fatty-acid composition and the risk of Alzheimer's disease: A longitudinal population-based study. *Eur. J. Clin. Nutr.* **2012**, *66*, 885–890. [CrossRef] [PubMed]
34. Conquer, J.A.; Tierney, M.C.; Zecevic, J.; Bettger, W.J.; Fisher, R.H. Fatty acid analysis of blood plasma of patients with alzheimer's disease, other types of dementia, and cognitive impairment. *Lipids* **2000**, *35*, 1305–1312. [CrossRef] [PubMed]
35. Goozee, K.; Chatterjee, P.; James, I.; Shen, K.; Sohrabi, H.R.; Asih, P.R.; Dave, P.; Ball, B.; ManYan, C.; Taddei, K.; et al. Alterations in erythrocyte fatty acid composition in preclinical Alzheimer's disease. *Sci. Rep.* **2017**, *7*, 676. [CrossRef]
36. Johnson, L.A.; Torres, E.R.S.; Impey, S.; Stevens, J.F.; Raber, J. Apolipoprotein E4 and Insulin Resistance Interact to Impair Cognition and Alter the Epigenome and Metabolome. *Sci. Rep.* **2017**, *7*, 43701. [CrossRef] [PubMed]
37. Goedeke, L.; Fernández-Hernando, C. microRNAs: A connection between cholesterol metabolism and neurodegeneration. *Neurobiol. Dis.* **2014**, *72*, 48–53. [CrossRef]

38. Jaouen, F.; Gascon, E. Understanding the role of miR-33 in brain lipid metabolism: Implications for Alzheimer's disease. *J. Neurosci.* **2016**, *36*, 2558–2560. [CrossRef]
39. Kumar, S.; Vijayan, M.; Reddy, P.H. MicroRNA-455-3p as a potential peripheral biomarker for Alzheimer's disease. *Hum. Mol. Genet.* **2017**, *26*, 3808–3822. [CrossRef]
40. Denk, J.; Oberhauser, F.; Kornhuber, J.; Wiltfang, J.; Fassbender, K.; Schroeter, M.L.; Volk, A.E.; Diehl-Schmid, J.; Prudlo, J.; Danek, A.; et al. Specific serum and CSF microRNA profiles distinguish sporadic behavioural variant of frontotemporal dementia compared with Alzheimer patients and cognitively healthy controls. *PLoS ONE* **2018**, *13*, e0197329. [CrossRef]
41. Zhang, X.; Liu, W.; Zan, J.; Wu, C.; Tan, W. Untargeted lipidomics reveals progression of early Alzheimer's disease in APP/PS1 transgenic mice. *Sci. Rep.* **2020**, *10*, 14509. [CrossRef] [PubMed]
42. Barupal, D.K.; Baillie, R.; Fan, S.; Saykin, A.J.; Meikle, P.J.; Arnold, M.; Nho, K.; Fiehn, O.; Kaddurah-Daouk, R. Sets of coregulated serum lipids are associated with Alzheimer's disease pathophysiology. *Alzheimer's Dement. Diagn. Assess. Dis. Monit.* **2019**, *11*, 619–627. [CrossRef]
43. Ooi, K.-L.M.; Vacy, K.; Boon, W.C. Fatty acids and beyond: Age and Alzheimer's disease related changes in lipids reveal the neuro-nutraceutical potential of lipids in cognition. *Neurochem. Int.* **2021**, *149*, 105143. [CrossRef] [PubMed]
44. Braga, A.A.; Bortolin, R.H.; Graciano-Saldarriaga, M.E.; Hirata, T.D.; Cerda, A.; de Freitas, R.C.; Lin-Wang, H.T.; Borges, J.B.; França, J.I.; Masi, L.N.; et al. High serum miR-421 is associated with metabolic dysregulation and inflammation in patients with metabolic syndrome. *Epigenomics* **2021**, *13*, 423–436. [CrossRef] [PubMed]
45. He, P.-P.; Jiang, T.; OuYang, X.-P.; Liang, Y.-Q.; Zou, J.-Q.; Wang, Y.; Shen, Q.-Q.; Liao, L.; Zheng, X.-L. Lipoprotein lipase: Biosynthesis, regulatory factors, and its role in atherosclerosis and other diseases. *Clin. Chim. Acta* **2018**, *480*, 126–137. [CrossRef] [PubMed]

8.2 Articles published by the doctoral candidate not included in the compendium but directly associated with the present doctoral thesis

8.2.1 Articles

Recent Evidence in Epigenomics and Proteomics Biomarkers for Early and Minimally Invasive Diagnosis of Alzheimer's and Parkinson's Diseases. Mayo S, Benito-León J, Peña-Bautista C, Baquero M, Cháfer-Pericás C. **Curr Neuropharmacol**. 2021;19(8):1273-1303. doi: 10.2174/1570159X19666201223154009.

Lipid peroxidation in neurodegeneration. Peña-Bautista C, Vento M, Baquero M, Cháfer-Pericás C. **Clin Chim Acta**. 2019 Oct;497:178-188. doi: 10.1016/j.cca.2019.07.037.

Free radicals in Alzheimer's disease: Lipid peroxidation biomarkers. Peña-Bautista C, Baquero M, Vento M, Cháfer-Pericás C. **Clin Chim Acta**. 2019 Apr;491:85-90. doi: 10.1016/j.cca.2019.01.02.

Plasma isoprostanoids assessment as Alzheimer's disease progression biomarkers. Peña-Bautista C, Álvarez L, Baquero M, Ferrer I, García L, Hervás-Marín D, Cháfer-Pericás C. **J Neurochem**. 2021 Jun;157(6):2187-2194. doi: 10.1111/jnc.15183.

Early neurotransmission impairment in non-invasive Alzheimer Disease detection. Peña-Bautista C, Torres-Cuevas I, Baquero M, Ferrer I, García L, Vento M, Cháfer-Pericás C. **Sci Rep**. 2020 Oct 2;10(1):16396. doi: 10.1038/s41598-020-73362-z.

Lipids as Early and Minimally Invasive Biomarkers for Alzheimer's Disease. Casas-Fernández E, Peña-Bautista C, Baquero M, Cháfer-Pericás C. **Curr Neuropharmacol**. 2022;20(8):1613-1631. doi: 10.2174/1570159X19666211102150955

Assessment of Lipid Peroxidation in Alzheimer's Disease Differential Diagnosis and Prognosis. Ferré-González L, Peña-Bautista C, Baquero M, Cháfer-Pericás C. **Antioxidants (Basel)**. 2022 Mar 14;11(3):551. doi: 10.3390/antiox11030551.

Assessment of Screening Approach in Early and Differential Alzheimer's Disease Diagnosis. Ferré-González L, Peña-Bautista C, Álvarez-Sánchez L, Ferrer-Cairols I, Baquero M, Cháfer-Pericás C. **Antioxidants (Basel).** 2021 Oct 22;10(11):1662. doi: 10.3390/antiox10111662.

Validated analytical method to determine new salivary lipid peroxidation compounds as potential neurodegenerative biomarkers. Peña-Bautista C, Carrascosa-Marco P, Oger C, Vigor C, Galano JM, Durand T, Baquero M, López-Nogueroles M, Vento M, García-Blanco A, Cháfer-Pericás C. **J Pharm Biomed Anal**. 2019 Feb 5;164:742-749. doi: 10.1016/j.jpba.2018.11.043.

Plasma alterations in cholinergic and serotonergic systems in early Alzheimer Disease: Diagnosis utility. Peña-Bautista C, Flor L, López-Nogueroles M, García L, Ferrer I, Baquero M, Vento M, Cháfer-Pericás C. **Clin Chim Acta**. 2020 Jan;500:233-240. doi: 10.1016/j.cca.2019.10.023.

Omics-based Biomarkers for the Early Alzheimer Disease Diagnosis and Reliable Therapeutic Targets Development. Peña-Bautista C, Baquero M, Vento M, Cháfer-Pericás C. **Curr Neuropharmacol**. 2019;17(7):630-647. doi: 10.2174/1570159X16666180926123722.

Reliable determination of new lipid peroxidation compounds as potential early Alzheimer Disease biomarkers. García-Blanco A, Peña-Bautista C, Oger C, Vigor C, Galano JM, Durand T, Martín-Ibáñez N, Baquero M, Vento M, Cháfer-Pericás C. **Talanta**. 2018 Jul 1;184:193-201. doi: 10.1016/j.talanta.2018.03.002.